

Environmental Assessment of the Alaskan Continental Shelf

**Annual Reports of
Principal Investigators
for the year ending March 1981**

Volume V: Transport



US DEPARTMENT OF COMMERCE
National Oceanic & Atmospheric Administration
National Ocean Service
Office of Oceanography & Marine Services



US DEPARTMENT OF THE INTERIOR
Minerals Management Service

Annual Reports of Principal Investigators

1981

GC
85.2
.A4
E57
1981
v.5

Environmental Assessment of the Alaskan Continental Shelf

Annual Reports of
Principal Investigators
for the year ending March 1981

Volume V: Transport



US DEPARTMENT OF COMMERCE
National Oceanic & Atmospheric Administration
National Ocean Service
Office of Oceanography & Marine Services



US DEPARTMENT OF THE INTERIOR
Minerals Management Service

ARLIS
Alaska Resources
Library & Information Services
Anchorage, Alaska

The facts, conclusions and issues appearing in these reports are based on interim results of an Alaskan environmental studies program managed by the Outer Continental Shelf Environmental Assessment Program (OCSEAP) of the National Oceanic and Atmospheric Administration (NOAA), U.S. Department of Commerce, and primarily funded by the Bureau of Land Management (BLM), U.S. Department of Interior, through interagency agreement.

DISCLAIMER

Mention of a commercial company or product does not constitute an endorsement by National Oceanic and Atmospheric Administration. Use for publicity or advertising purposes of information from this publication concerning proprietary products or the tests of such products is not authorized.

VOLUME V

TRANSPORT

<u>RU#</u>	<u>PI/Agency</u>	<u>Title</u>	<u>Page</u>
87	Martin, Seelye -University of Washington, Seattle, WA	The Interaction of Oil with Sea Ice in the Arctic Ocean	1
153	Cline, J., C. Katz, and H. Curl, Jr. -PMEL, Seattle, WA	Circulation Processes in Bristol Bay, Alaska, Using Dissolved Methane as a Tracer	29
435	Leendertse, J. J. and S.K. Liu -Rand Corporation, Santa Monica, CA	Modeling of Tides and Circulations of the Bering Sea	87
519	Kozo, T.L. -Tetra Tech, Inc., Pasadena, CA	Meteorology of the Alaskan Arctic Coast	109
526/ 77	Matthews, J.B. -University of Alaska, Fairbanks, AK	Characterization of the Nearshore Hydrodynamics of the Beaufort Sea and Chukchi Sea and Summer Studies of the Physical Oceanography of the Beaufort Sea Tracts for Sale #71	129
529/ 77	Naidu, A.S., L.H. Larsen, M.D. Sweeney, and H.V. Weiss -University of Alaska, Fairbanks, AK	Sources, Transport Pathways, Depositional Sites and Dynamics of Sediments in the Lagoon and Adjacent Shallow Marine Region, Northern Arctic Alaska	151
531	Wilson, D.E. et. al. -Kinnetic Laboratory, Anchorage, AK	Numerical Trajectory Modeling and Associated Field Measurements in the Beaufort Sea and Chukchi Sea Nearshore Areas	299
549	Schumacher, J.D., and C.A. Pearson, -PMEL, Seattle, WA	Bristol Bay Oceanographic Processes "Fluid Transport Processes in the North Aleutian Shelf and St. George Basin"	379

ANNUAL REPORT

Contract #03-5-022-67
Research Unit #87
Reporting Period:
1 April 1980 - 1 April 1981
Number of Pages: 27

THE INTERACTION OF OIL WITH SEA ICE IN THE ARCTIC OCEAN

Seelye Martin

Department of Oceanography WB-10

University of Washington

Seattle, Washington 98195

6 April 1981

REF: A81-06

I. Introduction

During the past year, in cooperation with Dr. Robin Muench of SAI/Northwest, we carried out an autumn and midwinter cruise in the Bering Sea. Appendices I and II describe the observations made by Dr. Muench; he coordinated both the placement of six over-winter current meters and the CTD research program during these cruises.

Second, during the midwinter LEG II SURVEYOR cruise, S. Martin carried out an observational program consisting of the tracking of ice-mounted radar transponders with the X-Band radar on the ship. The following section describes this program.

II. The Radar Buoy Experiment

A. Background: The purpose of this experiment was to determine the small-scale motion of ice floes near the ice edge in response to winds, waves, and tides. We carried out this study by mounting radar transponders on the ice floes, then tracking them with the X-Band radar on the ship. The transponders were contained inside and at the top of a 7.5 inch diameter, 10' long plastic pipe, which was sealed at both ends and contained rechargeable batteries and ballast in the tube bottom. To extend the battery lifetimes to 60 hours, the transponders had a duty cycle of 1 minute on, 2 minutes off. The buoys were also designed to float upright when they melted loose from the ice, and had a VINYL-FLOAT attached to them with a line to allow for pickup.

The buoys were mounted in the ice by drilling an 8" hole through the floe with a power auger, then dropping the buoy into the hole. When mounted in this way, about 5' of buoy stuck up above the ice. Using these buoys, we carried out the two related experiments. In the first, we deployed 4 buoys in a 2.4 mile long East-West line on floes near the ice edge and tracked the buoy

positions for 48 hours. In the second, we deployed 2 buoys on a 2.8 mile long North-South line and tracked them for 44 hours. In both cases we recorded the positions of each buoy at half-hour intervals. In the first experiment, the buoys remained within the ice floes at the edge; in the second, the buoys which were initially at the edge were carried rapidly southwest in an ice band by 20-40 kt winds where they melted out of the ice, so that we picked them up in open water.

B. Deployment Chronology

4 March: We deployed four buoys, called LUCY, MARY, DAVID, and SUZI within the pack ice near the edge along an East-West line from a small boat. The deployment took place between 1000 and 1500 hours; we mounted the buoys on floes with diameters of about 8 m, and thicknesses of about 1.2 m. We began our systematic logging of the buoy positions at 1500 hours. Between 1745-1800, we did a helicopter survey of the ice in which the floes were embedded. The survey flight showed that the buoys were in an ice strip adjacent to the main pack measuring about 1 nautical mile wide. The ice in this strip consisted of floes measuring 8-10 m in diameter and smaller which were floating in a 0.1 m thick slush ice layer.

5 March: We continued monitoring, from 1230-1330, we did a second helicopter survey flight in which we photographed each buoy from a 75' altitude. We also discovered that SUZI had moved away from the pack into a small cluster of floes.

6 March: At 1000, we did a final helicopter survey, and found that the former

brash and slush ice had refrozen into pancake and nilas. This refreezing was accompanied by a divergence of the pack which is also apparent in our buoy trajectories. We then carried out the buoy recovery. In the recovery, we steamed up to each buoy, then grappled the floe against the side of the ship. For the first two floes, we found that buoys LUCY and MARY were frozen into the ice, so that we were able to recover only the electronics. By careful digging out of the last two buoys we were able to recover them completely. This recovery took from 1100 to 1400. In the evening, we recharged the buoy batteries, and rigged two more buoys for deployment on the following day.

7 March: In the morning Quartermaster Edward LeMay spotted the shells of the buoys abandoned on the previous day. Between 1030 and 1200, we reoccupied these sites. Buoy MARY had been damaged by the attempt to auger it out the previous day so we abandoned it. We did, however, recover the shell of LUCY. We then installed a new buoy, JAREL, on the same floe from which we recovered buoy LUCY. We then steamed 3 miles north and installed the second buoy KURT at 1305, again on a floe of 10-12 m diameter. Following the installation, the wind picked up from the northeast at 20-40 knots which blew the buoys southwest at speeds of up to 1.3 knots.

8 March: Continued to track buoys, which moved away from the pack within a common band. The weather was too rough to fly; however, we did cruise around the band.

9 March: The band continued to move into warmer water. At 0500 we lost contact with JAREL, and by 0800, we had only a weak sporadic contact with KURT. Using these weak fixes, we steamed toward it, through heavy seas and 30 knot winds. First light showed that the ice band was reduced to remnants. Quartermaster LeMay again spotted buoy KURT in open water about 3 miles upwind of the band, and the buoy was recovered by the ship. We then steamed south on a dead-reckoning course based on the last known relative position of KURT-JAREL; Ensign Bill spotted JAREL about 3 miles down this course, and it was recovered by the ship at 0900.

In summary, during the course of our observations, we tracked the position of the floe marked by LUCY/JAREL from

4 March 1981 at 1600 (local)	59 18 29 N
	171 37 42 W

to

9 March 1981 at 0900	58 24 34 N
	173 28 13 W

for a straight line displacement over a 113 hour period of 78 nautical miles.

C. Preliminary Results: We obtained two data sets from this experiment, one from the 4 buoy array for conditions of light winds and a freezing and diverging pack, the second from the 2 buoy array for conditions of an ice band being advected by high winds southwest into warmer water where the band disintegrated.

What do we observe in a first look at this data set? First, there is a strong tidal signal present in all of the buoy tracks. This signal manifests itself as a periodic acceleration and deceleration of the buoy trajectories,

as well as periodic changes in the trajectory angle. Second, we observe a high coherence between the trajectories on the 3 nautical mile scale. Third, the first data set shows clearly a strong local divergence of the pack accompanied by the freezing of the slush ice surrounding the floes.

Fourth, comparison of the radar data from the second ice band observations with the pack ice interior data gathered from the satellite-tracked ice buoys deployed by Carol Pease clearly show that the ice bands move faster than the pack interior. For the twelve hour period immediately preceding the break-up of our band, we measured band velocities of 1.25 knots, while the satellite data from the interior showed ice velocities of 0.9 knots, so that the band velocities were 40% greater than the interior velocities. The cause of this greater velocity appears to be the momentum transferred to the band from the wind-waves. These waves, which are heavily damped by the ice in the bands, transfer their momentum to the ice band, causing it to move at a higher velocity.

Fifth, during our observations of the ice band, the two buoys remained between 2.7 and 2.9 nautical miles apart, while the band became thinner in the downwind direction. This implies that the cause of the thinning of the bands as they move downwind is not lateral spreading; rather the thinning is caused by the progressive erosion of the upwind side of the band by the warm water waves.

D. Acknowledgments: We are grateful to the Captain and crew of the SURVEYOR for their support of this work. We particularly acknowledge the help of the three watches, who put up with our monitoring the radar screen at half-hour intervals, and who demonstrated great skill in deployment and recovery of the buoys.

APPENDIX I

TEMPERATURE AND SALINITY OBSERVATIONS IN THE BERING SEA MARGINAL ICE ZONE

R.D. Muench, SAI/Northwest

Introduction and Program Objectives

As part of the coordinated OCSEAP research program aimed at understanding air/ice/water interactions in the Bering Sea Marginal Ice Zone (MIZ), water temperature and salinity observations have been obtained in autumn and mid-winter in the MIZ region and six recording current meters have been moored over winter in the MIZ. The objectives of these temperature and salinity observations include:

- Definition of the large-scale (i.e. of order hundreds of km) fields of temperature and salinity (and derived density) and relate these to regional oceanographic advective (transport) and diffusive (mixing) processes. This is to be carried out through water mass analyses and by comparing computed geostrophic baroclinic currents with moored current observations.
- Observation of small-scale (1-10 km) features (such as low salinity lenses and frontal structures) in the temperature and salinity distributions along the ice edge during winter and relate these where possible to regional oceanographic features, to ice motion and distribution, and to the wind field.
- Estimation of regional heat and salt balances, in conjunction with sea ice and meteorological data.
- Estimation of the effects upon the water column of convective processes associated with local winds and with ice freezing.
- Estimation of the effects of both large- and small-scale water circulation features upon ice motion and distribution in the MIZ.

Temperature and salinity observations in the Bering MIZ are being obtained through autumn, winter and spring shipboard field programs designed to measure regional distributions during autumn and spring and smaller-scale distributions along and south of the ice edge during winter. The autumn (November 1980) and mid-winter (February-March 1981) field programs have been successfully completed, as detailed in the following section. Achievement of the above objectives will also require the data from moored current meters deployed during November 1980 and scheduled for recovery in May or June 1981. The oceanographic data will be integrated with meteorological data and with ice distribution information obtained during winter 1981.

Completed Field Activities

Two successful field activities involving temperature and salinity observations have been carried out to date under this program: an autumn (November 1980) observation program of regional temperature and salinity distributions combined with current meter mooring deployments, and a mid-winter (February-March 1981) program of detailed temperature and salinity observations along the ice edge. The mid-winter program was carried out simultaneously with intensive observations of meteorological and sea ice features.

During the November 1980 program, 29 CTD casts were occupied in the portion of the Bering Sea normally occupied by the MIZ during winter (Figure I-1). Casts 1-12 and 17-29 of these were part of this program. Those in the vicinity of St. Lawrence Island (numbers prefaced by "NC") were carried out by Mr. R.B. Tripp of the University of Washington as part of a separate program, but nevertheless provide useful supporting data. These CTD data were acquired from the NOAA vessel DISCOVERER using a Plessey Model 9040 CTD system with calibration and processing procedures carried out as per OCSEAP specifications. The initial data processing was done by Ms. P. Morrison of the University of Washington. These November CTD data provide two transects extending across the shelf normal to the isobaths from about the shelf break to the 50-meter isobath and give a good representation of conditions over the central Bering Sea shelf including the MIZ. The observed distributions are discussed in the following section of this report.

In addition to the CTD stations occupied, 10 current meter moorings were deployed in November 1980 (Figure I-1). Those moorings numbered with a "NC" prefix are, again, related to another program but will provide useful supporting data after recovery. Details concerning the November 1980 CTD stations and mooring deployments are given in Tables I-1 and I-2.

During the February - March 1981 field program, 64 CTD casts (2-65, Figure I-1) were taken in the Bering Sea MIZ near the ice edge. (The initial single cast (1) was taken in the Gulf of Alaska near Unimak Pass for equipment calibration purposes.) The geographical location of the winter field work within the overall study region is indicated on Figure I-1; the winter CTD station work included occupation of the outer (southern) eight stations on the southeastern transect shown on Figure I-1, multiple occupation of a portion of this transect, and time series taken along the ice edge. A listing of the winter 1981 CTD stations is given in Table I-3.

The winter 1981 CTD data were taken from the NOAA vessel SURVEYOR using a Plessey Model 9040 CTD system; calibration casts were taken every third station. Preliminary processing of the data has not yet commenced and the discussion below of the temperature data is therefore considered preliminary. No attempt is made to discuss salinity or density data since they have not yet been de-spiked, calibrated, and corrected for CTD lowering rate.

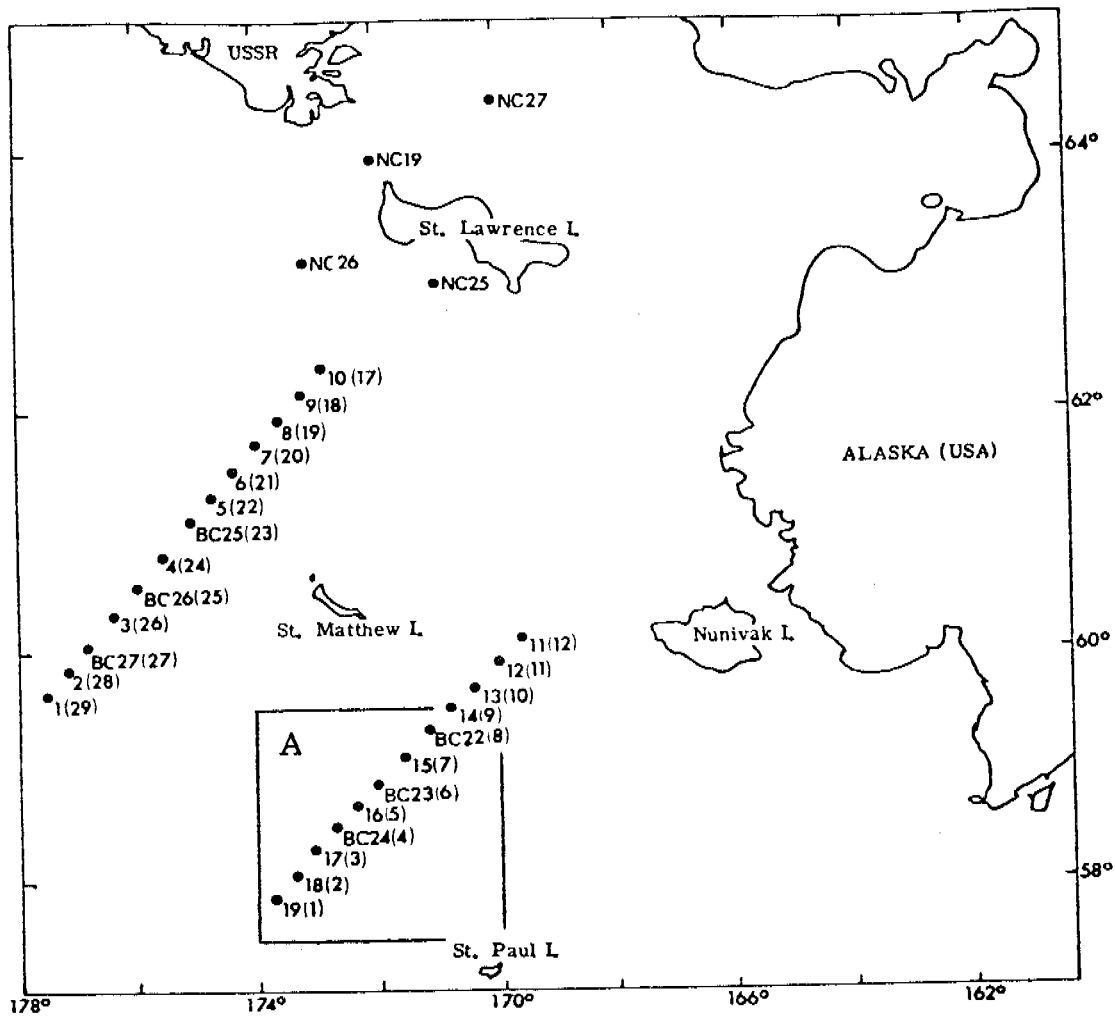


Figure I-1. Geographic locations of CTD stations (● with numbers only) occupied in the Bering Sea MIZ during November 1980 and moored current meter array (● with "BC" or "NC" prefixes) deployed at the same time. Parenthesized numbers are cast numbers which correspond to station names and are used in construction of the vertical sections shown in Figures I-3 to I-8. Rectangular box "A" shows the area covered by the February-March 1981 field program and shown on Figure I-2.

TABLE I-1

CTD STATIONS OCCUPIED IN NOVEMBER 1980

Consecutive Cast No.	Latitude (N)	Longitude (W)	Date (GMT)	JD (GMT)	Hour (GMT)	Bottom Depth (m)	Assigned Sta. No.
1	57-51.5	173-43.2	11-10	315	1440	137	19
2	58-03.8	173-21.7	11-10	315	1623	111	18
3	58-17.1	173-02.7	11-10	315	1759	110	17
4	58-28.1	172-41.1	11-10	315	1935	107	BC24
5	58-41.1	172-20.7	11-10	315	2159	97	16
6	58-51.8	171-59.3	11-10	315	2331	91	BC23
7	59-05.7	171-35.8	11-11	316	0154	82	15
8	59-18.0	171-12.7	11-11	316	0327	76	BC22
9	59-31.1	170-50.8	11-11	316	0526	73	14
10	59-42.1	170-27.1	11-11	316	0658	65	13
11	59-55.9	170-02.9	11-11	316	0823	53	12
12	60-08.1	169-38.8	11-11	316	1013	48	11
17	62-21.0	172-50.1	11-13	318	0207	58	10
18	62-08.9	173-12.6	11-13	318	0334	60	9
19	61-57.0	173-37.0	11-13	318	0509	65	8
20	61-45.1	173-58.9	11-13	318	0635	73	7
21	61-32.1	174-20.7	11-13	318	0759	80	6
22	61-19.9	174-44.0	11-13	318	0931	86	5
23	61-08.0	175-05.7	11-13	318	1057	92	BC25
24	60-51.2	175-34.3	11-13	318	1316	106	4
25	60-34.1	176-01.5	11-13	318	1503	119	BC26
26	60-19.7	176-24.9	11-13	318	1707	128	3
27	60-04.3	176-49.8	11-13	318	1858	142	BC27
28	59-52.2	177-09.8	11-13	318	2103	135	2
29	59-39.2	177-30.3	11-13	318	2238	207	1

TABLE I-2

CURRENT MOORING DEPLOYMENTS IN NOVEMBER 1980

Assigned Mooring ID	Latitude (N)	Longitude (W)	Date (GMT)	JD (GMT)	Hour (GMT)	Bottom Depth(m)	Meter Depth(m)	Meter Serial No
BC22	59-10.4	171-11.4	11-11	316	0357	76	51	1813
BC23	58-51.8	172-01.0	11-11	316	0007	95	52	3130
BC24	58-28.3	172-42.4	11-10	315	2021	107	59	3128
BC25	61-08.3	175-05.9	11-13	318	1128	95	52	3177
BC26	60-34.2	176-02.1	11-13	318	1531	119	52	3135
BC27	60-04.6	176-49.6	11-13	318	1927	142	61	3131

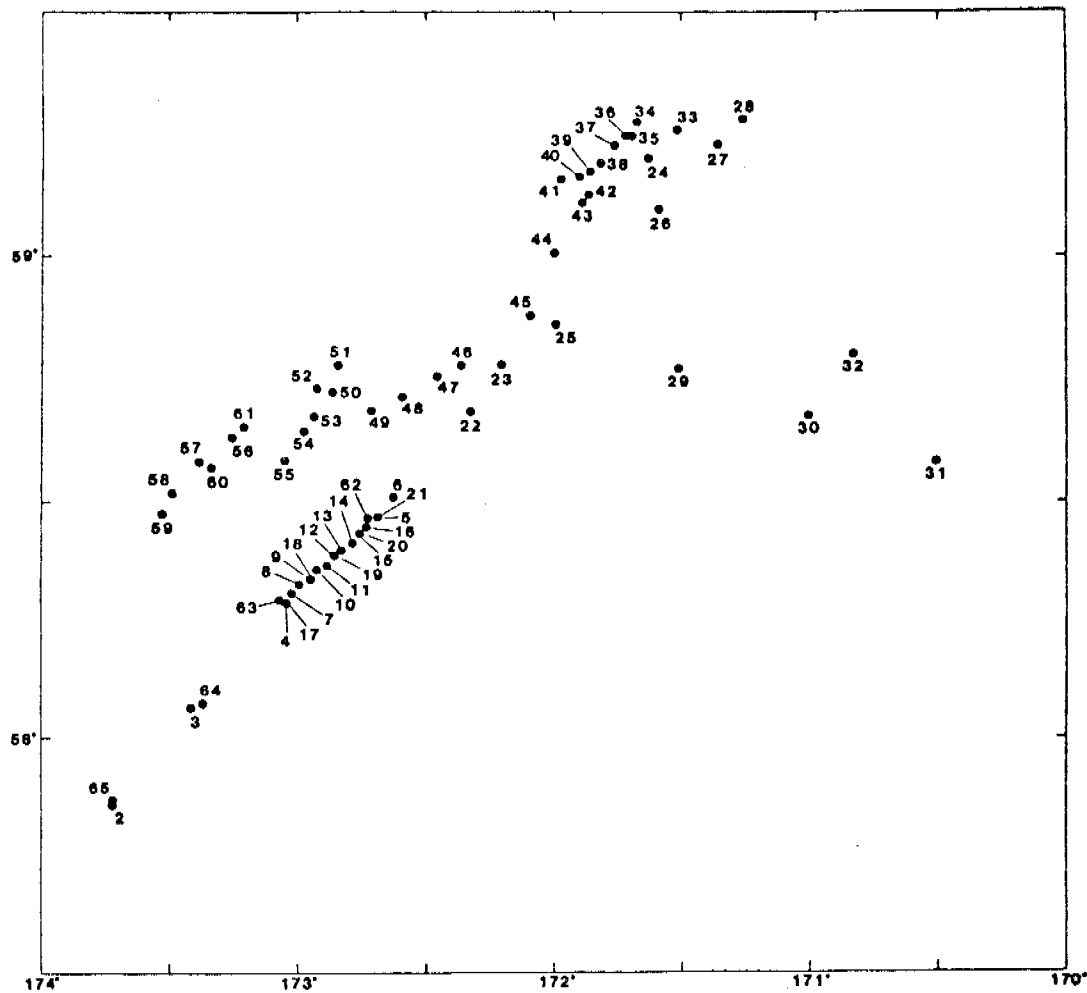


Figure I-2. Geographical locations of CTD stations occupied along the ice edge in the Bering Sea MIZ during February-March 1981. Location of the area shown on this figure within the Bering Sea is indicated on Figure I-1.

TABLE I-3
CTD STATIONS OCCUPIED IN FEBRUARY-MARCH 1981

Consecutive Cast No.	Latitude (N)	Longitude (W)	Date (GMT)	JD (GMT)	Hour (GMT)	Bottom Depth (m)	Assigned Sta. No.
1	55-36.3	158-59.7	2-23	54	2333	114	
2	57-51.7	173-43.0	2-26	57	1315	136	19
3	58-03.8	173-24.7	2-26	57	1610	113	18
4	58-17.1	173-02.9	2-26	57	1921	112	17
5	58-27.9	172-41.1	2-26	57	2116	109	BC24
6	58-30.6	172-37.6	2-26	57	2255	108	
7	58-18.4	173-01.5	2-27	58	0642	111	
8	58-19.4	172-59.7	2-27	58	0724	111	
9	58-20.1	172-57.3	2-27	58	0811	111	
10	58-21.3	172-55.5	2-27	58	0857	112	
11	58-21.9	172-53.1	2-27	58	0937	111	
12	58-23.2	172-51.7	2-27	58	1023	112	
13	58-23.9	172-49.8	2-27	58	1054	110	
14	58-24.8	172-47.2	2-27	58	1135	110	
15	58-25.9	172-45.9	2-27	58	1235	108	
16	58-26.8	172-43.8	2-27	58	1323	108	
17	58-17.2	173-02.6	3-01	60	0916	111	
18	58-20.2	172-56.6	3-01	60	1012	112	
19	58-23.1	172-50.9	3-01	60	1059	110	
20	58-26.1	172-45.1	3-01	60	1146	108	
21	58-28.2	172-41.1	3-01	60	1224	108	
22	58-41.1	172-19.6	3-01	60	1846	104	16
23	58-47.0	172-12.6	3-01	60	2200	101	BC23
24	59-11.9	171-37.9	3-02	61	2237	82	
25	58-52.0	171-59.2	3-03	62	0631	96	BC23
26	59-05.7	171-35.3	3-03	62	0827	83	
27	59-13.3	171-21.4	3-03	62	1048	81	
28	59-16.6	171-15.7	3-03	62	2037	78	BC22
29	58-46.5	171-30.8	3-04	63	0619	91	
30	58-40.6	171-00.7	3-04	63	0817	82	
31	58-34.9	170-30.7	3-04	63	1011	79	
32	58-48.3	170-49.9	3-04	63	1151	79	
33	59-15.5	171-31.2	3-04	63	1505	81	
34	59-16.4	171-40.7	3-05	64	0244	81	
35	59-14.7	171-41.8	3-05	64	0603	80	
36	59-14.7	171-43.1	3-05	64	0637	80	
37	59-13.4	171-45.4	3-05	64	0842	80	
38	59-11.4	171-49.0	3-05	64	1030	83	
39	59-10.3	171-51.4	3-05	64	1232	84	
40	59-09.6	171-54.0	3-05	64	1448	85	
41	59-09.3	171-58.1	3-05	64	1648	85	
42	59-07.5	171-51.9	3-05	64	2045	86	

Contin

TABLE I-3 (continued)

Consecutive Cast No.	Latitude (N)	Longitude (W)	Date (GMT)	JD (GMT)	Hour (GMT)	Bottom Depth (m)	Assigned Sta. No.
43*	59-06.7	171-53.2	3-06	65	0049	79	
44*	59-00.4	171-59.8	3-06	65	0449	93	
45*	58-52.9	172-05.6	3-06	65	1244	97	
46	58-46.9	172-22.1	3-08	67	0037	102	
47	58-45.4	172-27.7	3-08	67	0442	104	
48	58-42.8	172-35.6	3-08	67	0915	106	
49	58-41.3	172-43.0	3-08	67	1230	108	
50	58-43.6	172-51.8	3-08	67	1654	112	
51	58-47.0	172-50.5	3-08	67	1913	110	
52	58-44.0	172-55.5	3-08	67	2029	112	
53	58-40.6	172-56.1	3-08	67	2200	112	
54	58-38.7	172-58.6	3-08	67	2340	113	
55	58-35.1	173-03.0	3-09	68	0100	114	
56	58-37.8	173-15.3	3-09	68	0438	119	
57	58-34.9	173-23.1	3-09	68	0845	122	
58	58-31.1	173-29.6	3-09	68	1232	123	
59	58-28.7	173-31.5	ABORTED - Surface values only				
60	58-34.1	173-20.3	3-10	69	1940	121	
61	58-39.1	173-12.8	3-10	69	2348	119	
62	58-28.1	172-43.7	3-11	70	0236	108	BC24
63	58-17.4	173-04.1	3-11	70	0513	112	17
64	58-04.3	173-22.2	3-11	70	0703	113	18
65	57-52.1	173-43.3	3-11	70	0851	137	19

*Temperature record only, due to icing of conductivity cell.

Temperature, Salinity and Density Conditions
Observed in November 1980

Vertical distributions of temperature, salinity and density along the two CTD transects occupied in November 1980 are shown in Figures I-3 to I-8. The following features in the distributions were common to both transects:

- The water column was two-layered vertically in temperature, salinity and density, with the interface between layers occurring at 50-60 m. The water was vertically well mixed above and below the interface. The interface between layers was 5-10 m shallower at the northwest than at the southeast transect, and was about 10-m thick in most cases.
- There was a generalized and relatively uniform northward decrease in temperature, salinity and density in both the upper and lower layers. The ensuing horizontal gradients were approximately $0.01\text{ }^{\circ}\text{C}/\text{km}$, $0.003\text{ }^{\circ}/\text{oo}/\text{km}$ and $0.003\text{ sigma-t units}/\text{km}$, respectively.
- There was a tendency for slightly increased horizontal temperature and salinity gradients in both layers at the 80-90 m isobaths. However, this was not true for density due to the cancelling effects on the density gradient exerted by the opposing temperature and salinity gradients.
- At about the 80-m isobath, there was a 50-km wide "bolus" of water which was about $1\text{ }^{\circ}\text{C}$ colder than the surrounding water. This feature appeared on both transects, though the temperature of the bolus was about $2.5\text{ }^{\circ}\text{C}$ lower on the northwest transect.

While the major feature of the comparison between the two transects was the similarity in distributions, overall water temperature at the northwest transect was about $2\text{ }^{\circ}\text{C}$ lower than to the southeast. Salinity and density were similar between the two transects. In the southeast section, there was some indication of salinity finestructure at the interface between layers (stations 3, 4 and 8, Figure I-4); such finestructure was not evident anywhere in the transect to the northwest.

The cross-shelf horizontal density gradient evident in Figures I-5 and I-8 suggests that weak baroclinic northwestward flow may have been present. Dynamic topographies of the surface relative to both 50 dbar and 100 dbar (Figure I-9) reflect a weak northwestward baroclinic flow tendency, in agreement with conventional wisdom concerning circulation on the Bering Sea shelf. The weak southeasterly counterflow at the southern end of the northwest transect is probably connected with a bolus of relatively cold ($< 2.0\text{ }^{\circ}\text{C}$) water located in the lower layer (stations 25-28, Figure I-6). No attempt is made here to assign baroclinic current speeds, because of uncertainties in the geostrophic approximation by shallow depths.

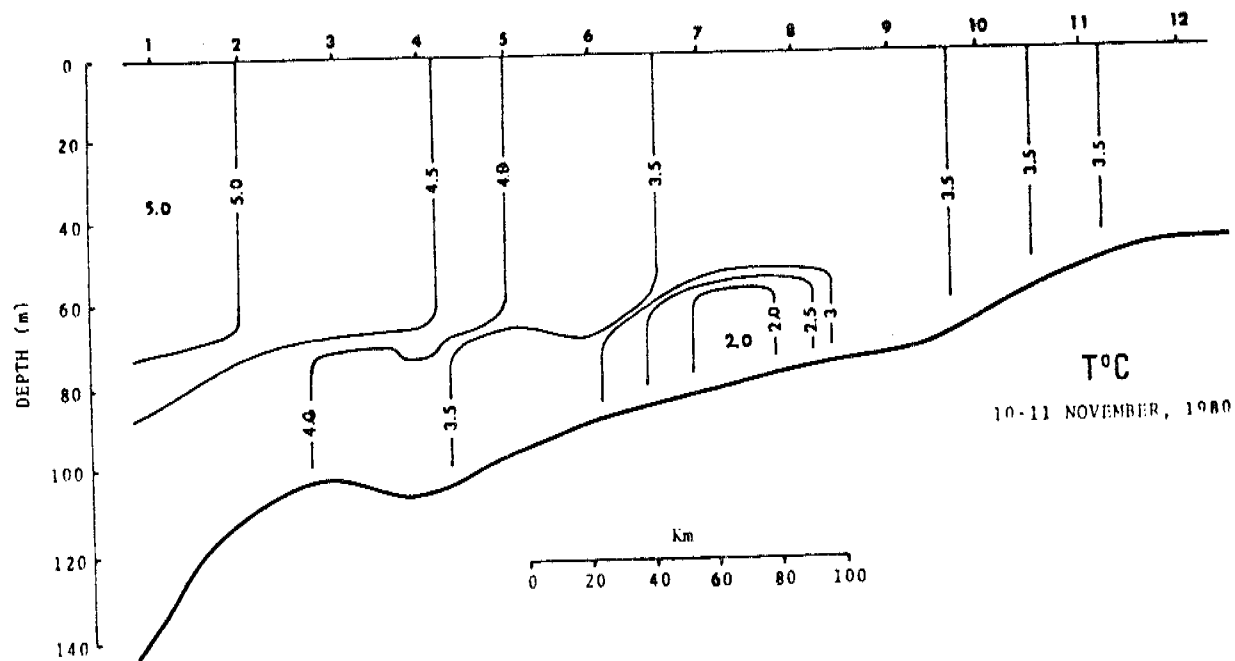


Figure I-3. Vertical distribution of temperature along a transect normal to the shelf break southeast of St. Matthew Island in autumn 1980. See Figure I-1 for station locations, referring to cast numbers.

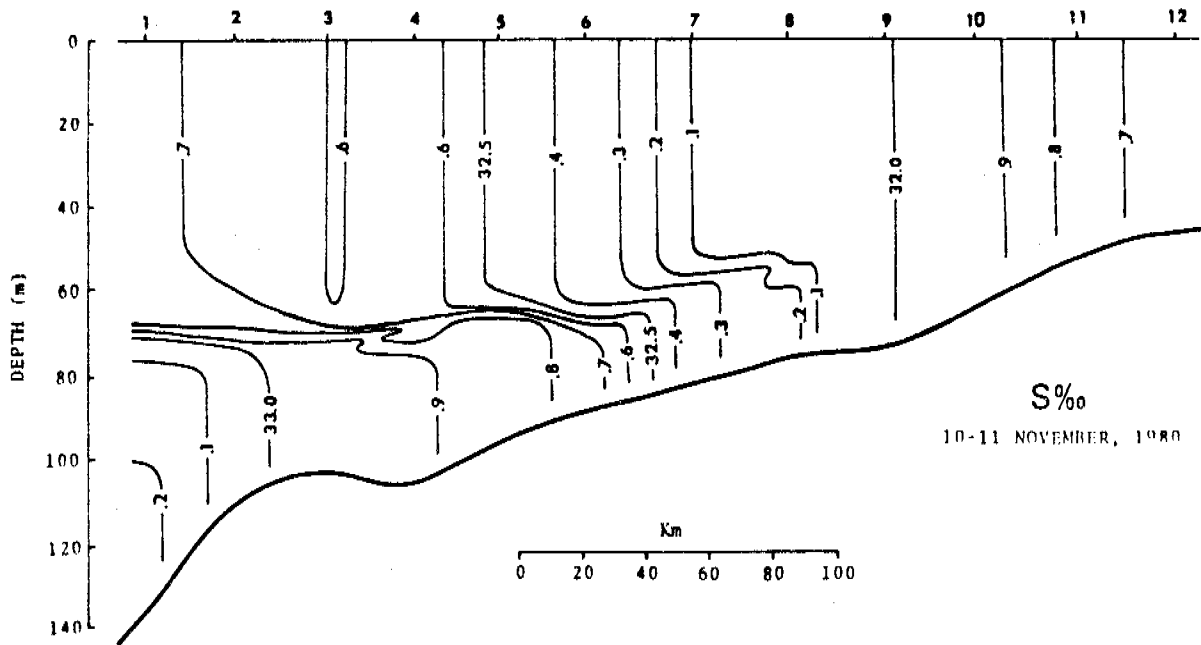


Figure I-4. Vertical distribution of salinity in same area as Figure I-3.

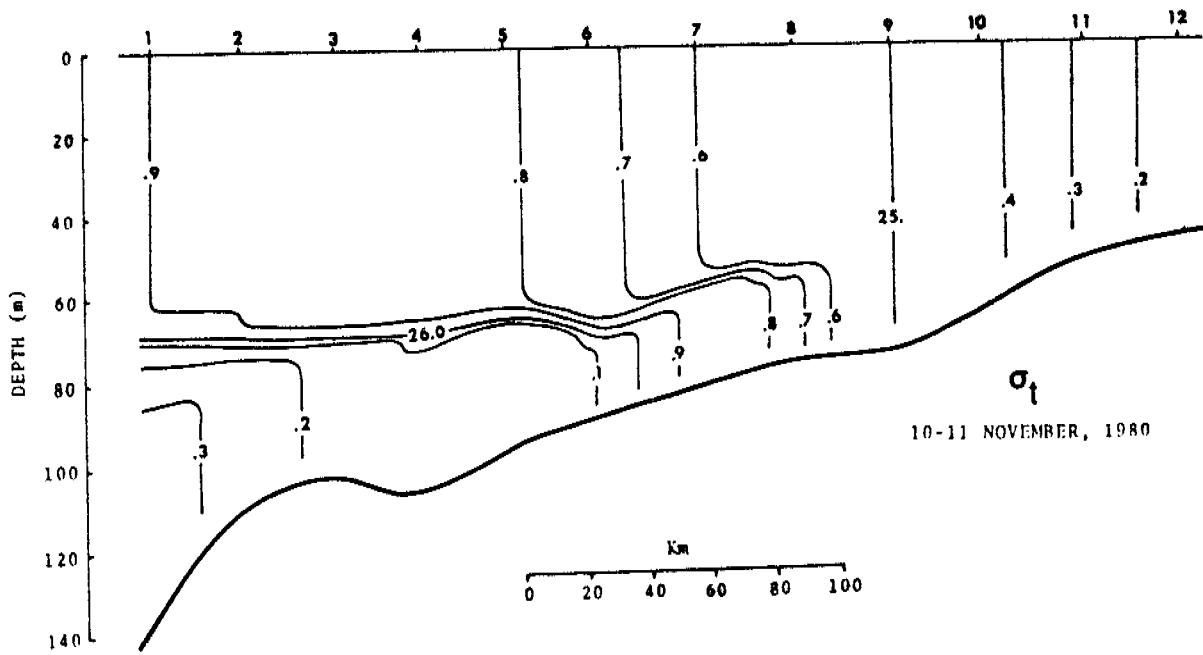


Figure I-5. Vertical distribution of density (σ_t) in same area as Figure I-3.

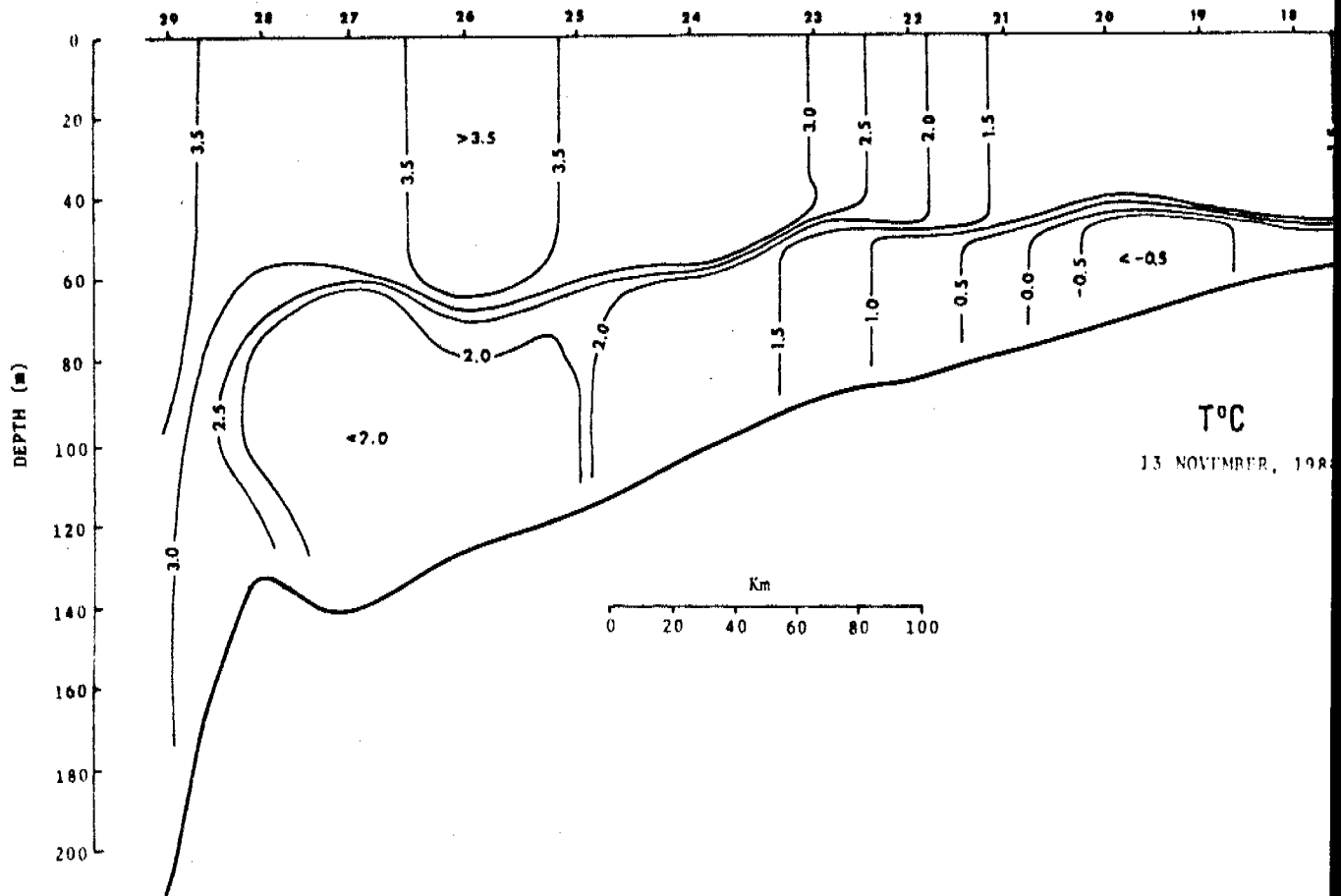


Figure I-6. Vertical distribution of temperature along a transect normal to the shelf break northwest of St. Matthew Island in autumn 1980. See Figure I-1 for station locations, referring to cast numbers.

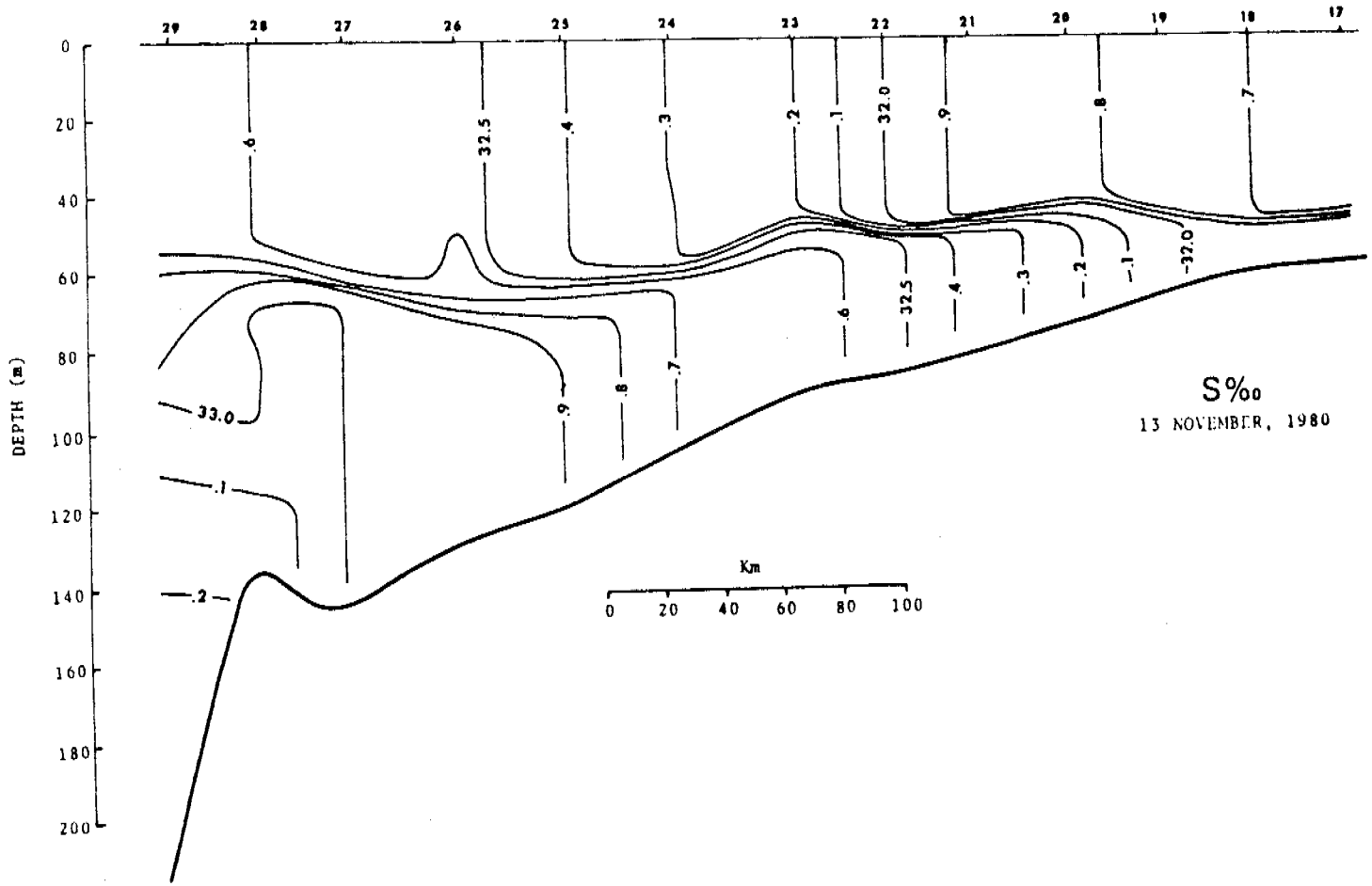


Figure I-7. Vertical distribution of salinity in same areas as Figure I-6.

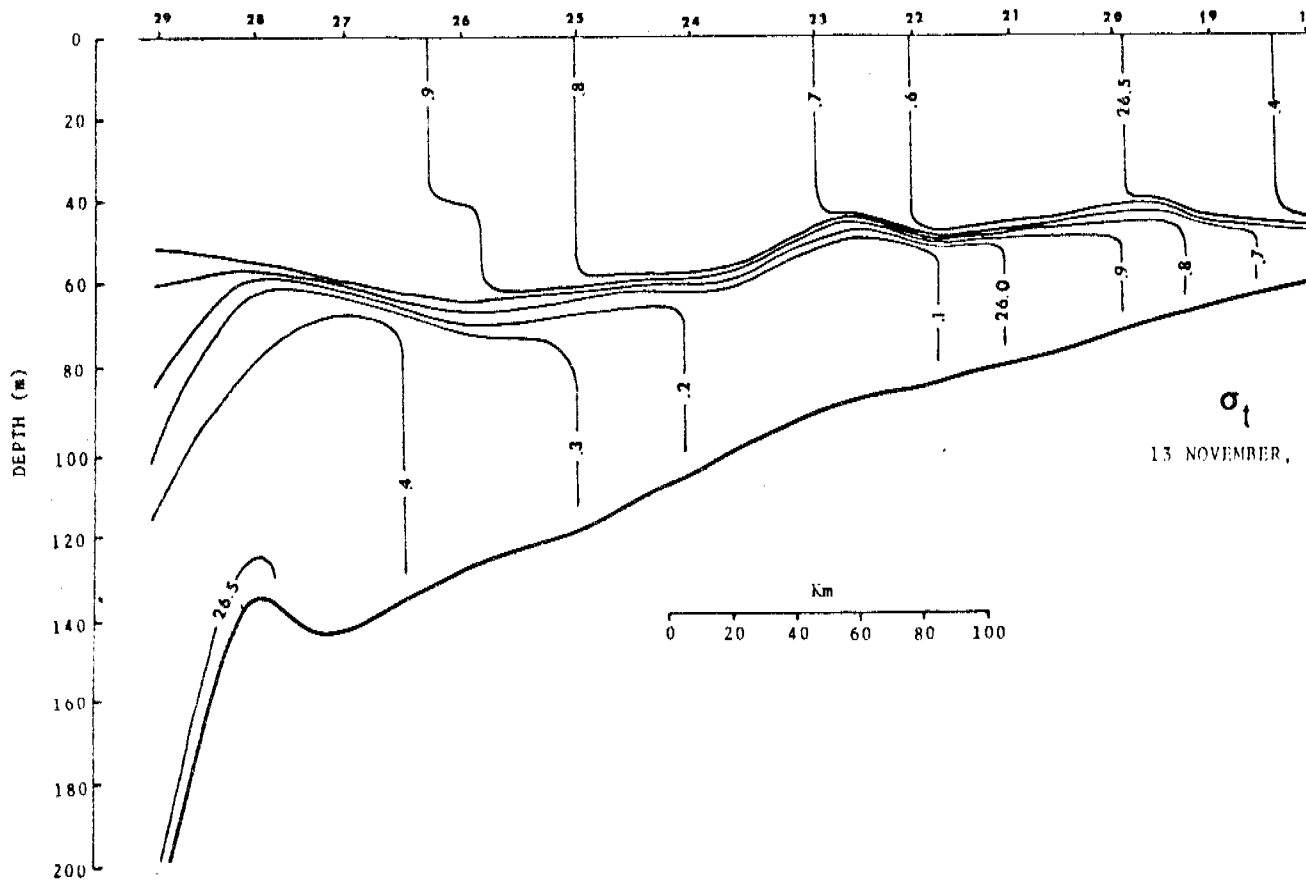


Figure I-8. Vertical distribution of density (σ_t) in same area as Figure I

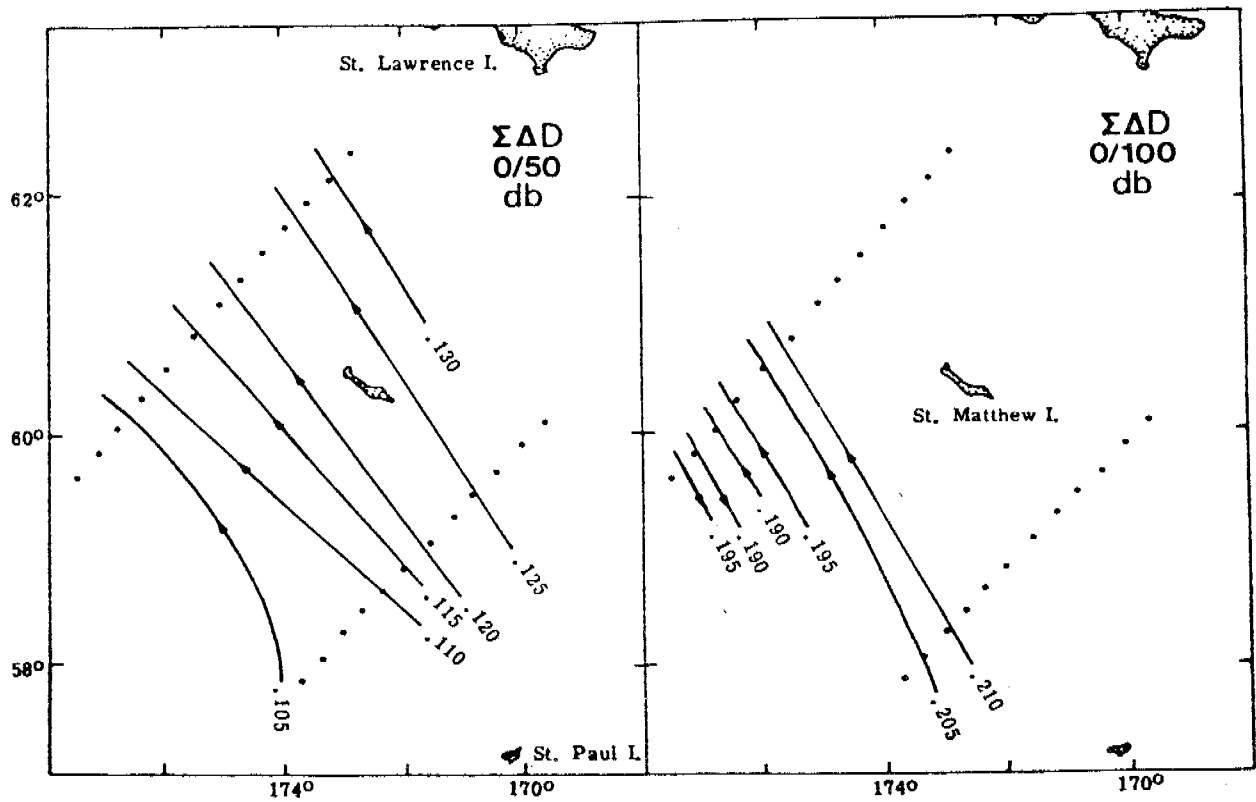


Figure I-9. Dynamic topography (in units of dynamic meters) of the surface relative to 50 and 100 dbar during November 1980.

Temperature Conditions Observed in February-March 1981

Temperature, salinity and density conditions were observed in the MIZ during this period. Since the salinity (and hence the derived density) data have not yet been processed, only selected aspects of the preliminary temperature data are presented here.

Figure I-10 shows a temperature transect which is useful both for a comparison with conditions observed in November 1980 and as an observation of relatively short-term (less than one week) changes. The transect between CTD casts 3 and 2 coincides with the portion of the November 1980 southeast transect between stations 18 and BC23 (see Figure I-1). The February-March transect was approximately bisected by the ice edge at the first of three separate occupations, at which time the edge was well-defined due to its northward compaction by south winds. It can be seen from the vertical temperature distribution along this transect (Figure I-10) that conditions varied from vertically homogeneous in temperature at the south end of the section (cast 3) to two-layered at all stations farther north. The earliest occupation of the section indicates considerable temperature structure in the upper layer, as opposed to the well mixed lower layer. This section was occupied just prior to the onset of a storm which resulted in strong (30-40 kt) southerly winds over a two-day period. The later occupation of the section indicates that vertical mixing of the upper water layer down to a sharper interface had occurred. The wind event did not appear to have radically altered heat content in the water; rather, it simply mixed it vertically. Stations occupied at the same locations as casts 17, 21 and 22 about a week later (not shown) indicate that conditions had begun to return to stratification similar to that before the storm, i.e. the interface had weakened and the upper layer was becoming stratified as opposed to well mixed. This "relaxation" was occurring during a period of northerly winds, low air temperatures, surface ice formation and organization of the ice into bands normal to the wind direction.

The temperature transect discussed above illustrates one of two major features of the mid-winter temperature structure: the transition from vertically well mixed south of the ice edge to stratified (or two-layered) beneath the ice edge. Farther north, the water column undergoes an additional transition from two-layered beneath the ice edge back to vertically homogeneous beneath the ice. This transition from two-layered back to homogeneous structure is illustrated in Figure I-11 which depicts a temperature time series obtained along the ice edge while the edge was progressing southward across the transition region. The transition from near vertical thermal homogeneity (cast 34) to a strongly two-layered structure (cast 41) is clearly indicated, though at cast 41 the bottom was barely deep enough to extend below the depth of the lower layer. Because the ship was drifting with the ice during this time series, it is impossible to ascertain whether this two-layering was developing in time, in space or both. The current records from mooring BC22 should, if recovered, aid in resolution of this by providing an estimate of advection in the vicinity of the CTD stations.

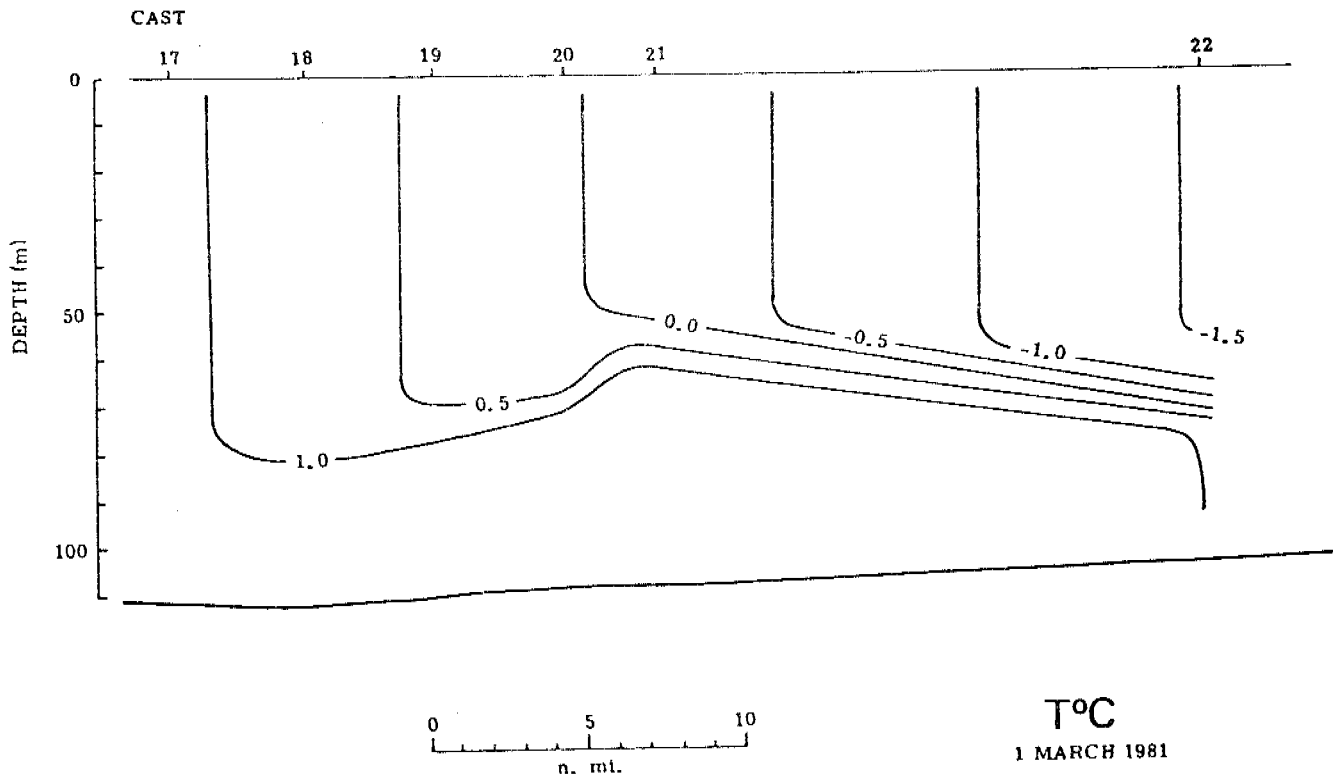
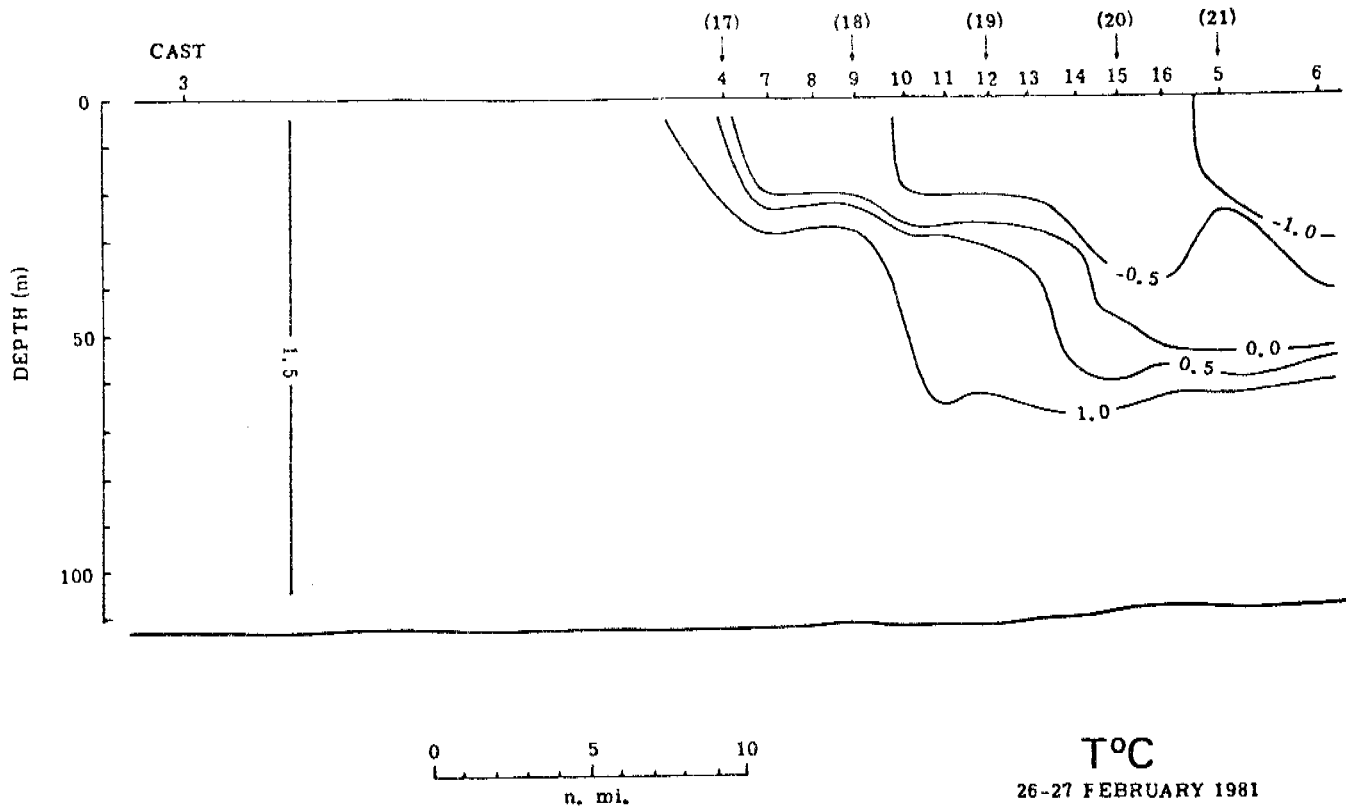


Figure I-10. Preliminary plots of vertical distribution of temperature at two times along the transect shown on Figure I-2.

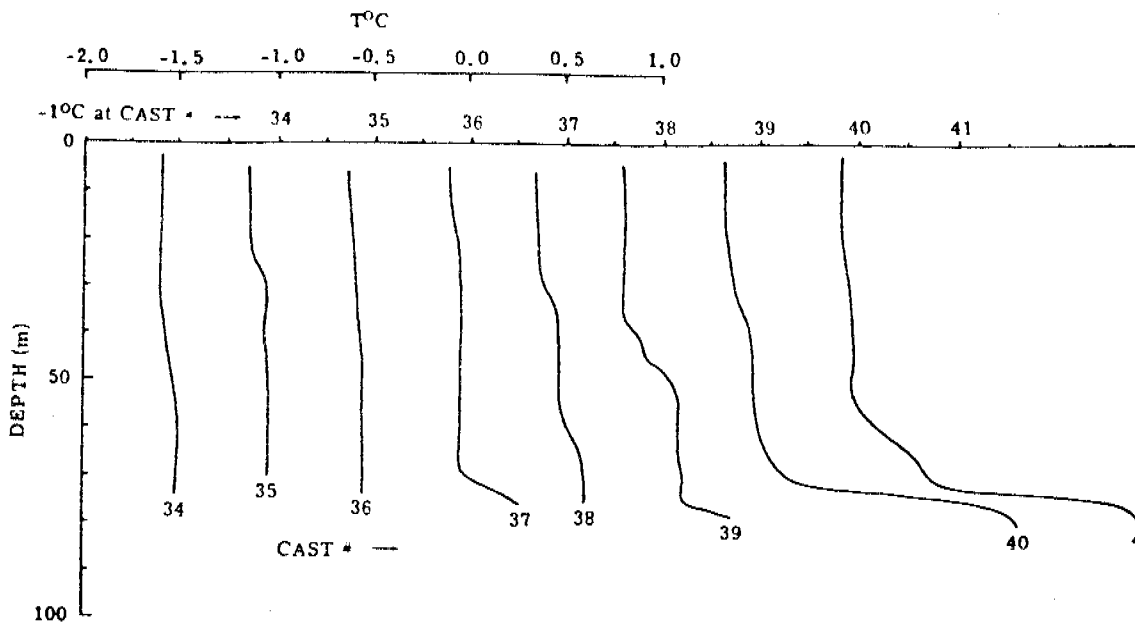


Figure I-11. Preliminary vertical temperature profiles obtained from the time series station at the ice edge. Cast locations are indicated on Figure I-2.

Summary of Results

A rigorous analysis of the CTD data obtained from the Bering Sea MIZ will require additional processing of mid-winter data and integration of all data with the results, which will not be available until summer 1981, of the moored current observations. Nevertheless, it is possible at this time to make the following tentative statements concerning temperature and salinity structure in the MIZ:

- During autumn 1980 the water was vertically two-layered in temperature, salinity and density from the shelf break to about the 80-m isobath. This layering had persisted, at least in temperature, at least until mid-winter 1981.
- Temperature, salinity and density decreased shoreward from the shelf break throughout the water column in autumn 1980. In mid-winter 1981, the temperature, at least, showed a similar shoreward decrease.
- MIZ water temperatures range from about 1.5 to 5 °C in autumn 1980, whereas by mid-winter temperatures had decreased to a range of about -1.7 °C to greater than 2 °C, with the lower temperatures being to the north. Temperatures well north of the ice edge were at the freezing point.
- In mid-winter the ice edge was underlain by a two-layered structure, while to the north and south the water was vertically homogeneous. This two-layered structure, also present during late autumn, appeared to be characteristic of the ice edge region.

Planned and Projected Future Activities

Activities for the remainder of FY81 include continuing processing and analysis of the CTD data from autumn 1980 and mid-winter 1981, and recovery, processing and analysis of the data from the over-winter current moorings deployed in November 1980. The CTD data obtained to date have provided excellent coverage for addressing problems of import to OCSEAP such as transport and dispersion processes associated with the Bering Sea MIZ. Successful recovery of the current data in early summer 1981 will provide, overall, a unique and extremely useful data set.

Activities in FY82 will depend upon the level of follow-on funding available. Due to the recovery of the current moorings relatively late in FY81, adequate analysis of these records cannot be completed this year. Therefore, additional funding will be required as stated in the RU87 proposal to continue the analysis into FY82. Also as stated in the proposal, a funding level of about \$40,000 will be necessary for adequate analysis of the CTD and current data.

APPENDIX II

ICE EDGE TRANSECT ON 7 MARCH 1981

R.D. Muench, SAI/Northwest

On 7 March 1981 a transect was made across the southern portion of the Berin Marginal Ice Zone (MIZ) on the NOAA ship SURVEYOR. The ship's course during this transect was 200 °T. Wind direction was 020 °T, and wind speed was fairly constant at about 12 kt. The ship was thus traveling directly downwind. Ship speed varied between about 6 and 9 kt, with lower speeds during passage through bands of ice and higher speeds in open water.

The MIZ transect was started at 0501Z on 7 March just NNE of 58°49.6N-172°09 and ended with a final exit from the ice at 0647 on 7 March. The last ice was exited at 58°39.0N-172°17.1W. The ice-water distribution along this transect was visually determined from the ship's bridge and is schematically indicated on Figure II-1. The along-track distance scale was computed using logged vessel speeds which were frequently changed because of varying ice conditions and therefore the scale is approximate. Widths of individual bands of ice and open water were computed using ship speed obtained from the LORAN and transit time across the feature. The two positions indicated locate the transect geographically and show that the distance covered was actually closer to 17 km than to the 23 km suggested by the distance scale. Based upon this comparison, the observed dimensions of the features are probably overestimated, by up to about 25 percent. No distance scale is attached to the cross-transect features illustrated.

Visual observation of the ice and water areas led to the following general observations:

- Ice-water and water-ice transitions were generally very sharp and well-defined, going from completely open water to complete ice coverage in 10 m or so.
- Within the ice bands ice cover was nearly complete with interstices between pans being occupied by what appeared to be newly-formed ice.
- The amount of ice older than a few days decreased steadily from north to south along the transect. South of the location indicated on the figure, no older ice was observed.
- At the windward ice edges, the transition was composed of closely packed pans. Leeward transitions were characterized by active ice formation, with newly formed pan-free ice extending of order 10-m downwind from the bulk of the ice made up of pans.
- Nowhere in the ice bands was there evidence, such as rafting or ridging, of compressive forces.

Schematic of Bering MIZ transect

7 March, 1981

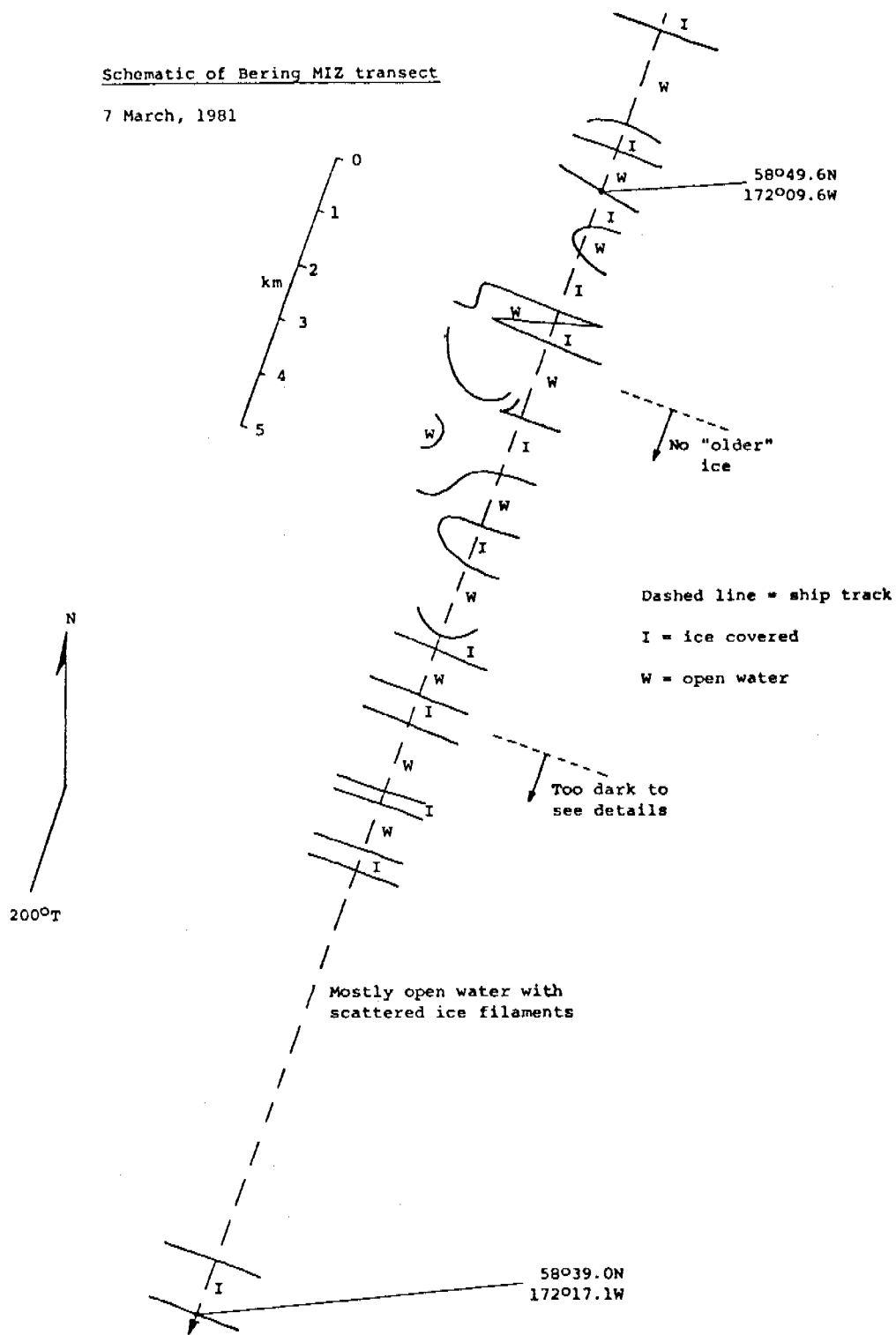


Figure II-1. Schematic showing ice distribution along ship's course normal to the MIZ on 7 March 1981.

- Within the open water areas, grease ice and pans were organized into bands parallelling the wind direction. These bands occupied only a small percentage of the open water area (less than 5 percent), and it was impossible to estimate whether there was a regular preferred spacing between the bands.
- Mean downwind extent of the open water areas was 1 km with a standard deviation of 0.5 km. Mean ice band extent was 0.5 km with a standard deviation of 0.34 km.
- The ice-water transitions generally were oriented roughly normal to the wind direction except as indicated schematically on the figure.

In summary, over the southernmost 20 km of the Bering MIZ newly formed ice and water occurred in alternate bands oriented roughly normal to the wind direction. Along-wind scales for these bands was of order 1 km, although the ice bands tended to be smaller than the water bands. Ice over in bands was nearly complete and the open water areas contained little ice with very sharp transitions between the ice and water areas.

ANNUAL REPORT

CIRCULATION PROCESSES IN
BRISTOL BAY, ALASKA USING DISSOLVED
METHANE AS A TRACER

Prepared by

Joel Cline, Charles Katz and Herbert Curl, Jr.

Pacific Marine Environmental Laboratory

7600 Sand Point Way N.E.

Seattle, Washington 98115

TABLE OF CONTENTS

	<u>Page</u>
Figures	31
1. GENERAL SUMMARY	33
1.1 Objectives of Program	33
1.2 Summary of Preliminary Observations	33
2. INTRODUCTION	35
2.1 Purpose of Study	35
2.2 Objectives	35
2.3 Relevance to OCSEAP	36
3. STUDY AREAS	37
3.1 Bristol Bay	37
3.2 North Aleutian Shelf	39
3.3 St. George Basin	40
4. METHODOLOGY	41
4.1 Sample Collection	41
4.2 Preconcentration	41
4.3 Gas Chromotography	42
5. RESULTS	42
5.1 North Aleutian Shelf	42
5.2 St. George Basin	54
6. DISCUSSION	62
6.1 Plume Model	62
6.1.1 Model Scenarios	66
6.1.2 Model Fit	69
6.2 St. George Basin	73
6.2.1 Vertical Methane Distribution	74
6.2.2 Near-Bottom Methane Plume	80
References	84

FIGURES

<u>Number</u>		<u>Page</u>
1	Regional setting of southeastern Bering Sea including Bristol Bay.	38
2	NAS stations occupied in August, 1980.	43
3	Surface salinity (g/kg) distribution along the NAS in August, 1980.	44
4	Surface concentration of dissolved methane (nL/L) along the NAS in August, 1980.	45
5	Vertical profiles of dissolved methane along two sections normal to the NAS. Sections IV and V are immediately east of Port Moller.	47
6	Distribution of methane across the entrance of Port Moller during a 24-hour tidal cycle. The vertical bars indicate 1 σ variation in the mean concentration at each station. The largest variation was observed at station PM-3, near the eastern side of Port Moller	48
7	NAS stations occupied in February, 1981.	49
8	Surface salinity distribution (g/kg) along the NAS in February, 1981.	50
9	Surface distribution of dissolved methane (nL/L) along the NAS in February, 1981.	52
10	Correlations between temperature ($^{\circ}$ C), salinity (g/kg), methane (nL/L) and tidal amplitude (m) at station PM-3 in February, 1981.	53
11	St. George Basin stations occupied in August, 1980. . . .	55
12	Vertical distribution of salinity (a), σ_t (b), methane (c) and temperature (d) along the PROBES Line in August, 1980. The middle front is located near PL 8-10.	56
13	Near-bottom distribution (B-5 m) of methane (nL/L) in St. George Basin in August, 1980. Maximum concentrations were found near stations PL-6 and SG-5.	57
14	St. George Basin stations occupied in February, 1981. . .	59
15	Vertical distribution of methane along a portion of the PROBES Line in February, 1981.	60
16	Near-bottom distribution (B-5 m) of methane (nL/L) in St. George Basin in February, 1981. Maximum concentration was observed at station SG-28; which is south of PL-6.	61

FIGURES

<u>Number</u>		<u>Page</u>
17	Model schematic of the NAS. The significant transport terms are horizontal diffusion, $K_y C''$, and horizontal advection, $V_x C'$. The well mixed coastal water is 10 km wide and 15 m deep.	67
18	Relative concentrations of methane, depth integrated, predicted from equation (2), assuming various mean velocities of (a) 5 cm s, (b) 7.5 cm s and (c) 10 cm s. Air-sea exchange of methane and biological oxidation are included in a single first order rate constant, $k = 4.6 \times 10^{-7}$ s. Source strength is set at 8-10 km. . .	68
19	A comparison of a observed methane distribution (solid lines) with the 7.5 cm s model scenario. Pulsing of the estuary leads to a strong time dependent source, which is not accomodated by the stationary model.	70
20	Tidal range and maximum ebb and flood tidal velocities at Entrance Point, Port Moller. The data presumably reflect conditions at mid-channel. Data are from the NOAA tide tables covering the observational period. . . .	71
21	Vertical density distribution at PL-6 on August 29, 1980 and September 3, 1980. Note the effects of salt fingering and double-diffusion.	75
22	Vertical distribution of dissolved methane at PL-6 on August 29, 1980 and September 3, 1980.	76
23	Estimated apparent vertical eddy diffusivity or a function of the buoyancy gradient. The Brunt-Vaaisela frequency was determined from the density distribution; K_z from the observed methane profile. The reciprocal square-root relationship suggests shear-induced turbulence.	78
24	A model fit to the depth integrated methane profile in the lower boundary layer ($\Delta z \approx 30$ m). The two case studies are (a) $\bar{u} = 2.5$ cm s ⁻¹ and (b) $\bar{u} = 5.0$ cm s ⁻¹ . The length of the source was assumed to be 30 km. The biological oxidation rate constant for the destruction of methane was set equal to 3.0×10^{-8} s ⁻¹	82

1. GENERAL SUMMARY

1.1 Objectives of Program

The goal of this study is to utilize dissolved methane as a Lagrangian tracer of petroleum introduced from point sources in Bristol Bay, Alaska. Previous baseline studies in this area revealed the presence of localized sources of methane in Port Moller, an estuary along the North Aleutian Shelf (NAS), and in the bottom waters of St. George Basin (SGB). Both the NAS and SGB are potential gas and oil lease areas and thus may eventually be subjected to a point source introduction of petroleum. In order to determine the fate and impact of spilled oil, it is of paramount importance to elucidate mean flow trajectories, velocities and turbulence regime.

1.2 Summary of Preliminary Observations

Two cruises have been conducted in Bristol Bay to date for this program. The first, in August, 1980, emphasized the NAS region. More time was dedicated to SGB in February, 1981, although the major effort was still on the NAS. On both occasions measurements of methane, suspended matter, mass field, currents (utilizing current meters) and microbiological methane production and consumption rates were made. Only observations from August are considered here in depth.

The major feature of the methane distribution on the NAS is the methane plume emanating from Port Moller in a well defined trajectory to the east. The plume could be traced to Port Heiden, approximately 150 km down the coast. Dissolved methane remains in the coastal zone and rarely penetrates more than 20 km

offshore. Assuming a stationary condition, the average mean velocity along the coast as calculated from a diffusion-advection model would be $7 \text{ cm s}^{-1} \pm 2 \text{ cm s}^{-1}$. Port Moller does not represent a uniform source of methane, but rather appears to pulse every 28 days, in concert with the occurrence of perigean tides. The aforementioned model allows for a scaled diffusion coefficient and predicts cross-shelf values ranging from $10^5 \text{ cm}^2 \text{ s}^{-1}$ to $10^6 \text{ cm}^2 \text{ s}^{-1}$. These values are systematically smaller than those computed for salt and is an artifact of the scale of the methane plume. However, when considering point source introductions of petroleum, dissolved methane is a useful tracer of these length scales.

The plume of methane observed in the near-bottom waters of St. George Basin was elongated in the northwest-southeast direction, apparently bathymetrically contained. Dissolved methane was uniformly distributed in the lower 30 m of the water column in agreement with other water column properties. Assuming a one-dimensional flux model with the surface flux as a boundary condition, apparent vertical eddy diffusivities (K_v) were calculated across the pycnocline. A plot of the apparent diffusivities versus the Brunt-Vaisela frequency gave a $-1/2$ power relationship suggesting shear induced turbulence. Two dynamic mixing regimes were apparent, the first in the upper portion of the pycnocline was characterized with K_v 's ranging $20\text{-}50 \text{ cm}^2 \text{ s}^{-1}$. The lower region was much less turbulent, with volumes ranging $0.2\text{-}0.5 \text{ cm}^2 \text{ s}^{-1}$. During periods of stratification, the lower boundary layer is well insulated from vertical exchange. Preliminary modeling efforts suggest a mean flow in the lower boundary layer of approximately 5 cm s^{-1} toward the northwest, in excellent agreement with current meter measurements. The penetration of the plume to the southeast, nearly to Unimak Pass, suggests periodic weakening or reversal of the mean northwest flow. It is apparent that along-shelf dispersion is more active than cross-shelf, which is in agreement with the distribution of

2. INTRODUCTION

2.1 Purpose of Study

The purpose of this program is to use naturally-occurring sources of dissolved methane as a Lagrangian tracer of mean circulation in selected subregions of Bristol Bay, Alaska. Regardless of the origin of the methane, point sources allow estimates to be made of trajectories, mean velocities and horizontal dispersion coefficients. Because of the nature of the methane sources, the behavior of other dissolved materials introduced from point sources (e.g., surface spills, well blowouts, etc.) can be elucidated. By analyzing the plume distribution of methane, correcting for biological consumption and air-sea exchange and introducing mean current velocities derived from current meter measurements, estimates can be made of the scale of turbulence.

2.2 Objectives

The principal goal of this study is to use dissolved methane as a quantitative tracer of circulation processes and mixing dynamics in selected areas of Bristol Bay, Alaska, a large embayment located in the southeastern Bering Sea. This report deals with two site specific areas of Bristol Bay, the NAS and SBG. Specifically, the objectives are:

1. To quantify the longshore mean velocity and cross-shelf dispersion coefficients along the NAS using a point source of methane emanating from the Port Moller estuary.
2. To estimate near-bottom current trajectories and lateral dispersion coefficients in St. George Basin, using a bottom source of methane as a tracer.

3. To estimate the depth dependent vertical eddy diffusivity in St. George Basin using a one-dimensional vertical flux model.
4. To analyze the distributions of methane in terms of a two-dimensional diffusion-advection model for the purpose of confirming mean current velocities and estimating the magnitude of horizontal and vertical processes.

2.3 Relevance to OCSEAP

The persistence of oil in Bristol Bay depends on several physical, chemical and biological processes that act in concert to disperse and degrade petroleum. These processes, each with their characteristic time scale (i.e., half-life), must be considered together in order to determine a characteristic time (or space) scale for the persistence of oil. Circulation and mixing processes are characterized by relatively short time scales and thus represent a first-order process. Given that the volume of spilled oil is small compared to the volume of water in the region, it is anticipated that harmful impacts due to petroleum development will be limited to space scales less than 100 km.

Utilization of methane as a diagnostic tracer of circulation and dispersion in support of the physical oceanography program, allows mesoscale mixing processes to be more clearly defined. In particular, these studies allow quantitative predictions of water mass trajectories, dispersion characteristics and water mass residence times required in order to quantitate the impact of oil on living resources.

3. STUDY AREAS

3.1 Bristol Bay

Bristol Bay is a shallow embayment located in the southeastern portion of the Bering Sea. The area and volume of the region, computed out to the 200 m isobath, is 419,000 km² and 30,000 km³, respectively, given a mean depth of approximately 70 m. Freshwater input occurs primarily from the Kuskokwim and Kvichak Rivers, located on the northern and eastern sides of the bay (Fig. 1), resulting in a 2⁰/oo salinity difference between the offshore waters and the near-shore areas (Schumacher et al., 1979).

Bristol Bay is characterized by a series of frontal features, primarily located at distinct bathymetric depths (Kinder and Schumacher, 1981). These fronts occur roughly at the 200 m (shelf break front), 100 m (middle shelf) and 50 m (inner front) isobaths (see Fig. 4-1; Kinder and Schumacher, 1981a). Mean circulation landward of the middle front is presumed weak ($\leq 2 \text{ cm s}^{-1}$) and hydrographic structures are largely determined by buoyancy input, wind stirring and tidal mixing (Kinder and Schumacher, 1981a, see their report for details). There appears to be a weak cyclonic circulation around the perimeter of Bristol Bay, largely confined to the coastal zone ($Z \leq 50 \text{ m}$).

Bristol Bay is partially ice covered in winter, usually beginning in protected bays in November and builds to a maximum in March. The spring melting results in considerable freshwater added to the surface (Schumacher et al., 1979). Maximum ice coverage is approximately 60%; thickness is usually less than 1 m. Details on hydrography and climate of the region can be found in reports by Kinder and Schumacher, 1981a; Kinder and Schumacher, 1981b; Coachman and Charnell, 1979; Overland, 1981; and references contained therein.

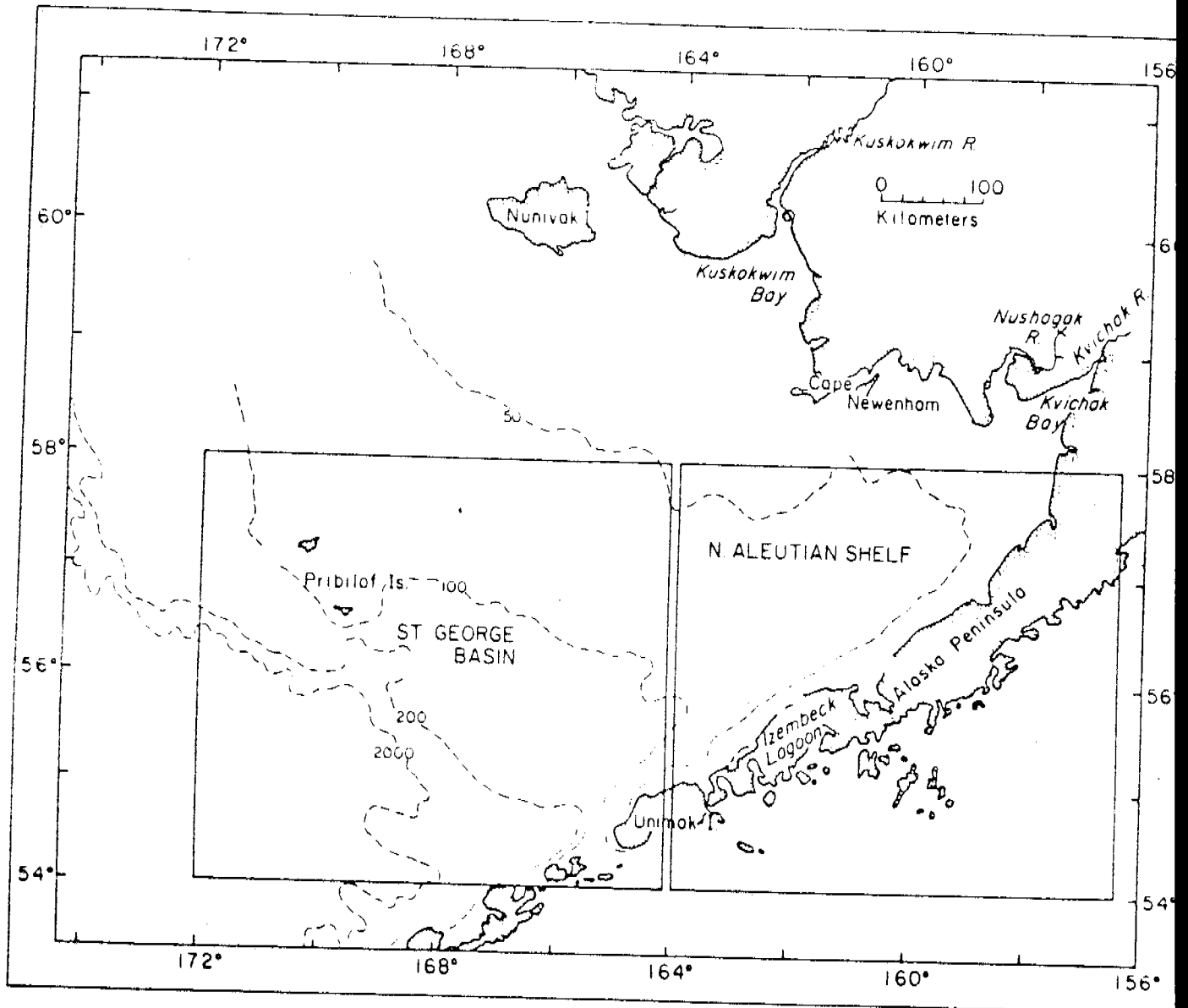


Figure 1. Regional setting of southeastern Bering Sea including Bristol Bay.

3.2 North Aleutian Shelf (NAS)

The NAS region encompasses the near shore areas from Unimak Island on the west to the Kvichak River on the east (Fig. 1). This region is characterized by a vertically well mixed coastal zone ($Z \leq 50$ m), which is hydrographically separated from the stratified regime located seaward. The breakdown of vertical stratification in the coastal zone is reportedly due to dissipation of tidal energy (Kinder and Schumacher, 1981a).

There is no apparent major source of freshwater along the NAS, except at the eastern extremity. There are undoubtedly numerous diffuse sources, including the possibility of submarine aquifers originating in the mountains of the Aleutian Chain. Mean velocities are estimated at no more than $3-5 \text{ cm s}^{-1}$ to the east (Schumacher et al., 1979), but there also appears to be strong seasonal variability in direction and magnitude (Personal communication, J. Schumacher).

The principal embayment along the NAS, Port Moller, is comprised of two arms, each approximately 38 km in length, with mean depths ranging from 5 m to 15 m. The western arm, Herendeen Bay, is the deeper of the two with a deep inner basin (approximately 100 m). Tidal currents within the Port Moller-Herendeen Bay complex are relatively strong, reaching maximum ebb and flood velocities of approximately 150 cm s^{-1} (Department of Commerce, 1981).

Previous measurements made in September-October of 1975 and again in July of 1976 (Cline, 1981), revealed that the Port Moller estuary represented a significant source of dissolved methane to the surface waters that could be traced down the coast (east) for distances of 200 km. The source of methane within Port Moller was not specifically known, but was believed to arise from methanogenesis in anoxic marine muds or possibly from the cannery operations

at Port Moller. Observations made in the summer of 1980 and again in winter of 1981 now shed some light on the source of methane.

3.3 St. George Basin

St. George Basin is an offshore basin located near the shelf break in Bristol Bay (Fig. 1). The axis of the basin is northwest-southeast, running roughly from Unimak Pass to the Pribilof Islands. The basin proper is largely contained between the 100-200 m isobaths.

The basin waters are separated from the inner shelf by the middle front at about 100 m and from the Bering Sea water located seaward of the 200 m isobath (Kinder and Schumacher, 1981a; see their Fig. 4-1). Dynamic topography are largely oriented parallel to the isobaths and reflect weak mean currents toward the northwest (Coachman and Charnell, 1979). Although seasonal variations do exist, surface and near-bottom mean currents are usually $\leq 5 \text{ cm s}^{-1}$ as confirmed from moored current meters (Coachman and Charnell, 1979; Kinder and Schumacher, 1981).

The waters overlying SGB appear to be seasonally stratified. There is a strong erosion and deepening of the pycnocline in winter. Because Alaska Stream-Bering Sea water penetrates the shelf seasonally (Kinder and Schumacher 1981), it is expected that the basin water is modified seasonally by cross-shelf advection and diffusion. Because the water column is seasonally stratified and characterized by weak mean currents, the injection of petroleum or other contaminants is of particular concern.

4. METHODOLOGY

4.1 Sample Collection

Water samples were collected using standard 5 L Niskin[®] bottles mounted on a General Oceanics Rosette sampler. Once on deck, water was transferred to clean 1 L glass-stoppered bottles such that air bubbles were not trapped. The samples were stored in the dark at approximately 5°C until analyzed, which was usually performed within one hour.

4.2 Preconcentration

The analysis of methane was accomplished using a procedure adopted from that originally proposed by Swinnerton and Linnenbom (1967). A detailed discussion of the methods used for analyzing methane and other LMW hydrocarbons can be found in Katz (1980). Dissolved methane was removed from approximately 250 mL of seawater by helium stripping. Gases removed from solution were passed through Drierite[®], Ascarite[®] and Tenax G.C.[®] traps to remove water vapor, carbon dioxide and heavier hydrocarbons. Methane was concentrated on an activated alumina trap at -196°C. After quantitative removal from solution, (~ 5 minutes at a helium flow rate of 100 mL min⁻¹) the trap was warmed to 100°C and the methane was backflushed directly into a gas chromatograph.

4.3 Gas Chromatography

Detection of methane was carried out on a Hewlett-Packard 5710A gas chromatograph equipped with dual flame ionization detectors. In order to insure separation of methane from the air gases (N₂ and O₂), chromatography was accomplished with an activated alumina 60-80 mesh column (1.8 m x 0.48 cm). Chromatography was completed in less than two minutes at a carrier flow rate

of 50 mL min^{-1} and the oven held isothermally at 100°C . Quantitation was accomplished by comparing the samples with methane standards of known concentration.

5. RESULTS

5.1 North Aluetian Shelf

The station grid occupied in August, 1980 is shown in Figure 2. Emphasis was placed on the vertical and horizontal distributions of salinity, temperature and dissolved methane. Several of the sections were occupied repeatedly during the duration of the study to provide temporal variability and model boundary conditions.

The surface salinity distribution along the NAS is shown in Figure 3. The salient features include low salinity water near the coast and the appearance of relatively high salinity water penetrating toward the east, offshore of the inner front. Just prior to sampling a major storm passed through the area (tropical storm Marge), which resulted in the temporary destruction of the inner frontal system and may have resulted in the patchy salinity distribution observed just east of Port Moller (personal communication, C. Pearson, PMEL). Port Moller appears to be the major source of freshwater between Izembek Lagoon and the Kvichak River. Port Heiden is undoubtedly a secondary source. Details on the hydrographic conditions during the observational period will be discussed by Schumacher et al. in their annual report.

The areal surface distribution of dissolved methane is shown in Figure 4. Concentrations of dissolved methane varied from near 4000 nL L^{-1} near the entrance of Port Moller to approximately 400 nL L^{-1} at the eastern extremity of the region (Kvichak Bay). Concentration seaward of the inner front were

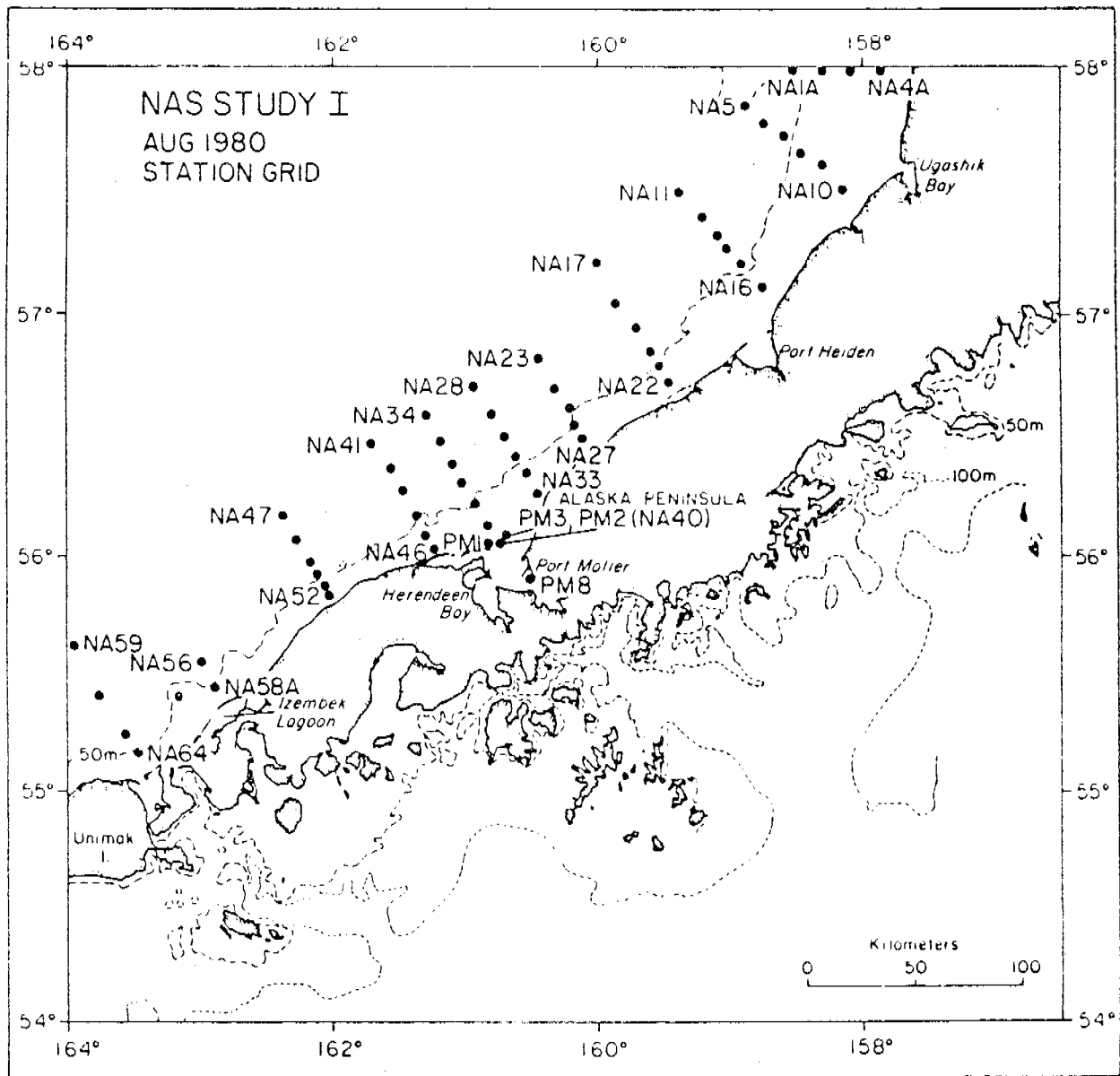


Figure 2. NAS stations occupied in August, 1980.

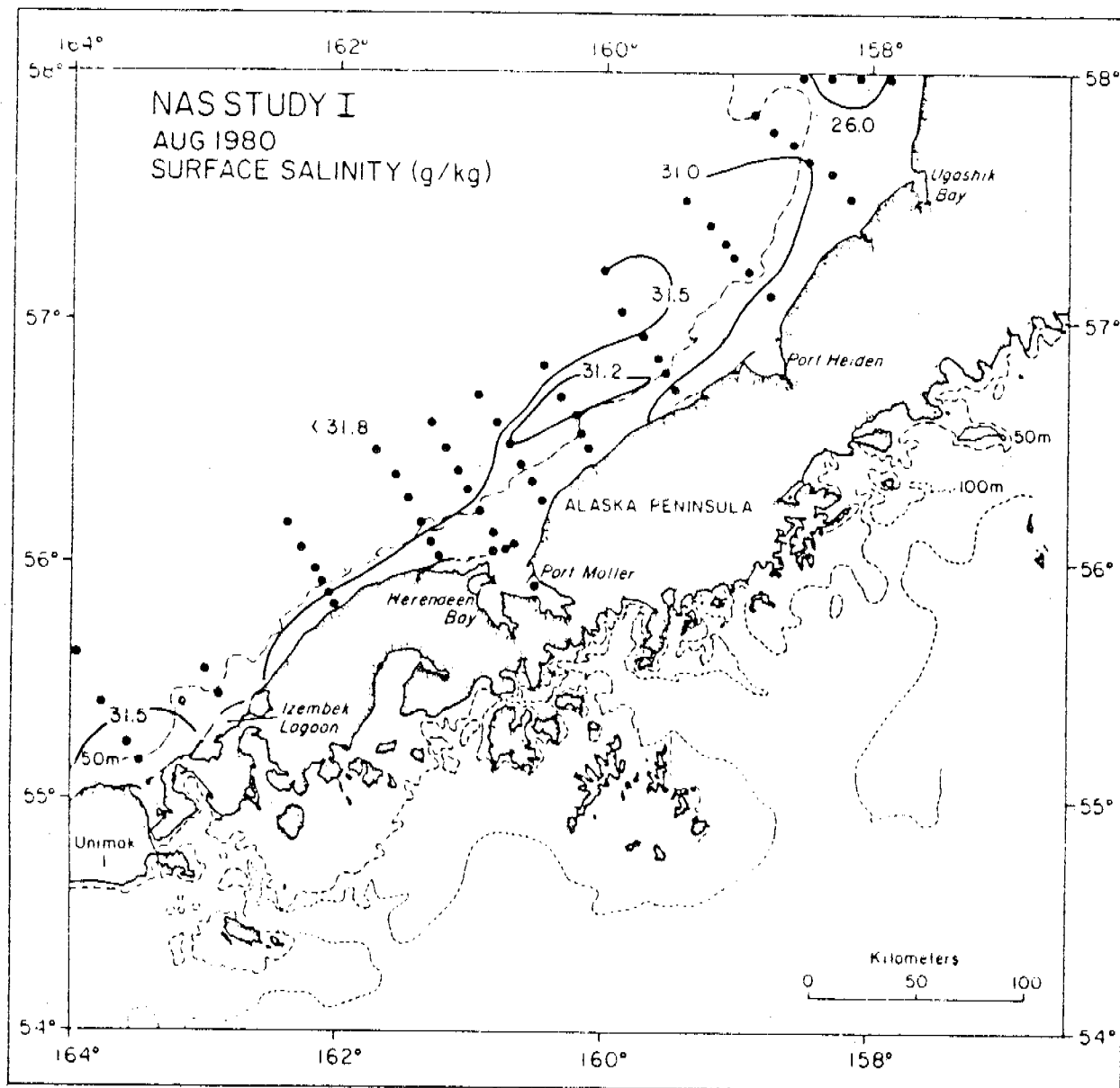


Figure 3. Surface salinity (g/kg) distribution along the NAS in August, 1980.

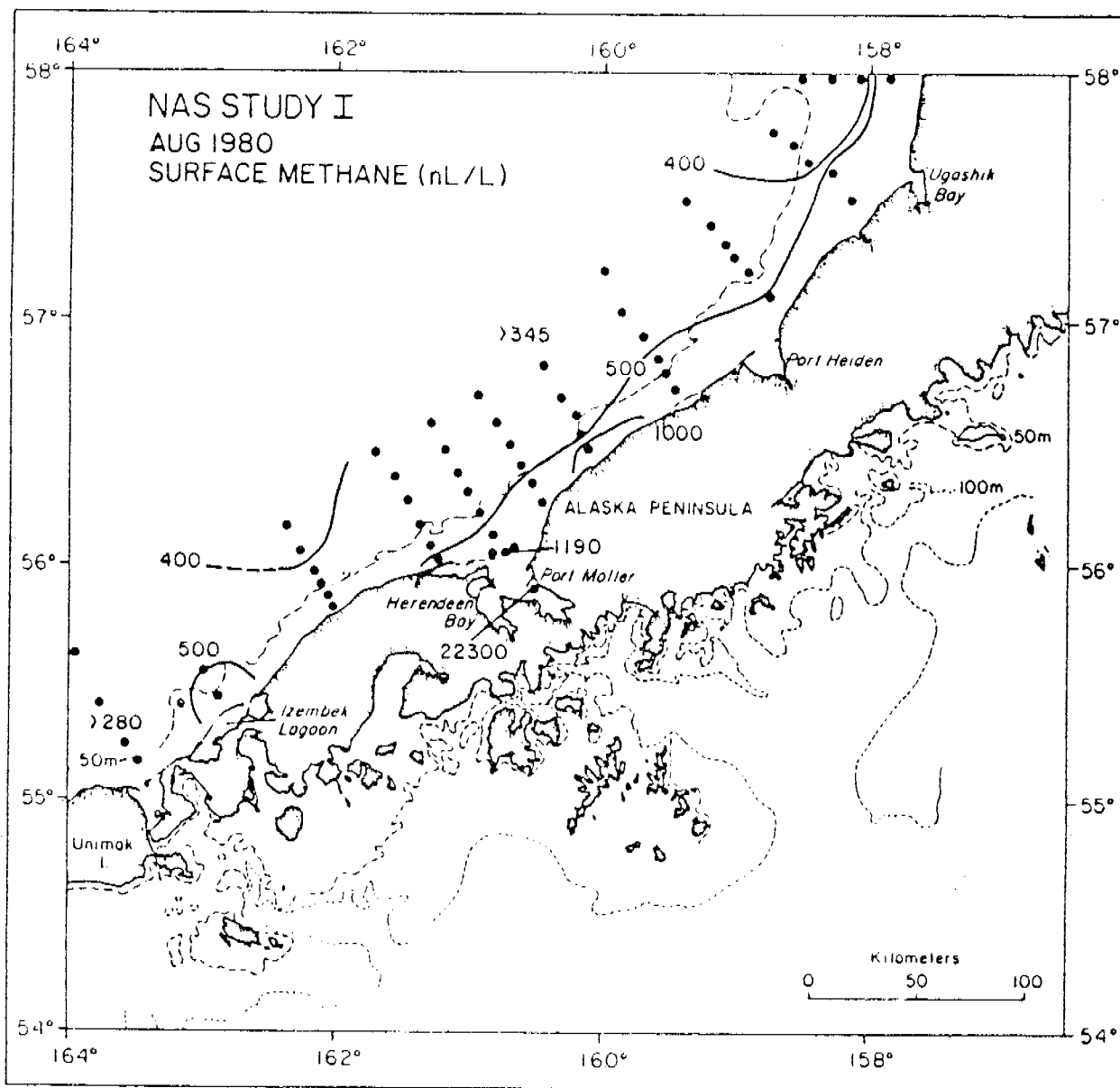


Figure 4. Surface concentration of dissolved methane (nL/L) along the NAS in August, 1980.

between 350-400 nL L⁻¹. Because the coastal zone was well mixed, the concentration of methane was vertically homogeneous, particularly near shore, as depicted in Figure 5. Surface intrusion of high methane, low salinity water is evident in several of the sections.

A minimal sampling program was conducted in the Port Moller estuary. The highest concentration of methane was found at the surface just south of the cannery located at Entrance Point. Here the concentration was near 22,000 nL L⁻¹ representing a supersaturation of 400%. Similar surface samples collected near the cannery pier were in the range of 4000-6000 nL L⁻¹, suggesting that the cannery may not be the major source of organic matter and subsequent production of methane.

In order to establish source boundary conditions for the transport of methane east along the coast, time series measurements were made across the entrance to Port Moller. A total of three stations (PM 1, 2 and 3) were occupied sequentially every two hours over a 24 hour time period. The results of this study are shown in Figure 6. Station NA-46, located on section line III just west of Port Moller, was occupied twice during the cruise. The PM stations were sampled at various stages of the tide. This diagram shows high methane water moving out alongshore to the east and being replaced by low methane water from the west. Because of shoals located near Entrance Point, it was not possible to evaluate the concentration field near shore, which is estimated by the dashed line. The shape of the curve shows strong lateral separation of the tidal flow into and out of Port Moller. The February 1981 NAS station grid is shown in Figure 7. The surface distribution of salinity, as observed in February, 1981, is shown in Figure 8. The mean salinity field is elevated compared to conditions in August, 1980, but similar

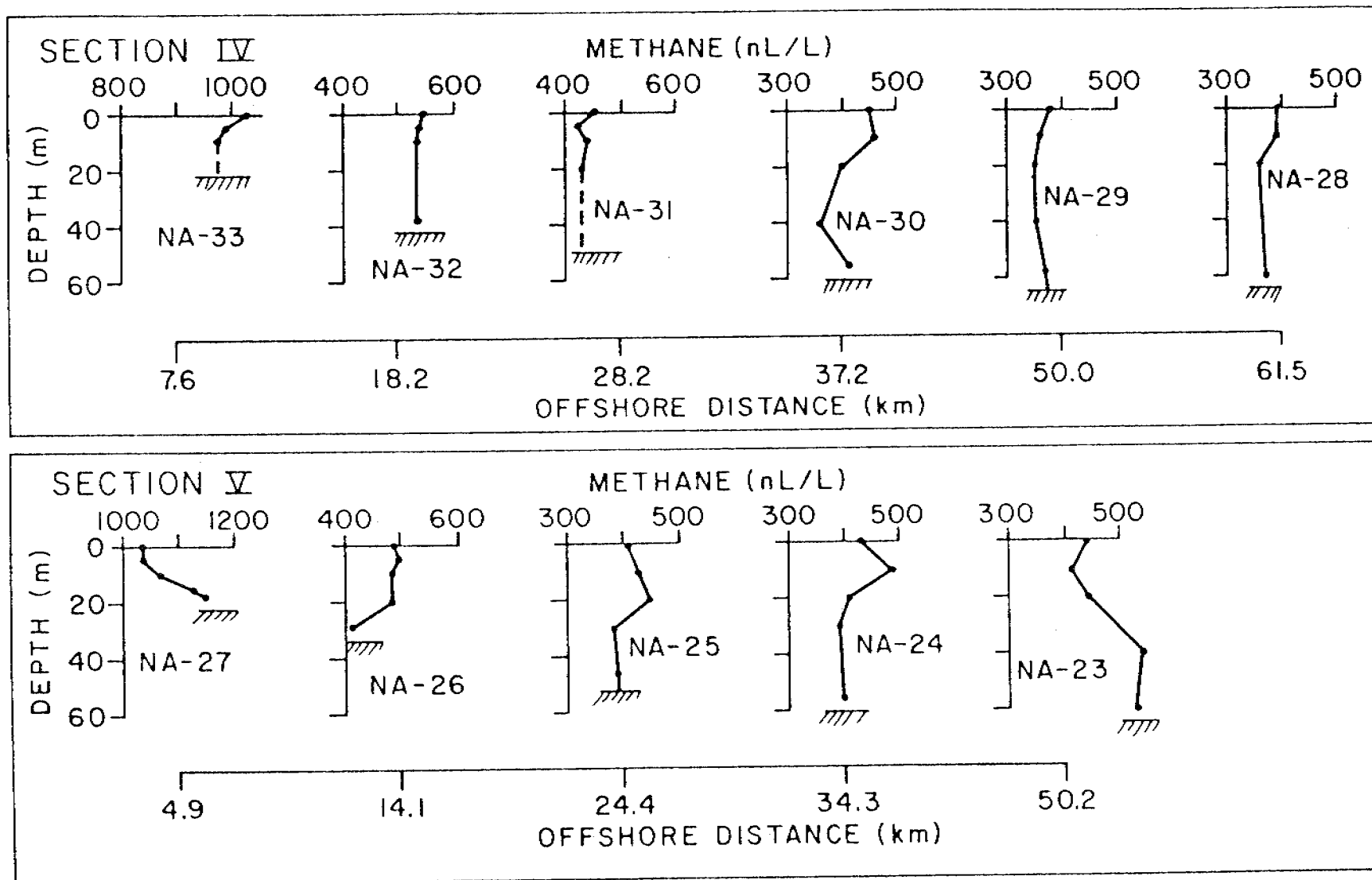


Figure 5. Vertical profiles of dissolved methane along two sections normal to the NAS. Sections IV and V are immediately east of Port Moller.

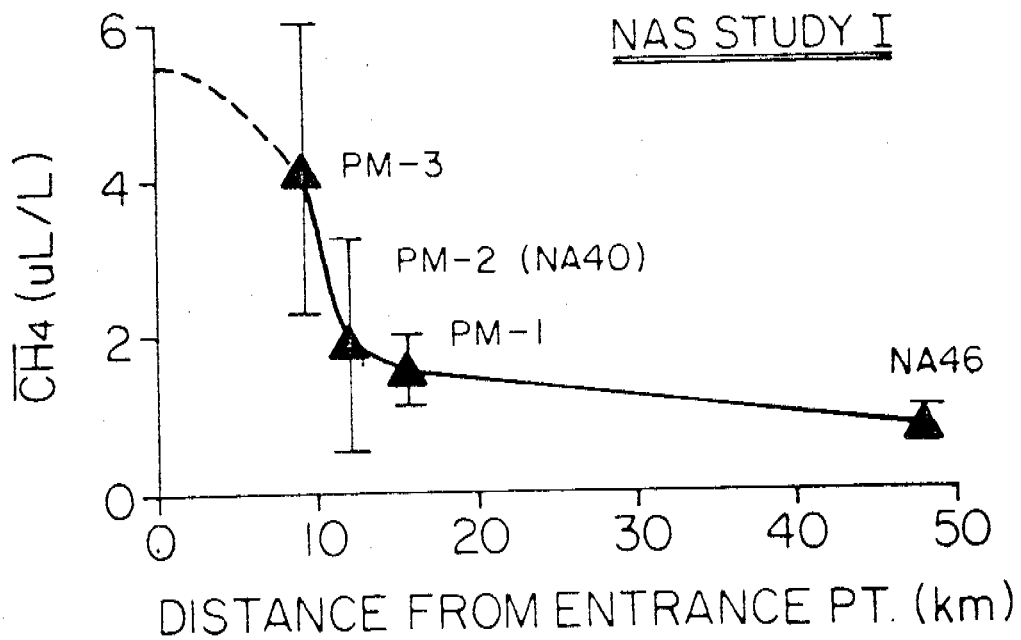


Figure 6. Distribution of methane across the entrance of Port Moller during a 24-hour tidal cycle. The vertical bars indicate 1 σ variation in the mean concentration at each station. The largest variation was observed at station PM-3, near the eastern side of Port Moller.

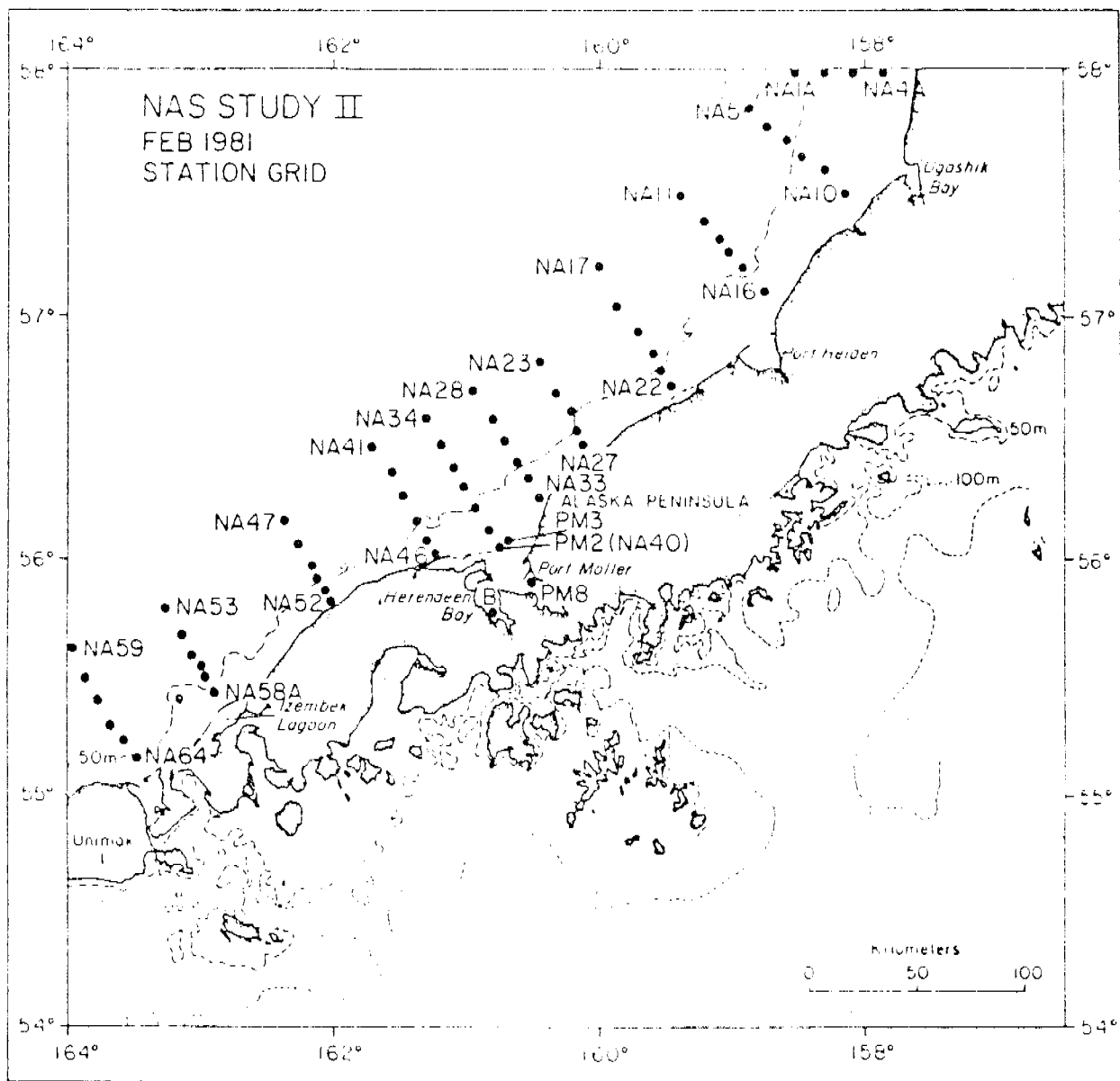


Figure 7. NAS stations occupied in February, 1981

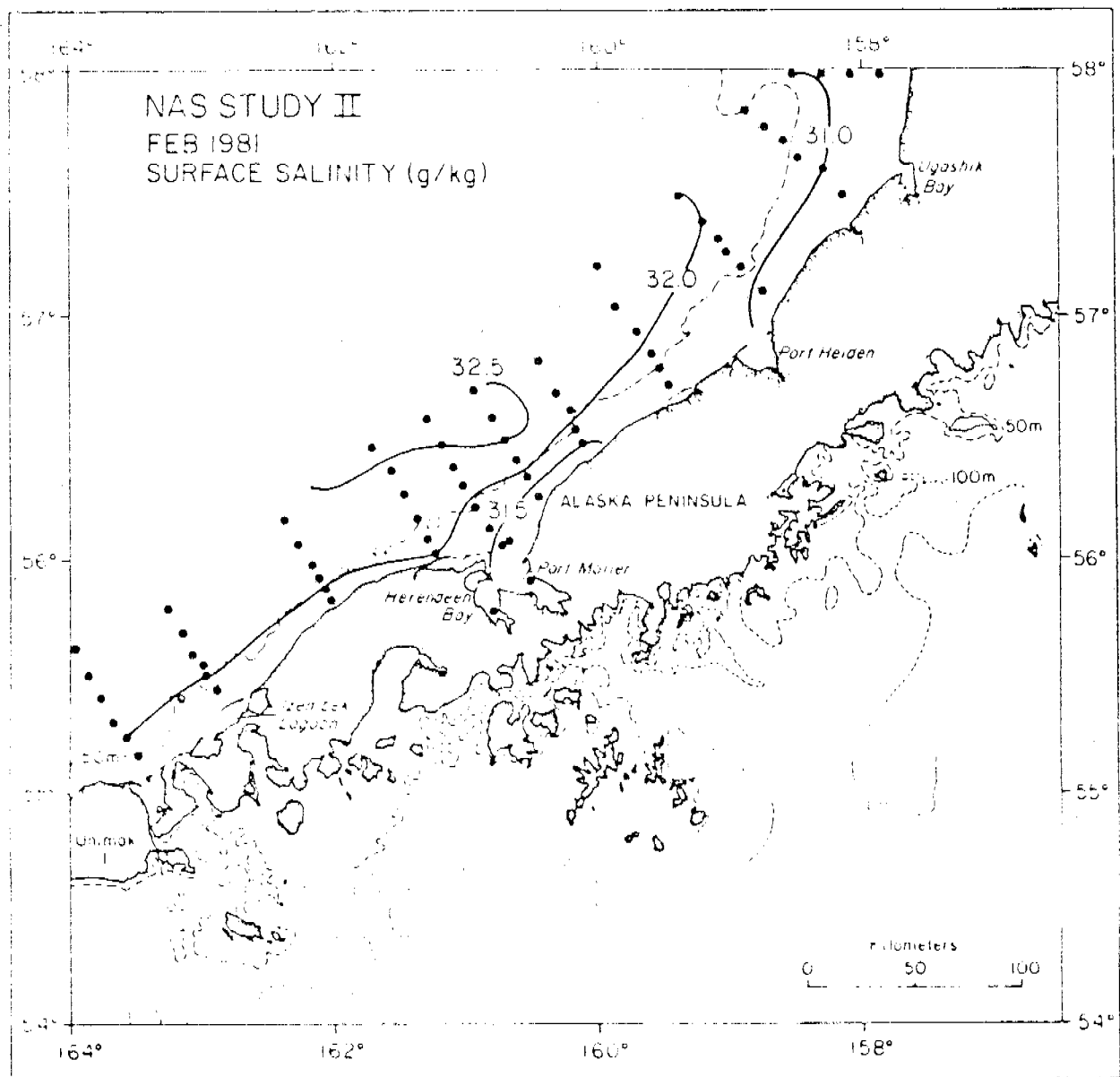


Figure 8. Surface salinity distribution (g/kg) along the NAS in February, 1981.

horizontal distributions are evident. The plume of brackish water fluxing from the Port Moller estuary is again evident, with higher salinity water found offshore.

The surface distribution of dissolved methane for the same period is shown in Figure 9. Concentrations of methane at the entrance were near 1200 nL L^{-1} , as compared to 400 nL L^{-1} observed in August, 1980. Similarly, offshore concentrations had decreased to 200 nL L^{-1} or about a factor of two relative to summer conditions. As observed previously in August, 1980, the methane flux from Port Moller was evident. The longitudinal gradient again decreased to the east. The reduced methane signature may be due to several factors, including a reduced microbiological production rate, more vigorous stirring of the surface layer due to seasonal increases in the scalar wind speed, or a reduced flushing of the estuary because of a seasonal decrease in the freshwater supply.

The highest concentration of methane ($23,800 \text{ nL L}^{-1}$) was observed in Herendeen Bay, the western arm of Port Moller. Apparently, the anoxic muds of this small basin (100 m deep; 22 m sill) provide a suitable environment for methanogenesis. Measurements of methane production rates in Herendeen Bay support this general conclusion (Griffiths, 1981). Thus, it appears that a substantial fraction of methane flux from the estuary is derived from Herendeen Bay. The previously reported high concentration of methane south of the cannery was probably due to complex tidal circulation in the estuary.

The methane flux from Port Moller is strongly correlated with low salinity water. This is graphically shown in Figure 10 for February, 1981 where correlations between salinity, methane and tidal amplitude are clearly depicted.

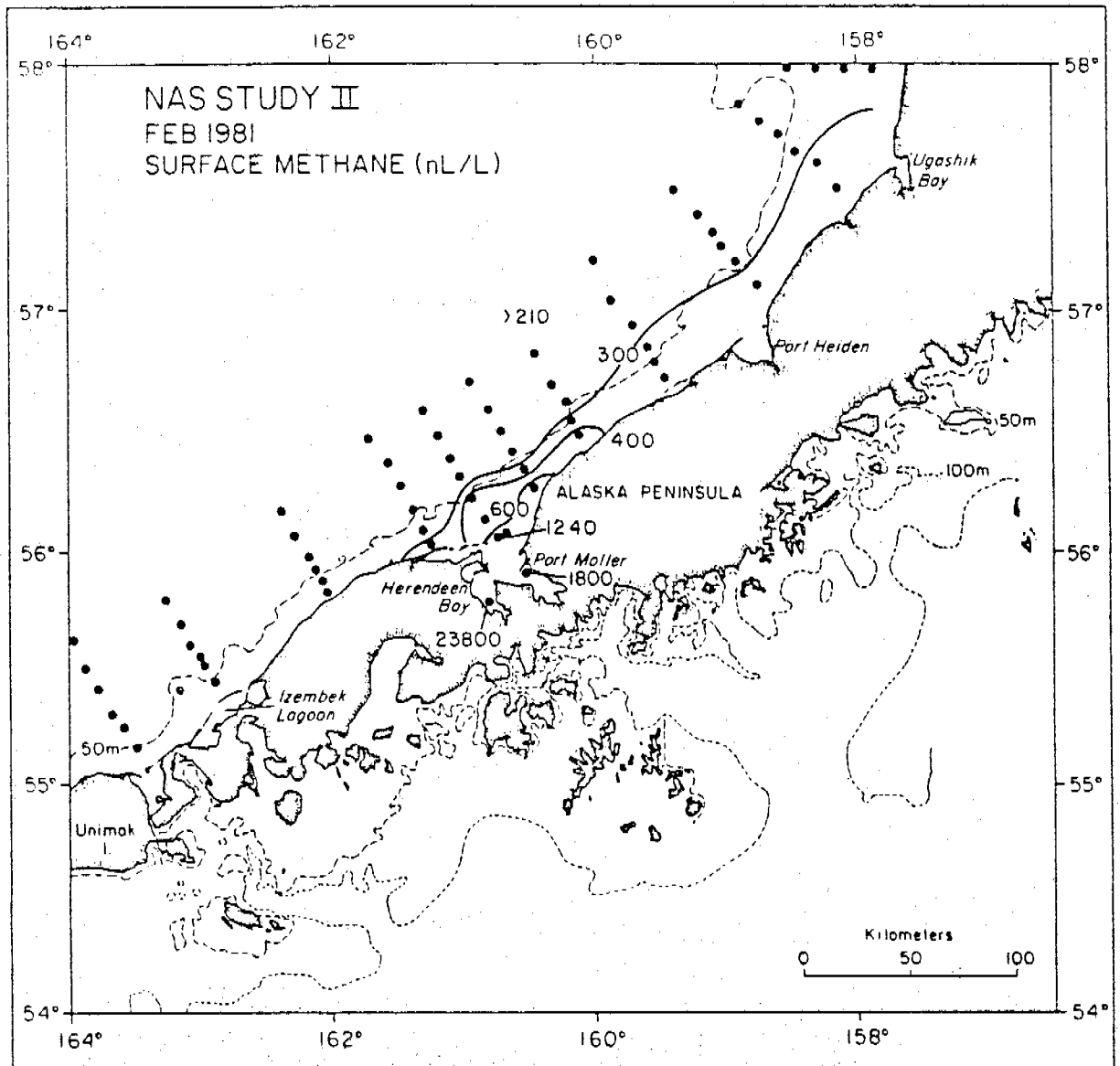
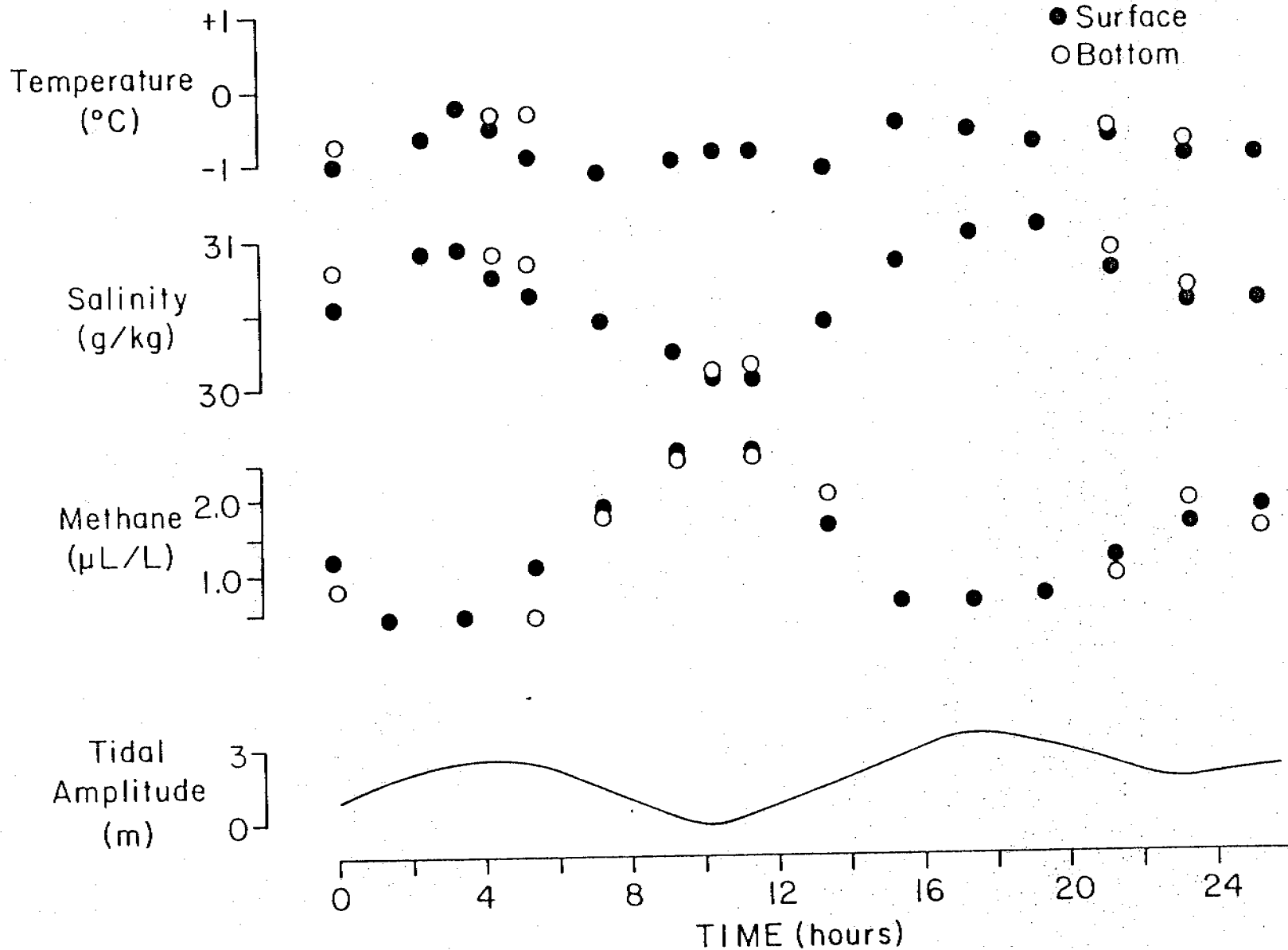


Figure 9. Surface distribution of dissolved methane (nL/L) along the NAS in February, 1981.

5-6 Feb 1981



53

Figure 10. Correlations between temperature (°C), salinity (g/kg), methane (nL/L) and tidal amplitude (m) at station PM-3 in February, 1981.

In the discussion section to follow, we will discuss these observations in terms of a two-dimensional steady state plume model. Only the August, 1980 data will be modeled as the data processing for the February, 1981 cruise has not progressed sufficiently to allow calculations to be made.

5.2 St. George Basin

Station locations for the August, 1980 cruise are shown in Figure 11. Detailed coverage of the area was not possible during this cruise because of the emphasis placed on the NAS. The station prefix - PL - refers to the PROBES line, which was occupied during this cruise and subsequent cruises.

The salinity distribution along the PL is shown in Figure 12a. This distribution suggests classical estuarine circulation with low salinity water at the surface underlain by high salinity water derived from offshore. Between station PL-4 and PL-24, the longitudinal salinity variation in the near-bottom waters was approximately 2⁰/∞. Positions of the outer, middle and inner fronts are roughly at stations PL-3, PL-9 and PL-20, respectively.

The vertical distribution of specific gravity (σ_t) is shown in Figure 12b. The location of the inner front, the boundary between the well-mixed coastal zone and the stratified inner shelf, is clearly indicated at PL-20.

The methane distribution along the PL is depicted in Figure 12c. A bottom source of methane is apparent near station PL-6 and a secondary maximum at station PL-14. Both features seem to correlate with isolated pools of cold water as shown in Figure 12d. Maximum near-bottom concentrations of methane are associated with water $\leq 4^\circ\text{C}$. Surface concentrations range from near 300 nL L offshore to approximately 500 nL L in the coastal zone.

The areal extent of the near-bottom methane plume in August, 1980 is shown in Figure 13. The highest concentration (2500 nL L⁻¹) was observed

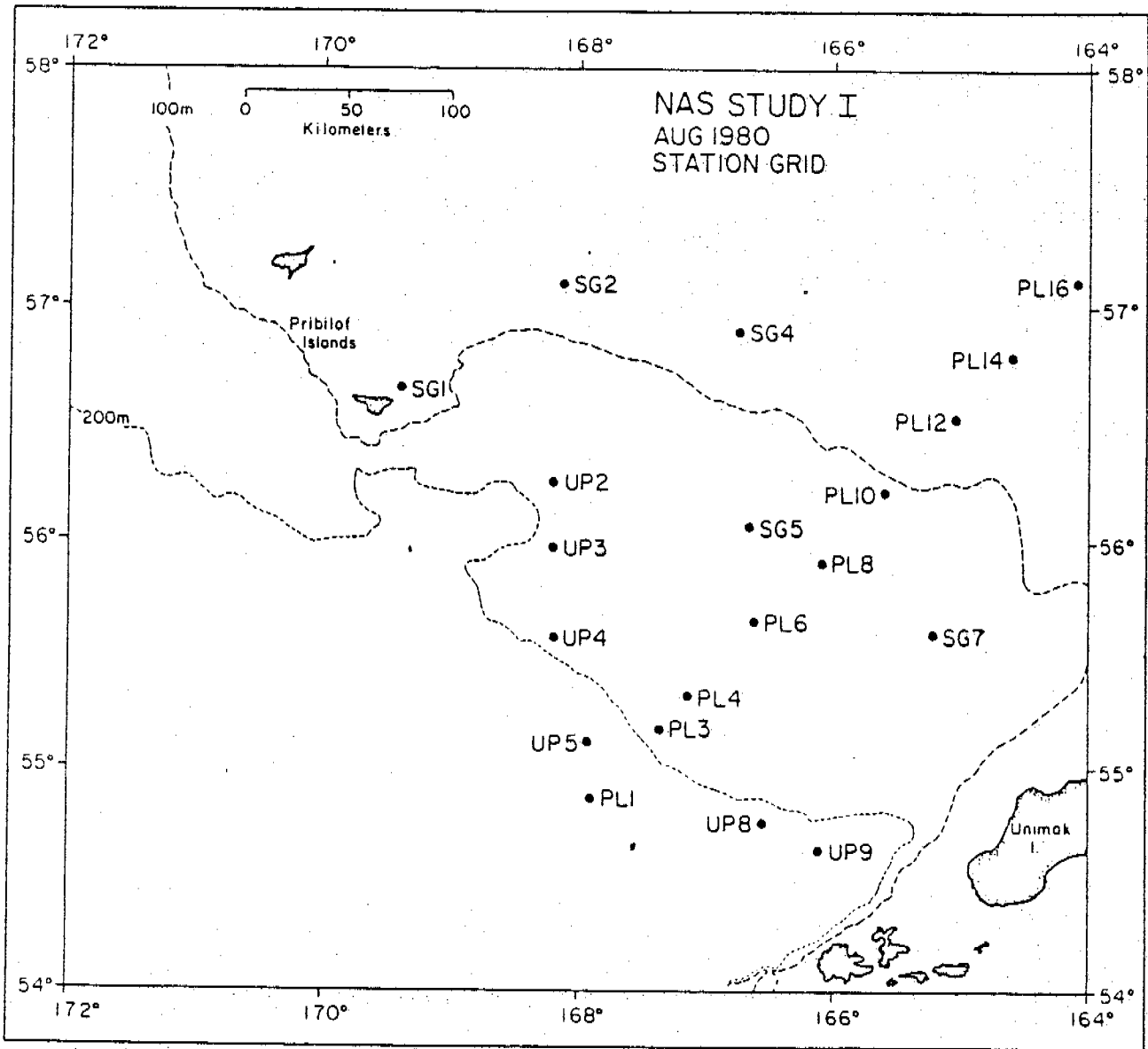


Figure 11. St. George Basin stations occupied in August, 1980.

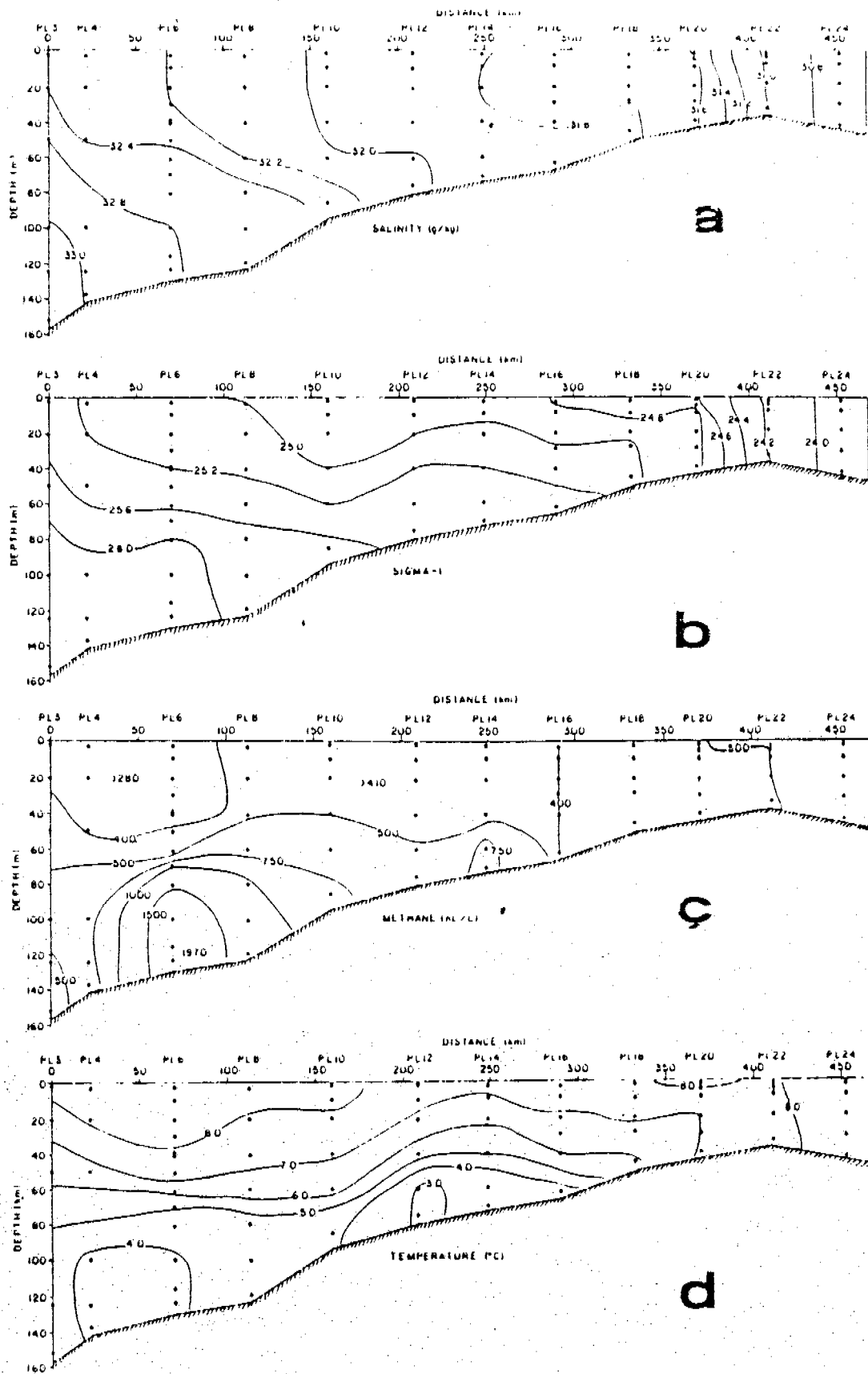


Figure 12. Vertical distribution of salinity (a), σ_t (b), methane (c) and temperature (d) along the PROBES Line in August, 1980. The middle front is located near PL 8-10.

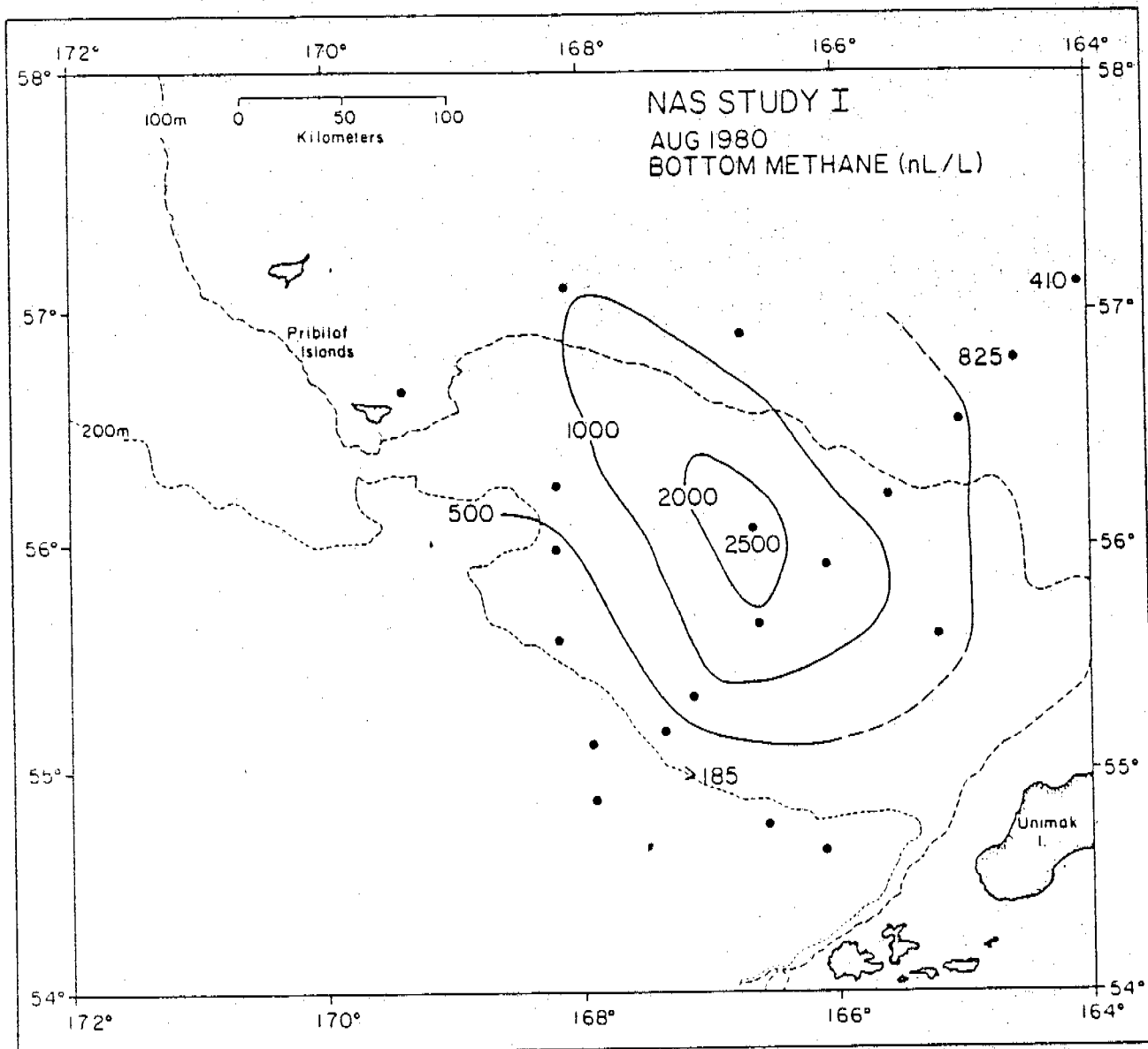


Figure 13. Near-bottom distribution (B-5 m) of methane (nL/L) in St. George Basin in August, 1980. Maximum concentrations were found near stations PL-6 and SG-5.

at SG-5, near PL-6. The plume trajectory shows a northwest-southeast orientation, which may be the result of anisotropic mixing or an elongated methane source. Although it is difficult to be precise, the plume structure appears to originate from a point source in the seafloor. If it is a gas seep, the methane appears to be of biological origin because of its compositional characteristics, that is, near absence of C_{2+} hydrocarbons.

The SBG station grid occupied in February, 1981 is shown in Figure 14. Because salinity, temperature and σ_t data were not available at the time of this writing, we are prepared to show only the vertical distribution of methane along the PL and the near-bottom concentration of methane in St. George Basin. The distribution of methane along the southwestern section of the PL is shown in Figure 15. Maximum near-bottom concentrations of methane were in excess of 500 nL L^{-1} compared to background values near 200 nL L^{-1} .

The near-bottom methane plume, shown in Figure 16, is quite similar to the distribution observed in August, 1980. Again it appears that methane arises from a point source near PL-6 and disperses along an axis parallel to the isobaths. Maximum concentrations of methane observed were approximately 1500 nL L^{-1} , or approximately 1/2 the value observed in August. Without knowing specifically the nature of the methane source (i.e., biogenic or thermogenic), it is reasonable to assume a temporal variability in source strength. However, erosion of the pycnocline in February relative to August would also result in reduced methane concentrations because of an increased vertical flux that would be accommodated by a concomitant increase in the air-sea exchange flux.

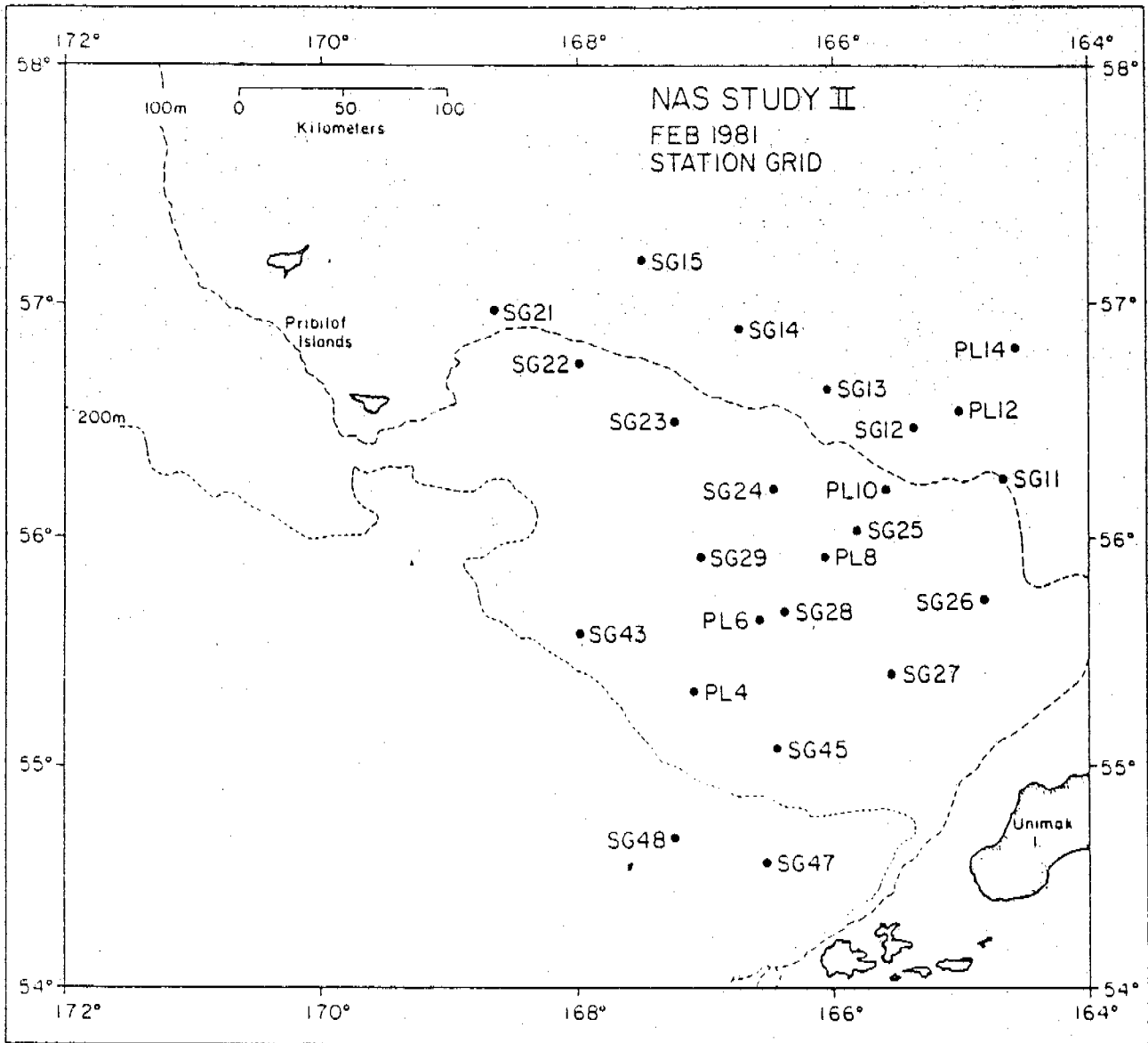


Figure 14. St. George Basin stations occupied in February, 1981.

09

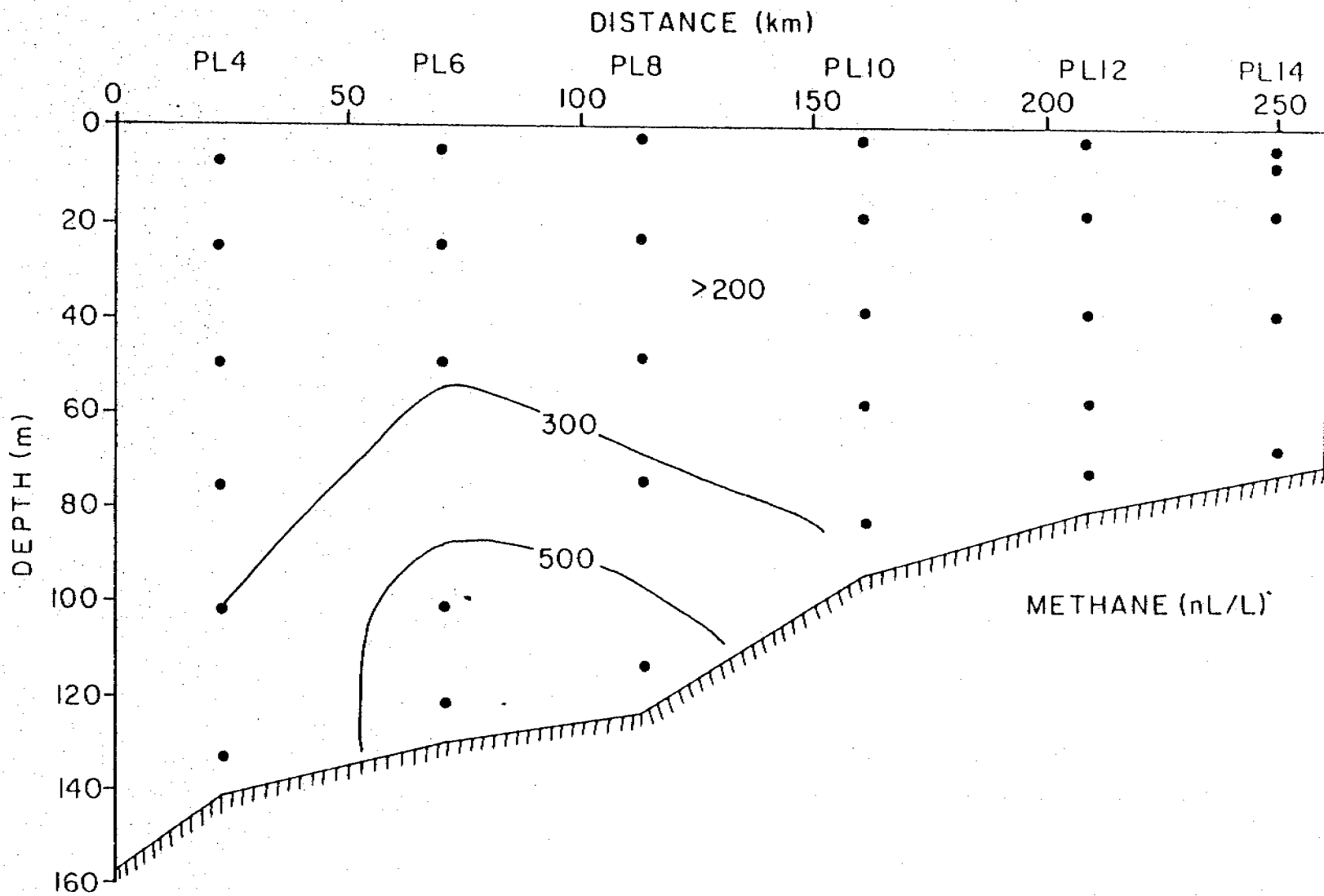


Figure 15. Vertical distribution of methane along a portion of the PROBES Line in February, 1981.

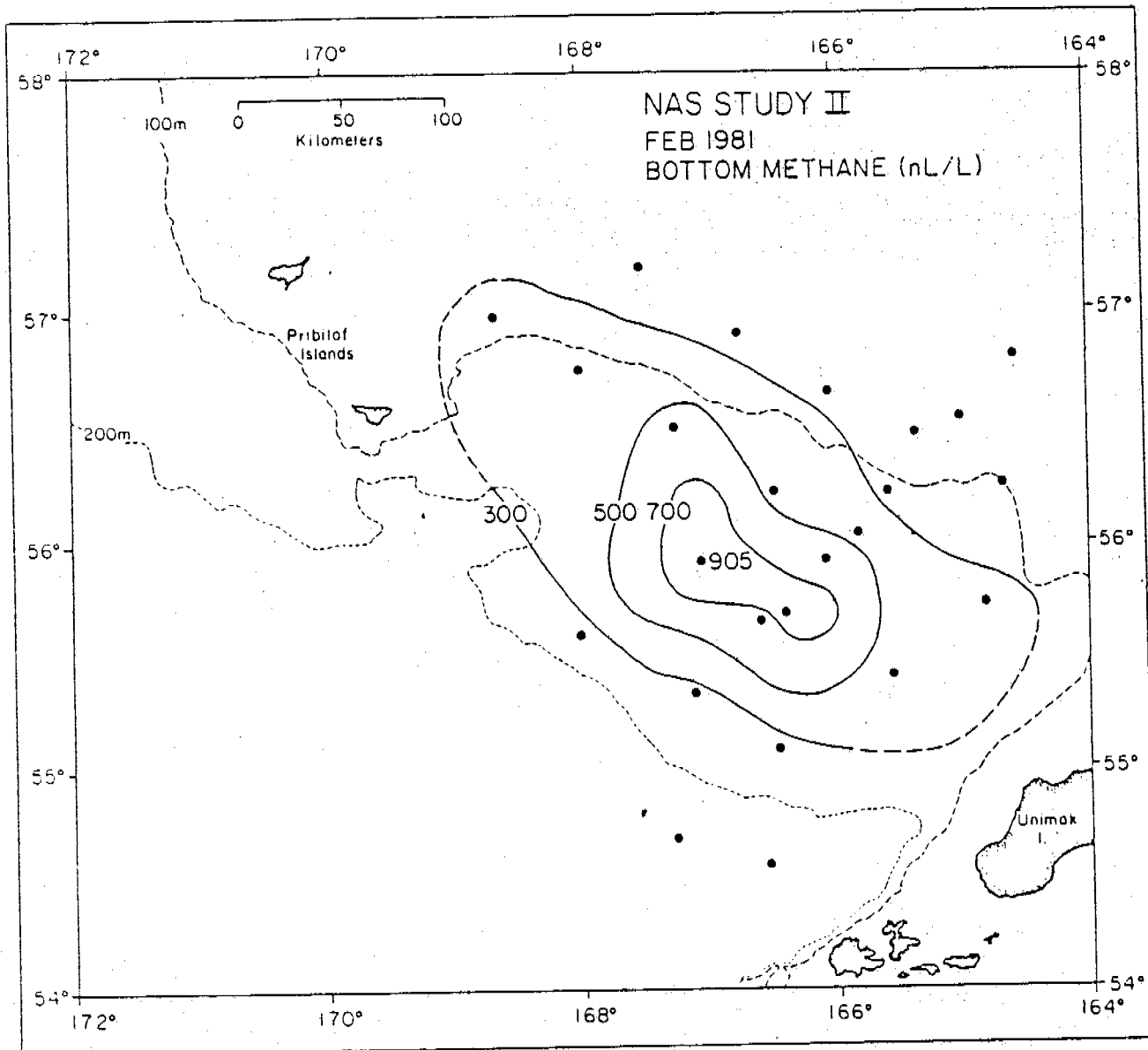


Figure 16. Near-bottom distribution (B-5 m) of methane (nL/L) in St. George Basin in February, 1981. Maximum concentration was observed at station SG-28; which is south of PL-6.

6. DISCUSSION

6.1 Plume Model

The distribution of dissolved methane along the NAS and in SBG is used to define limits on the horizontal and vertical eddy diffusivities and to compare mean flow velocities with those predicted from moored current meters. Because the program is still underway, only the August cruise data from the NAS will be considered in this report, but inferences about circulation processes in SBG will be made on the basis of preliminary data at hand.

To extract the salient spatial features of dissolved methane along the NAS, we adopted a stationary two-dimensional plume model described by Csanady (1973). The model has been used to predict the dispersion characteristics of wastewater injected from a pipe into a coastal zone. The model assumes stationary conditions, balances lateral diffusion against horizontal advection and includes a first order loss term. For stationary conditions:

$$\frac{\partial}{\partial y} \left[Ky \frac{\partial C}{\partial y} \right] - u \frac{\partial C}{\partial x} - kC = 0 \quad (1)$$

The solution to equation (1) for line source of length b is:

$$C = (C_0/2) \exp(-kx/u) [\operatorname{erf}(y^*_1) + \operatorname{erf}(y^*_2)], \quad (2)$$

$$\text{where } y^*_1 = \frac{b/2 + y}{0.1039(x/u)^{1.17}}$$

$$y^*_2 = \frac{b/2 - y}{0.1039(x/u)^{1.17}}$$

x = longshore direction

y = cross-shelf direction

u = longshore mean velocity

k = first order rate constant

C_0 = concentration of methane at the source

In the above model, we ignore diffusion in the x-direction and scale the horizontal diffusivity (K_h) in the y-direction according to the Lagrangian time scale. For simplicity, we assume that mixing is isotropic in the x- and y-directions. However, Okubo (1971) has shown that dispersion is enhanced in the direction of mean flow relative to dispersion across streamlines. The magnitude of the difference is approximately a factor of three for those coastal situations that have been studied. Furthermore, tidal currents are rectilinear along the shelf which likely results in an enhanced mixing alongshore. In the presence of a mean flow \bar{u} , it can be shown that:

$$\sigma_{rc}^2 = 2\sigma_x\sigma_y \quad (3a)$$

where σ_{rc} is the mean square radius of diffusing substance, σ_x and σ_y are the respective standard deviations of the plume in the x- and y-directions (Okubo, 1971). If we assume uniform horizontal mixing ($\sigma_{rc}^2 = 2\sigma_y^2$) the apparent diffusivity defined by Okubo is:

$$K_h = \sigma_y^2/4t \quad (3b)$$

or

$$K_h = \sigma_h^2/2t \quad (3c)$$

where $\sigma_h^2 = 2\sigma_y^2$ and t is the diffusion time. The characteristic time (or length) scale can be computed from $t = x/\bar{u}$. Substituting into (3c), we obtain:

$$K_h = \sigma_h^2 \bar{u}/2x \quad (3d)$$

Based on numerous dye patch studies, Okubo (1971) given estimates of K_h in terms of the characteristic length scale ℓ . He found that the 4/3 law tended to overestimate the magnitude of K_h and presented a log regression diagram that shows:

$$K_h \propto \ell^{1.1} \quad (3e)$$

or that

$$\sigma_{rc}^2 = 0.0108 t^{2.34} \quad (3f)$$

In equation (2), the horizontal eddy diffusivity is formulated in terms of the variance of the plume in the y-direction $Sy(\sqrt{2} \sigma_y)$. After substitution of $t = x/\bar{u}$ into (3f) we find:

$$\sqrt{2} s_y = 0.1039 t^{1.17} \quad (3g)$$

Based on the diffusion diagram given by Okubo (1971), we anticipate $10^5 \text{ cm}^2 \text{ s}^{-1} \leq K_h \leq 10^7 \text{ cm}^2 \text{ s}^{-1}$ for length scales between 10 and 100 km.

If we assume that K_h is proportional to the tidal excursion, which is approximately 10 km, then $K_h = 10^5 \text{ cm}^2 \text{ s}^{-1}$. Because cross-shelf mixing is orthogonal to the isopycnal surfaces, the magnitude of the apparent horizontal diffusivity in the y-direction should be less.

Dissolved methane may be lost from the water column via air-sea exchange and biological oxidation. Since both processes can be formulated in terms of first order kinetics, they are included in the model as a single term:

$$k = k_{a/s} + k_{\text{biol}} \quad (4)$$

Computation of $k_{a/s}$ requires knowledge of sea-surface roughness (a function of wind speed), the molecular diffusion and Bunsen solubility coefficients of methane as a function of salinity and temperature. All of these parameters are known to within 30% (Broecker and Peng, 1974), thus $k_{a/s}$ can be estimated (see Cline, 1981 for details on the calculation of $k_{a/s}$).

Biological oxidation rates of methane, not previously known for these waters, have been determined by RU# 595 headed by Dr. Griffiths. Water samples were inoculated with a known amount of $^{14}\text{CH}_4$ and incubated for 24 to 48 hours. The $^{14}\text{CO}_2$ given off after oxidation was counted and the rate constant computed. The kinetics generally obeyed a first order reaction when incubation time and substrate levels were varied.

By averaging all the biological oxidation rate determinations made at stations NA-20 through NA-46 (see Fig. 3), we compute a first order biological rate constant of $9.5 \pm 3.1 \times 10^{-8} \text{ s}^{-1}$. In contrast, the air-sea exchange term, $k_{a/s}$, was $3.7 \times 10^{-7} \text{ s}^{-1}$ assuming a mean wind speed at 10 m above the sea surface of 5.7 ms^{-1} and a mean mixed layer depth of 30 m (see Cline, 1981). Thus the air-sea exchange term is approximately four times the biological consumption term. The combined rate constant, k , is $4.6 \times 10^{-7} \text{ s}^{-1}$.

The model is formulated in terms of a line source of length b . If the depth of the mixed layer (Δz) is known, then the mass transport of methane out of Port Moller is simply:

$$Q_{\text{CH}_4} = (b) \cdot (\Delta z) \cdot (\bar{u}) \cdot (C_0) \quad (5)$$

where the mass transport Q has dimensions MT^{-1} . Thus, the model is sensitive to the boundary conditions: b , source length; Δz , mixed layer depth; \bar{u} , mean alongshore velocity; and C_0 , initial concentration at the boundary. Time

series measurements at the mouth of Port Moller were used to estimate b (8 to 10 km) and C_0 (4000 nL L⁻¹). The mean mixed layer depth (Δz) between shore and 10 km off shore was determined to be 15 m. The mean alongshore velocity (\bar{u}) was set so as to match the plume characteristics. The model does not take into account a time dependency of the source which appears to be applicable in light of the wave nature of the methane distribution along the NAS.

A schematic representation of the NAS and the major transport terms used in the model is shown in Figure 17. Because the water depth increases systematically as one moves offshore, the methane distribution in the 15 m surface layer must be vertically averaged to provide a realistic representation of the actual distribution. Under actual conditions, it appears that turbulent mixing in the coastal zone ($z \leq 50$ m) is sufficient to maintain vertical homogeneity in most water properties.

6.1.1 Model Scenarios

In this section we present three model scenarios which attempt to bracket the mean velocity field of the coastal zone. The three cases representing mean alongshore velocities of 5, 7.5 and 10 cm s⁻¹, are shown in Figures 18 a, b and c. We selected a 5% contour interval as the minimum detectable level based on a source strength of 4000 nL L⁻¹ and two times the ambient noise level in the methane data of 100 nL L⁻¹.

At a mean velocity of 5 cm s⁻¹, the effects of lateral diffusion are rather obvious in which the maximum excursion offshore is about 15 km (y) from a source length of 8 km (Fig. 18a). Maximum offshore penetration occurs at about 60-70 km downstream (x). Increasing the mean velocity causes the plume to elongate in the downstream direction, systematically

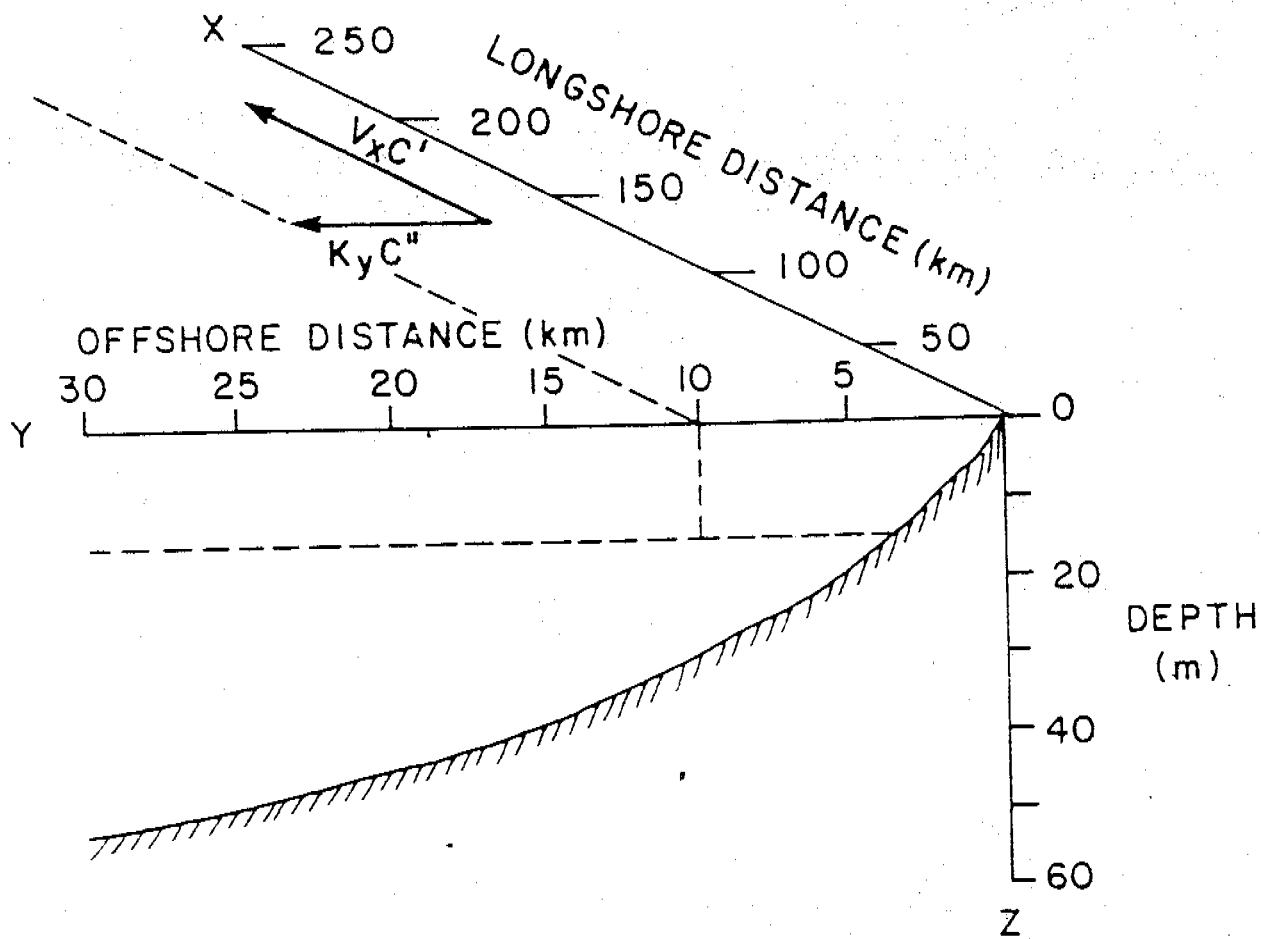


Figure 17. Model schematic of the NAS. The significant transport terms are horizontal diffusion, $K_y C''$, and horizontal advection, $V_x C'$. The well mixed coastal water is 10 km wide and 15 m deep.

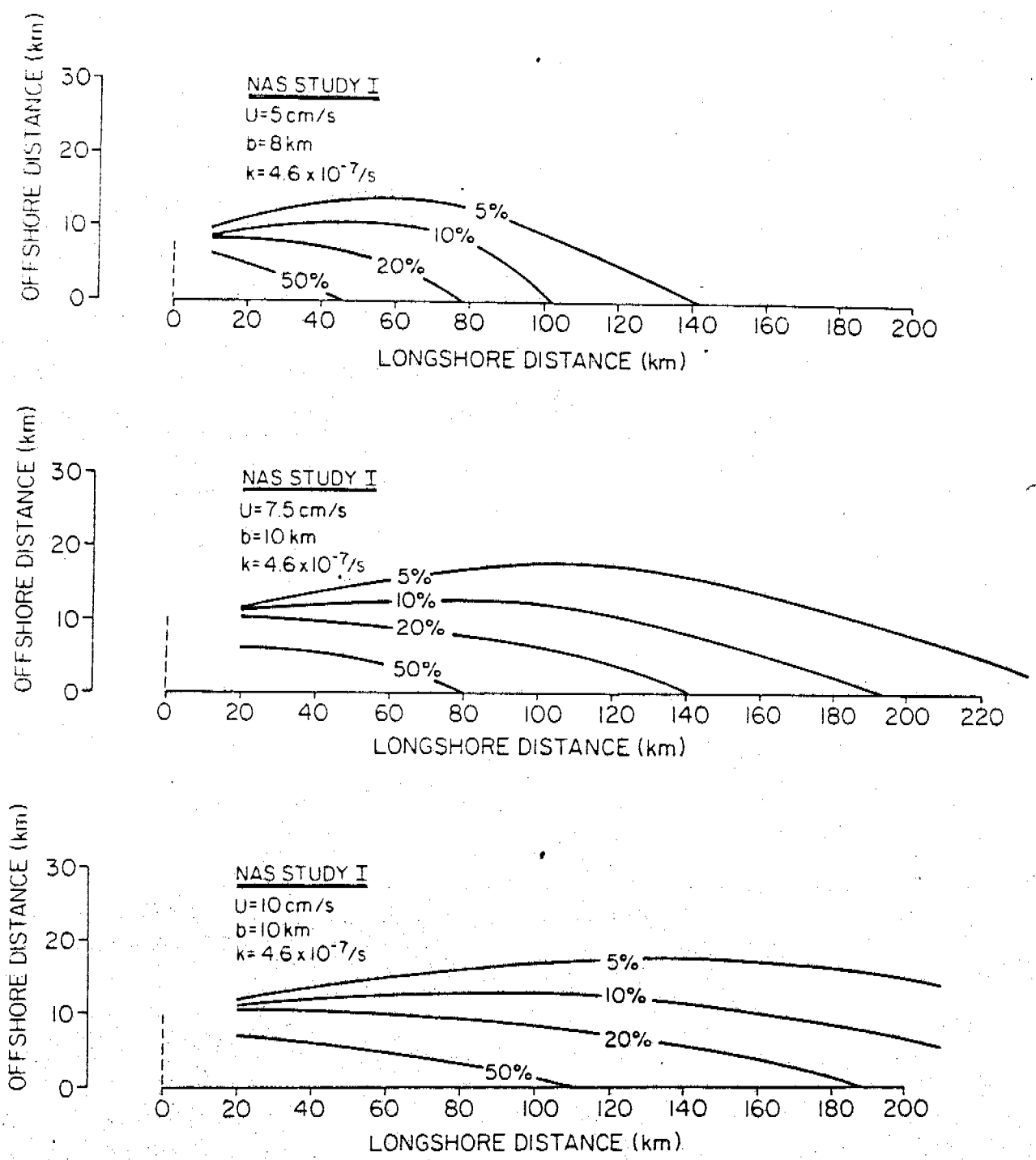


Figure 18. Relative concentrations of methane, depth integrated, predicted from equation (2), assuming various mean velocities of (a) 5 cm s, (b) 7.5 cm s and (c) 10 cm s. Air-sea exchange of methane and biological oxidation are included in a single first order rate constant, $k = 4.6 \times 10^{-7} \text{ s}$. Source strength is set at 8-10 km.

shifting the position of maximum excursion downstream (Figs. 18 b and c). As the velocity increases, lateral diffusivity becomes less important and the plume is contained largely within 10 km of shore or within the source distance b .

6.1.2 Model Fit

The depth averaged methane concentrations are shown in normalized form in Figure 19. Depth averaged concentrations at all stations outside the plume averaged $430 \pm 40 \text{ nL L}^{-1}$ (1σ). For comparison, we show the 10% isopleth for the model scenario of $\bar{u} = 7.5 \text{ cm s}^{-1}$ (Fig. 18b). Clearly, transport processes in the coastal zone are not as simple as the assumed model. The most serious discrepancy occurs at the input boundary, where episodically methane penetrates more than 10 km offshore. This results in a longitudinal wave structure. It is not clear whether accelerated pumping of the estuary occurs at selected tidal stages (e.g., perigean) or that some complex circulation occurs along the front between the well-mixed coastal zone and the more stratified water offshore.

Assuming a mean velocity of 7.5 cm s^{-1} , the node appearing at 105 km downstream is about 16 d downstream from the entrance to Port Moller. The daily tidal range and maximum tidal currents calculated for Entrance Point are plotted in Figure 20. The perigean tides, which occur every 28 d, appear to correlate well with the observed wave feature shown in Figure 19. Measurements, made along section VI (Fig. 19) on August 22, 1980, correlate well with the maximum perigean tidal excursion that occurred August 6-8, or about 16 d earlier. Because the station grid (Fig. 19) was occupied from east to west, section III (Port Moller) was occupied on August 24, 1980, about the time that a new perigean cycle was commencing (see Fig. 20). At about the same time however, the longshore winds were blowing toward the west (ap-

NAS STUDY I

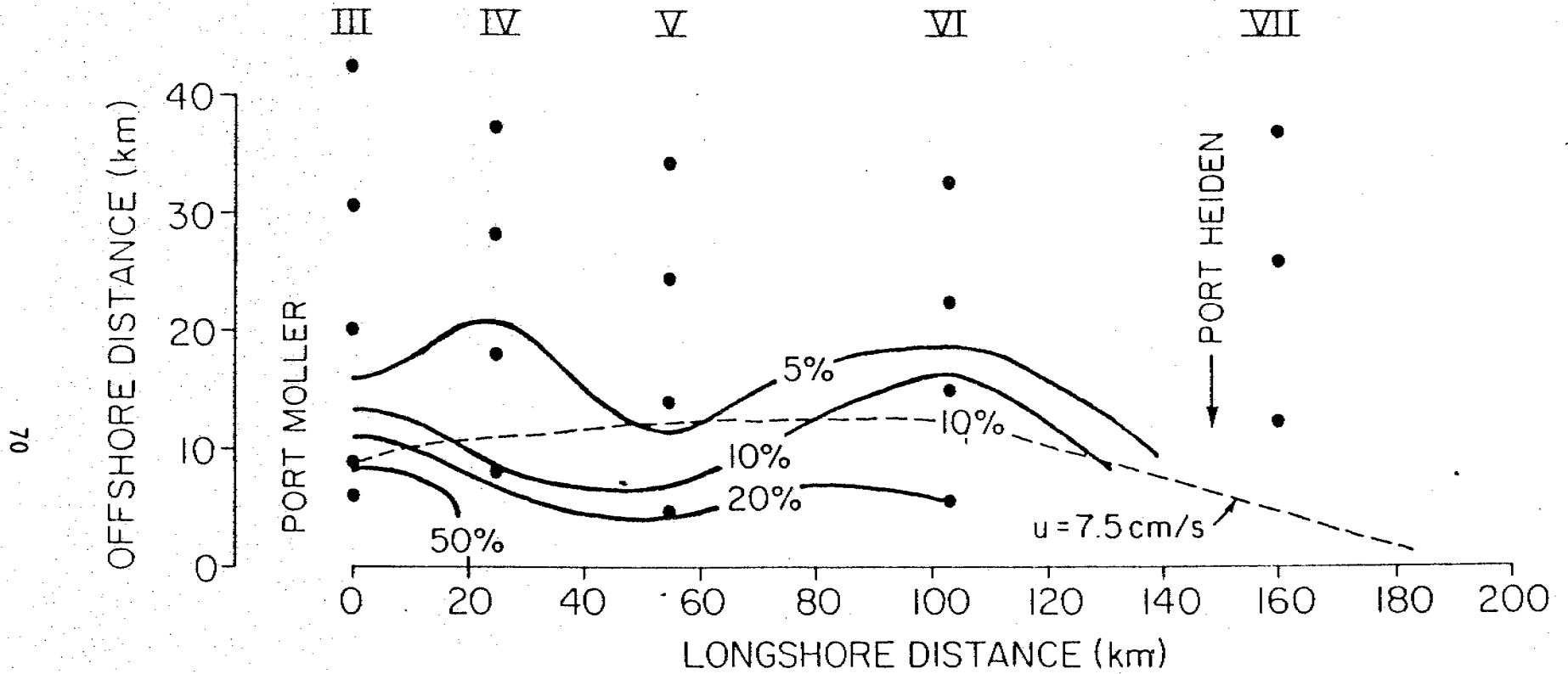


Figure 19. A comparison of a observed methane distribution (solid lines) with the 7.5 cm s model scenario. Pulsing of the estuary leads to a strong time dependent source, which is not accomodated by the stationary model.

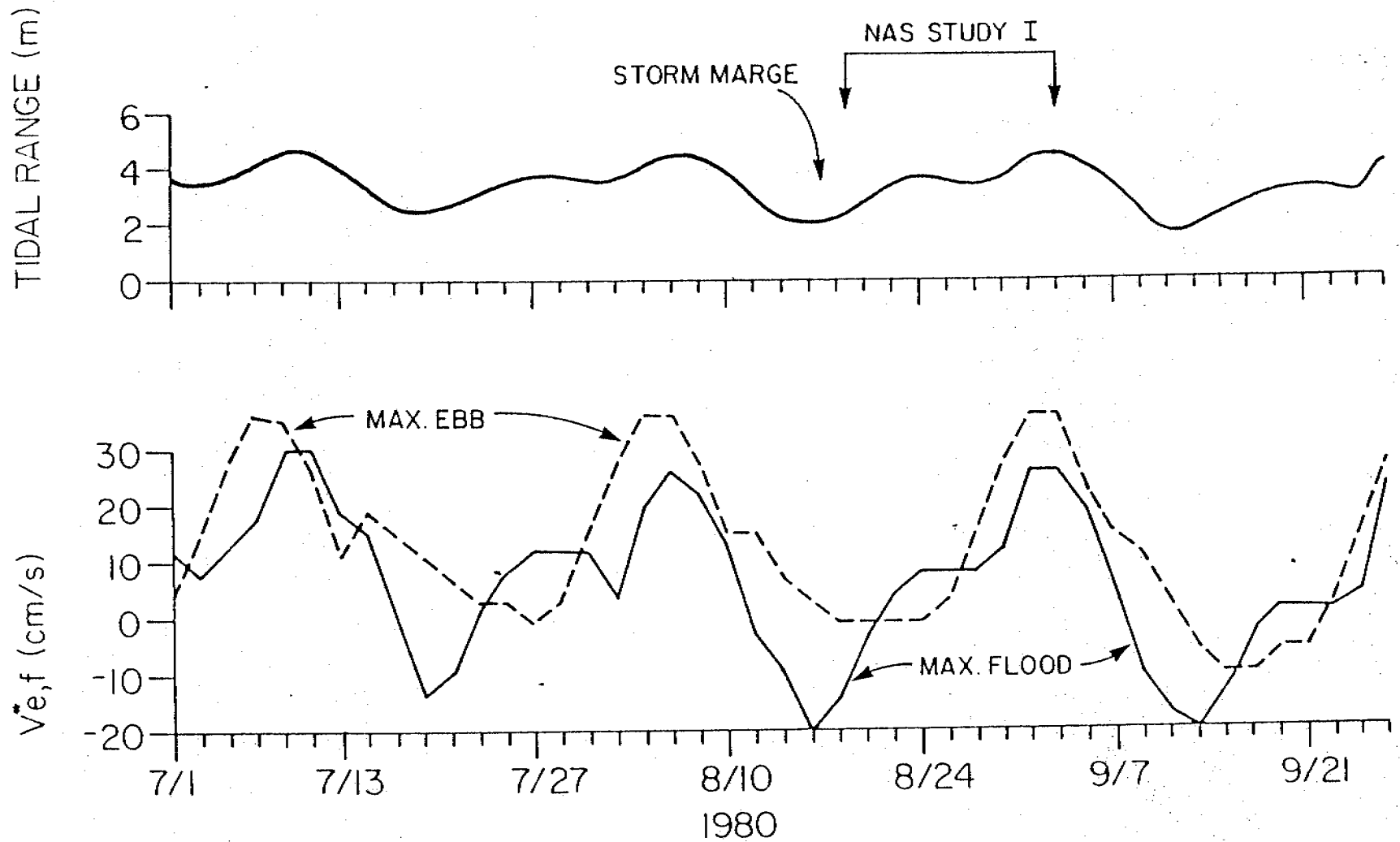


Figure 20. Tidal range and maximum ebb and flood tidal velocities at Entrance Point, Port Moller. The data presumably reflect conditions at mid-channel. Data are from the NOAA tide tables covering the observational period.

proximately 6 m s^{-1}), inducing a strong Ekman surface flux offshore (Pearson et al., 1981). Assuming a mean offshore surface velocity of 4 cm s^{-1} for the period August 21-24, dissolved methane would penetrate about 10 km offshore. This is roughly the distance shown in Figure 19, but undoubtedly both tides and wind-induced Ekman transport worked in concert to produce the observed distribution.

The reason why estuarine tidal pumping is an attractive mechanism for an efflux of methane from Port Moller is related to the probable methane source. It is now suspected that the major source of methane is in Herendeen Bay, a small isolated deep basin (approximately 100 m) with a shallow sill (approximately 22 m). Both the concentration of methane and the methane production rate (Griffiths, 1981) were highly elevated in this fjord-like bay in February, 1981. If flushing of this bay occurs primarily by tidal forces, we expect it to occur most likely during spring and perigean tidal cycles. During quiescent periods, the waters below sill depth would be stabilized, allowing methane concentrations to increase significantly. Obviously flushing would be enhanced by the presence of more dense water offshore, which presumably has a seasonal signature.

The distribution of methane as shown in Figures 4 and 19 suggests a mean drift east along the coast at a velocity of $5\text{-}10 \text{ cm s}^{-1}$. The characteristic time scale for these velocities is 17-35 d, thus our model predictions are not sensitive to tidal and subtidal events (2-10 d). Wind and current measurements made between August 20 and September 2 (13 d) suggest little mean current either east or west along the coast (Pearson et al., 1981). Surface mean currents are related to wind trajectories lasting for 2-4 d, causing directional Ekman transport along the coast (Pearson et al., 1981). The reasons for the disparity between measured mean current velocities and

the observed trajectory of the methane plume is not known, but several explanations are offered for discussion.

The current meter record is for 13 d and may not allow a statistical comparison to be made. There also may be difficulties associated with the extraction of subtidal frequencies ($0.001-0.002 \text{ hr}^{-1}$) when the energy spectrum is so heavily dominated by tides. It is also possible that non-linear tidal effects are present that lead to a net transport eastward along the NAS coastal zone. If non-linear tidal effects are not important, then tidally-induced diffusion would not result in the observed distribution, since we expect tidal energy to be isotropic in the x-direction.

While this dilemma has not been solved, it is hoped that these results might generate additional thought concerning transport mechanisms along the near shore areas of the NAS. The impact of spilled oil in this region, particularly on the beach and into the intertidal zone, depends critically on flow trajectories over temporal scales of a few days to a few months. Methane distributions are shown to be useful over time scales of 10-30 d.

6.2 St. George Basin

Seasonal observations conducted during the past five years have shown the existence of a localized bottom source of methane in SGB (see Figs. 13 and 16). The location is centered about $55^{\circ}40'N$ and $167^{\circ}00'W$. Unfortunately, the spatial station resolution during both the August and February cruises was too coarse to clearly identify the nature of the source. Horizontal diffusion coupled with episodic cross-shelf currents tend to confuse the exact nature of the source. One also could postulate a line or rectangular source which would not be inconsistent with the observed distributions.

6.2.1 Vertical Methane Distribution

Before describing a few of the prominent features of the methane distribution in SBG, we first address the vertical structure observed in August. At station PL-6 (see Fig. 11) located near the center of the middle shelf, the vertical density distribution (Fig. 21) reflects processes of salt fingering and double diffusion (Coachman and Charnell, 1977). Station PL-6 was occupied twice during the cruise, the time interval between visits was about 5 d. The points of interest are the well-mixed surface layer ($\Delta z_s \approx 30$ m) and bottom boundary layer ($\Delta z_b \approx 30$ m). Between these layers, the density gradient is sharp, but not uniform. Because of the degree of stratification present, a barrier to vertical transport of materials from the bottom boundary is expected. To quantify the magnitude of the relevant vertical transport parameter, K_v , within the pycnocline, we adopted a one-dimensional flux model describing the vertical distribution of dissolved methane. The vertical distribution of methane at station PL-6 for the two observational periods is shown in Figure 22. Measurements taken on September 3 were used in the model because they were more detailed.

The one-dimensional flux model assumes that the curvature in the methane profile is derived from a variable vertical eddy coefficient and not the result of in situ consumption. This assumption may or may not be valid, but as we show below, it places an upper limit on the magnitude of K_v . The essence of the model is that the methane is produced in the bottom boundary layer (or the underlying sediments). Most of the methane produced is removed (by horizontal diffusion and advection), however some fraction fluxes vertically through the pycnocline and is removed by air-sea exchange (stationary conditions). In the absence of horizontal or biological processes adding or removing methane, the model for the pycnocline is:

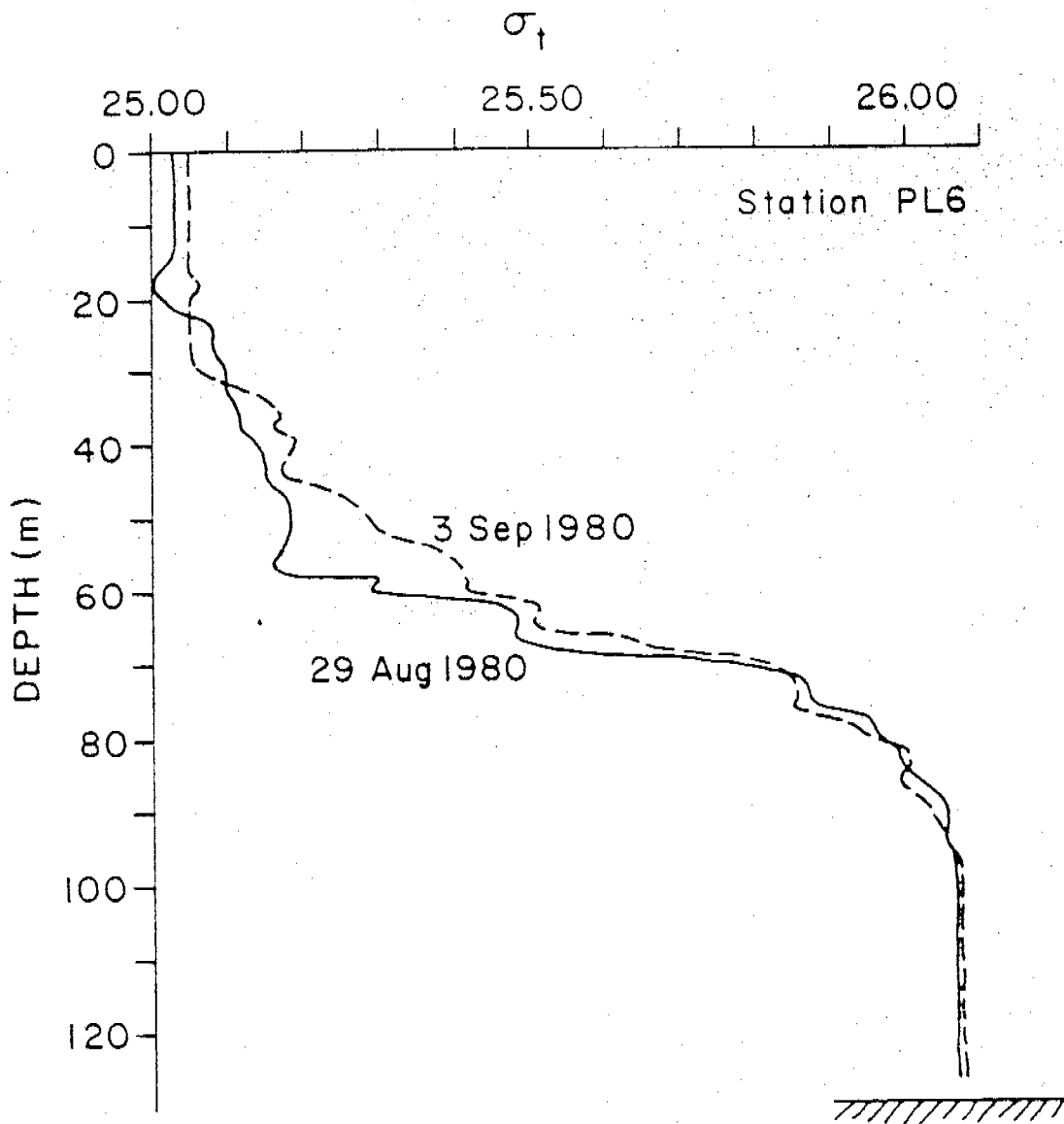


Figure 21. Vertical density distribution at PL-6 on August 29, 1980 and September 3, 1980. Note the effects of salt fingering and double-diffusion.

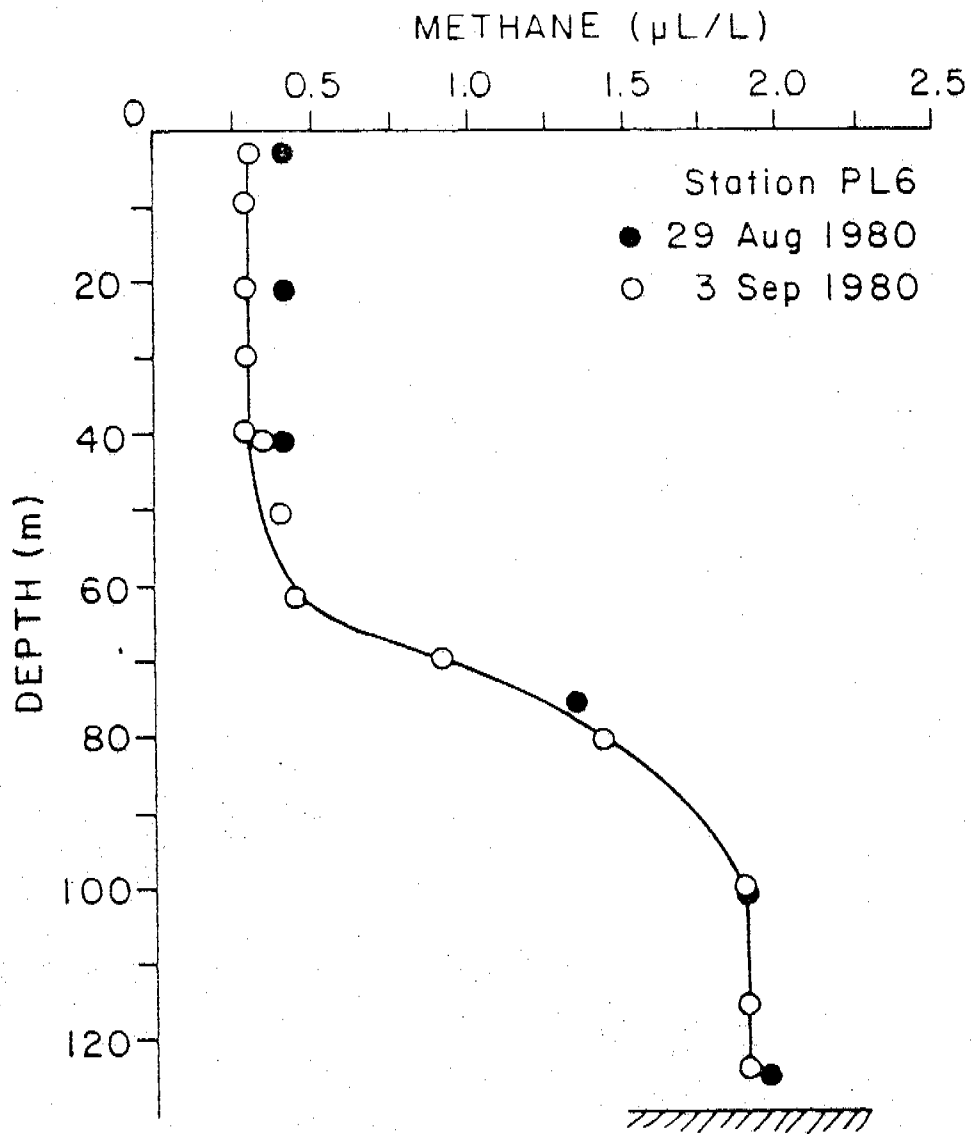


Figure 22. Vertical distribution of dissolved methane at PL-6 on August 29, 1980 and September 3, 1980.

$$K_V \frac{dC}{dz} = \text{constant} \quad (6)$$

where K_V is the depth dependent vertical eddy diffusivity. Since the flux across any horizontal plane is a constant, that constant must be equal to the air-sea exchange flux:

$$F_{a/s} = \frac{D}{\Delta h} (C - C') \quad (7)$$

where D is the molecular diffusivity of dissolved methane, Δh is the thickness of the stagnant film boundary layer and C' is the equilibrium solubility of methane at the surface. For the surface conditions during the cruise, $F_{a/s} = 1.9 \times 10^{-4} \text{ nL cm}^{-2} \text{ s}^{-1}$. The uncertainty in this value is no more than a factor of 2. To derive the functional dependence of K_V , the methane profile was smoothed by hand and a cubic spline function was fit to the curve. This function was then differentiated and used to calculate the gradient in equation (6).

Rather than present the estimated values of K_V as a function of depth, we plot them against the Brunt-Vaaisela frequency, a measure of stability (Welander, 1967). The relationship is shown in Figure 23. The data separate into two distinct groups, both of which show a reciprocal 1/2 power relationship. Based on the theoretical arguments presented by Welander (1967), this correlation implies turbulence induced by shear, which intuitively is not surprising. The dashed lines show the reciprocal 1/2 power relationship without data regression.

In the upper portion of the pycnocline ($24 \text{ m} < z < 50 \text{ m}$), K_V varies from about $20\text{-}50 \text{ cm}^2 \text{ s}^{-1}$. Because of the sluggishness of air-sea exchange, the methane flux model is not useful when vertical eddy diffusivities exceed

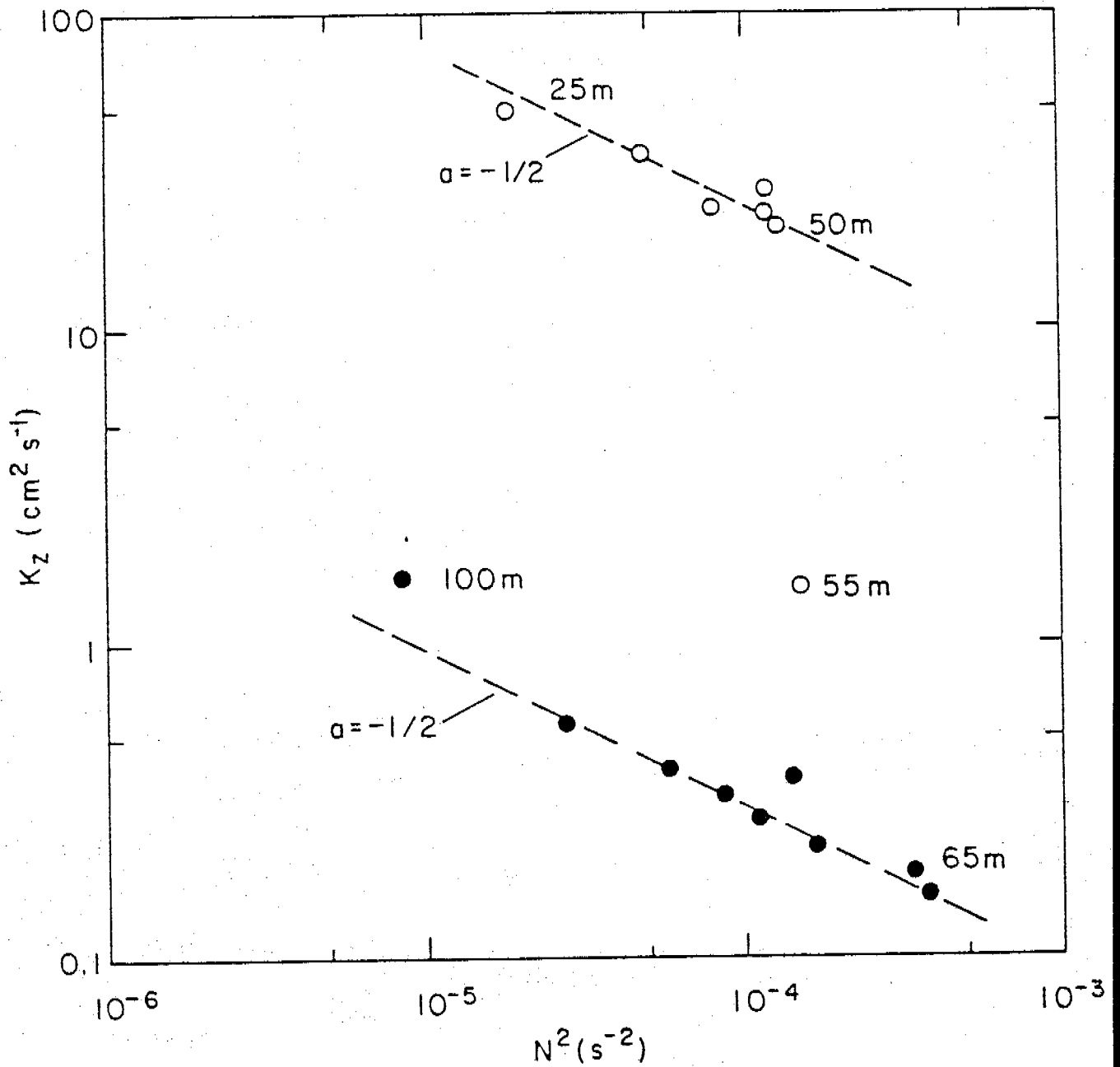


Figure 23. Estimated apparent vertical eddy diffusivity as a function of the buoyancy gradient. The Brunt-Vaaisela frequency was determined from the density distribution; K_z from the observed methane profile. The reciprocal square-root relationship suggests shear-induced turbulence.

$50 \text{ cm}^2 \text{ s}^{-1}$. In the lower portion of the pycnocline, K_v varies from 0.15 to $1 \text{ cm}^2 \text{ s}^{-1}$. Between these two regions, eddy diffusivity decreases rapidly and separates the water column into two distinct energy regimes. Near the surface, K_v is much larger because horizontal shear is the dominant mechanism by which energy is released to turbulent mixing. The lower region of the pycnocline is the principal concern in terms of bottom-released material. Between 65-95 m, the average K_v is about $0.3 \text{ cm}^2 \text{ s}^{-1}$ and will provide significant resistance to the vertical transport of dissolved and emulsified oil.

Returning to the model assumptions, boundary conditions could have been satisfied with either a bottom or surface flux. Microbial production rates in the sediments near PL-6 measured in August (Griffiths, 1981) gave an estimated surface flux of $5.8 \times 10^{-4} \text{ nL cm}^{-2} \text{ s}^{-1}$ or about a factor of 3 greater than the computed air-sea flux. As already noted, a large fraction of the methane is removed by lateral processes, hence the production rates quoted above are not unrealistic. If the methane is coming from a point source in the sea floor and is of thermogenic or paleomicrobial origin, then the measured production rates are not relevant to an understanding of the plume dynamics. Because of these uncertainties, we adopted an air-sea exchange flux as the boundary condition.

It has been assumed that there is no in situ methane consumption or production. If we now assume that biological oxidation occurs in the lower portion of the pycnocline ($65 \text{ m} < z < 95 \text{ m}$), the resultant methane concentration profile would show an increased curvature. Therefore, K_v would have to be even smaller than the estimated 0.15 to $1 \text{ cm}^2 \text{ s}^{-1}$. Thus, the model predicts a maximum value of K_v . This can be seen in the following model analogy. Assume that methane is produced in a lower boundary layer and con-

sumed according to first order kinetics (Griffiths, 1981) in the pycnocline. Further assume that K_V is depth dependent as before. The conservation of mass in the vertical is (steady state):

$$\frac{\partial}{\partial z} [K_V \frac{\partial C}{\partial z}] - kC = 0 \quad (8)$$

Performing the differentiation, we obtain after rearrangement:

$$\frac{\partial C}{\partial z} = \frac{kC - K_V (\partial^2 C / \partial z^2)}{\partial K_V / \partial z} \quad (9)$$

Considering the lower boundary region we have $\partial K_V / \partial z > 0$; $K_V > 0$ and $\partial^2 C / \partial z^2 < 0$, thus the gradient becomes:

$$\partial C / \partial z = (kC + |K_V (\partial^2 C / \partial z^2)|) / \partial K_V / \partial z. \quad (10)$$

Therefore, the methane gradient is increased by biological consumption in the lower boundary layer ($\partial^2 C / \partial z^2 < 0$) and our previous flux model ($k = 0$) must overestimate the magnitude of K_V .

6.2.2 Near-Bottom Methane Plume

We earlier showed the distribution of dissolved methane in the near-bottom waters of SGB (Fig. 13). Because the lower 30 m or so of the water column is well-mixed, the areal distribution shown in Figure 13 represents rather well the depth integrated distribution. Assuming that most of the methane arises from a single source (near SG-5 and PL-6), the distribution might be analyzed in terms of a lateral diffusive model or a longitudinal advection-lateral dif-

fusion model. Mean currents in the near-bottom waters more toward the northwest at $2-5 \text{ cm s}^{-1}$ (Kinder and Schumacher, 1981a). This mean current trajectory along shelf undoubtedly influences the observed orientation of the methane plume. We are not prepared at this time to analyze the methane plume in terms of a diffusion model with variable eddy diffusivities, but rather will use the diffusion-advection model already described for the NAS.

The model shown in equation (1), is modified slightly. Namely, the air-sea exchange flux is ignored since it is the lower boundary layer that is being analyzed. The source is estimated to be 30 km in length (cross-shelf) from Figure 13. Vertical diffusion is ignored and the mean velocity field is assumed to be in the range of $2.5-5 \text{ cm s}^{-1}$, based on current meter measurements. The results for the 2.5 cm s^{-1} case is shown in Figure 24a (dashed lines) and compared to the actual normalized distribution. A visual fit of the observed depth integrated data to a velocity field of 5 cm s^{-1} is much better, as shown in Figure 24b. Thus, the plume morphology suggests a mean velocity to the northwest of 5 cm s^{-1} in good agreement with the accepted current velocities. In all likelihood, however, anisotropic lateral mixing would give a similar result.

If we accept the premise that methane arises from a localized source ($b = 30 \text{ km}$), and the mean velocity field is near 5 cm s^{-1} , then the plume extension to the southeast is the result of complex mixing patterns not formally included in the model. Anisotropic lateral mixing ($K_y \neq K_x$), episodic reversals in mean flow and cross-shelf advection are all realistic options which, if included in the model, would probably give a realistic representation of the near-bottom methane distribution.

These results suggest that dissolved or emulsified petroleum compounds introduced into the near-bottom waters of SGB will move rectilinearly along

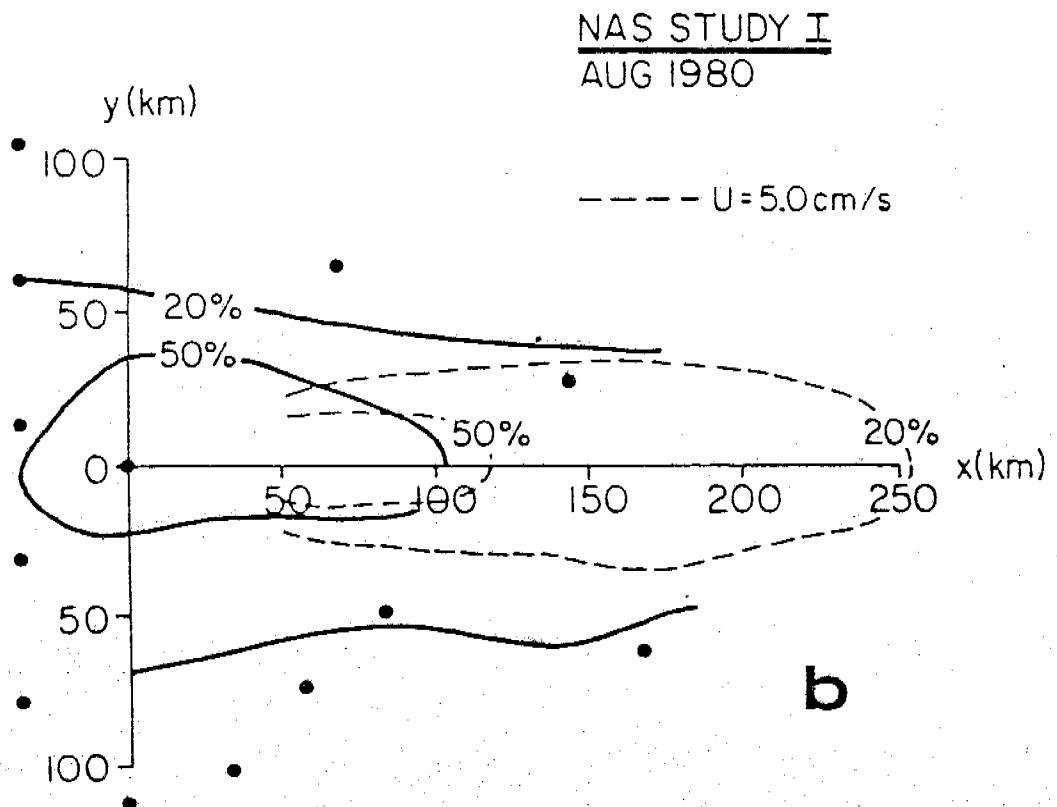
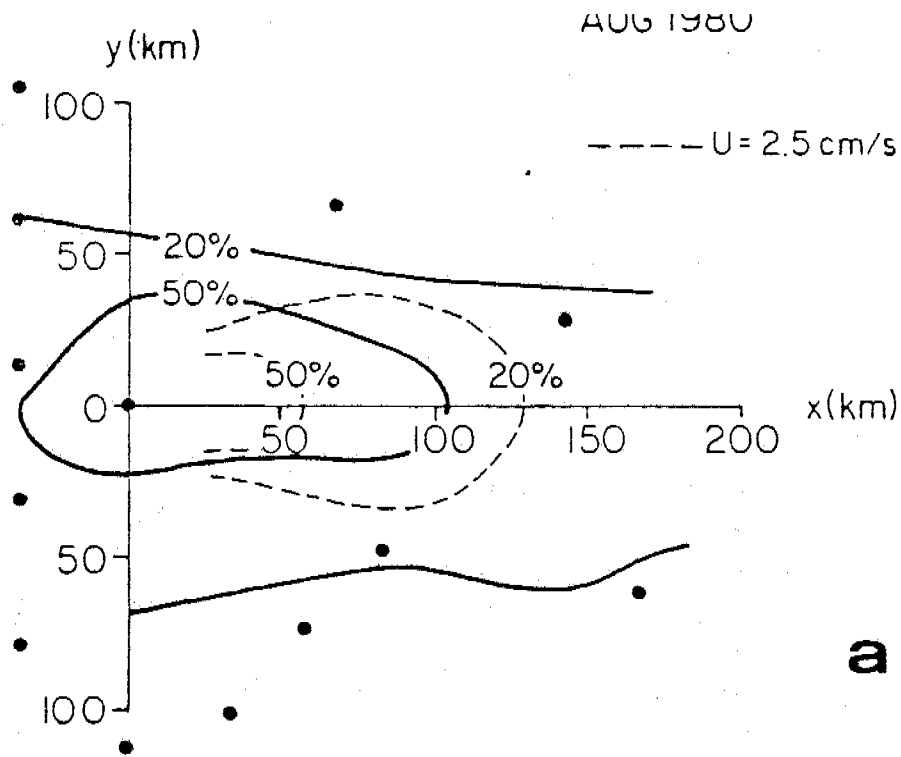


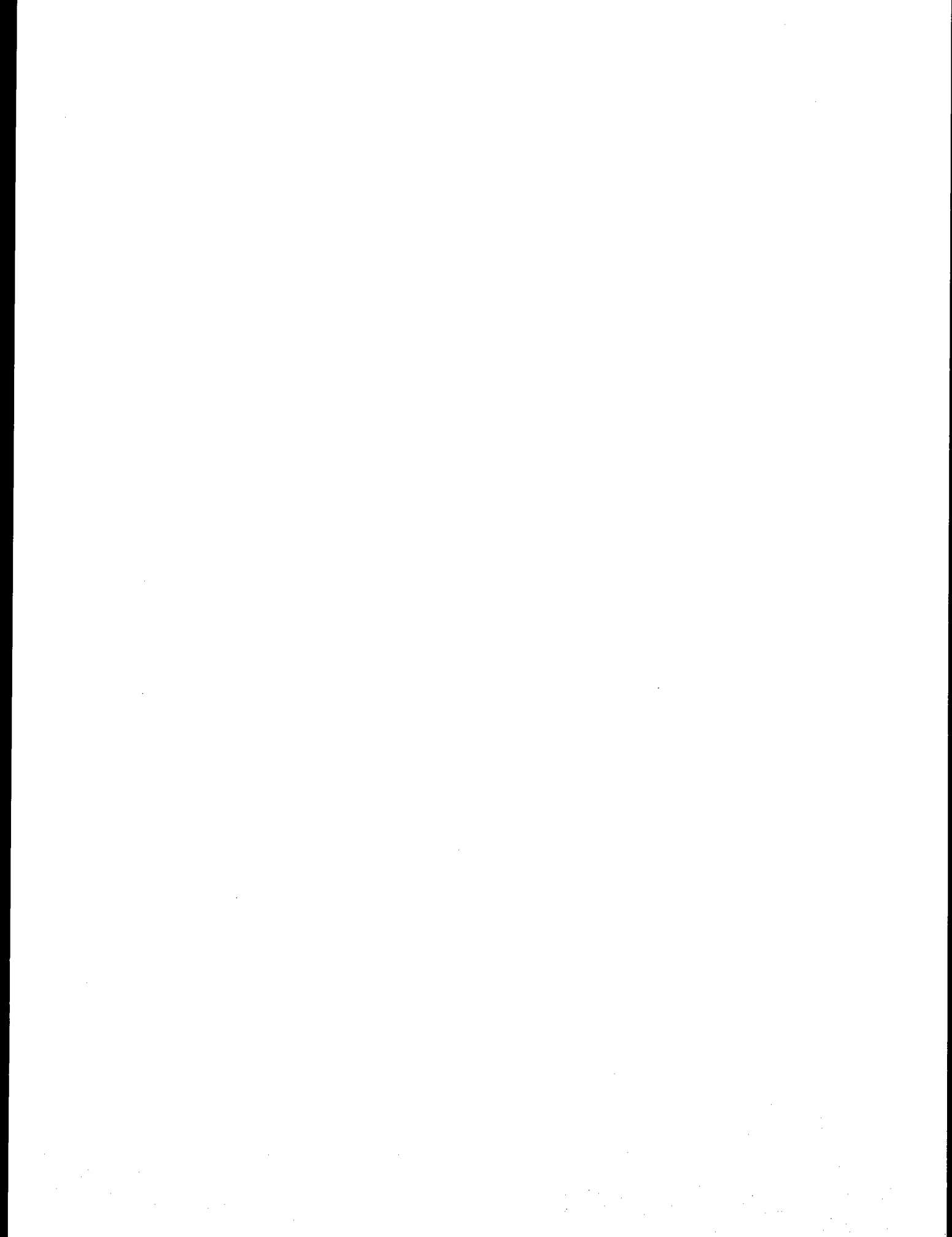
Figure 24. A model fit to the depth integrated methane profile in the lower boundary layer ($\Delta z \approx 30$ m). The two case studies are (a) $\bar{u} = 2.5 \text{ cm s}^{-1}$ and (b) $\bar{u} = 5.0 \text{ cm s}^{-1}$. The length of the source was assumed to be 30 km. The biological oxidation rate constant for the destruction of methane was set equal to $3.0 \times 10^{-8} \text{ s}^{-1}$.

the axis of the basin. There appears to be little on- or off-shelf penetration of methane which suggests that the outer and middle fronts are effective in restricting cross-shelf transport. We suspect that methane is introduced from a localized source, and thus, will mimic dissolved fractions of petroleum introduced in a similar manner.

REFERENCES

- BROECKER W.S., and PENG T.H. (1974) Gas exchange rates between air and sea. *Tellus* 26, 789-802.
- CLINE J.D. (1981) Distribution of dissolved LMW hydrocarbons in Bristol Bay, Alaska: Implication for future gas and oil development. In *The Eastern Bering Sea Shelf: Oceanography and Resources*, (eds D.W. Hood and J.A. Calder) Vol. I, pp 424-444, Dept. Commerce/NOAA/OMPA, 625 pp.
- COACHMAN L.K. and CHARNELL R.L. (1979) On lateral water mass interaction - A case study, Bristol Bay, Alaska. *J. Phys. Oceanogr.* 9, 278-297.
- CSANADY G.T. (1973) Turbulent diffusion in the environment. D. Reidel Publishing, Boston.
- DEPARTMENT OF COMMERCE (1981) Tidal current tables 1981. Pacific coast of North America and Asia. NOAA, *National Ocean Survey*, 260 pp.
- GRIFFITHS R.P. (1981) Microbial processes as related to transport in the North Aleutian Shelf and St. George lease areas. Annual Rept., OCSEAP/OMPA, 56 pp.
- KATZ C.N. (1980) Processes affecting the distribution of low molecular weight aliphatic hydrocarbons in Cook Inlet, Alaska. Master's Thesis, Univ. Washington, 131 pp.
- KINDER T.H. and SCHUMACHER J.D. (1981a) Hydrographic structure over the continental shelf of the southeastern Bering Sea. In *The Eastern Bering Sea Shelf: Oceanography and Resources*, (eds D.W. Hood and J.A. Calder) Vol. I, pp. 31-52, Dept. Commerce/NOAA/OMPA, 625 pp.

- OKUBO A. (1971) Oceanic diffusion diagrams. *Deep-Sea Res.* 18, 789-802.
- OVERLAND J.E. (1981) Marine climatology of the Bering Sea. In *The Eastern Bering Sea Shelf: Oceanography and Resources*, (eds D.W. Hood and J.A. Calder), Vol. I, pp. 15-22, Dept. Commerce/NOAA/OMPA, 625 pp.
- PEARSON C.A., BAKER E. and SCHUMACHER J.D. (1980) Hydrographic, suspended particulate matter, wind and current observation during reestablishment of structural front: Bristol Bay. EOA (Abstract)
- SCHUMACHER J.D., KINDER T.H., PASHINSKI D.H. and CHARNELL R.L. (1979) A Structural front over the continental shelf of the eastern Bering Sea. *J. Phys. Oceanogr.* 9, 79-87.
- SWINNERTON J.W. and LINNENBOM V.J. (1967) Determination of the C₁ to C₄ hydrocarbons in seawater by gas chromatography. *J. Chromatogr. Sci.* 5, 570-3.
- WELANDER P. (1967) Theoretical forms for the vertical exchange coefficients in a stratified fluid with application to lakes and seas. *Acta Geophysica* 1, 1-27.



MODELING OF TIDES AND CIRCULATIONS OF THE BERING SEA
National Oceanic and Atmospheric Administration

J. J. Leendertse and S. K. Liu, Principal Investigators
The Rand Corporation

March 31, 1981

Annual Progress Report

MODELING OF TIDES AND CIRCULATIONS OF THE BERING SEA (RU 435) National Oceanic and Atmospheric Administration

April 1, 1980 - March 31, 1981

J. J. Leendertse and S. K. Liu

During the reporting period our main efforts have been the generation of transfer functions for the oil trajectory analyses using the three-dimensional model of Norton Sound and St. George Basin for both ice-free and ice-cover conditions as well as performing oil trajectory analyses for these two areas. A total of twenty basic 3-D runs, 46 oil-spill simulations and 2,120 oil trajectories have been made. Duration of each oil spill was 30 days. The final results have been transmitted to the U.S. Geological Survey on seven magnetic tapes.

Norton Sound Simulations

Weather in the Norton Sound area has been characterized by three distinctive oceanic periods--from the end of May through the end of August, from the beginning of September through the end of November, and from the beginning of December through May. During the first period the waters of Norton Sound are characterized by a strong vertical density gradient, and the prevalent wind direction is from the southwest, with milder wind speed but greater direction variability than in the other two periods. During the second period, associated with surface cooling, the vertical density structure gradually disappears and predominant wind direction shifts from southwest to east and northeast, with high variability in both wind direction and speed. During the period between the end of November through May the generation and transport of ice presents another distinctive hydrodynamic characteristic in Norton Sound. The vertical column is nearly homogeneous except for certain surface salt input associated with ice generation near the northeast portion of the Sound. The predominant wind direction (north-northeast) during this period is quite persistent, while the average wind speed is the highest in the year.

Other than in the areas near the Yukon Delta and at the head of the Sound where shore-fast ice is found, Norton Sound is covered, to a variable extent, with ice floes. They range in size from a few meters to one or two kilometers. Except for a few occasions when the ice breakout occurs through the Bering Strait, the general direction of ice transport is to the west and southwest. Spatial variability of ice floe movement is substantial, particularly near the Yukon Delta and St. Lawrence Island, where ice-ice interaction between the ice floes and the shore-fast ice is very pronounced. Areas on the lee side of land, namely, the northeast Sound, south of Nome, and south of St. Lawrence Island, which are ice-producing areas, have the least extensive ice coverage.

To illustrate the ice's response to wind and tidal forces, we present certain computational results using the three-dimensional model with the finally adapted stress coefficients for air/ice and ice/water as they have been jointly selected by PMEL and Rand.

Figures 1 and 2 give the bottom topography of Norton Sound and the vertical layout of the model through a cross-section. Figures 3 and 4 show the horizontal ice thickness at the end of February. The initial ice coverage data has been obtained from long-term average conditions as compiled by NOAA and other published works. Area in the eastern and shallow portion of the sound are covered with shorefast ice. The movement of ice under the combined efforts of tidal current and 10-knot wind from NE is shown in Figure 4. Negligible movement occurs in the shorefast ice zone. In the meantime, the water in the surface layer (mean depth = 1.5 meters) beneath the ice (Figure 5) shows the combined effect of tidal forces and wind stress transmitted through the ice.

To study the inertial component of the ice's movement, the wind stress is exerted only during the first 12 hours of the day simulated. When combined with the tidal excursion, the transient movements of ice at selected locations are plotted in Figure 6. Notice the movements of ice in the eastern Sound is influenced by the underlying diurnal tidal excursion while the semi-diurnal tide exerts increasing influence near the southern and western open boundaries of the model.

On the other hand, the wind stress, transmitting through the ice, modifies the movements of underlying water (in addition to the local tidal residual components), making the diurnal displacements of water open-end curves. Since the NE wind stress was exerted only for the first half-day, the net movements of ice due to the wind-tide-combined effects (Figure 7) represents the half-day ice displacements during that period under the 10-knot wind from the NE.

Even though this is only under a simulated condition, it is typical for the predominant winter situation when the long-term average wind is approximately 10 knots from the northeast. Under such conditions the average ice drift is approximately 13-18 km per day (twice the amount shown in Figure 7) with variable drift angles. Under similar wind direction there have been two historical occasions where patterns of ice movements in the Sound were measured by satellite-imagery method. Figure 8 shows the patterns of ice movements from March 14-15, 1974 (Dupre, 1978) with marine wind direction coming from ENE.

The average wind speed during that period observed at Nome was 7.25 knots from NE. The equivalent wind condition over water would be 8.7 knots from ENE. The resulting wind stress is approximately 0.66 dynes per square cm.

For our simulation we used 10-knot wind with an equivalent stress value of 0.875 dynes/cm². The ratio of wind stress between March 14, 1974 and the value used in our simulation is approximately 0.75 to one.

The observed daily movement of ice in Figure 8 ranges from 9.5 to 14 km depending on the location. Considering 13-18 km of ice displacement under 25 percent higher wind stress, our simulation result agrees quite well with the observed data. Difference in drift direction is due to the slight difference in wind direction (NE vs ENE).

Similar conditions are also found on 30-31 March 1976 when the movement of ice was observed by Landsat imagery (Stringer and Hufford, 1980). The daily movements of ice ranges from 7 to 14.5 km while the pressure difference between Barrow and Nome was 0.4 inches (Fig. 9). Wind information during this period is still being analyzed (Stringer, personal communication).

Norton Sound Oil Trajectory Simulation

During the reporting period, a total of 920 oil trajectories have been made from 20 different launch points representing potential platforms, pipelines, and shipping routes. A typical simulation result for the Summer period (June-August) is presented in Figure 10. The weather scenario is represented by the wind vectors on top of the graph, direction relative to the model's orientation and length representing speed with each grid length for 15 knots. The first 9 days is dominated by strong winds from the S-SSW. Consequently, oil spill, if occurred near Pastol Bay, moves toward Golovin Bay. Yet, under the same scenario, oil, if spilled near St. Lawrence Island, would drift initially toward Cape Nome then divert passing Cape Woolley by the strong counter-clockwise net-circulation in the surface waters of Norton Sound. On each of the trajectories, circles denote launch points while dots mark daily displacements. Trajectories under 26 Summer weather scenarios launched from a hypothetical spill location situated in the middle of the lease area is plotted in Figure 11. Similar plots for the Fall (September-November) and ice-covered (December-May) periods are given in Figures 12 and 13.

St. George Basin Oil Trajectory Simulation

During the reporting period, a total of 1,200 oil trajectories have been made from 30 hypothetical spill locations representing platforms, pipelines, and tanker routes in the St. George Basin study area. A typical simulation result for the Summer period is presented in Figure 14. Bigger dots on each trajectory mark the tenth day of movements. In computing these trajectories, net transport through the Unimak pass derived from field data collected by PMEL has been incorporated in the computation. Forty trajectories from a launch point located in the middle of the lease area under Summer, Fall, and Winter weather are plotted in Figures 15, 16, and 17. Even under Winter's predominant NE wind, oil released from this location would travel over water, because, on the average, the 1,000-fathom line delineates the approximate ice's edge.

REFERENCES

1. Dupre, W. R. "Yukon Delta Coastal Processes Study," Annual Reports of Principal Investigators for the Year Ending March 1978. Environmental Assessment of the Alaskan Continental Shelf, Volume IX, Hazards, U.S. NOAA, October 1978, pp. 384-446.
2. Stringer, W. J. and G. Hufford, "On the Relationship Between Ice Motion in Norton Sound and Barometric Pressure Patterns," Prepared for NOAA-OCSEAP by Research Unit 267, October 1980.

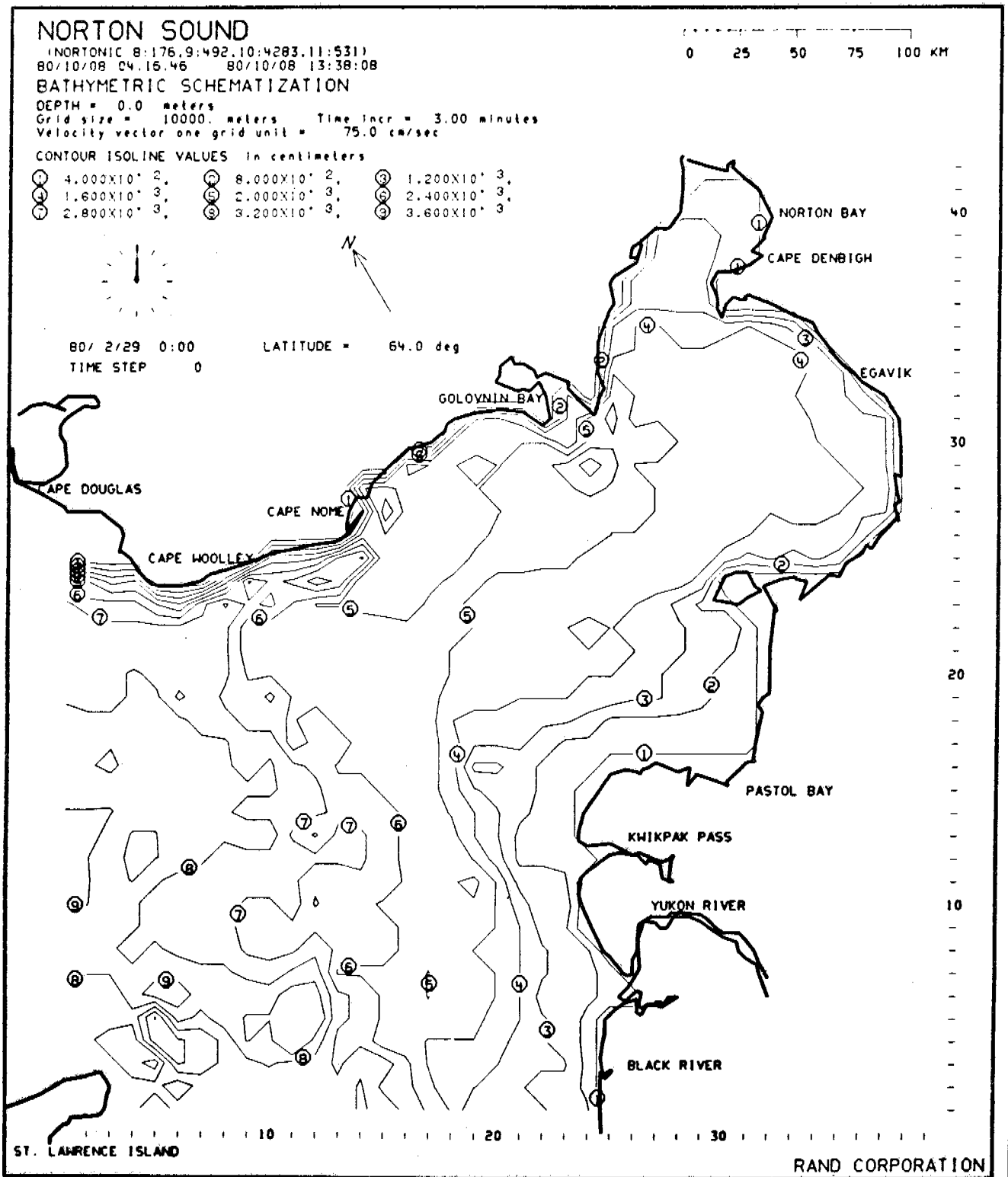


Fig. 1--Bottom topography of the three-dimensional model of Norton Sound.

NORTON SOUND

1NORTONIC 8:176.9:492.10:4283.11:5311
80/10/08 04:16:46 80/10/08 13:38:08

PRO FORMA PROFILE

Time incr = 3.00 minutes
Grid size = 10000. meters X 3.00 meters
Vertical scale distortion factor = 0.10
Velocity vector one grid unit = 50.0 cm/sec



80/ 2/29 0:00
TIME STEP 0

LATITUDE = 64.0 deg

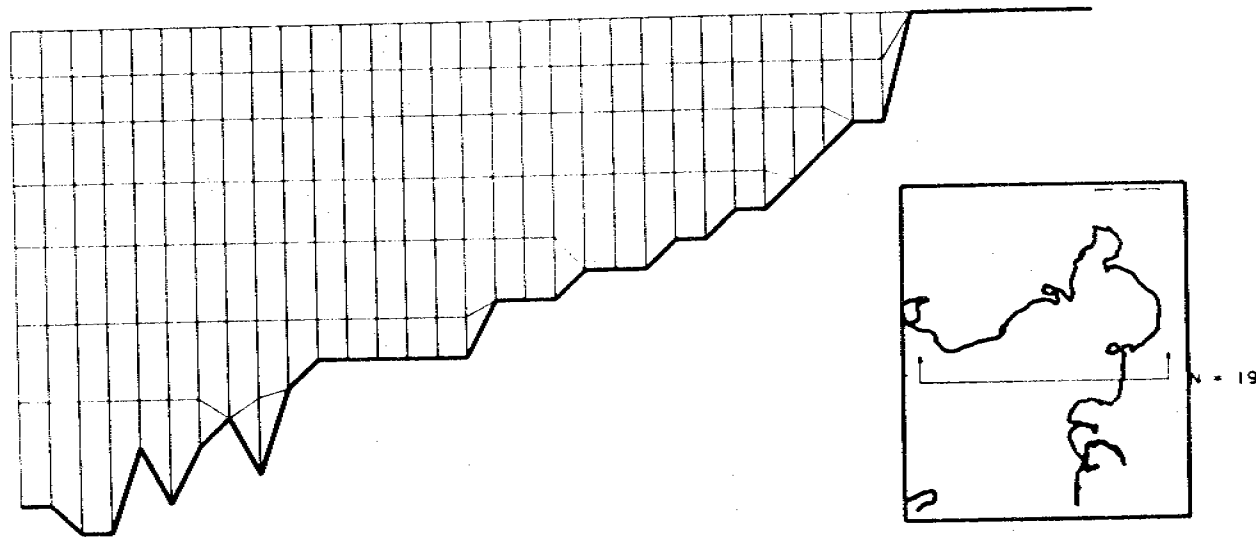


Fig. 2--Bottom profile through a model cross-section.

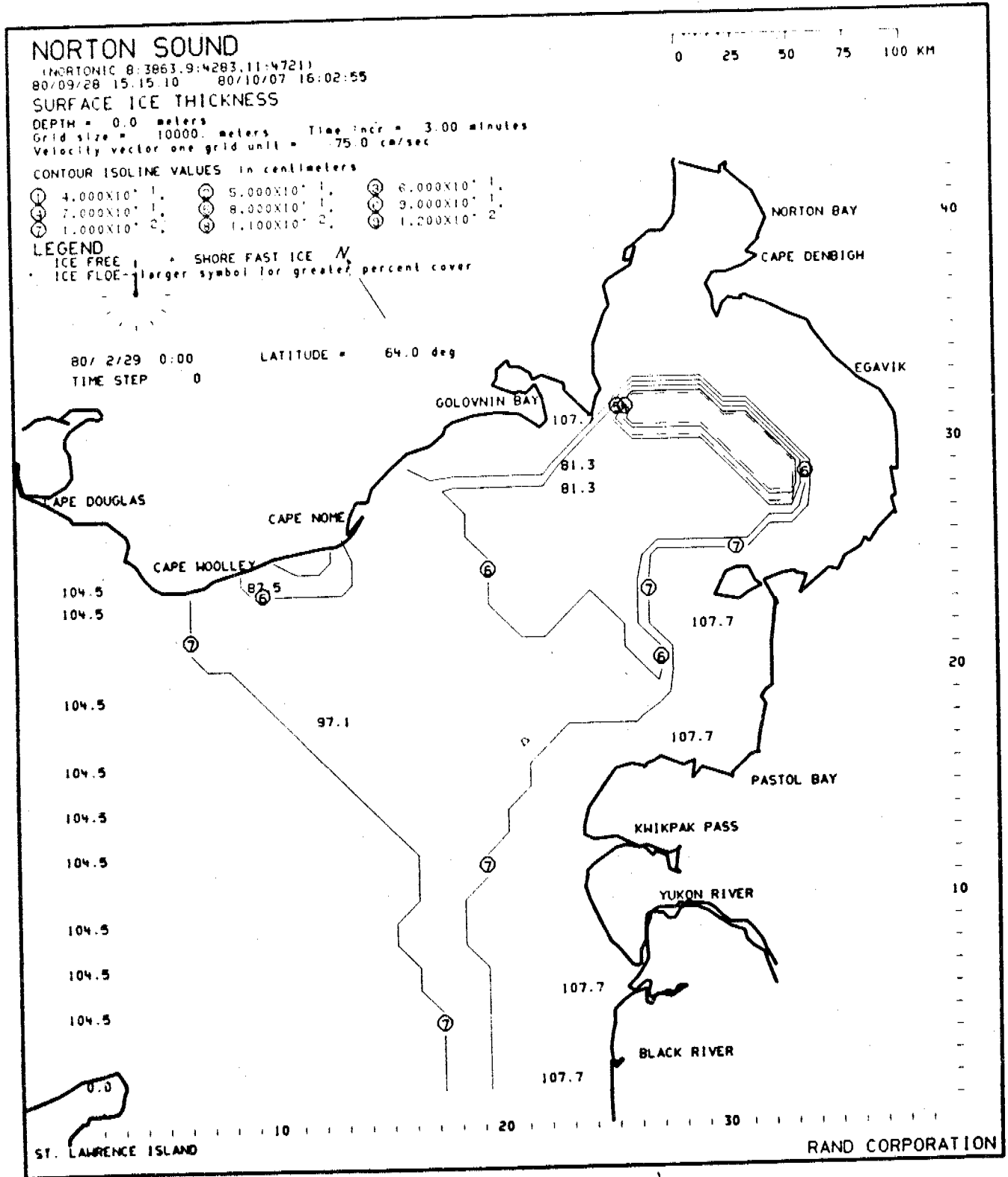


Fig. 3--Initial distribution of ice thickness. Area near the Yukon Delta and at the head of the Sound are covered by shore-fast ice. Areas near Golovin Bay and south of it are ice-producing areas.

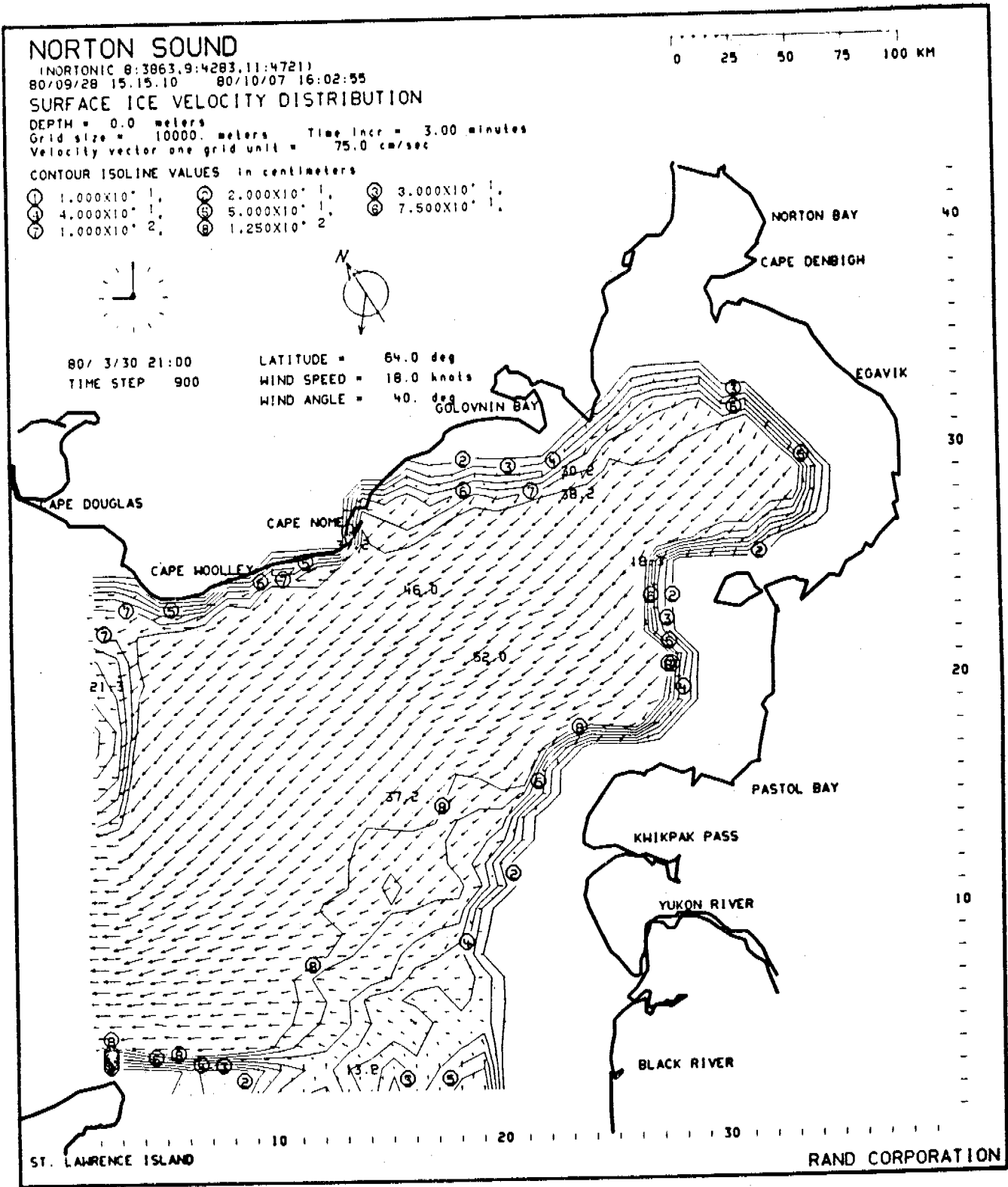


Fig. 4--Ice floe movement under NE wind (10-knots) combined with tidal movement. Displacements immediately neighboring shore-fast ice zones are limited with rotational behavior induced by strong ice-ice interactions.

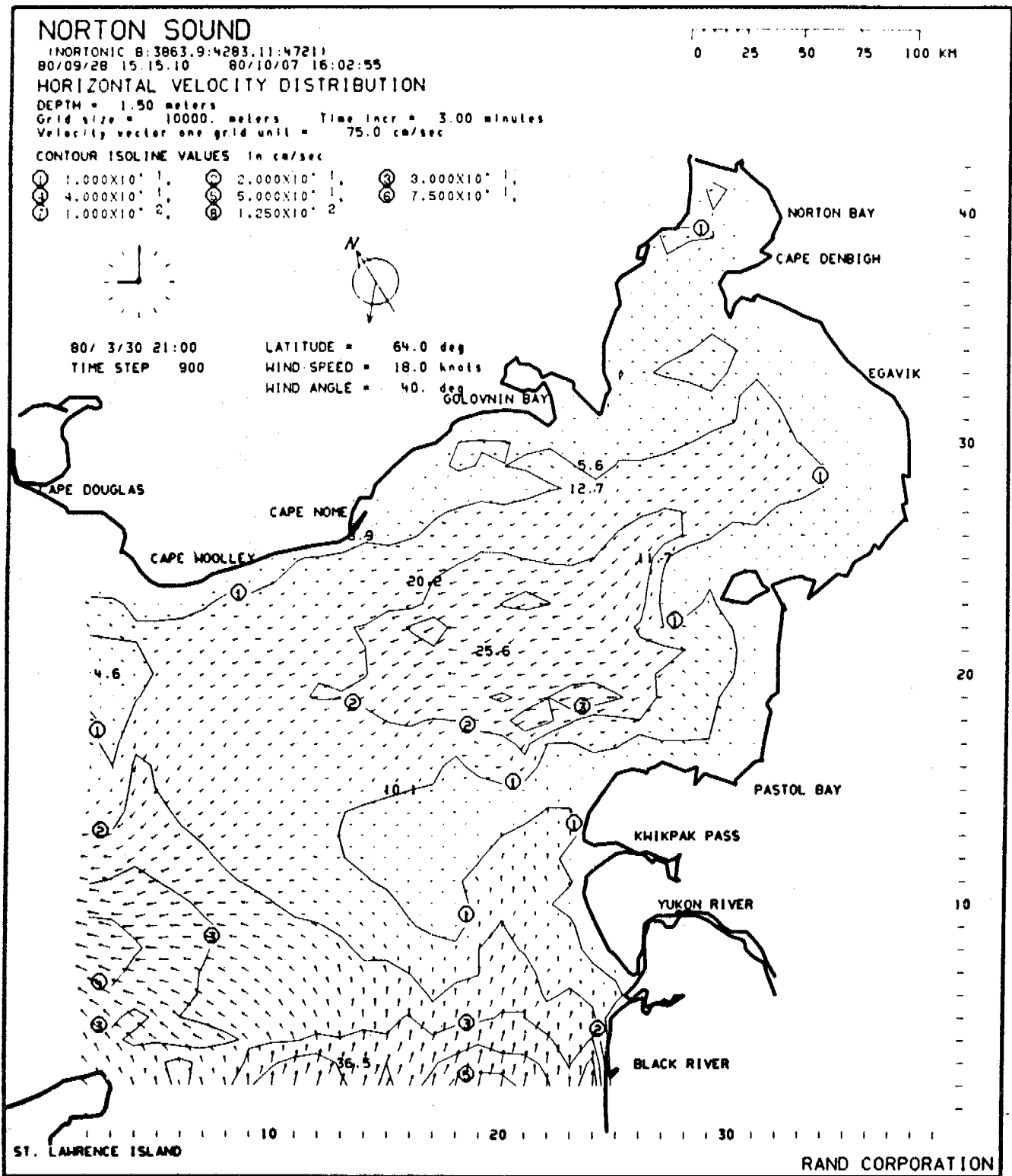


Fig. 5--Water movement beneath the ice. They are driven by tidal forces and wind stresses transmitted through the ice.

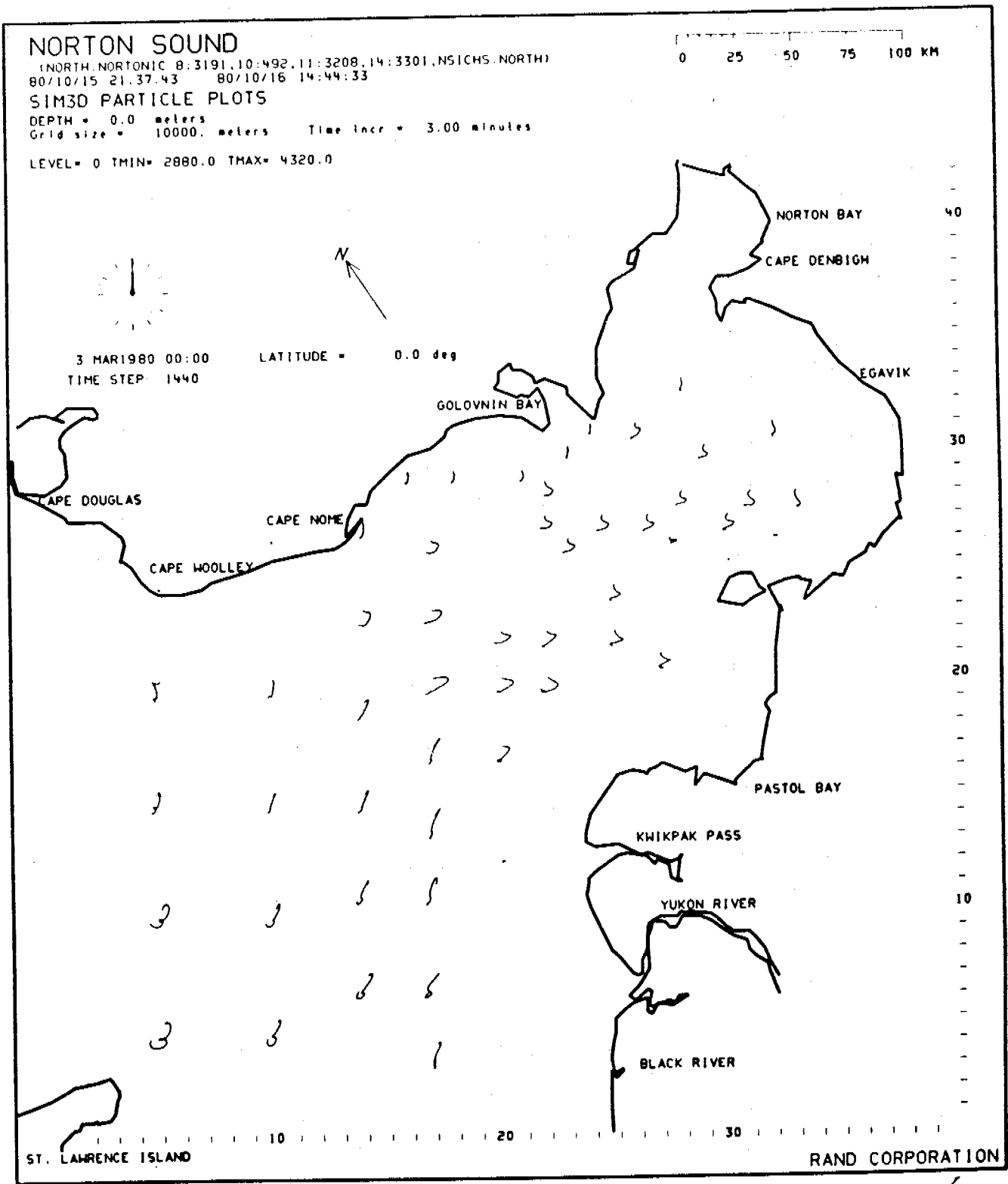


Fig. 6--24-hour ice trajectories driven by tidal excursion and 10-knot wind from NE for the first 12 hours.

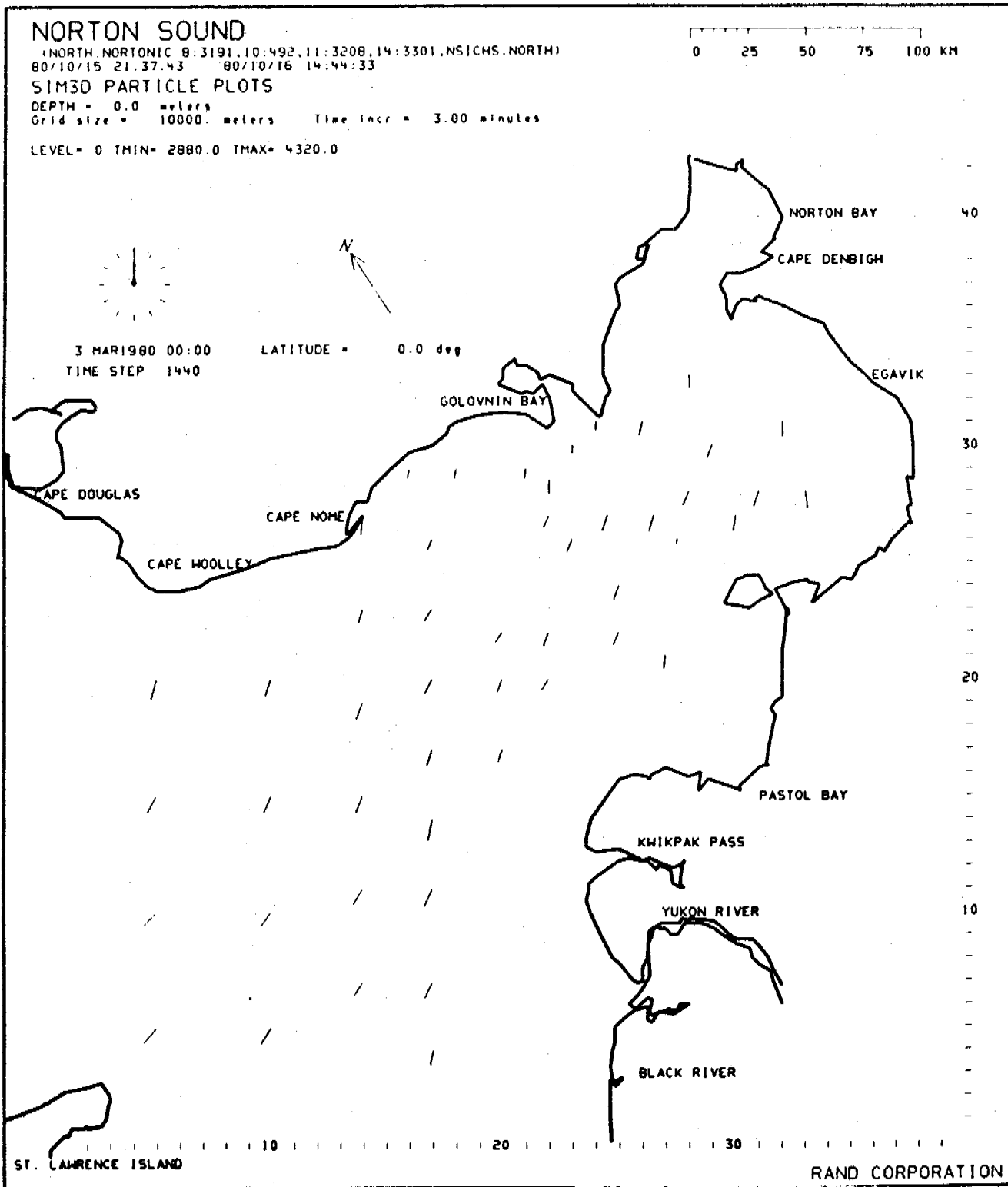


Fig. 7--24-hour net ice displacements induced by tidal-residual current and 10-knot wind from NE for the first 12 hours. Daily displacements under 24-hour wind stress would be approximately twice the amount shown.

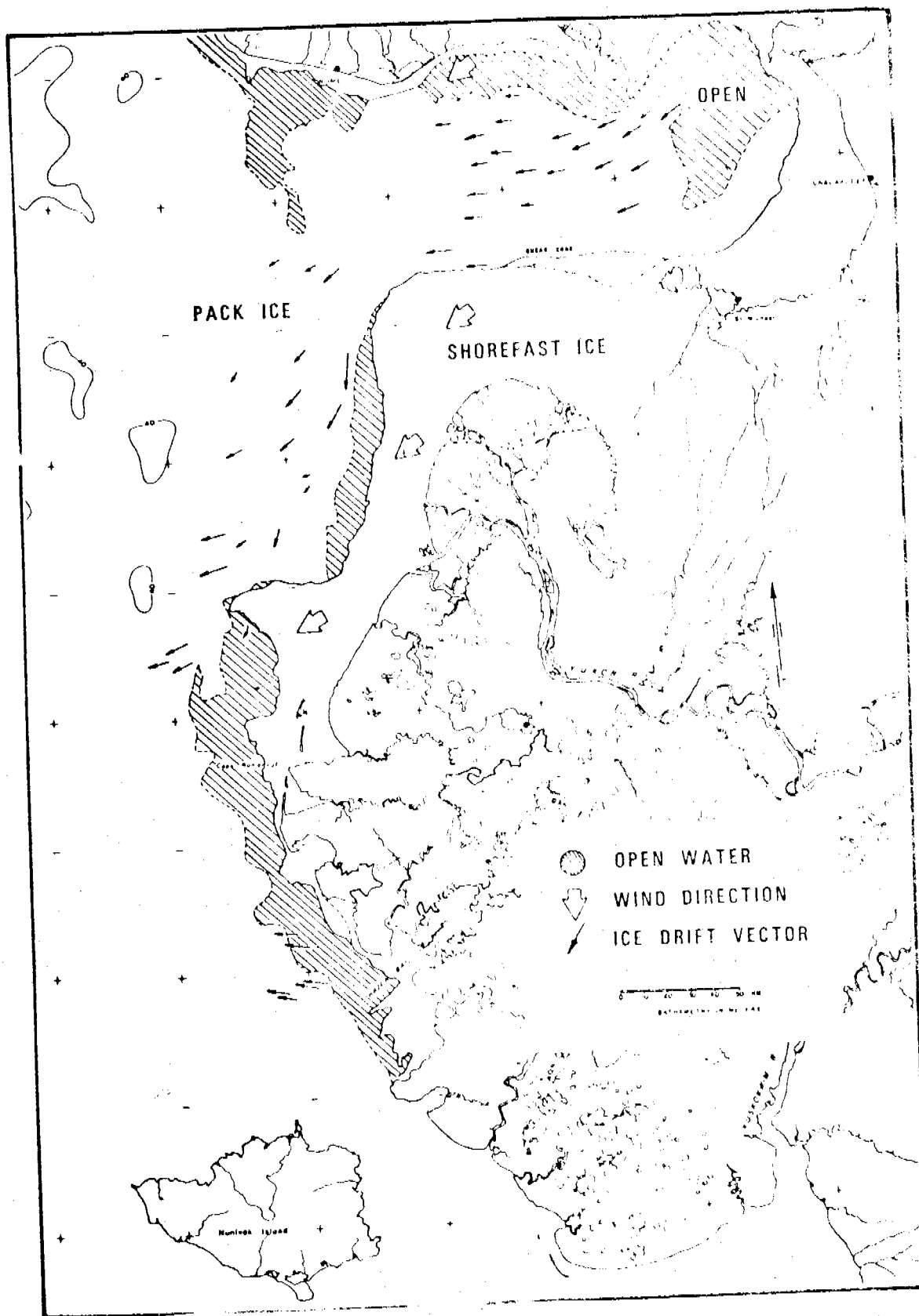


Fig. 8--The pattern of daily ice floe movement of 14-15 March 1974 measured by satellite-imagery method (Dupre, 1978). Wind stress is approximately 75% of those shown in Figure 7. Wind direction was from ENE as opposed to NE for the condition shown in Figure 7.

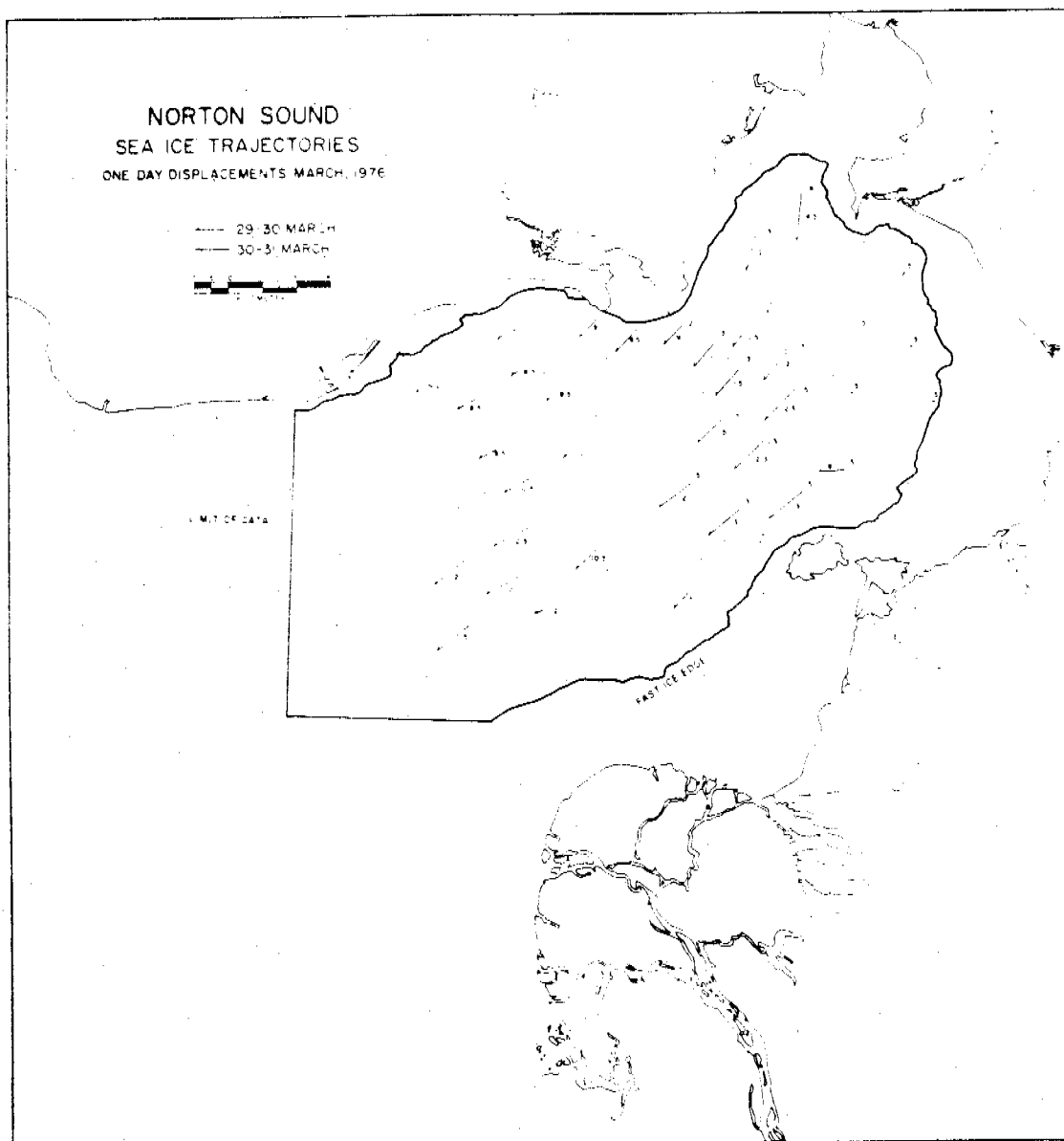


Fig. 9--The pattern of daily ice floe movement of 30-31 March 1976 (Stringer and Hufford, 1980) when the pressure difference between Barrow and Nome was approximately 0.4 inches.

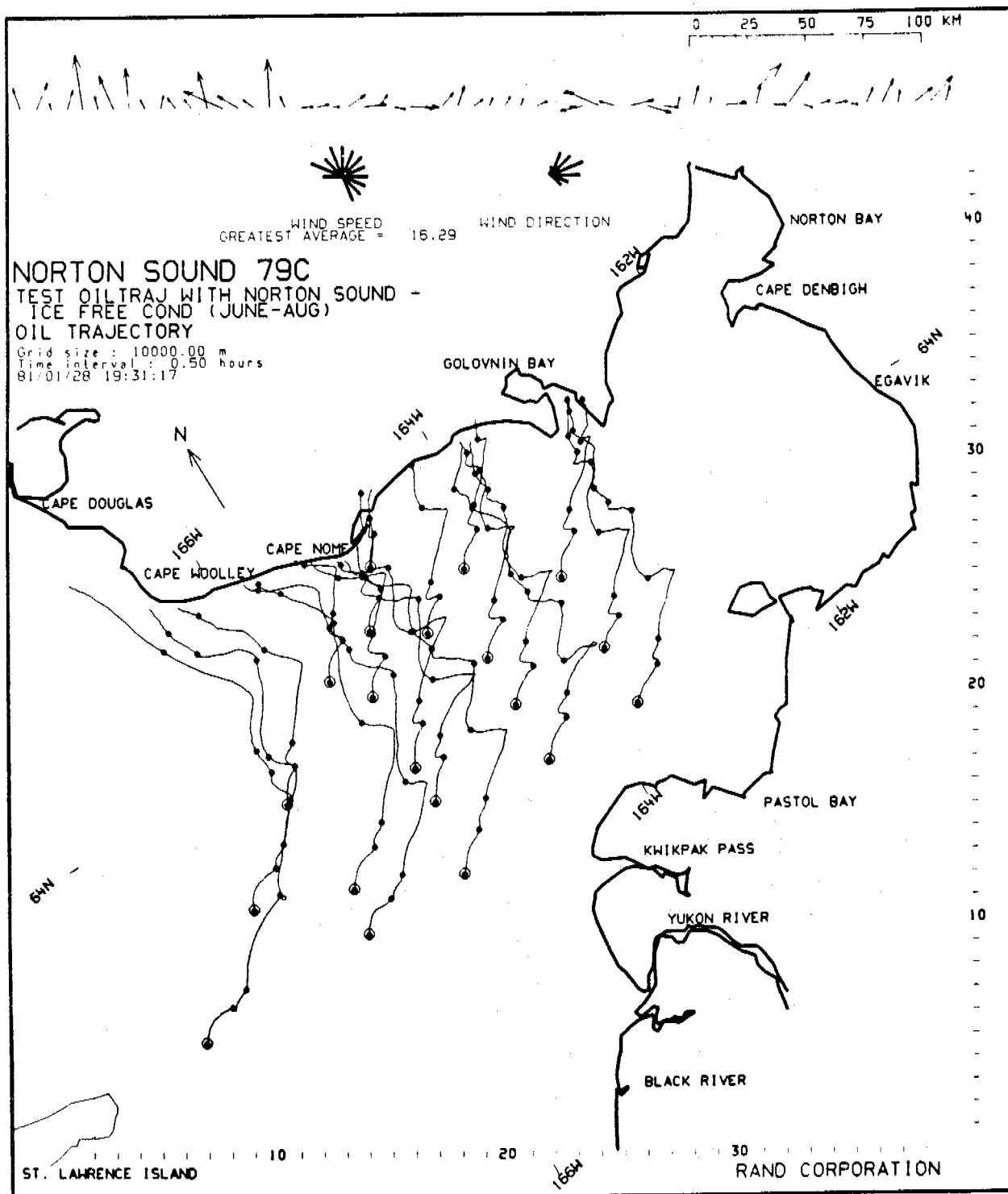
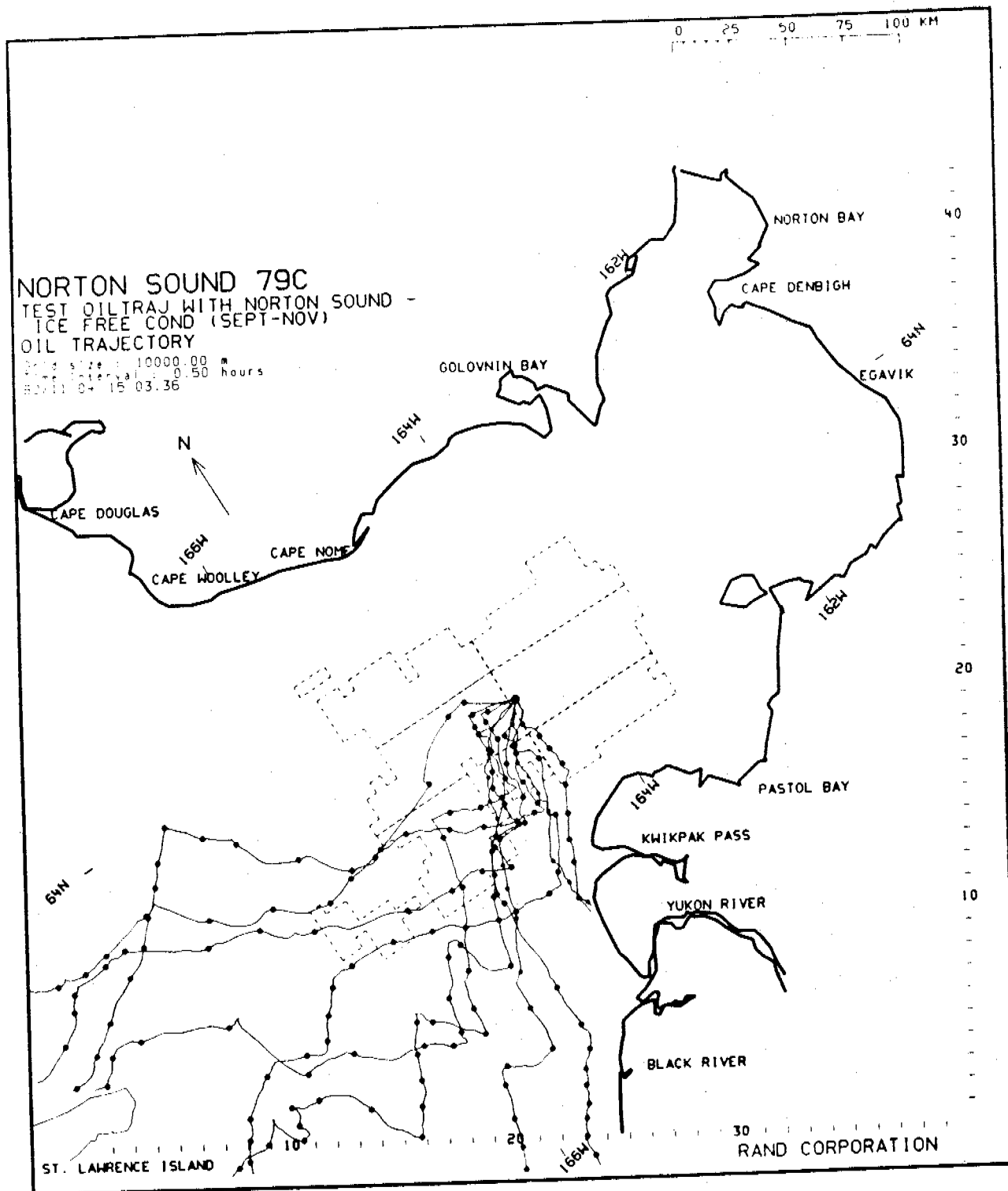


Fig. 10--A typical oil trajectory simulation result for the June-August period in Norton Sound. The weather scenario is represented by wind vectors on top of the graph, direction relative to the model's orientation and length representing speed with each grid length for 15 knots.



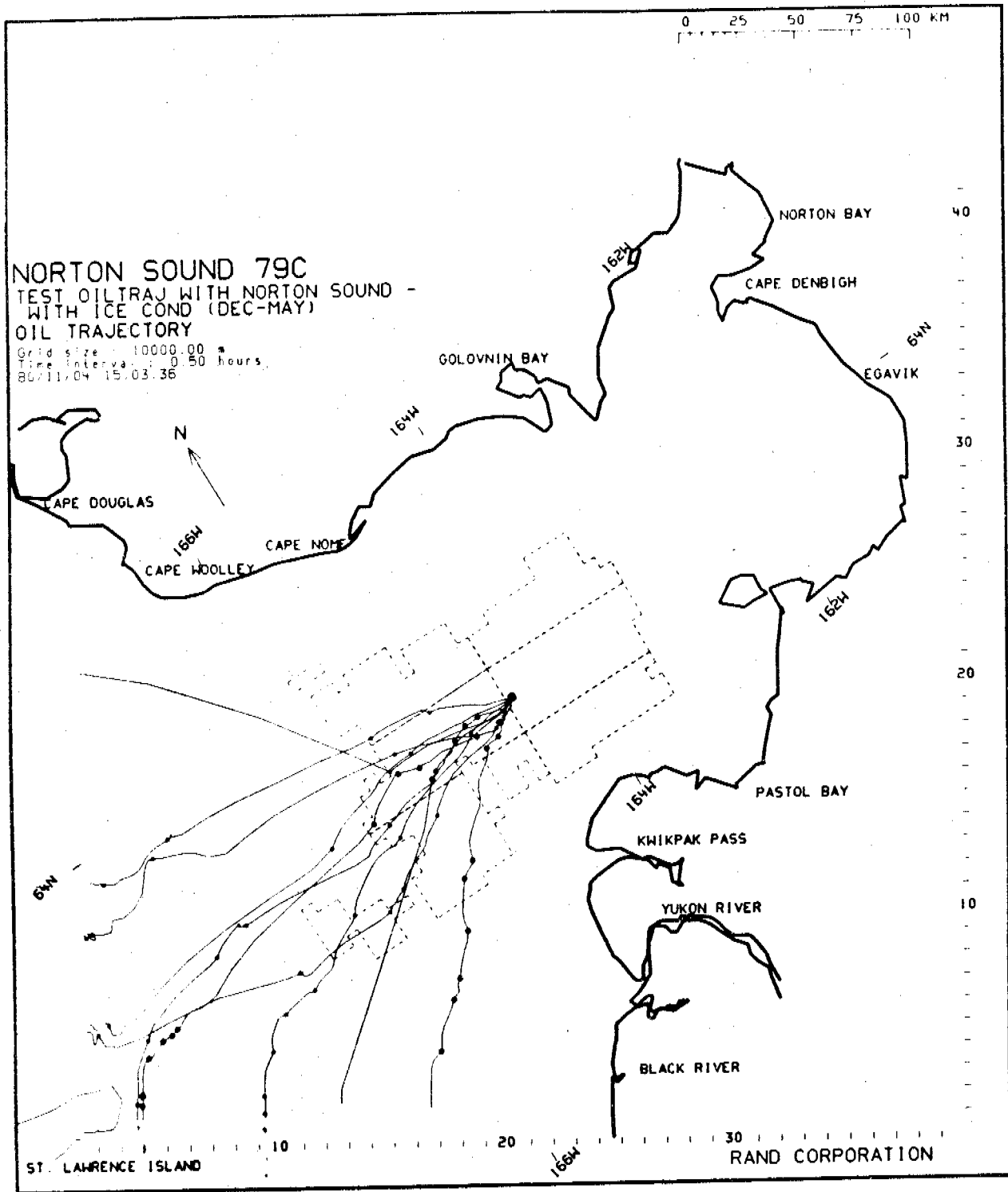


Fig. 13--Trajectories in ice-covered period under 10 weather scenarios launched from a hypothetical spill location situated in the middle of the Norton Sound lease area.

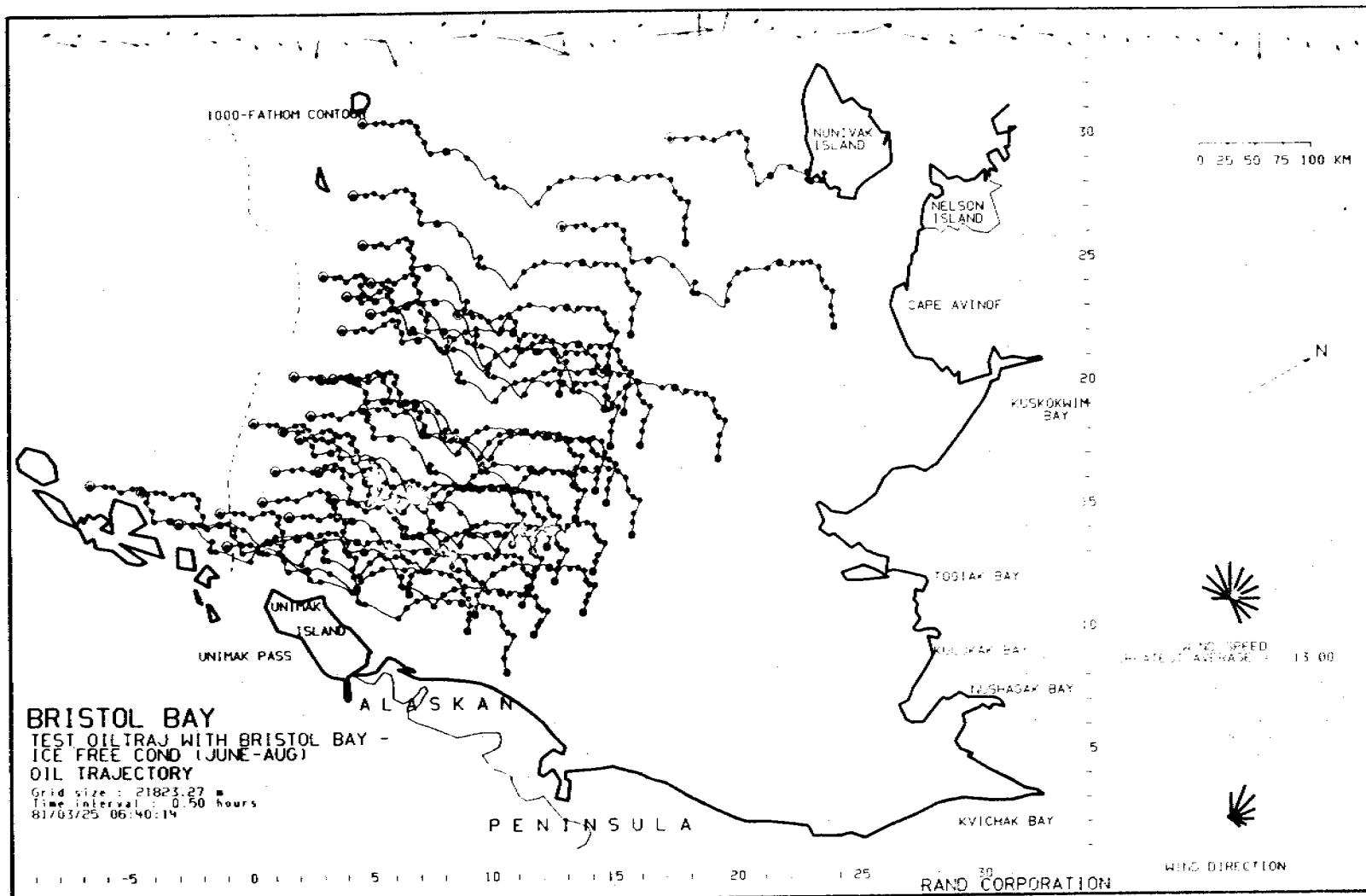


Fig. 14--A typical oil trajectory simulation result for the June-August period in St. George/Bristol Bay area launched from 30 hypothetical spill sites representing platforms, pipelines and tanker routes.

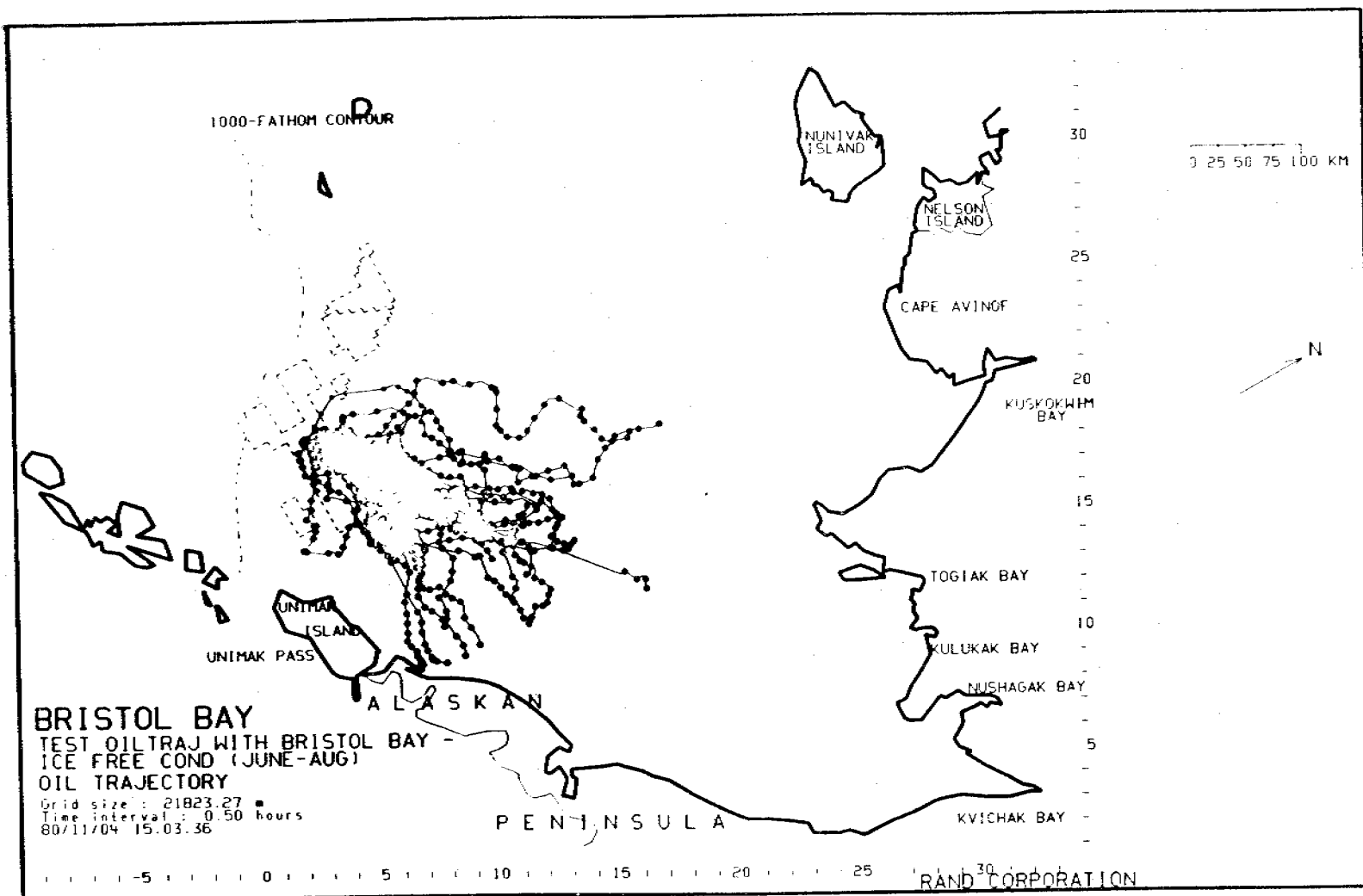


Fig. 15--Trajectories under 20 summer weather scenarios launched from a hypothetical spill location situated in the middle of the St. George lease area.

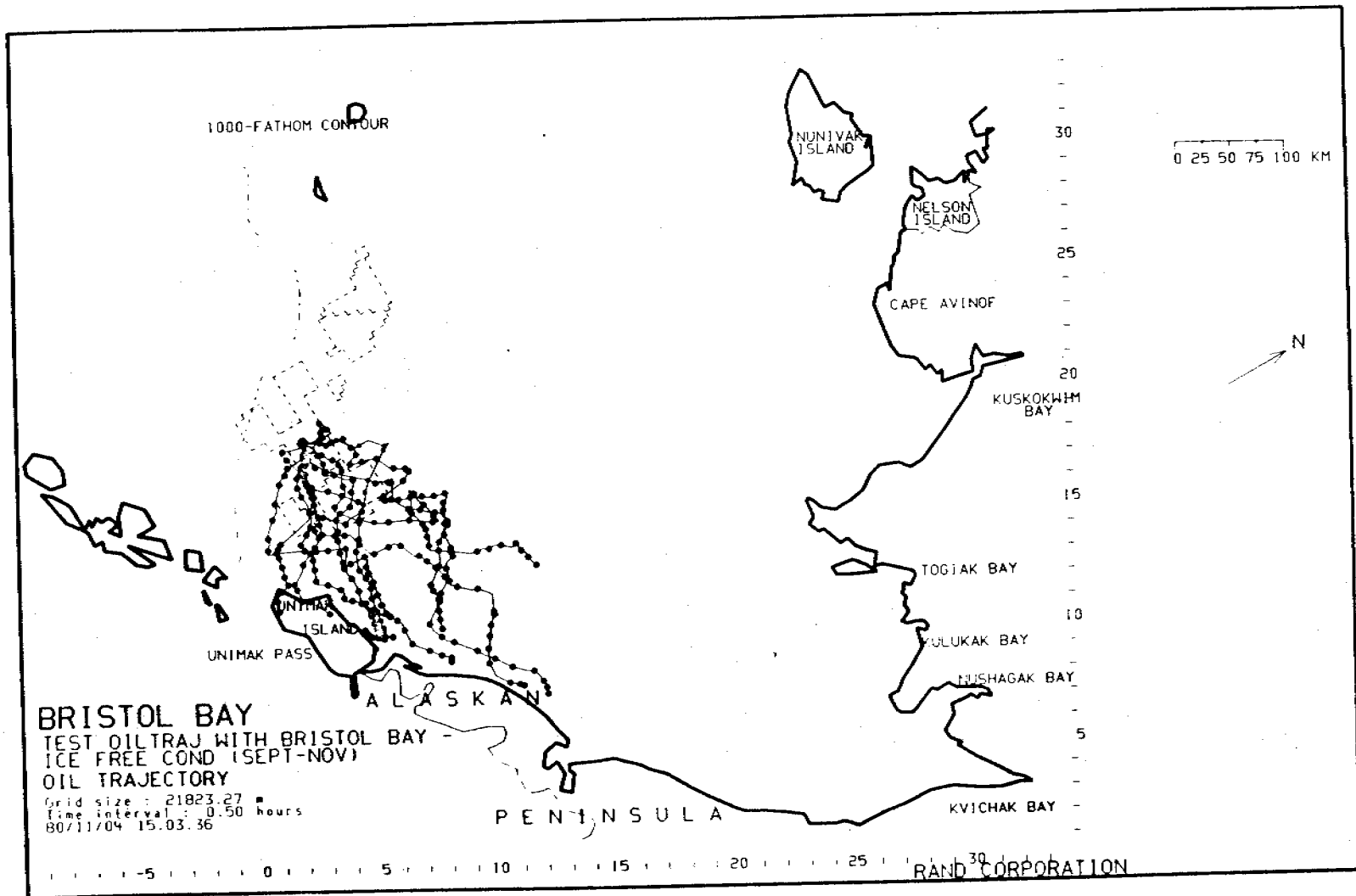


Fig. 16--Trajectories under 10 fall weather scenarios launched from a hypothetical spill site situated in the middle of the St. George Basin lease area.

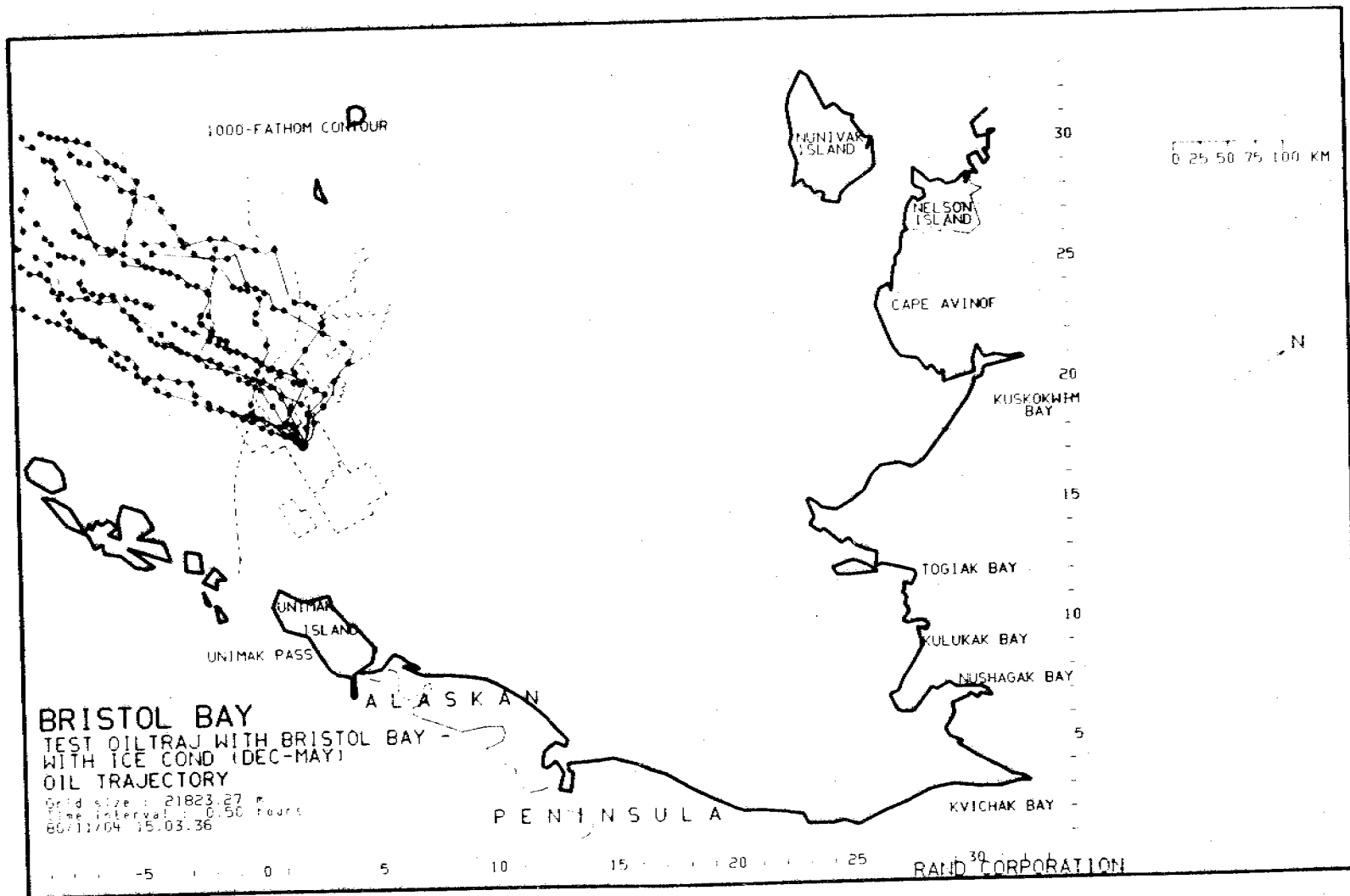


Fig. 17--Trajectories under 10 winter weather scenarios launched from a hypothetical spill site situated near the ice-edge in the middle of the St. George Basin lease area.

ANNUAL REPORT

Contract: 03-5-022-67 Task Order #13
Research Unit: 519
Reporting Period: 1 July 80 - 31 Dec 80
Number of Pages: 17

METEOROLOGY OF THE ALASKAN ARCTIC COAST

Thomas L. Kozo
Research Scientist

Tetra Tech, Inc.
Waterways and Harbors Division
630 North Rosemead Boulevard
Pasadena, California 91107

1 April 1981

CONTENTS

	Page
I. Summary.....	111
II. Introduction.....	111
III. Current State of Knowledge.....	112
IV. Study Area.....	114
V. Sources, Methods and Rationale of Data Collection.....	114
VI. Results.....	114
VII. Discussion.....	115
VIII. Conclusions.....	115
IX. Needs for Further Study.....	116
References.....	117
Figures.....	118- 127

I. Summary of objectives, conclusions, and implications with respect to OCS oil and gas development

The objectives of this summer Harrison Bay area program were fourfold:

A. To measure and analyze surface winds (10 meter elevation) for the purpose of deriving the wind field responsible for nearshore (water depths to 20 meters) surface water movement.

B. To derive the geostrophic wind from surface atmospheric pressure data and compare it to the simultaneously measured surface winds to assess the eventual real time surface wind prediction capabilities of a "permanent" OCS sponsored atmospheric pressure buoy network (on-land).

C. To examine the effects of the summer thermal contrast across the coastline on the resultant surface wind.

D. To establish a "permanent" mesoscale atmospheric pressure network to compute the geostrophic winds along the Beaufort coast.

Results of this study have shown that the surface wind field in the summer is strongly correlated at the measuring stations surrounding Harrison Bay. This mesoscale correlation implies that a minimum of surface wind measurement points could provide a reasonable data set for coastal current trajectory studies.

The comparison of geostrophic wind direction to surface wind direction is close except for days influenced by excessive thermal contrast leading to sea breeze effects.

The sea breeze is a summer mesoscale phenomenon important in determining the resultant surface wind field. This particular summer was unusual due to a persistence of moderate westerly surface winds and minimal sea breeze effects.

The effect of coastal winds on the summer nearshore circulation has relevance to transport of detritus, biota, spilled oil, and small ice floes. The sea breeze promotes bay flushing and upwelling by maintaining persistent NE to E surface winds.

The July 1980 deployment of two "permanent" on-land atmospheric pressure relaying buoys (utilizing the French System ARGOS) has shown the feasibility and utility of a pressure network for coastal studies with eventual real time monitoring capabilities.

II. Introduction

A. General Nature of the Study

This study was designed to measure surface winds and surface atmospheric pressures in the Harrison Bay area. The surface pressures were used to calculate geostrophic winds for comparison to actual measured surface winds. Causes of gross departures from calculations were investigated and those attributed to mesoscale phenomena were to be examined.

Measurements made during the 1980 field season served as input for Mathews (RU 526).

B. Specific Objectives

This study has specific objectives of:

1. Measurement of surface winds and atmospheric pressures in the Harrison Bay area from August through September and onset of bay re-freezing.
2. Derivation of the geostrophic wind from surface atmospheric pressure data (Kozo, 1979) for comparison to simultaneously measured surface wind at Harrison Bay.
3. Assessment of the extent of surface wind direction modification by the summer thermal contrast across the coastline.
4. Establishment of a "permanent" mesoscale atmospheric pressure network for calculation of geostrophic winds along the Beaufort Sea coast.
5. Establishment of a meteorological data base along the Beaufort coast for use by other OCSEAP investigators.

C. Relevance to Problems of Petroleum Development

Winds are the principle driving force for summer surface currents in the nearshore waters of the Alaskan arctic coast. Therefore, any attempt to predict current trajectories must include a prediction of the surface wind field. The summer ice pack edge (usually offshore several 100 km) serves as a source for small ice floes (roughly 30,000 kg) which are driven into the nearshore region by surface wind and resultant currents. The floes will exhibit movement in the nearshore region influenced by the combined effect of the large scale gradient wind and the sea breeze. Sea bed structures off the coast will be susceptible to ice damage when floes move into shallow water with a northerly velocity component. Oil spills that may result from the above accident, ship collisions, or other types of accidents will also be strongly influenced by the wind regime. Clean-up and containment operations will be made more difficult since local coastal winds will be hard to predict and sea breeze influence will diminish with distance seaward from the coast leading to surface current divergence or convergence effects as a function of large scale winds.

III. Current State of Knowledge

The Alaskan arctic coast in contact with the Beaufort Sea has five year-round weather reporting sites but only two are official NWS stations (Class A). These are Pt. Barrow and Barter Island, approximately 540 km apart. Located between Pt. Barrow and Barter Island are two Distant Early Warning (DEW) stations, Lonely and Oliktok, and one airport at Deadhorse routinely reporting supplementary data to the NWS but this information is mainly for post analysis and is not incorporated into twice-daily NWS pressure charts.

Before the offshore implantation of the Arctic Basin Buoy Array (University of Washington) in February 1979 (Kozo, 1980b), the traditional method of approximating the surface wind from the surface pressure field was of limited use since the only real-time surface pressure input data came from the above mentioned two Class A stations. Before the July 1979 implantation of a "permanent" OCS pressure station at Franklin Bluffs (Kozo, 1980a), no in-land pressure data existed near the Beaufort coast until south of the Brooks Range. Kozo (1977) earlier illustrated the increased detail in the pressure field when data from offshore buoys and additional temporary land pressure measuring sites were added to the NWS data set. For the next several years, the Arctic Basin Buoy Array will be maintained to provide offshore pressure data, and the station at Franklin Bluffs will provide an in-land pressure measurement for determination of reliable geostrophic winds along the Beaufort Sea coasts.

Estimation of the surface winds from the calculated geostrophic wind is complicated by the existence of an intermittent sea breeze circulation (Kozo, 1979) during the summer months. The summer sea breeze circulation is generated by a time varying but always positive land-sea temperature gradient (land temperature greater than the water temperature, Moritz, 1977). This results in a tendency to set up an along-shore component of the surface wind at the coast (a wind from $90^{\circ}T \pm 20^{\circ}$). Previous work (Kozo, 1977) from analysis of historical data suggests that the sea breeze occurs approximately 25% of the time in the summer months. The extent of offshore influence is less than 60 km (Hufford, 1979).

Recent developments are:

1. The Polar Science Center has established (February 1979) the Arctic Basin Buoy network (TIROS satellite) of surface pressure stations which marked the beginning of continuous pressure data from the Beaufort Sea at two locations 300 km north of the Alaskan arctic coast. This data is being analyzed to determine the extent and duration of mesoscale influences on the synoptic wind field.

2. Two buoys purchased by OCS were implanted in July 1980 (TIROS satellite-French System ARGOS). They are acting as fixed surface atmospheric pressure stations. One in-land station is located at Franklin Bluffs and the other has been placed on Narwhal Island offshore in the Beaufort Sea. Together with the Class A stations at Pt. Barrow and Barter Island, a system of pressure triangles for geostrophic wind calculation is now possible along the Beaufort coast year-round (see Figure 1). The pressure station combination triangle of Narwhal Island (McClure Islands), Franklin Bluffs and Pt. Barrow has a solution center (geometric center) over Harrison Bay (Figure 1) and was used to calculate geostrophic winds for this report. Other combinations (not shown), such as Pt. Barrow, Barter Island, and Franklin Bluffs triangle, would cover the Simpson Lagoon area while the Narwhal Island, Franklin Bluffs, and Barter Island triangle would serve the Brownlow Pt. area.

IV. Study Area

The study area for this past summer of 1980 can be seen in Figure 1 (within the triangle). It was specifically designed to cover the Harrison Bay area. Pressure stations are designated with a P while the W's indicate the locations of portable weather stations at Cape Halkett, Atigaru Pt. and Tolaktovut Pt. at surrounding Harrison Bay.

V. Sources, Methods and Rationale of Data Collections

The basic data collection period was from 1 August 1980 through 24 September 1980. The purpose was to provide meteorological data for the Harrison Bay area during current meter deployment up to the period of bay refreezing. Additional geostrophic wind data is available on a year-round basis for coastal positions mentioned in Section III.

Meteorology Research, Inc. (MRI) mechanical weather stations recorded surface wind speed, wind direction, and temperature at Cape Halkett, Atigaru Pt., and Tolaktovut Pt. (surrounding Harrison Bay, see Figure 1). A meso-scale surface pressure network was maintained (for August and September only) using Weather Measure and Belfort microbarographs at Lonely, Narwhal, Franklin Bluffs, and Oliktok. These microbarographs were serviced weekly and calibrated with two Negretti and Zambra precision digital barometers. Two "permanent" pressure stations were installed in July 1980 on Narwhal Island and Franklin Bluffs. These were buoys manufactured by Polar Research, Inc. (Santa Barbara, California). They communicate with the TIROS N satellite and data reduction is provided by the French System ARGOS. They were calibrated also with Negretti and Zambra precision digital barometers.

VI. Results

A. 1980 - Pressure Data and MRI Data

The MRI weather stations recorded average direction, wind run (converted to speed), and temperature on a strip chart from 1 August 1980 to 24 September 1980. One hour averages of these variables were selected for three-hourly intervals at 00, 03, 06, 09, 12, 15, 18 and 21 hours GMT. Pressure was also reported at three-hourly intervals (from continuous microbarograph output). The pressures were calibrated using Negretti and Zambra precision barometers as transfer standards and then were reduced to sea level pressure using the hypsometric equation, station altitude and mean air temperature. The pressure and wind data has been submitted to the OCS data bank in card form. Time series plots of surface wind, speed, surface wind direction, and temperature are presented below in Section VII. Pressure data from the implanted OCS buoys relies on system ARGOS output continuously averaging eight pressure values per day.

B. 1980 - Geostrophic Wind Data

The surface pressure data from the OCS buoys has been coupled to surface pressure data from Pt. Barrow and Barter Island to produce three-hourly geostrophic winds from triangular networks. Geostrophic winds for the Harrison Bay area have been compared to surface winds in the months of August and September. These data are presented in Section VII. Geostrophic wind data can now be calculated for the entire year at coastal sites if the need arises.

VII. Discussion

A. 1980 - MRI Data

Wind speeds (Figures 2 and 3), wind directions (Figures 2 and 3), and temperature (Figures 4 and 5) are shown for Tolaktovut Pt., Atigaru Pt., and Cape Halkett in the months of August and September. There is an expected close agreement in wind speed and direction between stations since their total separation is less than 50 km. The temperature from these stations also show close correlation. The data presented in the 1977-1980 annual reports show similar results. This summer was unusual in that there was a large percentage of winds with westerly components. In fact, as Figures 2 and 3 show, these winds persisted for a three-week period. This brought the ice edge so close to shore that ice filled Harrison Bay in August. Dome Petroleum Ltd. of Canada suspended drilling in the Beaufort Sea because of what were described as the worst ice conditions ever in the area (Oil & Gas Journal, 1980).

B. 1980 - Geostrophic Wind Data

Use of data from two OCS buoys (on-land) with concomitant NWS station data (Pt. Barrow) has allowed the calculation of three-hourly geostrophic wind through a two-dimensional least squares numerical fit technique (Krumbein, 1959). This pressure triangle can be seen in Figure 1 with its solution center in close proximity to Tolaktovut Pt.

Geostrophic winds calculated for the solution center are compared with actual measured surface winds (at Tolaktovut Pt.) for August and September 1980 in Figures 6 and 7, respectively. The correlation is extremely close for direction while speed of surface winds should be less than that of the simultaneously calculated geostrophic winds. Figures 8 and 9 are bivariate distribution tables of simultaneously occurring geostrophic wind directions and surface wind directions for August and September, respectively. Surface wind directions will be typically 20° less than the geostrophic wind direction due to frictional turning within the boundary layer. Therefore, most samples will be between the two diagonal lines. Shifts of 60° (resulting in northerly components of the wind) or greater are generally due to the mesoscale pressure gradient induced by the thermal contrast at the coast and sea breeze effects. The evidence here indicates the possible use of the pressure array as a prediction tool if a correction for the thermal contrast can be applied. Figures 10 and 11 are histograms of surface wind directions and geostrophic wind directions for the months of August and September 1980, respectively. The vertical axis is number of samples and the horizontal axis is in degrees from which the wind is blowing with each + column representing a 15° increment from 0 to 360. In both figures, the effect of thermal forcing on the surface wind can be seen by the increase in NE to E winds over the geostrophic directions (see Kozo, 1979).

VIII. Conclusions

This summer of 1980 was unusual in the severity of ice conditions due to an increase in the amount of westerly winds and the persistence of these wind directions for three weeks. There was a minimum of sea breeze activity

due to increased cloud cover in coastal areas and west wind velocities of a larger magnitude than typical years. This limited sea breeze activity led to a better correlation between calculated geostrophic winds and surface winds than would be expected in most years.

The utility of the mesoscale pressure network sponsored by O.C.S. can readily be seen and winter use during times of low coastal thermal contrast away from Mountain Barrier Effects (Kozo, 1980b) for Harrison Bay could be easily implemented.

IX. Needs for Further Study

The model developed by Kozo (1980) to predict surface wind from geostrophic winds including the thermal contrast at the coast should be further developed to predict surface current flow. In addition, an empirical function fit of surface currents in Harrison Bay to calculated geostrophic winds should be derived.

Studies in the winter months can now be carried out along the Beaufort coast since geostrophic winds can be calculated using combinations of pressure sites at Pt. Barrow, Barter Island, Narwhal Island, and Franklin Bluffs.

REFERENCES

- Brower, W.A., H.F. Diaz, A.S. Prechtel, H.W. Searby and J.L. Wise, 1977. Climatic Atlas of the Outer Continental Shelf Waters and Coastal Regions of Alaska, NOAA, NCC, EDS, Asheville, North Carolina, 409 pp.
- Hufford, G.L., 1979. Personal communication, OCS Office, Anchorage, Alaska.
- Kozo, T.L., 1977. Coastal meteorology of the Alaskan Arctic Coast. P.I., F. Carsey; OCS Contract 03-5-022-67, T.O. 11.
- Kozo, T.L., 1979. "Evidence for Sea Breezes on the Alaskan Beaufort Sea Coast", Geophysical Research Letters, Vol. 6, 849-852.
- Kozo, T.L., 1980a. Meteorology of the Alaskan Arctic Coast. P.I., T. Kozo, OCS Contract 03-5-022-67, T.O. 13.
- Kozo, T.L., 1980b. "Mountain Barrier Baroclinity Effects on Surface Winds Along the Alaskan Arctic Coast", Geophysical Research Letters, Vol. 7, 377-380.
- Krumbein, W.C., 1959. Trend surface analysis of contour-type maps with irregular control point spacing. J. Geophys. Res., 64, 823-834.
- Moritz, R.E., 1977. On a possible sea breeze circulation near Barrow, Arctic Alp. Res., 9, 427-431.
- Oil and Gas Journal, 1980. International Briefs, Penn Well Publishing Co., Tulsa, Oklahoma, Oct., p. 54.

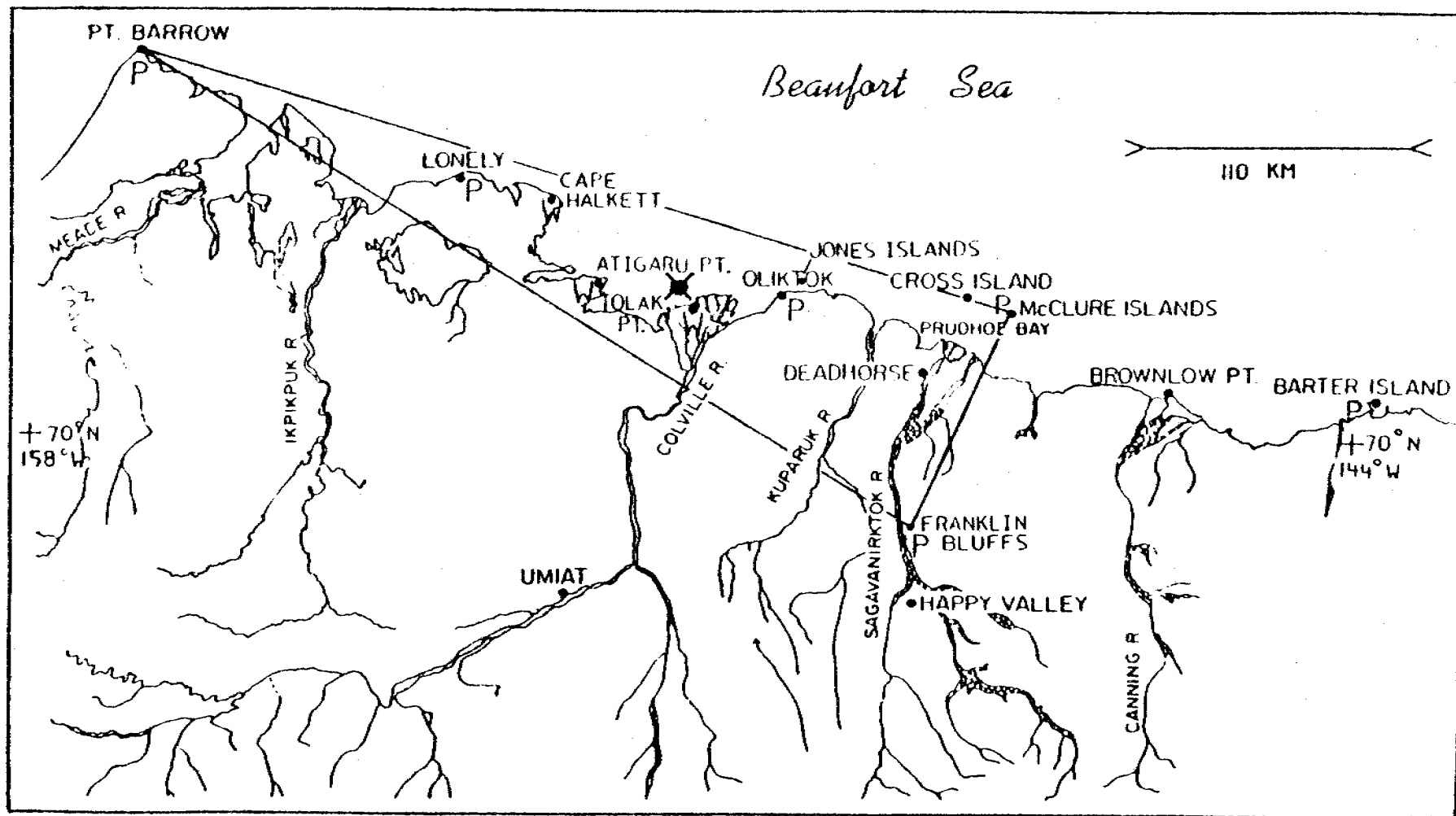
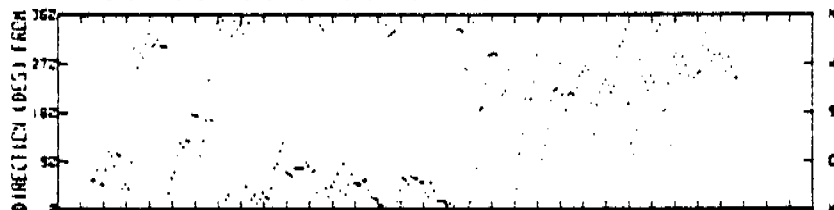
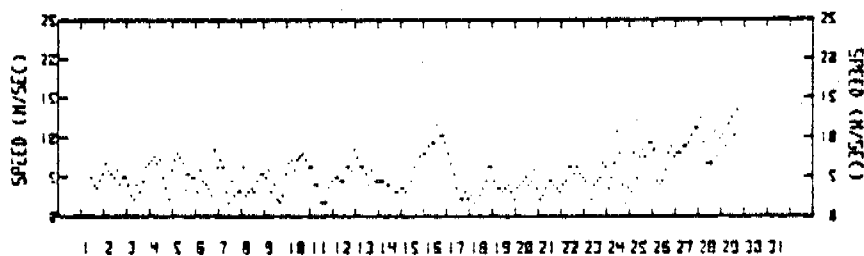


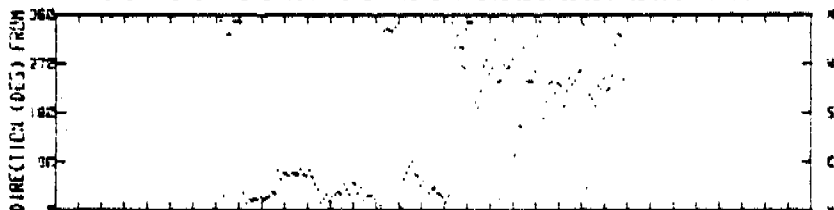
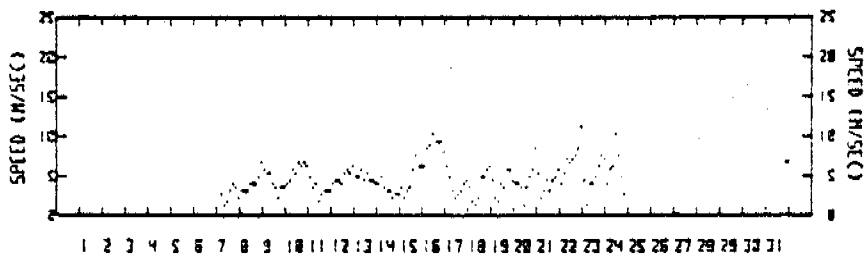
Fig. 1: Positions of the pressure stations (P) and portable weather stations (W) for August and September 1980. The Pt. Barrow-McClure Islands-Franklin Bluffs triangle has a geostrophic wind solution center (●) in Harrison Bay, just northwest of Tolaktovut Pt.

WIND SPEED & DIRECTION
AT: TOLAKTOVUT

AUGUST 1980



AT: CAPE HALKETT



AT: ATIGARU POINT

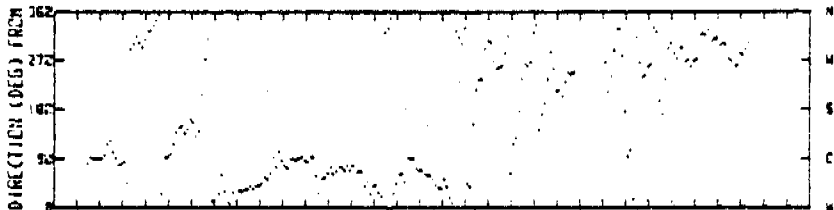
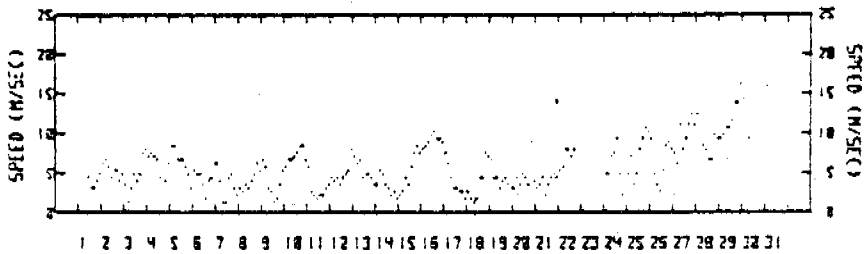
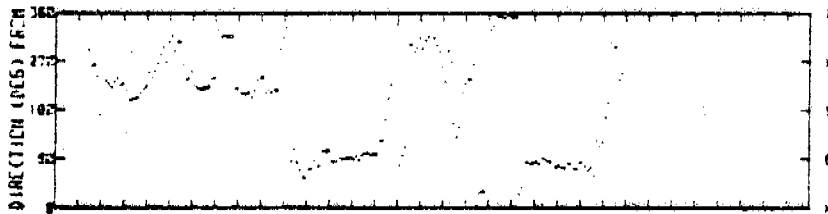
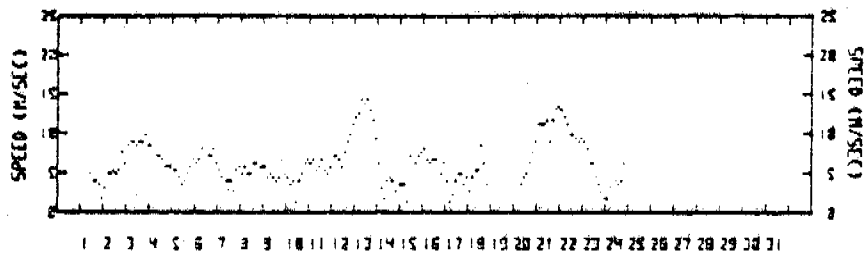


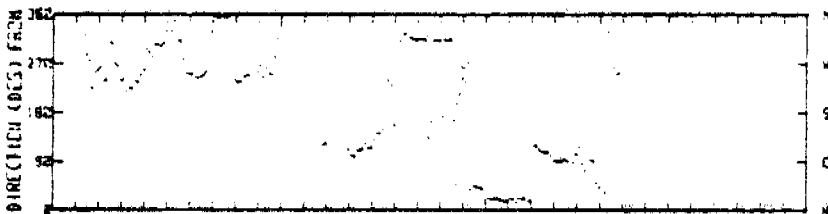
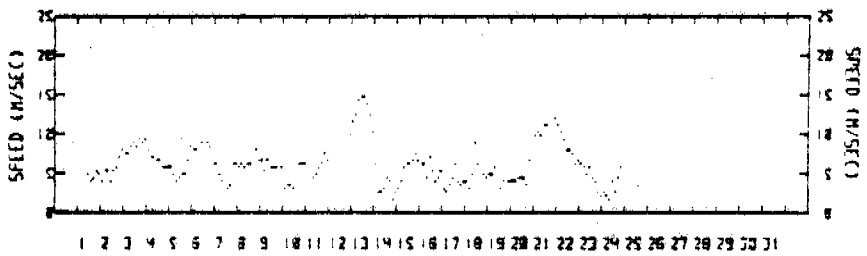
Fig. 2: Time series of surface wind speed and direction for Tolaktovut Pt., Cape Halkett, and Atigaru Pt. in August 1980

WIND SPEED & DIRECTION
AT: TOLAKTOVUT

SEPTEMBER 1980



AT: CAPE HALKETT



AT: ATIGARU POINT

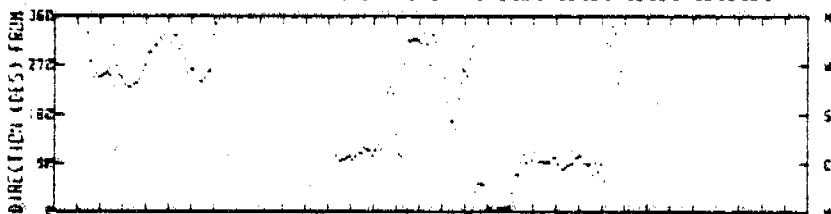
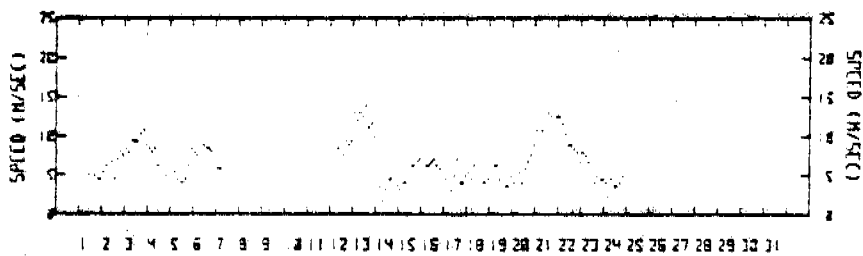
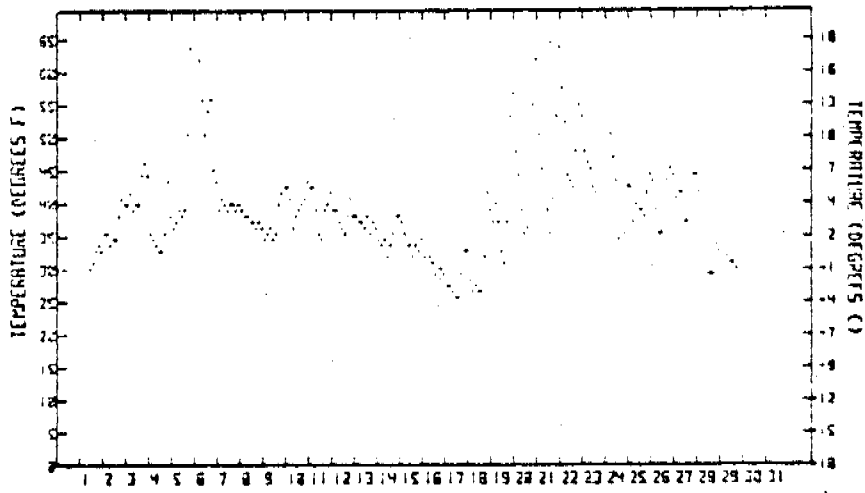


Fig. 3: Time series of surface wind speed and direction for Tolaktovut Pt., Cape Halkett, and Atigaru Pt. in September 1980 (note: no surface data collected after September 24, 1980)

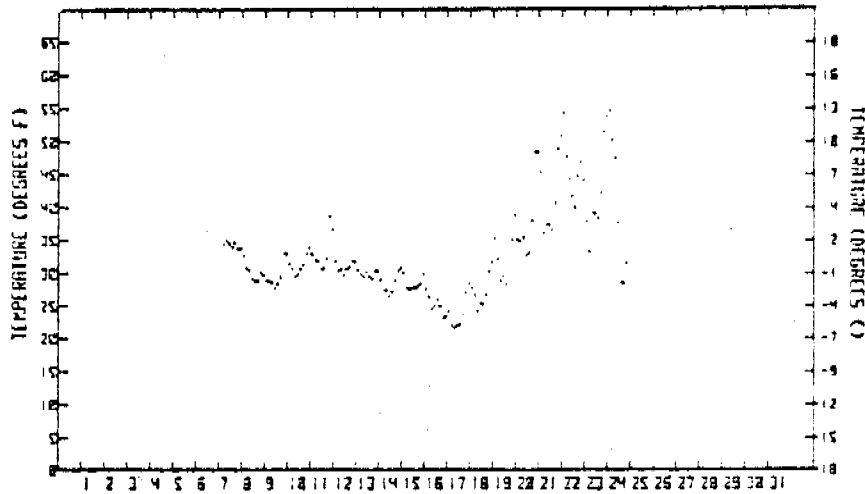
TOLAKTOVUT

AUGUST 1988



CAPE HALKETT

AUGUST 1988



ATIGARU POINT

AUGUST 1988

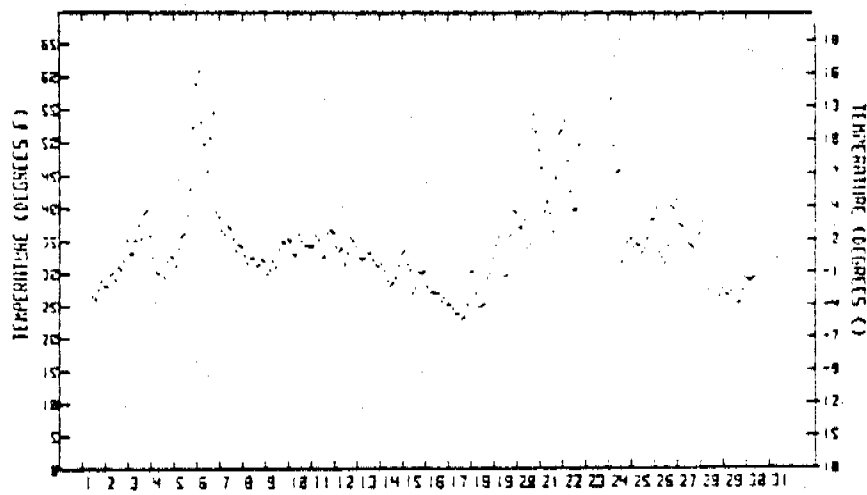
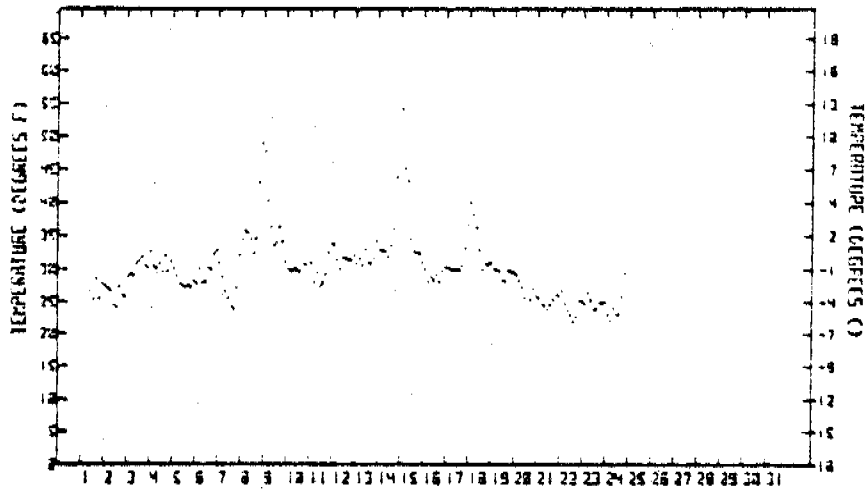


Fig. 4: Time series of surface temperature for Tolaktovut Pt., Cape Halkett, and Atigaru Pt. in August 1980

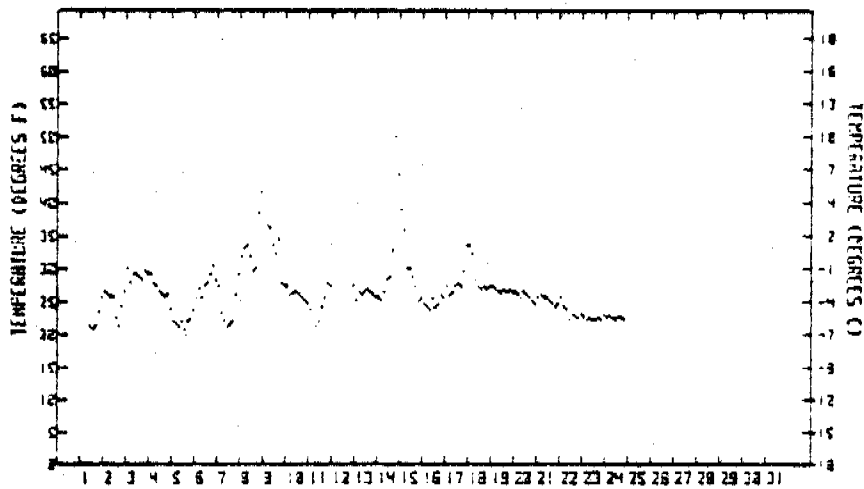
TOLAKTOVUT

SEPTEMBER 1980



CAPE HALKETT

SEPTEMBER 1980



ATIGARU POINT

SEPTEMBER 1980

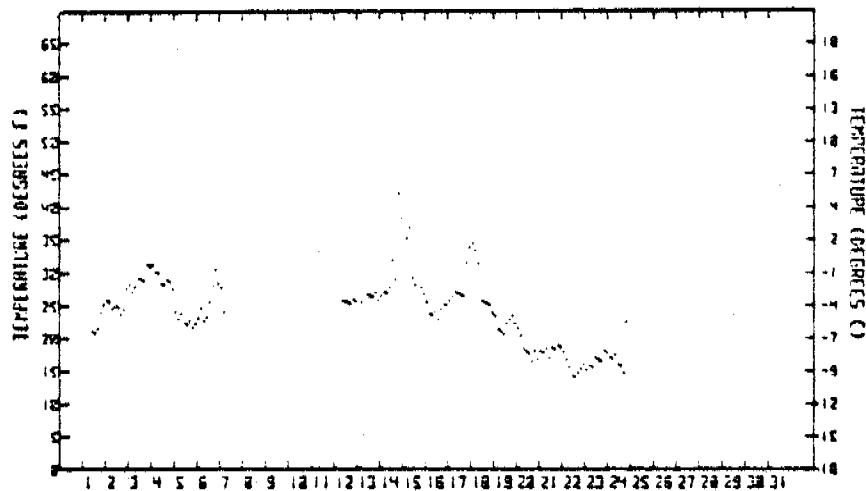
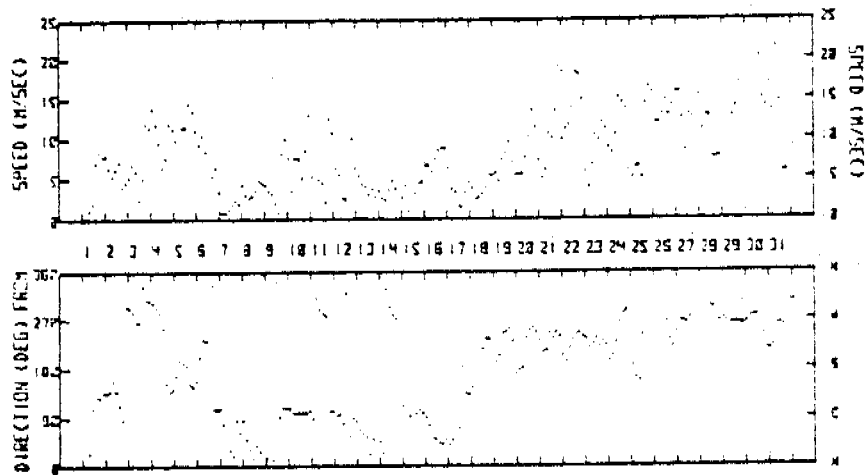


Fig. 5: Time series of surface temperature for Tolaktovut Pt., Cape Halkett, and Atigaru Pt. in September 1980

GEOSTROPHIC WIND SPEED & DIRECTION
AUGUST 1980



WIND SPEED & DIRECTION
AT: TOLAKTOVUT

AUGUST 1980

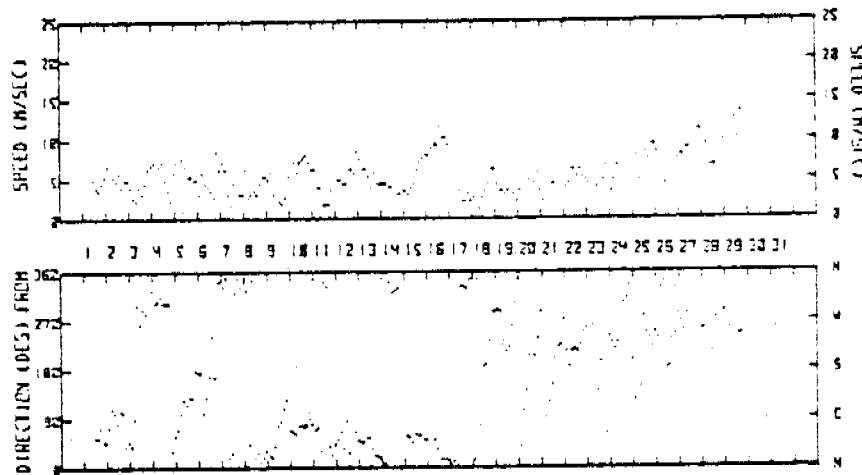
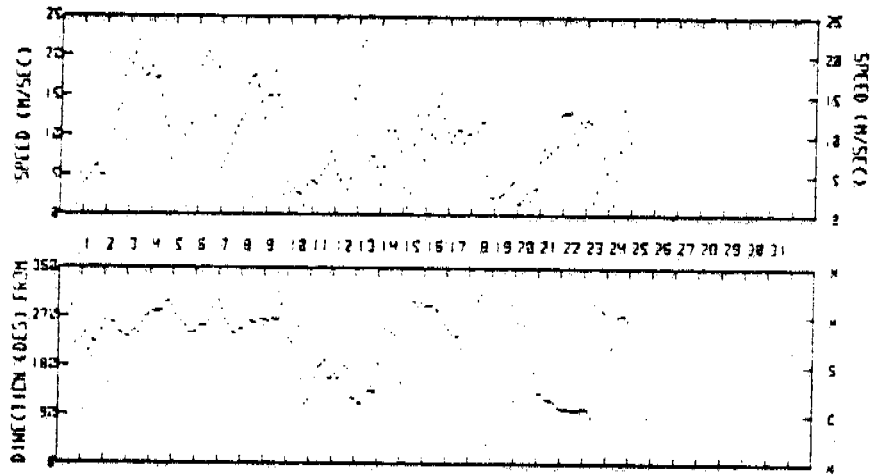


Fig. 6: Time series of calculated geostrophic winds for the solution center in Harrison Bay compared to measured surface winds at Tolaktovut Pt. in August 1980

GEOSTROPHIC WIND SPEED & DIRECTION
 SEPTEMBER 1980



WIND SPEED & DIRECTION SEPTEMBER 1980
 AT: TOLAKTOVUT

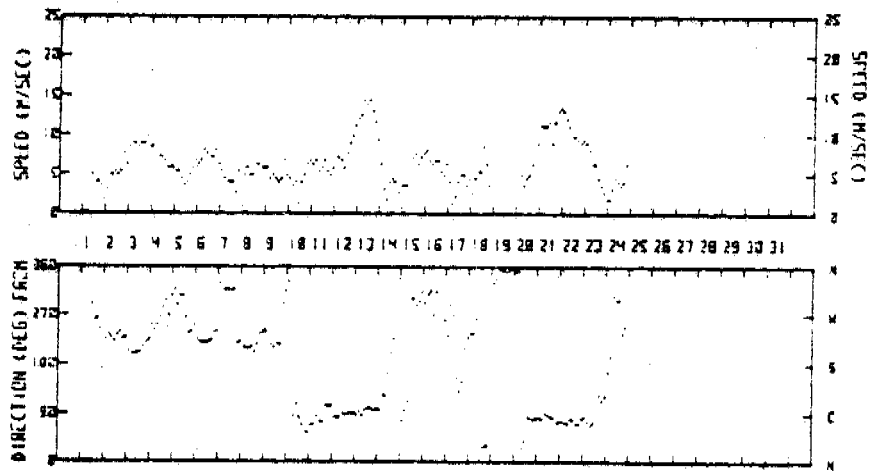


Fig. 7: Time series of calculated geostrophic winds for the solution center in Harrison Bay compared to measured surface winds at Tolaktovut Pt. in September 1980

SURFACE WIND DIR.

		0-30	30-60	60-90	90-120	120-150	150-180	180-210	210-240	240-270	270-300	300-330	330-360	
GEOS. WIND DIR.	330-360	2	1	1	3	0	0	0	0	0	0	1	0	
	300-330	1	1	0	0	0	0	0	0	0	0	3	1	
	270-300	0	1	1	0	0	0	0	0	3	6	6	2	
	240-270	0	0	0	0	2	3	3	9	15	6	4	1	
	210-240	1	0	1	1	2	2	7	11	5	2	0	2	
	180-210	0	0	0	1	2	0	1	4	0	4	1	1	
	150-180	2	3	0	3	2	2	3	7	3	3	0	2	
	120-150	1	3	3	4	0	1	0	0	0	0	1	2	
	90-120	1	10	12	1	1	0	0	0	0	0	0	4	
	60-90	2	5	3	0	0	0	0	0	0	0	2	1	3
	30-60	14	4	0	0	0	0	0	0	0	0	2	1	2
	0-30	3	3	1	0	0	0	0	0	0	0	0	1	1

Fig. 8: Bivariate distribution tables of simultaneously occurring geostrophic and surface wind directions for August 1980

SURFACE WIND DIR.

		0-30	30-60	60-90	90-120	120-150	150-180	180-210	210-240	240-270	270-300	300-330	330-360
GEOS. WIND DIR.	330-360	1	0	0	1	0	0	0	0	0	0	0	0
	300-330	2	0	0	0	0	0	0	0	1	0	1	0
	270-300	0	1	1	0	1	3	0	3	4	10	10	1
	240-270	1	0	1	1	2	0	6	27	5	1	2	2
	210-240	1	1	0	1	3	3	3	0	2	3	0	0
	180-210	0	1	2	3	0	0	0	0	2	0	0	0
	150-180	0	0	0	2	0	0	1	1	2	0	0	0
	120-150	0	0	0	0	0	0	0	0	0	0	0	0
	90-120	1	2	17	2	0	0	0	0	0	0	0	0
	60-90	0	0	1	0	0	0	0	0	0	0	0	0
	30-60	0	1	0	0	0	0	0	0	0	0	0	0
	0-30	0	0	0	1	0	0	0	0	0	0	0	0

Fig. 9: Bivariate distribution tables of simultaneously occurring geostrophic and surface wind directions for September 1980

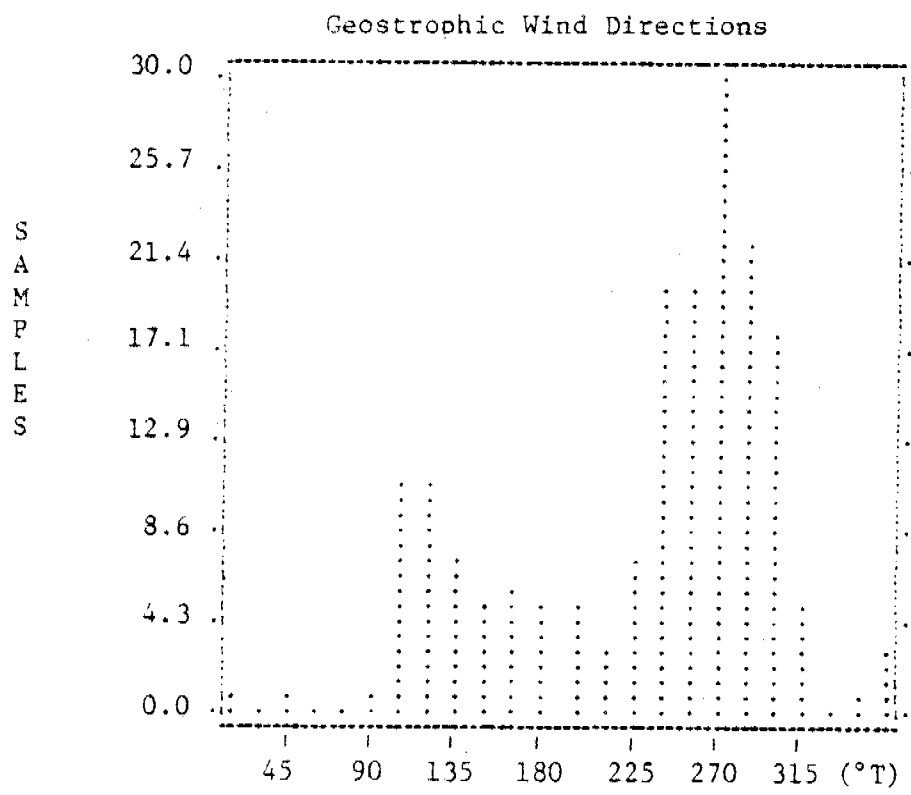
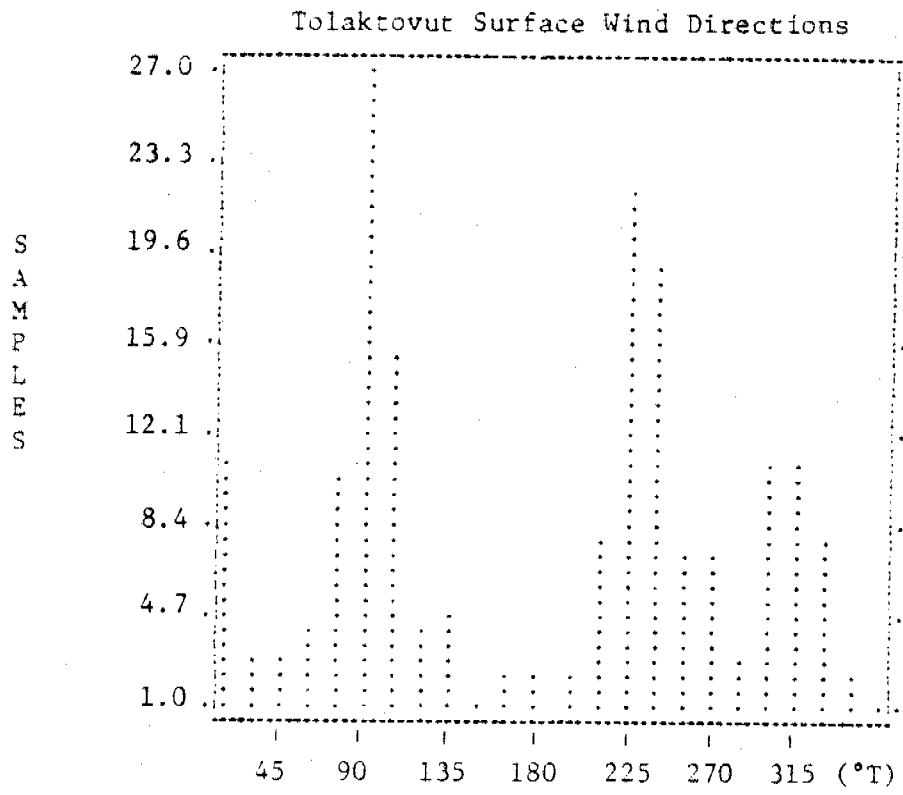


Fig. 10: Histograms of surface (Tolaktovut) and geostrophic wind directions for the month of August 1980

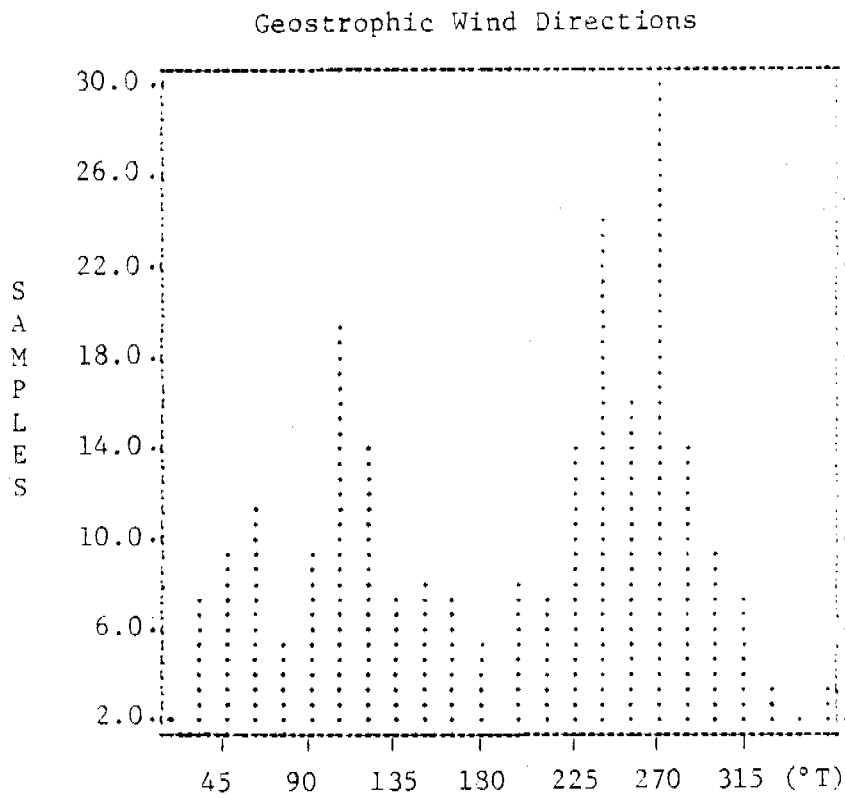
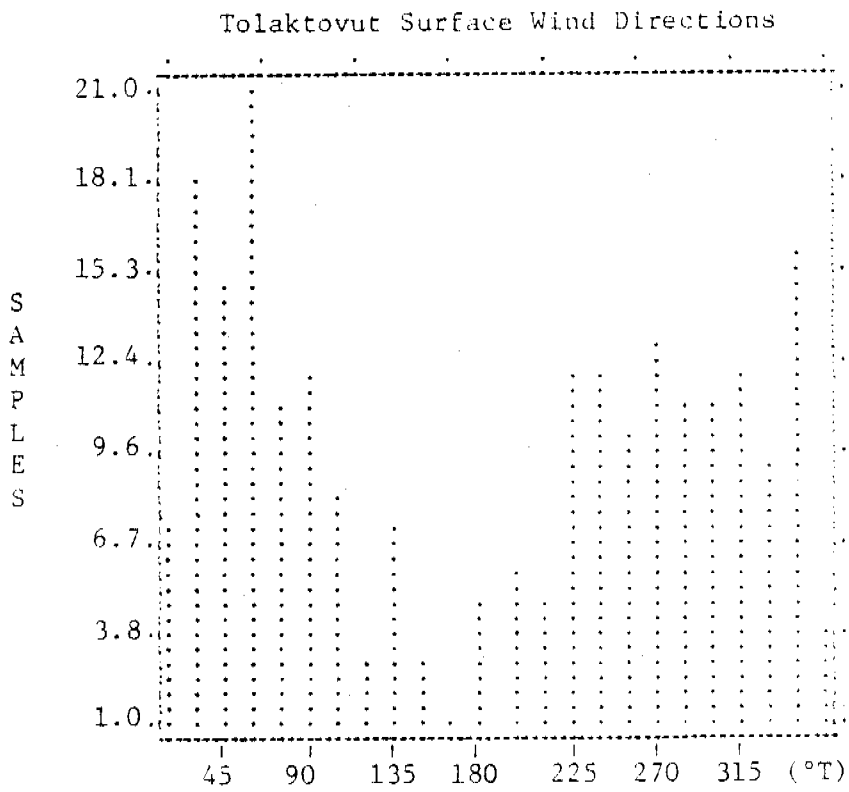


Fig. 11: Histograms of surface (Tolaktovut) and geostrophic wind directions for the month of September 1980

Annual Report

Contract #03-5-022-55
Research Unit #526-77
Task Order #13
Reporting Period: 1 April 1980
31 March 1981
Number of Pages: 19

CHARACTERIZATION OF THE NEARSHORE HYDRODYNAMICS
OF THE BEAUFORT SEA AND CHUKCHI SEA AND SUMMER
STUDIES OF THE PHYSICAL OCEANOGRAPHY OF THE BEAUFORT
SEA TRACTS FOR SALE #71

J. B. Matthews
Geophysical Institute
University of Alaska
Fairbanks, Alaska 99701

March 1981

I. SUMMARY

Data have been analysed for summer circulation characteristics in Harrison Bay. The bay is significantly different from other Beaufort Sea embayments previously studied in that it has no protective barrier islands and has major river upset.

Many instruments were lost during a summer storm which brought ice into the bay. However data from the instruments recovered clearly show two distinct regimes. In the first two weeks of August 1980 a two layer system prevailed with freshwater overlying more saline water. Nearshore water appeared to be separated from shelf waters at the 6 m isobath. Mean surface to bottom salinities differences were $5^{\circ}/\text{oo}$ in the range $25\text{-}30^{\circ}/\text{oo}$. Currents were variable with a net westward drift of 1 km/day.

Strong west winds for the second part of August resulted in a net eastward drift of 6 km/day to the east. The water mass became mixed with more saline waters driven on top of mixed brackish water. The salinity gradually dropped throughout the period indicating that Colville River water was trapped in Harrison Bay by the onshore winds.

A prototype instrument is being developed to reduce potential loss of data due to storm conditions and for work in the shear zone. Winter data from Harrison Bay and Steffansson Sound are being collected to allow comparison of water circulation in these two regions and to obtain details of a two layer system observed in earlier work.

II. INTRODUCTION

A. General Nature of Scope of Study

The general scope of the study is to provide physical oceanographic data on the coastal and estuarine regimes of the Beaufort Sea Shelf. Originally planned as an integral part of the "Beaufort Sea Barrier Island - Lagoon Ecological Process Studies", Research Unit 467, the project was expanded in FY79 to include winter studies in the Beaufort Sea. At the same time the work was extended beyond the barrier island lagoon system into the shear zone in order to bridge the gap to Aagaard's study region along the outer shelf (RU 91 and RU 151). In FY80 a major new oceanographic field study commenced in the Beaufort Sea sale area #71 (Harrison Bay). This project became part of the Harrison Bay field study and expanded the work into the winter season during FY81.

B. Specific Objectives

Major objectives for this report period have been to complete the recovery of instruments previously deployed and begin detailed analysis of any data collected. Within these overall objectives the specific objective of analyzing data from the Beaufort Sea Sale Tract #71 has been given first priority.

C. Relevance to Problems of Petroleum Development

The physical oceanographic processes determine the physical properties of the Beaufort Sea ecosystem. These processes, as well as determining the trajectories and movements of sediments, muds and spilled oil, control the flow of nutrients into and out of the ecosystem. The studies undertaken therefore have both direct and indirect relevance to the problems attendant to petroleum development.

III. CURRENT STATE OF KNOWLEDGE

Earlier work on the nearshore physical characteristics has concentrated on regions protected by barrier islands. Detailed work first began in shallow Simpson Lagoon, west of Prudhoe Bay and East of Oliktok Point. Summer circulation was shown to be wind-driven with currents being 3-4% of the windspeed and in the same direction. Summer water masses were shown to be derived from source waters in warmer ($>6^{\circ}\text{C}$) river water and cold ($<2^{\circ}\text{C}$), saline ($>30\text{‰}$) arctic ocean surface waters.

The river water was seen to mix slowly as it travelled westwards along the coast. In early summer (July) boluses of freshwater were recorded travelling through the barrier island channels and through the lagoons. The boundary between the brackish riverine water and the surrounding oceanic water was very sharp. Changes of 10‰ and 8°C can occur in less than the 5 minute sampling interval of our instruments.

By mid-August the volume of low salinity water in Simpson Lagoon was very much reduced. Salinities approached 30‰ and temperature fell to 0°C by early September when sea ice began to form.

Simpson Lagoon has only a few places with depths greater than 2 m. Consequently most of the lagoon is frozen solid by March or April. Brine exclusion from sea ice formation can produce pockets of very high salinities ($>40\text{‰}$).

Other work in Egg Island channel, the major channel of the Simpson Lagoon - Gwydyr Bay system, observed the flushing out of a winter's accumulation of brine. In late May salinities greater than 43‰ were measured in the bottom of Egg Island channel at 6 m depth under 2 m ice. On 5 June the Kuparuk River overflowed the sea ice to a depth of about 1 m as recorded on our sea level recorder. Subsequently over a period of 1 hour the salinity fell from 43‰ to 0‰ and the temperature rose from -2°C to 0°C . River water flowed in Egg Island channel for about 1 month after the first spring overflow. Subsequently, oceanic water returned and flowed into the lagoon as the winter ice broke up.

In later work we examined the circulation in Stefansson Sound and beyond the barrier islands. Stefansson Sound has water depths up to 8 m and consequently does not freeze to the bottom although it has a stable cover of landfast ice. Summer conditions showed similar wind-driven circulation to that observed in Simpson Lagoon. However winter measurements reported in the 1980 OCS report showed that seaward flowing layer of brine occurred in November and December. Maximum currents of 10 cm/sec were observed during a surge event with mean currents of about 2 cm/sec. The observations have been reported in Matthews (1981) and will be briefly summarized. Mean currents measured in 5 m water depth at 1.22 and 3.23 m depth were 1.91 and 1.34 cm/sec over a 50-day period. During the same time salinities rose at 0.04‰ per day from 32.5‰ , which is consistent with sea ice growth of about 0.8-1.0 cm per day. The currents flowed consistently at 50° true and did not reverse although a mean tidal current of 0.54 cm/sec was computed from the records.

These data suggested that a counter current flowing shorewards should exist immediately beneath the ice canopy. Such a current might influence the movement of oil or other floatables in the surface waters under the fast ice. Subsequent work has been aimed at verifying the existence of the surface current.

Beyond the barrier islands, on the basis of one record the currents showed a predominantly long-shore flow. Further analysis has been carried out on other instruments and is reported below.

In Summer 1980, in preparation for lease sale #71, an array of current meters and tide gauges was deployed in Harrison Bay. This region is significantly different from the lagoon and coastal regions studied previously. Most notable are the open nature of the Bay which has no protective barrier islands and the Colville River which empties into the southern part of the bay. The Colville is Alaska's largest river on the Arctic Ocean coast. Summer and winter circulation studies have been undertaken in Harrison Bay.

IV. STUDY AREA

The study area is shown in Figure 1. The Harrison Bay region is unprotected by barrier islands. Colville River enters at the south. The bathymetry changes from a generally east-west contour to a northeast-southwest trend off Harrison Bay.

V. SOURCES METHODS AND RATIONALE OF DATA COLLECTION

The data collection methods have been developed specially for this project and have been discussed extensively in previous reports. Briefly, we rely on moored recording current meters and tide gauges which can be deployed, serviced and recovered from helicopters. The instruments, floats, anchors and accessories are all arranged in modular units so they can be carried by helicopter and assembled on the ice. Aanderaa instruments were chosen because of their known performance characteristics in high latitude waters. Calibrations of all instruments is carried out both before and after each deployment.

Instrument arrays consisting of a surface and bottom current meter were deployed in three lines of three arrays. One line due north of Atigaru Point (A1, A2 and A3, Fig. 1), one due north of the Colville River off Tolaktuvut Point (C1, C2 and C3, Fig. 1) and one line due north beginning one mile west of Thetis Island (T1, T2 and T3 in Fig. 1). In a related study Kozo (RU 519) measured barometric pressure and 10 m winds at Cape Halkett, Atigaru Point and Tolaktuvut Point. Wind data was thus provided over the entire bay. This is necessary because National Weather Service data are not available for the region. Moreover the currents were anticipated being wind-driven. Barometer pressure measurements are necessary to correct the bottom-mounted pressure instruments.

The existence of a two layer system was anticipated in Harrison Bay, so top and bottom instruments were used. The array distribution was used to provide easy comparison with numerical model results.

Instruments have been deployed in November 1980 at T1 and A1 as well as in Stefansson Sound. By measuring winter circulation in both Stefansson sound and Harrison Bay we provide the ability to verify the two layer circulation in Stefansson Sound and compare Harrison Bay circulation with that of Stefansson Sound.

VI. RESULTS

The instrument packages deployed in late July 1980 were equipped with 3 mile, 3-year underwater pingers and surface radio beacons. An extensive search for the instruments was mounted in late August and early September. However, strong winds from the west had prevailed during the second part of August and into September. Ice was driven into Harrison Bay from the west. Observers aboard a research vessel in the Bay reported seeing one of our arrays under tow by an ice floe.

Three current meters were recovered two from A3 (Fig. 1) and one from T1. The A3 array was recovered south and east of its deployment point. The T1 array was recovered on outer Leavitt Island, east of the deployment point. The data from these instruments give a very good overview of both normal and storm conditions.

Figure 2 shows the temperature and salinity at the 3 m depth at A3 (Fig. 2) off Atigaru Point in 8 m water depth. Figure 3 shows the temperature salinity and current vectors at the same location at 6.25 m depth. Over the 31 days' record, the upper instrument recorded mean salinities and temperature of 24.0‰ and 3.08°C while the lower instrument recorded 25.19‰ and 4°C. During the first part of August a stratification was observed with about 5‰ difference between 3 and 6 m depth. During the second part of August the upper salinity was about 1‰ higher than the lower salinity and gradually falling.

The temperature records show the upper temperature about 2°C lower than the salinity at 6 m depth in the second part of August. On 3 and 4 August the 3 m temperature was between 1 and 2°C. At the same time a bolus of low salinity (<22‰) water passed the instrument array. Subsequently the temperature at 3 m rose to 3°C and remained above this 3°C for two weeks.

The rotor on the upper instrument did not function but the instrument at 6 m produced results. The vectors are shown in Figure 2. Maximum currents were 30 cm/sec with a mean current of 4 cm/sec towards the east. Variable currents occur in the first part of August with currents towards the south and east prevailing in late August.

The Thetis Island array was torn from its moorings and recovered near Spy Island (Fig. 1). Figure 4 shows the useful data through 13 August. Cessation of the record probably coincides with the movement of the array. Only one instrument deployed at 3 m depth in 5 m water was recovered. Higher salinity water prevailed until 11 August when water less than 22‰ appeared. This water with salinities near 12‰ and temperatures up to 6°C is clearly originating from the Colville River. Currents were variable and notably larger from 11 August onwards.

Areal coverage of water temperature and salinity were taken by Craig (RU 467). These data are shown in Figure 5. For all the data a two layer system was reported in the vertical and a nearshore and coastal water mass. The nearshore waters had lower salinities and higher temperatures; 25.1 ‰, 6.2°C and 27.2‰, 4.7°C for surface and bottom

waters. The dividing line between nearshore and coastal water masses coincided with the 6 m coastal offshore waters average 27.4‰ and 2.5°C in the surface and 28.7‰ and 1.9°C at the bottom.

VII. DISCUSSION

The results of the instrument recovery field expeditions were disappointing. Only three instruments of 18 have been recovered. Late August 1981 saw strong westerly winds blowing into Harrison Bay. Because the Bay is unprotected by barrier islands our instrument array with surface floats can be moved by ice floes. Both instrument arrays recovered were found east of their deployment positions. All arrays had radio beacons and underwater pingers. Moreover each instrument is individually buoyed. The chances of eventual recovery are quite good.

In order to evaluate the probability of instrument losses, we prepared statistics from our previous deployments. These are shown in Table 1. Overall recovery rate is 67%. Most notable is the 100% recovery rate for fall and winter deployments. Summer deployment recovery rates is 54% and for 1980 only 12%. The past summer was clearly by far the worst on record. This must be attributed to the adverse storm conditions in late August 1980.

In order to improve the situation we need to improve the data collection techniques for summer and spring. The major problem appears to be that data are recorded on in-situ tape recorders. If an instrument is not recovered all data are lost. A method of real time data collection would not depend on instrument recovery for retrieval of invaluable data. Ideally expendable telecommunicating devices are needed. We are investigating the possibility of interfacing our standard Aanderaa instrument packages to standard off-the-shelf satellite data transmission devices. The objective will be to obtain the same 100% data recovery for summer as well as for winter deployment.

The shear zone, beyond the 13 m isobath is an extremely hazardous region in which to work. The present field deployment was designed to avoid the shear zone because of the high potential for instrument loss. Much of lease sale #71 area lies beyond the 13 m isobath in the shear zone. If the satellite transmission system proves successful, the whole shelf region can be fully investigated. The times when instrument recovery are most difficult are the same periods when coastal navigation and industrial activity is also very arduous.

The data recovered from Atigaru Point and Thetis Island show two distinct regimes. The first part of August is the type of circulation observed during other summer work in the Beaufort Sea. Brackish water originating in the Colville River overlies more saline water near shore. The boundary between oceanic and near shore waters coincides with the 6 m isobath. The instrument off Thetis Island is close to the main channel on the Colville River and shows much lower salinity than the instruments off Atigaru Point in western Harrison Bay.

Figure 6 compares current transport and wind transport based on the current meter data from A3 (Fig. 1) and Kozo's wind data from Atigaru

Table 1. Instrument deployment and recovery statistics.

YEAR	DEPLOYED		RECOVERED		%REC	%CM's	%TG's
	CM	TG	CM	TG			
1977	3	1	2	1	75	66	100
1978 (summer)	14	11	14	11	100	100	100
1978-1979 (winter)	15	8	15	8	100	100	100
1979 (spring)	10	5	6	3	60	60	60
1979 (summer)	13	7	5	2	35	38	29
1979 (fall)	2	1	2	1	100	100	100
1980 (summer)	18	8	3	0	12	17	0
1980-1981 (winter)	12	2	12	2	100	100	100
TOTAL	87	43	59	28	67	68	65
TOTAL SUMMER	48	27	26	14	53	54	52
TOTAL WINTER	27	10	27	10	100	100	100
TOTAL SPRING	10	5	6	3	60	60	60
TOTAL FALL	2	1	2	1	100	100	100

Point. The wind record shows a wind from the northeast (south westerly transport) until 17 August after which a strong wind from the west (eastern transport) prevails. Easterly current transport begins about 18 August with very little net transport being recorded earlier in August. Water transport was only about 15 km to southeast in the first half of August compared to over 100 km to south west in the second part of the month.

The first part of August with its well defined two layer system and generally westerly drift is typical of other locations on the Beaufort Sea coast. Figure 7 shows the current transport off Thetis Island compared with the wind transport at Tolaktuvut Point and Cape Halkett. The current transport shows an excursion to the northeast and back between 6 August and 11 August which is not reflected in the wind record. The currents must result from some other driving mechanisms during this period.

From 17 August currents at Atigaru Point are towards southeast i.e. into Harrison Bay and towards the Colville River (Fig. 6). The salinity at Atigaru Point falls continuously from 17 August (Figs. 2 and 3). This suggests that the strong west winds are trapping the Colville River water in Harrison Bay resulting in the anomalously low salinity in early September. The two layer structure appears to have been destroyed also about 17 August. After that date the salinity at 3 m was consistently higher than that at 6 m and the density is uniform from top to bottom.

VIII. CONCLUSIONS

It is concluded that the oceanographic regime in Harrison Bay is significantly different from that in Stefansson Sound and Simpson Lagoon. This results from two major differences. Most importantly Harrison Bay is unprotected by barrier islands. Thus it is exposed to the strong westerly storm winds. In addition the Colville River, the largest north slope river enters southern Harrison Bay.

Under the prevailing easterly winds a variable current structure with generally westward drift is obtained. A two layer system forms from Colville River water overlying more saline and colder oceanic water near the 6 m isobath.

Under strong westerly storm conditions the water masses become well-mixed. Colville River water becomes trapped in the Bay resulting in much reduced salinity values if the winds persist.

IX. NEEDS FOR FURTHER STUDY

Data collection in summer in Harrison Bay is very hazardous as a result of the open nature of the Bay. No attempt was made to collect data seaward of the 10 m isobath. Summer and spring are the most difficult and hazardous periods for data collection and other activities in Harrison Bay and in the shear ice zone. Real time data collection techniques are needed for this important period. Plans are underway for the development of a prototype instrument. It is hoped that the instrument can be tested in winter and other models deployed during the following summer.

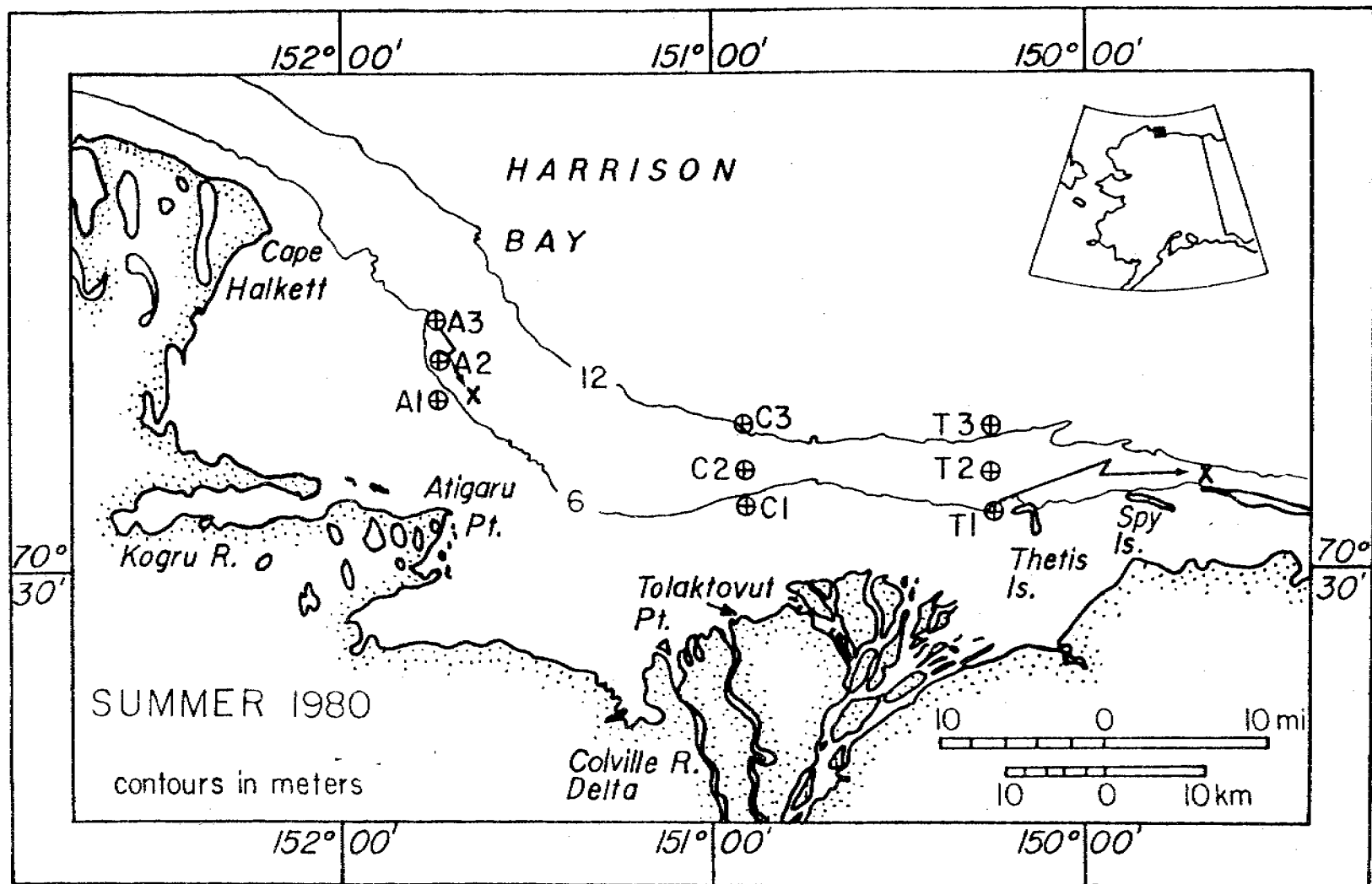


Figure 1. Harrison Bay Location map and instrument mooring locations

OFF ATIGARU POINT

WATER DEPTH = 7.92m

METER DEPTH = 3.09m

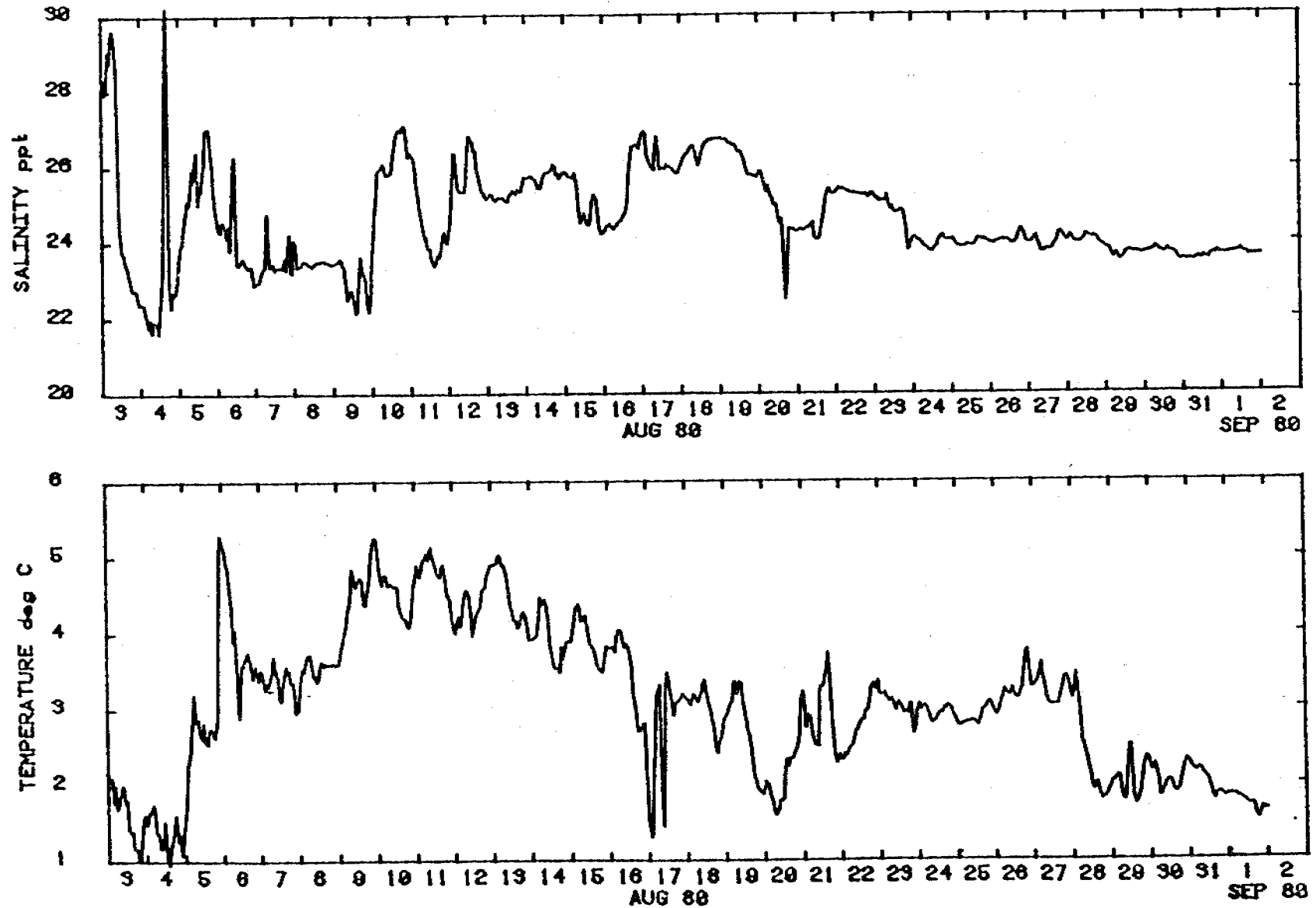


Figure 2. Salinity and temperature at 3 m depth in 8 m water at Station A3 in August 1980.

OFF ATIGARU POINT

METER DEPTH = 6.25m

WATER DEPTH = 7.92m

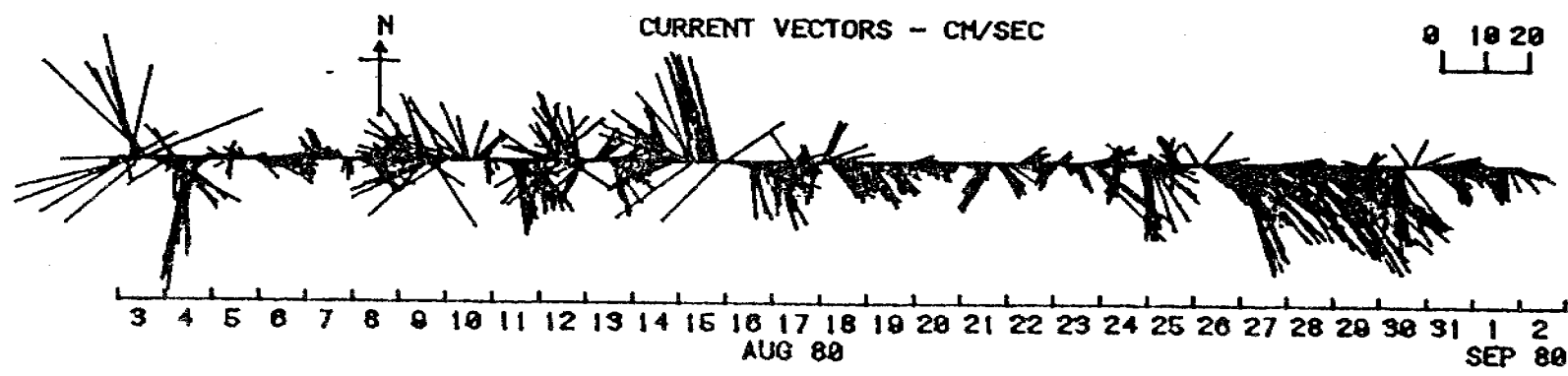
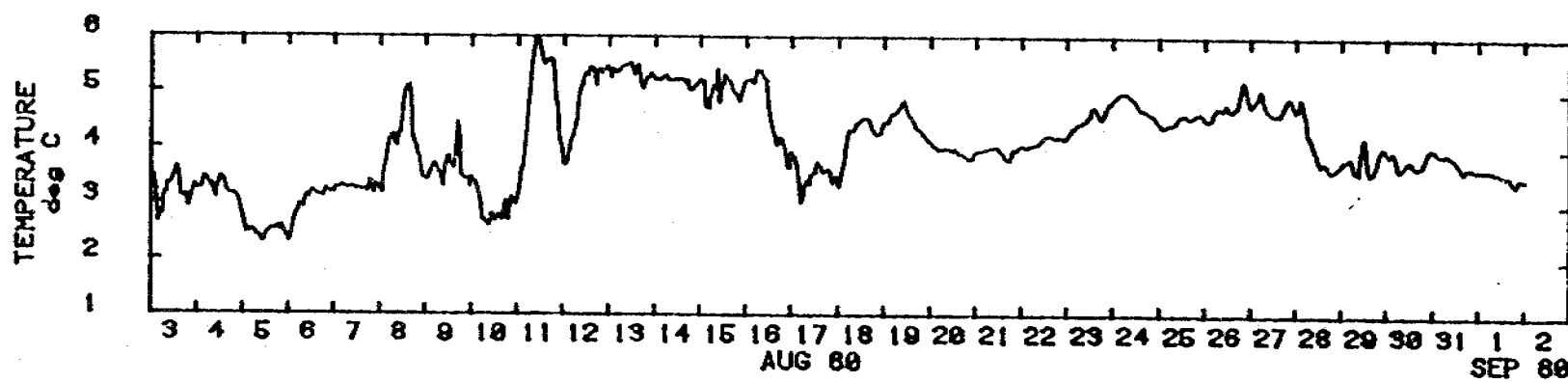
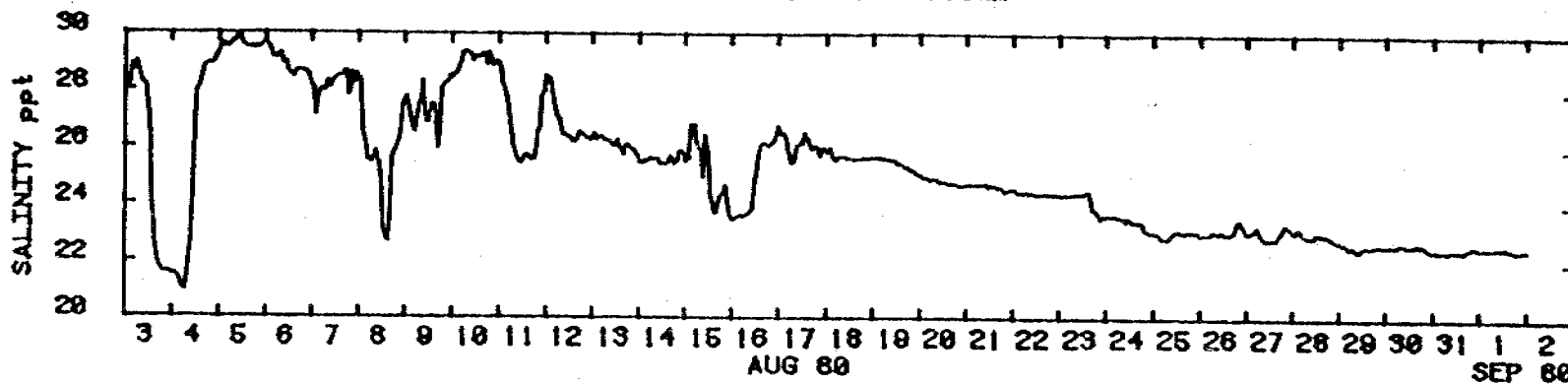


Figure 3. Salinity, temperature and current vector at 6.25 m depth in 8 m water at station

OFF THETIS ISLAND

WATER DEPTH = 5.18m

METER DEPTH = 2.95m

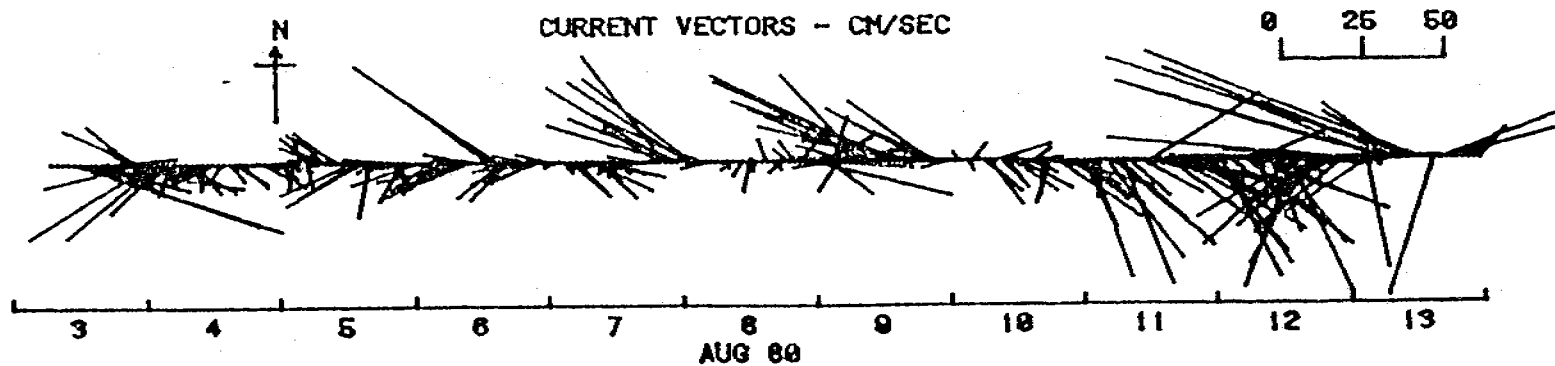
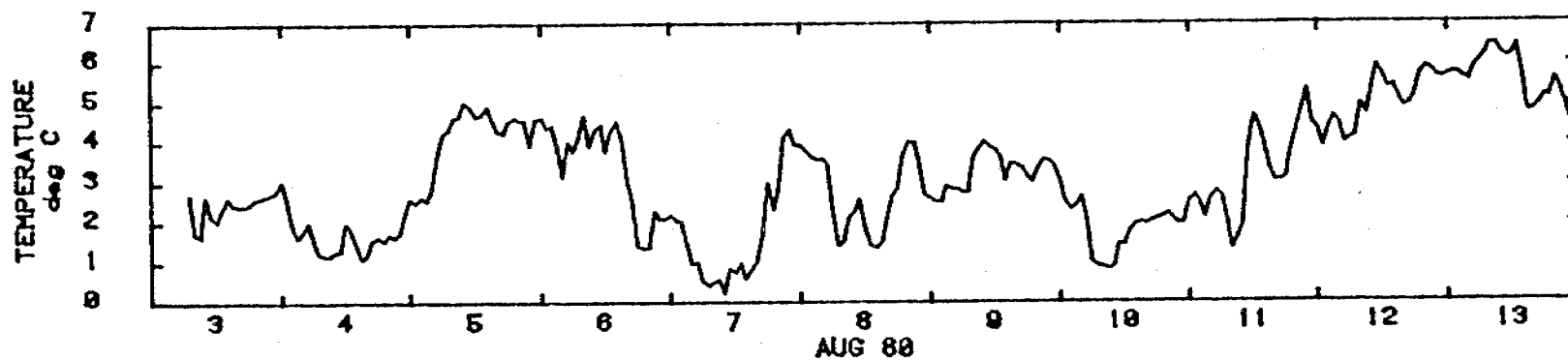
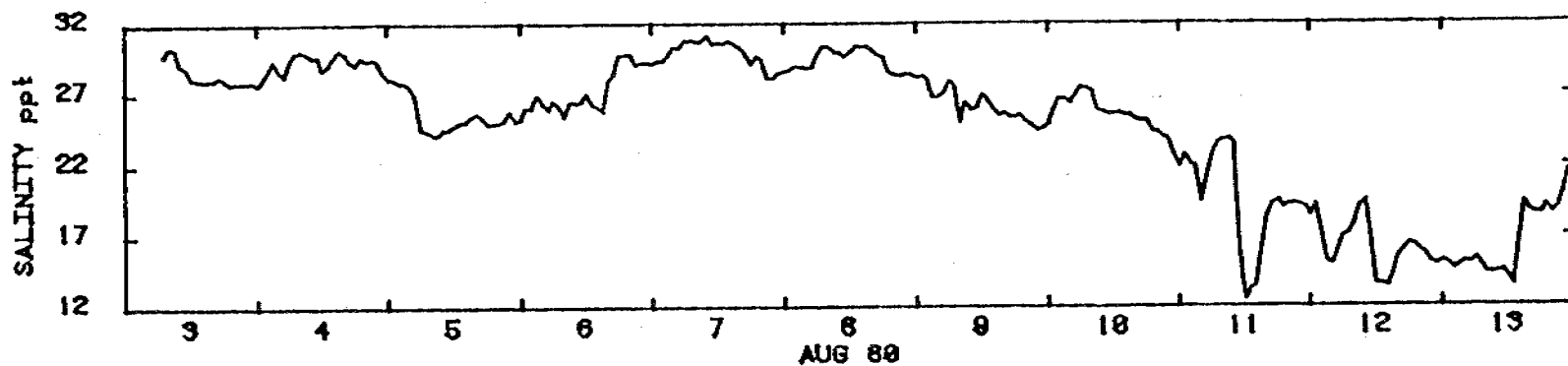


Figure 4. Salinity, temperature and current vectors at Station T1 at 3 m depth in 5 m water 3-13 August 1980.

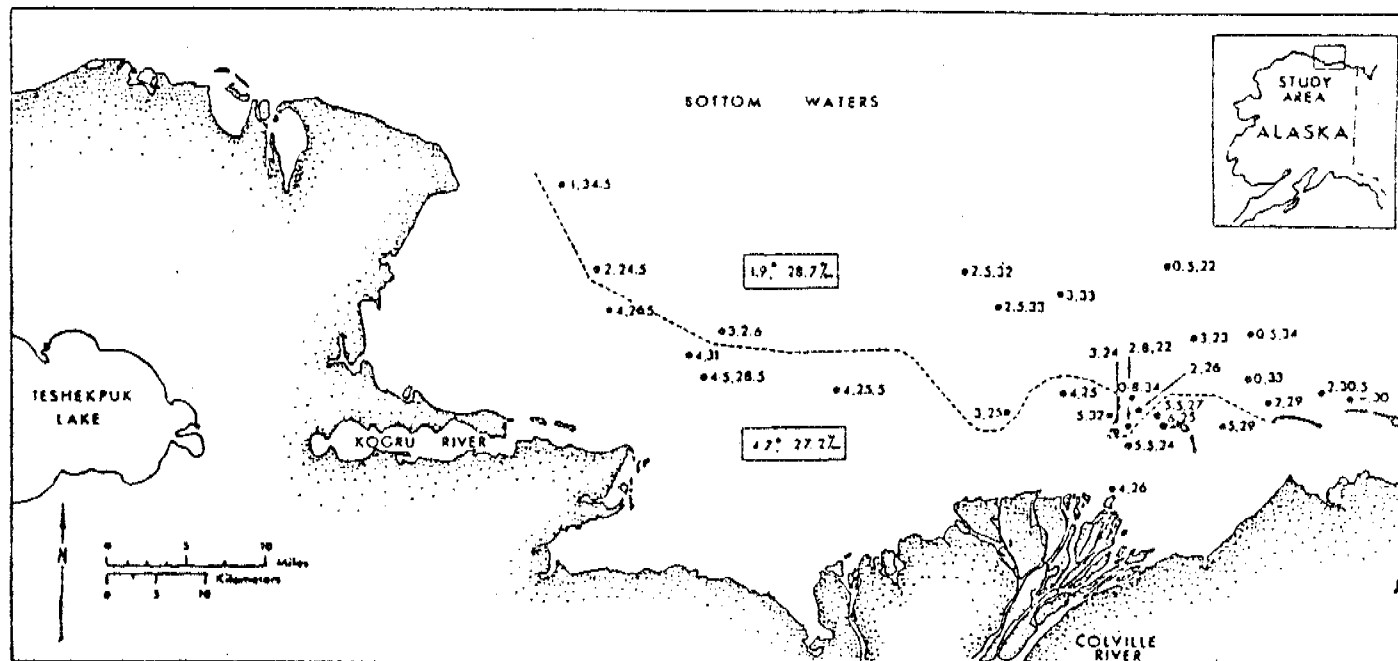
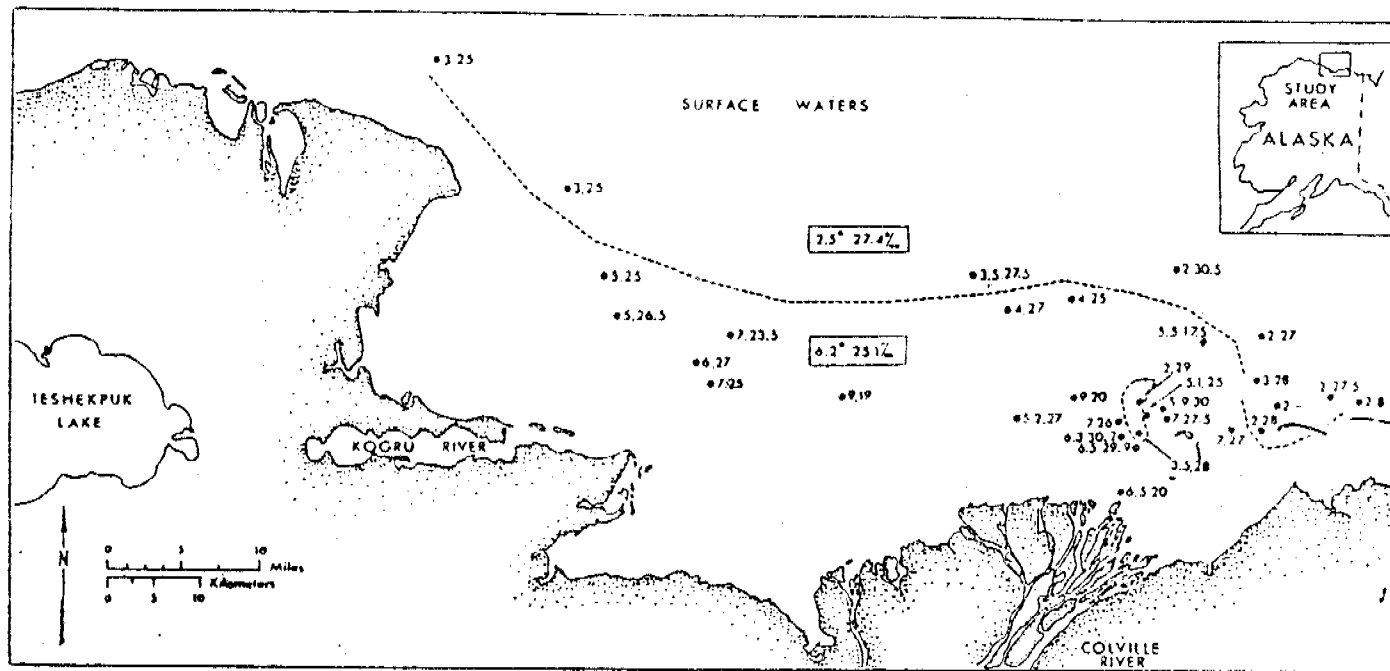
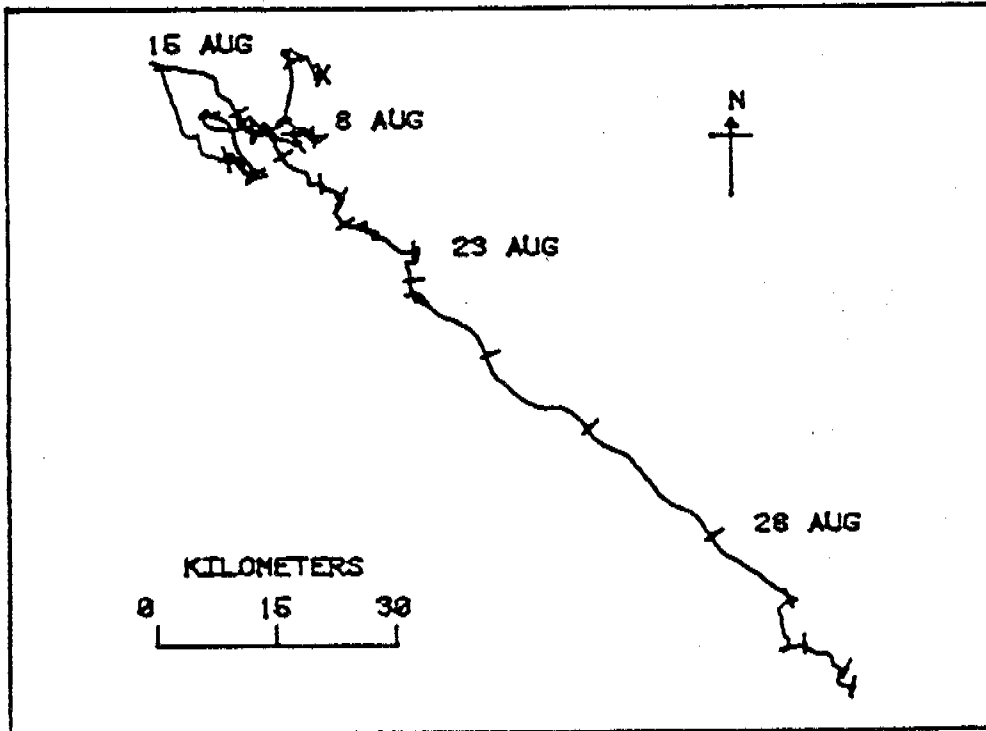


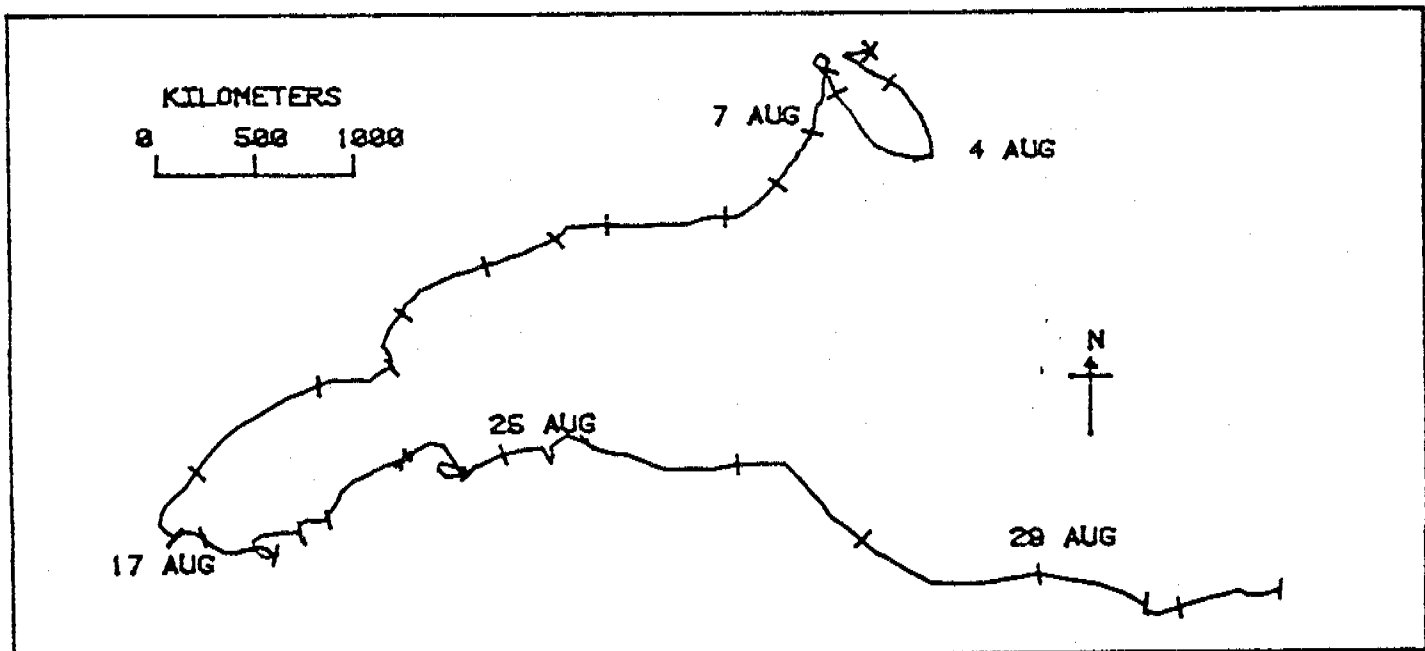
Figure 5. Surface and bottom salinity and temperature data from 3-19 August (After Craig RU 467 1981)

OFF ATIGARU POINT



3 AUG 80 TO 2 SEP 80
PROGRESSIVE VECTOR PLOT OF CURRENT TRANSPORT

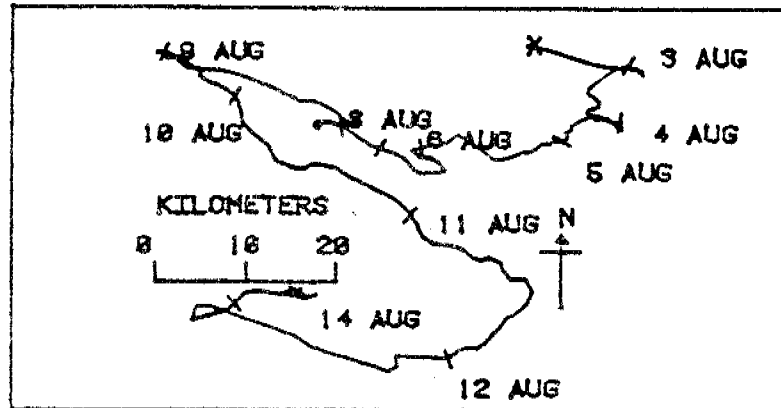
ATIGARU POINT



3 AUG 80 TO 2 SEP 80
PROGRESSIVE VECTOR PLOT OF WIND TRANSPORT

Figure 6. Current transport at A3 off Atigaru Point and wind transport at the point

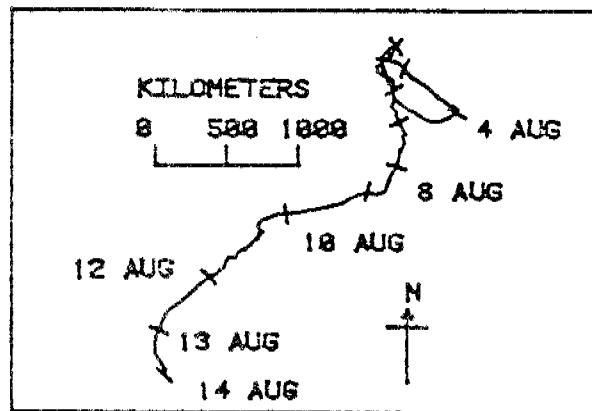
OFF THETIS ISLAND



3 AUG 88 TO 14 AUG 88

PROGRESSIVE VECTOR PLOT OF CURRENT TRANSPORT

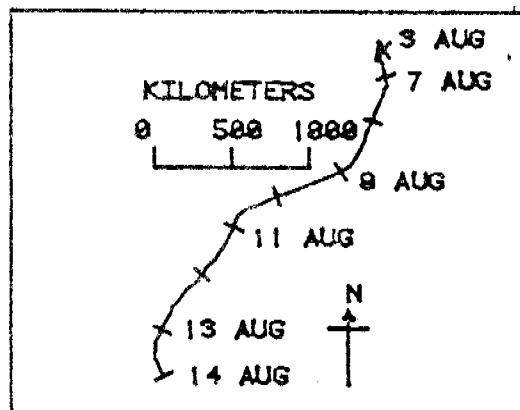
TOLAKTOVUT POINT



3 AUG 88 TO 14 AUG 88

PROGRESSIVE VECTOR PLOT OF WIND TRANSPORT

CAPE HALKETT



3 AUG 88 TO 14 AUG 88

PROGRESSIVE VECTOR PLOT OF WIND TRANSPORT

Figure 7. Current transport off Thetis Island and wind transport at Cap

X. SUMMARY

A. Ship or Laboratory Activities

1. Ship or Field Trip Schedule

a. Dates

1. 18 March-6 April 1980 to Mukluk Camp, Deadhorse
2. 3-5 August 1980
3. 1-10 September 1980
4. 3-7 November 1980

b. Name of Vessel
None

c. Aircraft
helicopters

2. Scientific Party

Stephen Petersen - UA Diver Tech; ArcTech Research Diver-Tech
Cliff Moore - UA Diver Tech; ArcTech Research Diver-Tech
Jeanette Moore - UA Diver Tech; ArcTech Research Diver-Tech
Ron Poirot - ArcTech Research Diver-Tech
Gary Meltvedt - UA, Technician
J. B. Matthews - UA, Principal Investigator

3. Methods

a. Field Sampling

Deployment of meters, and search and recovery attempts were made for all meters in the field

b. Laboratory Analysis

Analysis by computer in lab; methods described in earlier reports.

4. Sample Localities/Ship or Aircraft Tracklines
See Figure 1.

5. Data Collected or Analyzed

a. Number and Types of Samples/Observations

In August 1980, 18 meters and 8 tide gauges were deployed in Harrison Bay. In September, only 3 meters were recovered. The data recovered was from 1 array off Atigaru point, and one meter off Thetis Island. The salinity, temperature, current speed & direction were analyzed for all three meters. 14 more meters deployed Nov. 1980.

b. Number and Types of Analyses

See attached

Current meters analysed: 17

tide gauges analysed: 9

All edited, corrected, plotted & saved.

c. Miles of Trackline
none

XI. AUXILIARY MATERIAL

A. References Used (Bibliograph)

B. Papers in Preparation or Print

J. B. Matthews, 1981

The seasonal circulation of the Glacier Bay, Alaska fjord system.
Estuarine, Coastal & Shelf Science, Vol 12, pp 679-700, 1981.

J. B. Matthews, 1981

Observations of under-ice circulation in a shallow lagoon in
the Alaskan Beaufort Sea.

Ocean Management, Vol 6, pp 223-234, 1981.

J. B. Matthews

Observations of surface & bottom current movements in the Beaufort
Sea near Prudhoe Bay, Alaska

In Press, Journal of Geophysical Research

C. Oral Presentations

American Geophysical Union, Fall Annual Meeting

December 1980, "Under-Ice Circulation Patterns in the Nearshore
Beaufort Sea."

ANNUAL REPORT

Contract: #0302256
Research Unit: 52977
Task Order: #33
Reporting Period: 4/1/80-3/31/81
Number of Pages: 142

SOURCES, TRANSPORT PATHWAYS, DEPOSITIONAL SITES AND
DYNAMICS OF SEDIMENTS IN THE LAGOON AND ADJACENT
SHALLOW MARINE REGION, NORTHERN ARCTIC ALASKA

A. S. Naidu
Principal Investigator
Associate Professor of Marine Science
Institute of Marine Science
University of Alaska
Fairbanks, Alaska 99701

with

L. H. Larsen, M. D. Sweeney and H. V. Weiss

June 1981

TABLE OF CONTENTS

	LIST OF TABLES	154
	LIST OF FIGURES.	155
I.	SUMMARY OF OBJECTIVES, CONCLUSIONS AND IMPLICATIONS WITH RESPECT TO OCS OIL AND GAS DEVELOPMENT.	156
II.	INTRODUCTION	156
	General Nature and Scope of Study	156
III.	OBJECTIVES	157
	Relevance to Problems of Petroleum Development.	158
IV.	CURRENT STATE OF KNOWLEDGE	160
V.	STUDY AREA	160
VI.	SOURCES, METHODS AND RATIONALE OF DATA COLLECTION.	162
	Field Work and Samples.	162
	Laboratory Work	162
	Analytical Methods.	167
VII.	OTHER ACTIVITIES	168
VIII.	RESULTS.	169
IX.	DISCUSSION	182
	REFERENCES	193
	APPENDIX 1 - FIELD AND CRUISE REPORT	195
	APPENDIX 2 - REPORT OF AUGUST 1980 FIELD STUDIES IN HARRISON BAY.	202
	APPENDIX 3 - ASPECTS OF SIZE DISTRIBUTIONS, CLAY MINERALOGY AND GEOCHEMISTRY OF SEDIMENTS OF THE BEAUFORT SEA AND ADJACENT DELTAS, NORTH OF ARCTIC ALASKA.	207
	APPENDIX 4 - SEDIMENTATION RATE IN AN ARCTIC COASTAL REGION.	252
	APPENDIX 5 - CLAY MINERAL DISPERSAL PATTERNS IN THE NORTH BERING AND CHUKCHI SEAS	270

TABLE OF CONTENTS

CONTINUED

APPENDIX 6 - DISPERSAL PATTERNS OF CLAY MINERALS IN THE MARGINAL SEAS OF ALASKA	296
APPENDIX 7 - PARTITIONING OF HEAVY METALS IN LAGOON SEDIMENTS, NORTH ARCTIC ALASKA.	297

LIST OF TABLES

Table	I.	Statistical grain size distributions of Beaufort Lagoon sediments	170
Table	II.	Stratigraphic variations in gross texture of sediment cores taken from Simpson Lagoon and Harrison Bay	171
Table	III.	Revised data on the concentrations of certain metals in gross sediments from the bays, lagoons and sounds of the coastal region of the Beaufort Sea.	176
Table	IV.	Concentrations of some heavy metals in gross sediments from Harrison Bay and Simpson Lagoon	178
Table	V.	Concentrations of Fe, Mn, Cr and V in gross sediments of the Beaufort Lagoon, north arctic Alaska	179
Table	VI.	Concentration of some metals in total (T) and Chester and Hughe's extracts (che), and the percentages of extract of the total (% che).	180
Table	VII.	Stratigraphic variations in heavy metal contents in core SL8979-3 from Simpson Lagoon	181
Table	VIII.	Concentrations of organic carbon and nitrogen, and C/N ratios in continental margin and deep-sea sediments of the Beaufort Sea.	183
Table	IX.	Stratigraphic variations in organic nitrogen concentrations and in the C/N ratios in two Simpson Lagoon cores	187
Table	X.	Weight percentages of total and organic carbon, and carbonate in Beaufort Lagoon and Harrison Bay sediments.	188
Table	XI.	Weight percentages of total and organic carbon, and carbonate in some Beaufort Sea sediments	189
Table	XII.	Weight of particulate matter in continuous sections in sea ice cores, collected by Dr. T. Osterkamp from nearshore regions off the Lonely Dewline Station and in Norton Sound off Yukon Delta.	190
Table	XIII.	Concentrations of suspended particles in surficial water samples collected from the east Harrison Bay-Simpson Lagoon and Prudhoe Bay area in summer 1980.	191

LIST OF FIGURES

Figure 1.	Station locations for Beaufort Sea continental margin region	161
Figure 2.	Sample locations in Simpson Lagoon.	163
Figure 3.	Map showing the locations of sediment samples from the Beaufort Lagoon, north arctic Alaska	164
Figure 4.	Map showing location of stations in the Simpson Lagoon and Prudhoe Bay region from where water samples were collected synchronizing with the LANDSAT II and III satellite passages in August 1980	166

I. SUMMARY OF OBJECTIVES, CONCLUSIONS AND IMPLICATIONS WITH RESPECT TO OCS OIL AND GAS DEVELOPMENT

The primary objective of this program is to understand sediment dynamics, to characterize benthic substrate habitats, and collect geochemical data on certain biologically "critical" chemical attributes of sediments (e.g., C. and N) of the barrier island-lagoon complex and shelf of north arctic Alaska. Research has also been directed to assess the source and long-term directions of alongshore transport of sandy and clayey sediments (based on heavy mineral and clay mineral studies), as well as the stability and origin of the barrier islands along the Beaufort Sea coast. The additional objective of this program is to collect lithological and chemical baseline data from the contiguous area of the continental shelf of the Beaufort Sea. The chief purpose of this latter effort has been to fill in the data gaps relating to sediment dynamics and chemical baselines that exist on shelf sediments, principally between Barter Island and Demarcation Point.

All available granulometric, clay mineral and chemical data for the Beaufort Sea have been consolidated and summarized, and are being presented in a draft synthesis report (appended herewith). This report generally provides the summarized raw data either in tabulated form or on maps of Beaufort Sea. Attempts have been made to discuss the data very briefly; to avoid redundancy, they are not being repeated in this section. We believe that adequate baseline data have been gathered to detect heavy metal pollution and changes in sedimentation rates in the Colville Delta-Simpson Lagoon area on a site specific basis, as a possible consequence of oil and gas developmental activities in the Beaufort Sea nearshore. We hope to prepare a final (synthesis) report by December 1981 for submission to the OCSEAP office, and will then discuss in detail some of our observations made to date.

II. INTRODUCTION

General Nature and Scope of Study

This program (Research Unit 529) concerning sedimentological studies is part of a larger interdisciplinary research effort to study the

physicochemical and biological processes operative in the barrier island-lagoon as well as continental shelf ecosystem of the Alaskan Beaufort Sea. Additionally, the general scope of the overall program entails establishment of an ecosystem model which can be put to use in predicting possible impacts resulting from both petroleum exploration and exploitation activities in the barrier island-lagoon complex of the Beaufort Sea coast. Further details on the nature and scope of this study (RU 529) and associated investigations have been enumerated in the original proposals submitted by Naidu to the OCSEAP office in July 1979 and 1980. Briefly, the scope of the sedimentological studies (RU 529) includes understanding of the sediment dynamics, delineating environments based on lithological facies, estimating the C, N and carbonate contents in the substrate sediments, establishing the sources and alongshore transport directions of sediments, completing collection of baseline data on a suite of heavy metals for the Harrison Bay, Simpson Lagoon, Beaufort Lagoon, and adjacent open continental shelf environment of the Beaufort Sea.

III. OBJECTIVES

The overall objectives of this research unit are as follows:

1. Document and synthesize data on the grain size distributions, mineralogy, organic carbon, nitrogen, carbonate and first transition row metals in sediments of the nearshore environment of the Beaufort Sea lease area.
2. Define the source, probable migratory pathways and depositional sites of sand and clay-sized particles of the nearshore environment of the Beaufort Sea.
3. Estimate the sedimentation rates in the Simpson Lagoon and adjacent continental shelf area, via ^{210}Pb dating of sediment layers.
4. Acquire ground truth to help develop criteria that may be applied to quantify concentrations of suspended particles in the lagoons of north arctic Alaska, using LANDSAT images. This portion of the research is in collaboration with Dr. W. J. Stringer (OCSEAP RU 267).

Relevance to Problems of Petroleum Development

The exploitation of the petroleum reserves in the North Slope of Alaska has been well underway, and received additional impetus with the finding of new reserves in the Milne and Kuparuk fields. The present trend is towards exploration in the adjacent continental shelf of the Beaufort Sea and at the same time to develop plans for secondary recovery of Prudhoe Bay oil by the waterflooding procedure. As a consequence of the OCS petroleum and gas development activities, the nearshore and the open shelf ecosystem of the Beaufort Sea is bound to be subjected to some degree of anthropogenic perturbations. The industrial activities which most likely will be introduced in this area include the construction of artificial islands, causeways and wharfs for the use of drilling operations, and water treatment facility relative to the waterflood project, docking facilities, dredging for maintaining navigations and laying offshore pipelines, exploitation of gravel and sand deposits from several possible sources as construction and fill materials. These activities will almost certainly lead to changes in the present sediment budgets, including sediment accumulation rates, which in turn can trigger significant changes in the wave/current regime. Some of the possible effects of varying the hydrodynamic conditions and sedimentation rates on nutrient dynamics, feeding habits of the epibenthic communities (detritus versus suspension feeders), and the modeling of the ecosystem have been discussed earlier (OCSEAP RU 529-78). In another context the redox potential which is an important faunal boundary layer may be influenced by the depositional rate of sediments. Further, the concentrations, fluxes and resident times of pollutants in the coastal waters may be a function of the accumulation rate of sediments, since suspended particles are effective scavengers of pollutants and post-depositional mobilization of metals at the sediment-water interface is invariably redox controlled. For these reasons study of the dynamics of sedimentation and estimation of depositional rates merits careful consideration.

There is a strong possibility that a variety of pollutants will be introduced into the nearshore environment, resulting either from inadvertent blowouts, oil spills, coastal construction work and intensified navigation within the region, or intentional discharge of fluids, mud and cuttings

during drilling operations and discharge of effluents from water treatment plants associated with waterflood projects. Some of the pollutants thus discharged may prove toxic through direct assimilation by some faunal communities or indirectly through food chain transfer (Northern Technical Services, 1981). Collection of baseline concentrations of heavy metals and an understanding of the speciation of these metals is important, because such a collection can serve as an effective benchmark to monitor pollution in the above area. Additionally, dating of relatively recent sediment sequences (especially using Pb^{210} geochronology) coupled with measurements of heavy metal concentrations with sediment depth profiles have served a useful purpose in the detection of pollution resulting from anthropogenic activities, as surmised by Bruland *et al.* (1974), Erlenkunser (1974), Goldberg *et al.* (1978), Price *et al.* (1978), UNESCO (1978), Bertine (1978), Bertine *et al.* (1978), and Shirahata *et al.* (1980).

Further, it is to be expected that discharge of dredged spoils as well as drilling muds and cuttings during petroleum exploration and exploitation operations will enhance the suspended loads of waters, with possible deleterious effects on nearshore ecosystems (Schubel and Wise, 1979). However, without an adequate knowledge of the present baselines of suspended loads and trajectories of turbid sediment plumes, any significant industrial perturbations in the loads or trajectories and consequent impact on ecosystems cannot be comprehended.

Additionally, without cognition of the above it would be difficult to lay guidelines for discharge of dredge spoils to coastal waters of the Beaufort Sea. A useful and ready means for monitoring suspended loads and plume structures of surface waters is through study of LANDSAT images. However, reliable criteria have to be established first based on ground truth to quantify sediment loads from LANDSAT images, and this is one of the objectives of the present research unit.

If the response of the physical environment and biological resources of the area to the industrial changes can be properly assessed, or even predicted, it is quite possible that effective measures can be developed to protect or enhance existing resources. Therefore, unless satisfactory

answers are available to account for the sediment fluxes and sources, transport pathways and depositional sites of sediments, and unless adequate knowledge is developed to understand thresholds of sediment movements (as functions of wave-current energy flux), it would not be possible to quantitatively assess — or even speculate — the possible impacts of petroleum exploration and developmental activities on the Beaufort Sea nearshore ecosystem.

IV. CURRENT STATE OF KNOWLEDGE

Within the past ten years or so, considerable research has been accomplished on the processes and products of sedimentation in the continental margin area of the Alaskan Beaufort Sea. A major portion of this research has been accomplished by scientists from three institutions, namely the University of Alaska (Institute of Marine Science), the U.S. Geological Survey (Marine Geology and Alaska Branches, Menlo Park) and the Louisiana State University (Coastal Studies Institute). In a OCSEAP report, Naidu (in Burrell, 1977) has compiled a bibliography of sedimentological and related investigations that have been carried out in the Alaskan Beaufort Sea shelf and coastal area. Barnes *et al.* (1977) have summarized miscellaneous hydrologic and geologic observations as well as characteristics and changing patterns of ice gouging on the Beaufort Sea shelf. The arctic coastal processes and morphology, as studied by the LSU Group, have been condensed in a report by Wiseman *et al.* (1973). Results of more recent investigations, relative to Late Quaternary geologic history, sedimentation, mineralogy and geochemistry, supported by the BLM-NOAA environmental program in the Beaufort Sea coastal and shelf areas have been compiled in the 1977, 1978, 1979 and 1980 OCSEAP Annual and Quarterly Report Volumes, by LGL Ltd. (1980), as well as in the two Beaufort Sea synthesis volumes issued by the Arctic Project Office (Fairbanks). A third synthesis volume is in the preparation stage by the OCS-Arctic Project office.

V. STUDY AREA

The region of our investigations is confined to the inner continental margin of the Alaskan Beaufort Sea (Fig. 1). However, more intensive

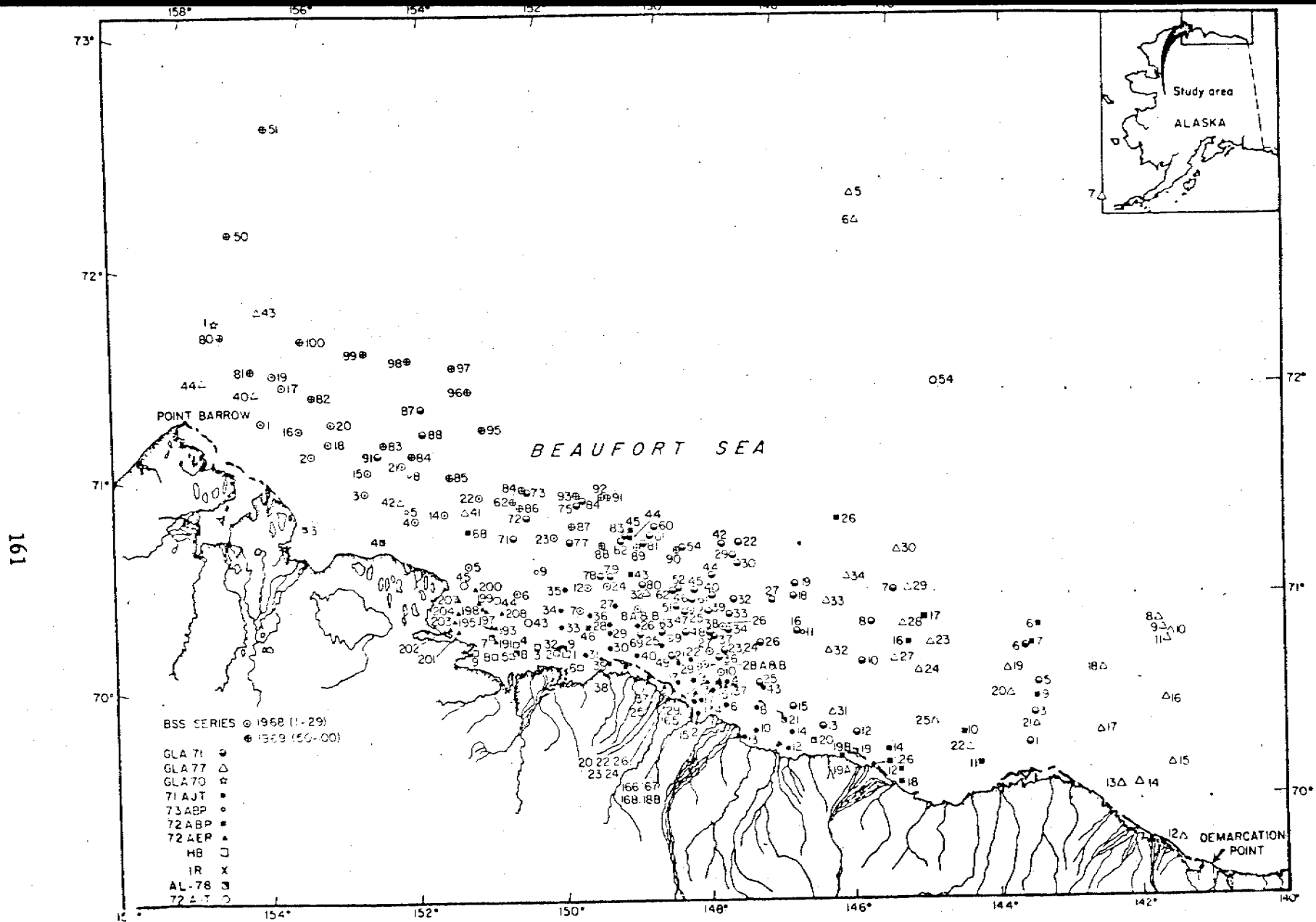


Figure 1. Station locations for Beaufort Sea continental margin region.

study has been limited to the Simpson and Beaufort Lagoon areas (Figs. 2 and 3, respectively).

VI. SOURCES, METHODS AND RATIONALE OF DATA COLLECTION

Field Work and Samples

Refer to Appendix 1 (Field and Cruise report) for details on field work and sample collection conducted between 26 July and 26 August 1980.

Refer to Appendix 2 for report on field studies in Harrison Bay by Dr. L. H. Larsen, under subcontract from this project (RU 529).

Laboratory Work

Laboratory work, since 1 April 1980, has included completion of calculations of the conventional statistical parameters of grain size distributions on Beaufort Lagoon and three Harrison Bay sediments.

In attempting to understand the distribution of nutrients in substrate particulates, nitrogen contents were measured in 93 surficial sediments samples which were collected and archived from a variety of nearshore and deep-sea areas of the Beaufort Sea. Based on organic carbon values recorded by us previously, the C/N ratios for some of the above sediment samples were computed. Further, to elucidate the diagenetic changes, nitrogen concentrations on 1-cm sections of one core sample from the Simpson Lagoon, were also analyzed.

Total carbon, organic carbon, and carbonate contents in 16 sediments from Beaufort Lagoon, 3 sediments from Harrison Bay, 26 sediments from Beaufort Sea were analyzed.

With the purpose of establishing baseline chemical data on a wide geographic data base, Fe, Mn, Cr, and V were analyzed in 17 gross sediment samples from Beaufort Lagoon. Additionally, Fe, Mn, Cu, Cr, Co, Ni, Zn and V were analyzed on the acetic acid-hydroxylamine hydrochloride extracts (Chester and Hughes, 1967) of the 17 sediment samples from the Lagoon.

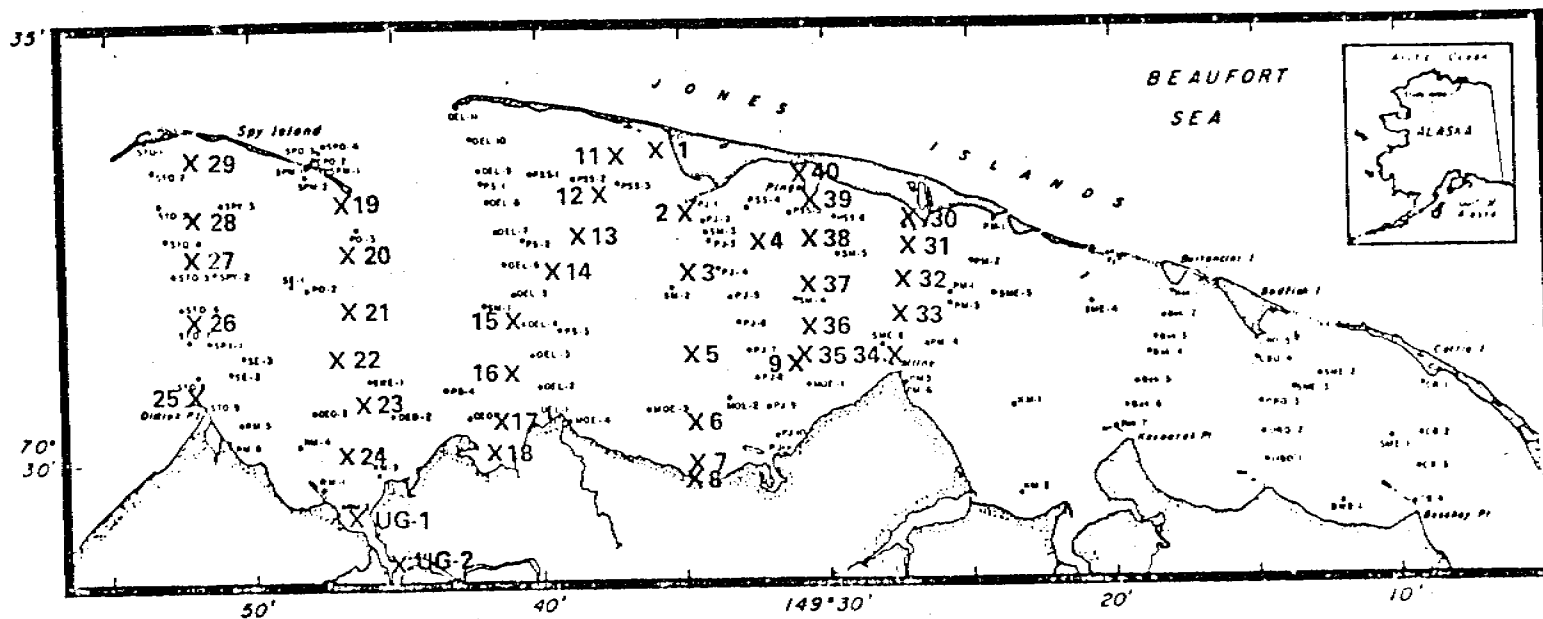


Figure 2. Sample locations in Simpson Lagoon. Locations depicted by heavy crosses indicate samples collected in Summer 1977. The remaining samples were collected by Tucker (1975).

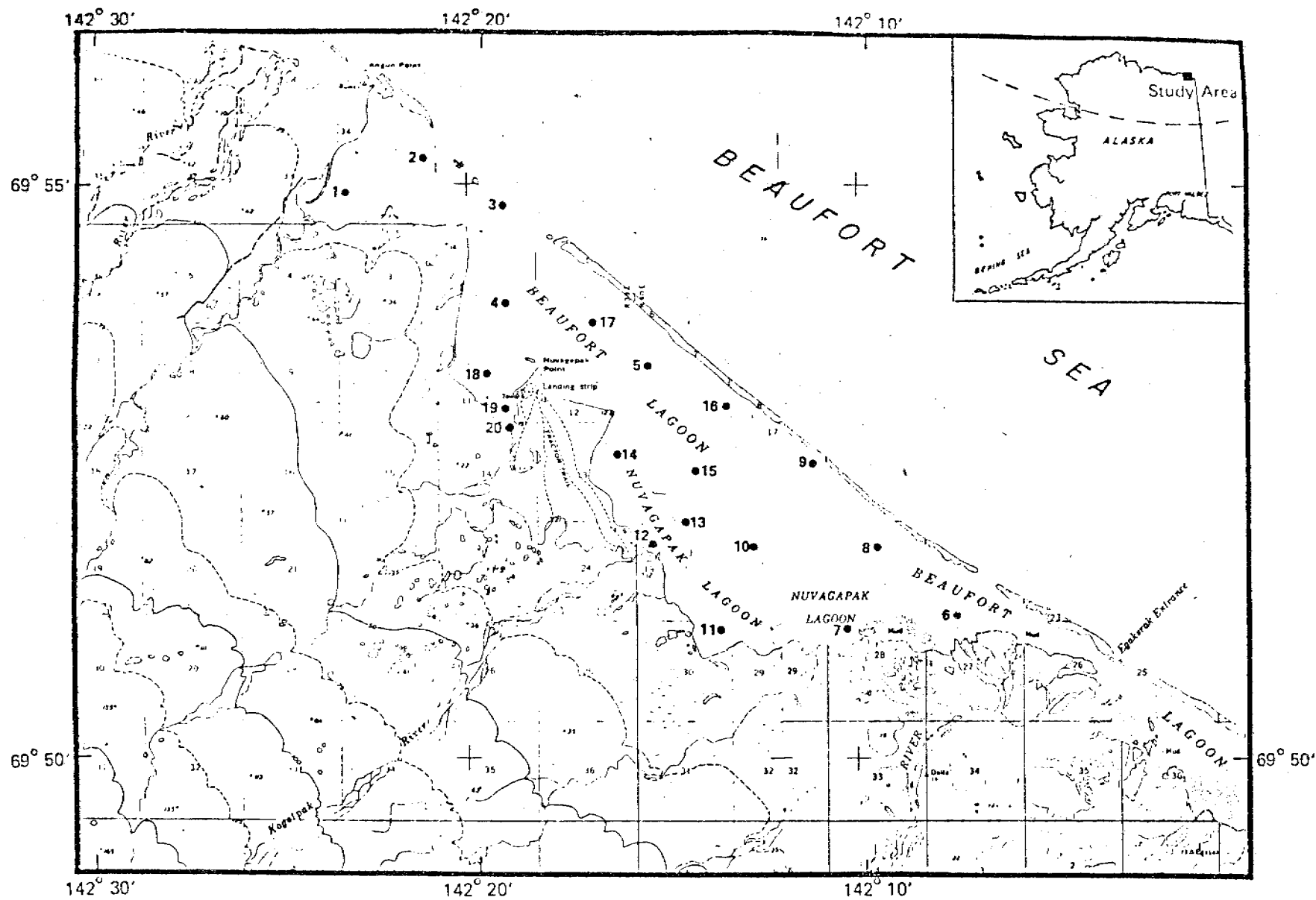


Figure 3. Map showing the locations of sediment samples from the Beaufort Lagoon, north arctic Alaska.

A suite of 54 sediment samples from the nearshore region of the Beaufort Sea (Burrell, 1977; Naidu, 1979) were rerun and revised for gross concentrations of the above eight metals. Trace-metal data reported earlier on the above samples were suspected to be in error. Additional baseline data on gross concentrations of the 8 metals were obtained on the surficial sections of core tops from Harrison Bay and Simpson Lagoon. Further, the stratigraphic variations in the metals were looked for via analysis of centimeter sections on a core sample that was retrieved from Simpson Lagoon in summer of 1979 (Naidu, 1980). On the basis of these elemental analysis and sedimentation rate estimation (as discussed below), fluxes of Fe, Mn, Cu, Cr, Co, Ni, Zn and V were computed for the Simpson Lagoon region.

During the past year, research has been continued to understand the fractionation pattern of the above listed eight metals in sediments of Simpson Lagoon. Presently, the analyzed data is being collated and synthesized.

For ^{210}Pb geochronologic work, relative to sediment depositional rate estimation, 9 cores were collected from Harrison Bay (refer to Appendix 1, Field and Cruise Report). One-cm continuous sections from the cores were separated. One split of each of the 1-cm sections was submitted to Dr. H. V. Weiss for ^{210}Pb assays, while a second split was subjected to gross (i.e., sand, silt and clay) textural analysis. The content of water in each of the core sections was estimated prior to forwarding the sections to Dr. Weiss.

As part of our investigations related to understanding of the geochemistry of Mn, water samples were collected by Dr. Weiss. Complementary to this task, splits of the water samples were taken for salinity, pH and organic carbon (both dissolved and particulate concentrations) measurements.

In continuation of our attempts to develop criteria to interpret suspension loads from LANDSAT images, water samples from a number of stations (Figure 4) were collected (refer to Appendix 1 for details), filtered, and amounts of particulates in them estimated.

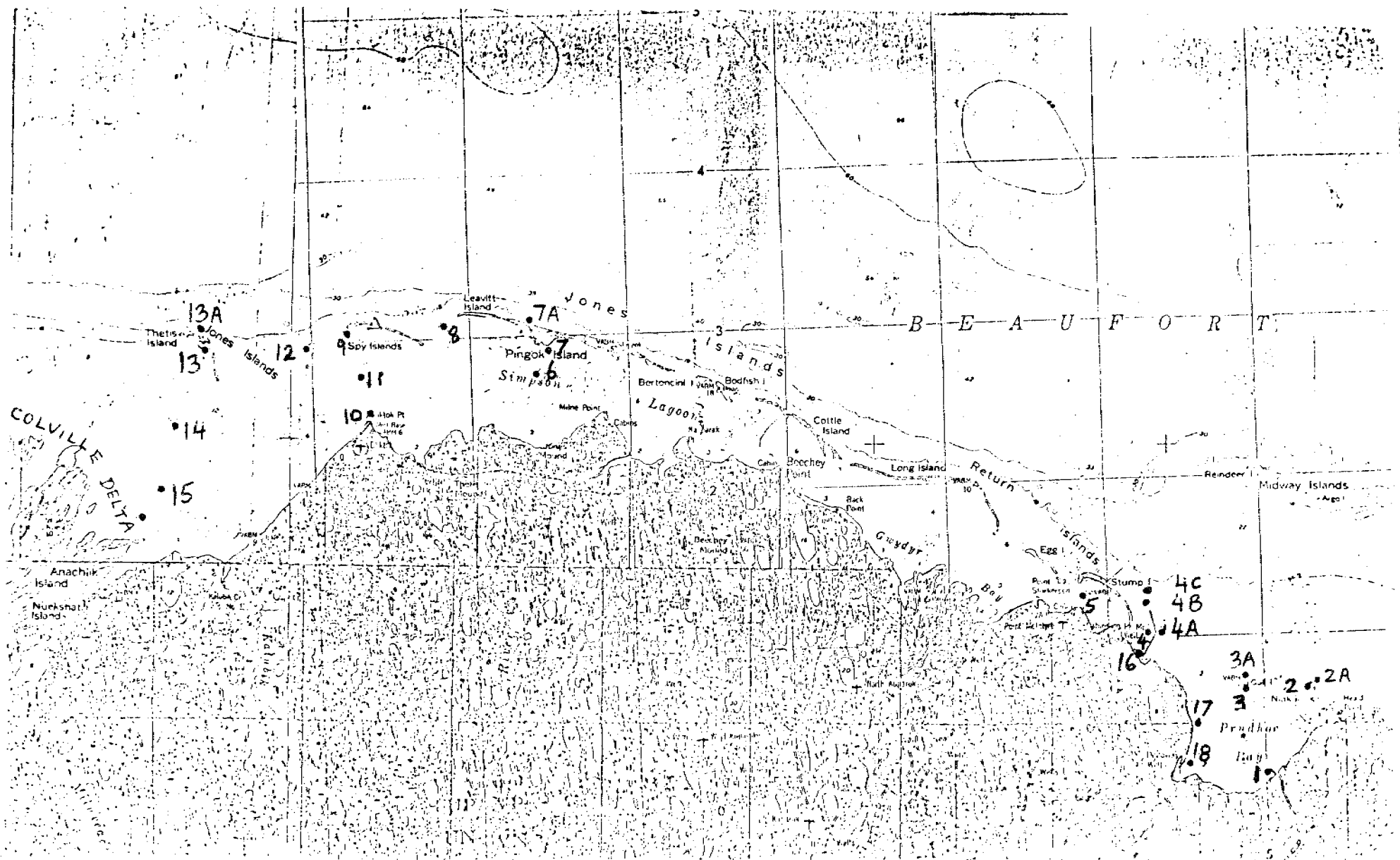


Figure 4. Map showing location of stations in the Simpson Lagoon and Prudhoe Bay region from where water samples were collected synchronizing with the LANDSAT II and III satellite passages in August 1980.

Three sea-ice cores were submitted to us by Dr. T. Osterkamp (RU 253) for estimation of particulate concentrations. Two cores were collected from the nearshore area off the Lonely Dewline station in North Slope, and a third core from Norton Sound off Yukon Delta. This analysis relates to our sediment dynamics study, particularly to understand processes of sediment entrainment in sea-ice.

All available published and unpublished lithological and chemical data have been compiled, and computer digitized maps showing distribution of various parameters in the Beaufort Sea have been generated.

In attempt to substantiate some of our interpretations on the sources of organic carbon and variations in the C/N ratios in sediments of the Beaufort Sea, stable carbon isotopes were analyzed and the $\delta^{13}\text{C}$ values computed on eight sediment samples. These sediments are considered representative samples from Harrison Bay, Simpson Lagoon, open continental shelf of the Beaufort Sea and the adjacent abyssal region of Canada Basin.

Analytical Methods

Grain size analysis was by the conventional sieving-pipetting technique, whereas computation of the statistical textural parameters were after Folk and Ward (1957). The gross metal analysis was performed on acidified solutions of ashed sediments, following HF-HNO₃ digestion (Rader and Grimaldi, 1961); precision and accuracy of the analysis are given in Naidu (1980). To understand metal speciation in sediments, a sequential extraction scheme was followed to isolate various chemical fractions of sediments. Details on the extraction scheme have been elaborated in Naidu (1980). The heavy metals concentrations in the acid solutions or extracts were measured by atomic absorption spectrophotometry, using a Perkin-Elmer, Model 603 unit or a Model 360 unit equipped with a HGA-2100 graphite furnace, or a Model 5000 unit fitted with a 500 Model graphite furnace.

The total carbon in sediments were run on finely pulverized dry samples, using a LECO carbon analyzer, whereas carbonate was analyzed manometrically (Hülsemann, 1966). The difference of the total and

carbonate-bound carbon yielded the organic carbon contents in sediments. The nitrogen concentrations, in finely pulverized sediments, were measured in a Coleman, Model 29B nitrogen analyzer using acetanalide as a standard.

Salinity and pH of the water samples collected in summer 1980 from the Colville Delta and Simpson Lagoon, were measured by using a Beckman, Model RC-19 Conductivity Bridge and a Model 601 ORION digital ionalyzer. Weights of dried particles retained on preweighed Nuclepore filter membranes, following filtration of water samples (constituting summer 1980 collections), were determined on a Cahn balance. A total of 53 samples were processed.

The analytical procedure for the determination of ^{210}Po and thus ^{210}Pb in sediments was based upon the procedures described by Koide *et al.* (1972) and Koide and Bruland (1975). Further details are enumerated in a manuscript recently submitted by us for publication (refer to Appendix 4).

Dissolved and particulate organic carbon contents in water samples from Colville Delta and Simpson Lagoon were provided by Dr. D. C. Burrell; the analysis was by the standard addition method, using an IR unit. Eight sediment samples were analyzed for stable carbon isotopes on an AEI MS 20 mass spectrometer. The $\delta^{13}\text{C}$ values were computed relative to "AER" standard ($^{13}\delta = 27.32$) supplied by Dr. P. Parker of the University of Texas, Port Aransas, Texas. The analysis was conducted for us by Mr. L. Michael Cheek, Stable Isotope Laboratory, Institute of Marine Science, University of Alaska, Fairbanks.

VII. OTHER ACTIVITIES

A. S. Naidu participated in the following workshops/meetings:

- (i) Third synthesis meeting on the Beaufort Sea, sponsored by the Arctic Project Office. It was held between 20 and 23 April 1981 at the Chena Hot Springs Resort.
- (ii) Adaptive Environmental Assessment (AEA) Workshop, to design an environmental monitoring program for Prudhoe Bay Oil Field Waterflood Project. It was held between 4 and 7 May 1981 at the Chena Hot Springs Resort and sponsored by CRREL (Fairbanks).

Attendance at both the above meetings was by invitation.

- (iii) Contributed two manuscripts for publication, and submitted additional abstracts of papers to two national/international meetings. Copies of the manuscripts and abstracts are submitted with this report as Appendices 4, 5, 6 and 7.
- (iv) Submitted two proposals to OCSEAP office; one requesting support for the summer 1980 field work and the second to support the ongoing research work (RU 529) for the period 1 October 1980 to 31 December 1981.

VIII. RESULTS

Statistical grain size parameters (after Folk and Ward, 1957) for a suite of Beaufort Lagoon and Harrison Bay surficial sediments are summarized in Table I. Stratigraphic variations in the sand, silt and clay contents are presented in Table II for 11 core samples collected from Simpson Lagoon and Harrison Bay. The latter analysis was in conjunction with our ^{210}Pb stratigraphic work.

Our geochemical studies have progressed well along the lines we had proposed. In Table III is shown a revised statement on the gross baseline concentrations of a suite of 8 heavy metals in surficial sediments of the Beaufort Sea inshore region. Additional baseline heavy metal data gathered on gross sediment samples from Harrison Bay and Simpson Lagoon are shown in Table IV. The concentrations of Fe, Mn, Zn, Cu, Ni, Co, Cr and V in gross sediments and in acetic acid hydroxylamine-hydrochloride extracts (Chester and Hughes, 1967) are indicated in Tables V and VI. Stratigraphic variations in the 8 heavy metals on a core sample from Simpson Lagoon are presented in Table VII. No systematic variations with core depth in the heavy metal concentrations were identified. Fluxes of the eight metals into the Simpson Lagoon sediments have been estimated (Appendix 3) based on average concentrations of the metals (Naidu, 1979, 1980; and also data in Tables IV and VII) and average sedimentation rate (Appendix 4) for the Lagoon.

The organic carbon and nitrogen contents, and C/N ratios for the continental margin and deep-sea sediments of Beaufort Sea and Canada basin

TABLE I

STATISTICAL GRAIN SIZE DISTRIBUTIONS (after Folk and Ward, 1957)
OF BEAUFORT LAGOON (BL series) AND HARRISON BAY (HB series) SEDIMENTS

Refer to Naidu (1980) and Figure 3 for sample locations

Sample No.	% Gravel	% Sand	% Silt	% Clay	Median	Mean	Sorting	Skewness	Kurtosis
HB- A	0.00	10.49	73.06	16.46	4.43	5.65	2.25	0.83	1.17
HB- B	0.00	96.50	2.11	1.39	3.13	3.17	0.28	0.32	1.27
HB- C	0.00	68.26	23.01	8.73	3.45	3.74	1.81	0.57	2.62
BL- 1	0.00	15.53	61.47	23.01	6.00	6.32	2.29	0.25	0.84
BL- 2	0.00	26.00	53.06	20.94	5.51	5.89	2.63	0.26	0.98
BL- 3	0.35	97.83	1.19	0.63	1.93	1.90	0.39	-0.09	1.02
BL- 4	0.00	7.53	66.42	26.05	6.28	6.67	2.31	0.29	0.94
BL- 5	0.00	53.94	28.45	17.61	2.66	4.22	3.33	0.66	0.76
BL- 6	0.00	77.76	15.52	6.72	2.56	3.08	1.74	0.81	5.34
BL- 7	0.00	97.11	1.68	1.22	2.49	2.50	0.39	0.08	1.22
BL- 8	0.00	98.53	0.59	0.88	1.89	1.91	0.38	0.10	1.01
BL- 9	0.00	32.86	52.23	14.91	4.65	4.92	2.67	0.25	0.89
BL-10	0.00	1.40	64.08	34.53	7.23	7.65	2.25	0.24	1.05
BL-11	0.00	1.61	59.73	38.66	7.43	7.58	2.26	0.08	0.87
BL-12	68.85	31.15	0.00	0.00	-2.56	-1.43	2.41	0.59	0.65
BL-14	0.00	15.74	60.60	23.66	6.12	6.34	2.40	0.17	1.00
BL-15	0.00	3.36	44.78	51.87	8.06	8.12	2.28	0.01	1.17
BL-16	0.00	9.07	68.09	22.85	5.90	6.40	2.26	0.32	1.06
BL-17	0.00	28.41	54.08	17.51	5.36	5.75	2.24	0.33	0.85
BL-18	0.54	36.96	42.19	20.32	6.18	5.65	2.91	-0.16	0.71
BL-19	62.09	37.91	0.00	0.00	-2.93	-1.76	2.67	0.54	0.53
BL-20	0.00	83.73	13.06	3.21	2.98	2.98	1.30	0.20	1.52

TABLE II

STRATIGRAPHIC VARIATIONS IN GROSS TEXTURE OF SEDIMENT CORES
TAKEN FROM SIMPSON LAGOON AND HARRISON BAY

Refer to Naidu (1980) and Appendix 1 for core location

Core Section (cm)	% Sand	% Silt	% Clay
<u>SL879-1</u>			
0- 1	57.97	28.03	13.99
1- 2	50.28	30.68	19.04
2- 3	48.79	31.95	19.26
3- 4	53.98	30.00	16.02
4- 5	42.01	38.44	19.54
5- 6	85.95	8.11	5.94
6- 7	95.56	2.34	2.10
7- 8	96.14	1.98	1.88
8- 9	89.27	6.99	3.74
9-10	61.82	28.05	10.13
10-11	44.67	41.06	14.26
11-12	38.47	47.38	14.16
12-13	43.07	45.58	11.35
13-14	40.54	47.87	11.59
14-15	27.56	56.40	16.04
15-16	20.91	57.24	21.85
16-17	12.47	63.58	23.95
17-18	22.82	59.44	17.74
<u>SL879-3</u>			
0- 1	9.25	62.31	28.44
1- 2	7.73	65.30	26.97
2- 3	8.38	75.68	15.94
3- 4	6.79	79.15	14.06
4- 5	15.00	73.34	11.66
5- 6	32.96	49.98	17.06
6- 7	26.08	57.22	16.70
7- 8	19.08	62.68	18.24
8- 9	27.69	52.74	19.57
9-10	42.93	35.85	21.22
10-11	47.22	31.59	21.19
11-12	47.28	30.66	22.06
12-13	45.36	32.75	21.88
13-14	49.77	30.44	19.79
14-15	53.37	27.29	19.34
15-16	56.81	22.99	20.20

TABLE II

CONTINUED

Core Section (cm)	% Sand	% Silt	% Clay
<u>SL879-3 (Cont'd)</u>			
16-17	60.07	21.36	18.57
17-18	72.00	14.22	13.78
18-19	75.56	11.67	12.77
19-20	49.32	26.55	24.13
20-21	49.78	28.72	21.50
21-22	42.55	4.10	53.35
22-23	43.85	33.01	23.13
23-24	43.03	33.59	23.38
24-25	41.94	34.52	23.54
<u>HB8083-1</u>			
0- 1	45.91	47.41	6.67
1- 2	40.45	50.96	8.59
2- 3	32.97	61.05	5.98
3- 4	35.96	58.42	5.61
4- 5	44.33	51.35	4.32
5- 6	72.55	23.57	3.88
6- 7	85.72	11.72	2.55
7- 8	84.60	15.30	0.10
8- 9	77.01	20.80	2.19
9-10	63.75	33.94	2.31
10-11	62.64	34.46	2.91
11-12	22.02	70.34	7.65
12-13	42.97	51.49	5.54
13-14	40.76	55.92	3.31
14-15	19.61	68.85	11.54
15-16	25.97	69.16	5.06
16-17	7.30	81.08	11.62
17-18	6.77	81.22	12.00
18-19	4.21	85.00	10.78
19-20	2.84	83.07	14.09
20-21	5.96	84.46	9.57
21-22	11.37	84.32	4.31
22-23	6.29	85.56	8.15
23-24	7.52	80.89	11.59
24-25	10.04	77.86	12.09
25-26	12.10	76.38	11.52

TABLE II

CONTINUED

Core Section (cm)	% Sand	% Silt	% Clay
<u>HB8083-2</u>			
0- 1	11.70	61.22	27.07
1- 2	11.79	57.39	30.82
3- 4	12.61	59.40	27.99
5- 6	8.98	58.29	32.73
6- 7	4.22	68.17	27.61
8- 9	6.59	67.89	25.52
9-10	3.12	65.25	31.62
11-12	31.50	58.44	10.06
12-13	19.64	67.42	12.94
14-15	11.74	66.99	21.27
15-16	13.70	60.63	25.66
17-18	17.86	61.84	20.30
<u>HB80810-1</u>			
0- 1	9.63	75.93	14.44
1- 3	12.56	72.69	14.75
3- 5	3.59	79.16	17.26
5- 7	4.41	70.45	25.14
7- 9	13.55	65.26	21.19
9-11	4.17	81.91	13.92
11-13	2.50	72.33	25.17
13-15	12.44	73.68	13.88
15-17	7.07	84.49	8.43
17-19	12.04	72.79	15.18
<u>HB80810-4</u>			
0- 1	41.77	53.16	5.07
1- 3	48.96	49.82	1.23
3- 5	58.41	39.92	1.67
5- 7	51.73	45.19	3.08
7- 9	45.12	52.11	2.76
9-11	22.86	68.37	8.77
11-13	44.02	51.13	4.85
13-15	59.74	35.28	4.98
15-17	59.95	36.22	3.84
17-18	61.16	34.74	4.11

TABLE II

CONTINUED

Core Section (cm)	% Sand	% Silt	% Clay
<u>HB80810-5</u>			
0- 1	86-31	9.94	3.75
1- 3	87-38	9.87	2.74
3- 5	91.59	6.26	1.3
5- 7	91.39	6.98	1.62
7- 9	86.45	11.76	1.79
9-11	95.36	3.26	1.39
11-13	93.50	4.56	1.94
13-15	88.25	9.34	2.41
15-17	88.20	8.47	3.32
17-19	88.58	7.18	4.25
19-21	81.63	14.38	3.99
<u>HB80810-6</u>			
0- 1	54.46	35.65	10.88
1- 3	70.82	25.12	4.07
<u>HB80810-7</u>			
0- 1	66.05	30.81	3.14
1- 3	55.48	40.49	4.03
3- 5	47.23	48.98	3.79
5- 7	27.94	66.53	5.52
7- 9	41.60	52.63	5.78
9-11	32.10	61.28	6.62
11-13	19.88	74.74	5.38
13-15	20.91	70.34	8.76
15-17	29.62	58.30	12.08
17-19	19.20	72.14	8.66
19-21	23.90	67.47	8.61
<u>HB80811-8</u>			
0- 1	36.48	56.05	7.46
1- 3	52.96	44.56	2.48
3- 5	37.80	51.85	10.35
5- 7	61.80	31.12	7.08
7- 9	66.07	29.63	4.30

TABLE II

CONTINUED

Core Section (cm)	% Sand	% Silt	% Clay
<u>HB80811-8 (Cont'd)</u>			
9-11	54.19	32.80	13.01
11-13	53.75	39.58	6.67
13-15	43.70	44.77	11.53
15-17	27.69	50.67	21.64
17-19	19.58	59.24	21.18
19-21	34.40	56.25	9.35
21-23	64.09	25.63	10.28
23-25	61.77	21.55	16.68
25-26	64.38	22.46	13.16
<u>HB80811-14</u>			
0- 1	9.05	63.11	27.84
1- 3	8.30	54.79	36.90
3- 5	5.87	54.01	40.12
5- 7	21.64	52.78	25.58
7- 9	69.18	26.98	3.83
9-11	90.30	6.23	3.47
11-13	43.25	38.16	18.58
13-15	27.78	41.46	30.76
15-17	13.30	56.48	30.22
17-18	65.88	17.57	16.54
18-19	93.23	3.70	3.07
19-21	43.46	34.33	22.21
21-23	15.59	55.23	29.18
23-25	8.78	62.24	28.97
25-27	7.65	64.28	28.06
27-29	1.64	59.86	38.50
29-30	12.13	58.19	29.67
30-32	8.50	57.78	33.72
32-33	46.82	25.81	27.37

TABLE III

REVISED DATA (from Naidu, 1979) ON THE CONCENTRATIONS
($\mu\text{g/g}$, except for Fe which is in $10^4\mu\text{g/g}$)
OF CERTAIN METALS IN GROSS SEDIMENTS FROM THE BAYS, LAGOONS,
AND SOUNDS OF THE COASTAL REGION OF THE BEAUFORT SEA

Refer to Naidu (1976) for station locations and water depths

Sample	V	Cr	Mn	Fe	Co	Ni	Cu	Zn
71-AJT- 1	59	36	240	1.8	6	24	9	54
71-AJT- 2	100	55	250	1.9	9	35	19	87
71-AJT- 3	110	59	250	0.8	8	36	22	82
71-AJT- 4	52	26	165	1.4	5	20	12	40
71-AJT- 5	69	39	240	1.3	6	22	11	49
71-AJT- 8	70	42	220	1.3	5	40	14	55
71-AJT-12	95	58	270	2.4	8	32	19	76
71-AJT-13	91	47	290	1.8	7	34	22	47
71-AJT-14	80	62	205	1.8	6.5	24	17	70
71-AJT-15	74	48	250	2.3	6.5	35	19	72
71-AJT-16	91	51	270	2.3	7.5	30	16	73
71-AJT-17	120	87	375	2.2	11	43	29	100
71-AJT-18	165	110	375	3.2	16	49	32	110
71-AJT-19	72	49	270	2.1	6.5	26	14	55
71-AJT-20	120	70	285	2.3	9.5	35	22	81
71-AJT-21	65	44	220	1.1	5.5	20	10	39
71-AJT-22	92	42	270	2.1	6	24	14	54
71-AJT-25	120	68	355	2.2	11	43	29	89
71-AJT-26	31	25	100	1.0	4	7	8	110
71-AJT-29	66	33	150	1.5	5.5	15	11	45
71-AJT-30	64	23	200	1.0	5.5	18	17	57
71-AJT-31	120	69	500	3.3	11	35	27	83
71-AJT-32	48	35	150	1.0	5.5	15	8	41
71-AJT-33	120	69	310	2.8	10.5	32	21	100
71-AJT-35	140	75	435	2.3	12.5	35	26	100
71-AJT-36	55	41	250	1.5	4	13	10	39
71-AJT-37	83	52	285	2.1	8	27	19	81
71-AJT-38	90	44	205	1.7	7	27	24	150
71-AJT-39	105	57	310	2.5	9.5	29	17	75
71-AJT-40	110	64	355	2.1	7.5	32	31	110
71-AJT-43	140	77	410	2.4	11	35	13	230
71- HB- 1	110	72	650	3.5	12.5	43	21	140
71- HB- 3	55	42	295	2.3	6	23	7	55
71- HB- 4	140	77	545	2.1	15	49	11	150
71- HB- 5	55	43	340	2.8	6	30	24	55
71- HB- 6	110	76	485	1.7	13	40	19	82
71- HB- 7	90	58	570	3.2	8.5	32	34	77
71-BSS-83	180	86	270	3.5	15	42	19	100
71-BSS-84	140	71	285	3.0	11.5	35	16	100
71-AER-15	83	48	355	2.1	8	30	14	77

TABLE III

CONTINUED

Sample	V	Cr	Mn	Fe	Co	Ni	Cu	Zn
72-AER- 20	55	42	150	1.1	5.5	35	22	47
72-AER- 22	110	55	280	1.8	8	33	14	90
72-AER- 23	74	43	170	1.7	6.5	24	14	66
72-AER- 24	80	42	205	1.5	6	24	11	71
72-AER- 25	70	42	160	1.8	6.5	20	12	56
72-AER- 26	240	130	375	4.8	18	59	83	160
72-AER-120	135	71	330	2.9	9.5	33	14	89
72-AER-134	150	85	355	2.8	13	37	18	100
72-AER-137	60	25	150	1.4	8	13	12	40
72-AER-166	87	50	260	2.2	6	26	19	81
72-AER-167	67	42	205	2.3	5	22	12	60
72-AER-168	100	48	270	2.1	6	29	24	82
70- BS- 21	105	54	285	1.7	7	28	19	78
70- BS- 22	110	55	285	2.6	8	29	20	78

TABLE IV

CONCENTRATIONS OF SOME HEAVY METALS IN GROSS SEDIMENTS
FROM HARRISON BAY AND SIMPSON LAGOON

Concentrations of all metals except Fe are in $\mu\text{g/g}$, whereas
that of Fe which is in $10^4\mu\text{g/g}$

Sample	Latitude (N)	Longitude (W)	Water Depth (m)	Zn	Co	Ni	Cu	Cr	V	Fe	Mn
<u>Harrison Bay</u>											
HB80810- 4	70°30'	151°15'	2.5	93	7	26	28	52	63	2.18	255
HB80811- 5	70°34'	151°30'	2.5	72	7	26	15	46	70	2.03	255
HB80811- 6	70°36'	151°51'	2.1	60	9	28	13	44	63	2.25	330
HB80811- 7	70°40'	152°15'	1.5	82	11	30	20	52	80	2.50	490
HB80811- 8	70°42'	152°00'	1.5	99	9	29	25	60	93	2.50	330
HB80811-10	70°37'	151°39'	4.2	171	7	23	20	42	70	2.05	235
HB-K0A	70°42'	151°00'	15	98	7	21	40	55	77	2.38	294
HB-K1A	70°44'	151°19'	16	70	13	34	35	84	160	3.30	647
HB-K1B	70°36'	151°15'	10	67	7	21	30	60	83	2.13	255
HB-K3C	70°45'	151°38'	11	66	11	31	35	65	108	2.83	353
HB-J3A	70°36'	150°32'	10	53	6	18	13	47	56	2.05	294
HB-J4B	70°35'	150°46'	10	114	13	36	30	81	136	3.48	650
HB-J5A	70°35'	150°57'	10	95	13	34	30	80	136	3.20	373
<u>Simpson Lagoon</u>											
SL8979-1	70°32'	150°07'	3.9	105	16	41	35	80	145	3.75	490
SL8979-2	70°31'	150°01'	3.6	89	13	31	25	68	118	2.73	255
SL8979-4	70°32'	149°53'	3.0	74	7	28	20	55	93	2.30	235
SL8979-7	70°32'	149°35'	2.6	83	9	28	30	51	90	2.25	320

TABLE V

CONCENTRATIONS OF Fe, Mn, Cr and V IN GROSS SEDIMENTS OF THE
BEAUFORT LAGOON, NORTH ARCTIC ALASKA

Refer to Naidu (1980) and Figure 3 for sample locations

Sample No.	Fe $10^4 \times \mu\text{g/g}$	Mn $\mu\text{g/g}$	Cr $\mu\text{g/g}$	V $\mu\text{g/g}$
BL- 1	2.30	250	60	135
BL- 2	2.55	275	58	130
BL- 3	1.75	215	30	85
BL- 4	2.65	310	65	140
BL- 4(D)*	2.75	310	68	135
BL- 5	2.30	350	48	95
BL- 6	2.50	365	48	105
BL- 7	2.70	465	48	130
BL- 8	1.60	330	25	60
BL- 9	2.75	375	58	120
BL-10	3.35	400	73	153
BL-11	3.50	465	94	170
BL-14	2.75	415	65	135
BL-14(D)*	2.75	415	65	135
BL-15	3.50	375	78	145
BL-16	2.80	375	65	135
BL-17	2.60	365	60	110
BL-18	2.85	350	65	125
BL-20	1.85	200	40	95
Average	2.62	348	59	123

*Duplicate analysis.

TABLE VI

CONCENTRATION OF SOME METALS IN TOTAL (T) AND CHESTER AND HUGHE'S EXTRACTS (CHE),
AND THE PERCENTAGES OF EXTRACT OF THE TOTAL (% CHE)

Concentrations of Fe are expressed in $10^4 \mu\text{g/g}$, whereas of other metals are in $\mu\text{g/g}$

Sample No.	Fe			Mn			Zn			Cu			Ni			Co			Cr			V		
	T	CHE	%CHE	T	CHE	%CHE	T	CHE	%CHE	T	CHE	%CHE	T	CHE	%CHE	T	CHE	%CHE	T	CHE	%CHE	T	CHE	%CHE
BL- 1	2.30	0.48	21	250	233	93	71	15	21	24	2.9	12	43	2.9	7	23	3.5	15	60	1.5	3	135	11	8
BL- 2	2.55	0.29	11	275	130	47	71	18	25	23	3.4	15	40	3.7	9	13	3.0	23	58	2.3	4	130	15	12
BL- 3	1.75	0.02	1	215	66	31	32	2.7	8	8	0.56	7	20	0.80	4	28	1.4	5	30	0.4	1	85	0.8	1
BL- 4	2.65	0.35	13	310	190	61	78	20	26	21	5.3	25	48	3.8	8	30	3.5	12	65	2.3	4	140	16	11
BL- 4 (D)	2.75			310			71			17			43		25				68			135		
BL- 5	2.30	0.20	9	350	205	59	58	13	22	16	4.5	28	33	2.7	8	20	3.0	15	48	1.3	3	95	8.5	9
BL- 6	2.50	0.11	4	365	218	60	62	5.2	8	20	3.0	15	35	2.3	7	22	2.8	13	48	1.0	2	105	2.3	2
BL- 7	2.70	0.08	3	465	221	48	65	5.1	8	19	2.4	13	40	1.5	4	22	1.9	9	48	0.9	2	130	2.1	2
BL- 8	1.60	0.03	2	330	178	54	32	2.8	9	13	1.1	9	18	0.96	5	10	1.3	13	25	0.3	1	60	0.8	1
BL- 9	2.75	0.25	9	375	195	52	72	15	21	28	4.4	16	40	3.3	8	26	3.8	15	58	1.5	3	120	9.3	8
BL-10	3.35	0.34	10	400	170	43	88	22	25	23	6.7	23	53	3.8	7	32	4.8	15	73	2.5	3	153	15	10
BL-11	3.50	0.45	13	465	258	55	102	23	23	28	7.2	26	58	3.8	7	35	5.0	14	94	2.0	2	170	9.8	6
BL-14	2.75	0.53	19	415	265	64	70	31	44	25	3.4	14	48	6.7	14	30	4.8	16	65	3.0	5	135	15.5	11
BL-14 (D)	2.75	0.49	18	415	258	62	65			20			49		28				65			135		
BL-15	3.50	0.51	15	375	193	51	90	22	24	21	7.0	33	53	3.2	6	32	5.0	16	78	1.8	2	145	14	10
BL-16	2.80	0.38	14	375	233	62	88	18	20	13	6.6	51	48	3.8	8	28	4.5	16	65	1.5	2	135	11	8
BL-17	2.60	0.38	15	365	230	63	75	15	20	21	5.7	27	45	3.5	8	25	3.8	15	60	1.3	2	110	8.8	8
BL-18	2.85	0.43	15	350	208	59	82	22	27	23	4.4	19	52	4.7	9	29	4.5	16	65	2.0	3	125	11	9
BL-20	1.85			200			42	9.4	23	10	1.3	13	30	2.7	9	15	3.0	20	40	1.3	3	95	2.0	2

TABLE VII

STRATIGRAPHIC VARIATIONS IN HEAVY METAL CONTENTS IN CORE SL8979-3
FROM SIMPSON LAGOON (refer to Naidu, 1980 for core location)

Concentrations of all metals except Fe are in $\mu\text{g/g}$, whereas
that of Fe is expressed as $10^4 \times \mu\text{g/g}$

Core Section (cm)	Zn	Co	Ni	Cu	Cr	V	Fe	Mn
0- 3	102	23	41	31	56	90	2.26	300
3- 6	98	20	39	29	45	81	1.83	240
6- 9	79	25	33	21	55	98	2.35	275
9-12	75	20	39	23	50	81	2.00	225
12-15	81	23	44	27	53	96	2.25	225
15-18	60	15	26	23	41	63	1.78	198
18-21	67	19	26	22	49	75	2.10	218
21-24	74	20	37	23	50	88	2.15	225
24-25	75	20	29	23	50	95	2.25	225

respectively, are summarized in Table VIII. One-cm sections of a sediment core from Simpson Lagoon were also processed for the above attributes and the results are given in Table IX. It would seem that there is a progressive seaward decrease in the C/N ratios (Table VIII).

In Tables X and XI total carbon, organic carbon and carbonate contents in sediments of Beaufort Lagoon, Harrison Bay and open Beaufort Sea are listed.

In continuation of our winter sediment dynamic studies, concentrations of sediment particles encapsulated in sea ice were measured. As mentioned earlier, one of these three samples was collected from the Norton Sound area off the Yukon River and the other two off the Lonely Dewline Station in Beaufort Sea by Dr. Osterkamp (RU 253). It is noteworthy that the concentrations of particulates (Tables XII) can be a few orders of magnitude higher in some ice core sections than those generally encountered in sea water from the above areas.

^{210}Pb assays by Dr. Weiss on the sediment core sections collected in summer 1980 have not been completed as yet. The ^{210}Pb data on summer 1979 samples have been consolidated into a manuscript (refer to Naidu and Weiss, Appendix 4).

The concentrations (mg/l) of particulate matter retained on Nuclepore membranes after filtering water samples that were collected in conjunction with the LANDSAT image studies, are summarized in Table XIII.

IX. DISCUSSION

All available data on grain size distributions, clay mineralogy and geochemistry of sediments have been consolidated, and a first attempt has been made to synthesize the data. The outcome of this effort is a Draft Synthesis Report which is included as Appendix 3. The latter report is brief and will serve as a basis for a full-blown final (synthesis) report to be submitted to the OCSEAP office, hopefully by December 1981.

The ^{210}Pb stratigraphic work on summer 1979 sediment cores and the sedimentation rates estimated on the basis of those data, have also been consolidated and communicated for publication (refer to Appendix 4).

TABLE VIII

CONCENTRATIONS (wt. %) OF ORGANIC CARBON AND NITROGEN, AND C/N RATIOS
IN CONTINENTAL MARGIN AND DEEP-SEA SEDIMENTS OF
THE BEAUFORT SEA

For locations of samples, refer to Naidu and Mowatt (1974),
Naidu (1979) and Figures 1, 2 and 3 of this report

Environment and Sample No.	Water Depth (m)	C (%)	N (%)	C/N
<u>Lagoon</u>				
SL877- 2	1.8	0.16	0.025	6.4
SL877- 3	2.6	1.13	0.114	9.9
SL877- 4	2.1	1.74	0.127	13.7
SL877- 5	1.8	0.89	0.055	16.2
SL877- 6	2.0	2.69	0.156	17.2
SL877- 7	0.9	0.27	0.019	14.2
SL877- 8	0.3	1.83	0.094	19.5
SL877- 9	1.5	2.19	0.156	14.1
SL877-11	2.1	0.45	0.100	4.5
SL877-12	2.1	1.65	0.094	17.6
SL877-13	2.4	1.10	0.088	12.5
SL877-14	2.3	1.40	0.089	15.7
SL877-15	1.8	0.30	0.084	3.67
SL877-17	0.6	0.59	0.098	6.0
SL877-18	0.5	3.12	0.201	15.5
SL877-19	3.2	0.42	0.023	18.3
SL877-20	2.6	0.35	0.026	13.5
SL877-21	2.9	1.47	0.103	14.3
SL877-22	2.4	1.59	0.090	17.7
SL877-23	2.4	2.18	0.125	17.4
SL877-24	1.5	0.83	0.063	13.2
SL877-25	2.6	1.99	0.093	21.4
SL877-26	2.9	1.14	0.097	11.8
SL877-27	3.1	1.13		
SL877-28	2.7	1.23	0.089	13.8
SL877-29	2.4	0.70	0.093	7.5
SL877-30	1.0	0.32	0.025	12.8
SL877-31	2.6	1.65		
SL877-32	2.3	1.56	0.091	17.1
SL877-34	1.5	0.09	0.013	6.9
SL877-35	2.0	1.66		
SL877-36	2.1	1.47	0.087	16.9
SL877-37	2.3	1.11		
SL877-38	2.3	1.00	0.100	10.0
SL877-39	2.0	1.36		
SL877-40	1.5	0.46	0.044	10.5

TABLE VIII

CONTINUED

Environment and Sample No.	Water Depth (m)	C (%)	N (%)	C/N
<u>Lagoon (Cont'd)</u>				
AJT71- 1		0.22	0.01	22.0
AJT71- 2		0.98	0.09	10.8
AJT71- 8		0.49	0.02	24.5
AJT71-12		0.84	0.10	8.4
AJT71-13		0.78	0.09	8.7
AJT71-14		0.59	0.05	11.8
AJT71-17		1.36	0.14	9.7
AJT71-38	1.5	1.51	0.13	11.6
AJT71-39	2.1	0.53	0.06	8.8
<u>Bay</u>				
AJT71-29		1.32	0.10	13.2
AJT72-44		0.54	0.09	6.0
AJT72-45		0.23	0.05	4.6
HB-1	3.2	1.13	0.09	12.4
HB-3	3.0	0.17	0.01	12.1
HB-4	3.0	1.40	0.13	11.0
HB-5	3.0	1.15	0.07	17.2
HB-6	2.8	1.15	0.07	17.2
HB-7	2.3	0.80	0.07	11.4
<u>Open Continental Shelf (>64 m)</u>				
ABP72-46		0.06	0.01	6.0
ABP73- 5		1.05	0.09	11.6
ABP73- 8		0.82	0.09	9.1
ABP73- 9		0.50	0.06	8.3
ABP73-23		0.60	0.06	10.0
AJT71-29		0.36	0.05	7.2
AJT71-33		0.67	0.07	9.6
AJT71-35		0.61	0.06	10.1
AJT71-40		2.25	0.18	12.5
BSS -82		0.77	0.08	9.6
BSS -85		0.73	0.06	12.1
BSS -87		0.77	0.12	8.3
BSS -89		0.81	0.10	8.1
GLA77-12		0.75	0.07	10.7
GLA77-14		0.71	0.07	10.1
GLA77-15		0.70	0.10	7.0

TABLE VIII

CONTINUED

Environment and Sample No.	Water Depth (m)	C (%)	N (%)	C/N
<u>Open Continental Shelf (Cont'd)</u>				
GLA77- 20		0.45	0.07	6.4
GLA77- 22		0.62	0.08	7.8
GLA77- 27		0.43	0.08	5.4
GLA77- 31		0.51	0.06	8.5
GLA77- 33		0.74	0.10	7.4
SMG -1344		0.66	0.07	9.4
SMG -1397		0.81	0.13	6.2
HB - 7	2.3	0.80	0.074	11.8
BSS - 88	30	0.80	0.091	8.8
BSS - 83	50	0.96	0.119	8.1
BSS - 62	44	0.63	0.076	8.3
GLA71- 1	26	0.89	0.080	11.1
GLA71- 3	45	0.98	0.062	15.8
GLA71- 12	26	0.64	0.085	7.5
GLA71- 25	26	Trace	0.093	
GLA71- 27	47	0.45	0.048	9.4
GLA71- 44	48	0.69	0.071	9.7
GLA71- 63	26	0.60	0.090	6.7
GLA71- 71	21	0.81	0.073	11.1
GLA71- 72	47	0.87	0.110	7.9
GLA71- 78	29	1.12	0.132	8.5
GLA71- 80	33	0.91	0.100	9.1
<u>Continental Slope (64-1,000 m)</u>				
BSS - 50		1.06	0.11	9.6
BSS - 80		0.96	0.15	6.4
BSS - 81		1.46	0.17	8.6
BSS - 95		1.47	0.17	8.6
BSS - 99		1.36	0.15	9.1
BSS - 100		1.16	0.12	9.6
GLA71- 5		0.42	0.09	4.7
GLA71- 6		0.76	0.14	5.4
GLA71- 8		0.16	0.06	2.7
GLA71- 22		0.66	0.15	4.4
GLA71- 58		1.00	0.15	6.7
GLA71- 85		1.33	0.16	8.3
GLA77- 11		1.06	0.15	7.1
GLA77- 16		0.67	0.08	8.4
GLA77- 18		0.31	0.06	5.2
GLA77- 19		0.76	0.12	6.0
GLA77- 23		0.83	0.09	0.2
GLA77- 28		0.92	0.11	8.4
GLA77- 29		0.63	0.12	5.3

TABLE VIII

CONTINUED

Environment and Sample No.	Water Depth (m)	C (%)	N (%)	C/N
<u>Deep-Sea (>1,000 m)</u>				
BSS -51	2477	0.91	0.13	7.0
BSS -97	1500	1.34	0.17	7.9
GLA71-20	2000	1.05	0.16	6.6
GLA71-21	2200	1.00	0.17	5.9
GLA71-57	1829	1.04	0.18	5.8
GLA71-86	2150	1.53	0.23	6.7
GLA77- 5	3593	0.78	0.10	7.8
GLA77- 6	3566	0.56	0.11	5.1
GLA77- 7	3566	0.58	0.09	6.4
GLA77- 8	2048	0.60	0.15	4.0
GLA77-30	1829	0.70	0.09	7.8
T3 - 1	3637	0.74	0.130	5.6
T3 - 2	3650	0.71	0.108	6.5
T3 - 3	3795	0.73	0.218	3.3
T3 - 4	3792	0.74	0.240	3.1
T3 - 5	3761	0.75	0.20	3.8
T3 - 6	3827	0.79	0.346	2.3
T3 - 7	3830	0.77	0.347	2.2
T3 - 8	3833	1.16	0.347	3.3
T3 - 9	3860	0.39	0.152	2.6
T3 -10	1705	0.39	0.111	3.5
T3 -11	1106	0.47	0.096	4.9
T3 -12	3835	0.79	0.125	6.3

Averages of C/N Ratios in Sediments from Various Environments

Deep-Sea (>1,000 m): 5.2

Continental Slope (64-1,000 m): 7.0

Open Continental Shelf (<64 m): 9.0

Lagoon: 13.2

Bay: 11.7

TABLE IX

STRATIGRAPHIC VARIATIONS IN ORGANIC NITROGEN CONCENTRATIONS (wt. %)
AND IN THE C/N RATIOS IN TWO SIMPSON LAGOON CORES

Refer to Naidu (1980) for core location

Core Section (cm)	Organic C (%)	N (%)	C/N
<u>Core Sample No. SL8979-7</u>			
0- 1	0.55	0.08	6.9
1- 2	0.45	0.09	5.0
2- 3	0.87	0.09	9.7
3- 4	0.85	0.08	10.6
4- 5	0.83	0.11	7.6
5- 6	0.76	0.11	6.9
6- 7	0.79	0.11	7.2
8- 9	1.11	0.09	12.3
9-10	1.23	0.12	10.3
10-11	1.27	0.10	12.7
11-12	0.94	0.09	10.4
12-13	0.48	0.08	6.0
13-14	0.89	0.08	11.1
15-16		0.13	
16-17		0.11	
17-18		0.08	
18-19		0.08	
19-20		0.10	

TABLE X

WEIGHT PERCENTAGES OF TOTAL AND ORGANIC CARBON,
AND CARBONATE IN BEAUFORT LAGOON AND HARRISON BAY SEDIMENTS

Refer to Naidu (1980) and Figure 3 for sample locations

Sample No.	Total Carbon	Organic Carbon	Carbonate
<u>Beaufort Lagoon</u>			
BL- 1	2.55	0.99	7.80
BL- 2	2.08	0.37	8.54
BL- 3	0.58	0.01	2.85
BL- 4	2.90	1.21	8.43
BL- 5	1.20	0.27	4.63
BL- 6	1.57	0.04	7.65
BL- 7	1.63	0.01	8.61
BL- 8	0.58	0.04	2.71
BL- 9	2.59	0.82	8.84
BL-10	2.54	0.62	9.63
BL-11	2.14	0.64	7.53
BL-14	5.56	4.28	6.40
BL-15	1.90	0.40	7.47
BL-16	2.57	0.74	9.15
BL-17	1.71	0.09	8.09
BL-18	2.39	1.21	5.89
BL-20	2.90	2.15	3.69
<u>Harrison Bay</u>			
HB-A	2.01	0.12	9.44
HB-B	0.30	0.03	1.35
HB-C	0.64	0.15	2.45

TABLE XI

WEIGHT PERCENTAGES OF TOTAL AND ORGANIC CARBON,
AND CARBONATE IN SOME BEAUFORT SEA SEDIMENTS

Refer to Naidu (1980) for sample location

Sample No.	Total Carbon	Organic Carbon	Carbonate
GLA71- 5	1.41	0.42	4.95
GLA71- 6	1.21	0.76	2.22
GLA71- 8	1.61	0.16	7.26
GLA71- 12	1.82	0.56	6.29
GLA71- 20	1.30	1.06	1.22
GLA71- 21	1.29	1.00	1.46
GLA71- 22	1.30	0.66	3.19
GLA71- 23	2.24	0.13	10.56
GLA71- 25	1.88	0.01	9.81
GLA71- 27	2.00	0.45	7.74
GLA71- 44	2.21	0.69	7.60
GLA71- 57	1.41	1.04	1.62
GLA71- 58	1.50	1.00	2.49
GLA71- 63	1.90	0.60	6.49
GLA71- 74	1.02	0.40	3.11
GLA71- 85	1.70	1.33	1.85
GLA71- 86	1.73	1.53	0.99
GLA77- 9	1.17	0.65	2.60
GLA77- 17	1.49	0.62	4.33
GLA77- 30	0.98	0.70	1.43
GLA77- 31	1.46	0.05	7.05
GLA77- 32	1.81	0.08	8.68
72AER-137	2.17	0.01	11.46
72AJT- 43	2.13	0.11	10.09
72AJT- 44	1.43	0.54	4.46
72AJT- 45	0.89	0.23	3.32

TABLE XII

WEIGHT OF PARTICULATE MATTER IN CONTINUOUS SECTIONS IN
SEA ICE CORES, COLLECTED BY DR. T. OSTERKAMP (RU 253) FROM NEARSHORE
REGIONS OFF THE LONELY DEWLINE STATION AND IN
NORTON SOUND OFF YUKON DELTA

Ice Core Section (mm)	Volume of Water Filtered (ml)*	Particulate Weight (mg)	Ice Core Section (mm)	Volume of Water Filtered (ml)*	Particulate Weight (mg)
<u>Lonely 1-R</u>			<u>Lonely 2-R</u>		
0- 70	61	15.28	0- 70	72	11.38
70- 140	82	105.97	70-140	70	36.81
140- 210	73	51.80	140-210	68	29.74
210- 280	88	28.34	210-285	73	88.18
280- 350	58	20.45	285-355	61	9.61
350- 420	64	33.79	355-450	101	11.43
420- 490	79	47.87	450-520	69	4.45
490- 560	60	35.45	520-590	73	5.00
560- 635	69	50.01	590-633	36	3.05
635- 710	71	9.06	633-703	68	4.25
635- 710	71	9.06	703-773	76	5.54
710- 780	80	4.77	773-818	40	1.71
780- 850	68	3.56			
850- 900	57	2.88	<u>Norton Sound</u>		
900- 975	46	3.11	0- 70		51.73
975-1025	52	2.96	70-140		59.60
1025-1095	64	5.25	140-210		82.56
1095-1175	72	5.12	210-260		1414.14
1175-1245	70	4.30	260-325		96.64
1245-1315	71	4.21	305-385		120.50
1315-1385	64	2.99	385-485		1470.57
1385-1400	34	1.57	490-560		2165.77
			560-630		292.35
			630-680		<132.07
			670-740		169.73
			740-810		133.86
			810-880		141.12
			880-930		108.78

* Volume of water obtained from melting various ice sections.

TABLE XIII

CONCENTRATIONS (mg/l) OF SUSPENDED PARTICLES IN SURFICIAL WATER SAMPLES
COLLECTED FROM THE EAST HARRISON BAY-SIMPSON LAGOON AND
PRUDHOE BAY AREA IN SUMMER 1980

Collection Date and Sample No.*	Station No.**	Suspension Wt. (mg/l)	Collection Date and Sample No.*	Station No.**	Suspension Wt. (mg/l)
8085- 1	1	4.56	80822- 1	2	5.70
8085- 2†	1	5.69	80822- 2†	2	6.71
8085- 3	2	6.52	80822- 3	2A	2.96
8085- 4	3	4.59	80822- 4	2A	2.42
8085- 5	4	9.10	80822- 5	3A	2.71
8085- 6	5	7.97	80822- 6	4A	4.20
8086- 1	6	2.46	80822- 7	4B	8.77
8086- 2	7	2.54	80822- 8	4C	2.39
8086- 3	8	2.48	80822- 9	16	3.34
8086- 4	9	2.62	80822-10	17	2.92
8086- 5	10	2.65	80822-11	18	2.75
8086- 6	11	2.51	80824- 1	15	4.82
8086- 7	12	1.80	80824- 2	13	10.83
8086- 8	13	2.64	80824- 3	14	5.11
8086- 9	14	54.72	80824- 4	13A	3.82
8086-10	15	2.13	80824- 5	12	3.00
			80824- 6	9	6.21
			80824- 7	11	5.42
			80824- 8	10	17.21
			80824- 9	8	3.84
			80824-10	7A	3.14
			80824-11	6	4.55

* The prefix (e.g., 8085) connotes the date of collection; for example 8085 represents a collection on 1980 August 5th.

** See Figure 4 for station locations.

† Duplicate.

As part of our long-term overall program to investigate composition, sources and depositional sites of clay minerals (and by implication fine-grained particles) of the marginal seas of Alaska, particularly the arctic region, hundreds of samples have been analyzed over the past 10 years. We have made an attempt to synthesize these data and the recent outcome of this effort has been the generation of one manuscript and an abstract (refer to Appendixes 5 and 6).

We have also attempted to summarize the data gathered to date on the partitioning of Fe, Mn, Zn, Cu, Co, Cr, Ni and V in surficial sediments of Simpson Lagoon. A summary of the results have been submitted as an abstract (refer to Appendix 7) to the symposium "Biological availability of Trace Metals" to be held in Richland, Washington, in 4-8 October 1981.

An attempt was made to develop criteria to infer and map the concentrations of suspended particles of surface waters for the open water season, for Prudhoe Bay area. This effort was based on ground truth collected by us on suspension weights for specific sites during summer 1980 synchronizing with the passage of the LANDSAT satellites over the sites. Additionally, Dr. W. J. Stringer arranged to obtain discrete values of reflectance for the area. Our analysis of the reflectance and suspension data indicated that the concentrations of particles recorded for the summer 1980 (Table XIII) period were lower than the threshold values that can be meaningfully correlated with the reflectance data. We have plans to duplicate the above study this summer, but this would be a limited effort because of lack of adequate funds in the current project.

The presence of particulate matter in sea ice (Table XII) in concentrations of a few orders of magnitude higher than ambient waters has been an enigma to investigators working on sea ice problems. We have no conclusive data to explain this interesting phenomenon.

REFERENCES

- Barnes, P., E. Reimnitz, D. Drake and L. Toimal. 1977. Miscellaneous hydrologic and geologic observations on the inner Beaufort Sea shelf, Alaska. U.S. Geol. Survey Open File Rept. 77. 477 pp.
- Bertine, K. K. 1978. Means of determining natural versus anthropogenic fluxes to estuarine sediments. *In* Biochemistry of Estuarine Sediments. Proc. UNESCO/SCOR Workshop, Melreux, Belgium. UNESCO, Paris. pp. 246-253.
- Bertine, K. K., S. J. Walawender and M. Koide. 1978. Chronological strategies and metal fluxes in semi-arid lake sediments. *Geochim. Cosmochim. Acta* 42:1559-1571.
- Bruland, K. W., K. Bertine, M. Koide and E. D. Goldberg. 1974. History of heavy metal pollution in southern California coastal zone. *Environ. Sci. Technol.* 8:425-432.
- Burrell, D. C. 1977. Natural distribution of trace heavy metals and environmental background in Alaskan shelf and estuarine areas. Annual Rept. to BLM-OCSEAP Office, Boulder. Inst. Mar. Sci., Univ. Alaska, Fairbanks. 204 pp.
- Chester, R. and M. J. Hughes. 1967. A chemical technique for the separation of ferro-manganese minerals, carbonate minerals and absorbed trace elements from pelagic sediments. *Chem. Geol.* 2:249-262.
- Erlenkunser, H. E. Suess and H. Willkomm. 1974. Industrialization affects heavy metal and carbon isotope concentration in recent Baltic Sea sediments. *Geochim. Cosmochim. Acta* 38:823-842.
- Folk, R. L. and W. C. Ward. 1957. Brazos River bar -- a study in the significance of grain size parameters. *J. Sedimentary Petrology* 27:3-26.
- Goldberg, E. D. *et al.* 1978. A pollution history of Chesapeake Bay. *Geochim. Cosmochim. Acta* 42:1413-1425.
- Hülsemann, J. 1966. On the routine analysis of carbonates in unconsolidated sediments. *J. Sedimentary Petrology* 36:622-625.
- Koide, M. and K. W. Bruland. 1975. The electrodeposition and determination of radium by isotope dilution in sea water and in sediments simultaneously with other natural radionuclides. *Anal. Chim. Acta* 75:1-19.
- Koide, M., K. W. Bruland and E. D. Goldberg. 1972. Th-228/Th-232 and Pb-210 geochronologies in marine and lake sediments. *Geochim. Cosmochim. Acta* 37:1171-1187.

- LGL Ltd. 1980. Beaufort Sea barrier island - lagoon ecological process studies: Final Report, Simpson Lagoon. Submitted to Arctic Project Office, Geophysical Institute, Univ. Alaska, Fairbanks. 678 pp.
- Naidu, A. S. 1979. Sources, transport pathways, depositional sites and dynamics of sediments in the lagoon and shallow marine region, northern arctic Alaska. Annual Report. Submitted to NOAA-OCSEAP Office, Boulder, Colorado. 81 pp.
- Naidu, A. S. 1980. Sources, pathways, depositional sites and dynamics of sediments in the lagoon and shallow marine region, northern arctic Alaska. Annual Report. Submitted to NOAA-OCSEAP Office, Boulder, Colorado. 86 pp.
- Northern Technical Services. 1981. Beaufort Sea drilling effluent disposal study. Prepared for the Reindeer Island Stratigraphic Test Well Participants under the direction of Sohio Alaska Petroleum Co., Northern Tech. Services (NORTECH), Anchorage. 329 pp.
- Price, N. B., S. J. Malcolm and J. Hamilton-Taylor. 1978. Environmental impacts of lead and zinc in recent sediments. *In Biogeochemistry of Estuarine Sediments*. Proc. UNESCO/SCOR Workshop, Melreux, Belgium, UNESCO, Paris. pp. 207-215.
- Rader, L. F. and F. S. Grimaldi. 1961. Chemical analysis for selected minor elements in Pierre Shale. U.S. Geol. Survey Prof. Paper 391-A, pp. A1-A45.
- Schubel, J. R. and W. M. Wise (eds.). 1979. Questions about dredging and dredged material disposal in the Chesapeake Bay. Marine Sci. Res. Center, State Univ. New York. 143 pp.
- Shirahata, H., R. W. Elias, C. C. Patterson and M. Koide. 1980. Chronological variations in concentrations and isotopic compositions of anthropogenic atmospheric lead in sediments of a remote subalpine pond. *Geochim. Cosmochim. Acta* 44:149-162.
- UNESCO. 1978. *Biogeochemistry of Estuarine Sediments*. Proc. 1976 UNESCO/SCOR Workshop, Melreux, Belgium. UNESCO, Paris. 293 pp.
- Wiseman, W. J. *et al.* 1973. Alaskan arctic coastal processes and morphology. Technical Report No. 149, Coastal Studies Inst., Louisiana State Univ., Baton Rouge. 171 pp.

APPENDIX 1

FIELD AND CRUISE REPORT

Contract: #03-022-56
Research Unit: #529
Task Order: #33
Reporting Period: 6/26/80-8/25/80
Number of Pages: 6

A. S. Naidu
Principal Investigator
Associate Professor of Marine Science

Institute of Marine Science
University of Alaska
Fairbanks, Alaska 99701

30 September 1980

I. TASK OBJECTIVES

The major objectives of this study are to understand the dynamics of sedimentation, to characterize benthic substrate habitats, and to elucidate the sources and depositional sites of terrigenous sediment particles in the lagoon and adjacent shelf area of north arctic Alaska. Additional goals of this program include completion of collection of baselines of a suite of heavy metals relative to sediments of the Beaufort Sea, understanding of the geochemical partitioning patterns of the heavy metals, and estimation of the rate of sedimentation in the above area.

II. OBJECTIVES OF FIELD WORK

The following were the overall objectives of the summer 1980 field work in the coastal area of north arctic Alaska.

- (1) To collect surficial water samples from known geographic locations, during the passage of LANDSAT II and III Satellites over the above locations.
- (2) To collect sediment core samples from the Harrison Bay for estimation of sediment depositional rates by the ^{210}Pb method.
- (3) To collect (on an opportunistic basis) sediment grab samples from the Harrison Bay for the purpose of collecting additional grain size distributions, clay mineralogy and chemistry of sediments.
- (4) To collect samples of suspended particles, *via* a rosette of traps on a time-series basis for the analysis of plant pigments and understanding of sediment fluxes.
- (5) To collect large samples of boulders along the arctic coast for the purpose of radiometric dating.
- (6) To collect representative samples of waters from the fresh, brackish and saline regimes of the Colville Delta for the analysis of manganese and organic carbon in the soluble and particulate phases.

III. FIELD PARTY AND CAMP LOCATIONS

<u>NAME</u>	<u>DATE</u>	<u>CAMP</u>
A. S. Naidu	July 26-29	Mukluk OCS
H. V. Weiss	August 13-25	Deadhorse
A. S. Naidu	July 29-August 9	Colville Village
H. V. Weiss	August 12	

<u>NAME</u>	<u>DATE</u>	<u>CAMP</u>
A. S. Naidu	August 10-11	R/V <i>D. W. Hood</i>
H. V. Weiss		
N. Wisemeyer	July 30-August 1 August 20-21	Mukluck OCS Deadhorse
D. C. Burrell	August 23-26	Mukluck OCS Deadhorse

IV. FIELD WORK

Collection of Water Samples

For the purpose of establishing ground truth that would assist in the mapping of the distributional pattern of suspended particle concentrations from LANDSAT images, surficial water samples were collected from a number of selected sites in the Simpson Lagoon and Prudhoe and Harrison Bays. These sample collections synchronized with the passage over the above locations of LANDSAT II and III Satellites. The two satellites which pass alternately over any one site at 9 days interval potentially made available to us 4 occasions, during the month of our stay in the field, to collect water samples at any one site. However, we could not collect water samples on more than two occasions at any one site because of inclement weather. Water samples in Prudhoe Bay area were obtained on August 5 and 22, 1980 while in the Simpson Lagoon and the contiguous east Harrison Bay region the collections were made on August 6 and 24, 1980. Additionally, a few samples were retrieved on our behalf by Mr. Paul Zimmerman (R.U. 537) on August 7, 8 and 13 from the west Harrison Bay, aboard the R/V *D. W. Hood*. We used a Cessna 206 plane on floats to collect the water samples, because a wide region had to be covered on any one day.

For the purpose of record it must be mentioned that we could not establish exact (\pm one or two meters) locations of the stations from which water samples were collected. Prior to the water collection a day was spent on August 30, 1980 to deploy buoys at some selected sites. The general strategy was to periodically collect surficial water samples from the buoy sites, synchronizing of course with the satellite passages

overhead. Additionally, it was planned to obtain the exact locations of the buoys at some later convenient time *via* the use of the miniranger aboard the R/V *D. W. Hood*. However, this was not possible because the miniranger on the R/V *D. W. Hood* was not operational almost all the time under contract to OCSEAP. Therefore, positioning of the buoy locations should be considered approximate (to within a 100 m of known geographic locations; refer to Fig. 1).

One litre aliquots of each of the water samples collected were filtered, at one of the field base camps, through preweighed Nuclepore membrane (0.4 μ m pore size). At one station replicate samples were collected to check our sampling precision. Temperature of all water samples were measured immediately after collection, and at each station a separate 100 ml water sample was obtained for measurement of salinity in the Fairbanks laboratory. The particulates collected on Nuclepore membranes will be dried and weighed in the Fairbanks Laboratory.

To further our understanding of the geochemical partitioning of Mn in nearshore waters of north Alaskan arctic a suite of water samples were collected on an opportunistic basis. Representative samples were obtained from the fresh, brackish and saline regimes of the Colville Delta as well as from the adjacent Simpson Lagoon. The water samples which were initially filtered through Nuclepore membranes (0.4 μ m pore size) at the base camp were preserved in 5% ultrex HNO_3 . These samples were retained by Dr. Weiss (NOSC, San Diego) for analysis of Mn by neutron activation. To support our geochemical program - especially pertaining to Mn distribution - 5 separate aliquots of water samples were collected from each of the above stations for the measurement of soluble and particulate organic carbon. These samples were provided to Dr. D. C. Burrell who processed them at Deadhorse camp for subsequent analysis of carbon in the Fairbanks laboratory. The pH of all the above samples were measured at the Deadhorse camp, while their temperatures were noted immediately after collection.

Collection of Sediment Core and Grab Samples

In continuation of our efforts to estimate the sediment accumulation rates and understand depositional processes in the Harrison Bay a number

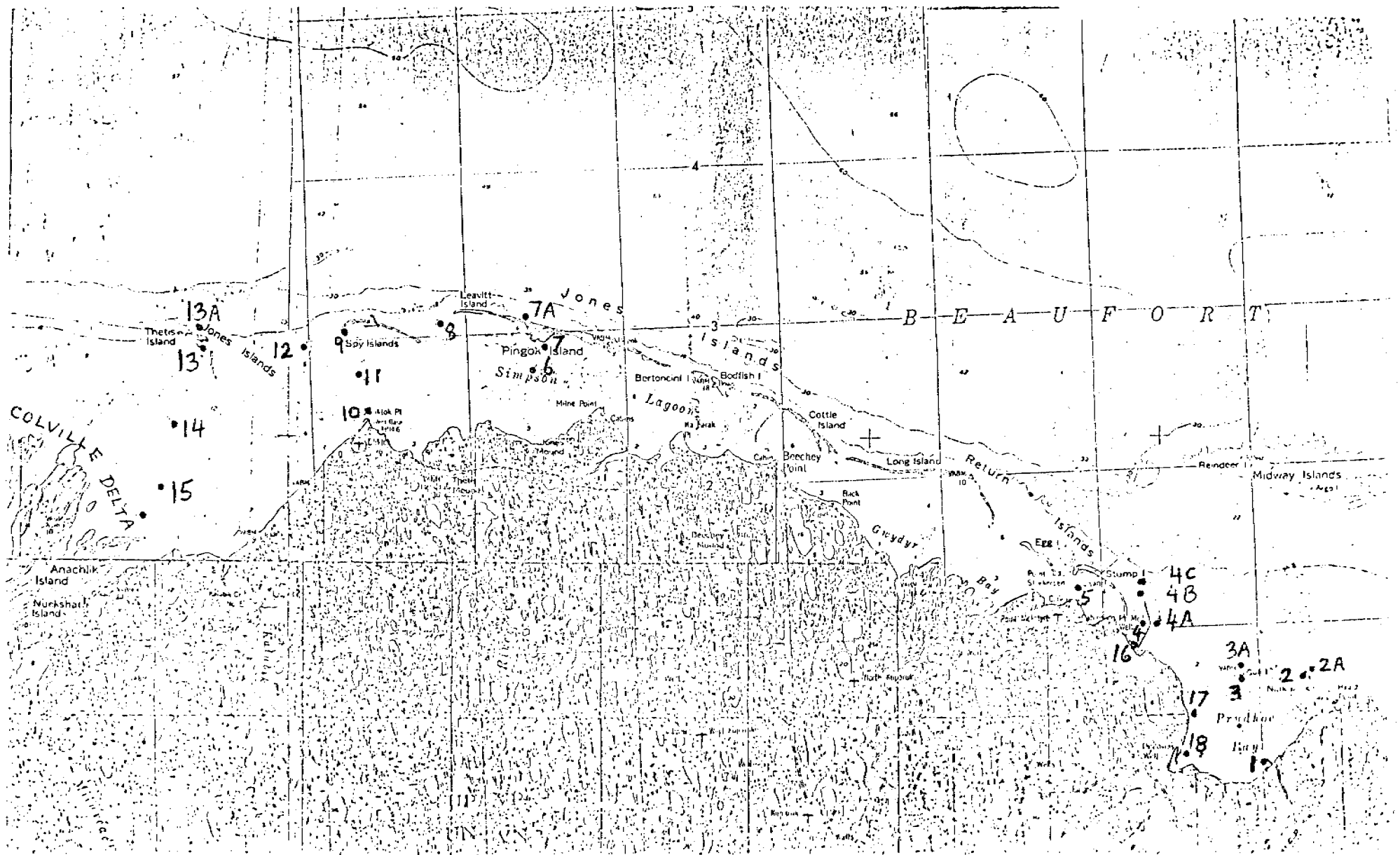


Figure 1. Map showing location of stations in the Simpson Lagoon and Prudhoe Bay region from where water samples were collected synchronizing with the LANDSAT II and III satellite passages in August 1980.

of sediment core samples were collected in the bay. A Phleger gravity coring unit which was initially used retrieved only a few inches of core samples, presumably because of low penetration on the stiff muddy or sandy substrate. Therefore, we had to take resort to a manually operated coring unit. Thus, total of 10 cores were collected, locations of which are given in Table I. In addition to the cores, grab sediment samples were obtained from the Harrison Bay at 6 random stations. We were also provided with Smith-McIntyre grab samples by Mr. G. Ruff (R.U. 6), and with several grab samples by Dr. Carter Broad (R.U. 356). Some of the above sediment samples will be processed for size distribution, clay minerals and trace metal contents with the purpose of establishing baseline data on a wider regional scale for the Harrison Bay.

Efforts to collect time-series samples of suspended particles *via* a rosette of sediment traps, under subcontract to Dr. L. H. Larsen of the University of Washington were not quite successful. A rosette of sediment traps was deployed at approximately 1/4 mile due north of the hut on the Thetis Island on July 30, 1980. The traps were, however, not sighted on August 20, 1980 when they were timed to surface up. They have been presumed lost. Further details on this particular field effort are expected from Dr. Larsen.

A one-half day trip was undertaken to the Flaxman Island in an attempt to further understand the distribution of boulders on that island, as well as to obtain additional large samples of dioritic and granitic boulders for the purpose of K-Ar radiometric dating. We also took side trips on two separate days to the areas in the vicinity of the east dock of Prudhoe Bay for collection of samples of boulders of Flaxman Formation, and also to retrieve samples of contemporary dune sands in the coastal hinterland adjacent to the dock.

One-cm sections of 7 cores, collected from the Harrison Bay, were cut and transferred into small preweighed glass vials. These samples were retained by Dr. Weiss (NOSC) for ^{210}Pb assays under an OCSEAP subcontract.

The field camp came to an end on August 25, 1980.

TABLE I

LOCATIONS OF CORE SAMPLES COLLECTED FROM THE HARRISON BAY
IN AUGUST 1980

Core sample No.	Latitude (N)	Longitude (W)	Water depth (m)
HB80810-1	70°31'	150°07'	1.5
HB80810-2*			1.5
HB80810-3*	70°32'	150°24'	2.1
HB80810-4	70°30'	151°15'	2.5
HB80810-5	70°34'	151°30'	2.5
HB80810-6	70°36'	151°51'	2.1
HB80810-7	70°40'	152°15'	1.5
HB80810-8	70°42'	152°0'	1.5
HB80810-9*	70°32'	151°30'	8.1
HB80810-10	70°37'	151°39'	4.2
HB80810-12	70°33'	151°21'	4.2
HB80810-13*	70°32'	151°6'	4.2
HB80810-14	70°33'	150°5'	2.4

*Attempts to collect sediment core samples from these locations were stymied by the stiff muddy or sandy nature of substrate. A few cm long cores were all that could be obtained and these samples should serve as representative grab samples for the locations indicated.

APPENDIX 2

REPORT OF AUGUST 1980 FIELD STUDIES IN HARRISON BAY

Submitted by

L. H. Larsen

Department of Oceanography
University of Washington
Seattle, Washington 98195

REPORT OF AUGUST 1980 FIELD STUDIES IN HARRISON BAY

Sediment traps were constructed for a deployment in Harrison Bay, Alaska. The deployment was scheduled for the ice-free period (August 1980). The sediment traps were not recovered from Harrison Bay. This short note describes the materials lost and includes details of the recovery attempt.

Eight PVC sediment traps (3" x 10") were fastened to a cylindrical stainless steel rosette (similar to a Niskin bottle rosette). The lids to the traps were cocked open and would be closed by an electronic timing device. The timer was housed in a deep-sea pressure case and attached to the sediment trap rosette. The timer, when fired, allows a current to pass through a circuit resulting in the corrosion of a stainless steel link to which the sediment trap lids are attached. There are sixteen available firing circuits on the electronic timer, thereby allowing up to sixteen separate trap closings. For the work in Harrison Bay, the sediment traps were cocked in pairs and each pair of traps was to be closed at an interval of 110 hours thus yielding a time-series of trap exposures (110, 220, 330 and 440 hours; August 1 - August 19).

A sketch of the sediment trap mooring is attached (Figure 1). Release of the mooring occurs when a second electronic timing package actuates an explosive cable cutter allowing the subsurface flotation to reach the surface. A canister of coiled line (20 meters) next to the explosive cutter remains attached to the anchor so the mooring cannot float away upon release. Moorings of a similar design with identical electronic timers have been deployed and recovered successfully ten times in the past ten months in Dabob Bay, Washington (water column=100 meters). The mooring in Harrison Bay also had a 75 meter weighted 'polypro' dragline stretched between the mooring anchor and a second 200 lb anchor. In case of release failure, the mooring could be retrieved by dragging over the polypro line with grappling hooks. During one release failure in Dabob Bay (1978) this dragging technique worked successfully even in 100 meters of water. A visual location of the mooring was provided by small surface floats which were attached to the line with a weak link (40 lb test monofilament) which would break in case passing ice caught the surface floats.

Sketch of Sediment Trap Mooring

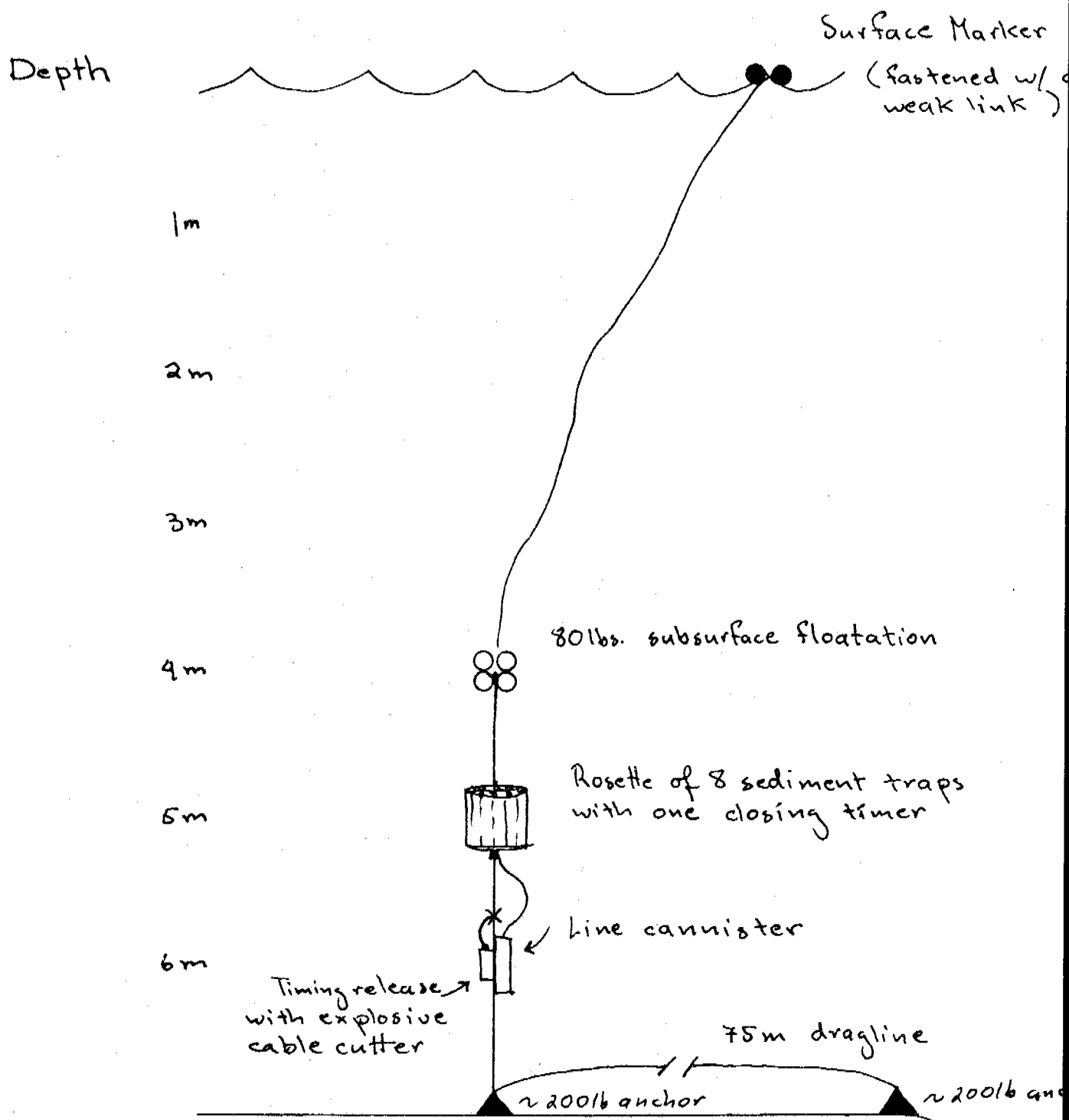


Figure 1.

The mooring was deployed from the R/V *Hood* on August 1, 1980, 1650 hrs, 0.45 miles north of the house on Thetis Island. The bearing was 330° (magnetic) and this fix was double-checked from the beach. The original location of the mooring was to be west of Thetis Island with navigation provided by a 'mini-ranger' system. However, the mini-ranger receiving unit on the R/V *Hood* was not operational and the house on Thetis Island provided the only good reflector for radar positioning as well as for visual fixes. For those reasons, the position north of Thetis Island was chosen. At the time of deployment, the floating ice was approximately 2-3 miles north of Thetis Island.

The recovery was originally scheduled via the R/V *Hood*; however, that vessel was not available and plans were changed to helicopter recovery. On the scheduled day of recovery (August 19), the ice had moved onto the northern beach of Thetis Island and recovery with the R/V *Hood* would have been difficult, if not impossible. Local observations noted that the ice had drifted south the previous week and at times had been even denser than on the day of recovery.

Our search for the mooring included a one-hour search of the immediate mooring vicinity using Boston wailer, one-hour helicopter search and two hours of dragging, again with the Boston wailer. Our logical conclusion is that the mooring had been dragged away by passing ice sometime during the previous week. The shallow water depth (7 meters) and the height of the mooring (3 meters) would certainly make this a likely assumption.

The lost equipment has a replacement value of \$3,000. The electronics system was completely tested prior to departure from Seattle and was in working condition.

Field operations were carried out by Nick Welschmeyer, a graduate student in the Department of Oceanography. He has considerable experience in deploying the sediment traps and had constructed the electronics in the system. Because he was most familiar with the equipment, I felt that the best bet was to have him in the field. In retrospect, it would have been better for both of us to have gone to the field. However, we had travel

funds for only a single person. This might have eliminated some logistic confusion which minimized contact between Nick Welschmeyer and Dr. Naidu.

Furthermore, we were under the impression that arrangements with the R/V *Hood* had been made for the deployment. This turned out not to be true and the deployment was made with the generous consent of Carter Broad who gave up a few hours of ship time.

Unfortunately, there was a misunderstanding among Carl Lorenzen, Nick Welschmeyer, who works for Carl, and myself concerning the total scope of the August operations. Following a discussion among Lorenzen, Larsen and Naidu, I was under the impression that two sediment trap systems would be brought north. We had planned to use traps which were to be recovered from the North Pacific in early July. These traps were not recovered, which left Lorenzen short of a second trap for deployment in the Colville River. However, I was not aware this loss would affect the August experiment since I did not know the total inventory. The situation regarding the August experiment had been left in limbo between Carl and myself because confirmation of the August experiment had not been made. The confirmation came the week prior to the deployment in Harrison Bay which did not give Carl time, under any circumstances, to construct a new trap. During this period, Nick Welschmeyer was involved in many cruises to Dabob Bay and it was difficult to contact him. Nevertheless, it is my fault that I was not aware that Welschmeyer was heading north with only a single sediment trap system.

APPENDIX 3

DRAFT SYNTHESIS REPORT

Contract: #03-5-022-56
Research Unit: #529
Task Order: 33
Number of Pages: 15

Aspects of Size Distributions, Clay Mineralogy and
Geochemistry of Sediments of the Beaufort Sea and
Adjacent Deltas, North Arctic Alaska

by

A. Sathy Naidu
Principal Investigator
Associate Professor in Marine Science

Assisted by
Michael D. Sweeney and Larry Klein
Graduate Students

Institute of Marine Science
University of Alaska
Fairbanks, Alaska 99701

May 1981

INTRODUCTION

This report consists of a brief synthesis of the salient points of the grain size distributions, clay mineralogy and geochemistry of continental shelf sediments of the Alaskan Beaufort Sea, as well as of the sediments from the adjacent marine facies of the North Slope deltas.

GRANULOMETRIC INVESTIGATIONS

Compilation, collation and synthesis of all data available from 1970 on the size distributions of sediments has been included in this report. The data gathered by Carsola (1954) have been purposely excluded because his grain size statistical analysis were based on a method different than those adopted since 1970. This synthesis is based on analysis of 330 samples from the open Beaufort Sea (Fig. 1), and about 100 analysis from the deltaic environment (e.g., lagoons, sound, bays, beaches, dunes, etc.). The locations of the latter suite are shown in Figures 2a, 2b, 3 and 4. Each of the values of gross textural attributes (e.g., percentages of gravel, sand, silt, clay and mud) as well as two conventional grain size statistical parameters, mean size and graphical standard deviation (after Folk and Ward, 1957) were digitally transferred onto maps of the Beaufort Sea and isopleths plotted. Broad regional variations in the granulometric compositions in the Beaufort Sea are graphically displayed in Figures 5 to 11. Generally, the middle and outer continental shelf areas are carpeted by poorly-sorted sandy muds (with almost equal proportions of silt and clay). Invariably size distribution curves of these sediments are positive-skewed to nearly symmetrical and platykurtic. The inner shelf and inland bays are characterized by silty-sand to sandy-silt

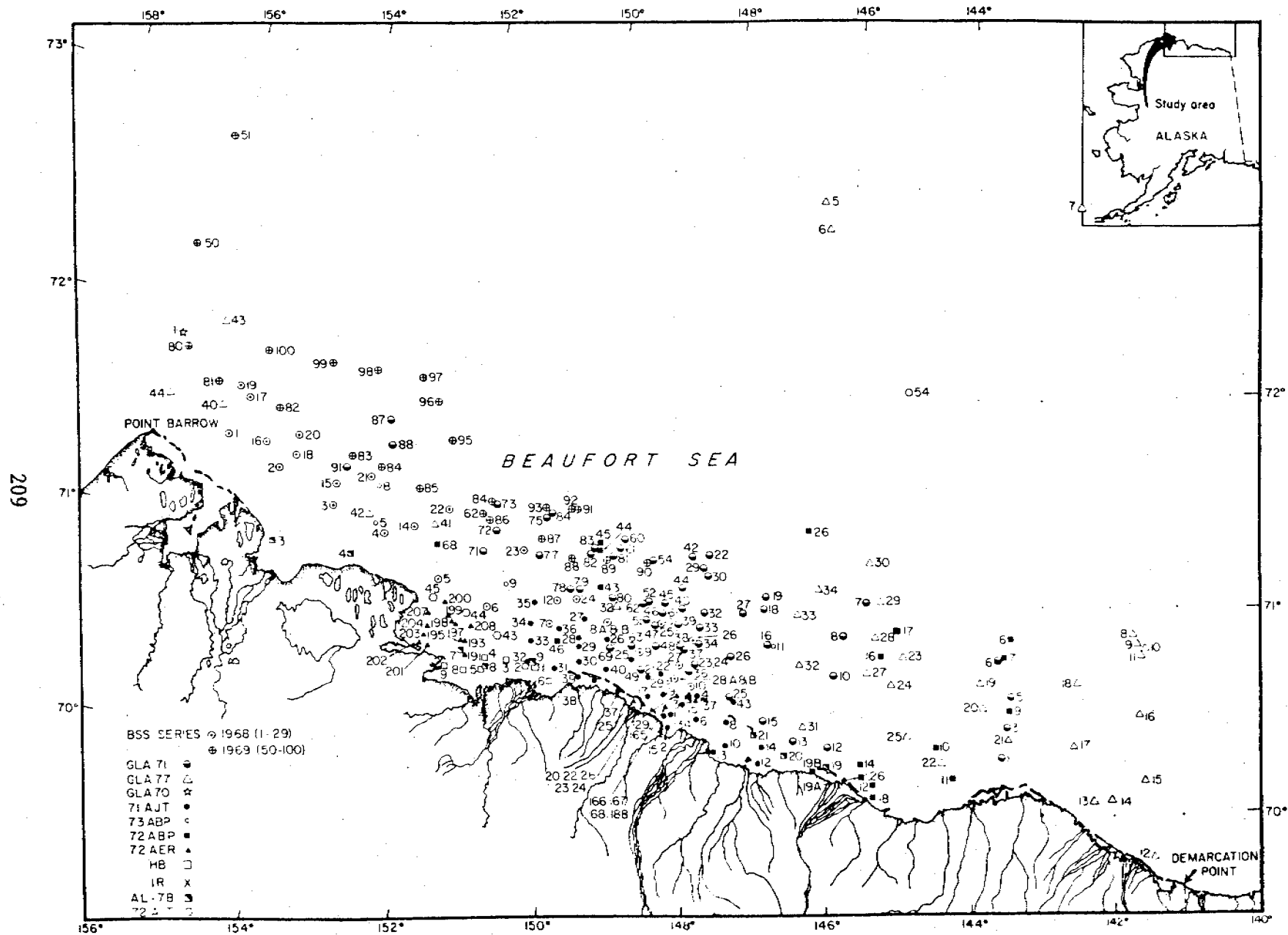


Figure 1. Station locations for Beaufort Sea.

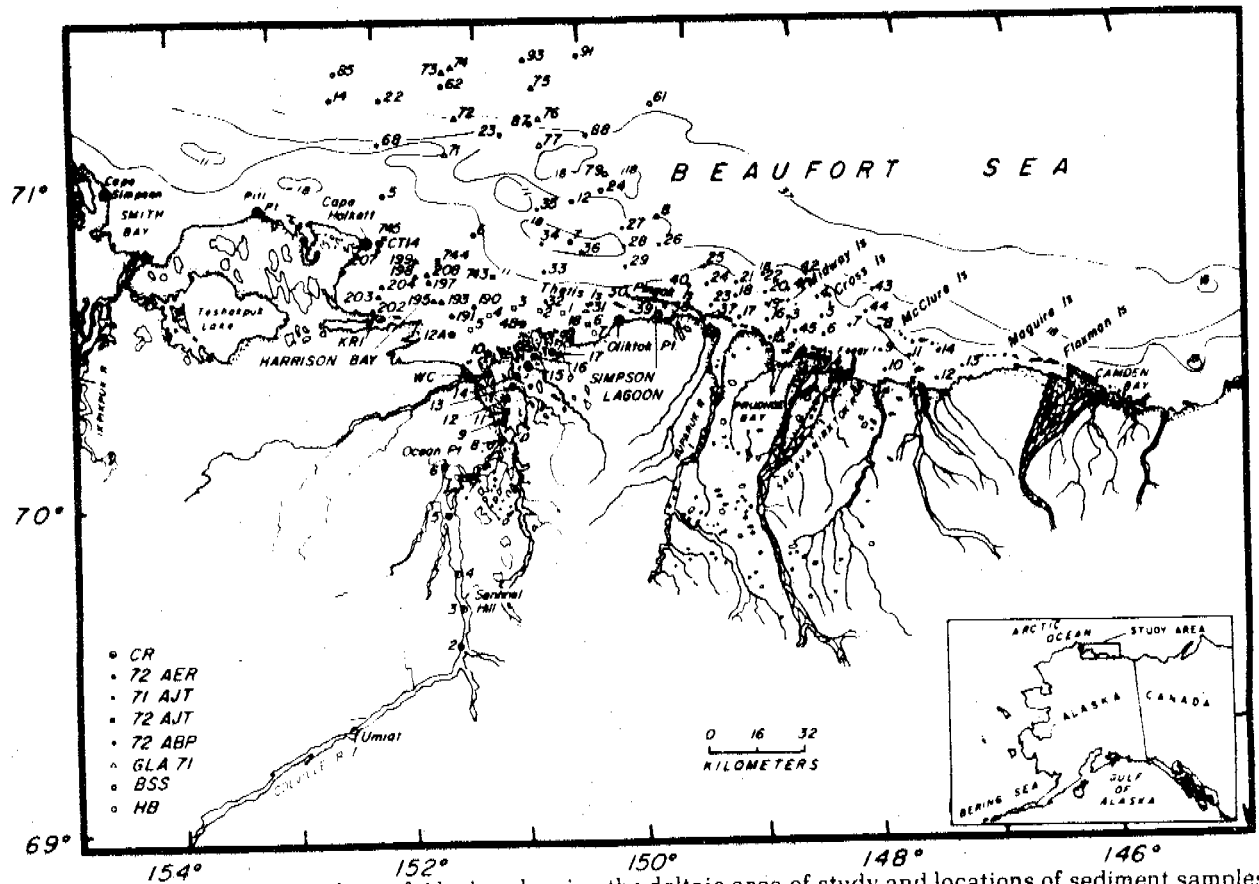


Figure 2a. Map of the North Slope of Alaska, showing the deltaic area of study and locations of sediment samples. The depth contours are in meters.

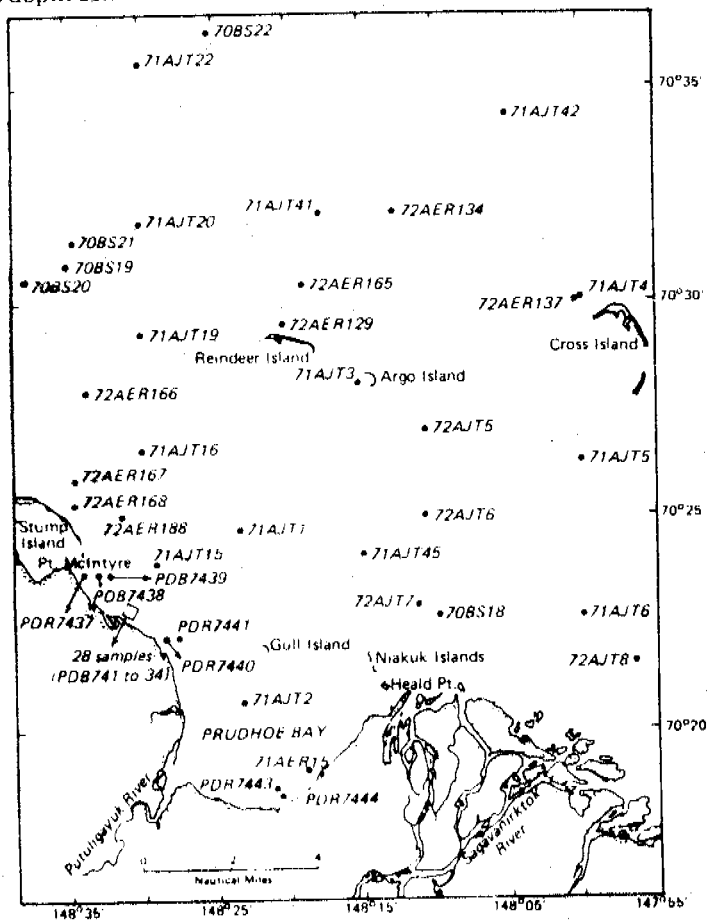


Figure 2b. Locations of sediment samples in the Prudhoe Bay and adjacent shallow marine environment of north arctic Alaska.

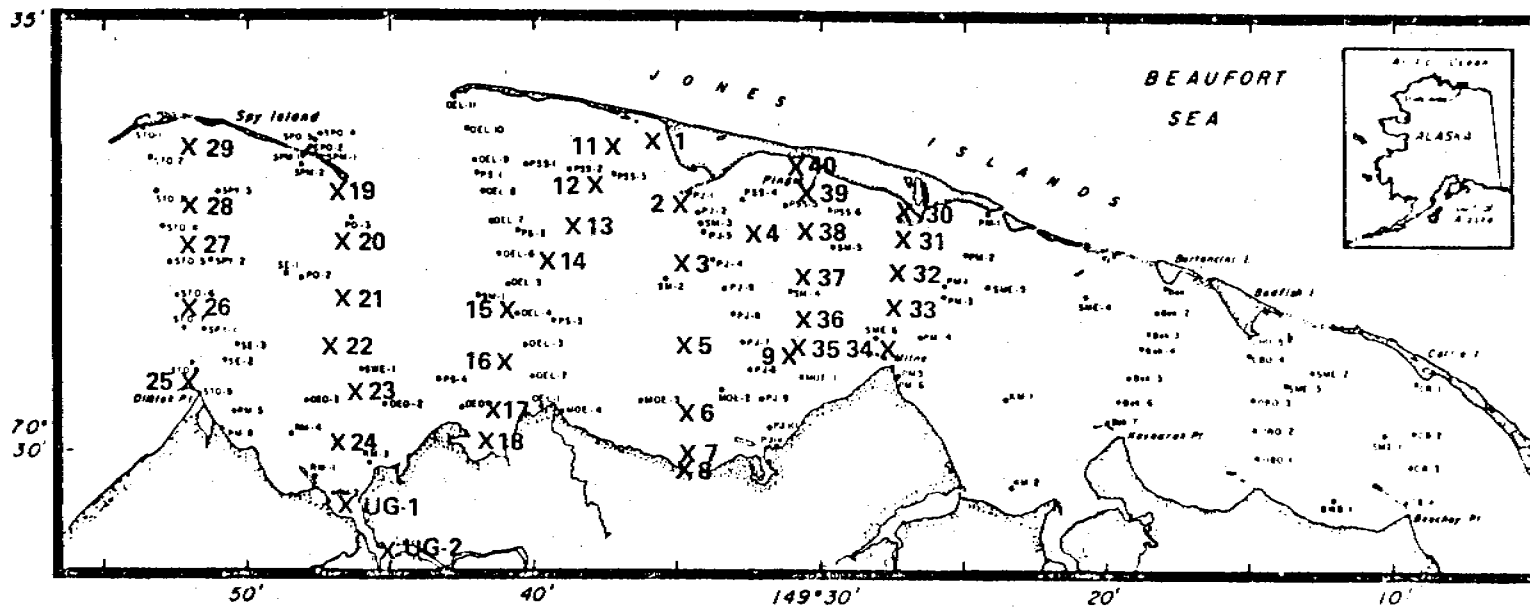


Figure 3. Sample locations in Simpson Lagoon. Locations depicted by heavy crosses indicate samples collected in Summer 1977. The remaining samples were collected by Tucker (1975) and size analysis data on them are already available.

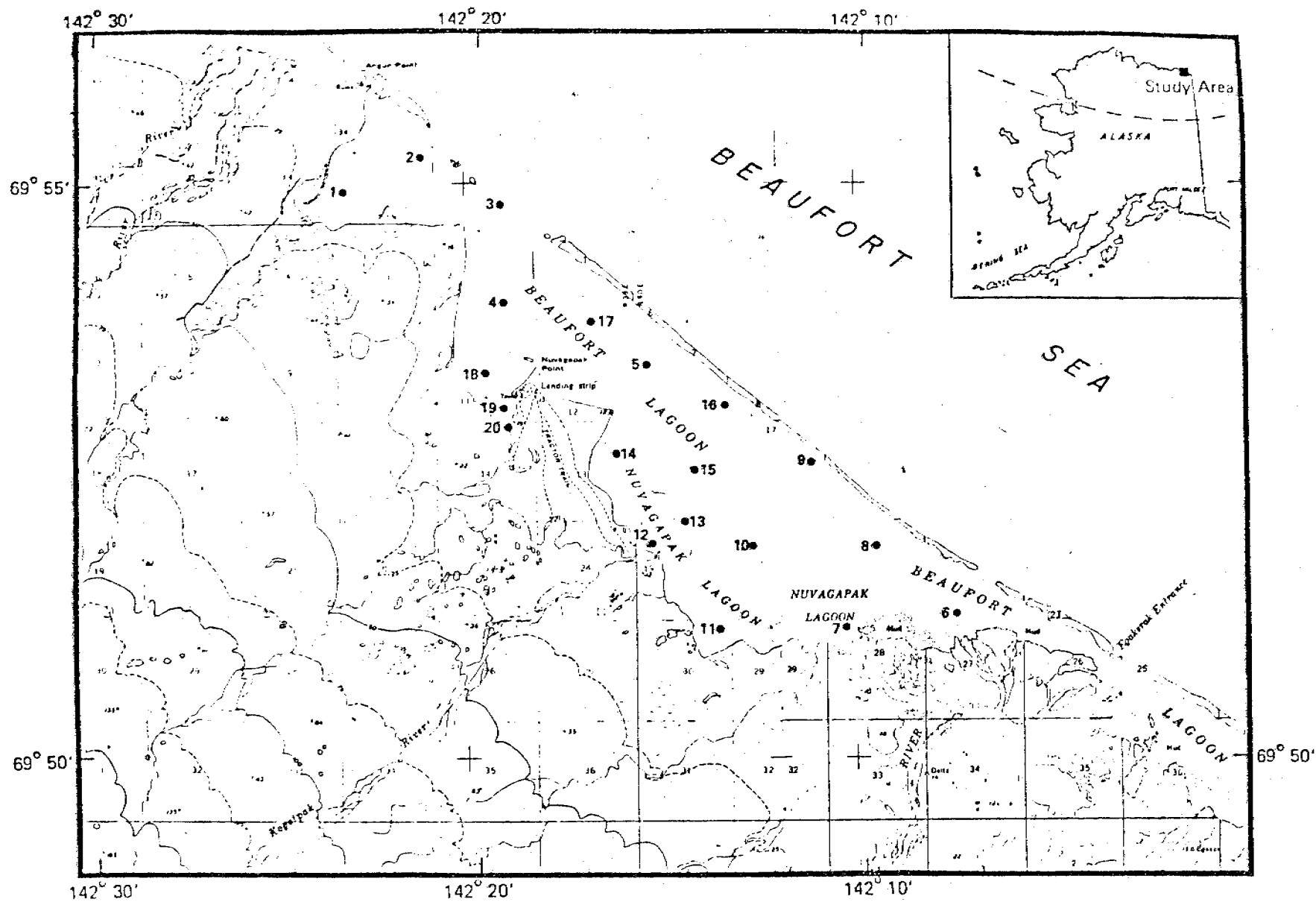


Figure 4. Map showing the locations of sediment samples from the Beaufort Lagoon, north arctic Alaska.

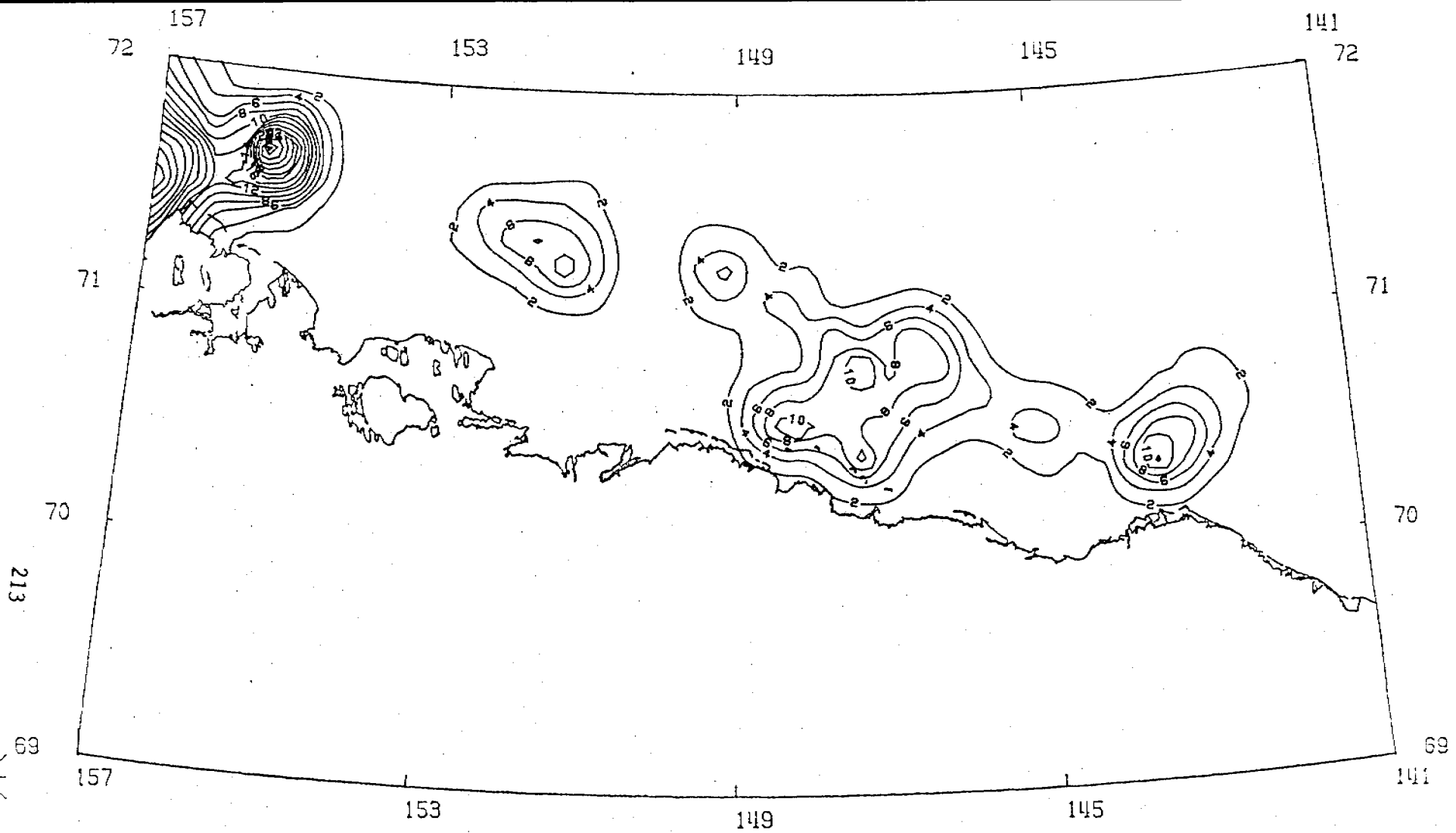


Figure 5. Map of the Beaufort Sea showing the distribution of gravel concentrations (wt. %).

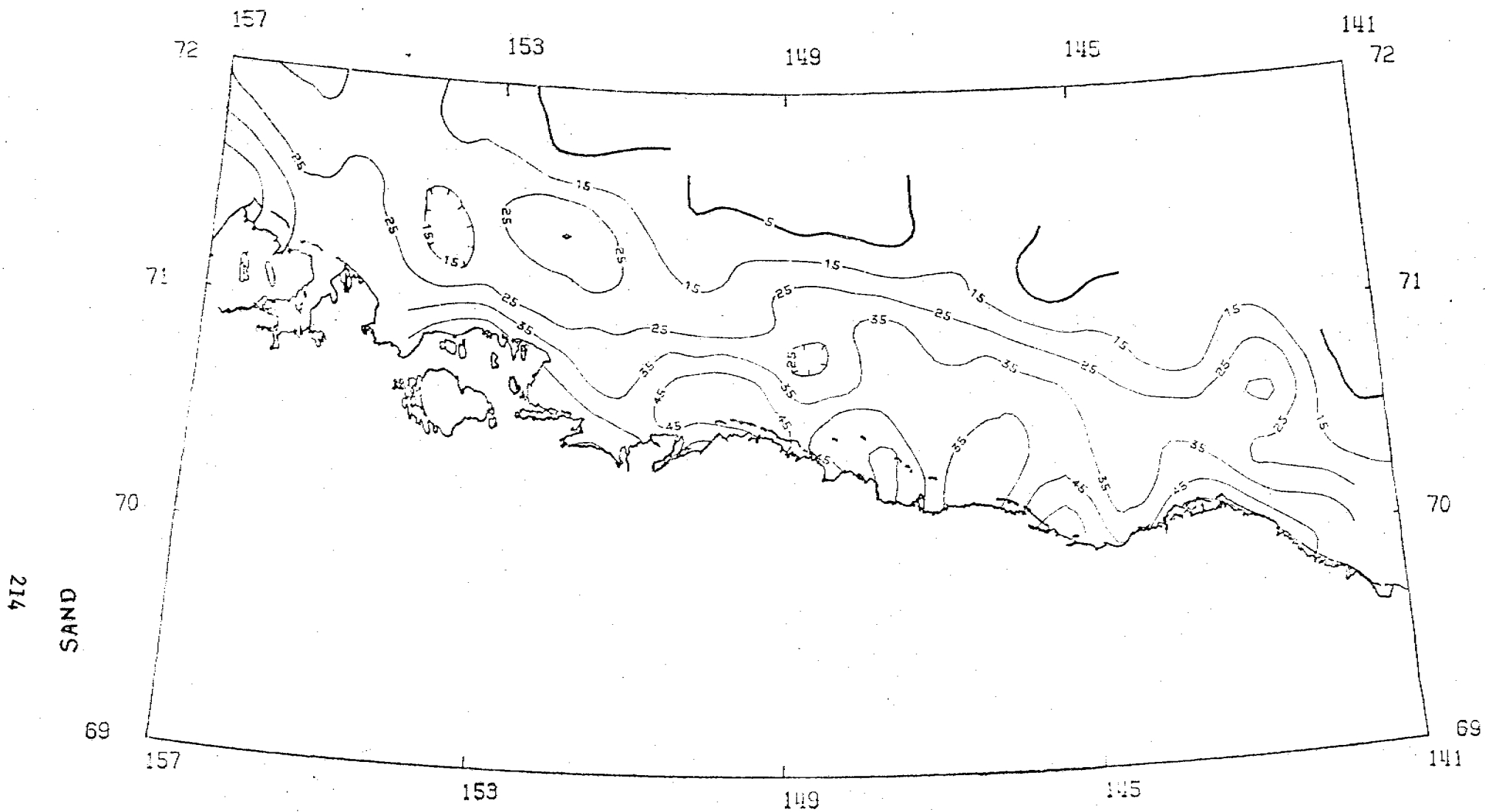


Figure 6. Map of the Beaufort Sea showing the distribution of sand (wt. %).

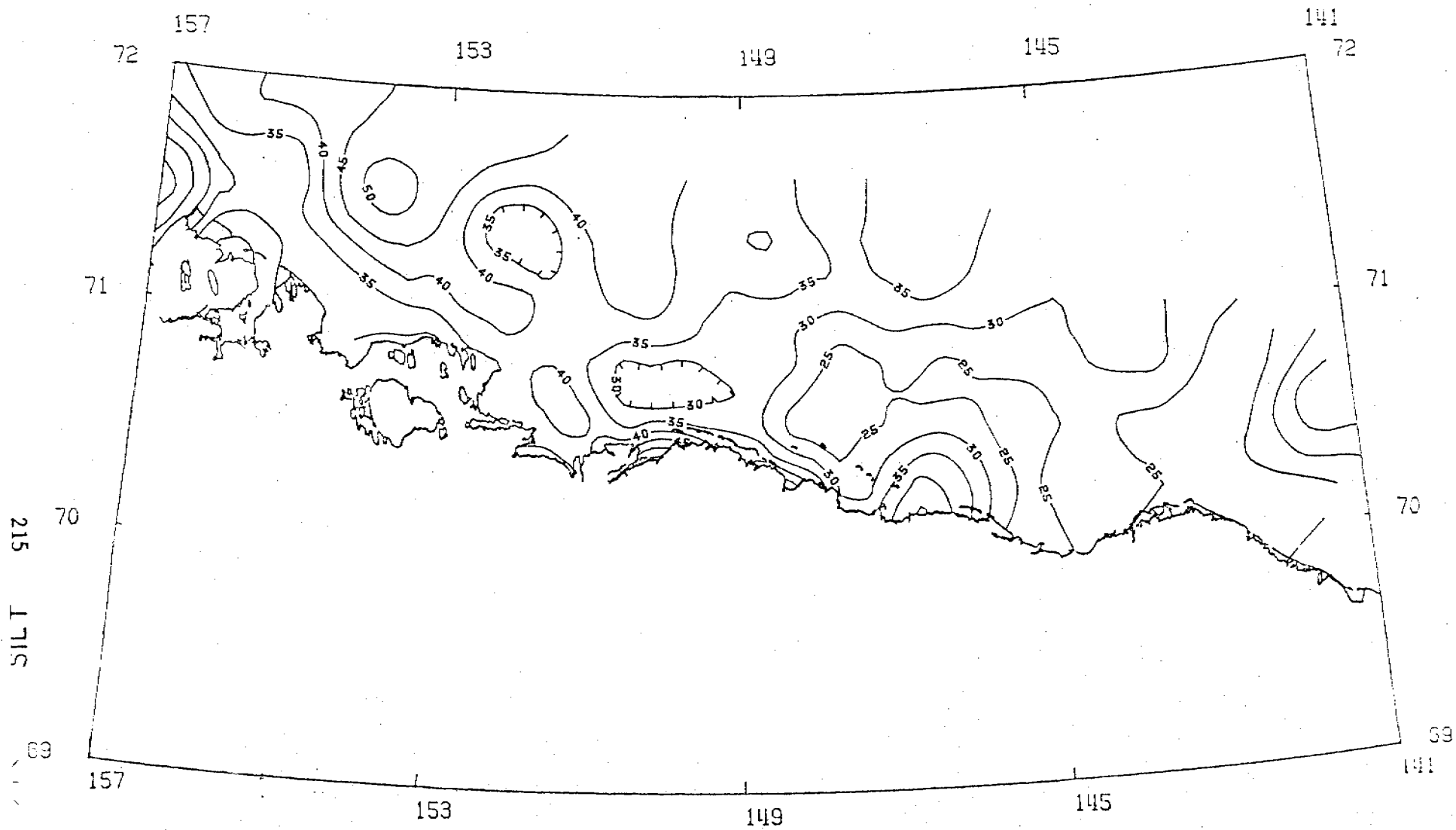


Figure 7. Map of the Beaufort Sea showing the distribution of silt (wt. %).

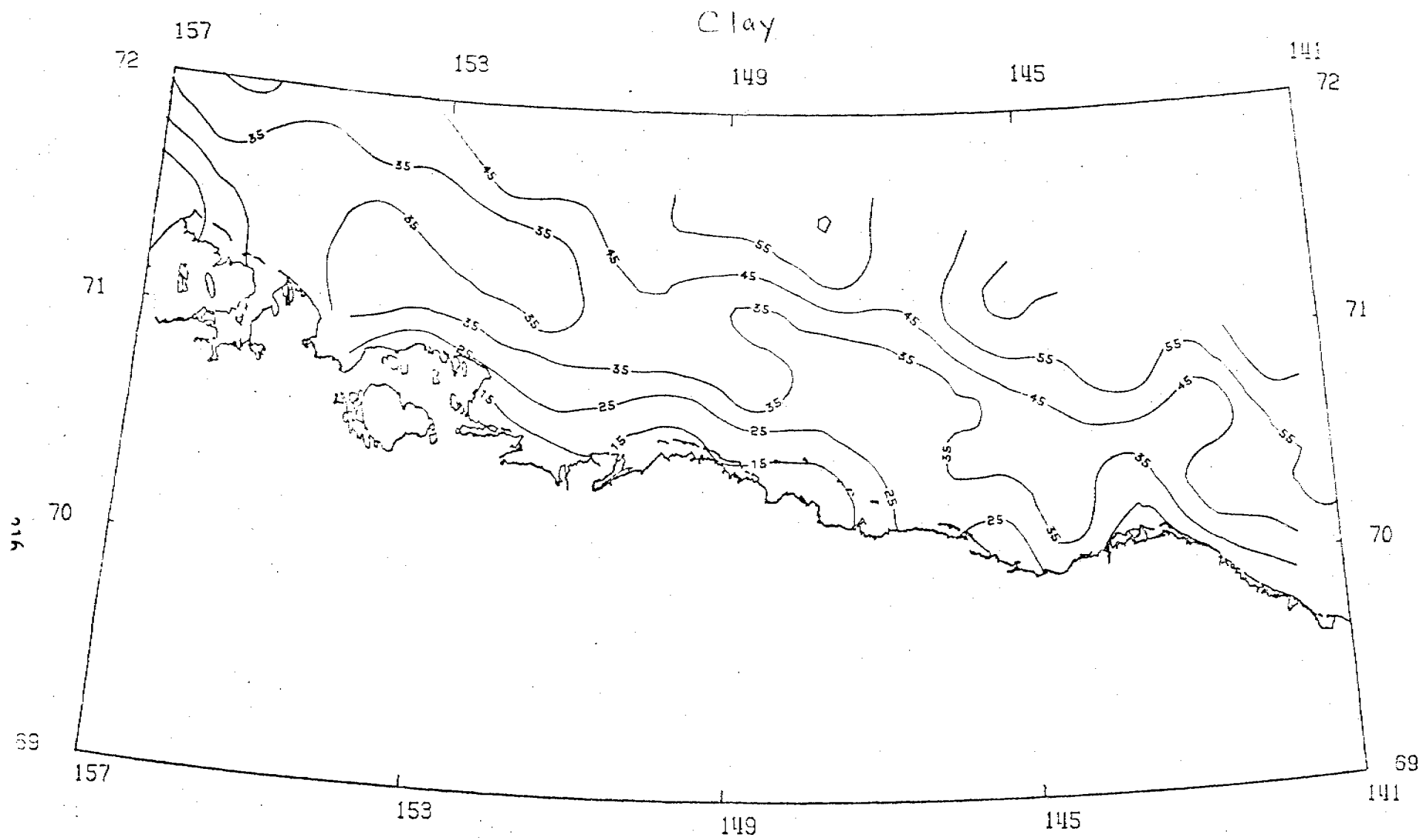


Figure 8. Map of the Beaufort Sea showing the distribution of clay (wt. %).

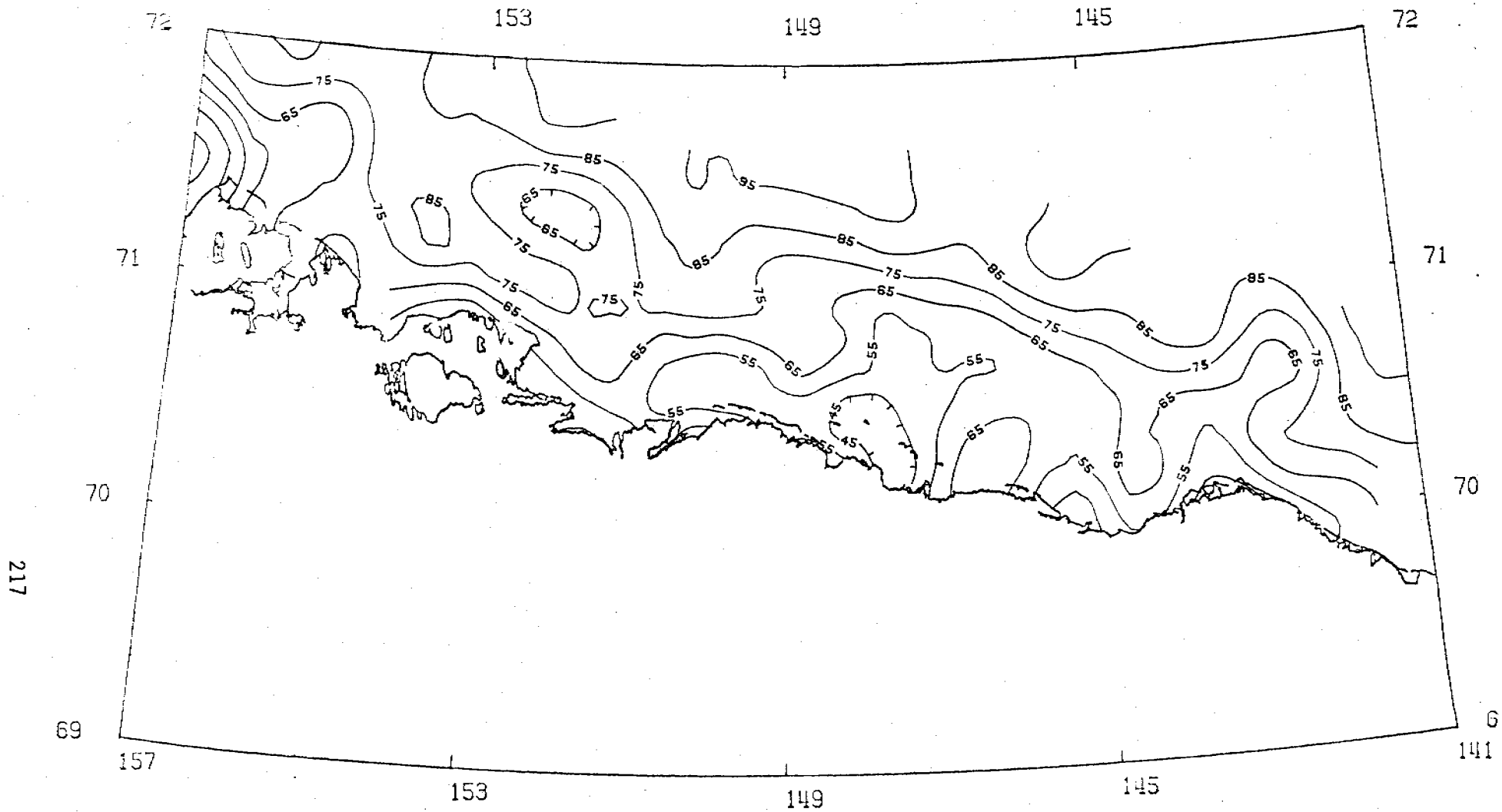


Figure 9. Map of the Beaufort Sea showing the distribution of mud (wt. %).

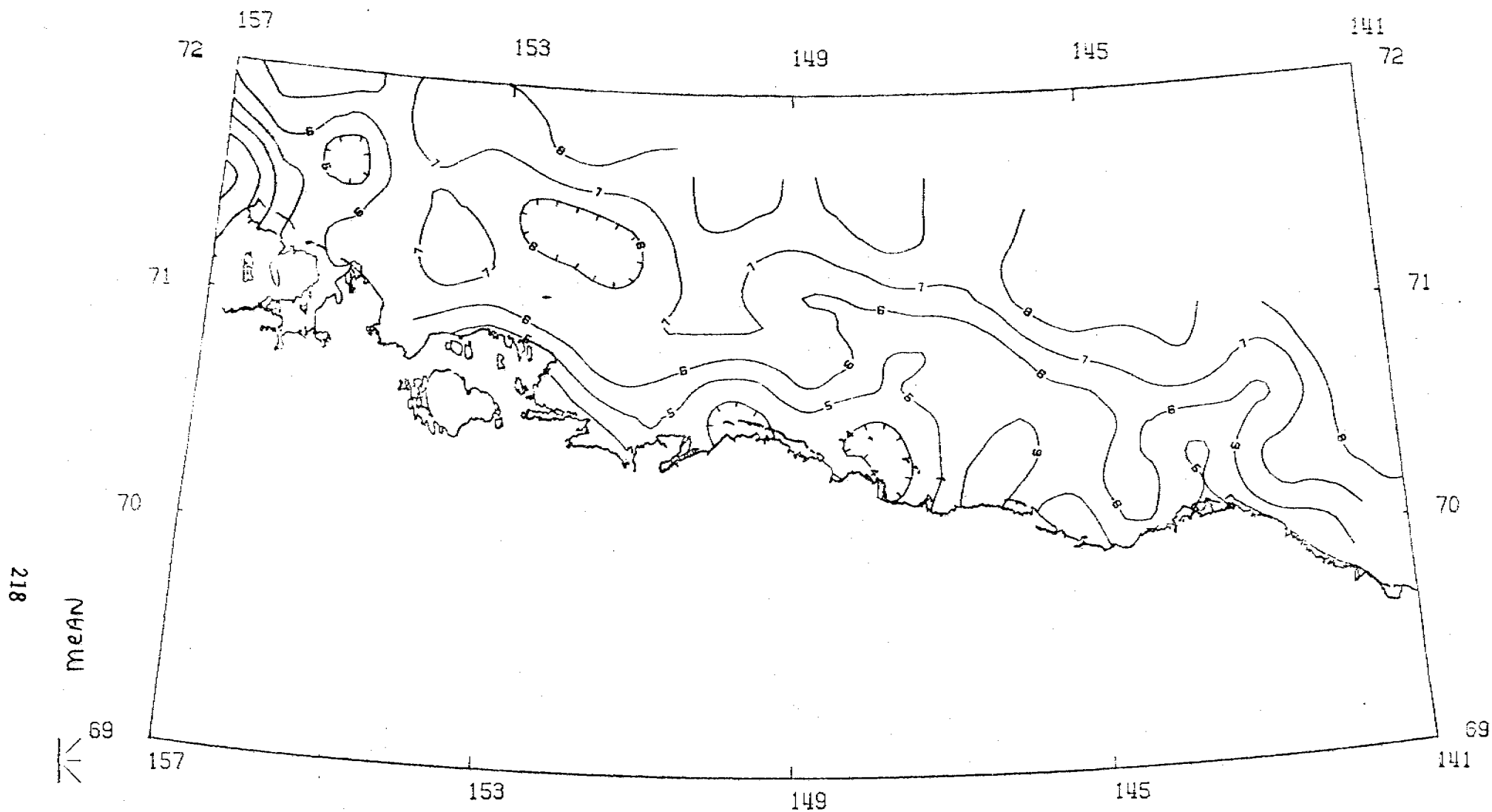


Figure 10. Map of the Beaufort Sea showing the variation of the phi mean size (M_z) of the sediments.

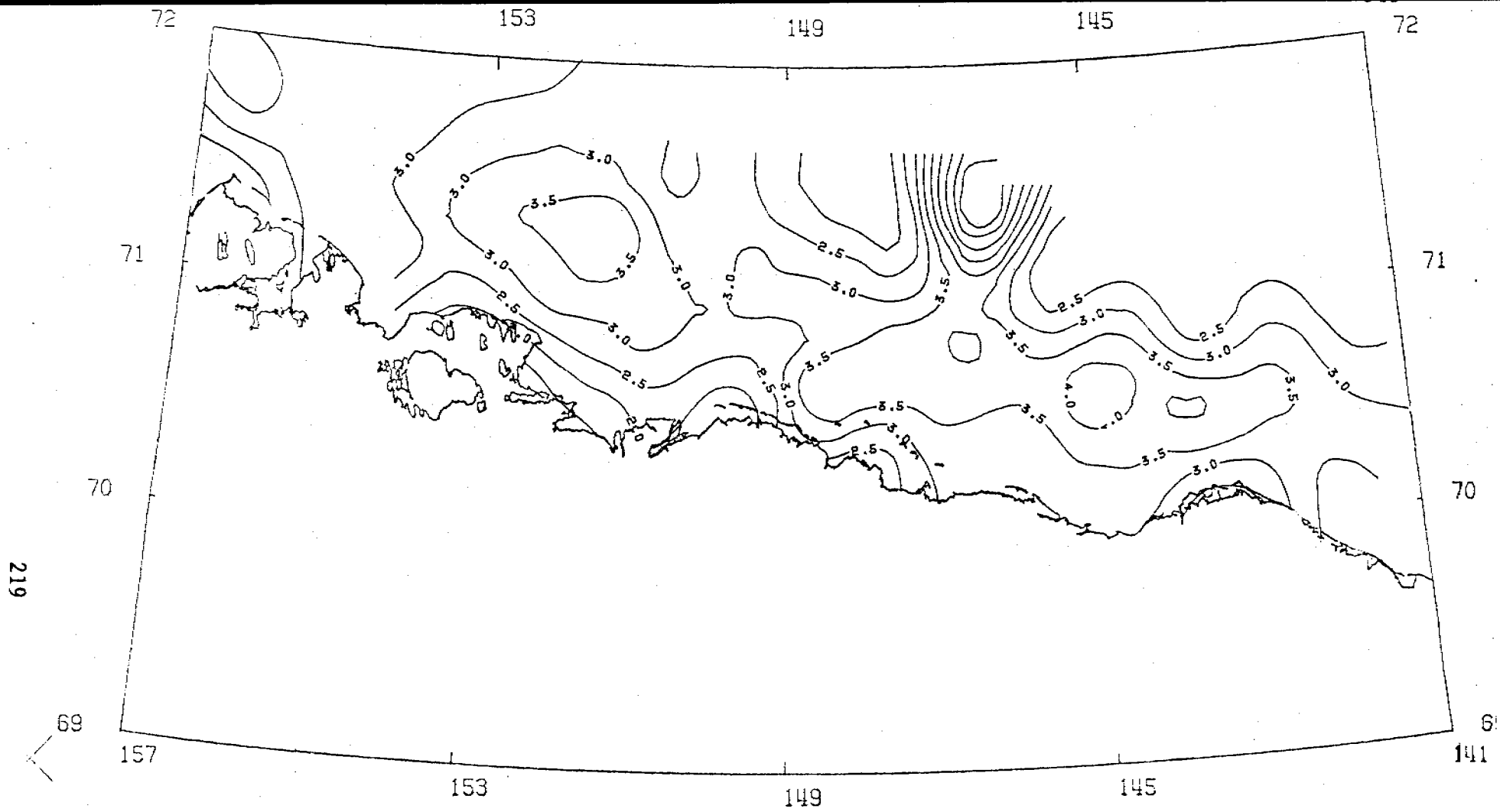


Figure 11. Map of the Beaufort Sea showing the variation in sorting of sediments.

substrate with minor clay and occasional gravel-size particles. No unequivocal lithological gradation is observed across the Beaufort Sea shelf. There are a few extensive regions within the middle shelf where significant amounts of gravel are encountered (Fig. 5). It is believed that the offshore gravels are relict deposits presumably transported by ice-rafting during Pleistocene higher sea-levels. These coarse deposits have not been blanketed by contemporary muds because of very low rates of sedimentation on that shelf portion. It would seem that the transport of gravel and sand size particles by ice-rafting is insignificant presently; however large volumes of terrigenous mud are being carried offshore by this mode.

STRATIGRAPHIC STUDIES ON CORE SAMPLES

The depositional processes in the Colville Prodeltic (?) area (Fig. 12) have been inferred from examination of the stratigraphy of unconsolidated cores (Figs. 13 and 14). It would seem that in the proximal end of the prodelta sediments have been depositing under fluctuating hydrodynamic conditions. This is evident from the presence of alternate bands and laminations of relatively high and low sand contents in cores PWB76-18, 19, 20 and 23. Additionally, it is suggested that in the area of the shelf from where these cores were retrieved reworking of sediments by bioturbation and/or ice gouging has not prevailed in recent times. This is inferred from the lack of stratigraphic homogeneity in the four core samples. However, core PWB76-1 (Fig. 13) which was retrieved from the Central Prudhoe Bay (Fig. 12) at 3 m water depth consists essentially of homogenous clayey silt with no evidence of sediment layering on basis of textural analysis. This would mean that

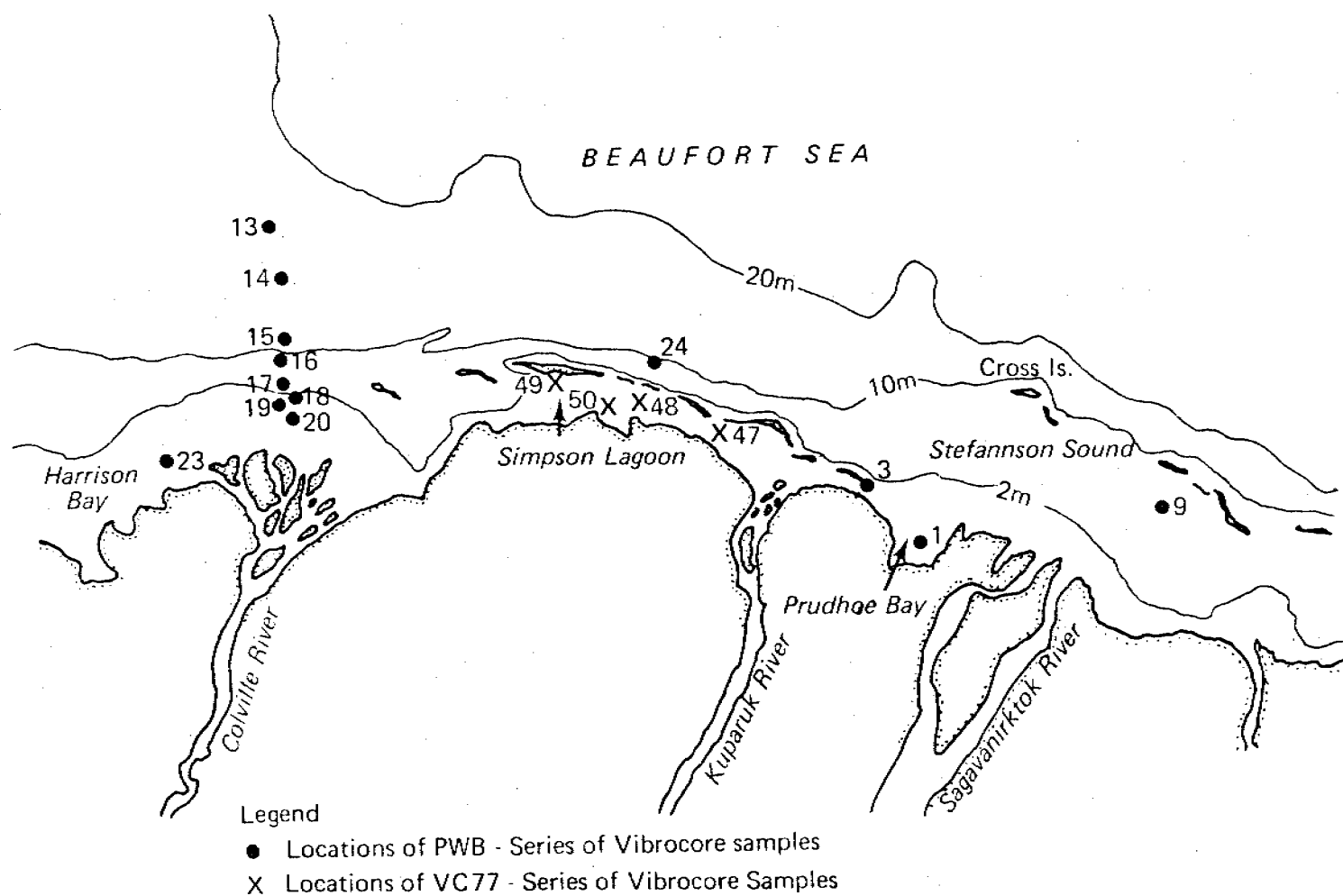


Figure 12. Locations of vibrocore sediment samples that have been collected by Drs. P. W. Barnes and E. Reimtz of the U.S. Geological Survey in 1976 and 1977. Splits of core samples from locations depicted by heavy dots have been provided to us for study.

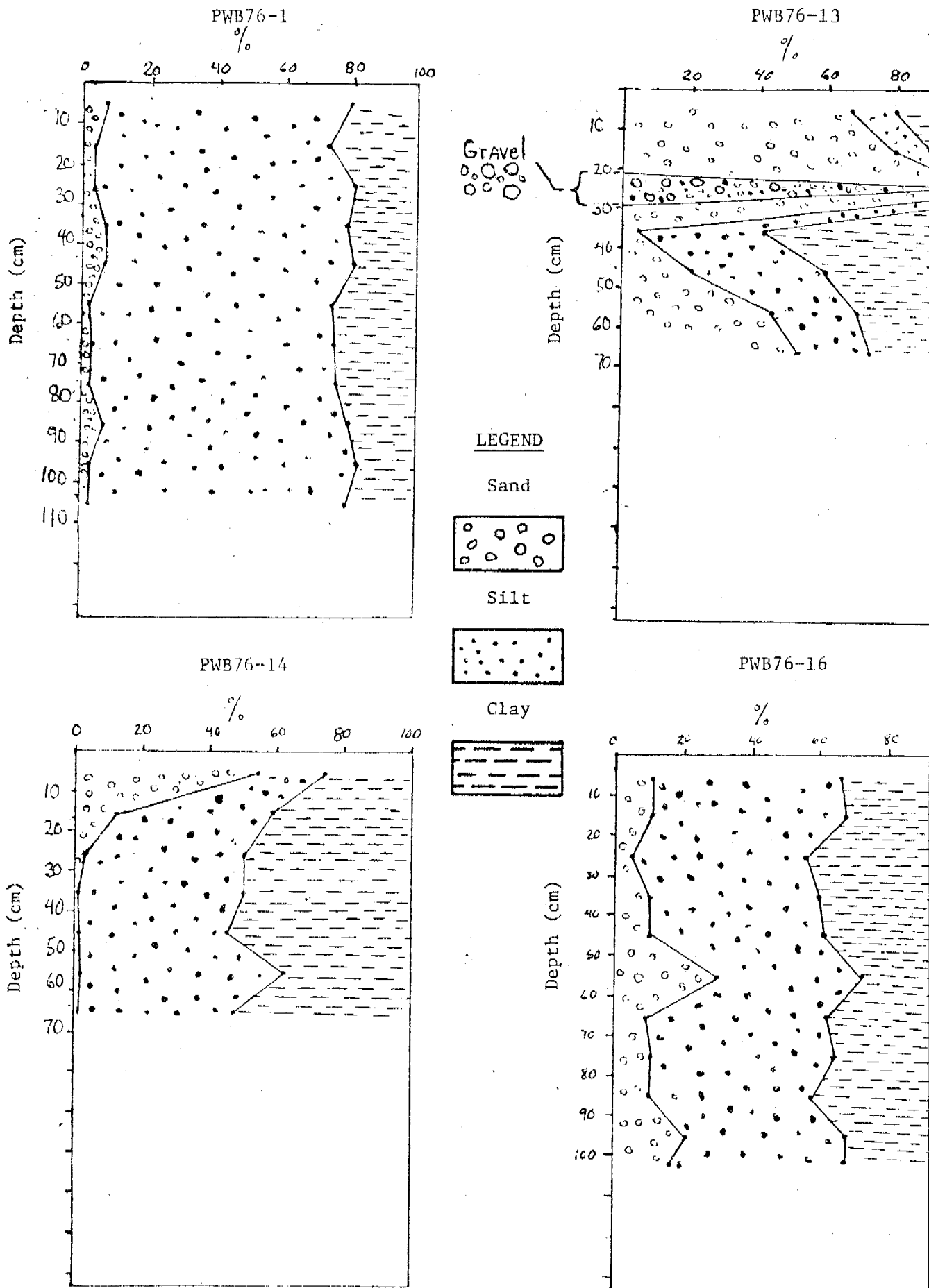


Figure 13. Variation of sediment texture with depth of PWB76 core samples.

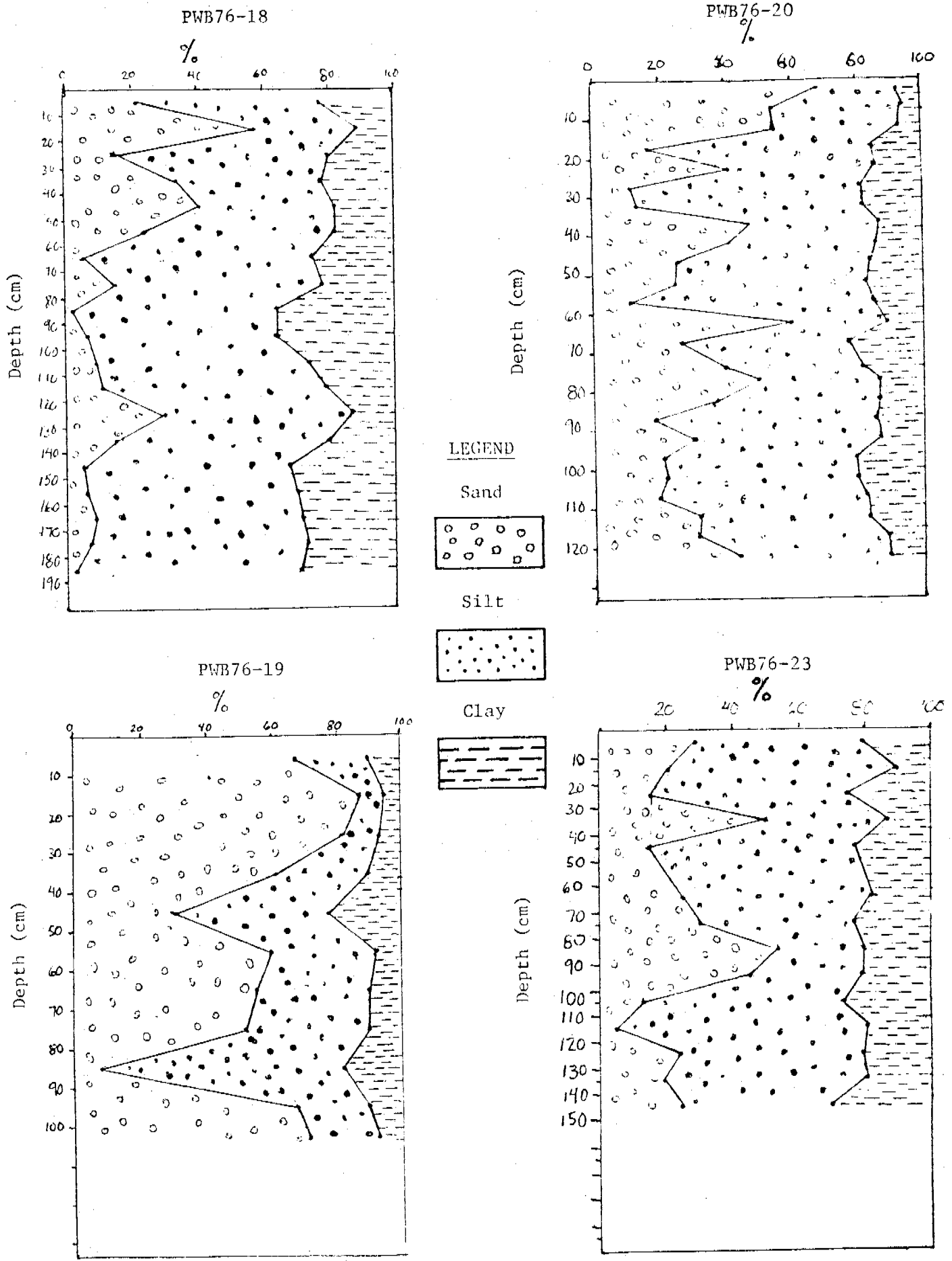


Figure 14. Variation of sediment texture with depth of PWB76 core samples.

sediments of the Prudhoe Bay have either not been completely free from reworking by ice gouging, or deposition in the bay has continued under similar hydrodynamic conditions during recent times.

Stratigraphic studies of short core samples (including lithological, structural and coarse-fractions changes) from the Simpson Lagoon (VC77-49 in Fig. 12) have assisted in the understanding of the lagoon evolution. It would seem most likely that the Simpson Lagoon has evolved from coalescing of several coastal lakes and subsequent inundation of the composite lake by the sea. The Pingok and the adjacent tundra blanketed islands which presumably represent remnant coastal highlands, delineated the inundated lakes from the open sea to form the present Simpson Lagoon. A ^{14}C date on a peat sample of lacustrine origin and separated at approximately 150 cm from top of Core VC77-49, suggests that the Simpson Lagoon is not older than 4500 years.

Deltaic Sediments

Grain size statistical parameters for contemporary sediment samples from several subfacies of the deltaic complex in north arctic Alaska were determined.

Results of the granulometric analysis of the various subenvironments are indicated in Table I. Evidently the deposits of the lagoon, bay and open shallow marine environments cannot be differentiated on the basis of the conventional grain size statistical parameters. However, the coastal beach, dune and deltaic plain sediments have distinctive lithologies. It is contended that textural relationships do not seem to be rigorously definitive with regard to delineating paleosedimentary environments of

TABLE 1. SUMMARIZED DATA ON THE TEXTURE OF RECENT DELTAIC SEDIMENTS ON, THE NORTH SLOPE, ARCTIC ALASKA. DESCRIPTIVE GRAIN SIZE PARAMETERS CALCULATED BY FOLKS (1958) METHOD

Environment	Gross Texture	Md (ϕ)	M _z (ϕ)	σ_1	Sk ₁	K _G
River Channel	Gravelly-sand to clayey-sand	-3.4 to 5.6	-2.4 to 5.9	Very poorly to poorly sorted	Positive to very positive	Platykurtic to extremely leptokurtic
Tundra Deltaic Plain (Marsh)	Structureless peaty organic muck, with sparse inorganic particles, and occasional frost- heaved gravels and collian sand	-	-	-	-	-
Mainland Coastal Beach	Gravel-gravelly- sand, and sand	-2.8 to 1.3	-2.8 to -0.6	Poorly sorted (many); moderat- ely sorted (few)	Continuous range from positive to negative	Platykurtic (predominantly) to leptokurtic
Bay	Sand, silty-sand and sandy-silt	2.8 to 6.6	2.9 to 6.8	Very poorly sorted to poorly sorted; few well sorted	Continuous range from positive to negative	Platykurtic to very leptokurtic
Lagoon	Sand, sandy-silt, silty-sand, and sand-silt-clay	2.2 to 6.2	2.1 to 7.0	Very poorly sorted; few well sorted	Most positive, few nearly symmetrical	Highly variable mesokurtic to extremely leptokurtic
Coastal Dune	Medium to fine sand	1.8	1.8	Well to very well sorted	Nearly symmetrical	Mesokurtic
Barriers	Gravel, gravelly- sand, and sand	-2.5 to -8.0	-1.5 to -8.0	Well sorted to very poorly sorted	Very positive to very nega- tive	(Not available)
Open Marine (Delta front platform?)	Sand-silt-clay to silty-clay	2.2 to 8.3	1.2 to 8.1	Very poorly sorted	Most posi- tive, few very positive	Platykurtic to extremely leptokurtic

polar deltas. The distinctive granulometric composition of North Slope coastal beaches is predominantly attributable to a local unique provenance (e.g., gravel-enriched Quaternary Gubik Formation underlying coastal tundra), rather than solely to depositional processes prevailing in the polar region.

The characteristics of Simpson Lagoon substrate are displayed in Figure 15. The Simpson Lagoon cannot be considered as a typical representative of arctic lagoons, at least as far as the sedimentary regime is concerned. By comparison the sediments of the Simpson Lagoon are relatively coarser, have higher organic carbon and expandable clay minerals, and lower heavy metal and kaolinite contents than the sediments of the lagoons near the Demarcation Point (type area: Beaufort Lagoon). These regional differences are attributed to differences in terrigenous sources of sediments of the various lagoons and the energy levels of the hydrodynamic conditions of deposition.

STRUCTURE AND ORIGIN OF TURBID PLUMES IN COASTAL AREAS IN LATE SUMMER

Satellite images clearly display that movement of turbid plumes along the nearshore lagoons and bays of north Alaskan arctic is either in the form of long continuous plumes or disconnected irregular streaks and wedges. With the exception of the Tigvarik Island area where an eastward moving gyre is apparent along most of the coast, the nearshore turbid plume is invariably seen to move westward. The latter water movement is impelled by the prevailing westward littoral currents. However, we are not quite sure whether the tongues of turbid plumes in the lagoons and bays in mid and late summer can be ascribed to fluvial discharge and thermoerosion of coastal bluffs and barriers. No such direct association is apparent from detailed scrutiny of several multi-year satellite

Legend

 > 50% Sand

 > 50% Mud

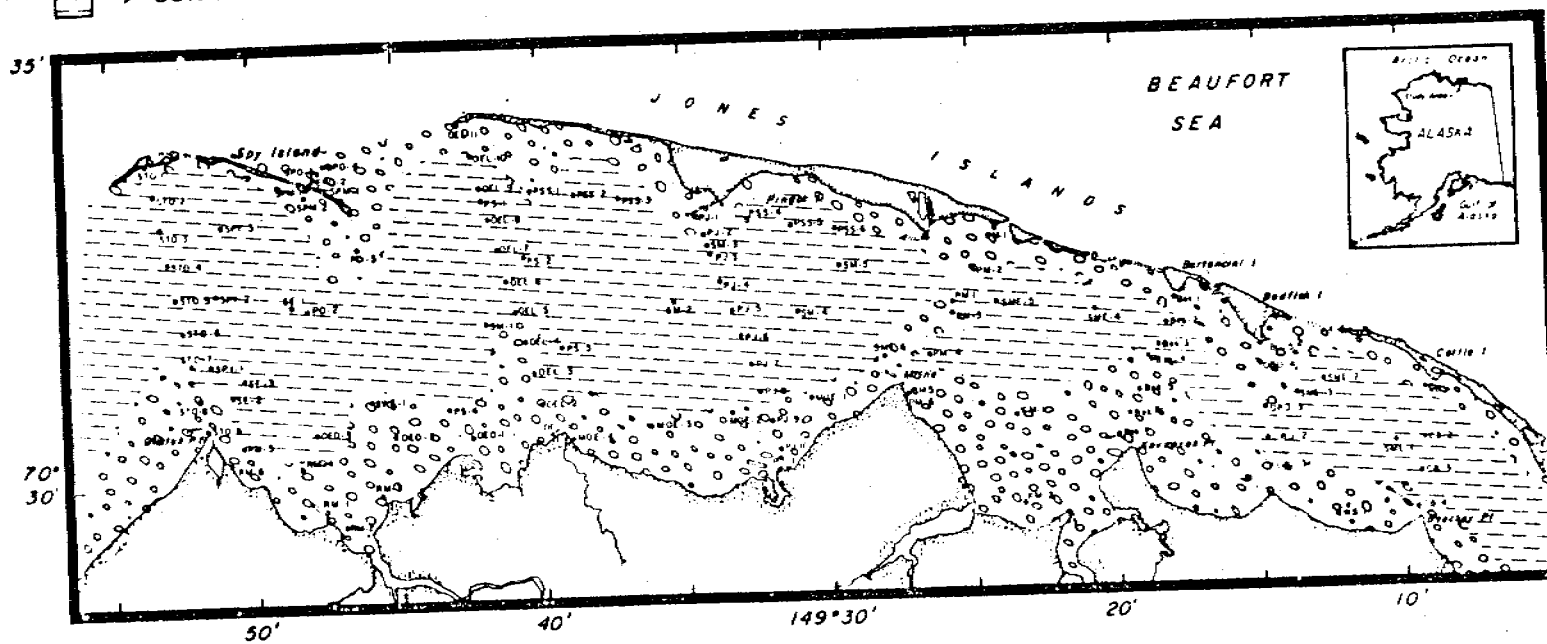


Figure 15. Characteristics of substrate lithology in Simpson Lagoon.

images, although invariably extensive turbid plumes do occur in the vicinity of large river mouths. It is important to note that comparatively fresh fluvial waters are discharged in late summer from mouths of the major distributary channels, while presence of relatively turbid waters can be delineated at some distance off the mouths. Additionally, the lagoon waters extending up to a few meters away from the coastal bluffs and barrier islands are observed to be relatively less turbid than the rest of the lagoon. A notable example is the Dease Inlet region. All these observations lead us to suspect that in mid and late summer when the fluvial outflow is low, much of the turbid coastal water is generated by resuspension of the cohesionless substrate particles from shallow-water regions by wave induced agitation. Since the region slightly off the river mouths are generally more shallow and are constituted by unconsolidated clays relatively high turbid waters are associated with such areas. Subsequent to resuspension the particles are carried westward in the form of a turbid plume.

Sedimentation Rates

Sedimentation rates have been estimated, based on ^{210}Pb dating techniques, for the Simpson Lagoon, Harrison Bay, a coastal lake and continental slope of the Beaufort Sea (Fig. 16). In the Harrison Bay the rate ranges between 0.60 cm yr^{-1} and 1.64 cm yr^{-1} . In the Simpson Lagoon there is a net decrease from 0.82 cm yr^{-1} in the western end to 0.52 cm yr^{-1} in the central lagoon due south of the Pingok Island. The lateral variations in the sedimentation rates within the contiguous bay-lagoon region is obviously a reflection of the volume of deposition of the Colville River debris. A few cores from the continental shelf were

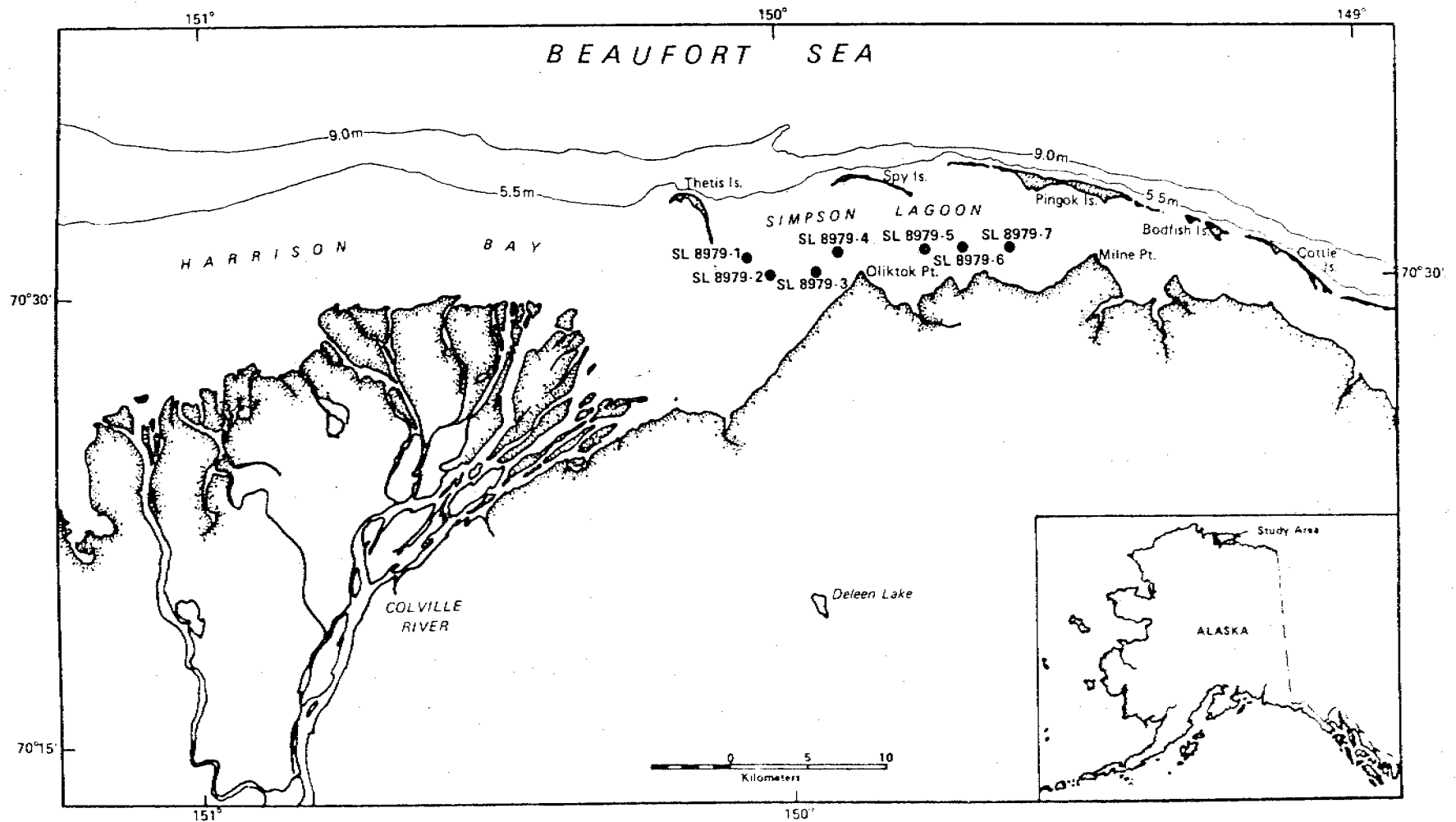


Figure 16. The area of study showing locations of the core samples in the Simpson Lagoon, east Harrison Bay and Deleen Lake.

also processed for the sedimentation rate estimation; however because of a lack of a clear-cut net linear exponential decay in ^{210}Pb , no meaningful rate could be obtained. Presumably, reworking of sediments by ice-gouging tends to homogenize the ^{210}Pb stratigraphy in the shelf region. In the continental slope the sedimentation rate, as it is to be expected, is relatively low (i.e., between 0.70 to 0.45 mm yr^{-1}).

Source and Origin of Erratic Boulders (Flaxman Formation) on Alaskan Beaufort Sea Coast

Results of the detailed petrographic studies on about 80 separate samples of boulder chips and visual inspection of hundreds of samples in the field have enabled us to define the composition of the boulders that are scattered on the beaches of the Pingok, Bodfish and Flaxman Islands, and in the vicinity of the Prudhoe Bay and lower Canning River. Based on knowledge of known rock types in the Brooks Range, Davidson, British and Romanzof Mountains and the MacKenzie River drainage area it would seem most unlikely that the boulder samples have their source in the hinterland of northern arctic Alaska or the adjacent northwest Canada (i.e., Great Slave and Bear Province of Canada). Based on the unique lithologic assemblage and the relatively old age of the pink granitic samples (i.e., about 2 million years) and the regional geology of the Canadian Archipelago it is contended that the boulders have a major source in the Coronation Gulf region of northern Canada. It is further surmised that the boulders were most probably ice-rafted to the Beaufort Sea coast, presumably during the Pelukian Transgression when the interglacial sea-level was significantly higher than the present time.

CLAY MINERALOGY OF THE BEAUFORT SEA

The predominant clay mineral is illite (45-70%) with relatively minor amounts of glycol expandable mineral, kaolinite, chlorite and mixed-layered phases. The dispersal patterns of the expandable mineral and the kaolinite/chlorite ratios in the continental shelf are exhibited as Figures 17 and 18. The sources of fine grained particles, as based on clay mineral studies, for the Simpson Lagoon are displayed in Figure 19. It is concluded that the observed clay mineral distributional patterns in the inner shelf and deltaic areas are related to the various terrigenous sources, the prevailing transport pathways and eventual depositional sites of fine grained particles. Clay mineral studies substantiate a net westward alongshore sediment drifts. The coastal region of Harrison Bay and the western-most portion of Simpson Lagoon are impacted by the clays from the Colville River, whereas the outer Harrison Bay, the eastern Simpson Lagoon, the inshore region off the Jones Island chain, and the Stepfanson Sound receive large fluxes of sediments from the Kuparuk and Sagavanirktok Rivers. Our ability to fingerprint the clay mineral assemblages of the various fluvial systems of the North Slope offers a unique criteria to interpret the disposition of paleochannels, and also of paleocurrent directions, for the Beaufort Sea nearshore.

SEDIMENT GEOCHEMISTRY

Organic Carbon and C/N ratios: The average contents (by dry weight %) of organic carbon and nitrogen and average C/N ratios of marine sediments for various environments of the north Alaskan arctic are presented in

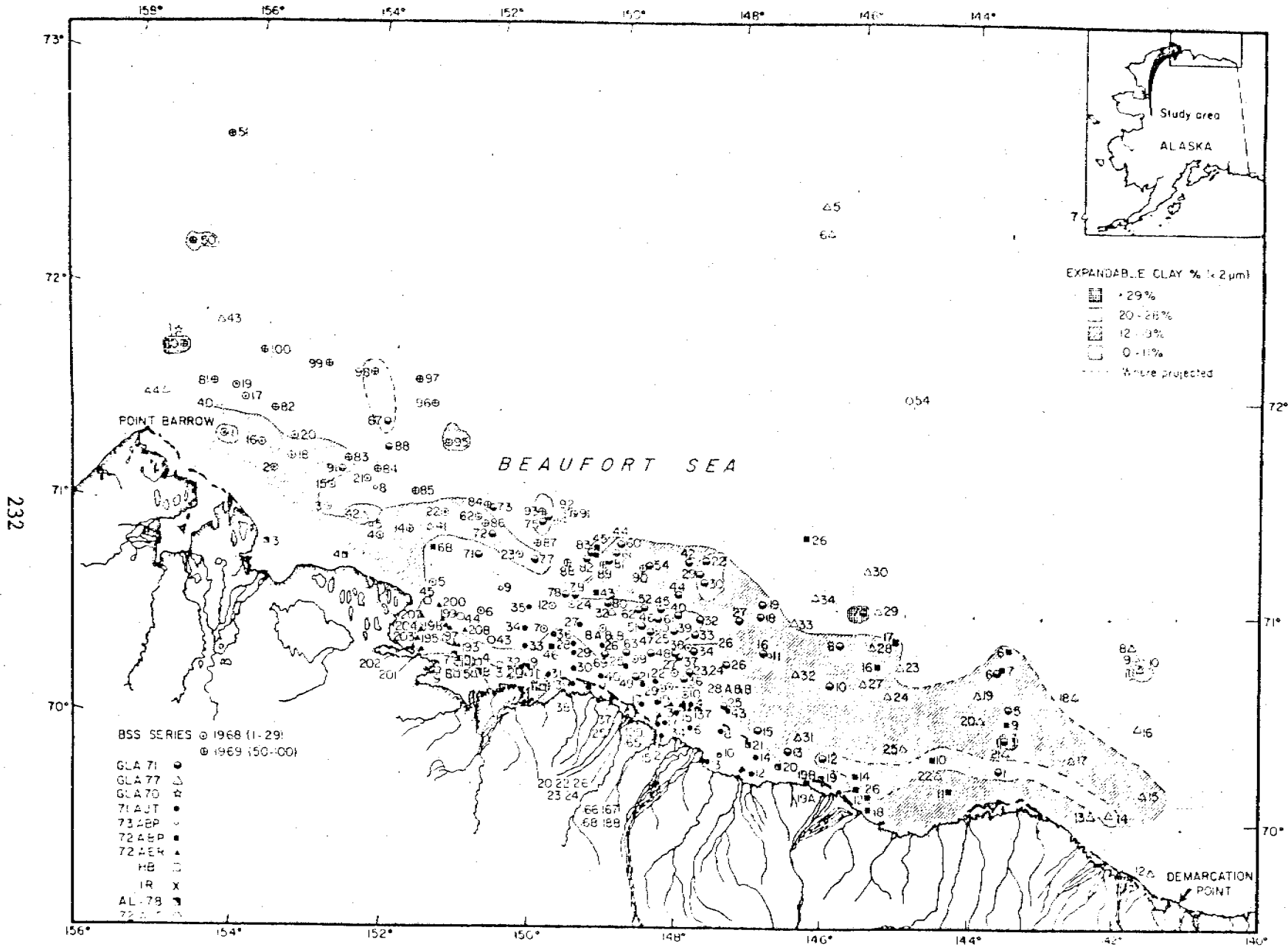


Figure 17. Expandable clay mineral distribution in Beaufort Sea surface sediments.

LEGEND

-  Colville Influx, Almost Entirely (90%)
-  Predominantly Colville (85%); with minor influx of Kuparuk (10%) & Sagavanirktok Rivers (5%)
-  Predominantly Kuparuk River (80%) with minor Sagavanirktok River Influx (15%) & Colville River (5% or less).

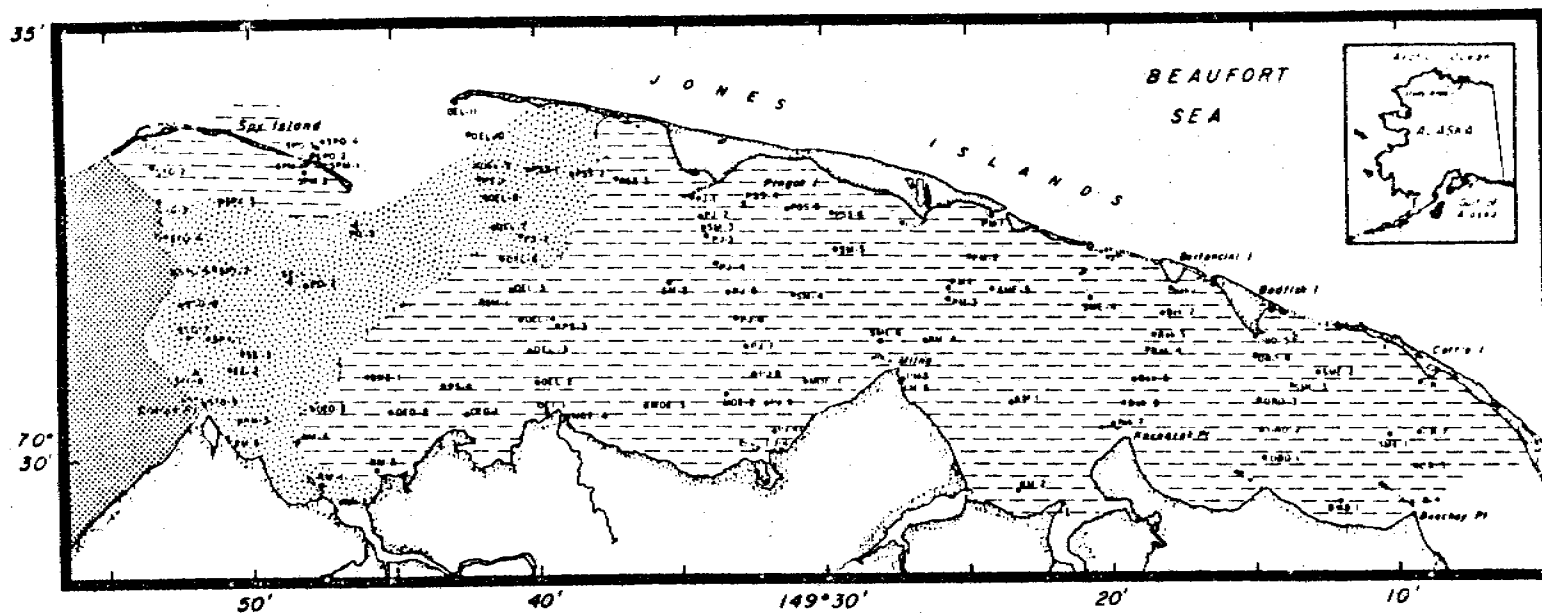


Figure 19. Sources of fine-grained (mud fraction) fluvial sediments* based on detailed clay mineral analysis.

* Sources of mud from coastal bluffs and barriers not considered.

Table II. The distribution pattern of organic carbon in the Beaufort Sea and the Simpson Lagoon are shown in Figures 20 and 21. The C/N ratios of the arctic deltaic sediments are slightly higher than the 8 to 12 ratios reported as typical for the low-latitude deltaic sediments. A net decrease in the C/N ratios of sediments from the nearshore to deeper waters has been recognized. It is surmised that the latter variations are most likely attributable to seaward decrease in the flux of terrigenous organic detritus. This is substantiated by the pattern of seaward variations in the stable isotope ratios ($\delta^{13}\text{C}$) of organic carbon in sediments.

Organic carbon in the particulate and dissolved phases of a few water samples have been analyzed. The content of particulate organic carbon (POC) in the Colville River fresh-water regime is $0.54 \text{ mg } \ell^{-1}$, whereas in the lower saline or brackish portion it is about $0.34 \text{ mg } \ell^{-1}$. In the east Harrison Bay and Simpson Lagoon the POC values are 0.28 and $0.31 \text{ mg } \ell^{-1}$, respectively. The dissolved organic carbon (DOC) in the Colville River and east Harrison Bay waters are 4.4 and $2.9 \text{ mg } \ell^{-1}$, respectively.

Carbonate Contents: The distributional pattern of carbonate contents (wt. %) in bottom sediments of the Beaufort Sea are illustrated in Figure 22. A net seaward decrease in carbonate contents is apparent.

Heavy Metal Geochemistry: The baseline concentrations of eight metals (e.g., Fe, Mn, Cu, Co, Cr, Ni, V and Zn) in four depositional facies (e.g., Continental shelf, Harrison Bay, Simpson and Beaufort Lagoons) of the Beaufort Sea are compared in Table III. More detailed fractionation patterns of the metals for the Simpson Lagoon sediments

TABLE II

AVERAGE CONTENTS (BY DRY WT. %) OF ORGANIC CARBON AND NITROGEN,
AND AVERAGE C/N RATIOS OF COASTAL TUNDRA PEAT, AND
SURFICIAL SEDIMENTS OF THE CONTINENTAL MARGIN
OF THE BEAUFORT SEA AND CANADA BASIN

Environment	Organic Carbon	Nitrogen	C/N Ratios
Harrison Bay	0.88	0.08	11.7
Simpson Lagoon	1.12	0.08	13.2
Open Beaufort Sea Shelf (21 m to 64 m)	0.73	0.08	9.0
Continental Slope (64-1000 m)	0.89	0.12	7.0
Deep-Sea (>1000 m)	0.81	0.17	5.2
Coastal Tundra Peat*	-	-	19.0*

* Average of C/N ratios of several samples provided by Dr. D. Schell (personal communication).

Organic Carbon Contents (wt. %)

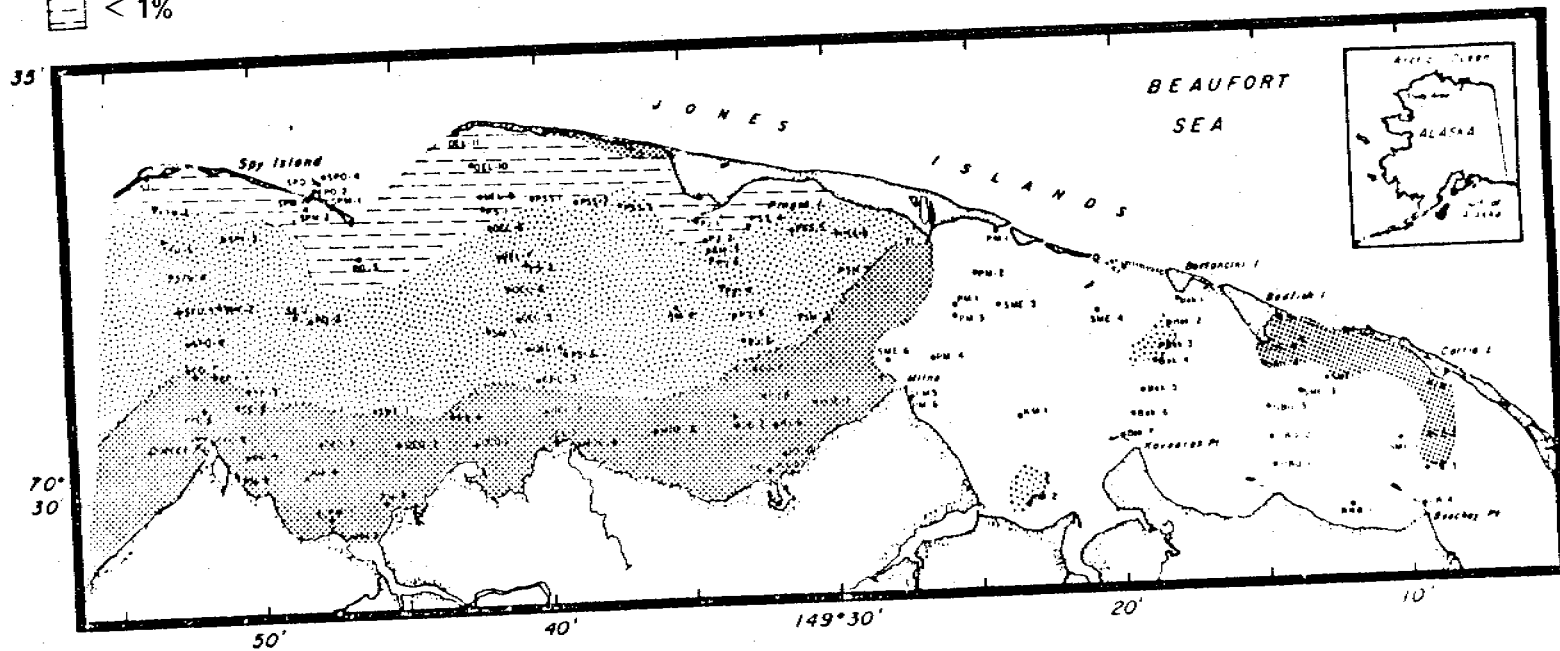
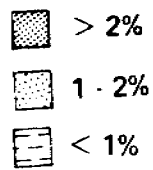


Figure 20. Organic carbon contents (dry weight percent) in substrate sediments in Simpson Lagoon.

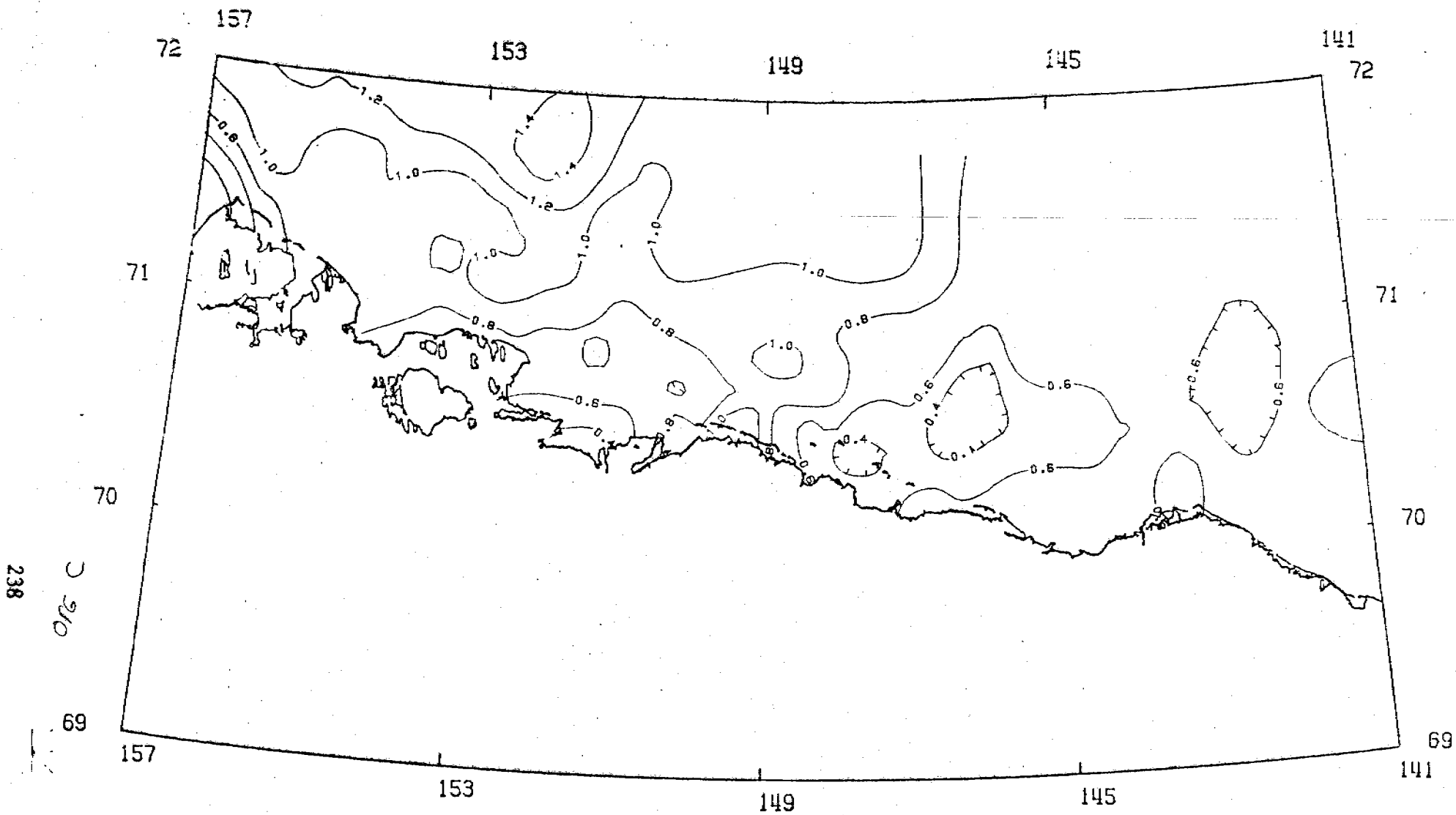


Figure 21. Map of the Beaufort Sea showing the distribution of organic carbon (wt. %) in bottom sediments.

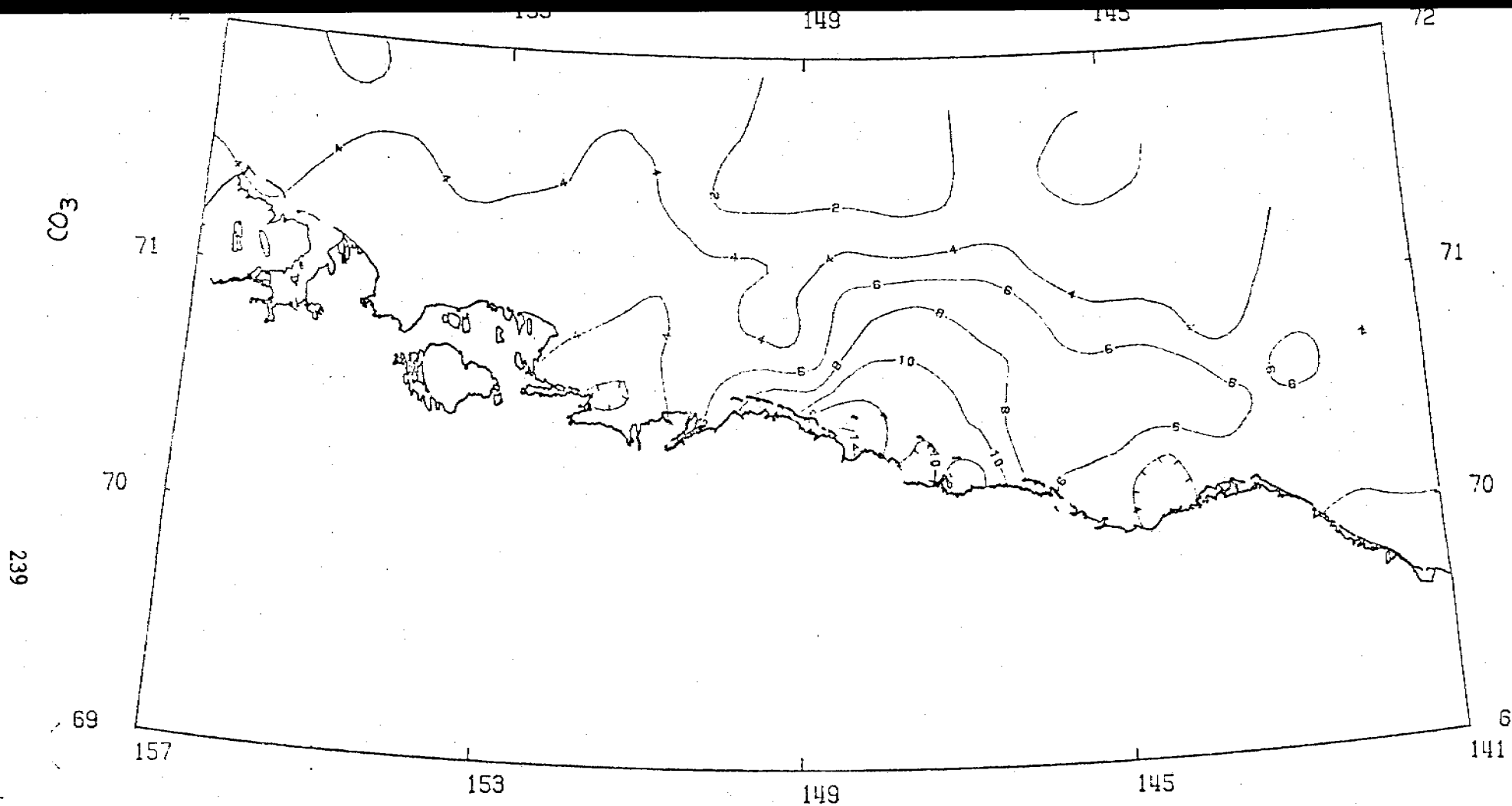


Figure 22. Map of the Beaufort Sea showing the distribution of carbonate (wt. %) in bottom sediments.

TABLE III

AVERAGE CONCENTRATIONS ($\mu\text{g/g}$, EXCEPT Fe WHICH IS IN 10 $\mu\text{g/g}$) OF SOME HEAVY METALS IN THE TOTAL (T) AND THE ACETIC ACID-HYDROXYLAMINE HYDROCHLORIDE EXTRACTS (E), WITH CALCULATED PERCENT EXTRACTABLE QUANTITIES (%E) FROM 54 SIMPSON LAGOON, 19 BEAUFORT LAGOON, 7 BEAUFORT SEA AND 7 HARRISON BAY (ONLY TOTAL) SEDIMENTS

Environment	V			Cr			Mn			Fe			Co			Ni			Cu			Zn		
	T	E	%E	T	E	%E	T	E	%E	T	E	%E	T	E	%E	T	E	%E	T	E	%E	T	E	%E
Simpson Lagoon	70	4	6	45	1	2	260	130	50	2.0	.22	11	8	2	25	23	3	14	17	3	18	76	13	17
Beaufort Lagoon	100	9	9	55	1.6	3	400	200	50	2.8	.31	11	10	3.5	35	30	3	10	27	4	15	80	15	19
Beaufort Sea Shelf	140	10	17	85	1.6	2	560	230	40	4.1	.42	10	16	3.9	24	40	3.7	9	33	8	24	112	21	19
Harrison Bay	108			67			410			2.8			10			28			30			80		

are shown in Table IV. The distributional patterns of the eight metals in the Beaufort Sea are displayed in Figures 23 to 30.

Partitioning of Fe, Mn, Zn, V, Cr, Ni, Cu, and Co in 54 arctic lagoon sediments was established. Average metal concentrations on HF-HNO₃ digests are 20,000 ppm Fe, 260 ppm Mn, 75 ppm Zn, 70 ppm V, 45 ppm Cr, 23 ppm Ni, 17 ppm Cu, and 8 ppm Co. A sequential extraction using MgCl₂ salt (EXCH), cation exchange resin (CER), a pH 2 hydroxylamine hydrochloride solution (NHH), acid ammonium oxalate (AAOX), sodium dithionite (DITH), and acetylacetone in benzene (ACETBEN) resolved the partitioning of the metals among the exchangeable phase, carbonate minerals, Mn oxides, amorphous and crystalline Fe oxides, and organic complexes, respectively. Of the total, 5% of Cr, 15% of V, 40% of Fe, Co, and Ni, 55% of Mn, and 60% of Cu constitute the extractables (E). The major portions of the E Fe (90%) and V, Cr, Co, Ni (70%) were removed by AAOX and DITH. Smaller fractions of the E Cu (50%) and Mn (30%) were mobilized by the latter two procedures. The ACETBEN step accounted for 25% of E Cu and 0.5% of E Ni. The combined treatments EXCH + CER + NHH contributed a minor portion of the E trace metals (20 - 30%). A major part of the E Mn (60%) and a very small fraction of the E Fe (4%) were recovered by these three mild treatments. Ni and Cu show significant correlations to the more easily extractable Mn phases.

Total metal abundances of the arctic lagoons are comparable with those of nonpolluted, temperate, nearshore sediments.

The "readily" extractable portions provide an estimate of each metal that is most likely not held in the crystal lattice, and which may be remobilized from sediments under alterations of certain physiochemical

TABLE IV

AVERAGES FOR PARTITIONING (IN PERCENT OF TOTAL CONTENT) OF SOME HEAVY METALS AMONG EXCHANGEABLE, CARBONATE STRUCTURE, AND COMBINED* EXCHANGEABLE, CARBONATE AND EASILY REDUCIBLE PHASES IN SIX SIMPSON LAGOON SEDIMENTS

	V	Cr	Mn	Fe	Co	Ni	Cu	Zn
Exchangeable	0.44	0.12	5	0.1	0.40	0.65	2.6	n/a
Carbonate structure	1.5	1.0	15	1.0	6	10	13	12
Exchangeable, carbonate structure and easily reducible	7	2.5	49	13	30	16	18	18

*The combined phase is identical to the acetic acid-hydroxylamine hydrochloride extract (E) above.

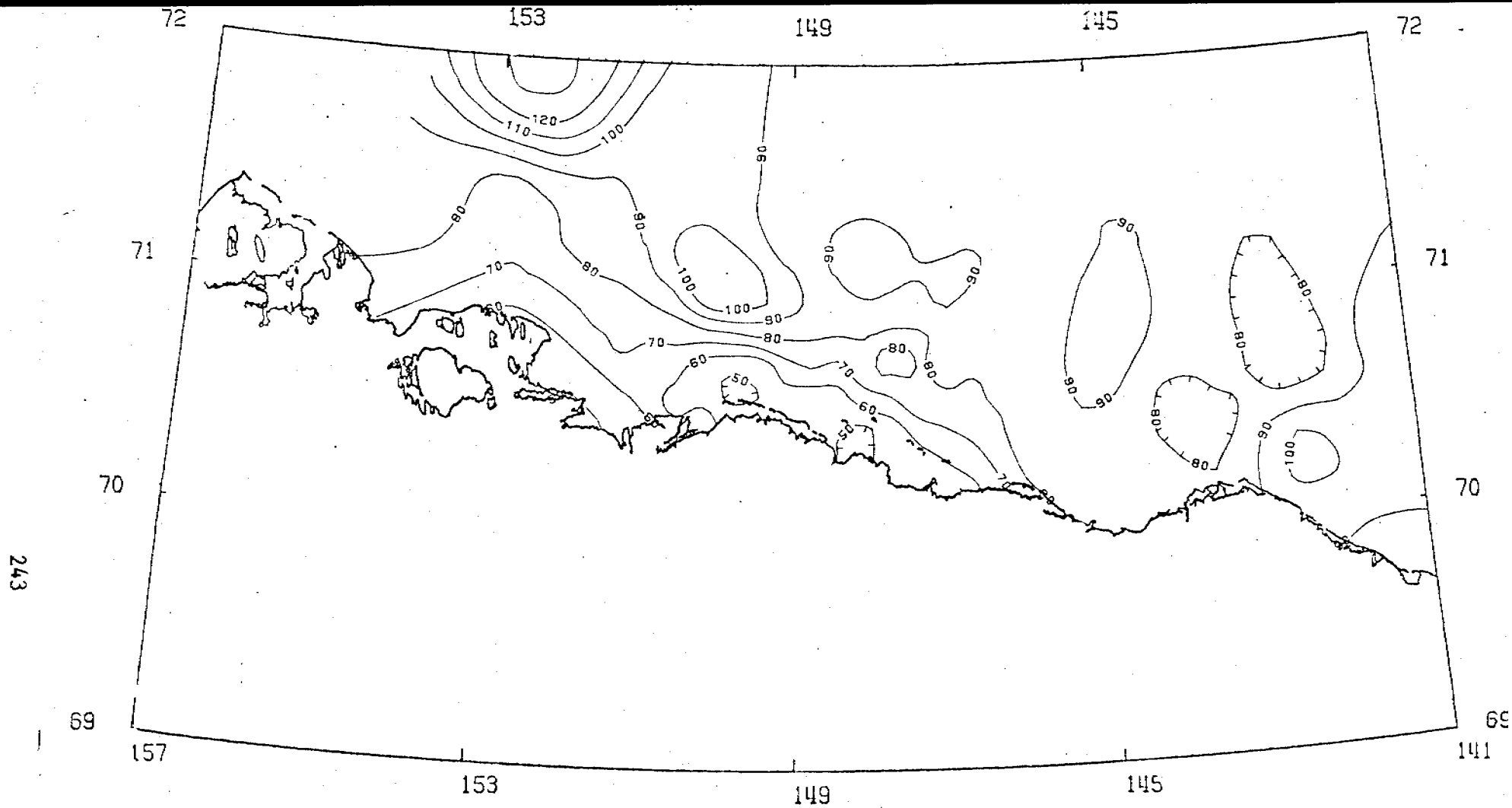


Figure 23. Map of the Beaufort Sea showing the variations in the concentrations ($\mu\text{g/g}$) of chromium in bottom sediments.

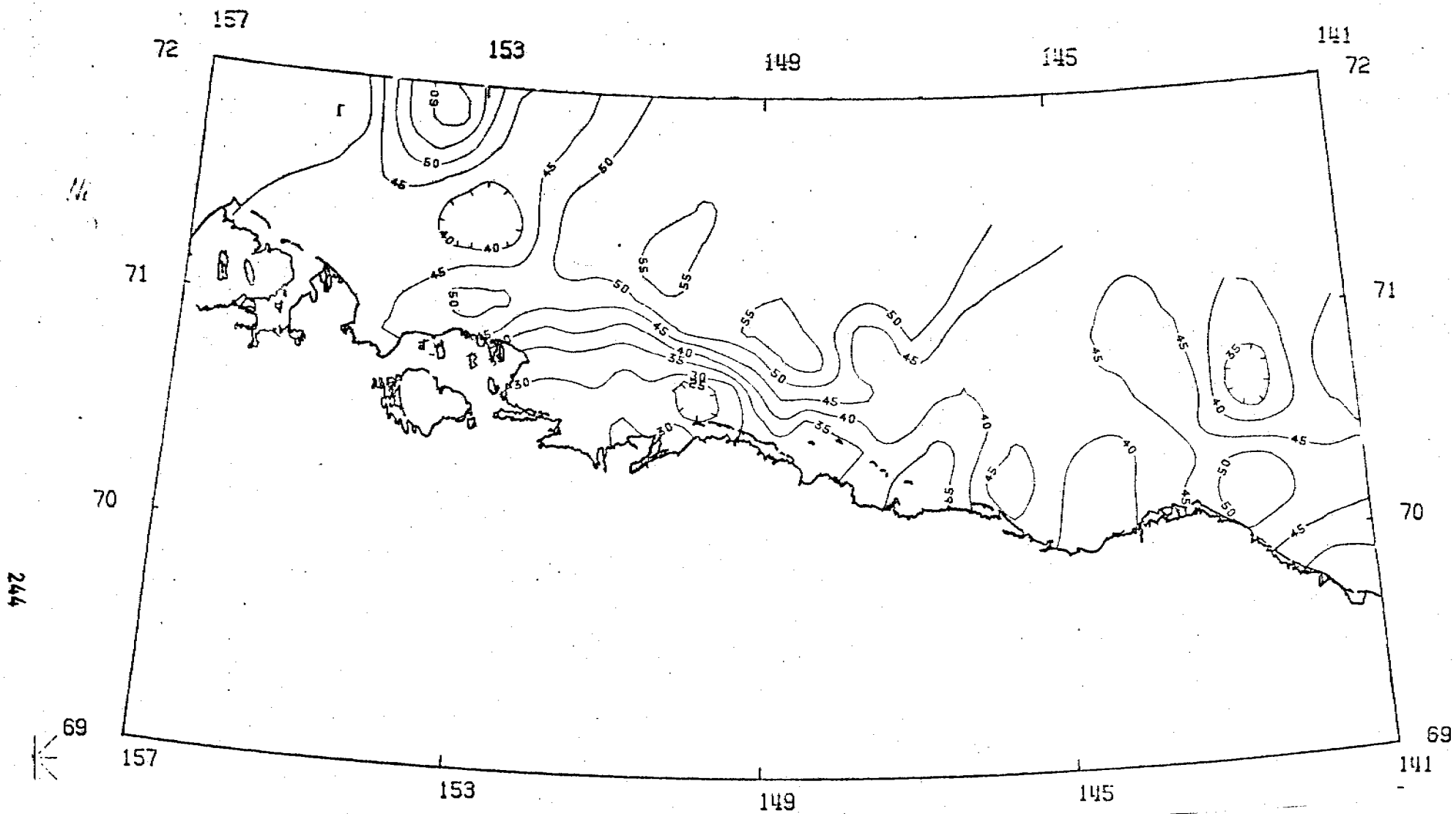


Figure 24. Map of the Beaufort Sea showing the variation in the concentrations ($\mu\text{g/g}$) of nickel in bottom sediments.

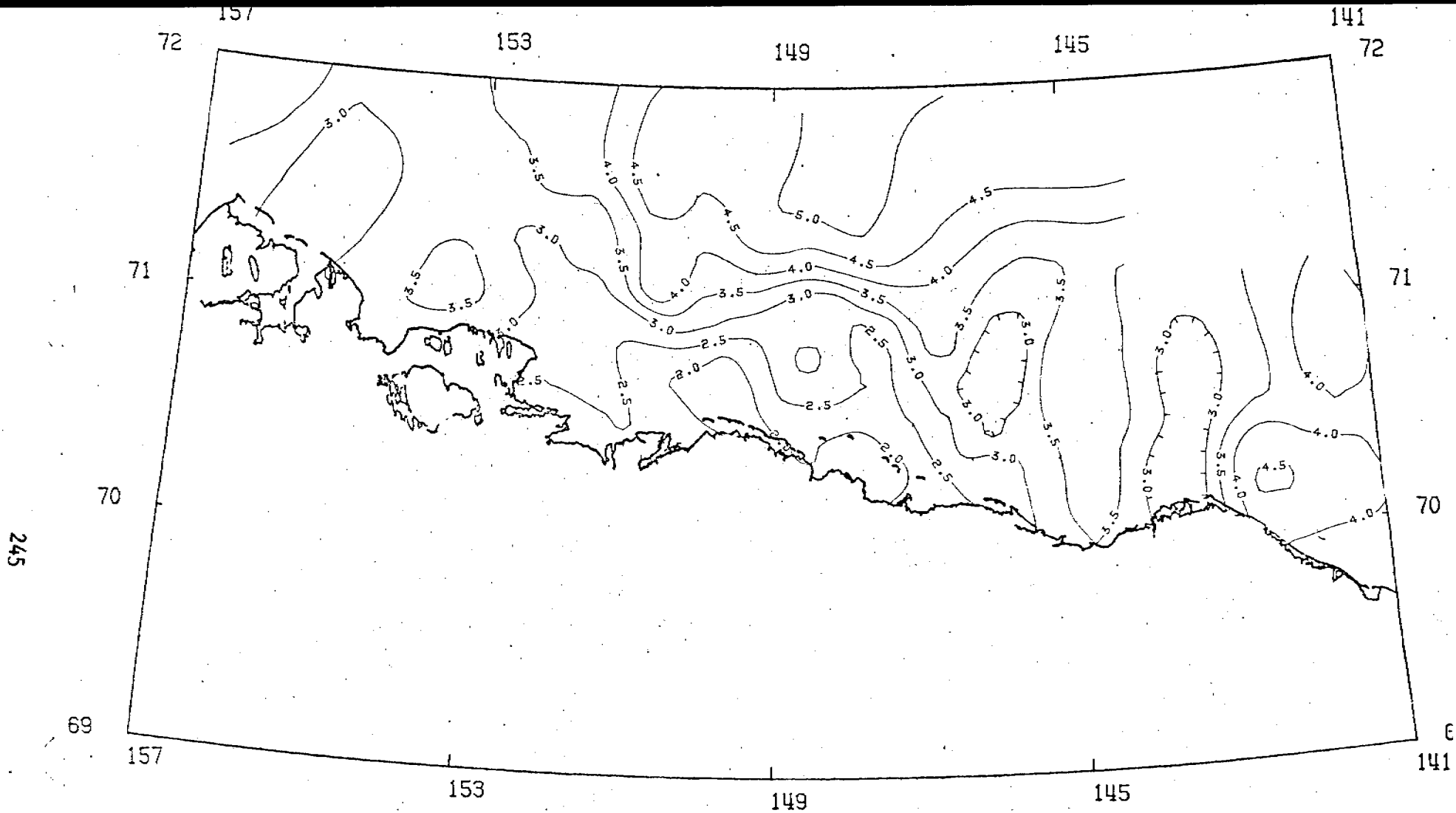


Figure 25. Map of the Beaufort Sea showing the variation of the concentrations ($10^4 \mu\text{g/g}$) of iron in bottom sediments.

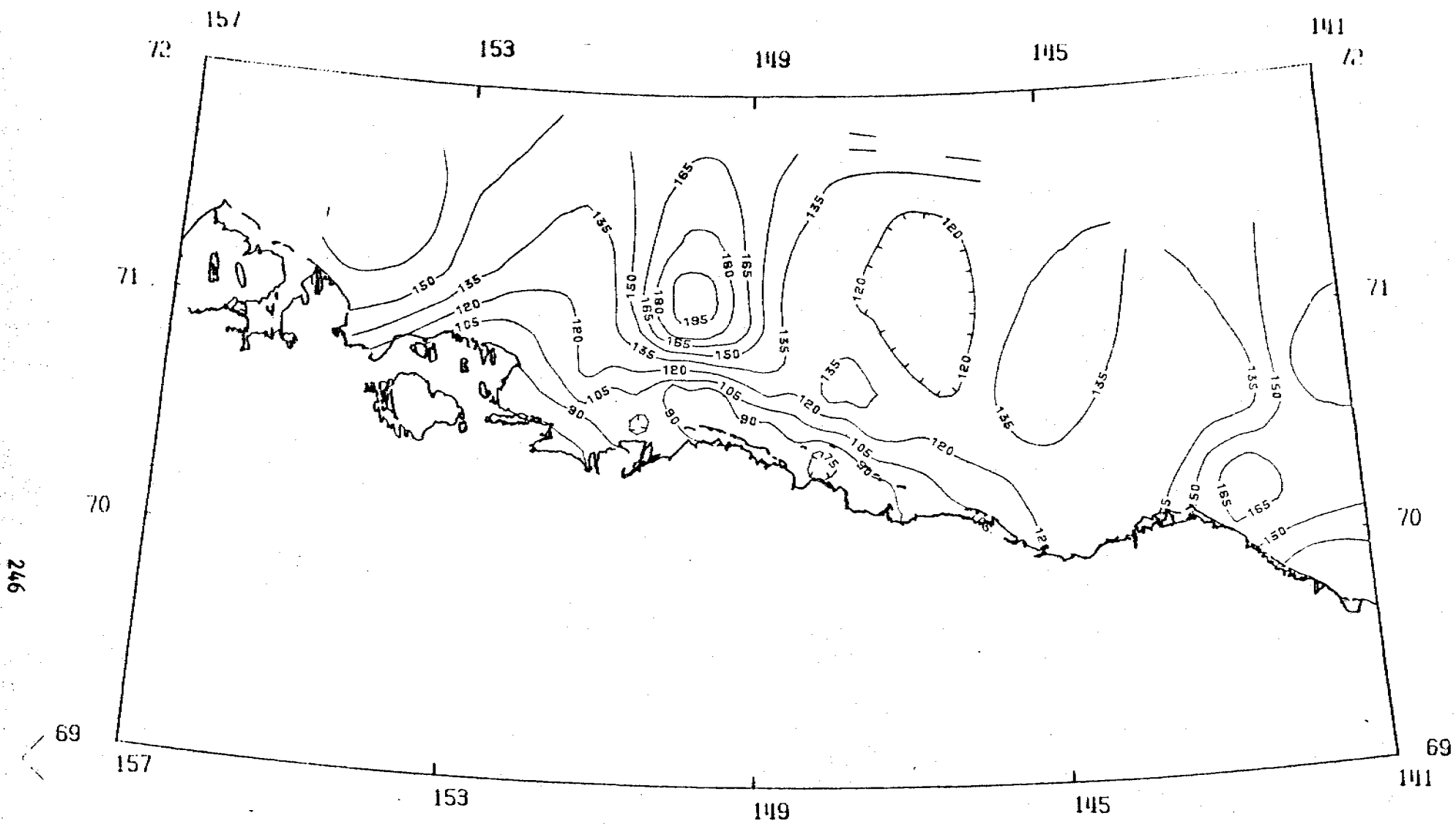


Figure 26. Map of the Beaufort Sea showing variation in the concentrations ($\mu\text{g/g}$) of vanadium in bottom sediments.

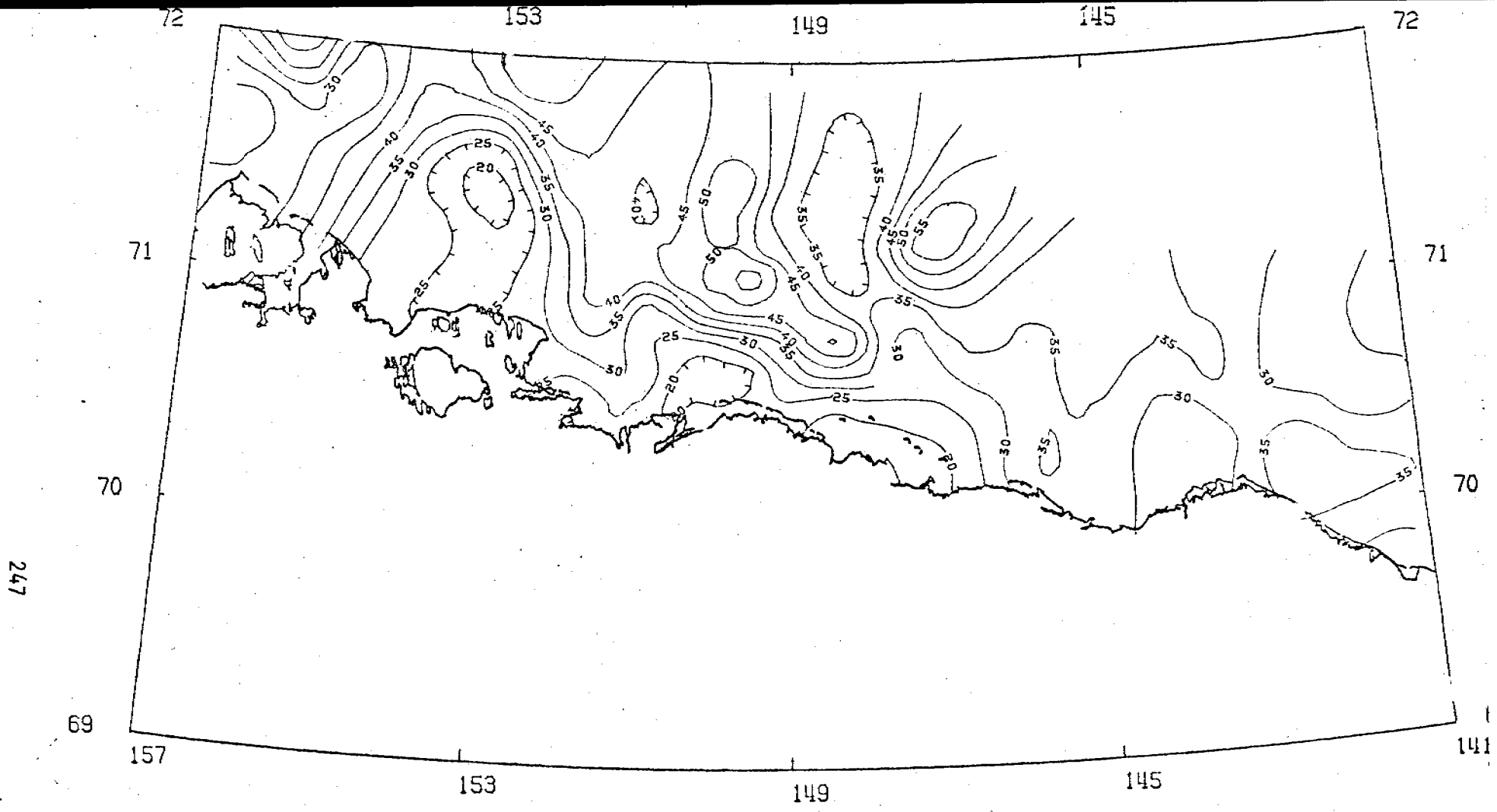


Figure 27. Map of the Beaufort Sea showing variation in the concentrations ($\mu\text{g/g}$) of copper in bottom sediments.

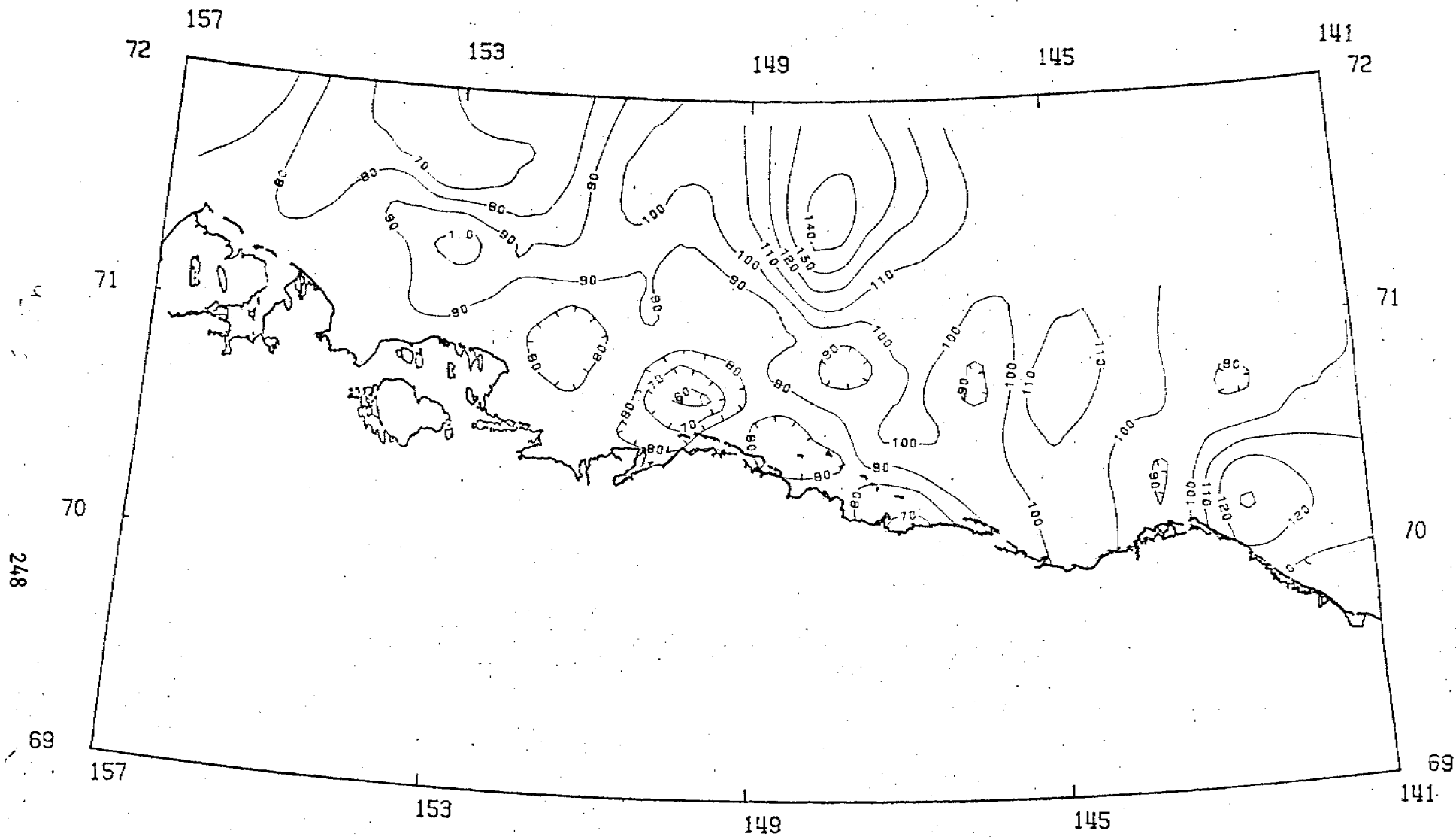


Figure 28. Map of the Beaufort Sea showing variation in the concentrations of zinc in the bottom sediments.

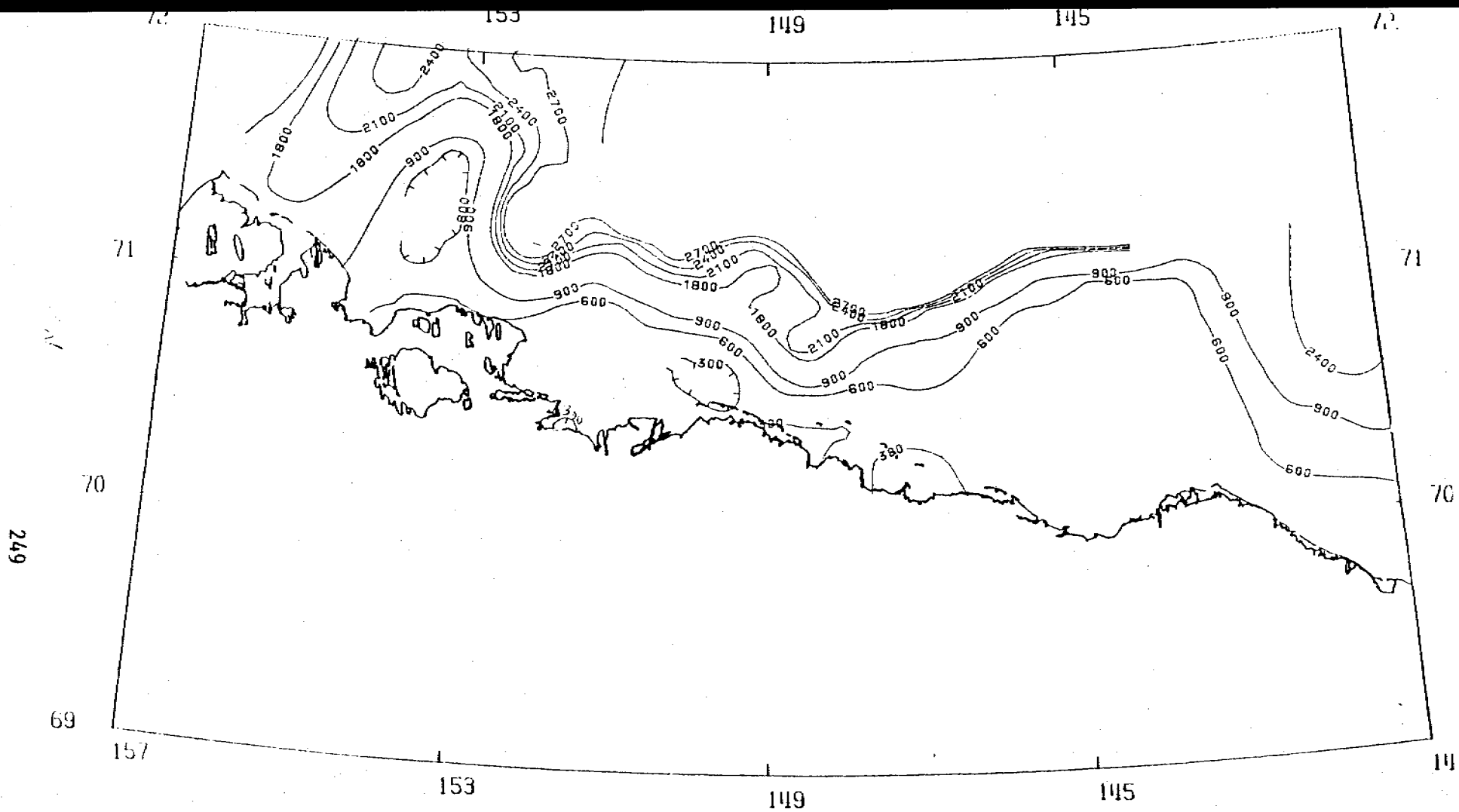


Figure 29. Map of the Beaufort Sea showing variation in the concentrations of manganese in bottom sediments.

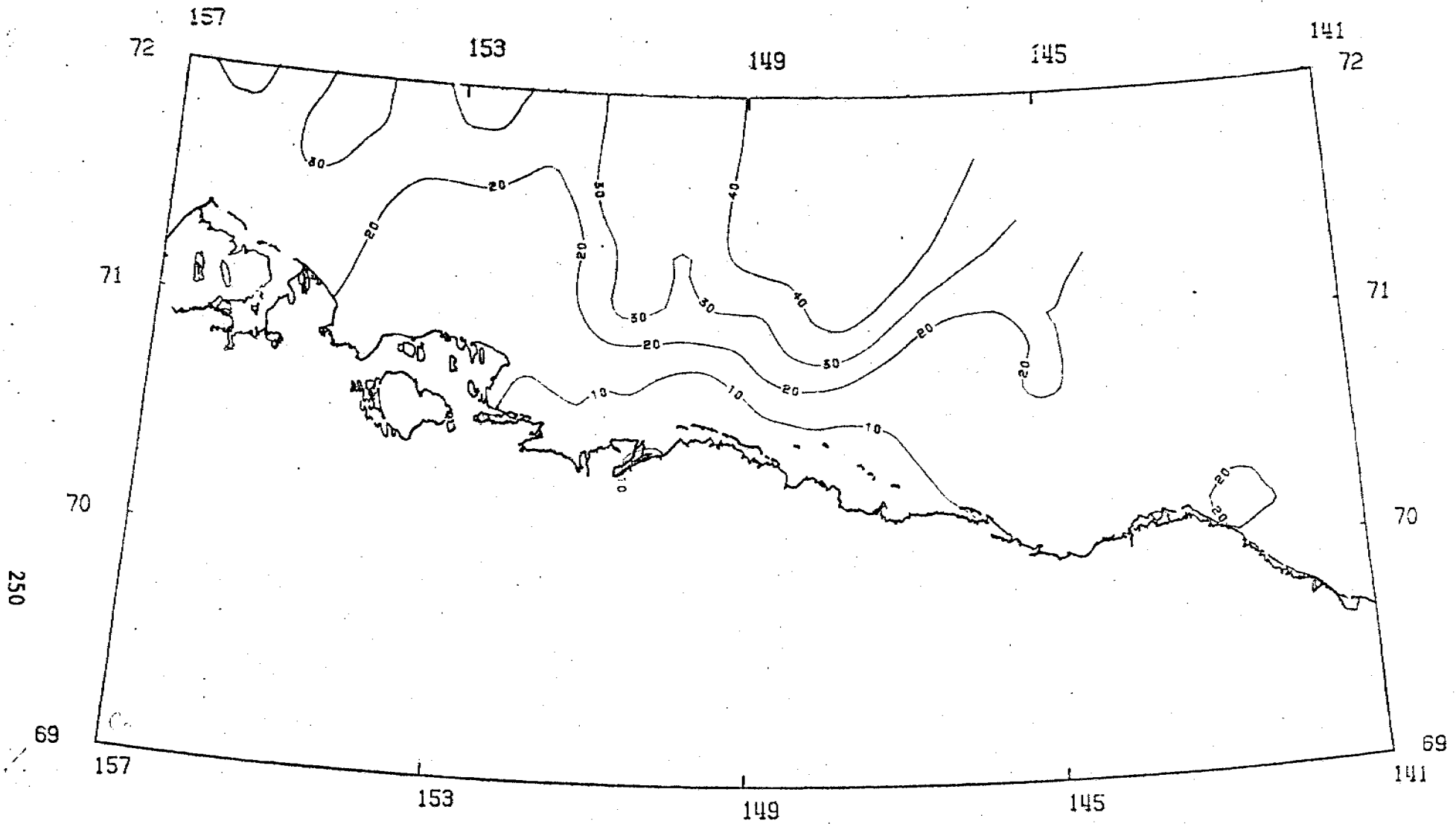


Figure 30. Map of the Beaufort Sea showing the variation in the concentrations ($\mu\text{g/g}$) of cobalt in bottom sediments.

conditions of the environment (e.g., decreased oxidation-reduction potential, reduced pH, dredging operations, etc.). The current fluxes of the eight metals into the Simpson Lagoon are listed in Table V. The metal inventories, their partitioning pattern and fluxes provide a bench mark to monitoring of pollution in the Beaufort Sea shelf and adjacent coastal areas.

TABLE V

AVERAGE FLUXES ($\mu\text{g cm}^{-2} \text{ yr}^{-1}$, EXCEPT Fe WHICH IS IN $10^4 \mu\text{g cm}^{-2} \text{ yr}^{-1}$), FOR TOTAL (T) AND ACETIC ACID-HYDROXYLAMINE HYDROCHLORIDE EXTRACTABLE (E) HEAVY METALS IN SIMPSON LAGOON SEDIMENTS

V		Cr		Mn		Fe		Co		Ni		Cu		Zn	
T	E	T	E	T	E	T	E	T	E	T	E	T	E	T	E
90	5.6	60	1.2	340	165	2.6	.29	9.6	2.5	30	4.2	22	4.0	100	17

APPENDIX 4

SEDIMENTATION RATE IN AN ARCTIC COASTAL REGION*

A. S. Naidu

Institute of Marine Science

University of Alaska

Fairbanks, Alaska 99701

H. V. Weiss

Department of Chemistry

San Diego State University

San Diego, California 92685

ABSTRACT

Seven marine coastal cores and one lake core were collected from a deltaic region in Northern Arctic Alaska and submitted to ^{210}Pb analysis. The resultant exponential decay, as a function of core depth, allowed for the determination of an upper limit of sedimentation rate in each of the cores but one. The ^{210}Pb activity levels in all cores were less than the levels generally observed in coastal sediments of nonpolar regions. An analysis of regional snows indicated that this deficiency was attributable to a reduced ^{210}Pb atmospheric flux in this Arctic environment.

INTRODUCTION

An estimation of the rates of sedimentation in Simpson Lagoon and east Harrison Bay, located in the Colville Delta region of North Arctic Alaska

*Submitted to the Journal of Geophysical Research for publication.

(Table 1, Figure 1), was undertaken. This information was desired in connection with our long-term investigations on the sources, transport pathways, depositional sites, and dynamics of sedimentation in ice-stressed deltas (Naidu, 1980).

The sedimentation rates were derived from ^{210}Pb measurements. The initial geochronological work with this nuclide was on permanent snow fields (Goldberg, 1963), and the approach was subsequently extended to the establishment of marine geochronology (Koide *et al.*, 1972). The basis for the procedure depends upon out-gassing of ^{222}Rn (half-life 3.8 days) to the atmosphere from ^{226}Ra precursor (half-life 16.22 years) in the regolith. Through a series of rapid decays ^{210}Pb (half-life 22.3 years) is formed, and the half-lives of the intermediate decay products are brief by comparison with the average residence time of the aerosol. Thus, essentially all atoms of ^{222}Rn are transformed into ^{210}Pb in the atmosphere. The ^{210}Pb is subsequently returned to the Earth's surface from the atmosphere with precipitation and dry fallout. Measurement of ^{210}Pb as a function of depth has been useful in establishing the chronology of recently deposited sediments in coastal marine sediments (Koide *et al.*, 1972, 1973; Bruland *et al.*, 1974) and in lakes (Krishnaswamy *et al.*, 1971; Robbins and Edgington, 1975; Von Damm *et al.*, 1979). However, the method has not been applied to marine or lake sediments in Arctic regions, and an aspect of this study is to ascertain the applicability of this methodology to the more extreme ice-stressed environment.

The sedimentation rate of seven cores recovered from the study area was determined. Upon comparison of the ^{210}Pb activities on their surfaces with those of other coastal regions, a relatively lower level was evident

Table 1

Locations and Water Depths (m) at Which Samples Were Collected, and Data
Summarizing Lithology of the Various Sediment Cores Analyzed

Core No.	Latitude (N)	Longitude (W)	Water Depth (m)	Gravel %		Sand %		Silt %		Clay %	
				Range	Average	Range	Average	Range	Average	Range	Average
SL8979-1	70°32'	150°07'	3.9	0 to 7.92	0.34	1.85 to 25.16	9.38	1.01 to 79.45	31.70	17.92 to 91.58	58.55
SL8979-2	70°31'	150°01'	3.6			45.47 to 7.81	27.30	28.38 to 72.43	51.20	9.74 to 39.12	21.50
SL8979-3	70°31'	149°57'	3.3			7.73 to 75.56	38.95	4.10 to 79.15	39.91	11.66 to 53.35	21.14
SL8979-4	70°32'	149°53'	3.0			20.34 to 72.32	40.18	8.37 to 67.84	44.52	9.21 to 25.47	15.30
SL8979-5	70°32'	149°45'	2.7			24.23 to 50.86	33.55	26.33 to 60.03	48.53	10.69 to 30.61	17.91
SL8979-6	70°32'	149°40'	2.6			12.96 to 42.95	29.26	31.58 to 78.32	55.81	6.92 to 25.47	14.83
SL8979-7	70°32'	149°35'	2.6	0 to 7.39	0.37	16.50 to 43.01	29.04	19.91 to 61.25	43.46	11.58 to 48.83	27.50

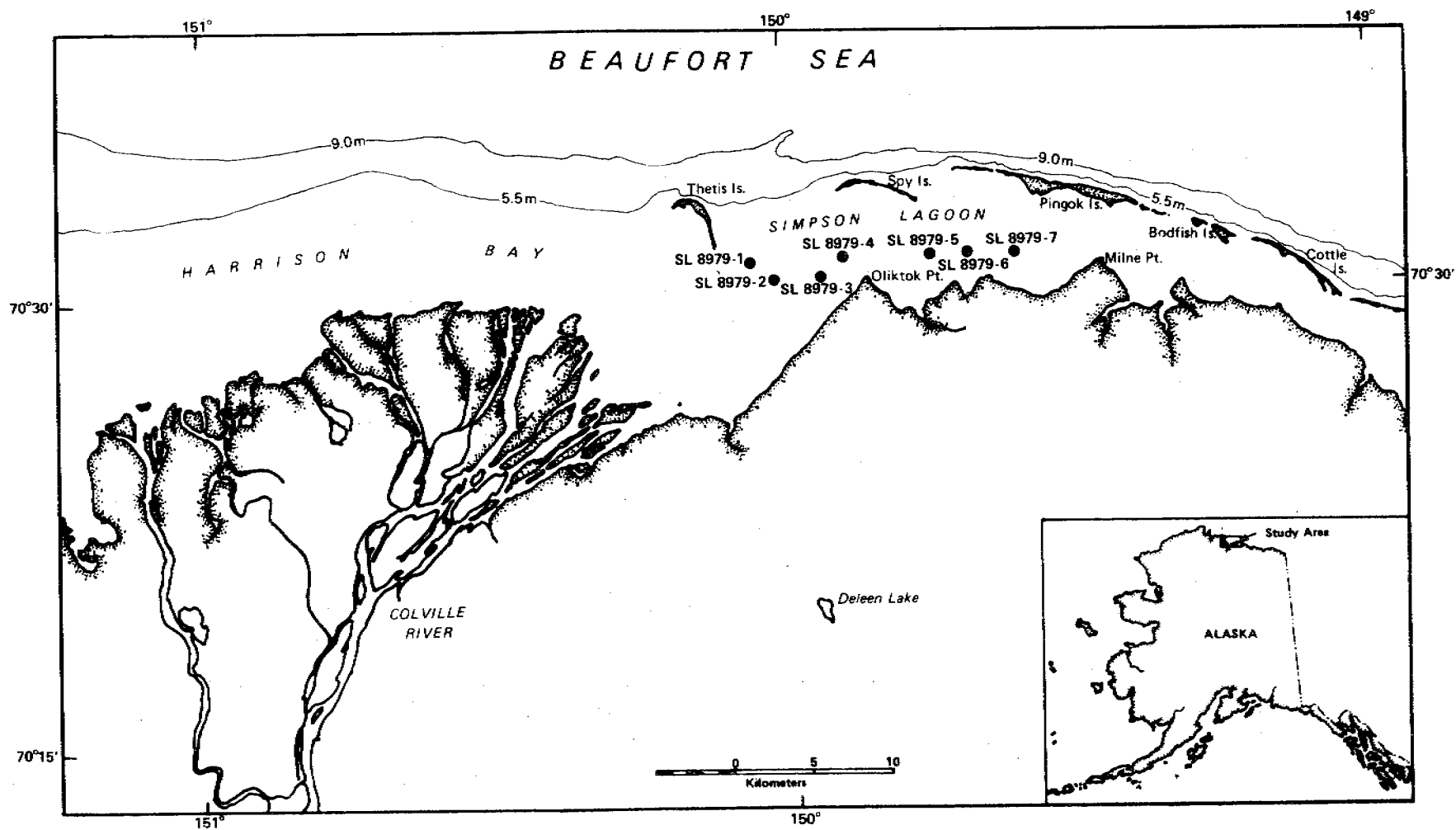


Figure 1. The area of study showing locations of the core samples in the Simpson Lagoon, east Harrison Bay and Deleen Lake.

for the sediments derived from the Arctic regime. To gain an understanding of the basis for this difference, measurement of ^{210}Pb was extended to include contemporary sediment from a coastal lake situated near the study area. The nuclide was also measured in snow deposits with the object of estimating the ^{210}Pb atmospheric flux in this environment.

DESCRIPTION OF THE STUDY AREA

Simpson Lagoon, which is contiguous with the Colville Delta, lies between a chain of barrier islands and the Arctic Coastal Plain Province of North Alaska (Figure 1). The most prominent climatic feature of this region is long, severely cold winters with ice cover that persists for 8 to 9 months of the year and cool summers for the remainder of the year. The lagoon is shallow (1 to 4 m deep), oriented parallel with the coastline and about 2.4 km long. Sediment and water mass characteristics are greatly influenced by the protracted duration of the yearly ice cover and the subsequent spring discharge of the adjacent rivers (Colville and Kuparuk). At breakup, usually in early June, the river melt waters flow over and under the lagoon ice, and the fluvial overflows on sea ice are largely confined to the lagoon and the adjacent bay. During spring and summer the terrigenous debris in the form of sandy mud reaches the lagoon primarily through suspension, river overflow and/or ice-rafting. However, most of the mud of this debris does not immediately settle, owing to the high turbulence prevailing, whereas the sand quickly deposits on the bottom. Most of the clay-size particles settle in the fall and winter months when wave and current actions have subsided considerably (Naidu and Mowatt, 1974).

MATERIALS AND METHODS

The coastal core samples were recovered from the Simpson Lagoon and east Harrison Bay region in August 1979 (locations shown in Figure 1). All cores were collected from waters deeper than 2 m (the depth to which the lagoon and bay waters generally freeze) to avoid possible perturbation of surficial sediment by ice gouging. The 5-cm diameter cores were collected from aboard the R/V *Natchik*; the westernmost with a Phelger corer, and the others by a manually driven unit. The deepest core obtainable was 33 cm. The sediment core sample from the coastal lake (Figure 1) was obtained from a 3.5 m depth with the manual device from a float plane. The snow deposits, about 30 cm deep, were gathered on January 15, 1978, from the frozen surface of the mouth of the Colville and Kuparuk Rivers.

Cores were sectioned into 1-cm segments and each was, in turn, split into two portions. One fraction (1-2 grams) was reserved for the ^{210}Pb analysis; the other was used for the size distribution analysis by the usual sieve-pipetting method.

Various methods are available for ^{210}Pb analysis. The one employed is similar to that described by Nittrouer *et al.* (1979) and depends upon its secular equilibrium with ^{210}Po . Sediment samples were dried at 110°C overnight, and a weighed aliquot (1-2 g), after spiking with ^{208}Po tracer, was ashed at $400\text{--}450^\circ\text{C}$ overnight. Snow samples were melted and acidified with conc. nitric acid to a final concentration of 0.16 N. One-liter aliquots were spiked with ^{208}Po and then slowly evaporated to dryness. Sediment and snow samples were further processed in the following manner: The residual was treated with about 30 ml each of conc. hydrochloric acid, aqua regia, and conc. hydrochloric acid, in that order. With each treatment,

the liquid was evaporated to dryness at simmering temperature. The final residue was prepared for autodeposition by its dissolution in 0.3 N hydrochloric acid. The alpha particles emitted by $^{208,210}\text{Po}$ deposited on silver discs were pulse-height analyzed with a surface barrier detector, usually for an overnight period.

RESULTS

The stratigraphic variations in the contents (wt.%) of gravel, sand, silt, and clay in the Simpson Lagoon and Harrison Bay cores have been reported elsewhere (Naidu, 1980). The sediment textures are variable both between and within cores. The mean and range of the size grades for the individual cores are indicated in Table 1. The average sand content of the least sandy core, 8979-1, was 9.12% with a range from 1.85 to 25.16% while for the most sandy core, 8979-4, the average sand value, was 40.03%, and the range from 31.35 to 72.32%. Gravel appeared in only two of the cores; five segments in the lower end of core 8979-1 and in a single segment (7-8 cm) in core 8979-7. The sediment from Deleen Lake was essentially muddy, with an organic content approximately 50%, as determined by weight loss upon thermal ashing, and a textural analysis was not performed.

The range of values for the ^{210}Pb disintegration rate, $\text{d m}^{-1} \text{g}^{-1}$, extended from 0.34 in Core 8579-3 to 5.44 for the Deleen Lake core. The error, as determined in replicate analyses, was 3 and 10% at the higher and lower disintegration rates, respectively.

The rate of sedimentation was determined from the slope of the least-squares fit to the logarithm of ^{210}Pb versus depth in the core. In a

number of cores, usually at a depth of 15 to 16 cm, and extending to the bottom, a divergence from linearity was evident. These values were not included in the computation. Table 2 presents a summary of the number and range of segments included in the least-squares fit, the slope, intercept, correlation coefficient (r) and the tabular r at the 99% confidence limit (Dean, 1977). The sedimentation rate and associated error were calculated from the slope and the standard error of the slope (Snedecor, 1950).

With exception of Core 8979-4 the data correlate with the linear equation. The sedimentation rate of the most westerly core (8979-1) was 1.6 cm y^{-1} while the rate for the others ranged from 0.5 to 0.8 cm y^{-1} . Their intercept values extended from 1.24 to $1.85 \text{ d m}^{-1} \text{ g}^{-1}$. A sedimentation rate of 0.9 cm y^{-1} was measured for the core from Deleen Lake. Plots of the data for the cores appear in Figure 2. The solid line in each, covers the region in the core over which linearity obtained.

The concentrations of ^{210}Pb in the snow on the Colville and Kuparuk Rivers were 5.4 ± 0.3 and 8.4 ± 0.4 , $\text{d m}^{-1} \text{ g}^{-1}$, respectively.

DISCUSSION

Variations of the ^{210}Pb values from the best-fit line for the coastal cores are greater than usually observed, and in excess of the error associated with the radiometric assay. These fluctuations are, in part, attributable to the relatively coarse texture of these sediments and to the changes in the degree of coarseness along the length of the cores. That relatively lower activity levels are associated with the coarser sandy particles has been reported a number of times (Nittrouer *et al.*,

Table 2

Sedimentation Rates of the Lake, Bay and Lagoon Cores, Including
Linear Coefficients, Number and Range of Linear Segments
and Correlation Coefficients

Sediment Core	Number of Linear Segments (n)	Linear Range (cm)	Intercept (a)	Slope (b)	Correlation Coefficient (r)	Tabular r at 99% level	Sedimentation Rate ₁ cm y ⁻¹
SL8979-1	30	0-33	1.77	-0019	0.75	0.46	1.64 +0.15 -0.13
SL8979-2	14	0-14	1.85	-0038	0.75	0.66	0.82 +0.13 -0.10
SL8979-3	9	10-19	1.22	-0.051	0.97	0.80	0.61 +0.01 -0.01
SL8979.4	11	0-11	-	-	0.26	0.74	-
SL8979-5	16	0-16	1.82	-0.054	0.91	0.62	0.58 +0.04 -0.04
SL8979-6	15	0-15	1.24	-0.042	0.75	0.64	0.74 +0.07 -0.06
SL8979-7	15	0-15	1.57	-0.060	0.89	0.64	0.52 +0.05 -0.04
Deleen Lake	21	0-21	4.86	-0.035	0.60	0.55	0.89 +0.15 -0.12

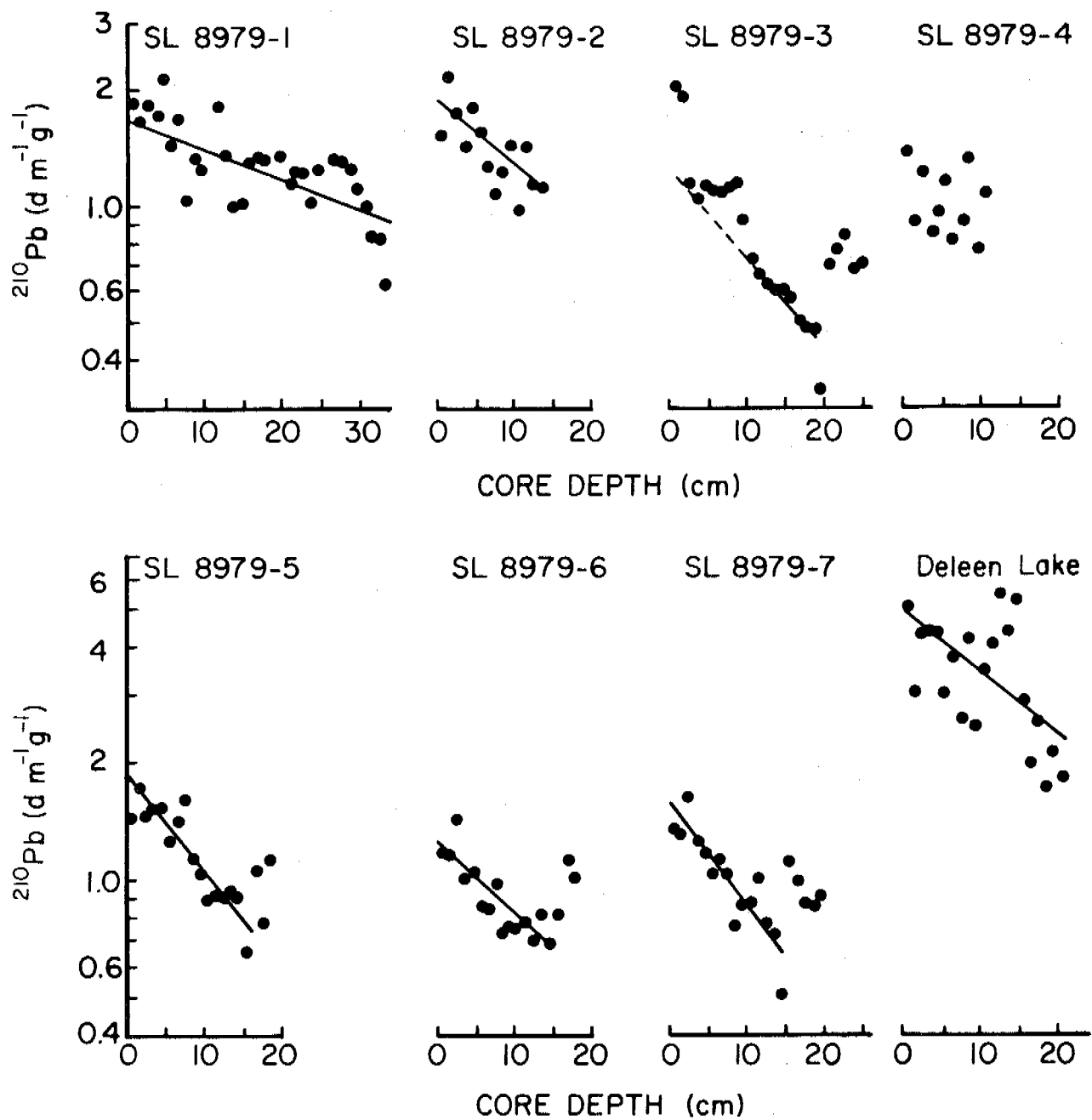


Figure 2. Profiles of ^{210}Pb activities for the 8 sediment cores investigated. Refer to Figure 1 for core locations.

1979; Kalesha *et al.*, 1980; Smith and Walton, 1980) and reflects the lesser capacity of these particles to scavenge ^{210}Pb from the water column. Yet, a calculation of ^{210}Pb in the core segments on a sand-free basis did not result in improvement in the least-squares fit. Still another factor that contributes importantly to the degree of variation relates to the rate of sedimentation as compared to the sample thickness. As an example, the rate of deposition measured in Core 8979-1 (1.6 cm y^{-1}) was greater than the 1-cm segment analyzed. Thus, the quantity of sediment assayed represented an amount that was deposited over only a fraction of a year. Recognizing that measurement of the ^{210}Pb flux for several consecutive years still results in an uncertainty of 10-50% (Turekian, 1977) a value that reflects only part of the annual flux is subject to appreciably greater error.

Nonetheless, for six of the seven cores, the data correlated with the linear equation. Further, the rates were not inconsistent with a decrease in sedimentation rate with increased distance from the Colville River, an important source of sediment in the study area.

Sedimentation rates were derived without benefit of correction for the quantity of background-supported ^{210}Pb . Thus, the rates presented represent upper limits of sedimentation.

The deviation from exponential decay occurred at a depth of 15 to 16 cm for Cores 8979-5, 6 and 7 and at 21 cm in Core 8979-3. In the latter core seven consecutive segments, from 2 to 9 cm are constant in ^{210}Pb activity. This relationship suggests the instantaneous accumulation of this layer. Under such circumstance the point of divergence from linearity would in effect shift upwards and thereby agree more closely with the

pattern in the other three cores. Thus, an event that occurred two to three decades ago may account for the elevated ^{210}Pb values. Whether the ^{210}Pb in this underlying layer was excess or ^{226}Ra -supported could not be established for reason of insufficient core length.

A comparison of the intercept values (Table 2) reveals that a substantially higher activity level prevails for the sediment from the lake. This difference is explainable, in part, by sediment composition. In contrast with the sandy muds characteristics of the lagoonal sediments the debris descending through the water column of the lake is largely organic and as such more effectively scavenges the ^{210}Pb (Lewis, 1977). Further, the lake serves as a reservoir for the atmospherically deposited ^{210}Pb whereas no such confinement exists in the coastal waters. Some of the sea ice is mobilized seaward out of the lagoons subsequent to its breakup in July (Naidu and Mowatt, 1974). Accordingly, the ^{210}Pb accumulation, beginning with the formation of the ice since the previous September, is transported away from the site of deposition and thereby could effect a partial depletion in the littoral environment.

That the surface marine sediments in the Arctic carry a lesser concentration of ^{210}Pb than the more temperate regions is apparent. For comparable sedimentation rates, representative values fall between $5 \text{ d m}^{-1} \text{ g}^{-1}$ in Narragansett Bay (Goldberg *et al.*, 1977) to $50 \text{ d m}^{-1} \text{ g}^{-1}$ in Santa Barbara Basin (Koide *et al.*, 1972) and Baja California (Koide *et al.*, 1973). Although scavenging efficiency and ice movement may be importantly involved to account for the difference in ^{210}Pb content between Deleen Lake and bay and lagoon sediments, the difference noted between the Arctic and other marine sediments may be influenced by an

an additional element. This conclusion is derived from a comparison of the data from Deleen Lake with that of other lakes.

The scatter in the data from Deleen Lake suggests some post-depositional sediment disturbance. The sediment was largely organic, of fluffy consistency, and thereby subject to mixing. Thus, the intercept value, $4.86 \text{ d m}^{-1} \text{ g}^{-1}$, is probably too low. However, were a correction possible, it seems doubtful that a value as high as $16 \text{ d m}^{-1} \text{ g}^{-1}$, which is the lowest of surface values recorded for a lake at temperate latitudes (Koide *et al.*, 1973), would be attained. More representative surface values of ^{210}Pb for sedimentation rates comparable to that of Deleen Lake range from $45 \text{ d m}^{-1} \text{ g}^{-1}$ for a Sierra Nevada subalpine pond (Shirahata *et al.*, 1980) to $85 \text{ d m}^{-1} \text{ g}^{-1}$ for Trout Lake in Wisconsin (Koide *et al.*, 1973).

Is the lower level of ^{210}Pb in Arctic sediment the result of a weakened atmospheric flux in the northern latitude? The measurement of this nuclide in surface waters of the oceans suggests that the flux at the higher latitudes is substantially less than in temperate zones (Schell, 1977). In addition, the measurement of ^{222}Rn , further supports the consideration of a reduced flux in the Arctic. The average ^{222}Rn flux is variously given as $0.7 \text{ atom cm}^{-2} \text{ sec}^{-1}$ (Israel, 1951) and $0.75 \text{ atom cm}^{-2} \text{ sec}^{-1}$ (Wilkening *et al.*, 1975). Fluxes measured in a northern region of the USSR (65°N , 40°E) by Kirichenko (1970), the Yukon Basin (65°N , 150°W) by Anderson and Larson (1974) and the Tanana Basin (65°N , 147°W) by Wilkening *et al.* (1975) are only 0.18 , 0.33 and $0.37 \text{ atom cm}^{-2} \text{ sec}^{-1}$, respectively.

Our analysis of snow samples for ^{210}Pb affirms the flux concept. The samples represented the accumulation of about 4 months of precipitation. Information available from the Lonely DEW Station and the weather station at Point Barrow, which are situated 130 and 260 km respectively to the west of the study area, indicated that snow, equivalent to 5.5 cm of water, was deposited over this time period (James L. Wise, personal communication). The average for the two snow samples, $6.9 \text{ d m}^{-1} \ell^{-1}$, leads to a flux of $0.08 \text{ d m}^{-1} \text{ cm}^{-2} \text{ y}^{-1}$ for the average annual precipitation of 12 cm y^{-1} in this region of the Arctic. It is understood that the calculation of a flux from data acquired over such limited duration could be uncertain by as much as a factor to two (Turekian *et al.*, 1977). However, this value contrasts sharply with a ^{210}Pb atmospheric flux of $1.0 \pm 0.2 \text{ d m}^{-1} \text{ y}^{-1}$ in the northeastern United States (Benninger, 1978), a region that has received concentrated study.

It is interesting to note that the ^{210}Pb atmospheric flux calculated for this region of the Arctic agrees with fluxes derived for permanent snowfield data from Greenland. At Camp Century (77°N , 61°W ; 1885 m elevation), at South Dome (63°N , 44°W ; 2700 m elevation), and at another Greenland site (77°N , 56°W ; 2000 m elevation) fluxes of $0.09 \text{ d m}^{-1} \text{ cm}^{-2} \text{ y}^{-1}$ (Crozas and Langway, 1966), $0.06 \text{ d m}^{-1} \text{ cm}^{-2} \text{ y}^{-1}$ (Koide *et al.*, 1979) and $0.11 \text{ d m}^{-1} \text{ cm}^{-2} \text{ y}^{-1}$ (Windom, 1969) were measured. However, whether or not the Greenland values reflect the flux at sea level, is not certain. It has been suggested (Turekian *et al.*, 1977) that the low fluxes could be a sign of effective scavenging of ^{210}Pb from air masses prior to their arrival at these altitudes.

CONCLUSIONS

Upper limits of sedimentation rates were measurable for six of the seven Arctic coastal marine sediments collected, although the ^{210}Pb activity level was unusually low. Factors such as the low scavenging efficiency of coarse granules and the movement of ice carrying entrained ^{210}Pb away from the site of deposition may account, in part, for the paucity of activity. The analysis of snows, however, indicates that the ^{210}Pb deficiency is compounded by an atmospheric flux to this environment that is appreciably depressed.

ACKNOWLEDGEMENTS

This work was supported largely by the Bureau of Land Management through interagency agreement with the National Oceanic and Atmospheric Administration under which a multiyear program responding to the needs of petroleum development of the Alaskan continental shelf is managed by the Outer Continental Shelf Environmental Assessment Program Office. We thank James Helmericks and the crew of the R/V *Natchik* for their help in the sample collection, and to Daniel L. Brooks of the OCS Arctic Project Office, Fairbanks for arranging the field logistics. James L. Wise of the Arctic Environmental and Data Center, University of Alaska, Anchorage kindly provided the snow precipitation data.

REFERENCES

- Anderson, R. V. and R. E. Larson, Atmospheric electricity and radon profiles over a closed basin and the open ocean, *J. Geophys. Res.*, 79, 3432-3435, 1974.
- Benninger, L. K., ^{210}Pb balance in Long Island Sound, *Geochim. Cosmochim. Acta*, 42, 1165-1174, 1978.
- Bruland, K. W., Pb-210 geochronology in the coastal marine environment, Ph.D. thesis, University of California, San Diego, 1974.
- Crozaz, G. and C. C. Langway, Jr., Dating Greenland firm ice cores with Pb-210, *Earth Planet. Sci. Lett.*, 1, 194-196, 1966.
- Dean, M. and Staff at Texas Instruments and the University of Denver Mathematics laboratory, Texas Instruments Decision Making Source Book, p. 2-18, Texas Instruments Inc., Publisher, 1977.
- Goldberg, E. D., Geochronology with ^{210}Pb , in radioactive dating, pp. 121-131, Int. Atomic Energy Agency, Vienna, 1963.
- Goldberg, E. D., E. Gamble, J. J. Griffin and M. Koide, Pollution history of Narragansett Bay as recorded in its sediments, *Estuarine and Coastal Mar. Sci.*, 5, 549-561, 1977.
- Israel, H., Radioactivity of the atmosphere. *In* Compendium of Meteorology, edited by T. F. Malone, pp. 155-161, Amer. Meteorol. Soc., Boston, 1951.
- Kalesha, M., K. S. Rao and B. L. K. Somayajulu, Deposition rates in the Godavari Delta, *Marine Geology*, 34, M57-M66, 1980.
- Kirichenko, L. V., Radon exhalation from vast areas according to vertical distribution of its short-lived decay products, *J. Geophys. Res.*, 75, 3539-3549, 1970.

- Koide, M., A. Soutar and E. D. Goldberg, Marine geochronology with ^{210}Pb ,
Earth Planet. Sci. Lett., 14, 442-446, 1972.
- Koide, M., K. W. Bruland and E. D. Goldberg, Th-228/Th-232 and Pb-210
geochronologies in marine and lake sediments, *Geochim. Cosmochim.
Acta*, 37, 1171-1187, 1973.
- Koide, M., R. Michel, E. D. Goldberg and C. C. Langway, Jr., Deposition
of artificial radionuclides in the Ross Ice shelf, Antarctica,
Earth Planet. Sci. Lett., 44, 205-223, 1979.
- Krishnaswamy, S., D. Lal, J. M. Martin, and M. Meybeck, Geochronology of
lake sediments, *Earth Planet. Sci. Lett.*, 11, 407-414, 1971.
- Lewis, D. M., The use of ^{210}Pb as a heavy metal tracer in the Sesquehanna
River system, *Geochim. Cosmochim. Acta*, 41, 1557-1564, 1977.
- Naidu, A. S., Sources, transport pathways, depositional sites and dynamics
of sediments in the lagoon and adjacent shallow marine region, Northern
Arctic Alaska, Annual Rept. submitted to the NOAA-OCSEAP Office,
Boulder, Colorado, 1-60, 1980.
- Naidu, A. S. and T. C. Mowatt, Depositional environments and sediment
characteristics of the Colville and adjacent deltas, Northern Arctic
Alaska, *In Deltas for Subsurface Exploration*, ed. M. L. S. Broussard,
pp. 283-289, Houston Geol. Soc., Texas, 1974.
- Nittrouer, C. A., R. W. Sternberg, R. Carpenter and J. T. Bennett, the use
of Pb-210 geochronology as a sedimentological tool: application to
the Washington continental shelf, *Marine Geology*, 31, 297-316, 1979.
- Robbins, J. A. and D. N. Edgington, Determination of recent sedimentation
rates in Lake Michigan using Pb-210 and Cs-137, *Geochim. Cosmochim.
Acta*, 39, 285-304, 1975.

- Shell, W. R., Concentrations, physico-chemical states and mean residence times of ^{210}Pb and ^{210}Po in marine and estuarine waters, *Geochim. Cosmochim. Acta* 41, 1010-1031, 1977.
- Shirhata, R., R. W. Elias and C. C. Patterson, Chronological variations in concentrations and isotopic compositions of anthropogenic atmospheric lead in sediments of a remote subalpine pond, *Geochim. Cosmochim. Acta*, 44, 149-162, 1980.
- Smith, J. N. and A. Walton, Sediment accumulation rates and geochronologies measured in the Saguenay Fjord using the Pb-210 method, *Geochim. Cosmochim. Acta*, 44, 225-240, 1980.
- Snedecor, G. W., *Statistical Methods*, p. 119, The Iowa State College Press, Ames, Iowa, 1950.
- Turekian, K. K., Y. Nozaki and L. K. Benninger, Geochemistry of atmospheric radon and radon products, *Ann. Rev. Earth Planet. Sci.*, 5, 227-255, 1977.
- Von Damm, K. L., L. Benninger and K. K. Turekian, The ^{210}Pb chronology of a core from Mirror Lake, New Hampshire, *Limnol. Oceanogr.*, 24, 434-439, 1979.
- Wilkening, M. H., W. E. Clements and D. Stanley, Radon-222 flux measurements in widely separated regions, *In The Natural Radiation Environment, II*, Ed., J. A. S. Adams, 2, 717-730, USERDA Conf. 720805, 1975.
- Windom, H. L., Atmospheric dust records in permanent snowfields: Implications to marine sedimentation, *Geol. Soc. Am. Bull.*, 80, 761-782, 1969.

APPENDIX 5

CLAY MINERAL DISPERSAL PATTERNS IN THE NORTH BERING
AND CHUKCHI SEAS*

A. S. Naidu¹, J. S. Creager² and T. C. Mowatt¹

¹Institute of Marine Science
University of Alaska
Fairbanks, Alaska 99701

²Department of Oceanography
University of Washington
Seattle, Washington 98105

Institute of Marine Science, Contribution No. 444, University of Alaska,
Fairbanks, Alaska.

*Accepted for publication (with minor revision) in *Marine Geology*.

ABSTRACT

Characterization of the clay mineralogic constituents of the $< 2 \mu\text{m}$ e.s.d. size fraction of contemporary marine and fluvial sediments from the north Bering Sea—Chukchi Sea region and adjacent land areas has resulted in delineation of suites dominated by broadly defined "illitic" and "expandable group" components, with lesser amounts of chlorite and kaolinite. Distribution patterns elucidated indicate net northward transport of sediments relatively enriched in the "expandable group" with predominant terrigenous source from the Yukon River system. This material is distributed across the study area in a medial zone along a general north-south trend, with peripherally decreasing relative amounts of this "expandable group" component, and concomitant relative increases in the "illitic" components. These patterns are consistent with known physical oceanographic and regional geologic relationships, in terms of sediment sources, transport processes, and depositional mechanisms.

The foregoing suggest, further, that consideration of the stratigraphic relationships of these clay mineral component-types, as a function of time, in relevant marine sediments north and south of the present Bering Strait, should be informative with respect to regional Quaternary paleogeography, as related to global sea level fluctuations during glacial and interglacial episodes.

INTRODUCTION

The potential usefulness of clay mineral studies in the understanding of several marine depositional processes has been amply demonstrated. The sources, dispersal pathways, transport agents (eolian, aquatic and ice), and depositional sites of fine-grained particles in oceans have been elucidated using clay mineral distributions (Biscaye, 1965; Gorbunova, 1966; Griffin *et al.*, 1968; Rateev *et al.*, 1969; Venkatarathnam and Biscaye, 1973; Andrew and Kravitz, 1974; Naidu and Mowatt, 1974; Wright, 1974; Windom, 1975; Venkatarathnam *et al.*, 1976; and Gibbs, 1977; among many others). Additionally, clay mineral stratigraphy of unconsolidated marine sediments has assisted in the inference of Cenozoic paleogeography of some ocean basins, submarine volcanic history, and with some constraints (Naidu *et al.*, 1971) also paleoclimate of continents adjacent to oceans (Turekian, 1968; Chamley, 1971; Jacobs and Hays, 1972; Jacobs, 1974; Latouche, 1978; and Hein *et al.*, 1976). In an excellent review Parham (1966) has implied that lateral variations in clay mineral assemblages can be a useful criterion to differentiate fresh water from saline water paleodeposits. In this paper we describe the dispersal pattern of clay minerals in the north Bering and Chukchi Seas of Alaska, and lend support to the conclusions of previous investigators that the Chukchi Sea is an important repository of the clays discharged by the Yukon River into the ocean. We also discuss the possible application of our findings to the elucidation of Quaternary marine transgressive-regressive history of the Chukchi Sea.

MATERIALS AND METHODS

Samples: Sediment splits from 294 grab samples, collected between 1959 and 1970 on various cruises from stations shown in Fig. 1, were analyzed for their clay mineral compositions. To elucidate terrigenous sources of clay mineral suites in the area of study, additional sediment samples from the Yukon, Kuskokwim, Kobuk and Noatak Rivers of Alaska, as well as from the deltaic area off the Kolyma River in East Siberia were taken for clay mineral analysis.

Analytical Technique: Details of the clay mineral analytical procedures utilized have been reported elsewhere (Naidu and Mowatt, 1974). In brief, the $< 2 \mu\text{m}$ e.s.d. particle size fraction of each sediment sample was separated from stable sediment suspensions by settling. Dispersion of the organic-freed (H_2O_2) clays was achieved in deionized-distilled water after removal of the salts by repeated washing. The $< 2 \mu\text{m}$ fractions were smeared on glass slides (Gibbs, 1965) and air dried. Glycolation was effected by vapour-phase exposure. Clay minerals were determined by analysis on a Phillips-Norelco X-ray diffractometer with a scintillation detector, using Ni-filtered copper K_α radiation.

Clay minerals were identified according to criteria outlined in Naidu and Mowatt (1974). Clay minerals that expanded upon glycolation and gave a basal diffraction peak in the neighborhood of 17 \AA were assigned to the Expandable Group. Ordinarily such expandable mineral phases are categorized in the Smectite Group, but we have refrained from this. Our detailed studies on several unglycolated and glycolated clay samples, saturated first either with 1N MgCl_2 or KCl solution, strongly suggest that some of the expandable clay mineral phases are neither smectite nor "stripped"

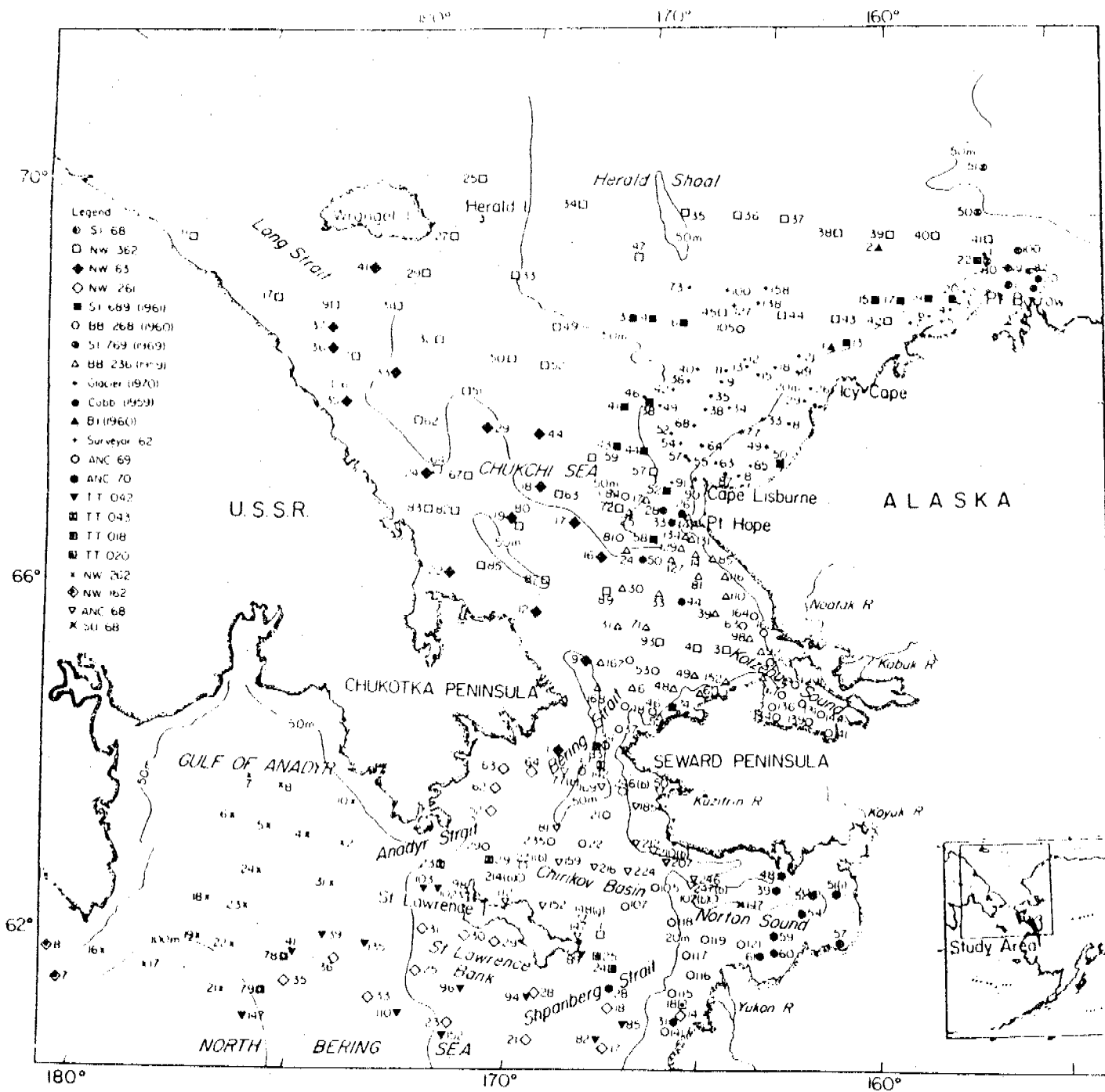


Figure 1. Map of the north Bering Sea-Chukchi Sea region, showing location of sediment samples analyzed for clay mineral assemblages.

chlorite. Instead they are most likely "degraded" (depotassicated) illite (Jonas, 1975) and/or mixed-layer expandable phases with interstratified "degraded" illite components. Additional tests, including step-wise heat treatment, prior to and after glycolation, indicate that clays with a series of broad peaks that coalesce with the low angle 2θ side of the 10 \AA peak are either mixed-layer illite-smectite or illite-chlorite, with varying amounts of "vermiculite". In the present study no attempt has been made to resolve and quantify all the above complex phases, and the relatively simple nomenclature adopted here serves a purely descriptive purpose. However, for comparison on a world-wide basis the "expandable clay mineral" sediment component in this paper may be assumed as essentially analogous to the "Smectite" Group as used by other workers.

Semi-quantitative estimation of the clay minerals (i.e., weighted peak area percents) was carried out following the method outlined by Biscaye (1965). Estimation of the relative abundances of chlorite and kaolinite in the clays was based on the resolution of the 3.5 \AA region doublet (Biscaye, 1964). Additionally, a measure of the crystallinity of the expandable clay mineral was obtained by calculating the v/p ratio, where p represented the height of the mineral peak above the background and v the depth of the 'valley' on the low angle side of the peak (Biscaye, 1965). Overall analytical precision was ± 5 percent.

Statistical Treatment of Data: The relative abundances of the clay mineral groups were plotted respective to the various stations, and based on these plots, the areal distributional trends for each of the groups were obtained. The different classes, constituting the various relative abundances for

each of the mineral groups, were delineated after ensuring that the groupings of the mineral abundance ranges within each class was significantly different statistically. This was verified by conducting 't' test of significance* between the various classes of abundance for a particular mineral group.

RESULTS

The distributional patterns of the weighted peak-area percentages of the expandable mineral phases and illite are shown in Figs. 2 and 3 respectively, whereas the variations of the kaolinite/chlorite ratios are displayed in Fig. 4. Some broad patterns in the distribution of clay mineral assemblages can be identified in the Chukchi and north Bering Seas. The St. Lawrence Bank, south of St. Lawrence Island, has the highest concentration of expandable minerals. From this region, towards both the Siberian and Alaskan coasts, the expandable mineral phases decrease in concentration, with the least amounts along the Chukotka and Seward Peninsular coasts. In the Bering Strait and contiguous Chukchi Sea, the expandable minerals are concentrated along a narrow band in the central region and are observed to decrease progressively coastward.

The distributional pattern of illite (Fig. 3) in the north Bering and Chukchi Seas generally runs counter to that of the expandable minerals. Between Icy Cape and Pt. Barrow, adjacent to the Alaskan continent, as well as around Wrangel Island in northwest Chukchi-East Siberian Sea (Fig. 3) the illite content is the highest (i.e., > 63 percent). No similar trends were apparent in the distributions of kaolinite or chlorite.

*Significance at 99% confidence level.

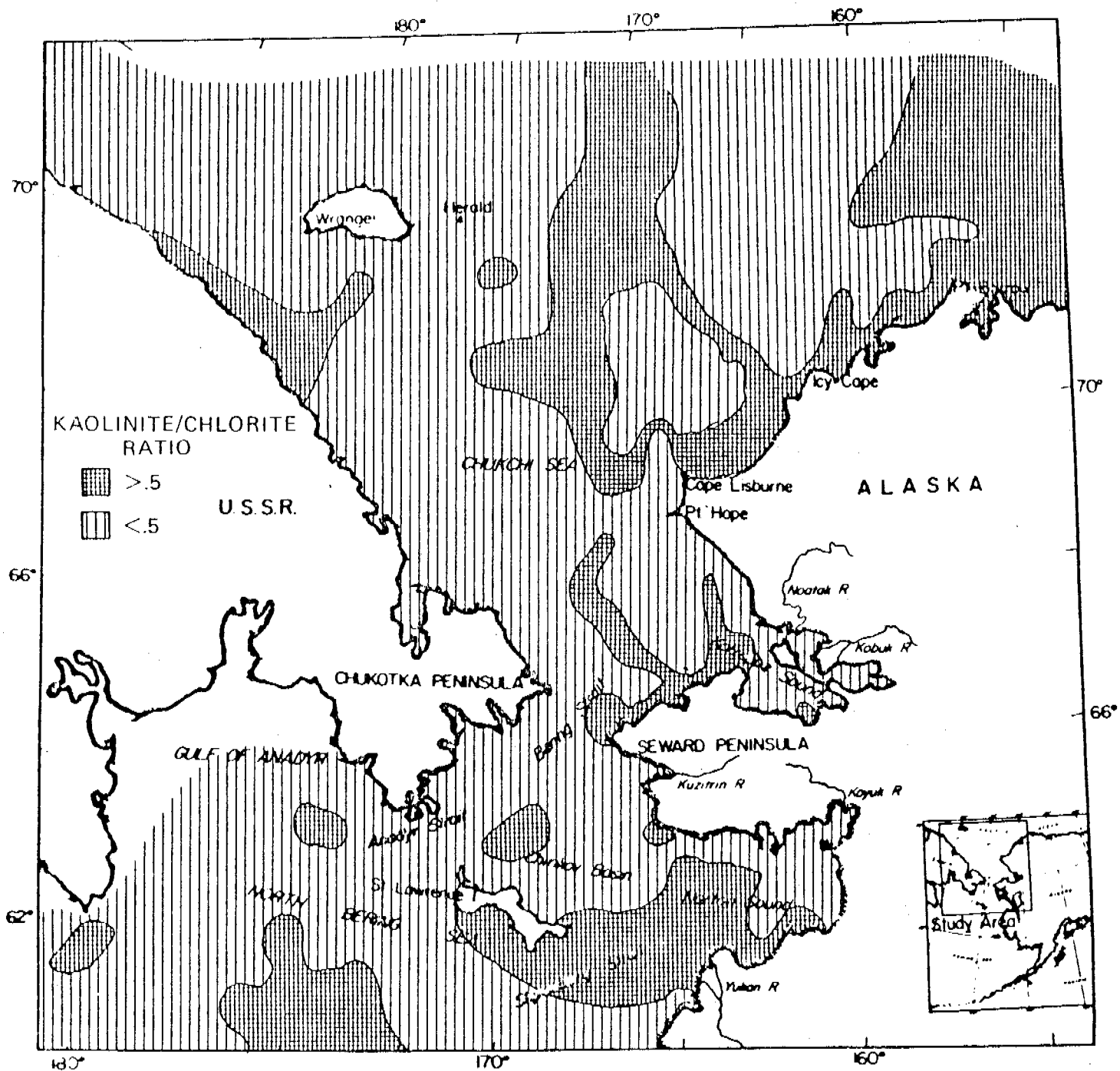


Figure 4. Distributional pattern of the kaolinite/chlorite ratios in the north Bering-Chukchi Sea.

Neither kaolinite nor chlorite was present in more than relatively minor amounts in any of the samples analyzed. However, the kaolinite/chlorite ratios (Fig. 4) are relatively higher adjacent to the Alaskan coast, with tongues projecting farther seaward off the bight between Cape Lisburne and Icy Cape, and also off northwest Seward Peninsula, and the Yukon River. Further scrutiny of the mineral distributions (Figs. 2 and 3) indicates that west of the Pt. Hope-Cape Lisburne Peninsula region and due south of Herald Shoal in the central Chukchi Sea the band of high amounts of expandable clay minerals--attended by low illite roughly bifurcates; one trend swerving westward and the other extending northeastward beyond Pt. Barrow into the Canada Basin.

DISCUSSION

Factors Influencing Clay Mineral Dispersal Patterns

It would seem that the observed distributional patterns of clay minerals in the north Bering and Chukchi Seas can be explained best on the basis of (a) the sources of the clay minerals, and (b) the transport pathways and depositional sites of the clay minerals as related to the prevalent regional and local water currents.

The presence of sediments with relatively high illite accompanied by low expandable minerals adjacent to the Bering Strait and Chukchi Sea coast is most likely related to a continental source that is enriched in illite and has a general paucity of the expandable mineral phases. This is corroborated by the clay mineralogy of the soils and sedimentary materials in the adjacent Alaskan hinterland (Campbell, 1966; Holowaychuk

et al., 1966; Kachadoorin, 1966) and of the bedloads of the rivers draining into the above coastal area (i.e., Kobuk and Noatak Rivers, Table 1). Additionally, the terrigenous debris discharged into the arctic coastal area of western Alaska is generally confined to the inshore region as suggested by ERTS imagery (Burbank, 1974). However, as mentioned earlier, in parts of the above coastal region, such as the bight between Cape Lisburne and Icy Cape and the inner shelf and northeast of Cape Prince of Wales, and Shismar Peninsula (Fig. 1), along the northwestern region of the Seward Peninsula sediment tongues typified by high illite and low expandable mineral components extend farther seaward onto the eastern Chukchi shelf. We believe that this is a manifestation of greater displacement seaward of terrigenous debris resulting from the presence locally of anticyclonic eddies and gyres (Fleming and Heggarty, 1966; Coachman *et al.*, 1975; Ingham *et al.*, 1972). In the northwest Chukchi Sea, surrounding Wrangel Island, are also deposits with notable concentrations of illite accompanied by low contents of expandable minerals. We ascribe this to the large amounts of clays rich in illite and poor in expandable minerals introduced through the Kolyma and Indigirka Rivers into the east Siberian Sea (Table 1; Naugler, 1967; Silverberg, 1972), and subsequent transportation of these clays to the Wrangel Island area by local east and southeast-set coastal currents (Sverdrup, 1929; Aagaard and Coachman, 1964; Coachman and Rankin, 1968; Coachman *et al.*, 1975). Continuation of this current through Long Strait and along the northeast Siberian and Chukotka Peninsula coast would also seem to explain the considerable illitic clays observed in the nearshore areas of the western Chukchi Sea and the regions adjacent to and southeast of Wrangel Island.

The presence of relatively high kaolinite/chlorite ratios adjacent to the northwest Alaskan coast is presumably attributable to the nature of sedimentary sequences in the onshore source terranes in these areas. In particular, the sedimentary rocks in the foothills north and west of the Brooks Range are likely contributors of kaolinite. Portions of these sequences consist in large part of coal-bearing rocks (Barnes, 1967), and contain appreciable proportions of kaolinite (Rao, 1980; Mowatt, unpublished data, 1981). The presence of high kaolinite/chlorite ratios off the Yukon Delta can be directly ascribed to the relatively high proportions of kaolinite that are being supplied locally by the Yukon River (Table 1) to this area.

We have no conclusive explanation for the highest concentration of the expandable clay minerals in the St. Lawrence Bank area (Fig. 2). Lisitsyn (1966) has maintained that the above region receives large volumes of sediments from the Kuskokwim River. Clay mineral analysis on 12 samples of Kuskokwim River sediments (Table 1) which show absence or traces of expandable mineral phases, do not support Lisitsyn's contention. A possible source in the south and southeast Bering Sea region seems unreasonable, as suggested by our clay mineral studies in those areas (Burrell *et al.*, 1981) and the isolated nature of the above tract with the high concentrations of expandable minerals. The Anadyr River of southeast Siberia also appears an unlikely source for the St. Lawrence Bank clays as attested by the regional variations in the v/p ratios of the expandable clay minerals. On an average the v/p ratio of the minerals in the Anadyr deltaic clays is 2.1 as opposed to 1.4 of the St. Lawrence Bank clays. In light of the above, we are tempted to

conclude that the latter clays are relict deposits, representing either (a) altered ash and/or soil from the St. Lawrence and adjacent basaltic islands or (b) Yukon River paleodeposits. The latter seems more acceptable, notwithstanding that the analysis of the $< 2 \mu\text{m}$ size fraction of modern Yukon clays discloses, on the average, slightly less expandable minerals than in the St. Lawrence Bank clays (Table 1 and Fig. 2). It is conceivable that in the past the finest size of the Yukon were deposited onto the St. Lawrence Bank. Consequent to such sorting of minerals based on size it could have been possible that relatively higher amounts of expandable minerals reached the St. Lawrence Bank in the past than can be accounted for on the basis of the average abundances of clay minerals in the $< 2 \mu\text{m}$ size particles of the modern Yukon River.* The observations of Knebel and Creager (1973) seem to lend support to our contention, inasmuch as they have reported that the Yukon distributaries have migrated northward since the Holocene Transgression, and that between 11,000 and 16,000 yrs. B.P. sedimentation on the St. Lawrence Bank was predominantly influenced by the terrigenous debris from the ancestral Yukon River. Another supporting piece of evidence is the very similar v/p ratios of the expandable minerals of the Yukon River and the St. Lawrence Bank. Our foregoing suggestions are also consistent with the observations of Matthews (1973), who has reported progressively increased concentrations of expandable mineral phases in successively finer particles of the Yukon River clays, which, of course, is a feature that has been observed in numerous other clay mineral suites elsewhere.

*It is noteworthy that analysis of the $< 2 \mu\text{m}$ fraction of a few Yukon deltaic clays independently by us and Moll (1970) showed between 32 to 35 percent of expandable mineral phases.

Table 1. Clay mineral concentrations (weighed peak-area percents) of the fluvial bedload or deltaic sediments of some major rivers supplying sediments to the north Bering and Chukchi Seas.

Deltaic Sediment	No. of Samples analyzed	Expandable	Illite	Chlorite	Kaolinite
Kobuk River ^a	2	4	66	27	3
Noatak River ^a	2	Trace	66	34	0
Yukon River ^a	6	21	41	26	12
Kuskokwim River ^a	12	Trace	60	35	5
Kolyma River ^a	1	5	59	27	9
Kolyma-Indigirka Delta ^b	5	3	71	21	5

^aThis study.

^bAfter Silverberg (1972).

We feel that the narrow belt extending along the central Chukchi Sea, consisting of relatively high proportions expandable clay minerals (Fig. 2), accompanied by low proportions of illite (Fig. 3), represents the depositional site of clays originating from the north Bering Sea. Considering all possible sources (Table 1) we contend that the Yukon River is the primary source of the clays flushing through the Bering Strait. A net northward displacement of the Bering Sea water, induced by the Alaskan Coastal and Bering Sea Currents, through the Bering Strait has been amply demonstrated (Fleming and Heggarty, 1966; Coachman and Aagaard, 1974; Coachman *et al.*, 1975; among many others). This flow which is on the order of about 1.5 Sv (Coachman *et al.*, 1975), achieves velocities sufficiently high to transport clay particles. The transport direction of the above waters is also confirmed by the drift-bottle experiments conducted in the Bering Strait-Chukchi Sea region by Fleming and Heggarty (1966). We believe (as do Nelson and Creager, 1977) that a significant portion of the total sediment discharged by the Yukon River (96.8×10^6 tons) is caught in the northward-set currents, and eventually deposited in the central Chukchi Sea. This implies that most Yukon clay bypasses the Chirikov Basin, Norton Sound and adjacent Norton Bay area. This is essentially supported by the generally sandy nature of the Basin substrate (Creager and McManus, 1967; McManus *et al.*, 1969); the relatively high illite content, accompanied by a paucity of expandable clay minerals, documented in the bay and adjacent coastal region (Figs. 2 and 3); the presence of a notably thin blanket of Holocene muds of Yukon derivation in Norton Sound (Nelson *et al.*, 1974); and also the Yukon River plume structure (Burbank, 1974).

In another context it is of interest to note that in the Chukchi Sea the abundance pattern of the expandable clay minerals (Fig. 2) is closely correlatable with the net directions of the prevalent water currents (Coachman *et al.*, 1975), as well as with the dispersal trend of the water mass derived from the Bering Sea. The relatively darker meandering water mass, as depicted in the IR imagery of Figure 5, undoubtedly represents the trajectory of the Alaskan Coastal-Bering Shelf current component in the Chukchi Sea, composed chiefly of the warmer Yukon outflow. The presence of the latter outflow can be further substantiated on the basis of salinity and temperature measurements (Coachman *et al.*, 1975). The existence of the above correlations further corroborate our interpretations relating to the long-term net transport pathways and major depositional sites of the Yukon clays in the central Chukchi Sea. Our latter conclusions are also compatible with and, strongly substantiated by, a number of additional observations based on presence of turbid bottom waters in the central Chukchi Sea (McManus and Smyth, 1970), ERTS imagery (Burbank, 1974; Sharma *et al.*, 1974), sediment texture (McManus *et al.*, 1969), heavy mineralogy (McManus *et al.*, 1974), and the Holocene history of the north Bering and Chukchi Seas relative to the Yukon sediment supply (Nelson and Creager, 1977).

Possible Implication of Clay Mineral Dispersal Patterns on Elucidation of the Quaternary Paleogeography of the Chukchi Sea and Adjacent Regions.

It would seem from our foregoing conclusions, relative to dissemination of the Yukon clays through the Bering Strait, that clay mineral stratigraphic studies may offer potential criteria for the elucidation of the

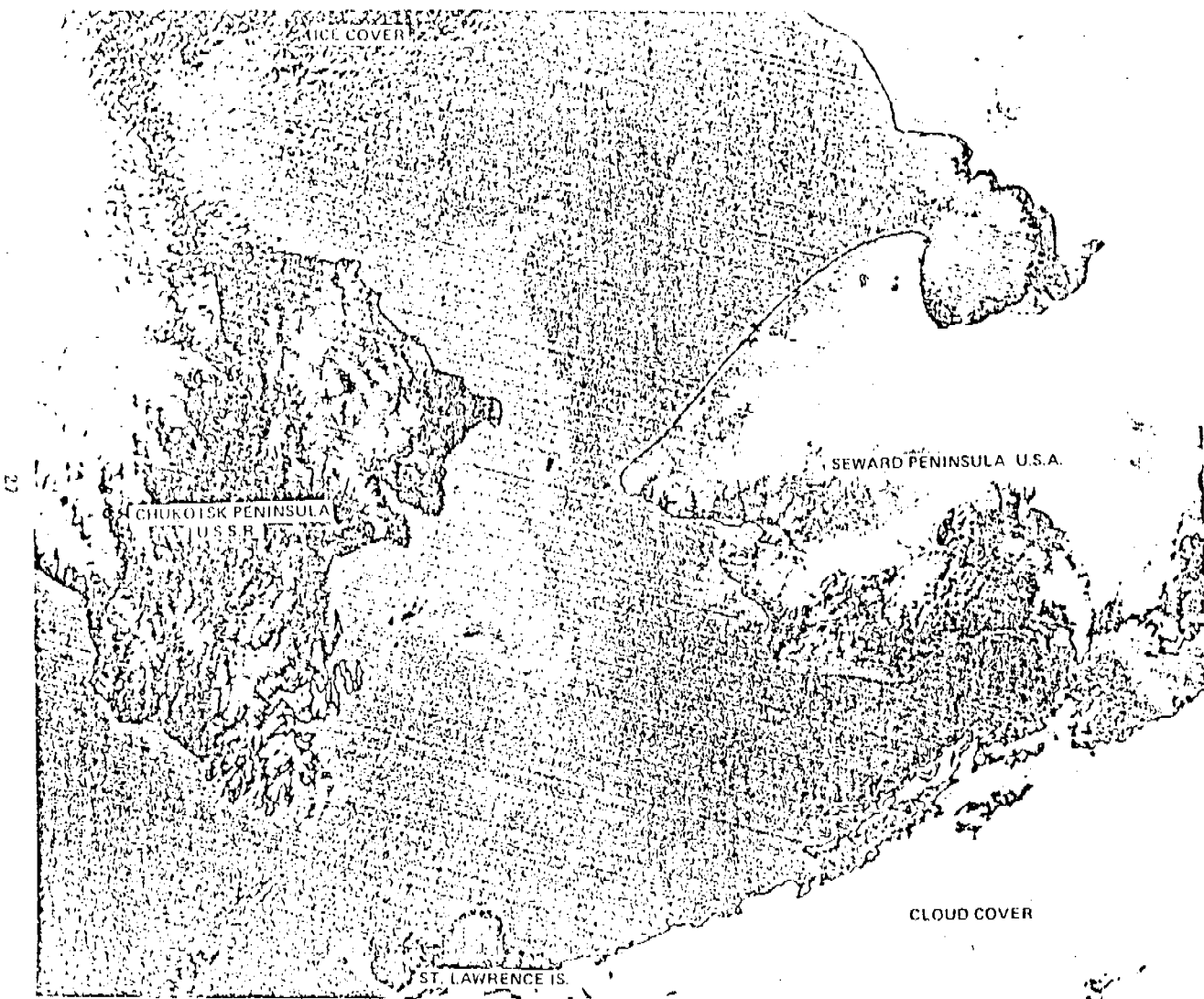


Figure 5. IR imagery showing the flow pattern of water masses from the north Bering Sea to the Chukchi Sea, through the Bering Strait. NOAA-3 VHRR IR image obtained on October 22, 1974.

Quaternary transgressive-regressive history of the Chukchi Sea. It is now well documented that the Bering Strait and contiguous shallow marine areas (e.g., Beringia of Hopkins, 1967) were subaerially exposed intermittently during the Quaternary, consequent to eustatically depressed sea levels coinciding with world-wide glaciation (Scholl and Sainsbury, 1961; Hopkins, 1967, 1972, and 1973; among several others). Assuming that a net northward displacement of Bering Sea waters was sustained during lowered sea-level periods of the Quaternary, it would seem justified to make some general predictions. One would reasonably anticipate a hiatus in the supply of Yukon River clay, attended by relatively larger fluxes of debris from the ancient Kobuk and Noatak Rivers, to the Chukchi Sea during times of marine regressions when the Bering Strait presumably remained closed. Likewise, it seems reasonable to suggest a resumption in the supply of Yukon River clay to the Chukchi Sea attended upon the periodic opening of the Strait, coinciding with interglacial marine transgressions. The foregoing scenario, although perhaps somewhat simplistic, nevertheless would seem to imply that marked stratigraphic shifts in the concentrations of Yukon River deposits in dated sections of core samples of southcentral Chukchi Sea could provide criteria to elucidate the more recent transgressive-regressive history of that sea. Thus, sediment sequences with relatively greater proportions of the Yukon River assemblage (i.e., containing high contents of expandable mineral phases), accompanied by a paucity of Noatak-Kobuk components (i.e., relatively enriched in illite) would most likely be anticipated in transgressive deposits, and vice versa. In another context, clay mineral stratigraphy in the southcentral Chukchi Sea region may have

a potential use in the understanding of the paleocurrent vectors in the Bering Strait and vicinity, because we have characterized and distinguished the clay mineral assemblages of the dominant fluvial systems contributing terrigenous materials to that area. Our future plans call for investigations to verify some of the above concepts.

CONCLUSIONS

The mineralogy of the $< 2 \mu\text{m}$ clay-sized fractions of a large number of marine sediment samples from the Chukchi Sea-north Bering Sea region, together with sediment samples representative of the major fluvial systems presently contributing sediments to the ocean in this region, as well as hinterland rock-types in selected areas, has been investigated. The resultant characterization of these sediments is consistent with the results of our previous work in adjacent regions (Bristol Bay, Beaufort Sea, Canada Basin, etc.). Additionally, this characterization has permitted examination of regional distribution patterns of these materials, as well as made possible the attendant consideration of the explanation of these distributions in terms of sediment sources, transportation processes, and depositional mechanisms. The distributions elucidated are quite consistent with the known physical oceanographic and regional geologic relationships within the study area.

As an ancillary, the above information seems to provide a potentially useful means to investigate further certain aspects of Quaternary paleogeography in this region. In particular, interpretations concerning eustatic sea level changes attendant upon global glacial/interglacial episodes, and the opening and closing of the Bering Strait (i.e., submergence/emergence of Beringia) to the northward marine transport of sediments from the Bering Sea to the Chukchi Sea should be considered in light of the stratigraphy of the clay minerals in the relevant marine sediments in the Chukchi and Bering Seas. The latter information is presently lacking, and should be obtained.

ACKNOWLEDGEMENTS

We thank M. D. Sweeney and Nam Veach for running some of the X-ray analysis. Charles R. Geist provided valuable help in the statistical treatment of the data. This research work was funded partly by the Office of Marine Geology, U.S. Geological Survey, Menlo Park, through Contract No. 14-08-0001-14827, and by the State of Alaska appropriation to the Institute of Marine Science, University of Alaska, Fairbanks. Additional support was provided by the Bureau of Land Management through interagency agreement with the National Oceanic and Atmospheric Administration under which a multiyear program responding to the needs of petroleum development of the Alaskan continental shelf is managed by the Outer Continental Shelf Environmental Assessment Program Office. The IR image of the Bering Sea region was kindly provided by Kristina Ahlnaes. We are grateful to Richard W. Roberts for supplying splits of samples from the collection of the Department of Oceanography, University of Washington, Seattle (supported by NSF Grant OCE 78-24898), and to Hans C. Nelson for a few sediment samples from the region off the Yukon Delta.

REFERENCES

- Aagaard, K. and Coachman, L. K., 1964. Notes on the physical oceanography of the Chukchi Sea. *In*: U.S. Coast Guard Oceanogr. Rept. No. 1, U.S. Govern., Printing Office, Washington, D.C., pp. 13-16.
- Andrew, J. A. and Kravitz, J. H., 1974. Sediment distribution in deep areas of the northern Kara Sea. *In*: Yvonne Herman (ed.), *Marine Geology and Oceanography of the Arctic Seas*, Springer-Verlag, N.Y., pp. 231-256.
- Barnes, F. F., 1967. Coal resources of Alaska. U.S. Geol. Surv. Bull. 1232-B, 89 pp.
- Biscaye, P. E., 1964. Distinction between kaolinite and chlorite in recent sediments by X-ray diffraction. *Amer. Mineralogist.*, 49:1281-1289.
- Biscaye, P. E., 1965. Mineralogy and sedimentation of recent deep-sea clay in the Atlantic Ocean and adjacent seas and oceans. *Geol. Soc. Amer. Bull.*, 76:803-832.
- Burbank, D. C., 1974. Suspended sediment transport and deposition in Alaskan coastal waters, with special emphasis on remote sensing by the ERTS-1 satellite. M.S. Thesis, Univ. Alaska, Fairbanks, 222 pp.
- Burrell, D. C., Tommos, K., Naidu, A. S. and Hoskin, C. M., 1981. Some geochemical characteristics of Bering Sea sediments. *In*: D. W. Hood and J. A. Calder (eds.), *The Eastern Bering Sea Shelf: Oceanography and Resources*. U.S. Dept. Commerce, p. 305-319.
- Campbell, R. H., 1966. Areal geology. *In*: N. J. Wilimovsky and J. M. Wolfe (eds.), *Environment of the Cape Thompson Region, Alaska*, USAEC Div. Tech. Inf. Ext., Oak Ridge, Tenn., pp. 57-84.
- Chamley, H., 1971. Sur la sedimentation argileuse profonde en Mediterranée. *In*: D. J. Stanley (ed.), *The Mediterranean Sea: A Natural Sedimentation Laboratory*, Dowden, Hutchinson and Ross, Inc., Stroudsburg, Penn., pp. 387-399.
- Coachman, L. C. and Rankin, D. A., 1968. Currents in Long Strait, Arctic Ocean. *Arctic* 21:27-38.
- Coachman, L. K., Aagaard, K. and Tripp, R. B., 1975. *Bering Strait, the Regional Physical Oceanography*. Univ. Washington Press, Seattle, Wash., 186 pp.
- Creager, J. S. and McManus, D. A., 1967. Geology of the floor of Bering and Chukchi Seas--American Studies. *In*: D. M. Hopkins (ed.), *The Bering Land Bridge*, Stanford Univ. Press., Stanford, Calif., pp. 7-31.
- Fleming, R. H. and Heggarty, D., 1966. Oceanography of the southeastern Chukchi Sea. *In*: N. J. Wilimovsky and J. M. Wolfe (eds.), *Environment of the Cape Thompson Region, Alaska*, U.S. Atomic Energy Comm., Washington, D.C., pp. 697-754.

- Gibbs, R., 1965. Error due to segregation in quantitative clay mineral X-ray diffraction mounting techniques. *Amer. Mineralogist*, 50:74-751.
- Gibbs, R. J., 1977. Clay mineral segregation in the marine environment. *J. Sed. Petrology*, 47:237-243.
- Gorbunova, Z. N., 1966. Clay mineral distribution in the Indian Ocean sediments (In Russian). *Okeanologia*, 6(2):267-275.
- Griffin, J. J., Windom, H. and Goldberg, E. D., 1968. The distribution of clay minerals in the world ocean. *Deep-Sea Research*, 15:433-459.
- Hein, J. R., Scholl, D. W. and Gutmacher, C. E., 1976. Neogene clay minerals of the far NW Pacific and southern Bering Sea. *In: S. W. Bailey (ed.), AIPEA Proc., 1975 Inter. Clay Conf., Mexico City. Applied Publ. Ltd., Illinois, pp. 71-80.*
- Holowaychuk, N., Petro, J. H., Finney, H. R., Farnham, R. S. and Gersper, P. L., 1966. Soils of Ogotoruk Creek watershed. *In: N. J. Wilimovsky and J. M. Wolfe (eds.), Environment of the Cape Thompson Region, Alaska, USAEC Div. Tech. Inf. Ext., Oak Ridge, Tenn., p. 221-273.*
- Hopkins, D. M., 1967. *The Bering Land Bridge. Stanford Univ. Press, Stanford, Calif., 495 pp.*
- Hopkins, D. M., 1972. The paleogeography and climatic history of Beringia during late Cenozoic time. *Inter-Nord.*, 12:121-150.
- Hopkins, D. M., 1973. Sea level history in Beringia during the past 250,000 years. *Quaternary Res.*, 3:520-540.
- Ingham, M. C. *et al.*, 1972. An ecological survey in the eastern Chukchi Sea; September-October 1970. U.S. Coast Guard Rept. No. 50, CG 373-50, Washington, D.C., 206 pp.
- Jacobs, M. B., 1974. Clay mineral changes in Antarctic deep-sea sediments and Cenozoic events. *J. Sed. Petrology*, 44:1079-1086.
- Jacobs, M. B. and Hays, J. D., 1972. Paleoclimatic events indicated by mineralogical changes in deep-sea sediments. *J. Sed. Petrology*, 42:889-898.
- Jonas, E. D., 1975. Crystal chemistry of diagenesis in 2:1 clay minerals. *In: S. W. Bailey (ed.), Proc. Inter. Clay Conf., 1975, Mexico City, Mexico. Applied Publ. Ltd., Wilmette, Illi., p. 3-13.*
- Kachadoorin, R., 1966. Engineering geology of the Chariot site. *In: N. J. Wilimovsky and J. M. Wolfe (eds.), Environment of the Cape Thompson Region, Alaska, USAEC Div. Tech. Inf. Ext., Oak Ridge, Tenn., p. 85-96.*
- Knebel, H. J. and Creager, J. S., 1973. Yukon River: evidence for extensive migration during the Holocene Transgression. *Science*, 179:1230-1232.

- Latouche, C., 1978. Clay minerals as indicators of the Cenozoic evolution of the north Atlantic Ocean. Proc. VI Inter. Clay Conf., 1978, Oxford, England, Elsevier Sci. Publ. Co., Oxford, England, pp. 271-279.
- Lisitsyn, A. P., 1966. Recent sedimentation in the Bering Sea: U.S.S.R. Acad. Sci., Inst. Oceanology (English translation: Israel Program for Scientific Translation), 1969, 614 pp.
- Matthews, M. D., 1973. Flocculation as exemplified in the turbidity maximum of Acharon Channel, Yukon River Delta, Alaska. Ph.D. Dissertation, Northwestern Univ., Evanston, Illi., 88 pp.
- McManus, D. A., Kelley, J. C. and Creager, J. S., 1969. Continental shelf sedimentation in an arctic environment. Geol. Soc. Amer. Bull., 80:1961-1984.
- McManus, D. A. and Smyth, C. S., 1970. Turbid bottom water on the continental shelf of the northern Bering Sea. J. Sed. Petrology, 40:869-873.
- McManus, D. A., Venkatarathnam, K., Hopkins, D. M. and Nelson, C. H., 1974. Yukon River sediment of the northern most Bering Sea shelf. J. Sed. Petrology, 44:1052-1060.
- Moll, R. F., 1970. Clay mineralogy of the north Bering Sea shallows. Rept. No. USC-Geol 70-2, submitted to U.S. Geol. Surv., Menlo Park, Calif., 101 pp.
- Naidu, A. S., Burrell, D. C. and Hood, D. W., 1971. Clay mineral composition and geologic significance of some Beaufort Sea sediments. J. Sed. Petrology, 41:691-694.
- Naidu, A. S. and Mowatt, T. C., 1974. Clay mineralogy and geochemistry of continental shelf sediments of the Beaufort Sea. In: J. C. Reed and J. E. Sater (eds.), The Coast and Shelf of the Beaufort Sea, Arctic Inst. North Amer., Arlington, Virg., pp. 493-510.
- Naugler, F. P., 1967. Recent sediments of the east Siberian Sea. M.S. Thesis Univ. Washington, Seattle, 71 pp.
- Nelson, C. H., Hopkins, D. M. and Scholl, D. W., 1974. Cenozoic sedimentary and tectonic history of the Bering Sea. In: D. W. Hood and E. J. Kelley (eds.), Oceanography of the Bering Sea, Inst. Mar. Sci. Occas. Pub. No. Univ. Alaska, Fairbanks, 485 pp.
- Nelson, C. H. and Creager, J. S., 1977. Displacement of Yukon-derived sediment from Bering Sea to Chukchi Sea during Holocene time. Geology, 5: 141-146.
- Parham, W. E., 1966. Lateral variations in clay mineral assemblages in modern and ancient sediments. In: Proc. Inter. Clay. Conf., 1966, Jerusalem, Israel, Vol. 1, pp. 135-145.
- Rao, P. D., 1980. Petrographic, mineralogical and chemical characterization of certain arctic Alaskan coals from the Cape Beaufort region. M.I.R.L. Rept. 44, Univ. Alaska, Fairbanks, 66 pp.

- Rateev, M. A., Gorbunova, Z. N., Lisitsyn, A. P. and Nosov, G. L., 1969. The distribution of clay minerals in the oceans. *Sedimentology*, 13:21-43.
- Scholl, D. W. and Sainsbury, C. L., 1961. Subaerially carved arctic sea valley under a modern epicontinental sea. *Geol. Soc. Amer. Bull.*, 72: 1433-1436.
- Sharma, G. D., Wright, F. F., Burns, J. J. and Burbank, D. C., 1974. Sea surface circulation, sediment transport, and marine mammal distribution, Alaska continental shelf. ERTS Final Rept., Nat. Tech. Inf. Service Rept. E74-10711, 77 pp.
- Silverberg, N., 1972. Sedimentology of the surface sediments of the east Siberian and Laptev Seas. Ph.D. Dissertation, Univ. Washington, Seattle, 184 pp.
- Sverdrup, H. U., 1929. The waters on the north-Siberian shelf. The Norwegian North Polar expedition with the "Maud" 1918-1925. Scientific results, Vol. 4, Bergen, Norway, A. S. John Griegs Boktrykkeri, 131 pp.
- Turekian, K. K., 1968. *Oceans*. Prentice-Hall, Inc., New Jersey, 120 pp.
- Venkatarathnam, K. and Biscaye, P. E., 1973. Clay mineralogy and sedimentation in the eastern Indian Ocean. *Deep-Sea Res.*, 20:727-738.
- Venkatarathnam, K., Henderson, L. and Biscaye, P., 1976. Clay mineralogy and sedimentation in the western Indian Ocean. *Deep-Sea Res.*, 23: 949-961.
- Windom, H. L., 1975. Eolian contributions to marine sediments. *J. Sed. Petrology*, 45:520-529.
- Wright, P. L., 1974. The chemistry and mineralogy of the clay fraction of recent sediments from the southern Barents Sea. *Chem. Geol.*, 13: 197-216.

APPENDIX 6

DISPERSAL PATTERNS OF CLAY MINERALS IN THE MARGINAL SEAS OF ALASKA*

A. S. Naidu and T. C. Mowatt
Institute of Marine Science
University of Alaska
Fairbanks, Alaska 99701

ABSTRACT

The $<2\mu\text{m}$ e.s.d. of about 700 sediment samples from the major rivers and marginal seas of Alaska (constituting 74% of the United States continental shelf) were analyzed by X-ray diffraction for clay mineralogy. The clay mineral assemblages in the Gulf of Alaska and Bering Sea are consistent with the latitudinal trends suggested for world oceans. In the Beaufort and east Chukchi Seas kaolinite concentrations are similar or higher than in mid-latitudes. The clay mineral concentrations and dispersal patterns are attributed to terrigenous source and prevailing currents.

The Gulf of Alaska has three mineral suites. The illitic and chloritic glaciomarine sediments of fjords and eastern shelf are locally derived, from argillites, and greywackes subjected to mild chemical weathering. A discernible increased concentration of glycol-expandable clay minerals (GECM) in the north Gulf is ascribed to the Copper River. This flux is transported up to northeast Kodiak and central Prince William Sound by the Alaska coastal current. The western Gulf derives its sediments from the Alaska Peninsula and the Aleutians, as attested by the notable increase in GECM and illite/chlorite ratios.

In southeast Bering Sea a progressive northwestward decrease in GECM, from 65 to 11%, is caused by gradual decreased sediment supply from the Alaska Peninsula and Aleutian andesites and a complementary increase in illite from the Kuskokwim River. The Yukon River is the predominant clay source for the north Bering Sea, as signified by an abrupt increase in GECM (20 to 35%) and kaolinite. Clay mineralogy conveys that the central Chukchi Sea is the major repository of the Yukon clays, and this has implication for interpretation of the Quaternary paleogeography of Beringia.

In Beaufort Sea, influence of different fluvial inputs and their current dispersals are sharply defined. A westward sediment drift in Alaskan portion is evident. In the Mackenzie Delta the drift is north-eastward. An apparent seaward increase in illite/smectite ratio in the Colville Delta is ascribed to reconstitution of depotassicated illite by K^+ adsorption in saline waters. An isolated smectite-rich deposit in central Beaufort shelf is presumably relict.

*Accepted for Proceedings of the Seventh International Clay Conference, Pavia and Bologna, Italy, in 6-12 September 1981 (full paper will be published in the Proceeding Volume).

APPENDIX 7

PARTITIONING OF HEAVY METALS IN LAGOON SEDIMENTS, NORTH ARCTIC ALASKA*

M. D. Sweeney and A. S. Naidu
Institute of Marine Science, University of Alaska
Fairbanks, Alaska 99701 (907) 479-7032

ABSTRACT

Partitioning of Fe, Mn, Zn, V, Cr, Ni, Cu, and Co in 54 arctic lagoon sediments was established. Average metal concentrations on HF-HNO₃ digests are 20,000 ppm Fe, 260 ppm Mn, 75 ppm Zn, 70 ppm V, 45 ppm Cr, 23 ppm Ni, 17 ppm Cu, and 8 ppm Co. A sequential extraction using MgCl₂ salt (EXCH), cation exchange resin (CER), a pH 2 hydroxylamine hydrochloride solution (NHH), acid ammonium oxalate (AAOX), sodium dithionite (DITH), and acetylacetone in benzene (ACETBEN) resolved the partitioning of the metals among the exchangeable phase, carbonate minerals, Mn oxides, amorphous and crystalline Fe oxides, and organic complexes, respectively. Of the total, 5% of Cr, 15% of V, 40% of Fe, Co, and Ni, 55% of Mn, and 60% of Cu constitute the extractables (E). The major portions of the E Fe (90%) and V, Cr, Co, Ni (70%) were removed by AAOX and DITH. Smaller fractions of the E Cu (50%) and Mn (30%) were mobilized by the latter two procedures. The ACETBEN step accounted for 25% of E Cu and 0.5% of E Ni. The combined treatments EXCH + CER + NHH contributed a minor portion of the E trace metals (20 - 30%). A major part of the E Mn (60%) and a very small fraction of the E Fe (4%) were recovered by these three mild treatments. Ni and Cu show significant correlations to the more easily extractable Mn phases.

Total metal abundances of the arctic lagoons are comparable with those of nonpolluted, temperate, nearshore sediments.

* Abstract submitted to the 4-8 October 1981 Symposium in Richland, Washington, entitled: BIOLOGICAL AVAILABILITY OF TRACE METALS.

ANNUAL REPORT

Contract: NA79RAC00086
Research Unit: 531
Reporting Period:
1 April 1980 - 1 October 1981

NUMERICAL TRAJECTORY MODELING AND
ASSOCIATED FIELD MEASUREMENTS IN
THE BEAUFORT SEA AND CHUKCHI SEA
NEARSHORE AREAS

Donald E. Wilson, J.C.H. Mungall,
Stephen Pace, Philip Carpenter,
Howard Teas, Toby Goddard
Robert Whitaker, Patrick Kinney


Donald E. Wilson
Principal Investigator

KLI-81-9
9 November 1981

Kinnetic Laboratories Inc.
519 West Eighth Avenue, Suite 205
Anchorage, Alaska 99501

TABLE OF CONTENTS

	<u>Page</u>
LIST OF FIGURES	302
LIST OF TABLES	304
SUMMARY	305
QUASI-OPEN WATER SPILL MOVEMENT PREDICTION	306
Introduction	306
Current Modeling	306
Sea Level Changes	306
Currents	307
Trajectory Modeling	307
Modeling Applicability	311
Model Verifications	311
Trajectory Results	313
BEAUFORT SEA DROGUE TRACK EXPERIMENTS, 1979	322
Introduction	322
Experiment 1	322
Experiment 2	327
Experiment 3	327
Conclusions	335
PRUDHOE BAY DIFFUSIVITY MEASUREMENTS, 1979	337
Introduction	337
Experimental Procedure	337
Winds	337
Analysis	340
Conclusions	351

TABLE OF CONTENTS (Continued)

	<u>Page</u>
HARRISON BAY DIFFUSIVITY MEASUREMENTS, 1980	353
Introduction	353
Experimental Procedures	353
Winds	353
Analysis	356
Results	356
NUMERICAL MODELING; MAPPING GRID FOR CHUKCHI SEA	361
Introduction	361
Methods	361
Results	362
CRUISE REPORT, CHUKCHI SEA COAST 1981, R.V. <u>D.W. HOOD</u>	367
Introduction and Objectives	367
Methods	367
Chronology of the Cruise	369
Results	378

LIST OF FIGURES

	<u>Page</u>
1. Southern Harrison Bay Setdown/Setup Resulting from Steady Winds of 24 Hour Duration	309
2. Central Harrison Bay Currents and Direction Resulting from Steady Winds of 24 Hour Duration	310
3. NOAA Calculations: 1977 Winds	314
4. NOAA Calculations: 1978 Winds	315
5. NOAA Calculations: 1980 Winds	316
6. NOAA Calculations: 1977 Winds	317
7. NOAA Calculations: 1978 Winds	318
8. NOAA Calculations: 1980 Winds	319
9. Cottle Island Winds	323
10. Narwhal Island Winds	324
11. Drogue Tracking Experiment No. 1: Harrison Bay Area (18-22 August 1979)	325
12. Drogue Tracking Experiment No. 2: Stockton Islands Area (26-28 August 1979),	328
13. Drogue Tracking Experiment No. 3: Steffanson Sound Area , (30 August - 2 September 1979) Drogues 1,2, and 4	331
14. Drogue Tracking Experiment No. 3: Steffanson Sound Area (30 August - 2 September 1979) Drogues 3,5, and 6	332
15. Prudhoe Bay Diffusivity Measurement Location Map	338
16. Ellipses and Mean Times of Drifters 1 - 9 (25 August 1979)	341
17. Ellipses and Mean Times of Drifters With 4 and 9 Excluded (25 August 1979)	342
18. Enlarged Drifter Location Map: 5,000 Feet Between Large Crosses	343

LIST OF FIGURES (Continued)

	<u>Page</u>
19. Enlarged Drifter Location Map: 5,000 Feet Between Large Crosses	344
20. Variances Computed Using All Drifters	349
21. Variances Computed Using All Drifters With 4 and 9 Excluded	350
22. Harrison Bay Diffusivity Measurement Location Map	354
23. Raw Ellipses of Drifters 1 - 9 (20 August 1980)	357
24. Interpolated Ellipses of Drifters 1 - 9 (20 August 1980)	358
25. Variances Computed Using All Drifters	359
26. Sample Chukchi Sea Grid	365
27. Chukchi Sea Coast Study Sites (August - September 1981)	368

LIST OF TABLES

	<u>Page</u>
1. Steady 24-Hour Wind Results: Setup/Setdown in Southern Harrison Bay, Current Speed and Direction in Central Harrison Bay	308
2. Wind Classification	312
3. Milne Point Slick Movement Summary	320
4. Experiment No. 1: True Bearings	322
5. Experiment No. 2: True Bearings from Tigvariak Island	329
6. Experiment No. 2: True Bearings from Foggy Island and Point Gordon	330
7. Experiment No. 3: True Bearings from Bullen Point	333
8. Experiment No. 3: True Bearings from Foggy Island Bay and Heald Point	334
9. Analysis of Beaufort Sea Drogue Trajectories, 1979	336
10. Cottle Island Winds	339
11. Mean Times - All Drogues, Five Groups	345
12. Mean Times - Less Drogues 4 and 9, Five Groups	346
13. Mean Times - All Drogues, Last Four Groups	347
14. Mean Times - Less Drogues 4 and 9, Last Four Groups	348
15. Tolaktovut Point Winds	355
16. Mean Times - All Drogues	360
17. Mapping Constants Required for Chukchi Sea Grid Generation	363- 364
18. Equipment Deployment and Retrieval Log, Chukchi Sea, 1981	370- 371
19. C/STD Transect Log	373

SUMMARY

Nearshore physical oceanographic tasks were accomplished by RU 531 since April 1980 in both the Beaufort Sea and Chukchi Sea areas.

The major task accomplished in the Beaufort Sea was furnishing a selected set of predicted oil spill trajectories for use in the Environmental Impact Statement for Lease Sale 71 (Harrison Bay area). This task involved the construction and operation of a numerical hydrodynamic model of the inshore area. Real wind data, furnished by Tom Kozo (RU 519), were utilized. The set of predicted trajectories were submitted (in the form of 9-track data tapes) to the U.S. Geological Survey, Water Resources Division, which is using them as input to aid estimating impacts of spills on regional resources.

Experimental drogue trajectory and drogue dispersion data from nearshore areas in the Beaufort Sea were also worked up and interpreted during this period.

For the Chukchi Sea, an orthogonal computational grid has been numerically constructed for use in storm surge and other future modeling tasks. However, the major effort this summer has been the field effort along the Chukchi nearshore area from Point Lay to Barrow. Current meter moorings, a tide gauge, drogue tracking and dispersion experiments, and STD transects were accomplished from the inshore survey research vessel, D.W. HOOD. These data, which include a major negative storm surge event, are now being reduced and interpreted. These actual data will be used as a guide to refine the physical concepts inherent in predicting oil spill trajectories in the nearshore areas along the Chukchi Sea coast.

QUASI-OPEN WATER SPILL MOVEMENT PREDICTIONS

Introduction

The general approach used in the prediction of oil spill tracks is performed in two steps. The first step is the calculation of current tables, either one or two for each of 16 evenly-distributed wind directions. The second step involves accessing these tables on the basis of an appropriate wind speed and direction record (either real or statistically generated).

The following scenario discussion will start with a description of the current-prediction process and results, and will continue with a brief description of the tracking program along with some generalizations. Lastly, some sample plots and results will be presented.

Current Modeling

Depth-mean currents were predicted for the Harrison Bay/ Prudhoe Bay region using a 60 x 26 grid of 2 x 2 nautical mile squares. The grid was later extended to cover the entire lease area. Runs were typically made for 24 hours of real time, by which time the currents had nearly settled down to their steady-state values (a consequence of the shallow, wind-driven nature of the region). Verification of the currents, to be discussed below, was accomplished through comparison between measured and predicted progressive vector diagrams for currents at a fixed point. In addition to currents, sea level changes were also computed, these values being of interest in the estimation of shoreline inundation. A brief summary of the results is included in the two following sections, since they may be of use in the estimation of oil spill scenarios to cover cases other than those presented in this chapter.

Sea Level Changes

Changes in sea level along the coast are often associated with storms. Should a spill reach the shore during a storm, a surface slick could be deposited on surfaces above or below the normal coastline, i.e., on low-lying salt marshes or on shallow mudflats. Typical values of the sea level change to be expected are listed in Table 1, for 15 and 30 knot winds that have been blowing steadily for 24 hours. The results are relative to a zero sea level occurring along a line parallel to the shore and some 50 miles from it. Furthermore, the model has not been verified for elevations, only for currents.

As can be seen in Figure 1, the setup/setdown is a non-linear function of wind speed. Maximum values are ± 0.6 ft and ± 2.2 ft for 15 and 30 knot winds respectively. Maximum setup and setdown occur respectively for winds from $337^\circ/360^\circ$ and $157^\circ/180^\circ$ true. Using the values in Table 1, interpolated as necessary, the degree of inundation or recession can be estimated from the topographic maps.

Currents

Also listed in Table 1 are typical currents associated with a steady 15 or 30 knot wind that has been blowing for 24 hours. The location chosen is in central Harrison Bay ($70^\circ 36'N$, $151^\circ 19'W$). The results are shown in Figure 2. As can be seen, the currents have values ranging between 0.1 and 0.4 ft/sec for 15 knot winds, and 0.3 and 0.9 ft/sec for 30 knot winds. The currents, for the most part, tend to be parallel to the coast, with little difference between current directions for 15 and 30 knots. As will be seen, there will be little or no tendency for pollutants within the water column to be transported towards the shores opposite the lease area.

Slick movement is not included in the above. Typically, this is computed by adding to the above vectors a second vector equal to some $3/100$ of the wind speed in the direction of the wind.

Trajectory Modeling

As briefly discussed earlier, real or statistically-generated winds are provided to the trajectory model along with a set of current maps. A random start time within the record of 3-hourly winds is selected, and the first speed and direction are read. The nearest of the sixteen sectors is then selected, and an interpolation or extrapolation is performed to obtain an estimate of the depth-mean current. To this value can be optionally added a wind-induced surface slick component. The spill is then moved using the above values subject to the geometry of the region. Implicit in this approach is the assumption of negligible response time (3 hours or less) of the water column. The next wind record is then read, and the process is repeated until the particle reaches the shore or leaves the modelled region. A fresh random start time is then computed and the procedure is repeated a sufficient number of times so that a reasonable estimate of spill track distributions and shoreline hit distributions can be obtained. In the case of this particular lease area, the tracks will be used by the U.S. Geological Survey, Water Resources Division, for estimating the impact of spills on the resources of the region.

Table 1. Steady 24-hour wind results: Setup/setdown in southern Harrison Bay (70°26'N, 151°28'W), current speed and direction in central Harrison Bay (70°36'N, 151°19'W).

Wind Direction (°T)	15 knots			30 knots			Speed Ratio	Direction Difference
	Setup (ft)	Speed (ft/s)	Direction (°T)	Setup (ft)	Speed (ft/s)	Direction (°T)		
000	0.5	0.3	104	2.1	0.6	101	2.0	-3
022	0.3	0.1	068	1.7	0.4	060	4.0	-8
045	0.1	0.2	319	1.1	0.6	313	3.0	-6
067	-0.1	0.3	302	0.5	0.8	298	2.7	-4
090	-0.2	0.4	298	-0.4	0.9	293	2.25	-5
112	-0.4	0.4	295	-1.1	0.9	291	2.25	-4
135	-0.6	0.4	293	-1.7	0.9	289	2.25	-4
157	-0.6	0.3	290	-2.2	0.8	287	2.7	-3
180	-0.6	0.2	282	-2.2	0.6	282	3.0	0
202	-0.4	0.1	242	-1.6	0.3	245	3.0	3
225	-0.1	0.2	136	-0.9	0.5	132	2.5	-4
247	0.1	0.3	118	-0.7	0.7	118	2.3	0
270	0.3	0.4	114	0.5	0.9	114	2.25	0
292	0.4	0.4	111	1.2	0.9	112	2.25	1
315	0.5	0.4	109	1.8	0.9	109	2.25	0
337	0.6	0.3	107	2.1	0.8	106	2.7	-1
							$\bar{x}=2.59$ $\sigma=0.49$	$\bar{x}=-2.37$ $\sigma=2.92$

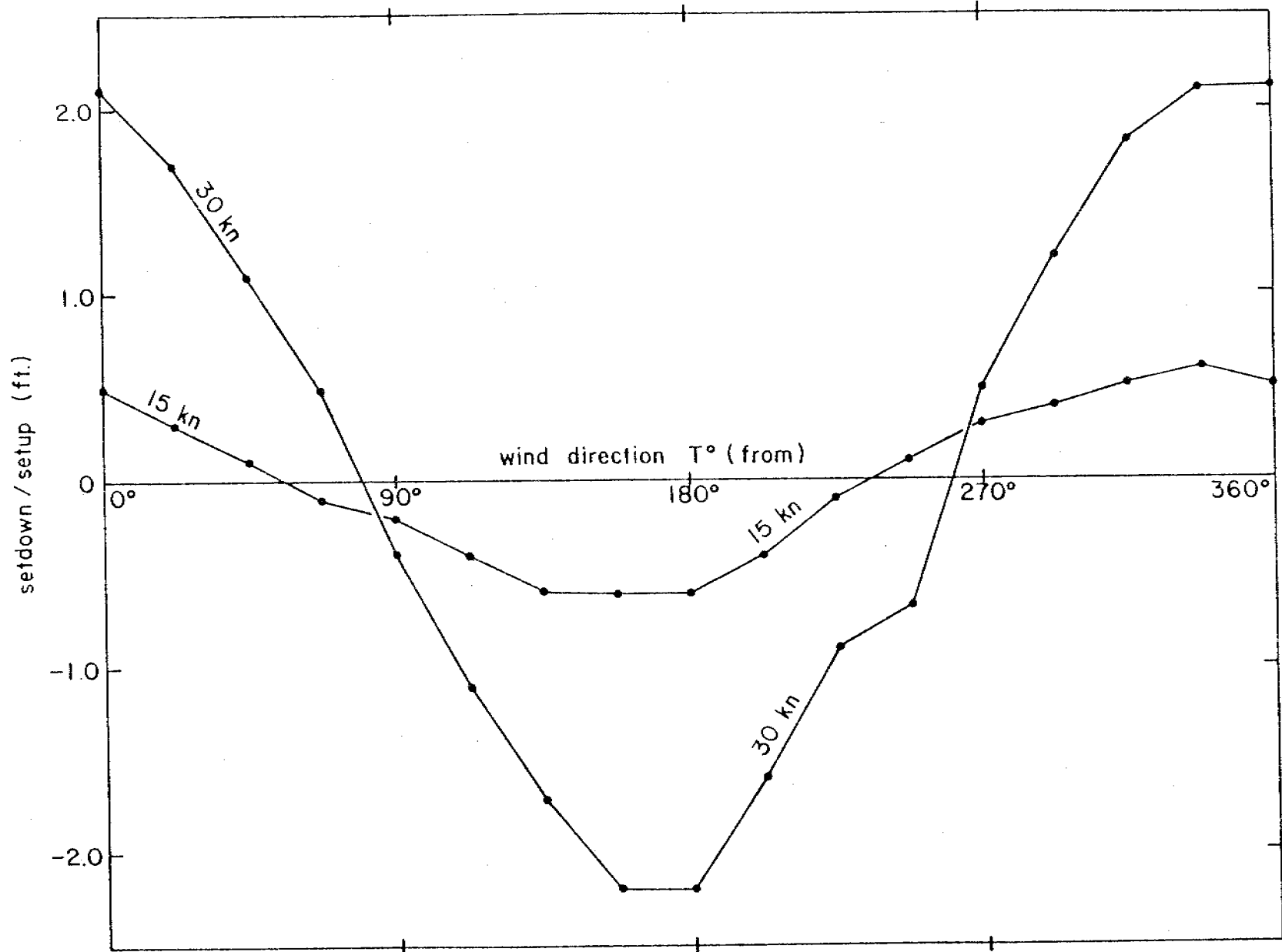
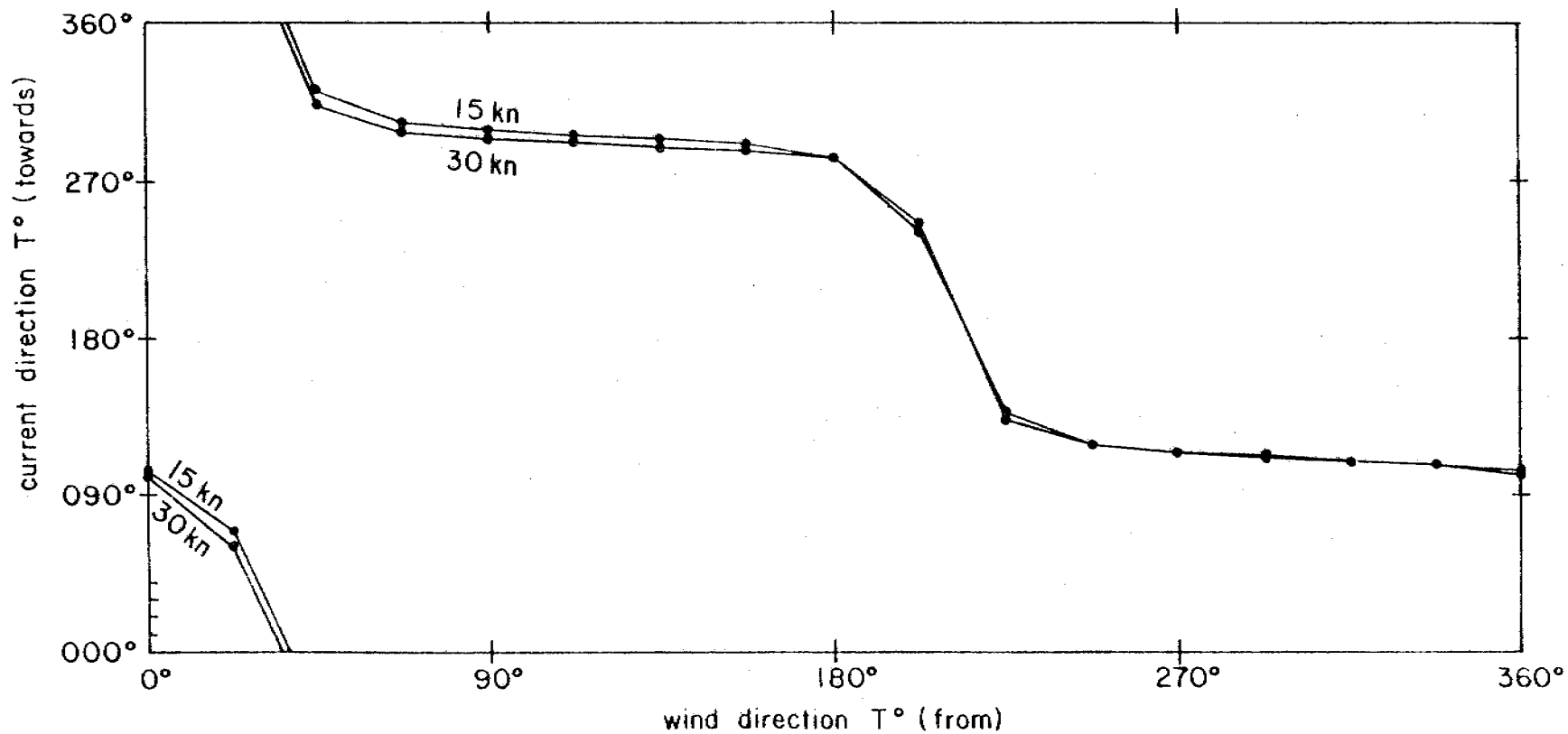
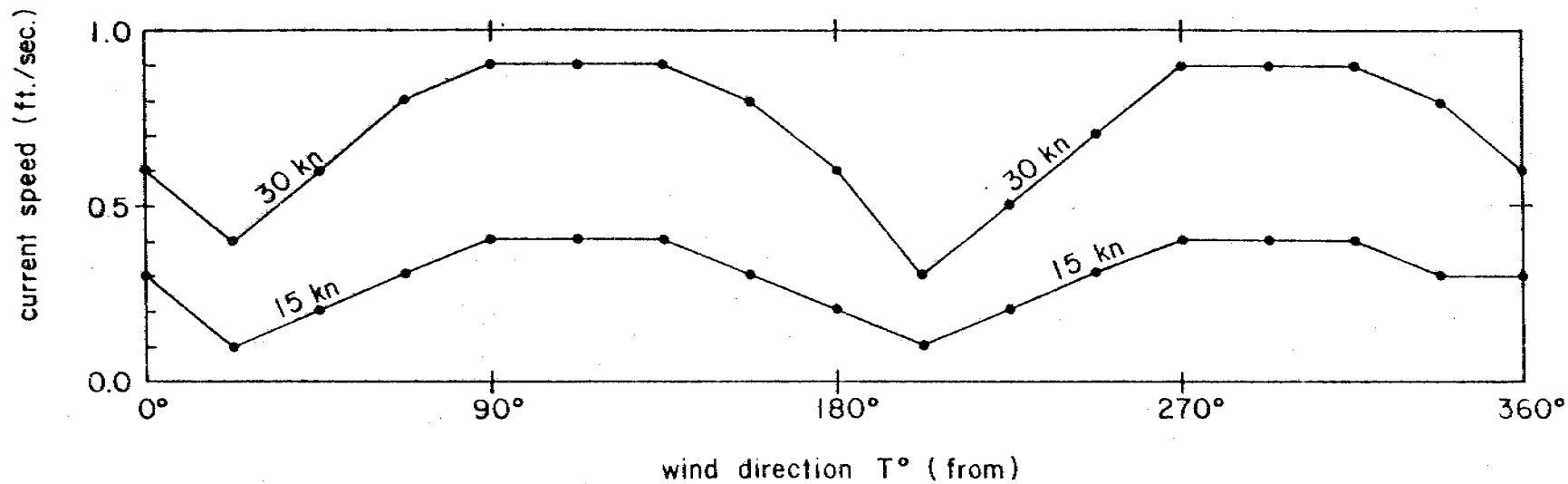


Figure 1. Southern Harrison Bay Setdown/Setup Resulting From Steady Winds of 24 Hour Duration



Modeling Applicability

Of obvious concern is the general applicability of both the models---current prediction and trajectory prediction---to the problem. In open water situations the models are limited only by tuning (selection of friction coefficient for the current model, selection of wind drift factor, and turning angle for the trajectory model). In mid-winter neither model is suitable or, in fact, necessary if one is concerned only with oil that does not go into solution (as was shown in the winter oil spill scenario). A more questionable situation exists when modeling those times of year when partial ice coverage exists.

When the pack ice edge has receded offshore for some miles, leaving an open extent of water, the problem can be fairly easily handled in the U.S.G.S. Water Resources Division model. The ice edge is merely treated as another shoreline, and a summary can be produced of the frequency with which spills produced by the trajectory model encounter each segment of this artificial shore. Grounded ice can similarly be treated, using data from satellite photos (Bill Stringer) or from direct observations (Peter Barnes, Erk Reimnitz).

More difficult to assess is the problem of ice scattered throughout the "open" water region. Intuitively one suspects that the open water method may hold up to an ice concentration of, say, three- or four- tenths. Beyond this, an ice aggregation model may have to be used. Of particular interest, both practical and academic, is the subject of oil or ice movement caused by direct wind action. Work by Flow Research indicates that ice tends to travel to the right of the wind in a manner not associated with Ekman theory. Similarly, the U.S.G.S. Water Resources Division is of the opinion that, as an average, an oil slick tends to move 20° to the right of the wind. (To each of these vectors, one must add an appropriate surface current in order to arrive at a velocity vector relative to the sea bed.)

Model Verification

Confidence in the overall capability of the pair of models to realistically simulate spill tracks must be estimated through verification. For the models described above, this has been achieved through comparison between progressive vector diagrams derived from current meters moored in Harrison Bay and simulated progressive vector diagrams as computed from depth-mean currents for fixed points using the trajectory model. When this was done for two current meter records, one off Atigaru Point and the other off Thetis Island, the measured and computed excursions of the progressive vector plots for two weeks of motion agreed to within 30 percent. When one considers that particle movement is accomplished by assuming that the

Table 2. Wind Classification

Year	Start Date	Number of Hours	Location	Wind-Type
1977	July 24	765	Cottle Isl	Strong ENE winds: 1 week negative surge, 90% steadiness factor.
1978	July 21	1008	Cottle Isl	Typical Easterly winds: typical average wind data for month of August (compared to 20 yr. wind average).
1980	August 1	1308	Tolaktuvut	Strong Westerly winds: persistence in westerly direction (~70%) was high from August 15 to September 10.

depth-mean currents respond instantly to the wind, the agreement is impressive, and is a result of the quick response time of the water to changes in wind conditions.

Trajectory Results

In the computations described in this chapter, three real wind years have been used. These winds (provided by Tom Kozo of Tetra Tech, Inc.) are for quasi-open water periods in 1977, 1978, and 1980. A description of the winds is given in Table 2. The approach of using real winds instead of statistically generated winds was chosen as being best suited for the scenarios on account of the need for each discipline to see visual summaries of the consequences of various wind types. A more statistically-oriented summary will be provided by the U.S.G.S. at a later date.

Trajectory simulations are presented for each of the three wind-types. For each wind-type, two computations are shown: trajectories computed assuming that the spill travels entirely within the water column at a rate dictated by the depth-mean current, and trajectories that additionally include surface slick movement. It is felt that various disciplines may require one or the other information mode.

Since the actual tracks taken by spills will depend on the initial position of the spill, it is impractical in this presentation to cover too many cases. Instead, examples will be shown for the case of a spill originating in quasi-open water at a site some 6 miles off Milne Point, at $70^{\circ}39'N$, $149^{\circ}15'W$. Six plots are shown, with 25 randomly started spills in each plot tracked for a maximum of one month.

Figures 3, 4, and 5 show simulated spills occurring at random times in the open-water months of 1977, 1978, and 1980, respectively. No surface slick movement effects have been included; the spill is assumed to move with the depth-mean current which, following Figure 2, tends to be parallel to the coast. The three figures reflect the wind tendencies during the three years: easterly, typical (predominantly from the east), and westerly. Of particular interest is Figure 4 for typical winds. The figure shows that under those circumstances, spills transported by the water column alone will typically affect a region offshore between 10 nm to the east and 50 nm to the west.

Figures 6, 7, and 8 again show, respectively, simulated spills occurring at random times in the open-water months of 1977, 1978, and 1980. An additional surface slick vector has been added equal to 0.03 times the wind-speed vector. Figures 6 and 7 have been computed assuming the spills will stop once they hit the shore. A numerical summary is given in Table 3, with the transit times referring to the time between the spill release and the first contact with the shore.

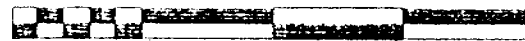
BEAUFORT SEA

NOAA CALCULATIONS

1977 WINDS

WIND DRIFT FACTOR = 0 $\times E-3$
10 0 10 20 30

KINETIC LABORATORIES INC.



NAUTICAL MILES

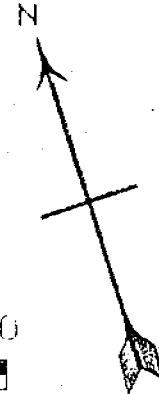
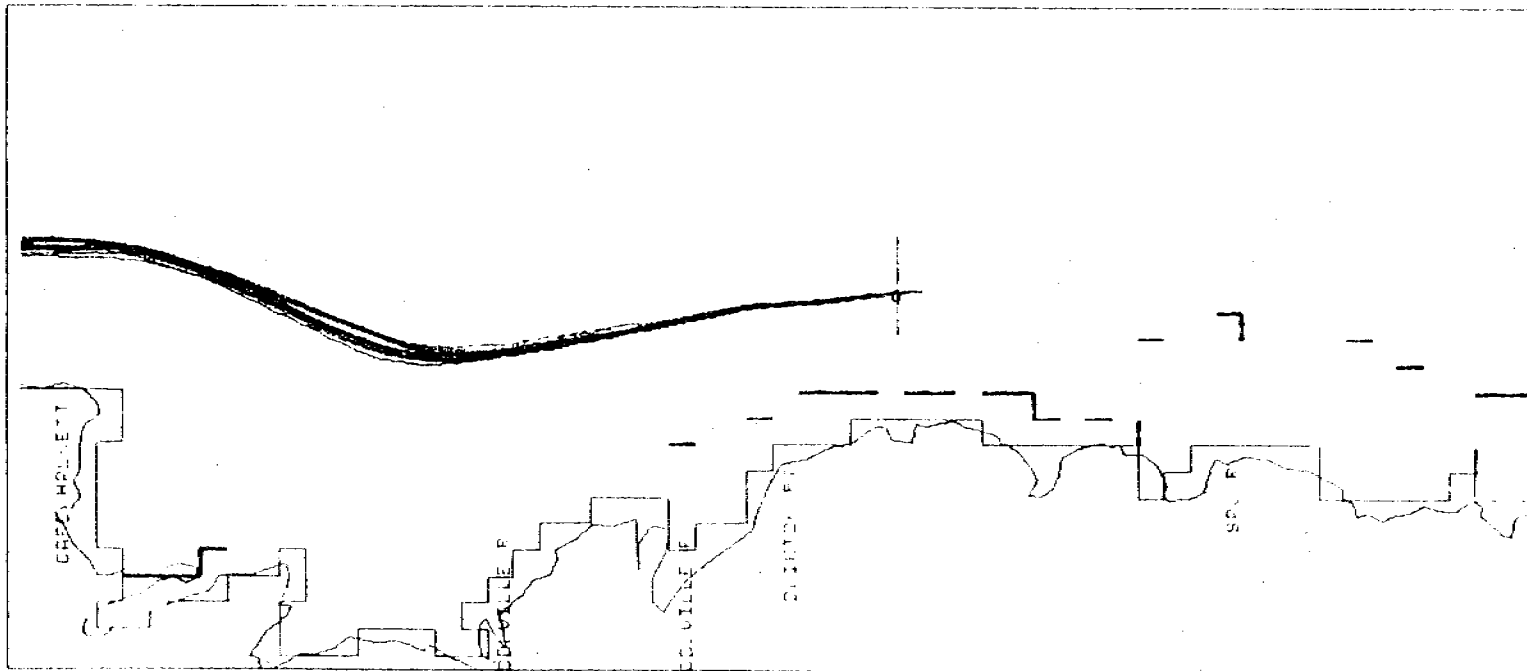


FIGURE 3



BEAUFORT SEA

NOAA CALCULATIONS

1978 WINDS

WIND-DRIFT FACTOR = 0 X E-3

10 0 10 20 30

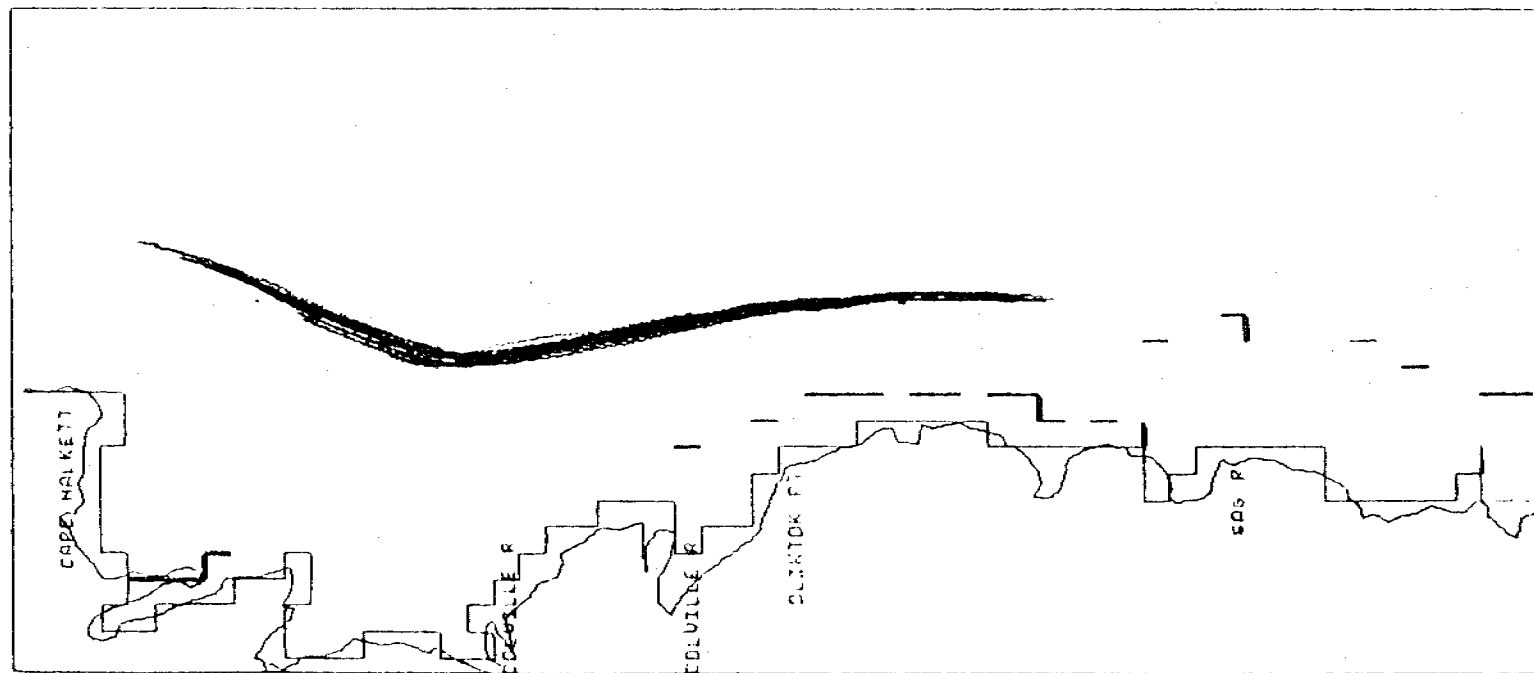
KINNETIC LABORATORIES INC.



NAUTICAL MILES



FIGURE 4



BEAUFORT SEA

NOAA CALCULATIONS

1980 WINDS

WIND DRIFT FACTOR = 0 X E-3

10 0 10 20 30

KINNETIC LABORATORIES INC.



NAUTICAL MILES

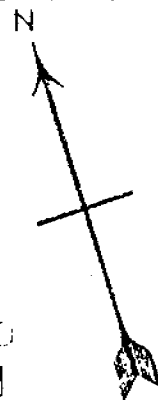
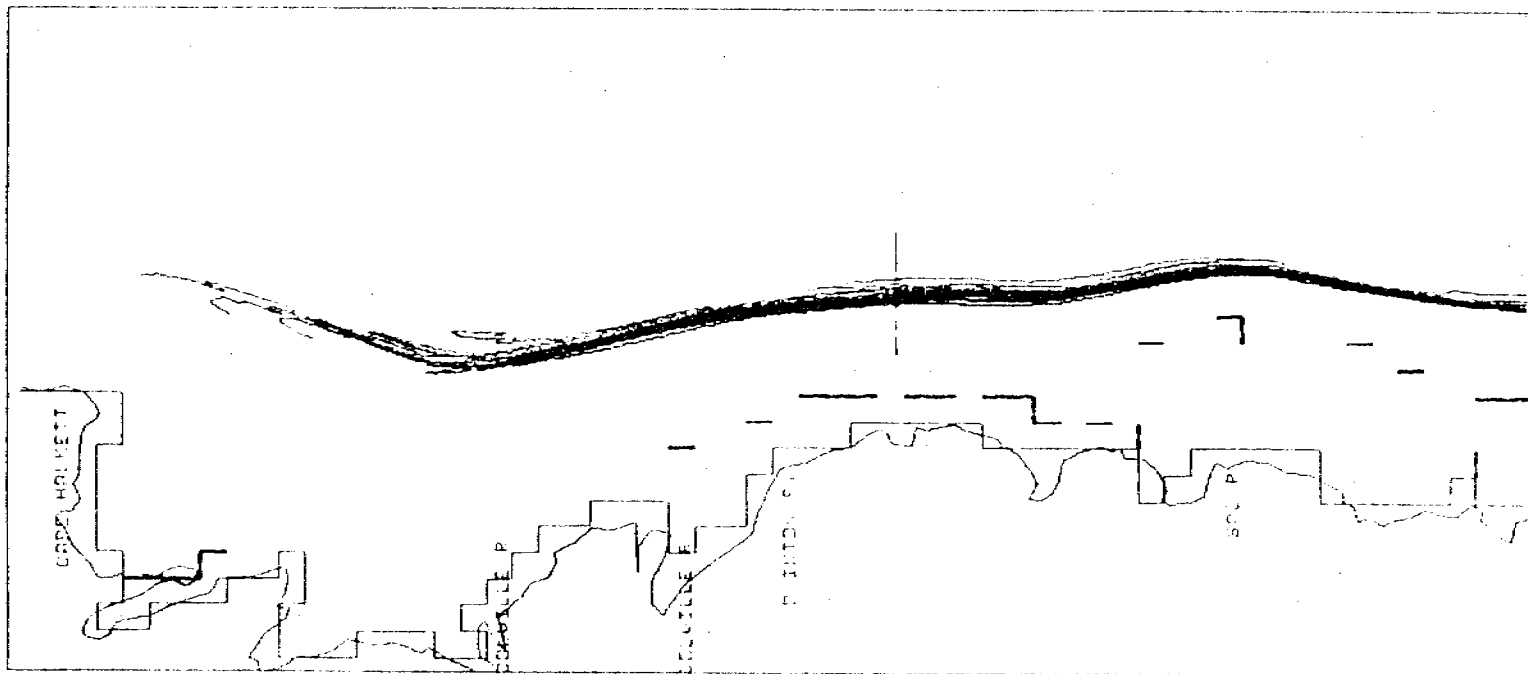


FIGURE 5



BEAUFORT SEA

NOAA CALCULATIONS

1977 WINDS

WIND-DRIFT FACTOR = 30 X E-3

10 0 10 20 30

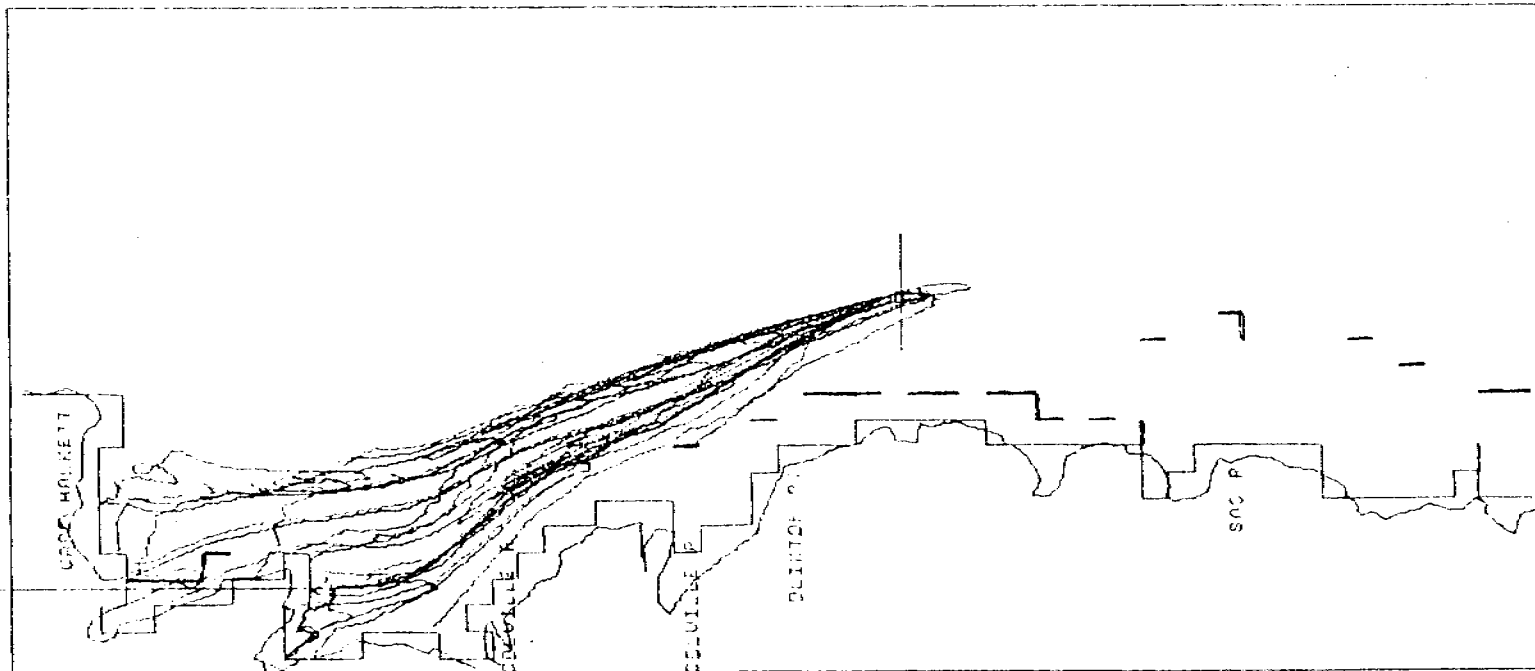
KINNETIC LABORATORIES INC.



NAUTICAL MILES



FIGURE 6



BEAUFORT SEA

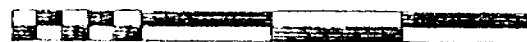
NOAA CALCULATIONS

1978 WINDS

WIND-DRIFT FACTOR = 30 X E-3

10 0 10 20 30

KINNETIC LABORATORIES INC.



NAUTICAL MILES

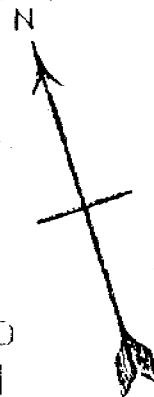
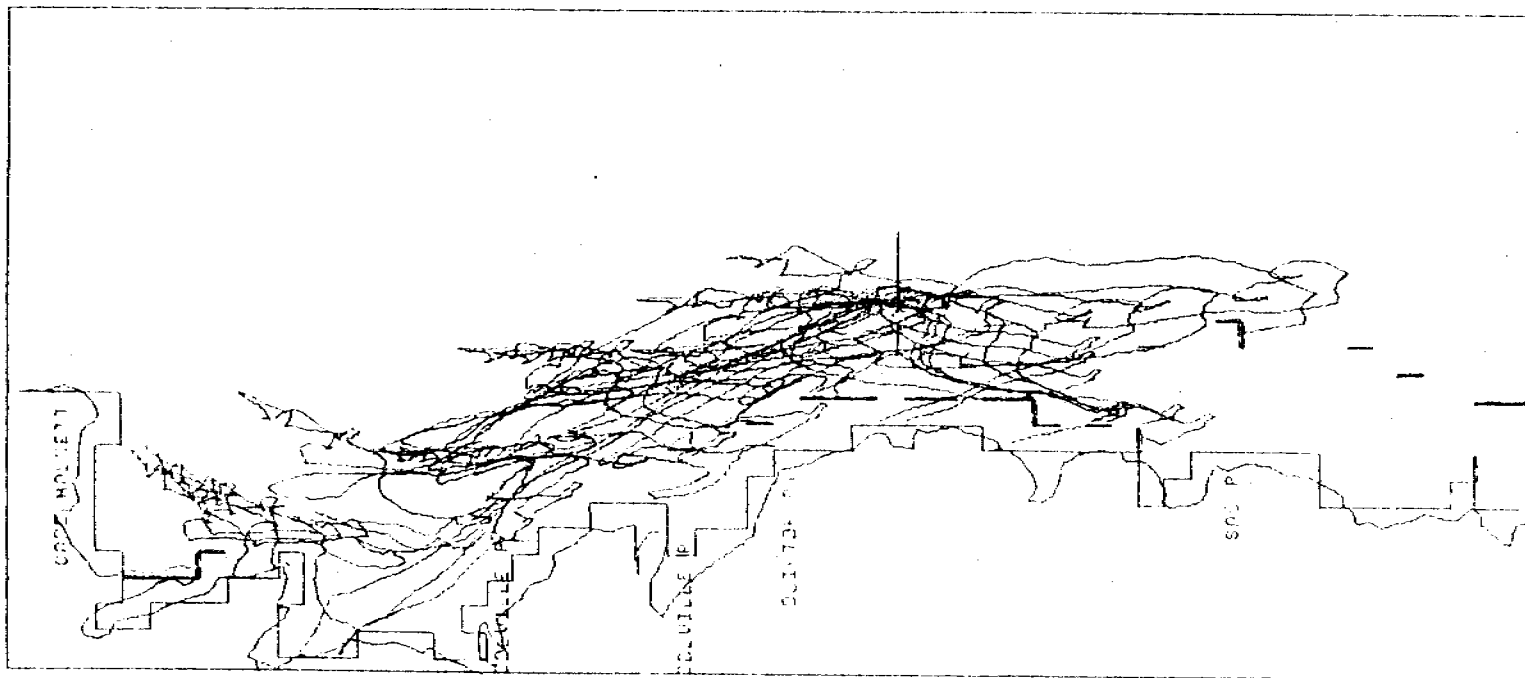


FIGURE 7



BEAUFORT SEA

NOAA CALCULATIONS

1980 WINDS

WIND-DRIFT FACTOR = 30

X E-3

10 0 10 20 30

KINETIC LABORATORIES INC.



NAUTICAL MILES

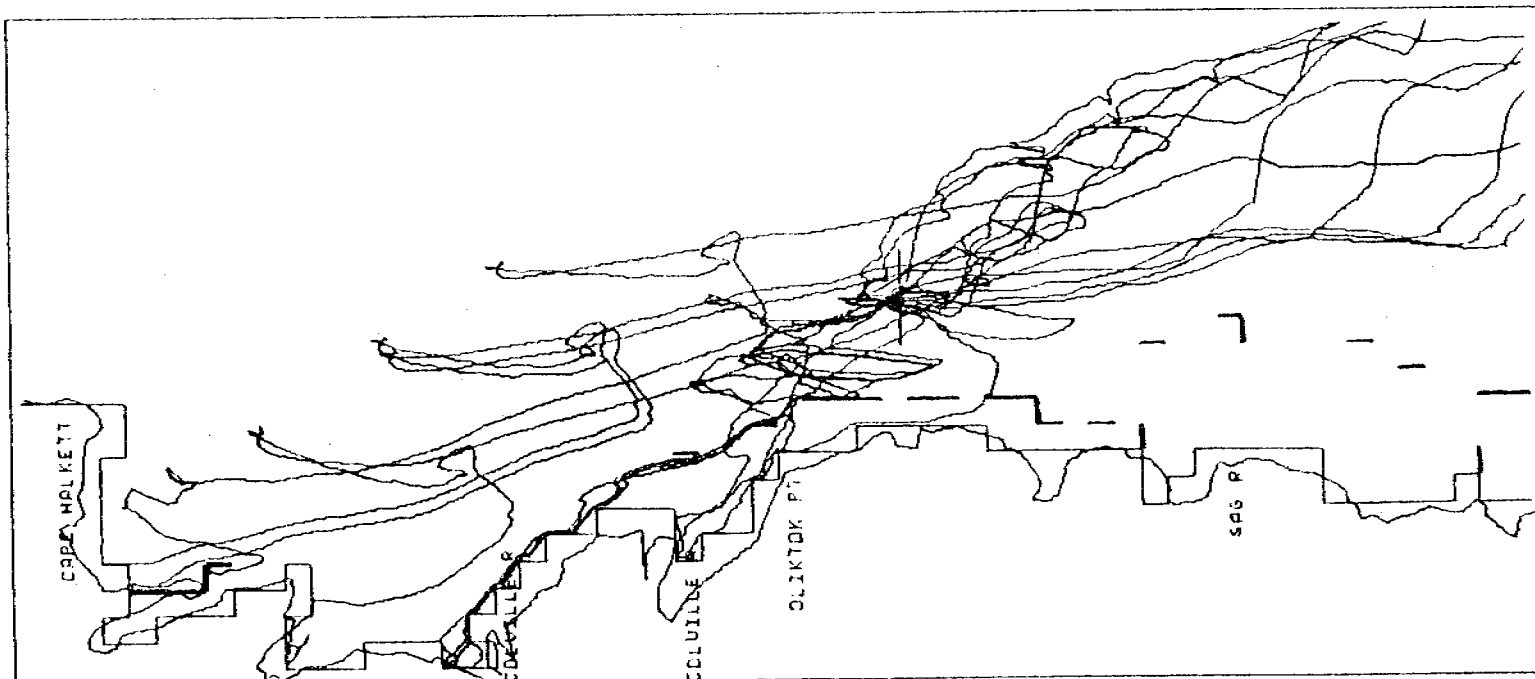
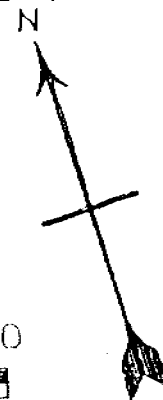


Table 3. Milne Point Slick Movement Summary*

	Year:	1977	1978	1980
	Wind Type:	Easterly Storms	Typical ENE Prevailing	Westerly Storms
# reaching north boundary		0	0	3
# reaching east boundary		0	0	3
# reaching west boundary		0	0	0
# reaching shore or islands		25	25	19
transit time (mean, days)		7.6	12.5	7.0
transit time (standard deviation)		1.9	6.9	6.1

* Position: 70°39'N, 149°15'W

For the most part, the figures are self-explanatory. Strong easterly winds will cause the central and western parts of Harrison Bay to be impacted, typical winds will extend the previous impact region eastwards to the Sagavanirktok River region, and a year with a trend of offshore westerly winds will cover a region extending from Harrison Bay to the middle of Simpson Lagoon, with perhaps 25 percent of the spills going northeast towards the pack ice. Transit times (based only on 25 spills in each case) have, for the three wind conditions, means and standard deviations as shown in Table 3.

When detailed statistics have to be obtained, a single wind record is used. For this particular study, the single record was obtained by concatenating the wind records for 1977, 1978, and 1980; and taking 1 length of the 1977 wind record, 5 lengths of the 1978 record, and 1 length of the 1980 wind record. This was done so as to conform with information from Tom Kozo (personal communication) that, based on a 20-year average, the three seasonal types of wind tend to occur 1 year 10, 7 years in 10, and 2 years in 10, respectively.

When 100 spills are run using this concatenated wind field along with a wind drift factor of 0.03, the mean and standard deviations for the transit times came to 5.6 and 3.7 days, respectively, with 7 percent of the spills reaching the pack ice towards the northeast.

For purposes of risk analysis, 100 spills from each of 45 possible locations have been computed and their track coordinates sent to the U.S.G.S. Water Resources Division. When these hypothetical spill cases have been analyzed by the U.S.G.S., a more sophisticated view of the situation will be possible. Until then, the above techniques should provide some guidelines; those wishing to make their own predictions will probably achieve a fair degree of realism by making use of velocities interpolated from Table 1, to which should be added the appropriate slick drift correction.

BEAUFORT SEA DROGUE TRACK EXPERIMENT, 1979

Introduction

Radio-beacon equipped free-drifting buoys were released during three different experiments in order to ascertain typical nearshore current velocities. Each buoy contained either a 4 MHz or 6 MHz transmitter that emitted a characteristic "beep" capable of being tracked by shore-based Radio Direction Finding (RDF) stations. In a typical experiment, 3 to 7 buoys would be released from a taxiing float-plane at appropriate points between the shore and the ice-edge (some 3-5 miles offshore). Two stations (each consisting of a two-man team, tents, RDF set, etc.) would be located at points satisfying the criteria of float-plane accessibility and navigational line-of-position (LOP) quality. Due to the short base-line that resulted from the combination of small offshore buoy location and need for at least 30° between LOP's, frequent station movement was desirable---a requirement that could not always be dealt with due to poor flying conditions.

Experiment No. 1 - 18 August to 22 August 1979

The first tracking experiment was started in a period of easterly winds (see Figures 9 and 10) with the objective of studying flow trajectories into Harrison Bay. Three buoys were released off the eastern end of Pingok Island:

6209.0 Khz buoy	~1 mile offshore
6200.0 Knz buoy	~2 miles offshore
6236.0 Knz buoy	~3 miles offshore

Due to mechanical problems, only a poor connection was possible between the hull and the current drogue of the 6200.0 Khz buoy. Probably the failure of this connection and the subsequently assumed horizontal position caused this buoy to go off the air prematurely.

Regrettably, after moving the two stations to the west on 20 August, the wind changed direction and blew from the west. The consequent wave heights made it impossible to relocate the stations in time to achieve good LOP's.

The resulting bearings from each station are shown in Table 4. Due to lack of sun and absence of landmarks, compasses had to be used to establish reference angles. The bearings shown in Table 4 and in subsequent tables are in

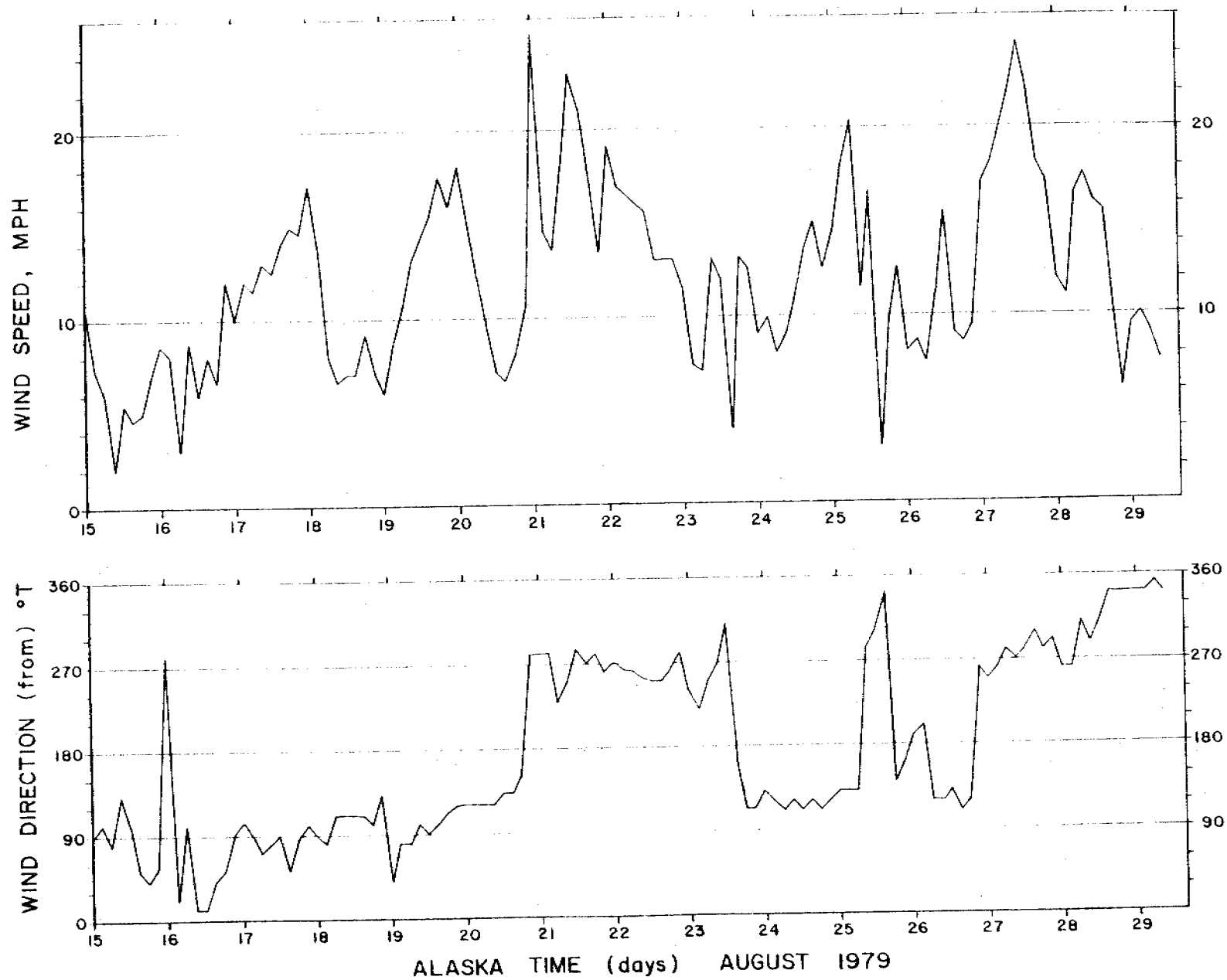
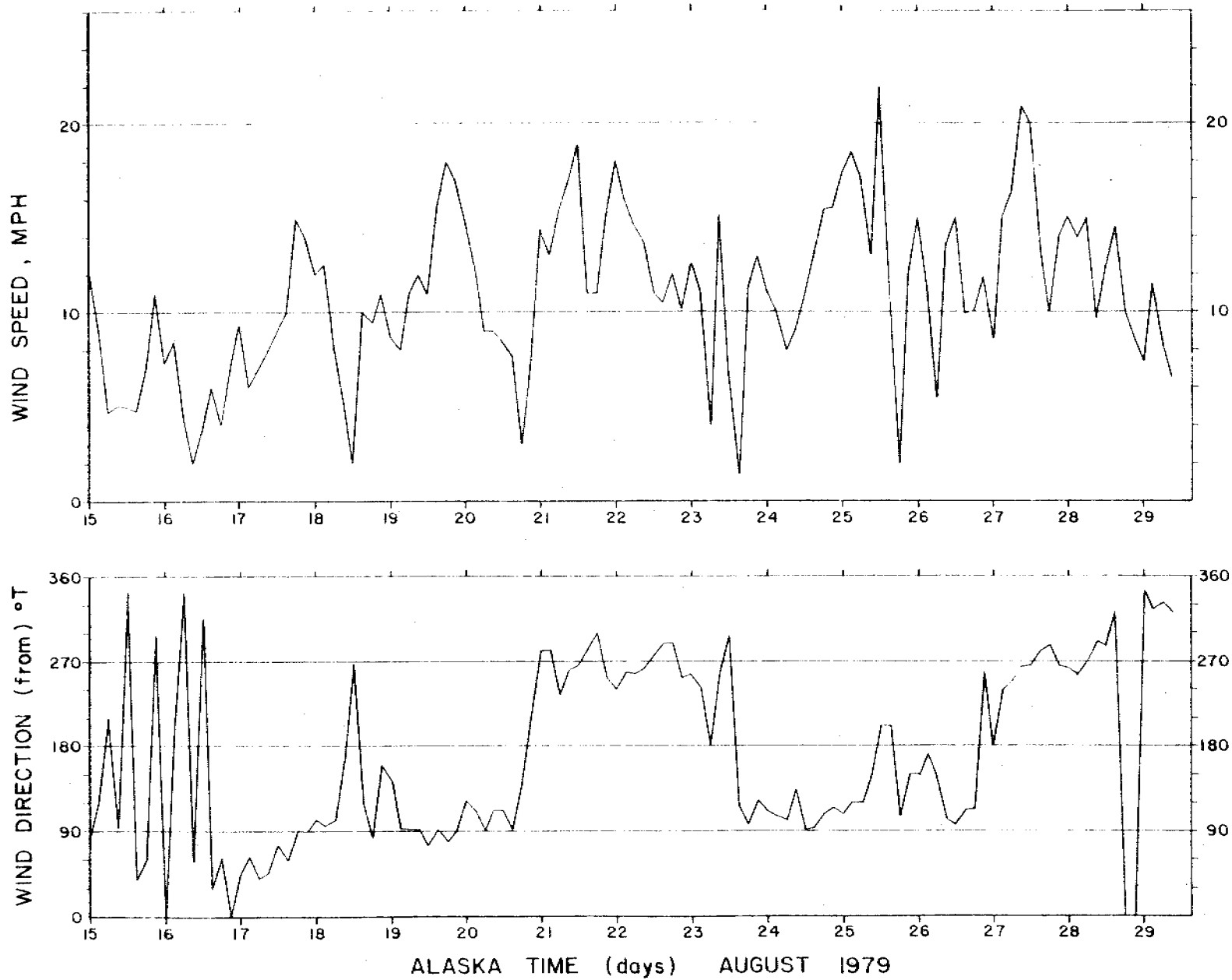


Figure 9 . Cottle Island winds
Source: Tom Kozo, University of Washington

324



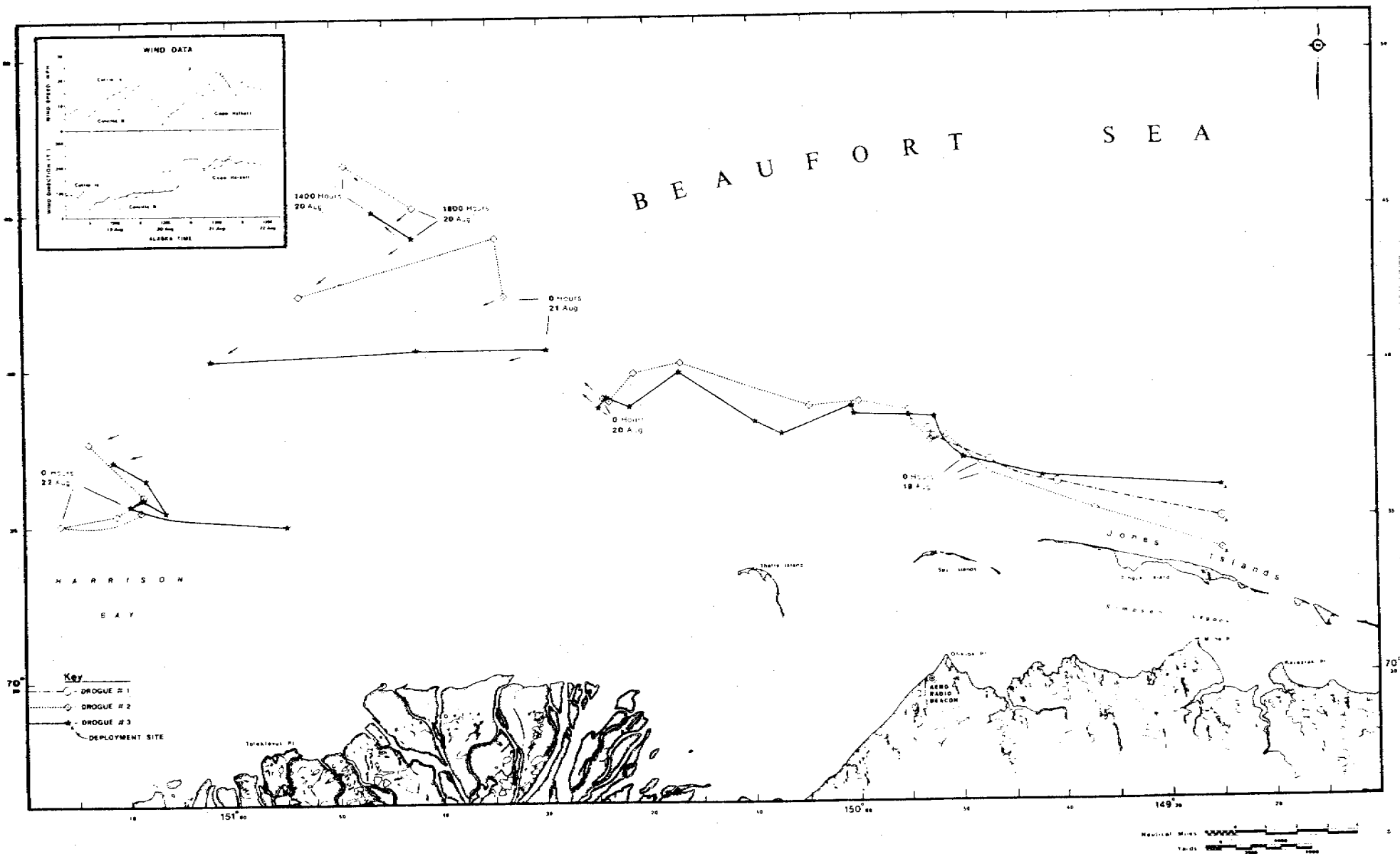


Figure 11. Drogue Tracking Experiment No. 1: Harrison Bay Area. (18-22 August 1979)

Table 4.

Experiment No. 1. True Bearings

Date	AK Time	Buoy Frequency in Khz						
		6200	6209	6236	6200	6209	6236	
		Colville Village (70°26.2'N, 150°22.6'W)			Milne Point (70°30.8'N, 149°27.4'W)			
18 Aug. 79	2000	063	069	058				
	2200	058	062	057	321	324	319	
19 Aug. 79	0000	054	056	053	313	311	310	
	0200	049	049	048	309	311	310	
	0400	047	049	043	310	309	310	
	0600	off air	045	039	off air	309	305	
	0800	"	043	037	"	310	306	
	1000	"	037	036	"	307	298	
	1400	"	032	028	"	303	298	
	1800	"	017	014	"	-	-	
	2200	"	355	356	"	300	299	
	20 Aug. 79	0200	"	340	340	"	297	294
0600		"	330	328	"	294	294	
1000		"	327	324	"	294	293	
					Eskimo Islands (70°34.5'N, 151°53.5'W)			
1400		"	326	320	"	060	064	
1800		"	324	317	"	065	067	
					Cape Halkett (70°50.8'N, 152°18.7'W)			
2200		"	106	112	"	068	071	
21 Aug. 79		0200	"	100	107	"	069	075
		0600	"	103	105	"	073	077
	1100	"	121	121	"	076	079	
	1400	"	122	121	"	084	082	
	1800	"	124	122	"	086	086	
	2200	"	127	122	"	-	084	
22 Aug. 79	0200	"	127	123	"	087	085	
	0600	"	123	119	"	086	088	

degrees TRUE, as computed by adding 30° to the RDF set bearings (in turn based on magnetic reference bearings). The sudden change of angle at Cape Halkett at 1100 hours, 21 August cannot be explained: it could be real, or it could be due to a failure of the bearing readout circuitry. (The set had to have repairs made to the power supply after the experiment.)

Experiment No. 2 - 26 August to 28 August 1979

The second experiment had to be conducted with only one RDF set, the other having been taken to Prudhoe Bay for repairs. This required considerable work on the part of the pilot (Jim Helmericks) and the field party (Dale Harber, Steve Pace, and Howard Teas). Buoy positions could only be established by the "running" fix method. One buoy (4144.8 Khz) was placed on Jeanette Island (70°22'N, 147°25'W) in the McClure Islands group so as to provide an RDF bearing check. In addition, four free-drifting buoys were released as follows:

4125.6 Khz buoy	~1 mi W of Lion Pt, Tigvariak Island
4162.2 Khz buoy	~1 mi W of Pole Is, Stockton Islands
4187.6 Khz buoy	~1 mi S of Karluk Is, McClure Islands
4222.3 Khz buoy	~1.5 mi W of Karluk Is, McClure Islands

RDF angles (as in Experiment 1) are shown in Tables 5 and 6, along with the theoretical angles computed using latitudes and longitudes of the reference buoy (4144.8 Khz) and of the stations. The rather wide scatter between the measured and computed angles can be attributed variously to operator problems (mostly due to the awkward running fix method), RDF set problems, and perhaps magnetic reference bearing problems.

Experiment No. 3 - 30 August to 2 September 1979

The third and last experiment, carried out with two RDF sets, was hampered both by nearshore ice and poor flying weather. Six free-drifting buoys were deployed in the McClure Islands group as follows:

4118.3 Khz buoy	2.5 mi ESE of Karluk Island
4245.6 Khz buoy	2 mi ESE of Karluk Island
4295.6 Khz buoy	0.5 mi ESE of Karluk Island
4274.1 Khz buoy	1 mi SW of Jeanette Island
4183.2 Khz buoy	2 mi SW of Jeanette Island
4137.6 Khz buoy	3 mi SW of Jeanette Island

The 4144.8 Khz buoy continued to act as a check.

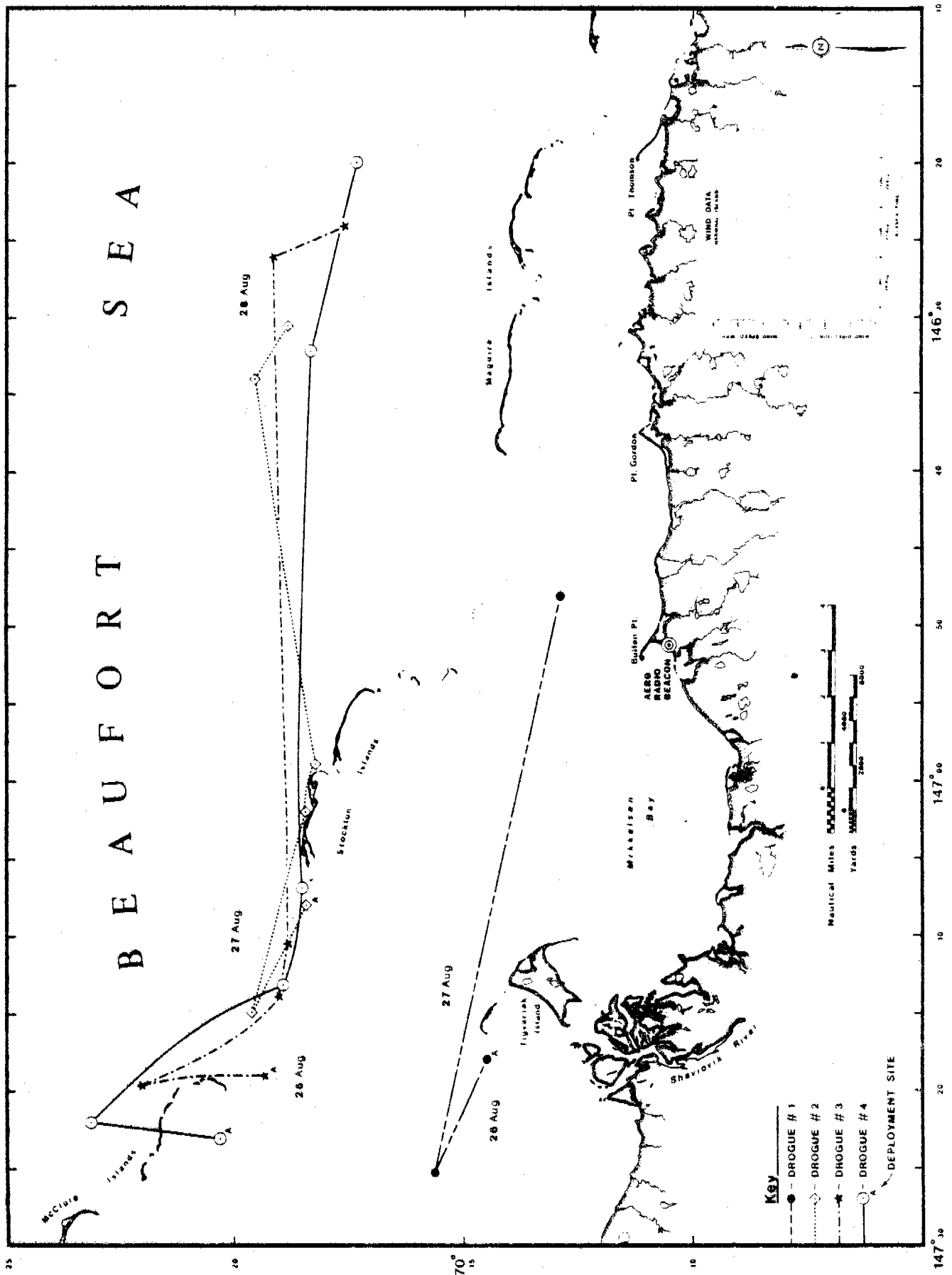


Figure 12. Drogue Tracking Experiment No. 2: Stockton Island Area. (26-28 August 1979)

Table 5.

Experiment No. 2. True Bearings (Uncorrected) from Tigvariak Island

Date	AK Start Time	AK End Time	Buoy Frequency in Khz				
			4125.6	4144.8	4162.2	4187.6	4222.3
			Tigvariak Island (70°12.7'N, 147°16.0'W)				
26 Aug. 79	1525	1605+	321	332	014	340	331
27 Aug. 79	1130	1155+	069	338	058	016	020
27 Aug. 79	1650	1735+	087	338	061	036	047
28 Aug. 79	1035	1055+	no signal	342 346	064	069	069
28 Aug. 79	1630	1650+	"	346	072	078	080

Note: True bearing of buoy with frequency of 4144.8 Khz should be:
342° T from Tigvariak Island.

Table 6.
 Experiment No. 2. True Bearings (Uncorrected) from Foggy Island and Point Gordon

Date	AK Start Time	AK End Time	Buoy Frequency in Khz				
			4125.6	4144.8	1462.2	4187.6	4222.3
			Foggy Island (70°16.9'N, 147°47.0'W)				
26 Aug. 79	1645	1710+	099	054	075	060	057
27 Aug. 79	1245	1310+	095	052	081	076	077
27 Aug. 79	1828	1907+	091	045	075	071	073
			Point Gordon (70°11.1'N, 146°37.0'W)				
28 Aug. 79	1140	1155+	no signal	305	008	026	014
28 Aug. 79	1730	1745+	"	306	018	036	045

NOTE: True bearing of buoy with frequency of 4144.8 Khz should be:
 055°T from Foggy Island
 304°T from Point Gordon

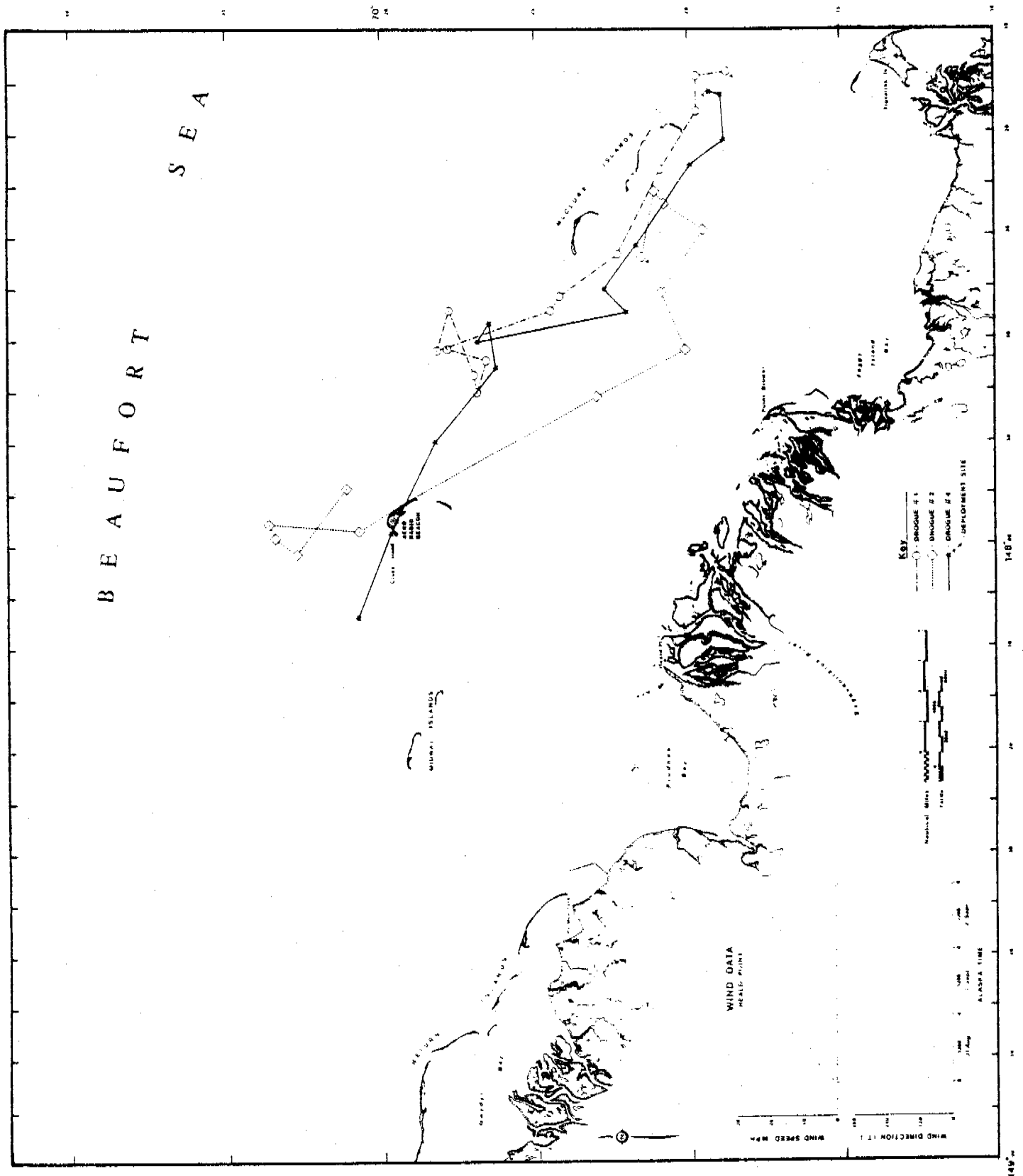


Figure 13. Drogue Tracking Experiment No. 3: Stefansson Sound Area. Drogues 1, 2, and 4. (30 August-2 September 1979)

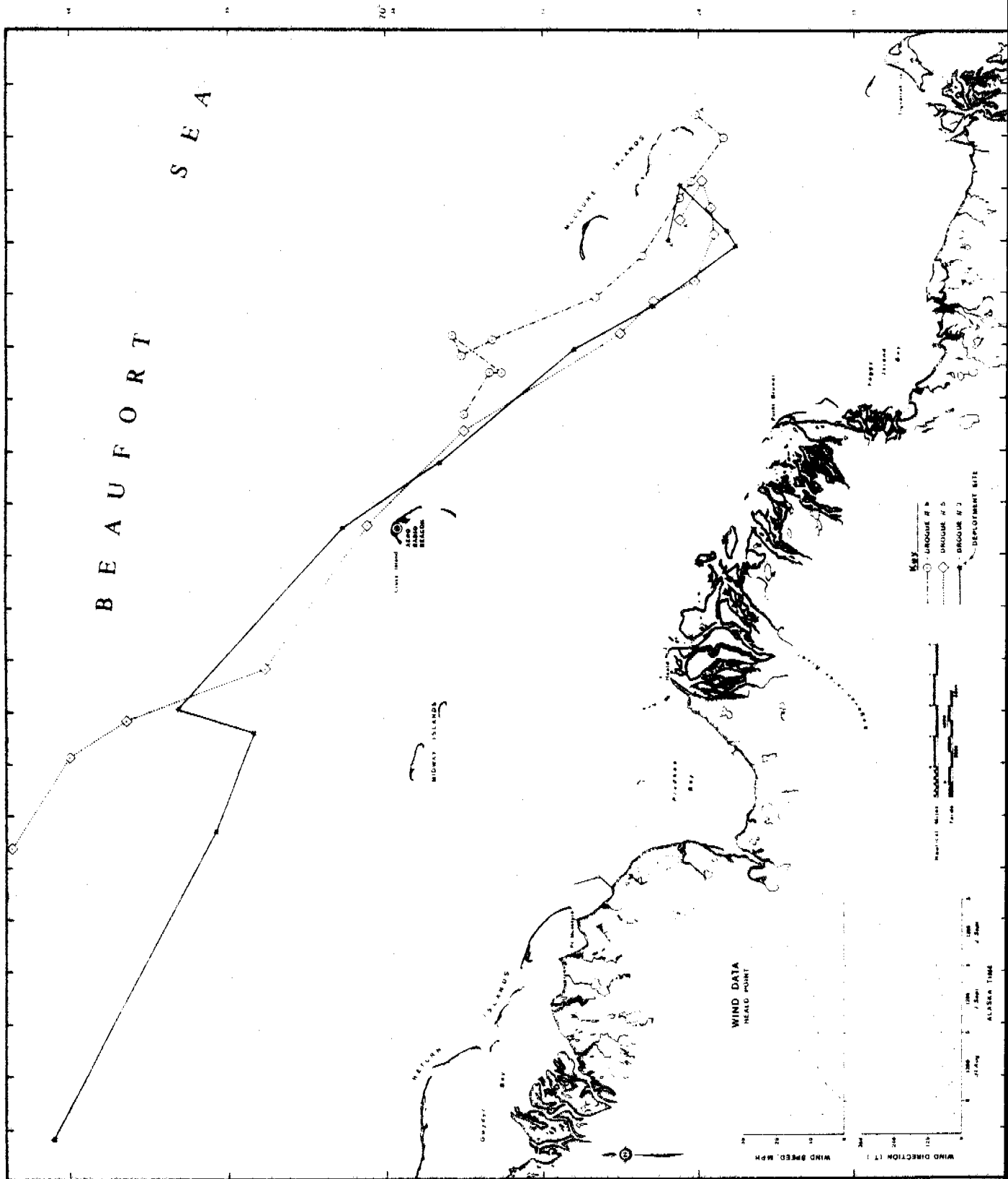


Figure 14. Drogue Tracking Experiment No. 3: Stefansson Sound Area Drogues 3, 5, and 6. (30 August-2 September 1979)

Table 7.

Experiment No. 3. True Bearings (Uncorrected) from Foggy Island Bay and Heald Point

Date	AK Start Time	AK End Time	4118.3	4137.6	4144.8	4183.2	4246.6	4274.1	4295.6
Foggy Island Bay (70°12.2'N, 147°41.0'W)									
30 Aug.79	1820	1940	047	027	026	030	048	033	042
31 Aug.79	0004	0121	043	026	026	027	043	030	032
31 Aug.79	0628	0720+	030	024	025	024	034	024	027
31 Aug.79	1209	1248	016	011	026	014	018	015	017
31 Aug.79	1755	1848	008	000	026	009	010	010	009
Heald Point (70°20.8'N, 148°12.3'W)									
1 Sept.79	0010	0120+	002	348	025	357	359	000	358
1 Sept.79	0620	0722	356	339	025	344	357	347	356
1 Sept.79	1230	1336	053	016	083	023	061	025	055
1 Sept.79	1800	1912	052	014	080	352	056	357	056
2 Sept.79	0010	0015+	051	013	080	348	040	351	054
2 Sept.79	0600	0718	056	026	081	338	023	349	048
2 Sept.79	1200	1256	053	no signal	082	321	007	343	021

Note: True bearings of buoy with frequency of 4144.8 Khz should be:
 029°T from Foggy Island Bay
 085° from Heald Point

Table 8.

Experiment No. 3. True Bearings (Uncorrected) from Bullen Point

Date	AK Start Time	AK End Time	4118.3	4137.6	4144.8	4183.2	4246.6	4274.1	4295.6
			Bullen Point (70°11.3'N, 146°51.0'W)						
30 Aug. 79	1800	1850+	306	300	303	299	301	297	298
31 Aug. 79	0000	0100+	305	301	306	294	299	297	301
31 Aug. 79	0600	0700+	305	296	307	293	302	296	302
31 Aug. 79	1200	1300+	302	296	306	267	301	295	301
31 Aug. 79	1800	1900+	306	293	308	299	303	299	304
1 Sept. 79	0000	0100+	303	295	305	300	196	297	306
1 Sept. 79	0600	0700+	303	299	300	298	301	298	302
1 Sept. 79	1200	1320+	303	303	303	301	303	300	305
1 Sept. 79	1800	1910+	301	303	303	301	300	299	300
2 Sept. 79	0005	0110+	301	303	303	299	301	304	302
2 Sept. 79	0600	0710+	302	303	304	297	299	304	301
2 Sept. 79	1200	1310+	305	no signal	303	296	298	304	no signal

NOTE: True bearings of buoy with frequency of 4144.8 Khz should be:
313°T from Bullen Point

In spite of the difficulties (Bullen Point was manned by one person, Steve Pace, in circumstances made difficult by high winds), the experiment went well, with little scatter in the reference angles from Foggy Island Bay and Heald Point. The explanation for the consistently smaller reference angles at Bullen Point is not known.

Conclusions

A tabulated analysis of the drogue trajectory results is shown in Table 9. Although the resulting speed data is somewhat fragmented due to the experimental field difficulties, the median speeds fall predominately in the range of 0.10 to 0.25 m/sec with an extreme to 0.86m/sec. Based upon the corresponding winds measured on shore, comparable speed values computed by the model reported in the first section of this report fall closer to the low end of this median range. Offshore wind data were not available, but these winds could have been somewhat higher than those measured on land. Directional data of the drogues were about as expected given the transient nature of the wind directions recorded during the tracking experiments.

Table 9. Analysis of Beaufort Sea Drogue Trajectories, 1979.

Time	Mean Wind		Mean Drogue Movement		Number of Drogues
	Speed, m/sec	Direction T	Speed, m/sec	Direction T	
0200 Aug.19- 0400 Aug.19	3.6	60	0.15	W	3
0600 Aug.19- 0800 Aug.19	4.4	75	0.10	W	2
2200 Aug.19- 0200 Aug.20	4.1	108	0.13	NW	2
2200 Aug.20- 0200 Aug.21	7.3	245	0.86	E	2
1400 Aug.21- 1800 Aug.21	9.0	270	0.15	SE	2
1600 Aug.26- 1200 Aug.27	6.2*	110*	0.57	SE	3
1200 Aug.27- 1800 Aug.27	8.6*	250*	0.13	ESE	3
1800 Aug.27- 1100 Aug.28	9.4*	280*	0.40	E	3
1100 Aug.28- 1700 Aug.28	7.5*	265*	0.21	SE	3
1800 Aug.30- 0000 Aug.31	1.8	65	0.07	NW	6
0000 Aug.31- 0600 Aug.31	1.5	64	0.11	NW	6
0600 Aug.31- 1200 Aug.31	3.1	74	0.23	NW	6
1200 Aug.31- 1800 Aug.31	4.9	53	0.15	NW	6
1800 Aug.31- 0000 Sept.1	4.9	55	0.22	NW	6

* Source: Tom Kozo, University of Washington

PRUDHOE BAY DIFFUSIVITY MEASUREMENTS, 1979

Introduction

A precision small scale drifter tracking experiment was conducted in Prudhoe Bay (see Figure 15) during the summer open water season on 25 August 1979. The objective of the experiment was to determine values for the eddy diffusion coefficients as needed for realistic diffusion modeling. Due to weather and logistic constraints, only half a day was available for actual tracking. Although this did not reduce the validity of the results, since after a certain period of time inhomogeneity sets in, it meant that the experiment was not repeated.

Experimental Procedure

Nine drifters were constructed using 20-square ft sails, weighted at the bottom. Weights were adjusted so that a minimum of float area was presented to the wind. Identification flags were used in order that the position of each drifter could be determined uniquely. A Motorola Miniranger radar frequency range-range system was used, with transponders being placed as high as possible on the operations building on the end of the ARCO West Dock ($70^{\circ}24'1.2''N$, $148^{\circ}31'3.6''W$), and on a tower on Heald Point ($70^{\circ}20'51.6''N$, $148^{\circ}12'1.2''W$). Height and aiming problems resulted in a maximum effective range of about 12,000 meters.

The drifters were deployed initially at 1630 hours, 25 August 1979 in 18 feet of water in the approximate form of a cross. The initial separation between drifters was of the order of 40 meters. The initial centroid location was at $70^{\circ}25'34.2''N$, $148^{\circ}14'37.2''W$. The drifters were visited at hourly intervals, with ranges being obtained from the Miniranger as the boat passed by each drifter at low speed. The experiment continued for some five hours, after which time the drifters had moved sufficiently far to the west so that the Heald Point transponder no longer provided a range reading.

Winds

Winds at Cottle Island (as provided by Tom Kozo of the Polar Science Center, University of Washington), as shown in Table 10, were primarily from the south-east and south-south-east over the measurement period. The average velocity was 11.5 mph from 150° . Prior to the measurement the wind had been blowing from the north-west for some nine hours.

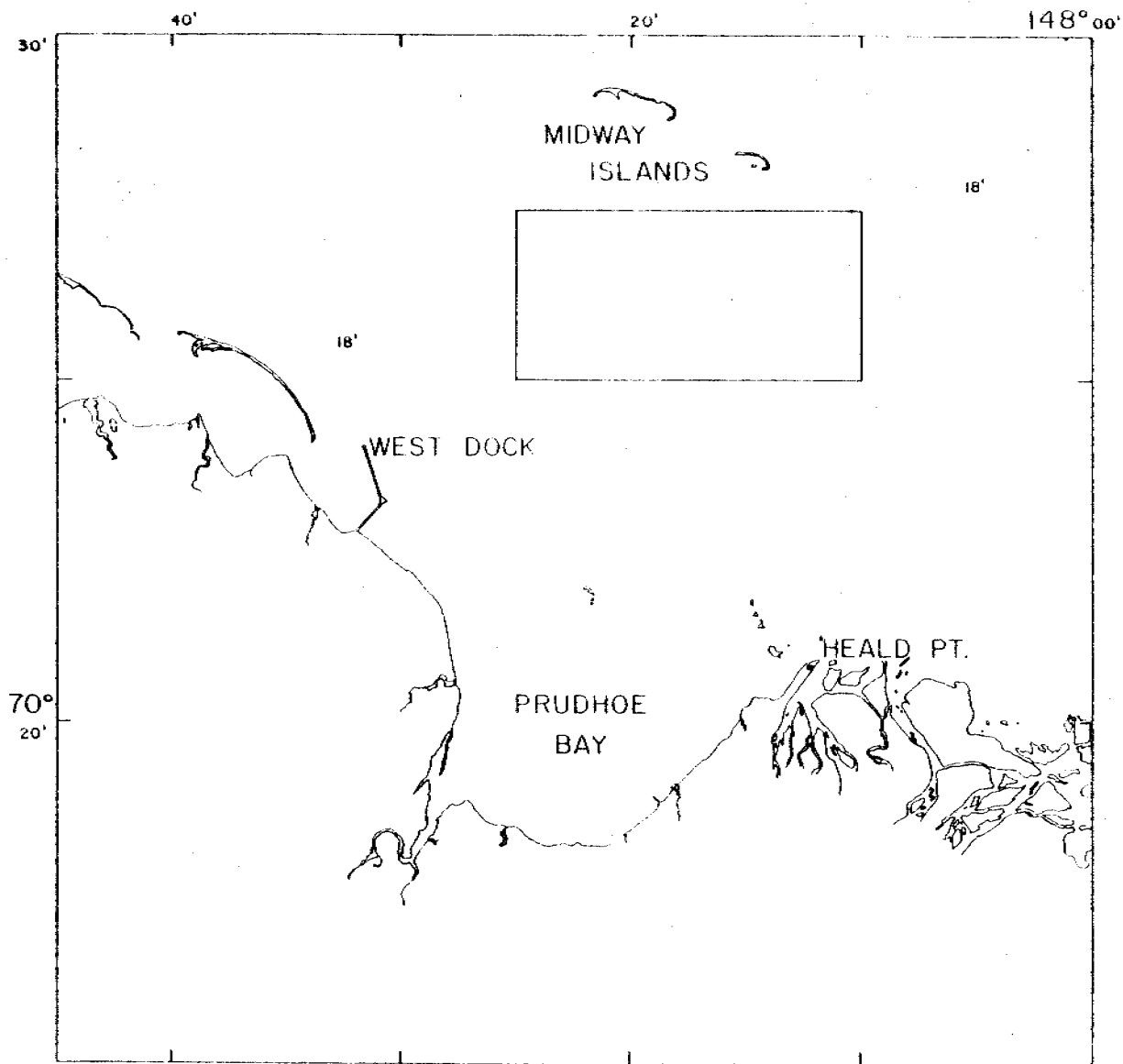


Figure 15 Prudhoe Bay diffusivity measurement location map.

Table 10. Cottle Island Winds.

	Hour Alaska Time	Direction (From) Degrees True	Speed Miles Per Hour
25 Aug. 1979	0000	130	14.5
	0300	130	18.0
	0600	130	20.5
	0900	280	11.5
	1200	300	16.5
	1500	340	3.0
	1800	130	9.5
	2100	160	12.5
26 Aug. 1979	0000	190	8.0
	0300	200	8.5
	0600	120	7.5

Analysis

The data were analyzed following the methods of Okubo et al. (1) and Ichniye et al. (2). The range-range position data were converted first to latitude and longitude (using spherical trigonometry) and then to localized cartesian coordinates. Variances σ_x^2 , σ_y^2 and covariances σ_{xy} were then computed. From these values major and minor ellipse semi-axes lengths σ_x^2 and σ_y^2 , were computed by rotation such that σ_{xy} vanished.

It was found that two drifters, 4 and 9, appeared to move somewhat anomalously. Calculations were therefore made with all nine drifters and with drifters 4 and 9 excluded. Figures 16 and 17 show the general movements of the centroids, along with the computed ellipses. Figures 18 and 19 show similar ellipse formation on a larger scale, and also show the individual drifter locations. It is at once apparent that the dispersion tends to be greatest approximately in the direction of the current.

The computed data are summarized in Tables 11 through 14. In addition to separate computations being made for the entire group and for the entire group less drifters 4 and 9, computations were repeated using all five times, and then with the first time excluded. The tables show the data used in drawing Figures 20 and 21. The major and minor ellipse axes are a and b , respectively. The methods developed by Okubo and others involve the computation of diffusivities based on the set $a^2/4$ yielding the eddy diffusivity K_x , $b^2/4$ yielding K_y , and $ab/4$ yielding the mean eddy diffusivity \bar{K} .

The resulting eddy diffusivities are shown below in units of 10^4 cm²/sec.

	<u>5 groups</u>		<u>last 4 groups</u>	
	<u>all drifters</u>	<u>less 4 & 9</u>	<u>all drifters</u>	<u>less 4 & 9</u>
K_x	1.99	1.550	2.31	1.890
K_y	0.74	0.078	0.84	0.053
\bar{K}	1.22	0.400	1.40	0.440

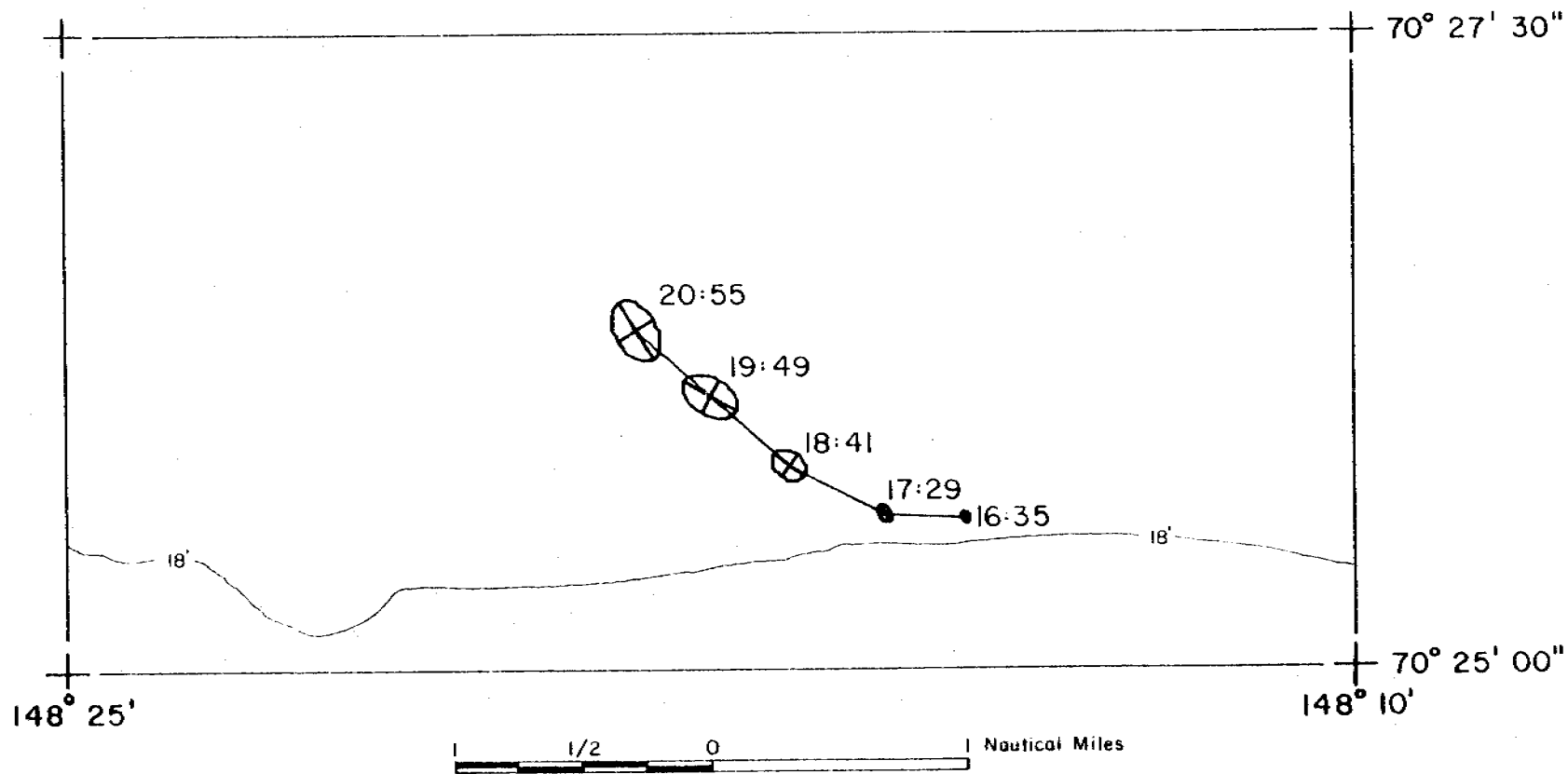


Figure 16. Ellipses and mean times (25 August 1979) of drifters 1 - 9. Boundary corresponds with that shown in Figure 15.

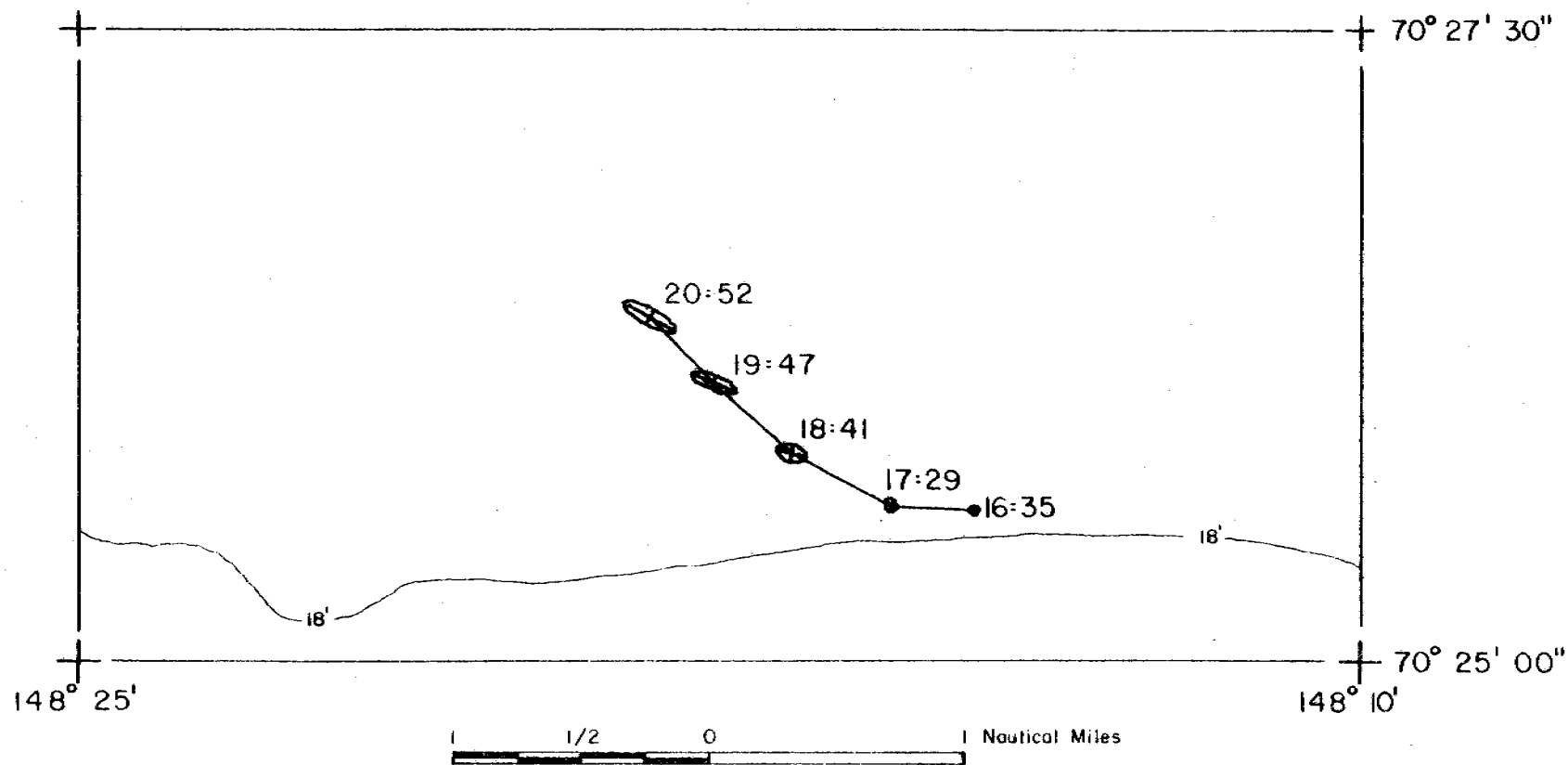


Figure 17. Ellipses and mean times (25 August 1979) of drifters with 4 and 9 excluded. Boundary corresponds with that shown in figure 15.

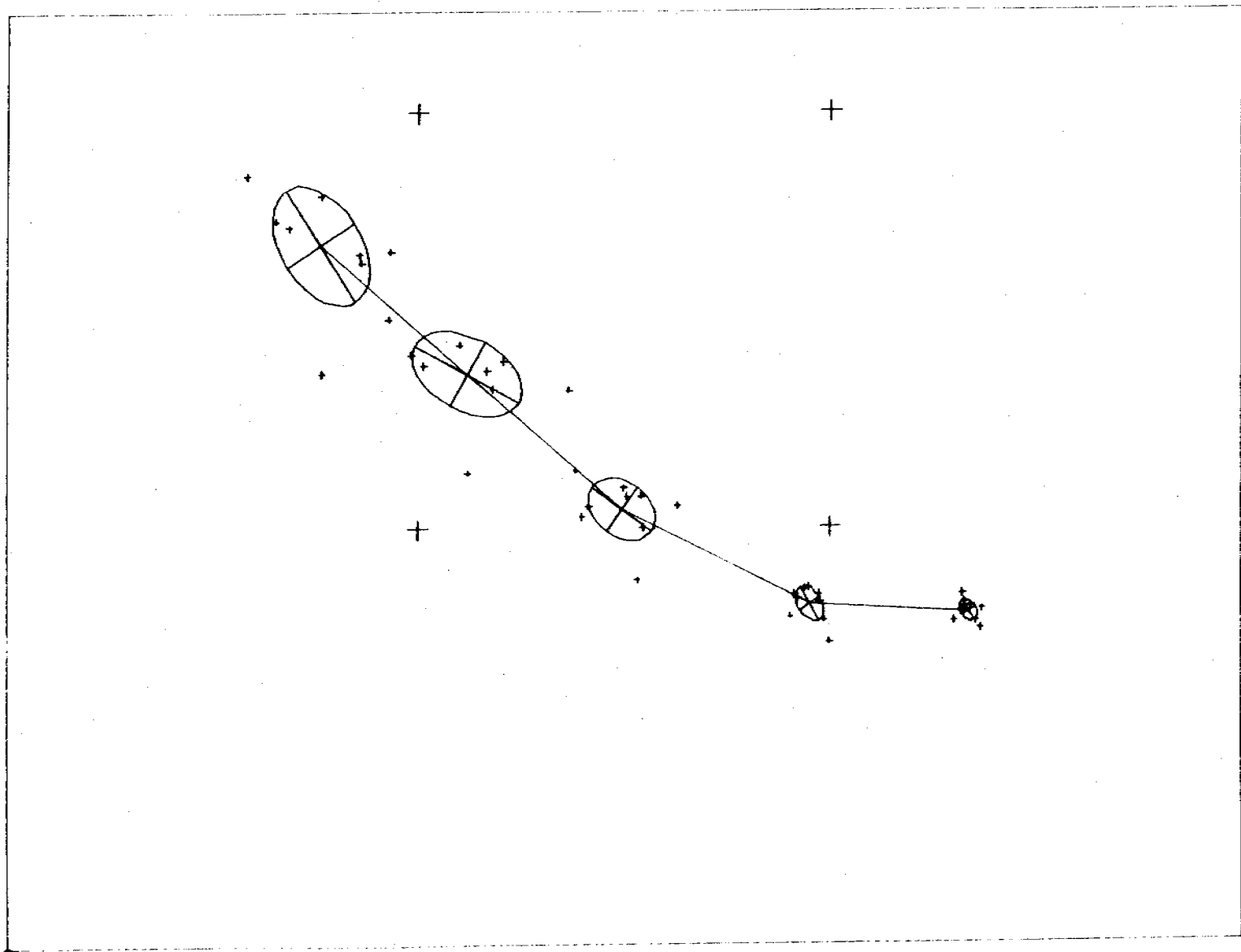


Figure 18. Enlarged drifter location map (all drifters); 5000 ft between large crosses.

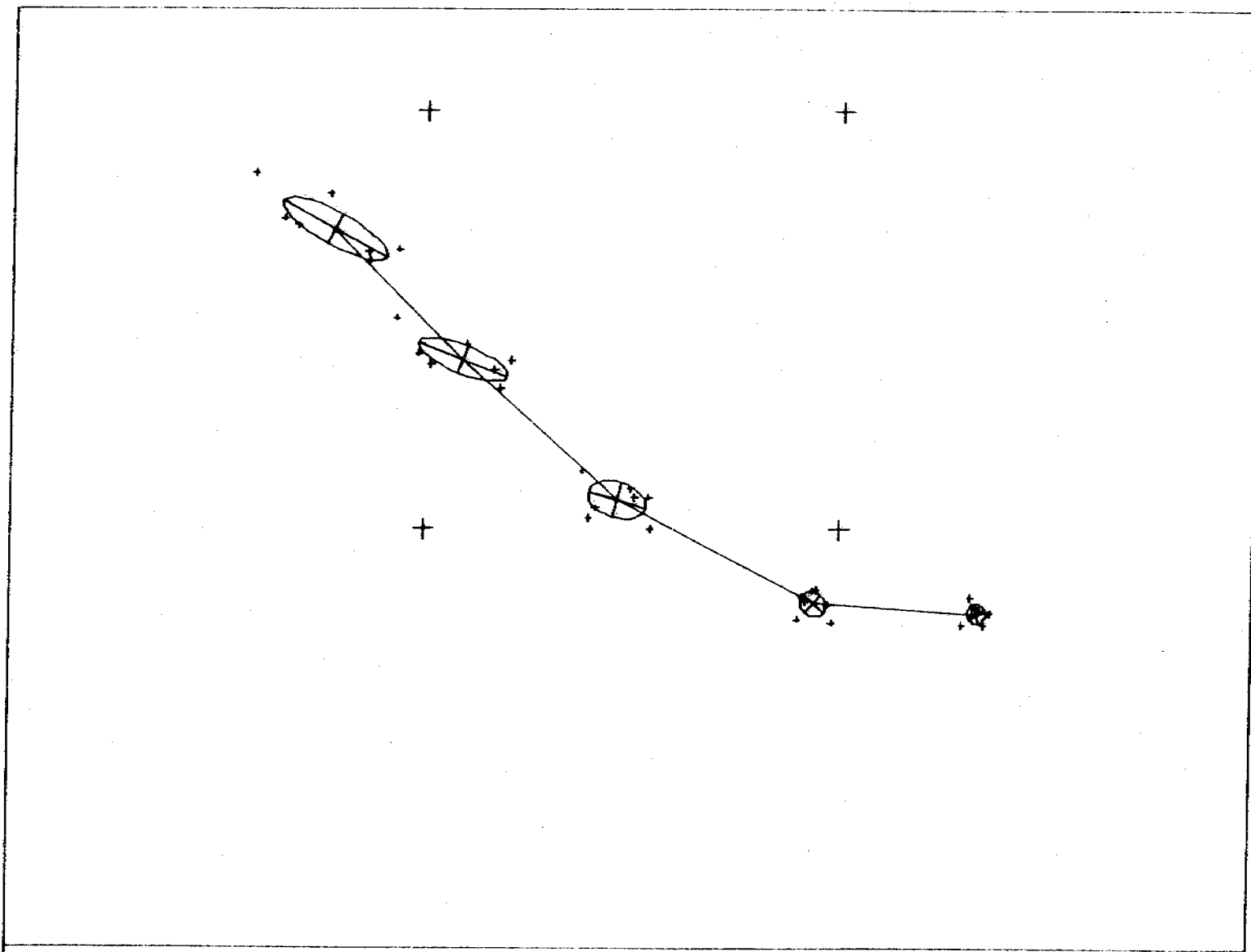


Figure 19. Enlarged drifter location map (with drifters 4 and 9 excluded):
5000 ft between large crosses.

Table 11.

Mean times - all drogues
5 groups

Time hours	Major Axis a m	Minor Axis b m	$a^2/4$ m^2	$b^2/4$ m^2	$ab/4$ m^2
0.0	84.0	59.9	1764	897	1258
0.9074	144.2	84.2	5198	1772	3035
2.0963	274.3	197.8	18810	9781	13564
3.2297	437.3	266.3	47808	17729	29113
4.3297	484.5	297.5	58685	22127	36035

x in seconds

$$a^2/4 = -3841 + 3.98314x$$

$$b^2/4 = -850 + 1.48711x$$

$$ab/4 = -1916 + 2.43465x$$

$$\text{slopes: } \frac{1}{2} \frac{d}{dt} (\sigma_x^2) = 1.99 \times 10^4 \text{ cm}^2/\text{sec}$$

$$\frac{1}{2} \frac{d}{dt} (\sigma_y^2) = 0.74 \times 10^4 \text{ cm}^2/\text{sec}$$

$$\frac{1}{2} \frac{d}{dt} (\sigma_x \sigma_y) = 1.22 \times 10^4 \text{ cm}^2/\text{sec}$$

Table 12.

Mean times - less drogues 4 & 9
5 groups

Time hours	Major Axis a m	Minor Axis b m	$a^2/4$ m^2	$b^2/4$ m^2	$ab/4$ m^2
0.0	73.1	66.2	1336	1096	1210
0.9143	102.3	85.8	2616	1840	2194
2.1143	222.9	129.0	12421	4160	7189
3.2119	349.3	106.2	30503	2820	9274
4.2952	436.6	121.4	47655	3684	13251

x in seconds

$$a^2/4 = 4545 + 3.09176x$$

$$b^2/4 = 1529 + 0.15692x$$

$$ab/4 = 566 + 0.79863x$$

$$\text{slopes: } \frac{d}{dt}(\sigma_x^2) = 1.55 \times 10^4 \text{ cm}^2/\text{sec}$$

$$\frac{d}{dt}(\sigma_y^2) = 0.078 \times 10^4 \text{ cm}^2/\text{sec}$$

$$\frac{d}{dt}(\sigma_x\sigma_y) = 0.40 \times 10^4 \text{ cm}^2/\text{sec}$$

Table 13.

Mean times - all drogues
last 4 groups

Time hours	Major Axis a m	Minor Axis b m	$a^2/4$ m^2	$b^2/4$ m^2	$ab/4$ m^2
0.0	95.5	76.5	2280	1463	1826
0.9074	164.5	56.9	6765	809	2340
2.0963	361.5	177.8	32671	7904	16069
3.2296	398.8	239.5	39760	14340	23878
4.3083	426.1	302.5	45390	22877	32224

x in seconds

$$a^2/4 = -11255 + 4.61559x$$

$$b^2/4 = -3159 + 1.68410x$$

$$ab/4 = -6114 + 2.79275x$$

$$\text{slopes: } \frac{1}{2} \frac{d}{dt} (\sigma x^2) = 2.31 \times 10^4 \text{ cm}^2/\text{sec}$$

$$\frac{1}{2} \frac{d}{dt} (\sigma y^2) = 0.84 \times 10^4 \text{ cm}^2/\text{sec}$$

$$\frac{1}{2} \frac{d}{dt} (\sigma x \sigma y) = 1.40 \times 10^4 \text{ cm}^2/\text{sec}$$

Table 14.

Mean times - less drogues 4 & 9
Last 4 groups

Time hours	Major Axis a m	Minor Axis b m	a ² /4 m ²	b ² /4 m ²	ab/4 m ²
0.0	76.7	64.7	1471	1047	1241
0.9143	111.2	80.6	3091	1624	2241
2.1143	242.1	120.8	14653	3648	7311
3.2119	380.6	99.5	36214	2475	9467
4.2952	475.2	115.5	56454	3335	13252

x in seconds

$$a^2/4 = -12471 + 3.77261x$$

$$b^2/4 = 2114 + 0.10670x$$

$$ab/4 = -303 + 0.87325x$$

$$\text{slopes: } \frac{1}{2} \frac{d}{dt} (\sigma x^2) = 1.89 \times 10^4 \text{ cm}^2/\text{sec}$$

$$\frac{1}{2} \frac{d}{dt} (\sigma y^2) = 0.053 \times 10^4 \text{ cm}^2/\text{sec}$$

$$\frac{1}{2} \frac{d}{dt} (\sigma x \sigma y) = 0.44 \times 10^4 \text{ cm}^2/\text{sec}$$

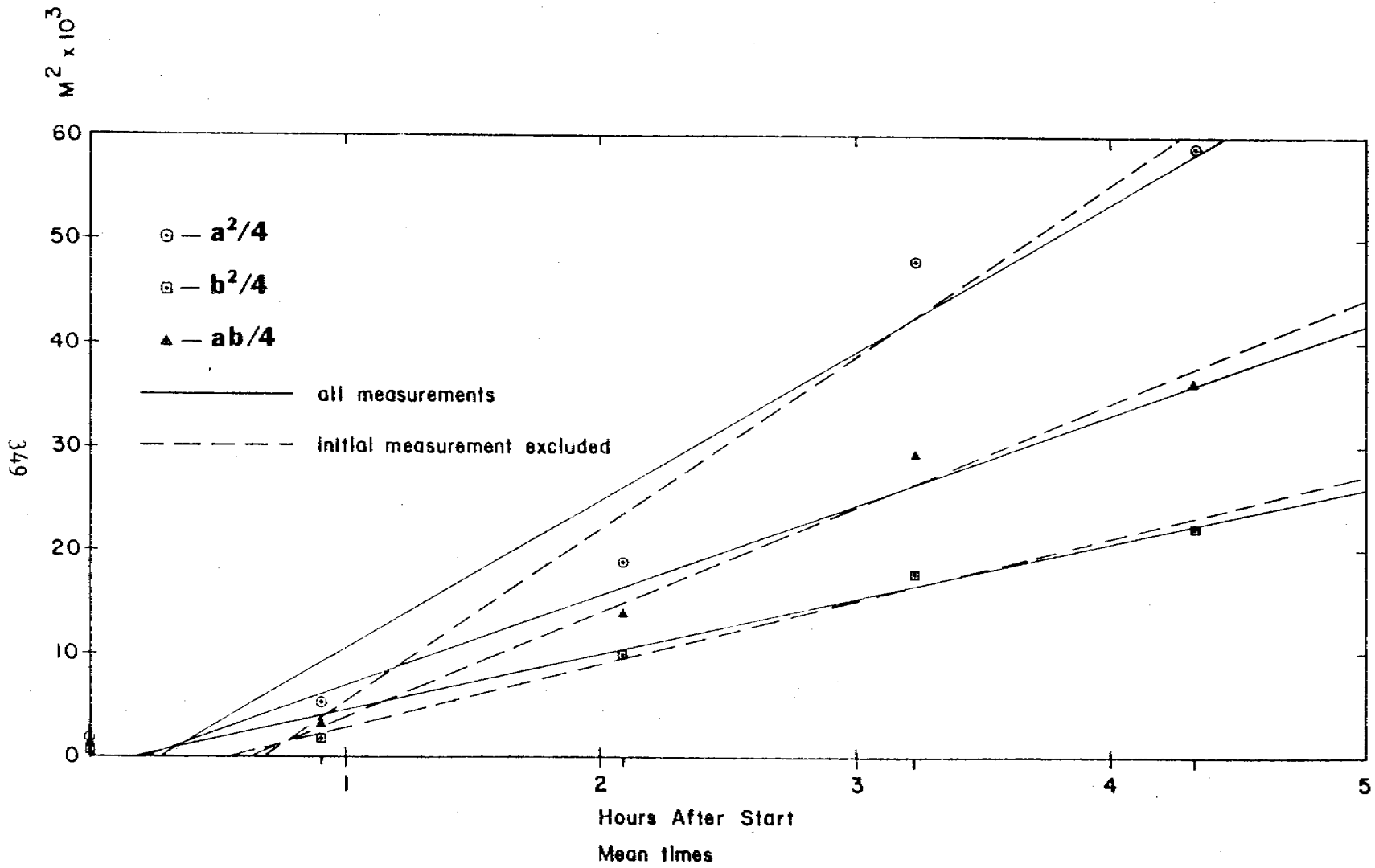


Figure 20. Variances computed using all drifters.

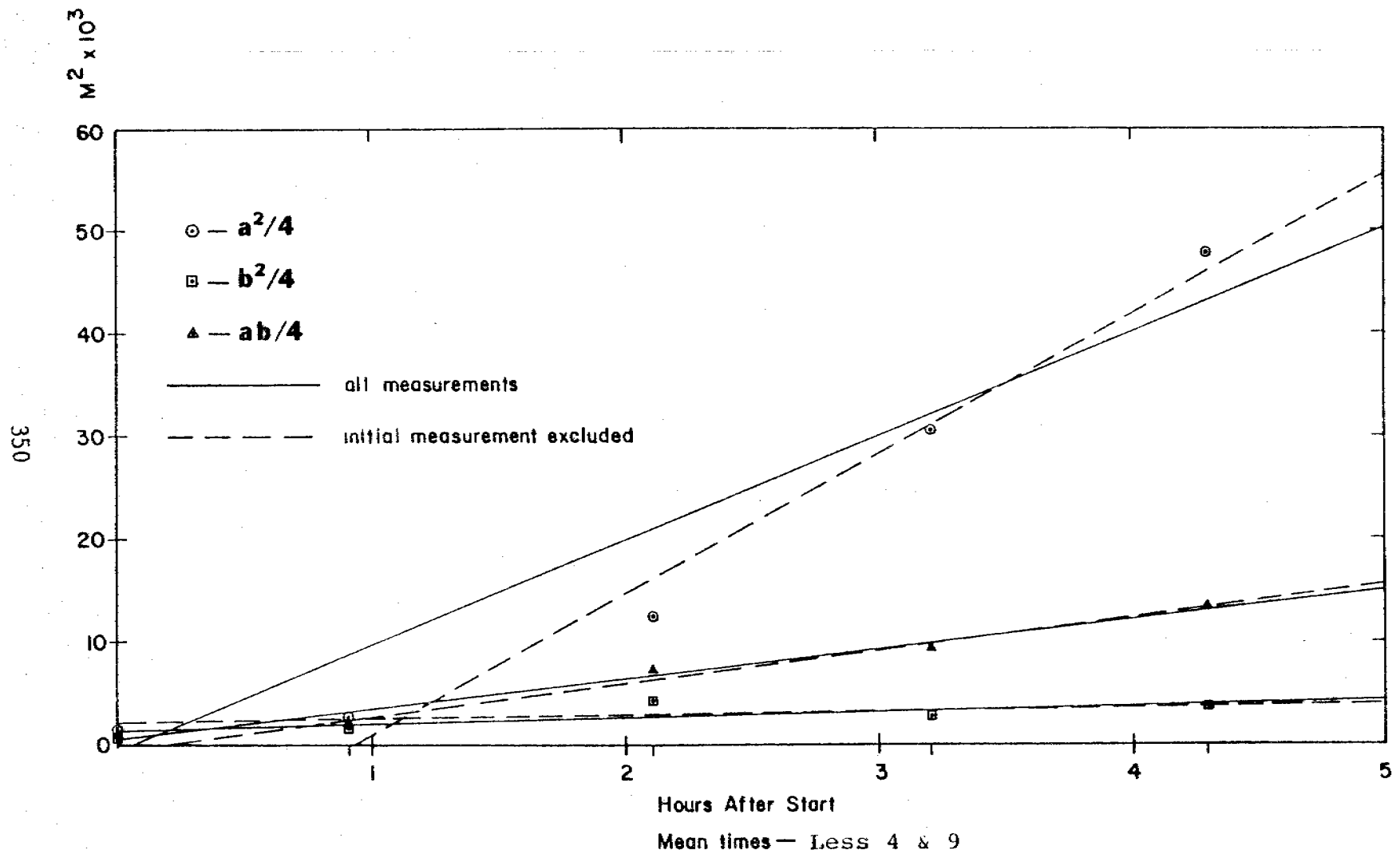


Figure 21. Variances computed using all drifters less 4 and 9.

Conclusions

In general, the order of magnitude of the computed eddy diffusivity is 10^4 cm²/sec, with numbers ranging from 0.05×10^4 cm²/sec to 2.31×10^4 cm²/sec. Although these may seem small when compared to oceanic values, the values are consistent with the length scales (separation between drifters) involved. The four-thirds power law of Ichiye and Olsen [see Hill (3), p. 819] is:

$$F(\ell) = 0.02461 \ell^{4/3},$$

where ℓ is the neighbor separation in centimeters, and $F(\ell)$ is the diffusivity in centimeters squared per second. On substituting typical separation limits, 50×10^2 cm and 500×10^2 cm, one obtains respectively 0.2×10^4 cm²/sec and 4.5×10^4 cm²/sec -- values consistent with measured values.

If one selects the calculations made with drifters 4 and 9 excluded, the eddy diffusivities based on the five groups are: approximately 1.55×10^4 cm²/sec for the major axis; 0.078×10^4 cm²/sec for the minor axis; and 0.40×10^4 cm²/sec for the overall eddy diffusivity. The values for the two axes are consistent with a major axis to minor axis length ratio of 4.5, as can be seen in Figure 21. The major axis lies approximately along the trajectory formed, with the direction and eccentricity being related to current shear.

In the absence of additional experimental evidence, it is suggested that use be made of the pronounced diffusion tendency discussed above. In particular in trajectory simulations, a Monte Carlo technique might be used in which a quasi-random offset is computed for each particle. The probabilities would be based on two distributions, one related to $K_x = 1.55 \times 10^4$ cm²/sec in the general current direction, and $K_y = 0.078 \times 10^4$ cm²/sec perpendicular to the current direction.

1. Okubo, A., C.C. Effesmeyer, J.M. Helseth (1976).
Determination of Lagrangian Deformations from Analysis
of Current Followers. J. Phys. Oceanog. 6:524-527.
2. Ichiye, T., C. Mungall, M. Inoue, D. Horne (1978).
Gulf of Mexico Dispersion Calculations. Texas A & M
University, Department of Oceanography, Report 78-10-T.
3. Hill, M.N., ed. (1963). The Sea, Volume 1: Physical
Oceanography. Interscience Publishers, New York.

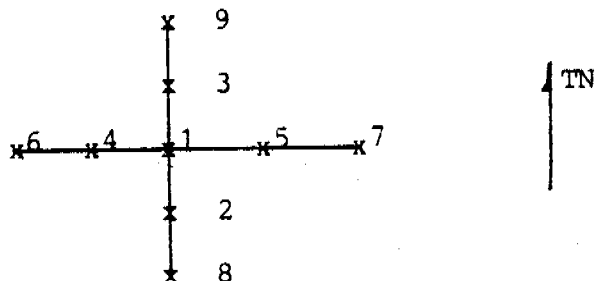
HARRISON BAY DIFFUSIVITY EXPERIMENTS, 1980

Introduction

Following diffusivity measurements made during the open water season of 1979 in Prudhoe Bay, a similar experiment was performed in Harrison Bay in 1980. The same windowshade-type drogue sails were used in both years, and identical data reductions have been used.

Experimental Procedure

Nine windowshade-type drogues were released in Harrison Bay on the morning of 20 August 1980. The initial position ($70^{\circ}33'3''N$, $150^{\circ}44'0''W$) was some five miles north of the northernmost part of the Colville River delta (Figure 22). The water depth was some 20 feet. Weather conditions were sunny and mostly calm. The drogues (identical to those usually tracked by a radio direction finding set in previous years) were deployed in the form of a cross as follows:



Precision tracking was achieved through the use of a Motorola Miniranger microwave range-range system with transponders located at Tolakturat, Oliktok, and Atigane. Reception was not good and considerable time was lost in trying to capture signals. Positions were measured five times over a four-hour period.

Winds

Winds at Tolaktovuk Point (provided by Tom Kozo of Tetra Tech. Inc.) as shown in Table 15, were primarily from the SSW-SW over the measurement period. The average velocity was 6.7 miles per hour. One day prior to the experiment the wind direction changed from the northwest to the southwest.

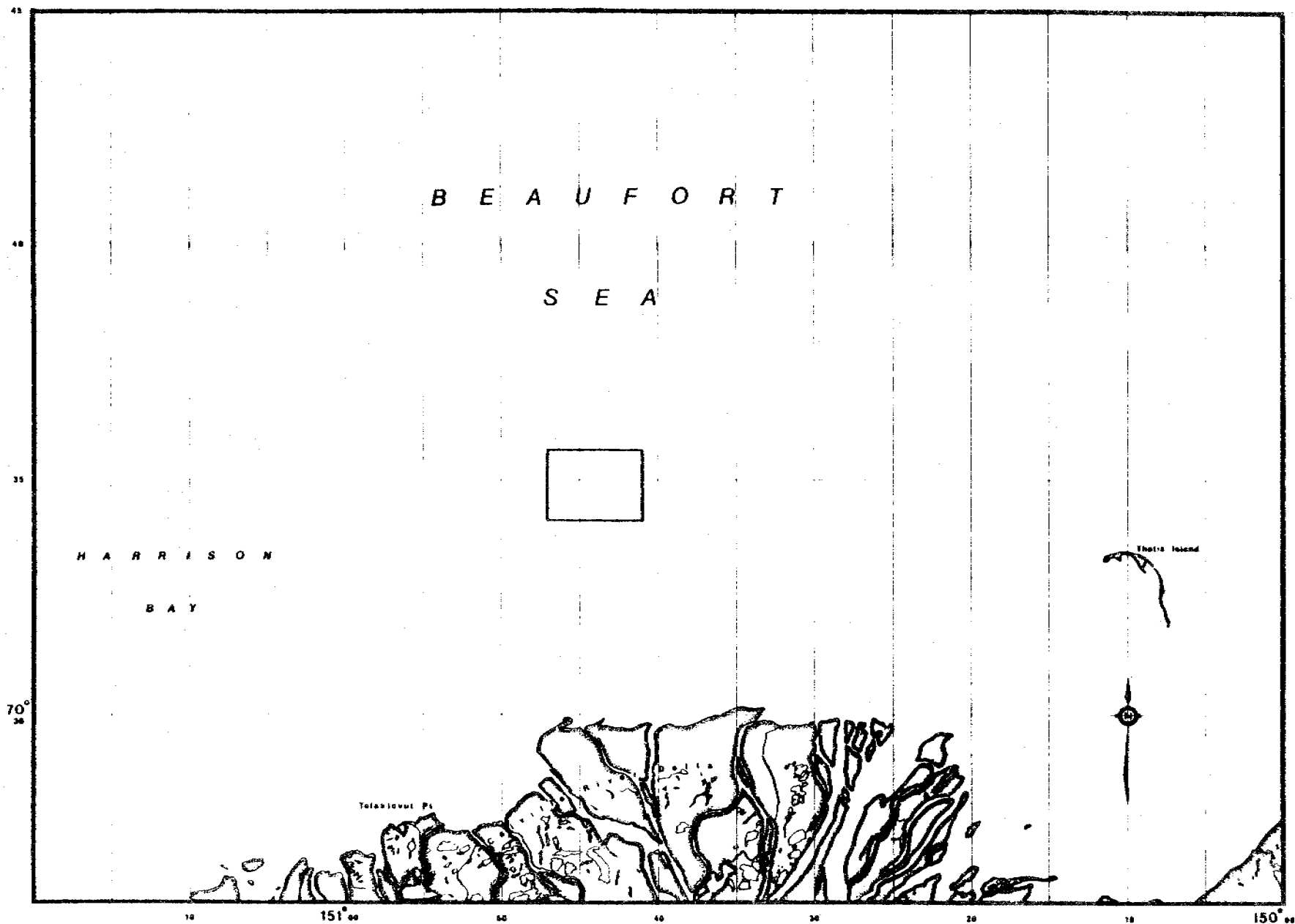


Figure 22. Harrison Bay Diffusivity Measurement Location Map

Table 15 . Tolaktovut Point Winds

	Hour Alaska Time	Direction (From) Degrees True	Speed Miles per Hour
20 August 1980	0000	344	5.0
	0300	40	12.8
	0600	105	14.4
	0900	139	16.0
	1200	205	17.6
	1500	228	14.4
	1800	205	16.0
	2100	236	20.8

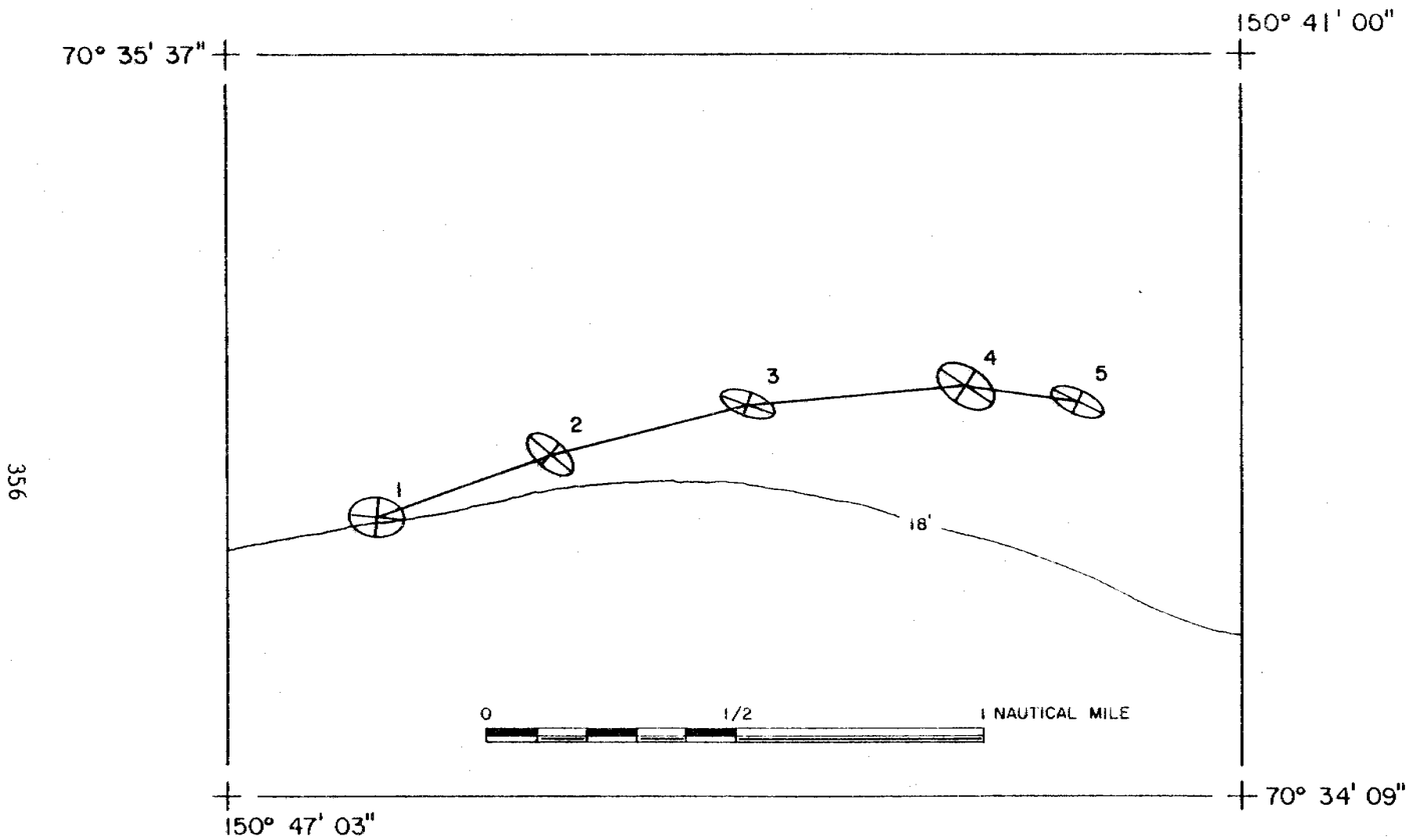


Figure 23. Raw Ellipses of Drifters 1 - 9 (20 August 1980)
Boundary corresponds with that shown in Figure 22.

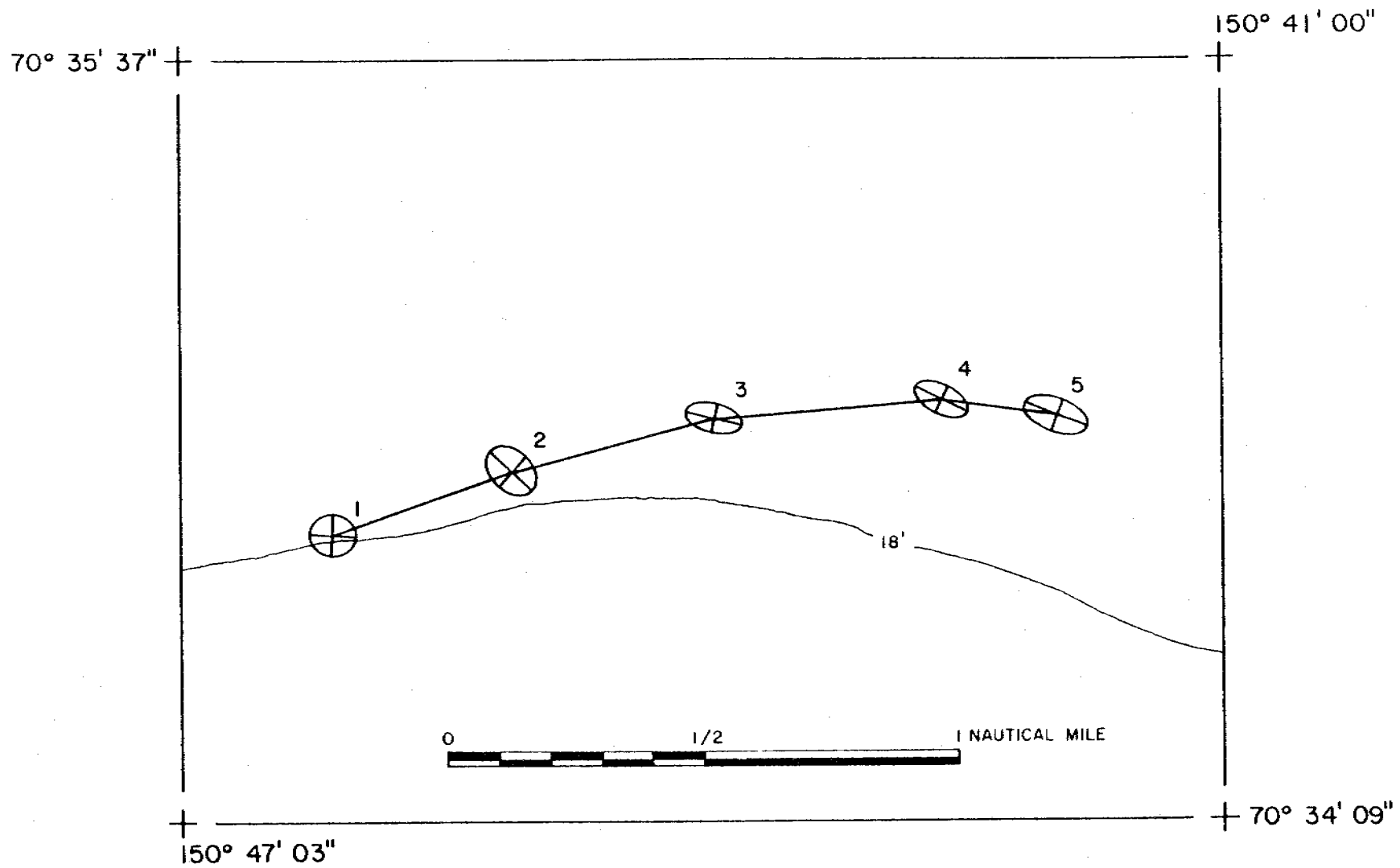


Figure 24. Interpolated Ellipses of Drifters 1 - 9
(20 August 1980)
Boundary corresponds with that shown in Figure 22.

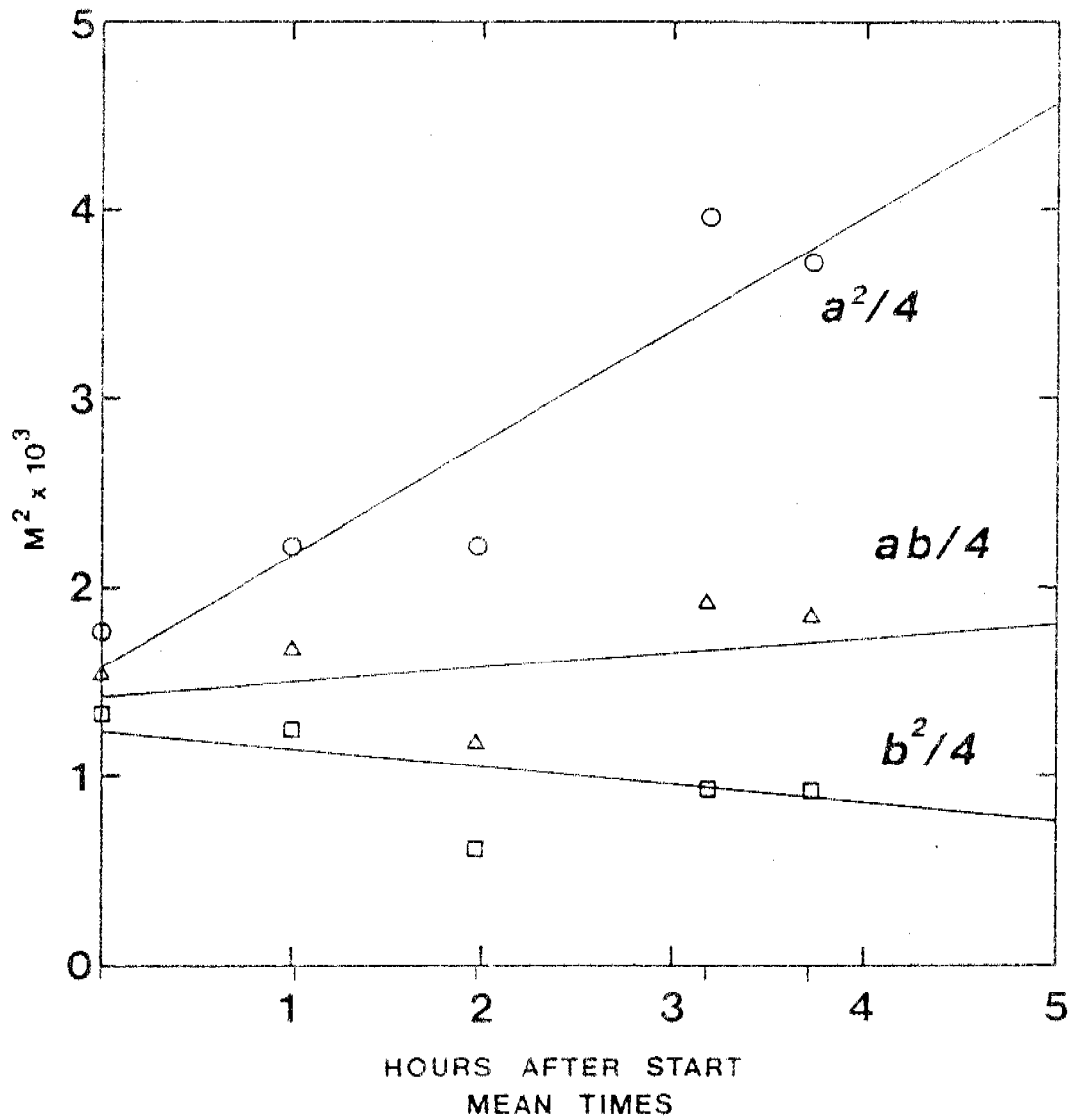


Figure 25. Variances Computed Using All Drifters

Table 16. Mean Times - All Drogues

Time (hours)	Major Axis, a (meters)	Minor Axis, b (meters)	a ² /4 (m ²)	b ² /4 (m ²)	ab/4 (m ²)	Wind Speed (m/s)	Wind Direction, from (°T)	Depths, Total (ft)
0.0	83.9	72.9	1760	1329	1529	3.5	200	20-22
1.0074	94.3	70.8	2223	1253	1669	3.0	224	20-23
1.9797	94.3	49.5	2223	613	1167	2.0	217	21-24.5
3.1796	125.7	60.7	3950	921	1907	3.0	217	24-25.5
3.7222	121.8	60.3	3709	909	1836	-	-	24-25

Correlation: 0.93 -0.65 0.48
Slope: 598 -123 91

$$a^2/4 = 1591 + 0.166t \quad (t \text{ in seconds})$$

$$b^2/4 = 1248 - 0.034t$$

$$ab/4 = 1441 + 0.025t$$

$$\text{Slopes: } 1/2 (d/dt) (\sigma_x^2) = 830 \text{ cm}^2/\text{sec}$$

$$1/2 (d/dt) (\sigma_y^2) = -170 \text{ cm}^2/\text{sec}$$

$$1/2 (d/dt) (\sigma_x \sigma_y) = 130 \text{ cm}^2/\text{sec}$$

NUMERICAL MODELING: MAPPING GRID FOR CHUKCHI SEA COAST

Introduction

Applying ordinary numerical techniques to model the nearshore flow in the Chukchi Sea as well as the circulation in general requires significant computer resources. This will always be the case when sharp gradients and large scale motions are portrayed on rectangular grids, as required by the complex shoreline of the Chukchi coast. Atmospheric modelers have struggled with this problem for decades. Apparently, they often choose nested grids. Others select finite elements or coordinate transformations (stretched grids) to reduce computer costs.

Methods

For the case of the Chukchi coast we chose the coordinate transformation approach primarily because it is very adaptable to any numerical model. Any finite difference model can utilize the transformed system by simply transforming the model equations. The solution technique need not be altered. Readers are referred to Reid, et al (1977) for details concerning transformation of the model equations. We will discuss the coordinate transformations only.

Briefly, the procedure consists of two steps. The first step consists of the actual conformal mapping and the second step produces the computing grid. The mapping is defined by establishing the coefficients that minimize the overall error between the given coordinates and those obtained from the following expansions:

$$X = A_0 + C_0 \xi - D_0 \psi + \sum_n (A_n \cosh(n\psi) - D_n \sinh(n\psi)) \cos(n\xi) \\ + \sum_n (B_n \sinh(n\psi) + C_n \cosh(n\psi)) \sin(n\xi),$$

$$Y = B_0 + C_0 \psi + D_0 \xi + \sum_n (B_n \cosh(n\psi) + C_n \sinh(n\psi)) \cos(n\xi) \\ + \sum_n (D_n \cosh(n\psi) - A_n \sinh(n\psi)) \sin(n\xi),$$

where X and Y are approximations to the given coordinates, and ξ , and ψ are the mapped coordinates.

The region to be transformed extended from Cape Prince of Wales to Point Barrow on the East and from East Cape to MysShimdta (177 W), then northward to the north side of Wrangel Island for the western boundary. The eastern and western boundaries were digitized (in inches) from nautical chart No. 16003. Because of the high latitudes involved, the digitized coordinates were subjected to an inverse mapping to account for the Mercator distortion.

One hundred and sixteen points were needed to define the eastern boundary, but only 62 points were required for the western boundary due to its simplicity. Both sets of points reflected some subjective smoothing of small scale features. However, subsequent attempts to conformally map the region (using the routine CONFORM which is available from the Waterways Experiment Station, Vicksburg, Miss.) suggested that the convergence rate would be enhanced with more points on the western boundary. The western points were linearly interpolated to give 123 total points. The convergence rate is critical since the numerical mapping routine is an iterative procedure and requires considerable computer time. The final run on 110 iterations (took about 6 min. of AMDAHL V6 time) gave an average variance of less than 5nmi. This indicates the fit is relatively good considering the complicated eastern boundary of the Chukchi seacoast.

Results

The resulting mapping constants required for the Chukchi Sea grid generation are given in Table 17.

Now that the constants and coefficients given in Table 17 have been obtained, a very inexpensive routine (the routine GRID, also available from the Waterways Experiment Station) can be employed to generate computing grids. Literally, if the computing grid generated is not appropriate or is lacking in any respect, the input to the mapping routine can be readily modified to produce another computing grid. It must be emphasized that the grid generation routine is inexpensive.

As an example, the computing grid shown in Figure 26 was produced (using less than one minute of AMDAHL V6 time) to illustrate the conformal mapping technique and its ability to provide variable resolution over an extensive area. Notice that sharp gradients can be resolved in the central portion of the Chukchi coastline while not carrying this resolution toward the west. This results in less computer requirements to model the Chukchi sea.

Table 17. Mapping Constants Required for Chukchi Sea Grid Generation.

Note: SCALAT, SCALON, DUMMY, SCAL, DFAC7, DUMMY

B B0
 Bn Cn
 etc. etc.

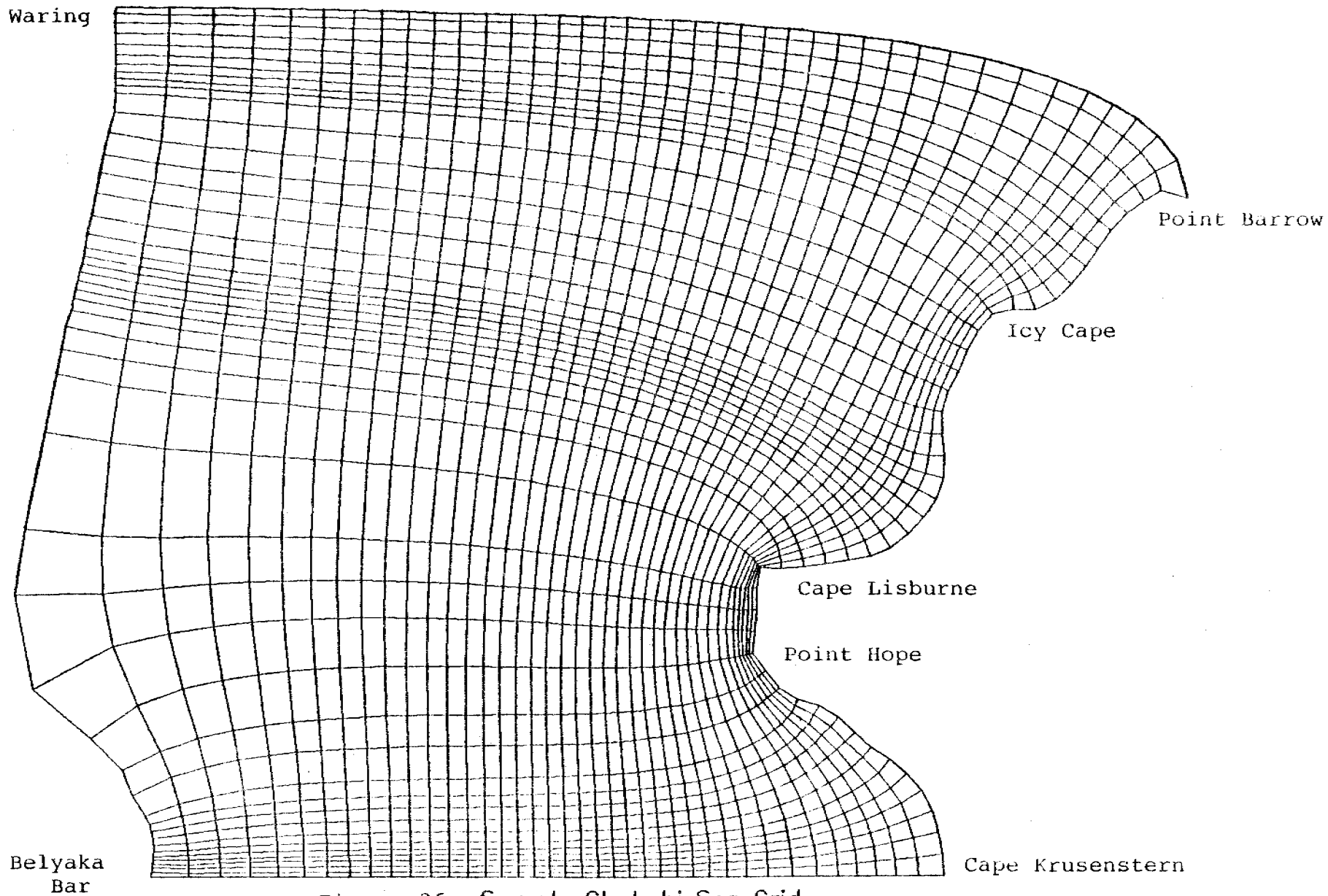
0.124296E+03	0.106066E+01	0.835917E+02	0.705592E+03	-0.172555E-01	0.1037
0.5094880E+03	0.2536362E+03				
0.4632817E+02	0.5447133E+02				
0.1461939E+02	0.5996958E+01				
-0.4842135E+00	0.5228670E+00				
0.1799836E+00	0.1983455E+00				
0.2990571E-01	0.2965861E-02				
0.1273740E-01	0.1957162E-01				
0.1093549E-02	0.5743208E-03				
0.3580367E-03	0.1663855E-03				
-0.4528514E-04	0.4438321E-05				
0.1679949E-04	0.1344103E-04				
0.2925335E-05	0.1034118E-06				
0.7065794E-06	0.1366576E-05				
0.6569280E-07	0.8127476E-08				
0.2324395E-07	0.7191591E-08				
-0.2215033E-08	0.4429770E-07				
0.2444194E-08	0.1985556E-08				
0.7532186E-09	0.4760813E-09				
0.1149636E-09	0.2013248E-09				
0.1209911E-10	0.7110333E-11				
0.3305260E-11	0.5152053E-12				
-0.1246955E-11	0.2702250E-12				
0.1942657E-12	0.4601267E-13				
-0.1906439E-14	0.5742206E-13				
-0.1352319E-13	0.6725545E-14				
-0.5521261E-14	0.9021094E-14				
0.1249254E-14	0.1537555E-14				
-0.5231469E-15	0.2678241E-15				
-0.4891655E-16	0.7575871E-16				
-0.1625935E-16	0.1731934E-16				
-0.5358301E-17	0.3552210E-17				
-0.4393363E-18	0.1199899E-17				
-0.2611640E-18	0.2984505E-18				
-0.5771539E-19	0.2639901E-18				
-0.1392722E-19	0.1986394E-19				
-0.1893418E-20	0.4262294E-20				
-0.1603293E-20	0.9126339E-21				
-0.1930369E-21	0.2757075E-21				
-0.8227249E-22	0.9204179E-22				
-0.2398099E-22	0.8326164E-23				
-0.2954646E-23	0.5968414E-23				
-0.5401404E-24	0.7734889E-24				
-0.2657521E-24	0.7758186E-25				
0.9129534E-27	0.7836200E-25				
-0.167635E-25	0.5391244E-26				
-0.5942772E-27	0.5575717E-27				
0.3770840E-27	0.4424344E-28				
0.1320085E-27	0.1391709E-27				
0.1756112E-29	0.5229173E-29				
0.1130915E-29	0.4824795E-29				
0.1523144E-29	0.1584031E-29				
0.3923751E-30	0.7357177E-30				
0.1991781E-30	0.9751553E-31				
0.6254502E-31	0.5089270E-31				
0.7554647E-32	0.1694077E-31				
0.4020135E-32	0.1829192E-32				
0.7737475E-33	0.5785776E-33				
0.1510609E-33	0.3080251E-33				

Table 17. (Cont.)

0.9123253E-34	0.6062432E-34
0.2159994E-34	0.1870119E-34
0.3519810E-35	0.5850639E-35
0.1176940E-35	0.7063679E-36
0.2212975E-36	0.2099451E-36
0.3012955E-37	0.6935033E-37
0.1572057E-37	0.1041983E-37
0.2761232E-38	0.1671375E-38
0.2035449E-39	0.4998255E-39
0.4624855E-40	0.6464363E-40
-0.9620330E-41	-0.3334787E-41
-0.5925531E-41	-0.5789563E-42
0.3556443E-42	-0.8611739E-42
-0.2706847E-42	-0.2194135E-42
-0.1361212E-42	-0.2873298E-43
-0.1753719E-43	-0.4911939E-43
-0.8374739E-44	-0.5954244E-44
-0.2352674E-44	-0.1620859E-44
-0.1230712E-45	-0.4407799E-45
-0.2122757E-45	-0.1769770E-45
-0.6954457E-46	-0.3640462E-46
-0.1186350E-46	-0.2286284E-46
-0.4621586E-47	-0.3454025E-47
-0.1309816E-47	-0.3240540E-48
-0.1686079E-48	-0.3155980E-48
-0.7380911E-49	-0.8721028E-49
-0.1738533E-49	-0.1045087E-49
-0.2203735E-50	-0.4851890E-50
-0.7309953E-51	-0.5170502E-51
-0.1537850E-51	-0.9518449E-52
0.1666053E-54	0.3300528E-52
-0.4588907E-53	-0.4397514E-54
-0.8053490E-54	0.5709087E-54
0.3086707E-54	-0.3409447E-54
-0.2998678E-55	0.7114789E-55
0.4515940E-56	0.2051914E-55
0.1094933E-55	0.1414646E-56
0.1150543E-56	0.2583483E-56
0.3781687E-57	0.7007595E-57
0.2307107E-57	0.4101819E-58
0.2801242E-58	0.5529506E-58
0.1085033E-58	0.1457144E-58
0.5338240E-59	0.2598605E-59
0.8345476E-60	0.1264378E-59
0.2213853E-60	0.3067286E-60
0.8309976E-61	0.3019339E-61
0.8431742E-62	0.1808961E-61
0.2977387E-62	0.3822304E-62
0.1241214E-62	0.3907865E-62
0.8576749E-64	0.2541256E-63
0.2225148E-64	0.3526460E-64
0.1143432E-64	-0.5479506E-65
-0.2008297E-65	0.2479775E-65
0.0	0.2550033E+00
	0.1854014E+01
	0.1996982E+01

Point
Waring

364



Belyaka
Bar

Cape Krusenstern

Figure 26. Sample Chukchi Sea Grid

The salient point here is not the sample grid, but rather the constants and coefficients listed in Table 17. Any modeler can produce his own computing grid using these values and a numerical routine (Grid). Moreover, any existing finite difference computer code can be easily modified to accommodate the transformed model equations.

Reid, R.O., A.C.Vastano, R.E.Whitaker, and J.J.Wanstrath(1977). Experiments in Storm Surge Simulation. In Goldberg, E.D. et. al. (eds.). The Sea. Volume 6. Marine Modeling. Wiley & Sons, N.Y. pp.145-168.

CRUISE REPORT, CHUKCHI SEA COAST 1981, R.V. D.W. HOOD
(3 August to 10 September)

Introduction and Objectives

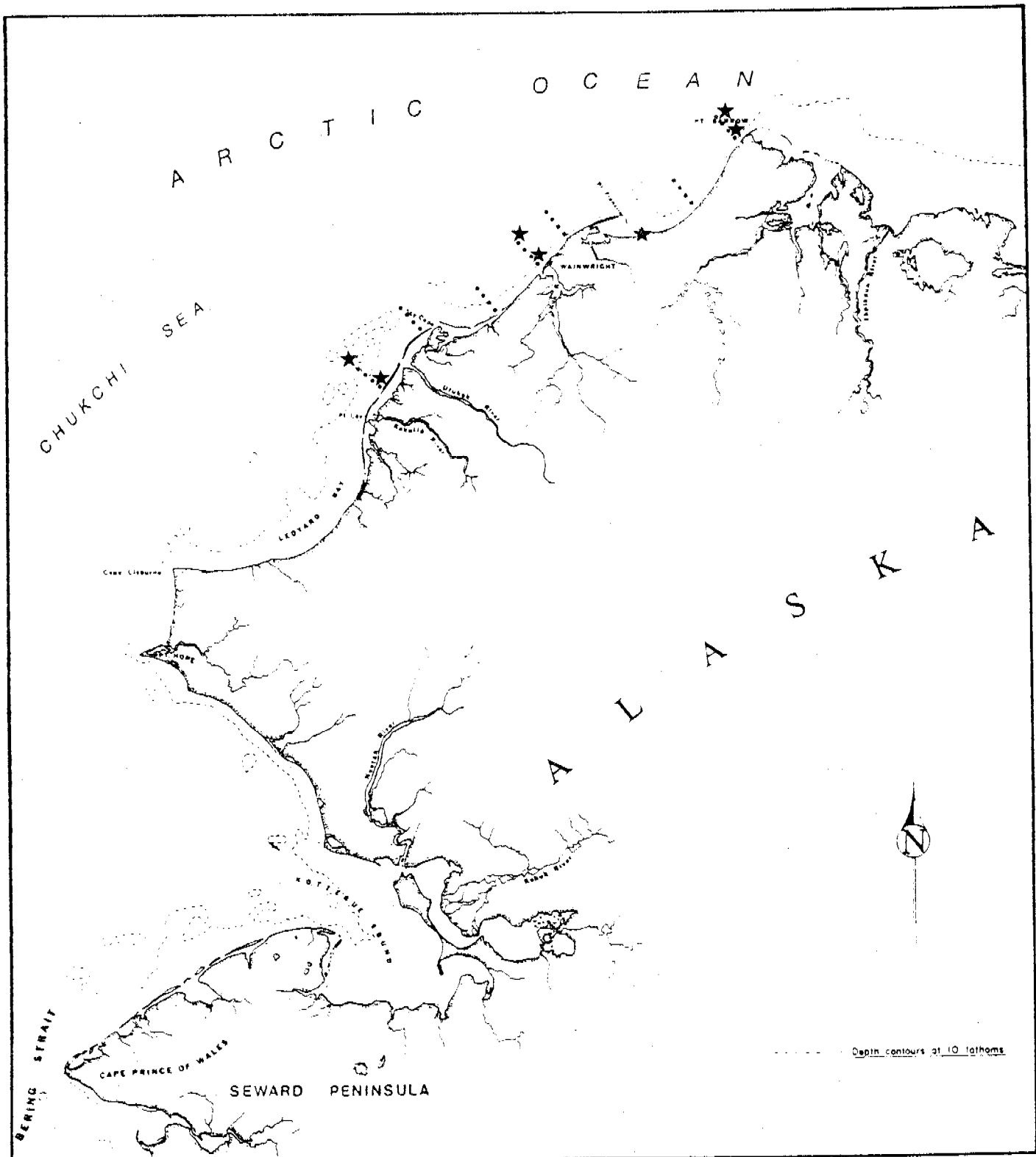
Objectives for summer field efforts of RU 531 were jointly set by the NOAA Project Offices in Fairbanks and Juneau during a re-evaluation in May and June of NOAA's priorities. As a result of this evaluation, a field effort in the Chukchi Sea nearshore area was confirmed. Because of unavailability of NOAA ship support, logistics and vessel were provided by RU 531 based upon the infore vessel D.W. HOOD.

Prior to major modeling efforts for trajectory predictions pertinent to the Chukchi Sea nearshore area, additional field observations were felt to be essential to better elucidate the basic physics involved before model construction. Based upon the excellent but limited nearshore data previously available available (e.g., Coachman et al 1975, Wiseman et al 1973, Wiseman and Rouse 1980, Mountain et al 1976, Ingham et al 1972), the following specific cruise objectives were set:

1. Obtain moored current meter data from nearshore stations along the Chukchi Sea coast from Barrow to Ledyard Bay.
2. Obatin sea level data.
3. Obtain hydrographic (density) profile on transects perpendicular to the coast concurrent with the current meter data.
4. Perform Lagrangian drogue dispersion studies and long-range drogue tracking experiments in the areas of interest along the coast.
5. Interpret and correlate the results with available meteorological data being gathered during the same time in this region.

Methods

Current data were obtained by deploying and retrieving current meters along the Chuckchi seacoast during the initial and final stages of the study (Figure 27). Prior to the deployment of a current meter string, two meters were attached to bridles and an appropriate length of stainless steel cable complete with subsurface floats, an acoustic pinger, a primary anchor (250 lbs), a tag line (600 ft), and a secondary anchor (40 lbs). Each meter was positioned at



- ★ Instrument Mooring Locations
- C/STD Transects

Figure 27. Chukchi Sea Coast Study Sites (August - September 1981)

lengths along the string according to ice hazards present at the surface and the density structure of the water column as previously determined by C/STD transect.

Current meter station locations were established and relocated with a Motorola Miniranger III system. The system consisted of two shore-based battery powered transponders which transmitted distance information to a portable readout located on the D.W. HOOD. Positions at sea were triangulated by distances from known transponder sites on shore.

Current meter recovery depended on relocating the position of deployment, checking for the presence and actual location of the acoustic pinger attached to the string, marking the spot of pinger transmission with a bouy and weighted line and, finally, snagging the tag line stretched from the primary anchor to the secondary anchor with a grapnel hook. Expected acoustic releases were not made available to RU 531 by NOAA due to a shortage of supply.

Nearshore density profiles of the water column were acquired with an InterOceans C/STD system (model 513D). Surface water samples were taken during each transect to calibrate the salinity values of the C/STD system, and a reversing thermometer was used to check surface temperature values.

Drogue dispersion studies and long-range RDF tracking studies were performed as previously described in the earlier chapters of this year-end report.

A Chronology of the Cruise

A four man crew of scientists doubled as boat crew during the cruise. Oceanographers Stephen Pace (Captain), Philip Carpenter, Howard Teas, and Toby Goddard served as the crew and Sam Stoker handled onshore logistics.

The following account is based on notes taken from the log of the D.W. HOOD and those notes taken by members of its crew. As originally planned, the length of the cruise was to be 30 days, starting in the first week of August and ending in the first week of September. The vessel was to begin and end the cruise at Prudhoe Bay in time to allow other commitments to be fulfilled at the end of the season in the Beaufort Sea. However, major storms which occurred near the end of August necessitated adjusting the planned scope of work, and lengthening the cruise in order to accomplish the necessary tasks. On the plus side, the data that was retrieved contains these storm events, including a major negative storm surge event.

Table 18. Equipment Deployment and Retrieval Log, Chukchi Sea, 1981

Date		Instrument*	Location		Meter Depth (feet)	Bottom Depth (feet)	Comments
Deployed	Retrieved		Latitude	Longitude			
7 Aug 81	7 Sep 81	Aanderaa CM	71°19'31"N	156°45'19"W	57	63	[Barrow onshore] Station located by by pinger after moved (by ice?) 2,000 meters.
7 Aug 81	Missing	Aanderaa CM	71°19'31"N	156°45'19"W	37	63	Top meter missing. Possibly broken free by iceberg.
7 Aug 81	8 Sep 81	Aanderaa CM	71°23'27"N	156°50'52"W	220	270	[Barrow offshore] Difficult recovery, rough seas and currents.
7 Aug 81	8 Sep 81	Aanderaa CM	71°23'27"N	156°50'52"W	70	270	Difficult recovery, rough seas and currents.
9 Aug 81	3 Sep 81	Aanderaa tide gauge	70°48'39"N	158°22'12"W	6	6	[Peard Bay] Easily found by Zodiac crew.
11 Aug 81	2 Sep 81	G.O. CM (film)	70°37'36"N	160°08'12"W	43	50	[Wainwright onshore] Easily recovered.
11 Aug 81	2 Sep 81	G.O. CM (film)	70°37'36"N	160°08'12"W	17	50	Easily recovered.

* Abbreviations: CM = current meter; G.O. = General Oceanics.

Table 18 . (continued)

Date		Instrument	Location		Meter Depth (feet)	Bottom Depth (feet)	Comments
Deployed	Retrieved		Latitude	Longitude			
11 Aug 81	2 Sep 81	G.O. CM (film)	70°42'46"N	160°22'48"W	97	120	[Wainwright offshore] Snagged meter string w/dragline between Hood & Zodiac drifting in 2 knot current & 2-3 ft. seas. Grapnel hook didn't work on cobble bottom.
11 Aug 81	2 Sep 81	G.O. CM (film)	70°42'46"N	160°22'48"W	32	120	
14 Aug 81	Lost	Aanderaa CM	69°54'33"N	162°52'30"W	27	30	[Akunik Pass onshore] Station missing or floats damaged. No clear pinger signal.
14 Aug 81	Lost	Aanderaa CM	69°54'33"N	162°52'30"W	8	30	Station missing or floats damaged. No clear pinger signal.
14 Aug 81	Lost	Aanderaa CM	70°00'30"N	163°07'42"W	37	63	[Akunik Pass offshore] Mini-Ranger batteries discharged. No pinger signal in area reached by dead reckoning. No pinger signal rec'd by R.V. Oceanographer in correct area. Station assumed missing or pinger and float malfunctioning.
14 Aug 81	Lost	Marsh- McBirney CM	70°00'30"N	163°07'42"W	16	63	

* Abbreviations: CM = current meter; G.O. = General Oceanics.

Shortening the scope of the project was based on a series of priorities set previous to the cruise. Theoretically, those objectives of lowest priority would be sacrificed first in favor of finishing the project within the given time frame. The lower priority objectives were the long-range RDF drogue tracking and drogue dispersion studies, while the higher priority objectives included the current meter and sea level data and the density profiles established with the C/STD.

3 August. The beginning of the cruise was uneventful and the sea conditions were mild as the D.W. HOOD weighed anchor at the East Dock facility in Prudhoe Bay at 10 p.m. and departed for Point Barrow on the Chukchi seacoast. By 12 p.m. the vessel had negotiated the channel near West Dock and was headed west along the outer barrier islands of Simpson Lagoon.

4 August. During the Beaufort Sea crossing to Point Barrow, sea and wind conditions remained calm. Multi-year ice was absent along the 50 foot contour of Harrison Bay and the 40 foot contour of Smith Bay. However, a tongue of multiyear floe ice with coverage of 25-33 percent extended to within two miles of Cape Simpson, blocking the eastward advance of several sea-lift tugs and barges.

5 August. The HOOD arrived in Elson Lagoon in the early morning hours, completing the 180 nautical mile journey in under 24 hours of running time. At the town of Barrow some oceanographic gear was offloaded in preparation for air transport to Wainwright, while the rest was prepared for immediate deployment on board the HOOD. Additional scientific personnel, P. Carpenter and T. Goddard, joined the crew.

6 August. The crew prepared for the first set of meter deployments to take place offshore of Barrow. Suitable sites for miniranger transponders were located and equipped, while preparations continued for meter deployments and C/STD casts aboard the HOOD. Foggy, windy weather, and nearshore multi-year ice movement forced an early anchorage in Elson Lagoon for the night.

7 August. As the weather continued foggy and windy (10-15 knots), the crew deployed a string of two Aanderaa current meters in shallow water and a second similar string in the Barrow canyon (Table 18). Prior to current meter deployments, several C/STD casts were taken in a transect extending from nearshore to the edge of the ice margin offshore (Table 19).

8 August. Winds had subsided and seas were calm by morning as the HOOD completed a second C/STD transect off Skull Cliffs and entered Peard Bay to deploy a tide gauge at the eastern end. Winds and seas increased while inside Peard Bay, trapping the HOOD until seas subsided.

Table 19. C/STD TRANSECT LOG

Date	Area	Cast Depths (feet)	Station Distances from Land in Nautical Miles	Weather Observations
7 Aug 81	Barrow	57	1	Wind: 4-6 knots, 300° mag Air temperature: 37°F
		90	2	
		90	3	
		90	4	
		90	5	
8 Aug 81	Skull Cliffs	35	1	Wind: 10 knots, 020° mag. Air temperature: 44°F
		54	2	
		60	3	
		65	4	
		67	5	
		75	7	
10 Aug 81	Pt. Belcher	65	1	Wind: 5-6 knots, 020° mag Air temperature: 49°F
		90	2	
		90	3	
		90	5	
		90	7	
13 Aug 81	Pingorarak Pass	24	1	Wind: 0-2 knots, 0° mag. Air temperature: 47°F
		37	2	
		47	3	
		55	5	
		67	7	
14 Aug 81	Akunik Pass	24	1	Wind: 16-20 knots, 300° m Air temperature: 44°F
		45	3	
		52	5	
		60	7	
		60	9	
14 Aug 81	Icy Cape	36	1	Wind: 10 knots, 010° mag. Air temperature: 46°F
		44	2	
		47	4	
		54	6	
		70	8	
2 Sep 81	Wainwright	45	1	Wind: 10-12 knots, 020° m Air temperature: 45°F
		60	2.5	
		70	3.5	
		75	4.5	
		90	6.5	
		90	8.5	

9 August. Winds and seas increased, and the HOOD remained at anchor where scheduled equipment checks and maintenance were performed during daylight hours. During the evening wind velocities dropped to 10 knots and seas decreased, allowing safe passage through the narrow channel at Sea Horse Islands the next morning.

10 August. The HOOD continued south to Point Belcher where another C/STD transect was recorded before continuing on to the DEW-Line site at Wainwright Lagoon. The HOOD was not welcome at the DEW-Line site, and fuel and supplies previously arranged for by NOAA and deposited there were difficult to recover.

11 August. Under threat of filing a report for breach of security by the U.S.A.F. commander at the DEW-Line site (Major Manning), the HOOD took on its first fueling and supplies since departure at Prudhoe Bay. Later in the afternoon the crew successfully deployed two strings of meters seaward of the Wainwright Lagoon entrance (Table 18) and then returned to safe anchorage within the lagoon as wind velocity increased during the evening.

12 August. Winds increased to 20-25 knots out the the northeast during the day forcing the HOOD into a maintenance program while at anchor within Wainwright Lagoon. Wind velocities then dropped at night, leaving calm conditions at dawn.

13 August. With calm conditions, HOOD headed south to Pingorarak Pass where a fourth C/STD transect was recorded before continuing on toward Icy Cape and Akunik Pass. Safe anchorage was made in the south channel of the lagoon after negotiating the shallow entrance at Akunik Pass in the evening hours.

14 August. Following a lengthy discussion the previous night, the opinions carried which cautioned respect for both the requests of the Point Lay villagers and the notorious weather south of Icy Cape. A compromise was reached between cruise plan expectations and caution based on immediate field experience. As a result, Akunik Pass was the southernmost extent of the project's objectives, and the scope of the project was reduced to exclude the greater part of Ledyard Bay. During the early morning hours, miniranger transponder sites were established along the barrier island to the north of Akunik Pass, maintenance was performed on the HOOD, and programming problems were solved on the Marsh-McBirney current meter prior to deployment. The last two strings of meter were deployed seaward of Akunik Pass as winds increased to 30 knots from the north, and a C/STD transect was completed before the HOOD gained safe anchorage behind Akinuk Pass for the evening.

15 August. The winds subsided during the previous night and the HOOD headed north to Icy Cape, performing a C/STD transect before arriving at Wainwright Lagoon for the evening.

16 August. In the morning a second fueling of the HOOD and reorganization of the gear was performed near the DEW-Line site. Gear for meter deployment was offloaded and replaced with equipment for the drogue dispersion and the long range RDF studies.

17 August. The first of the major storms arrived with wind velocities over 35 knots from the west, sea heights and wind chop of 3-5 feet, and blowing snow. Consequently, the HOOD remained at anchor in Wainwright Lagoon waiting for suitable weather for a dispersion drogue study.

18 August. Storm winds continued unabated from the west at 35 knots and greater. HOOD remained safely anchored in Wainwright Lagoon.

19 August. Storm winds slackened during the afternoon, but sea conditions remained hazardous. HOOD waited at anchor in the protection of Wainwright Lagoon.

20 August. Under calm sea and wind conditions a drogue dispersion study was initiated five miles seaward of the Wainwright Lagoon inlet. The study results relied on accurate miniranger coordinates and the ability to visually sight twelve drogue spars from the HOOD's crows nest. The dispersion study ended after twelve hours of daylight. In preparation for the longer range RDF drogue study, six drogues were repositioned at one and two mile intervals in a transect ranging from 8.5 miles offshore to within 2 miles of the Wainwright Lagoon entrance.

21 August Another set of equipment changes was made near the DEW-Line site at Wainwright. The bulk of the RDF drogue tracking equipment was left onshore in preparation for recovering the current meters at Wainwright and Akunik Pass. However, one set of running fixes was attempted during the evening hours of the 21st and early morning hours of the 22nd on the six drogues left offshore. RDF fixes were taken whenever the opportunity presented itself, thereby monitoring the progress of the drogues over a long period of time.

22 August. Increased wind speeds up to 30 knots from the southwest and rough seas prevented the HOOD from traveling south to Akunik Pass and the vessel remained at anchor in Wainwright Lagoon as the skipper departed to Fairbanks for a planned rest.

23 August. Winds abated during the morning hours and the HOOD attempted to recover the nearshore string of meters off Wainwright in the early evening hours. The attempt was unsuccessful because the miniranger batteries were low on power and the relocating system did not function.

24 August. Recharging the transponder batteries from the vessel's electrical system was required before the miniranger system could be use' again. As the HOOD sailed south to Akunik Pass the batteries were placed on a charging system. Upon arriving at the pass, the batteries' condition was checked as they were deployed with the transponders in anticipation of recovering the current meters on the following morning.

After negotiating the pass at Akunik, the HOOD's crew was visited by two upset villagers from Point Lay. The villagers felt their earlier warnings of encroachment had been ignored by the HOOD. Immediately after the visit the crew of the HOOD attempted to recover two meter strings and depart the area.

The recovery attempt during the evening of the 24th and morning of the 25th was unsuccessful because the batteries powering the transponder unit onshore were not fully charged. Regardless of the miniranger failure, the crew continued its search for the meters using the pinger locator without success.

25 August. No signals were received on the pinger locator and further attempts were abandoned when wind velocities increased to 30-40 knots by mid-morning. The HOOD returned to the shelter of Akunik Pass as seas continued to increase in height.

26 - 29 August. Winds and seas continued to rise and virtually trapped the HOOD at Akunik Pass for a four-day period. Wind velocities increased to 60 knots as the ship's barometer (uncorrected) rose to 1032 mb. Skies were clear and the wind from the northeast dropped the water level inside the lagoon by about 2.5 feet, creating a difficult anchorage for the HOOD.

30 August. In the morning winds dropped to 16-20 knots and the HOOD escaped Akunik Pass when water level resumed normal depths. The HOOD sailed north to Wainwright without having recovered the current meters at Akunik Pass.

31 August. The skipper rejoined the crew as the mate left for a planned rest in Fairbanks. The charging problem of the transponder batteries was solved as the HOOD refueled and was resupplied in Wainwright Lagoon.

1 September. The offshore string of meters at Wainwright was located using the miniranger and pinger locator.

However, after dropping a marker buoy on the spot, the grapnel hook failed to pickup the 600 foot tagline attached to the meter string. Conditions were not favorable to hooking as a form of recovery in the area; currents of approximately two knots carried multiyear ice through the area exposing marker floats and complicating drag procedures. The hook continually bounced over the cobble bottom, occasionally impaling a mass of soft coral or an anemone. The HOOD returned to Wainwright Lagoon for the evening.

2 September. During the morning hours the nearshore meter string off Wainwright was recovered after briefly relocating the deployment spot with the miniranger, marking the spot with a buoy, checking the accuracy with the pinger locator and dragging the grapnel hook over the tagline. The afternoon hours were spent rigging for the recovery of the offshore meter string off Wainwright. The second recovery attempt for the meters offshore took place in moderate winds and current. A weighted dragline was stretched 800 feet between the HOOD and the ZODIAC one half mile up current of the marked current meter location. As the vessels drifted to either side of the marker buoy they closed the arc of dragline and both ends of the line were winched aboard the HOOD. The bight of the dragline caught a meter and the entire string was safely recovered. The evening was spent completing a final C/STD transect off Wainwright.

3 September. The HOOD left Wainwright Lagoon and sailed north to Peard Bay, retrieving the tide gauge deployed in the northeast corner of the embayment. Winds increasing to 25 knots and rising seas prevented safe navigation of the Sea Horse Island channel. The HOOD remained at anchor inside Peard Bay.

4 - 5 September. The HOOD remained at anchor as heavy seas and high winds continued from the northeast.

6 September. As winds dropped to 16-20 knots the HOOD escaped Peard Bay and traveled north to Barrow. After arriving at Barrow during the evening, the HOOD anchored in the lee of an icebreaker (ARCTIC CHALLENGER) and the tug (GUARDSMAN) in drifting multiyear ice, strong currents, 20 knot winds, and blowing snow.

7 September. The nearshore meter string was recovered after relocating the deployment spot with the miniranger, marking the spot with a buoy, checking the accuracy with the pinger locator, moving the marker buoy 2,000 meters to a shallower location, and catching the meter string with the grapnel hook. Although the string was recovered, the uppermost instrument package was missing. The loss of the surface current meter occurred possibly as a result of drifting ice. The string was recovered at a distance of 2,000 meters from its location of deployment and the remaining current meter vane was severely damaged.

8 September. The offshore meter string at Barrow was recovered during marginal operating conditions. The string was located with the miniranger and pinger locator, and marked with a buoy. The meters were recovered after the grapnel hook unexpectedly snagged the marker buoy line which in turn had snagged a meter on the string.

After recovering the string the HOOD returned to Barrow where equipment and personnel were offloaded in preparation for return to Prudhoe Bay. Toby Goddard departed as the mate, Howard Teas, returned from Fairbanks. Plans were laid for the return of the HOOD to Prudhoe Bay and a final attempt at recovery of the two meter strings deployed off Akunik Pass. Pace and Carpenter were to return the HOOD to Prudhoe Bay after loading equipment at Barrow. Teas would board the NOAA vessel, OCEANOGRAPHER, at Barrow on its way to Nome, stopping in the Akunik Pass area to recover the missing meters.

9 September. The HOOD left Barrow, avoided rough seas in the Beaufort by running inside Elson Lagoon to Sanigaruak Pass, and continued on the Thetis Island for a brief rest.

10 September. The HOOD continued on to the East Dock facility at Prudhoe Bay and completed offloading procedures before ending the cruise.

9 - 28 September. H. Teas boarded the OCEANOGRAPHER on the 12th and continued on toward Nome after a thorough (though fruitless) search of the Akunik area for the current meter strings. At no time during the search was a pinger signal detected even though the areas of deployment were accurately relocated. Either the meters were no longer in the area of deployment or the pingers associated with the missing strings failed to transmit a signal. At the time of deployment the pinger locator was not available and could not be used to check proper operation of the pingers. Word of current meter recovery by Point Lay residents has been subsequently received through the Alaskan Whaling Commission at Point Barrow and efforts are underway to retrieve these instruments.

Results

Current meter stations and hydrographic stations are summarized in Tables 18 and 19, respectively. Essentially, 7 of 12 current meters plus the water level meter were recovered with long-term data records. Hydrographic transects were made during the cruise as was one drogue dispersion/tracking experiment.

The data resulting from this cruise are being processed and will be interpreted along with available meteorological data taken during the same time frame.

Within the restraints of the storm events and physical locale, the D.W. HOOD performed well because of its ability to handle a variety of heavy equipment in rough seas. Also, its design allowed entry into the shallow water embayments and operation among the icefloes endemic to the Chukchi seacoast.

1. Coachman, L.K., K. Aagaard, R.B. Tripp (1975). Bering Strait: the Regional Physical Oceanography. University of Washington Press, Seattle. 172 pp.
2. Wiseman, Wm. J. Jr. and L.J. Rouse Jr. (1980). A Coastal Jet in the Chukchi Sea. Arctic 33: 21-29.
3. Wiseman, Wm. J. Jr., J.M. Coleman, A. Gregory, B.A. Hsu, A.D. Short, J.H. Suhayda, C.D. Walters Jr., and L.D. Wright (1973). Alaskan Coastal Processes and Morphology. Coastal Studies Institute Technical Report 149. Louisiana State University, Baton Rouge. 171 pp.
4. Mountain, D.G., L.K. Coachman, K. Aagaard (1976). On the Flow Through Barrow Canyon. J. Phys. Oceanog. 6: 461-470.
5. Ingham, M.C., B.A. Rutland, P.W. Barnes, G.E. Watson, G.I. Divoky, A.S. Naidu, G.D. Sharma, B.L. Wing, and J.C. Quast (1972). Websec-70: an Ecological Survey in the Eastern Chukchi Sea. September-October 1970. U.S.C.G. Oceanographic Report No. 50. 206 pp.

SIXTH ANNUAL REPORT

Bristol Bay Oceanographic Processes (BBOP)
"Fluid Transport Processes in the North Aleutian
Shelf and St. George Basin"

J. D. Schumacher
C. A. Pearson

Pacific Marine Environmental Laboratory
Environmental Research Laboratories, NOAA
3711 15th Ave. N.E.
Seattle, WA 98105

Contract No. R7120849
Research Unit: 549
Period: 1 April 1980 to 1 April 1981
Number of Pages: 308

Table of Contents

I. Summary	381
II. Objectives	382
III. Study Area	382
IV. Present Status (see appendicies A to F)	
V. Cooperation	383
VI. Publications from OCSEAP Work	383
VII. Needs for Further Study	387
VIII. Conclusions	397
IX. Milestone Update	398
A. A Review of Circulation Patterns, Property Distributions and Processes over the Outer Shelf Domain	399
B. Effects of Wave-Induced Mooring Noise on Tidal and Low-Frequency Current Observations	422
C. Cruise Report, NASTE Cruise #2; RP-4-SU-81A Leg I; 20 January to 19 February 1981	438
D. Preliminary results from current, hydrographic and meteorological data: Unimak Pass, Alaska	459
E. CTD and SPM observations during reestablishment of structural front: Bristol Bay, Alaska.	504
F. Guide to R2D2: Rapid Retrieval Data Display	529

I. Summary

During the present reporting period, 1 April 1980 to 1 April 1981, the following activities were completed:

1. An AGU presentation entitled "CTD & SPM observations during reestablishment of a structural front: Bristol Bay, Alaska" by Pearson, Baker and Schumacher was presented by J. D. Schumacher. The abstract was published in Transactions of the American Geophysical Union (EOS), Vol. 61(46): 1002. A more complete manuscript, which includes analysis of wind and current observations, was prepared (see Section IV. E). One result relevant to vertical transport of oil was that even during vertically stratified (summer) hydrographic conditions, storms can mix the entire middle shelf water column. In this process, the vertical flux of oil would be greatly enhanced. In concert with increased suspended matter concentrations throughout the water column, this could result in large quantities of oil reaching the sensitive benthic community. We note that at the Asilomar Workshop, the only mechanism by which oil was transported to the bottom was detrital rain. Storm related transport is likely to be greater in magnitude and occur over a much shorter (several days) period of time.

2. A manuscript, entitled "Preliminary results from current, hydrographic and meteorological data: Unimak Pass, Alaska" by Schumacher, Pearson and Overland was written (see Section IV. D). One conclusion is that flow was generally into the Bering Sea, however, there were strong current pulses in the opposite direction. These reversals constituted about 25% of the observations and were a response to regional scale meteorological forcing. Although regional scale winds contribute to mass transport through Unimak Pass, surface winds generated by the atmospheric pressure gradient and channeled through the Pass will likely be in the opposite direction (see Figure 14, Preliminary Results from Current, Hydrographic and Meteorological Data: Unimak Pass, Alaska. In Section IV. D). Prediction of Oil trajectories, often modeled as the superposition of wind-drift, surface wave (Stoke's drift) and current vectors will be complex in Unimak Pass: surface transport may be of opposite direction to dissolved oil transport. Analyses of wind observations during ship transit through Unimak Pass and surface atmospheric pressure charts could determine when down pressure gradient winds exist, their magnitude and their relation to regional wind patterns. We note that such winds are not unique to the Pass, they also exist at Cold Bay and perhaps at Port Moller. Understanding the nature of these channeled winds, in particular their length scale over the coastal domain and impact on coastal currents is critical to near-shore trajectory modeling and spilled oil response strategies.

3. A review of existing knowledge regarding circulation patterns, property distributions and processes over the outer shelf domain was prepared by J. D. Schumacher (see Section IV. A.) for the St. George Basin synthesis meeting to be held in April 1981.
4. An article (see Section IV.B) which presents substantial evidence that wave-induced noise does not seriously contaminate tidal and averaged sub-tidal frequency currents recorded by Aanderaa current meters accepted for publication in Deep-Sea Research. The results of the paper imply that current records, when acquired in a manner used by this RU, are a relatively accurate depiction of the natural environment.
5. A guide for use of R2D2 (Rapid Retrieval Data Display) was prepared by Carl Pearson (see Section IV.F). This "cookbook" not only facilitates the use of R2D2's current and hydrographic data sets (which includes 2845 hydrocasts in the Bering Sea), but also provides a clear definition of all analysis products available to the user.

II. Objectives

The general objective of this research unit is to provide physical oceanographic data and interpretations leading to improved understanding of transport processes in the study region. Specific objectives are:

1. Calculation of statistics of near shore currents using current meter data. This includes finding tidal constituents and vector mean currents.
2. Calculation of near shore baroclinic and barotropic currents, using CTD, bottom pressure, and current meter data.
3. A qualitative description of the front found near the 50 meter isobath and an estimation of its possible affect on oil spill trajectories.
4. A description of the currents inferred from examination of the FY80 Unimak Pass records.
5. Transmittal of processed data to the Rand Corporation to refine the numerical circulation model.

III. Study Area

This RU is presently conducting field operations, analysis and interpretation of data collected over the southeastern Bering Sea shelf. Emphasis is on transport processes along the Alaska Peninsula (North Aleutian Shelf lease area) and over the outer shelf domain between Unimak Pass and the Pribilof Islands (including much of the St. George Basin lease area).

V. Cooperation

In order to determine fate and possible impact of spilled oil, it is necessary to understand the important transport mechanisms in a given lease area. To acquire such knowledge requires an interdisciplinary effort including direct observations of wind, current and bottom pressure, inferred net transport using methane distribution where source/sink rates are suggested by microbial action and observations of suspended particulate matter and its flux. Cooperative efforts have been undertaken prior to field operations and have resulted in two highly successful cruises, a presentation at the Fall 1980 AGU meeting (see Section IV.) and a report of results from Unimak Pass (see Section IV). The synthesis of various information related to oil transport over the St. George Basin will be conducted on 28-30 April 1981.

VI. Publications from OCSEAP funded studies

The following is an update of the publication lists presented in the Sixth Annual Report: Gulf of Alaska Study of Mesoscale Oceanographic Processes (GAS-MOP) by Schumacher and Pearson (1980) and the Fifth Annual Report: Bristol Bay Oceanographic Processes (B-BOP) by Schumacher et al (1980). Where appropriate, either an abstract or executive summary is also presented.

Coachman, L.K., T.H. Kinder, J.D. Schumacher and R.B. Tripp, 1980. Frontal systems of the southeastern Bering Sea shelf. In: Stratified Flows Second IAHR Symposium, Trondheim, June 1980, vol. 2, Tapir, Trondheim; pp 917-933.

Schumacher, J.D., C.A. Pearson, L.K. Coachman and R.B. Tripp, 1980. Fifth Annual Report: Bristol Bay Oceanographic Processes. In Envir. Assessment of the Alaskan Continental Shelf, Annual Reps. of PI's for the year ending March 1980: Vol. ?, Transport: 183 pp.

Pearson C.A., J.D. Schumacher and R.D. Muench, 1981. Effects of wave-induced mooring noise on tidal and low frequency current observations. In Press, Deep-Sea Res. (See Section IV.B)

Schumacher, J.D. and C.A. Pearson, 1980. Sixth Annual Report, Gulf of Alaska Study of Mesoscale Oceanographic Processes (GAS-MOP). In Envir. Assessment of the Alaskan Continental Shelf, Annual Reps of PT's for the year ending March 1980; Vol. ?, Transport: 170 pp.

Reed, R., R. Muench and J.D. Schumacher, 1980: On baroclinic transport of the Alaskan Stream near Kodiak Island. Deep-Sea Res., 27.

Deep-Sea Research, Vol. 27A, pp. 509 to 523
Pergamon Press Ltd 1980. Printed in Great Britain

0198-0149/80/0701-0509 \$02.00/0

On baroclinic transport of the Alaskan Stream near Kodiak Island*

R. K. REED†, R. D. MUENCH†† and J. D. SCHUMACHER†

(Received 17 May 1979; in revised form 25 January 1980; accepted 10 February 1980)

Abstract—Near Kodiak Island the Alaskan Stream, a southwestward-flowing boundary current, exhibits no significant alongshore variability in volume transport; hence the region is suitable for examination of temporal changes in flow. Seventeen CTD (conductivity-temperature-depth) sections occupied during 1975-79 were used to compute baroclinic transport by two methods: (1) referred to 1500 dbar or the deepest common level; and (2) adjusted to 1500 dbar by the method of Jacobsen and Jensen. The second method gave larger values and less variability than the first. The mean adjusted volume transport was $12 \times 10^6 \text{ m}^3 \text{ s}^{-1}$, and maximum and minimum values were 17 and $8 \times 10^6 \text{ m}^3 \text{ s}^{-1}$.

Baroclinic transport computed from the CTD data showed no seasonal signal, even though wind-stress curl in the Gulf of Alaska increases by an order of magnitude from summer to winter. A combination of changes in location of the stream along the continental slope and failure to adjust the transport to 1500 dbar seems to have caused some of the previously inferred variability. It appears that the baroclinic flow does not consistently spin up or down seasonally because of insufficient response time at these high latitudes.

Schumacher, J.D. and R.K. Reed, 1980. Coastal flow in the northwest Gulf of Alaska: the Kenai Current. J. Geophys. Res., 85: 6080-6688

JOURNAL OF GEOPHYSICAL RESEARCH, VOL. 85, NO. C11, PAGES 6680-6688, NOVEMBER 20, 1980

Coastal Flow in the Northwest Gulf of Alaska: The Kenai Current

J. D. SCHUMACHER AND R. K. REED

*National Oceanic and Atmospheric Administration, Environmental Research Laboratories
Pacific Marine Environmental Laboratory, Seattle, Washington 98105*

Recent data from the northwest Gulf of Alaska reveal a coastal current which flows westward along the Kenai Peninsula (mainly within 30 km of shore), enters Shelikof Strait, and exits to the southwest of Kodiak Island. This flow, which we call the Kenai Current, has a large seasonal variation in baroclinic transport and maximum surface speed; transport is typically about $0.3 \times 10^6 \text{ m}^3/\text{s}$ but exceeds $1.0 \times 10^6 \text{ m}^3/\text{s}$ in fall, with concurrent speed increases from 15-30 cm/s to over 100 cm/s. The coastal flow is clearly distinct from the offshore Alaskan Stream; its seasonal signal is mainly related to a cross-shelf pressure gradient, which responds to an annual hydrological cycle. Current records from Shelikof Strait substantiate the presence of an annual signal and indicate that wind forcing has maximum effect from December through February, but it does not appear to augment flow at other times.

Muench, R.D. and J.D. Schumacher, 1979. Some observations of physical oceanographic conditions on the northeast Gulf of Alaska continental shelf. NOAA Tech. Memo ERL-PMEL-17: 84 pp.

SOME OBSERVATIONS OF PHYSICAL OCEANOGRAPHIC CONDITIONS
ON THE NORTHEAST GULF OF ALASKA CONTINENTAL SHELF*

By R. D. Muench¹ and J. D. Schumacher

Contributors: S. P. Hayes
R. L. Charnell²
G. Lagerloef
C. A. Pearson

Pacific Marine Environmental Laboratory

ABSTRACT. Circulation and hydrographic conditions on the northeast Gulf of Alaska continental shelf between Yakutat and Prince William Sound, Alaska, were investigated using current, temperature and salinity observations obtained in 1974-77. Flow on the shelf was westerly, with mean currents highest at the shelf break and decreasing toward the coastline. Mean current speeds near the shelf break were about 15 cm s^{-1} in winter and decreased to about 5 cm s^{-1} during summer. These seasonal variations were due primarily to variations in intensity of the wind-stress-driven Gulf of Alaska subarctic gyre. Prominent fluctuations in flow were superposed upon the westerly mean flow, and were at times sufficiently large to lead to reversals to easterly flow. These fluctuations were larger relative to mean flow during summer than in winter; the stronger mean flow in winter was sufficient to maintain westward flow at all times despite the larger fluctuations. Fluctuations in flow were apparently driven primarily by local wind forcing, though propagation of mesoscale eddies from the central Gulf of Alaska onto the shelf was probably a contributing factor.

¹Now at SAI/Northwest, 13400B Northrup Way, Bellevue, WA 98005.

²Deceased.

*Contribution No. 450 from the NOAA/ERL Pacific Marine Environmental Laboratory.

Lagerloef, G.S.E., R.D. Muench and J.D. Schumacher, 1981. Low frequency variations in currents near the shelf break, northeast Gulf of Alaska. In press J. Phys. Oc.

ABSTRACT

We present current observations from 20, 50, 100 and 175 m depths obtained over a 3-year period near the northeast Gulf of Alaska shelf break, and emphasize a 2-year continuous segment from 50 m depth. These records indicate that a moderate ($\sim 16 \text{ cm s}^{-1}$ at 50 m) mean flow was directed, at all depths, alongshelf toward the northwest. Variance was high and had nearly normal distributions in along and cross-shelf components. The mean alongshelf speed varied from $\sim 12 \text{ cm s}^{-1}$ in summer to $\sim 20 \text{ cm s}^{-1}$ in winter and a more distinct seasonal cycle was evident in monthly kinetic energies of wind and current. Very low frequency (VLF) ($< 0.1 \text{ cpd}$) current fluctuations were prominent flow features and were vertically coherent between 50-m and 100-m depth (coherency squared > 0.8 at 95% level). Fluctuating kinetic energy of the current contained in the VLF band was a significant fraction (34%) of the total kinetic energy and displayed an increase over the 2 years with no seasonal trend. Trends in the wind kinetic energy in the VLF band were much different and most ($\sim 66\%$) of the VLF current kinetic energy was not correlated with that of the winds. These current fluctuations were probably related to oceanic scale features such as eddies or meanders in the Alaska Current.

Reed, R.K. and J.D. Schumacher, 1981. Sea level variations in relation to coastal flow around the Gulf of Alaska. In Press, J. Geophys. Res.

ABSTRACT

Adjusted sea level deviations at six tide stations around the Gulf of Alaska were examined in light of our recent knowledge of the flow regime. On the east side of the Gulf, a maximum in the deviations seems to be caused by winter barotropic flow on the shelf. On the north side of the Gulf, the maximum in fall is apparently produced by a marked increase in flow of the baroclinic coastal current. Farther west the seasonal sea level signal is appreciably reduced.

Reed, R.K. J.D. Schumacher and C. Wright, 1981. On coastal flow in the northeast Gulf of Alaska: In Press, Atmosphere-Ocean.

ABSTRACT

Seasonal maps of geopotential topography and salinity at 10 m were prepared for a region in the northeast Gulf of Alaska near Yakutat. Coastal waters in this region receive considerable runoff in late summer, but the dilution does not result in a greatly intensified coastal flow. Baroclinic coastal flow in the northeast Gulf appears to be weaker than the coastal flow (Kenai Current) to the west along the Kenai Peninsula and in Shelikof Strait.

Hydrographic Structure Over the Continental Shelf of the Southeastern Bering Sea

Thomas H. Kinder¹ and James D. Schumacher²

¹ Naval Ocean Research and Development Activity
National Space Technology Laboratories Station,
Mississippi

² Pacific Marine Environmental Laboratory,
Environmental Research Laboratory/
National Oceanic and Atmospheric Administration
Seattle, Washington

ABSTRACT

We synthesize recent work conducted over this exceptionally broad (~500 km) shelf which generally has only slow mean flow (≤ 2 cm/sec). Hydrographic structure is little influenced by this flow, but rather is formed primarily by boundary processes: tidal and wind stirring; buoyancy input from insolation, surface cooling, melting, freezing, and river runoff; and lateral exchange with the bordering oceanic water mass. Three distinct hydrographic domains can be defined using vertical structure to supplement temperature and salinity criteria. Inshore of the 50 m isobath, the coastal domain is vertically homogeneous and separated from the adjacent middle domain by a narrow (~10 km) front. Between the 50 m and 100 m isobaths, the middle domain tends toward a strongly stratified two-layered structure, and is separated from the adjacent outer domain by a weak front. Between the 100 m isobath and the shelf break (~170 m depth), the outer domain has surface and bottom mixed layers above and below a stratified interior. This interior has pronounced finestructure, as oceanic water intrudes shoreward from the weak haline front over the slope, and shelf water (middle domain) intrudes seaward across the 100 m isobath. These domains and their bordering fronts tend to persist through winter, although the absence of positive buoyancy often makes the middle shelf vertically homogeneous.

INTRODUCTION

We selected the title hydrographic "structure" rather than simply "hydrography" because we wish to emphasize the structure, or organization, inherent in the hydrographic distributions. This approach focuses on the shapes of vertical profiles, or rather classes of shapes (e.g., two-layered), rather than on values of temperature and salinity or their correlation (TS diagrams). Thus, we find a large region of the shelf where the temperature and salinity are

vertically homogeneous throughout the year, although the values of temperature and salinity fluctuate over a wide range. We concentrate on the persistent vertical homogeneity and label this region a hydrographic domain. Because vertical profiles control the hydrostatic stability of the water column and because stability influences vertical mixing, this approach is physically meaningful and useful.

We also concentrate on characteristics of small size on what can be called the spatial variability. Thus the fronts that separate regions of uniform hydrographic structure (hydrographic domains) are discussed in some detail, as is the finestructure over the outer shelf. One front, for example, has a width of only 1 km and the finestructure has a typical vertical extent of 5 m. It is now possible to resolve such features and fronts and finestructure because samples are taken closer together than formerly.

Our emphasis on hydrographic structure and small spatial scales is not opposed to examination of other properties or broader spatial scales, but complementary to it. Our description of the shelf hydrographic structure is more meaningful in considering the shelf environment from a climatic point of view. We mostly ignore changes at intervals longer than annual, although interannual hydrographic variability is significant (e.g., Overland, Niebauer, and Ingraham in this volume). The major features that we discuss here, however, were observed both in 1976 (the winter of 1975-76 was exceptionally cold, with

Circulation Over the Continental Shelf of the Southeastern Bering Sea

5

Thomas H. Kinder¹ and James D. Schumacher²

National Space Technology Laboratories Station,

¹ Naval Ocean Research and Development Activity,
Bay St. Louis, Mississippi

² Pacific Marine Environmental Laboratory,
Environmental Research Laboratories/National
Oceanic and Atmospheric Administration
Seattle, Washington

ABSTRACT

Using extensive direct current measurements made during the period 1975-78, we describe flow over the southeastern Bering Sea shelf. Characteristics of the flow permit us to define three distinct regimes, nearly coincident with the hydrographic domains defined in the previous chapter. The coastal regime, inshore of the 50 m isobath, had a slow (1-5 cm/sec) counterclockwise mean current and occasional wind-driven pulses of a few days' duration. The middle regime, bounded by the 50 and 100 m isobaths, had insignificant (<1 cm/sec) mean flow but relatively stronger wind-driven pulses. The outer regime, between the 100 m isobath and shelf break (~170 m), had a 1-5 cm/sec westward mean and low-frequency events unrelated to local winds. Over the entire shelf most of the horizontal kinetic energy was tidal, varying from 60 percent in the outer regime to 90 percent in the coastal regime. About 80 percent of the tidal energy was semidiurnal.

Mean flow over the shelf is well described qualitatively by dynamic topographies, and shallow current data from both coastal and outer regimes agree quantitatively as well. Two meteorological conditions that force the observed current pulses have been identified. In summer eastward-traveling low atmospheric pressure centers caused low-frequency pulses in the middle regime, and weaker pulses in the coastal regime. In winter, outbreaks of cold and dry continental air forced pulses within the coastal and middle regimes.

INTRODUCTION

Until recently, few direct current measurements were available over this shelf, so that ideas about flow were based partly on indirect methods and partly on intuition (see the historical review which follows). Since 1975, however, we and many colleagues have gathered numerous direct current measurements with

concurrent hydrographic data. We are thus able to base our characterization of the flow over this shelf on plentiful information. Our analysis of this suite of data (Table 5-1) is still incomplete. We expect further analysis building on this preliminary report to improve understanding, but not to change fundamentally the conclusions that we present here.

The most important discovery as a result of these new data is the existence of three distinguishable flow regimes over the shelf. These flow regimes correspond closely to the hydrographic domains outlined in the preceding chapter. The coastal regime is shoreward of the 50 m isobath, the middle regime is between the 50 m and 100 m isobaths, and the outer regime is between the 100 m isobath and the shelf break. Seaward of the shelf break lies the oceanic regime. Although they nearly coincide, for clarity we refer to flow *regimes* and hydrographic *domains* in this and the previous chapter.

We emphasize the characteristics of these regimes as we examine the frequency distribution of the horizontal kinetic energy, the mean circulation, and seasonal variations. Before discussing our findings, we review the physical setting, highlight earlier work, and discuss our measurements.

Setting

The southeastern shelf is bounded by the Alaska Peninsula, the Alaskan mainland, the shelf break

Tides of the Eastern Bering Sea Shelf

Carl A. Pearson,¹ Harold O. Mofjeld,² and Richard B. Tripp³

¹ National Ocean Survey, assigned to:
Pacific Marine Environmental Laboratory/NOAA
Seattle, Washington

² Pacific Marine Environmental Laboratory/NOAA
Seattle, Washington

³ Department of Oceanography
University of Washington
Seattle, Washington

ABSTRACT

The acquisition of a substantial amount of pressure-gauge and current-meter data on the Bering Sea shelf has permitted a much more accurate description of the tides than has previously been possible. Cotidal charts are presented for the M_2 and, for the first time, the N_2 , K_1 , and O_1 constituents, and tidal current ellipse charts for M_2 and K_1 . S_2 , normally the second largest semidiurnal constituent, has not been included because it is anomalously small in the Bering Sea. The tide enters the Bering Sea through the central and western Aleutian Island passes and progresses as a free wave to the shelf. Largest tidal amplitudes are found over the southeastern shelf region, especially along the Alaska Peninsula and interior Bristol Bay. Each semidiurnal tide propagates as a Kelvin wave along the Alaska Peninsula but appears to be converted on reflection in interior Bristol Bay to a Sverdrup wave. A standing Sverdrup (Poincaré) wave resulting from cooscillation in Kuskokwim Bay is evident on the outer shelf. The semidiurnal tides are small in Norton Sound where there is an amphidrome. The diurnal tides, which can have only Kelvin wave dynamics, cooscillate between the deep basin and the shelf. Amphidromes are found between Nunivak Island and the Pribilof Islands, and west of Norton Sound. Throughout most of the shelf the tide is of the mixed, predominantly semidiurnal type; however, the diurnal tide dominates in Norton Sound.

Tidal models by Sünderman (1977) (a vertically integrated M_2 model of the entire Bering Sea) and by Liu and Leendertse (1978, 1979) (a three-dimensional model of the southeastern shelf incorporating the diurnal and semidiurnal tides) are discussed. Good qualitative agreement is found between the models and observations.

INTRODUCTION

As with most continental shelves, the tides and tidal currents on the eastern Bering Sea shelf play important roles in such oceanographic processes as the maintenance of the density structure, sediment resuspension and transport, and the distributions of benthic and intertidal organisms. A knowledge of the tides and tidal currents is therefore necessary in order to understand the region's oceanography. The tides of the Bering Sea have been of interest to physical oceanographers and astronomers for a long time (e.g., Jeffreys 1921, Munk and MacDonald 1960, Cartwright 1979). This interest has been based on the premise that the vast continental shelves of the Bering Sea (Fig. 8-1), with their proximity to the Pacific Ocean, act as a major sink of the world's tidal energy. Yet many aspects of the tides and tidal currents in the Bering Sea have remained unknown because inadequate data made it impossible to draw definitive cotidal charts or to obtain reliable boundary conditions for numerical models. Fortunately, in recent years a large number of pressure-gauge and current-meter observations have been made on the eastern Bering Sea continental shelf, and the new data make possible a more detailed description of the tides in the eastern Bering Sea.

Kinder, T.H., J.D. Schumacher and D.V. Hansen, 1980: Observations of a baroclinic eddy: an example of meso-scale variability in the Bering Sea. *J. Phy. Oc.*, 10: 1228-1245.

1228

JOURNAL OF PHYSICAL OCEANOGRAPHY

VOLUME 10

Observation of a Baroclinic Eddy: An Example of Mesoscale Variability in the Bering Sea

THOMAS H. KINDER

Naval Ocean Research and Development Activity, Code 331, NSTL Station, MS 39529

JAMES D. SCHUMACHER

Pacific Marine Environmental Laboratory, Environmental Research Laboratories, NOAA, Seattle, WA 98105

DONALD V. HANSEN

Atlantic Meteorological and Oceanographic Laboratories, Environmental Research Laboratories, NOAA, Miami, FL 33149

(Manuscript received 26 March 1979, in final form 27 March 1980)

ABSTRACT

Drift buoys with shallow (17 m) drogues, released during May 1977 and tracked by satellite, delineated an eddy in the southeastern Bering Sea. Located above complex topography having a depth range of 200 to 3000 m, the eddy had a diameter of about 150 km. Mean rotational speeds ~50 km from the eddy's center were 20 cm s^{-1} , but speeds up to 50 cm s^{-1} were measured. A CTD survey during July defined the eddy from 200 to 1500 m depth in temperature and salinity distributions, but no hydrographic evidence for the eddy existed at the surface. A geostrophic calculation relative to 1500 m agreed qualitatively with drifter data, but was -5 cm s^{-1} less than mean drifter speeds. Examination of the *T-S* correlation showed that water masses at the eddy's core were the same as those at its periphery, in contrast with a cyclonic ring observed nearby in July 1974. The last drifter left the eddy in October, and a second CTD survey in February 1978 showed that the eddy had either dissipated or moved.

An earlier STD survey of the region in summer 1971 had shown neither an eddy like that seen in 1977 nor a ring like that seen in 1974. In spite of the ubiquitous inclusion of permanent eddies and steady currents in Bering Sea circulation schemes, recent evidence from synoptic data suggests that the hydrographic and velocity fields are highly variable on scales of 50 to 200 km and a few weeks to a few years. While we do not understand the generating mechanism for this eddy, current instability, wind forcing and topographic interaction all remain plausible candidates. Because of the eddy's size and location, we believe that it formed within the southeastern Bering Sea.

EXECUTIVE SUMMARY

This report presents a summary of the major findings of Outer Continental Shelf Environmental Assessment Program research into physical oceanographic conditions in the northwest Gulf of Alaska. The stress is on circulation features, since water circulation plays a major role in the path and dispersal of surface contaminants, a problem of major impetus for the OCSEAP program. Reference is made throughout this summary section to Figure 1, which summarizes the net circulation regime as deduced from this study. On the figure, arrows depict sense of net flow while the numbers represent a typical range of current speeds, in centimeters per second, which might be encountered in that region. In general, the smaller numbers represent spring-summer conditions while the larger numbers represent autumn-winter conditions. It is stressed here that instantaneous flow observed at a given time need not agree with our simplified graphical depiction. The patterns shown are, rather, indicative of mean conditions and of a normal response to the dynamics which we feel exert dominant control over the system.

The results can be summarized as follows:

1. The Alaskan Stream is a major regional oceanic circulation feature. It flows southwesterly, roughly coincident with the shelf break and slope, with mean speeds of 50-100 cm sec⁻¹. Its width is about 50 km, and its computed annual mean baroclinic volume transport is about $12 \times 10^6 \text{ m}^3 \text{ sec}^{-1}$. There was no significant annual variability detected either in baroclinic current speed or volume transport. There were eddy-like perturbations observed in the current, at times, which appeared to be related to bottom

topography. A principal driving force for the Alaskan Stream is the wind stress curl over the Gulf of Alaska, which forces the North Pacific subarctic gyre. The Alaskan Stream is the intensified, northwestern leg of this gyre.

2. Dominant circulation on the banks south and southeast of Kodiak Island is predominantly driven by the Alaskan Stream. This includes a poorly defined, weak ($5-10 \text{ cm sec}^{-1}$) anticyclonic circulation over Portlock Bank, and a complex flow regime connected with the bank-trough region to the southwest. This bank-trough flow, which apparently represents a bathymetric effect upon the inshore edge of the Alaskan Stream, consists of shoreward flow along the upstream (northeastern) sides of the troughs and a compensatory seaward flow along the downstream (southwestern) sides. The coastal southwesterly flow at the head of Kiliuda Trough reflects this residual circulation, but is probably also due in part to a baroclinic coastal wedge consequent to freshwater input along the south coast of Kodiak Island.

3. A nearshore southwesterly flow along the Kenai Peninsula, the Kenai Current, is a baroclinic coastal current driven by the density field created by freshwater input along the Alaskan coast. This flow is 20-30 km in width and attains maximum current speeds in autumn following the annual period of maximum coastal precipitation and freshwater input. This flow is at its annual minimum during spring and early summer.

4. Flow through Shelikof Strait is southwesterly, with observed speeds during winter ($\sim 20 \text{ cm sec}^{-1}$) twice those in summer ($\sim 10 \text{ cm sec}^{-1}$). No flow reversals were observed during winter; during summer, the weaker mean flow was accompanied by occasional reversals. This flow is driven in part by the Kenai current upstream and in part by a large-scale alongshore pressure gradient established by the Alaskan Stream. The flow through Shelikof Strait continues to the southwest in a well-defined channel bounded by

relatively shallow banks, merging with the Alaskan Stream some 200 km southwest of Kodiak Island.

5. Circulation in lower Cook Inlet is dominated by the southwesterly flow into Shelikof Strait, which is constrained by bottom topography to traverse an arcuate east-west path across the lower Inlet. Off Cape Douglas, this flow merges with a weaker southward current generated by the freshwater input to upper Cook Inlet, creating a particularly intense southward flow in the region off Cape Douglas. Flow in the central lower inlet out of these two well-defined currents is weak and highly variable.

6. Currents throughout the study region are characterized by speed and direction fluctuations having time scales between about 2 days and a week. These fluctuations are probably related either to meteorological factors or to propagation of ocean eddies across the shelf, though the exact mechanisms are uncertain. In regions such as Shelikof Strait, with a strong mean flow, these fluctuations are of lesser significance relative to the mean flow, leading to speed fluctuations but only minor perturbations to direction. In regions of weak mean flow, such as in central lower Cook Inlet and on Portlock Bank, the fluctuations both in speed and direction are the dominant flow characteristics.

7. Tidal currents vary widely in magnitude throughout the study region. Tidal current effects in Shelikof Strait are minimal because of the standing wave nature of the tidal wave there, and tidal currents become small as the coast is approached south of Kodiak Island. Lower Cook Inlet is characterized, conversely, by large tidal currents particularly in the passages north and south of the Barren Islands due to the near-resonant conditions which lead to extremely large tides in upper Cook Inlet. Tidal currents are also significant in comparison with mean flow on the banks south of Kodiak Island.

8. Winds are controlled by the interaction between large-scale north-eastward migrating cyclonic low pressure systems and regional topography. Over the banks south of Kodiak Island, observed winds appear to agree reasonably well with geostrophic winds computed from the atmospheric surface pressure distributions. In lower Cook Inlet, winds are orographically channelled into two orthogonal paths whose axes are aligned with upper Cook Inlet-Shelikof Strait and Barren Islands-Kamishak Bay. This leads to a complex wind pattern there which results from the interaction between these orthogonal flows. Katabatic (drainage) winds may be important locally, particularly in lower Cook Inlet and Shelikof Strait, and wake effects perturb the wind field downstream from such features as Augustine Island.

The picture presented here of major circulation features in the northwest Gulf of Alaska is one of extreme complexity. The various possible combinations of mean, low frequency fluctuating and tidally fluctuating flow lead to a regime wherein prediction of instantaneous flow is impossible. We believe, however, that the flow field has been sufficiently well defined to allow a good prediction of seasonal mean flow. Combined with knowledge of the local and regional wind field, this allows at least an approximate predictability of contaminant dispersion and trajectory.

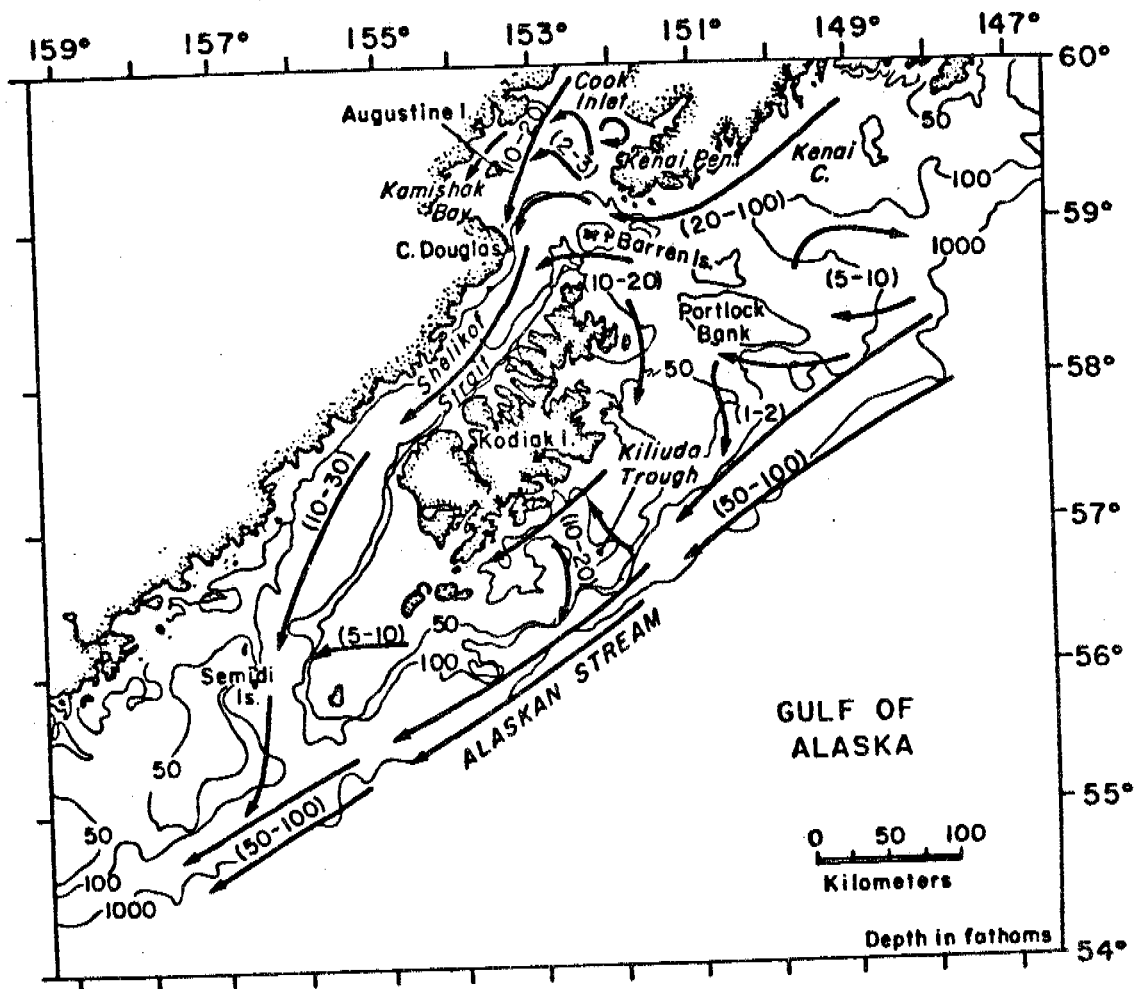


Figure 1. Schematic diagram of net circulation in the northwest Gulf of Alaska. Arrows indicate direction of mean surface flow, and numbers in parentheses indicate approximate range of speeds in cm sec⁻¹.

VII. Needs for Further Study

Upon completion of field operations in June 1981, we will have collected the data sets required to meet our specific goals. Undoubtedly analysis of the data will generate new questions, however, the information required by BLM can be supplied by analysis interpretation and very importantly, synthesis of information from all NASTE RU's. Thus, for FY82, we propose to analyze and interpret physical oceanographic data and then combine such results with results from the other programs.

VIII. Conclusions

Field work in the Bristol Bay region has yielded more complete understanding of the physical oceanography. This understanding is reflected in Section IV of this report (present status), in previous reports, and in the publications listed in Section VI. Some major conclusions from field operations during 1980 (see Section IV for more details) are:

- 1) Vector mean flow through Unimak Pass is from the Gulf of Alaska to the Bering Sea and exhibits a strong seasonal trend. Forcing for vector mean flow appeared to be coastal flow along the Alaska Peninsula while low-frequency fluctuations were highly coherent with changes in the atmospheric pressure gradient normal to the pass.
- 2) Although tides dominate horizontal kinetic energy over the north Aleutian shelf, sub-tidal flow in the near-surface ($\sim 5\text{m}$) layer was highly coherent with wind.
- 3) Storms can mix the middle shelf domain water column at least 50 km from shore. Subsequent reestablishment of "mean" hydrographic conditions resulted from a combination of cross-shelf fluxes and tidal mixing.

IX. Milestone Update: RU 549, Schumacher and Pearson
 0 planned completion date; X actual completion date

Milestone	1980					1981						
	O	N	D	J	F	M	A	M	J	J	A	S
I. Field Operations:												
Cruise #2				—								
Cruise #3								—				
II. Reports:												
Cruise Report #1		0										
Cruise Report #2								0				
Cruise Report #3										0		
Unimak Pass			0									
Results from Aug 80 to Jan 81								0*				
R2D2 Guide				0				X				
Results from vertical mixing experiment (TP3)				X(AGU)				0				
Results from Jan to June 81												Due Jan 1982
III. Meetings:												
PI Workshop						0						
St. George Basin Synthesis meeting								0				

398

* ... wind and pressure records were collected and are now in quality control.

IV. Present Status

IV. A

A REVIEW OF CIRCULATION PATTERNS

PROPERTY DISTRIBUTIONS AND

PROCESSES OVER THE

OUTER SHELF DOMAIN

by

J. D. Schumacher

1. Introduction

The eastern one half of the Bering Sea is underlaid by a vast, relatively flat and shallow shelf (figure 1). The southeastern portion of this shelf includes the "outer shelf" domain which has been defined (Kinder and Schumacher, 1981a) as that portion of the shelf between Unimak Pass and St. George Island, and from the shelf break (~170m) landward to the 100m isobath. The domain area is about $5 \times 10^4 \text{ km}^2$ with a volume of $6 \times 10^3 \text{ km}^3$. This shelf supports one of the world's richest fisheries and also has potentially large quantities of petroleum in the St. George basin lease area. The Bureau of Land Management, through the Outer Continental Shelf Environmental Program (OCSEAP), has funded physical oceanographic studies designed to elucidate important transport processes in this region.

This report is a summary of results from OCSEAP and Processes and Resources of the Bering Sea Shelf (PROBES) studies, including the following publications: Coachman and Charnell, (1977,1979); Kinder and Coachman, (1978); Coachman, Kinder, Schumacher and Tripp, (1980); Kinder, Schumacher and Hansen (1980); Kinder and Schumacher, (1981a,1981b); Pearson, Mofjeld and Tripp, (1981); and several recent PROBES (Coachman, 1979,1980) and OCSEAP (Schumacher and Pearson, 1981) unpublished reports.

2. Circulation

Forcing mechanisms for shelf flow include interactions with oceanic currents, baroclinicity, winds and tides. The domain is bounded on the west by the Bering Slope Current which flows parallel to the shelf break from near Unimak Pass to near Cape Navarin. The current is broad (~200 km) with speeds of 5 to 15 cm/sec and transports $\sim 5 \times 10^6 \text{ m}^3/\text{sec}$ (Kinder, Coachman and Galt, 1975). During summer 1977, six satellites tracked drifters (drogued at 17 m) were deployed over the shelf/slope region north of Unimak Pass. The results (figure 2) indicate that over the basin meso-scale (10-100 km radius) eddies were present. Maximum speeds were $\sim 50 \text{ cm/sec}$, however, vector mean speeds were 5 to 15 cm/sec towards the northwest with even lower (1 to 3 cm/sec) vector movement over the shelf (Kinder, Schumacher and Hansen, 1980). There is no evidence that the Bering Slope Current flows over the shelf proper; however, interactions between eddies and bathymetry can result in along-shelf pressure gradients which could drive cross-shelf barotropic flow (Csanady, 1978; Beardsley and Winant, 1980).

Kinder and Schumacher (1981a) have summarized current data (figure 3) and note that tides dominate horizontal kinetic energy (HKE), accounting for 60 to 80% of the total kinetic energy. Over the outer shelf domain, low frequency flow accounted for 20 to 40% of the energy (frequencies in these bands match those of weather phenomena, say 2 to 10 days, and of longer period variability of the Bering Slope Current). As shown in figure 3, vector mean flow generally has a larger component parallel to the bathymetry and a lesser cross-shelf flow component (see also Table 1, adapted from Kinder and Schumacher, 1981a). These authors noted that the current records contain little or no seasonal signal at any frequencies. The increase in kinetic energy of the wind was not reflected in current spectra. Although there were year to year changes in low

frequency energy, these occurred at period longer than 10 days and hence were probably associated with changes in oceanic forcing. Further, there was little spatial or vertical coherence except at tidal frequencies.

Current records in the spring of 1980 from either side of the middle front (Coachman, 1980) showed that over a period of one month there was a convergence of 3 cm/sec at the middle front. This helps to maintain the characteristic isopleth distributions marking the front and requires an upwelling at the middle front to preserve continuity. But the convergence was not steady over a period of a few days; there was one 2-day period when the current records indicate divergent flow. Such perturbations appeared to be related to onshore/offshore winds. An example of non-steady currents which imply convergence is shown in Figure 4. The record in panel (A), which was obtained from the outer shelf domain, indicates a vector mean cross-shelf flow of 2 cm/sec. The record from the middle shelf domain (B) shows a vector mean current less than 1.0 cm/sec.

Tidal frequencies contained most of the energy over the outer shelf and roughly 80% of this energy was semi-diurnal and 20% diurnal with ellipses major axes directed cross-shelf (cf. figure 5 and TABLE 1B, from Pearson, Mofjeld and Tripp, 1981). The observed tidal speeds (10 to 30 cm/sec) result in tidal excursions of about 5 to 7 km. Tides are considered to be primarily responsible for the cross-shelf flux of salt required to maintain the observed mean salt balance; over most of this shelf, tidal diffusion appears to be the dominant transport mechanism (Coachman *et al.*, 1980).

Three current meters, deployed in March 1980 and recovered in August 1980, provide the only direct observations of current from Unimak Pass (figure 5). Preliminary results (Schumacher, Pearson and Overland, 1981) indicate that unlike currents on the outer shelf, there was a strong seasonal signal:

TABLE 1A
SUMMARY OF CURRENT RECORDS

Mooring	Water Depth (m)	Meter Depth (m)	Scalar Speed (cm/sec)		Mean Speed ¹ Along Cross (cm/sec)		Record Length (Days)	Period
BC-3A	115	20	29.0	1.8	2.7	130	11/7/75-3/16/76	
BC-3B	116	25	27.8	2.7	0.9	9	3/17/76-3/25/76	
		105	17.4	1.1	0.5	73	5/29/76-5/28/76	
BC-3C	114	20	31.8	9.4	14.2	123	5/29/76-9/28/76	
		100	20.5	4.7	4.7	123	5/29/76-9/28/76	
BC-13A	122	20	20.6	2.6	2.0	69	3/22/76-5/29/76	
		100	11.9	1.3	0.9	87	3/22/76-6/16/76	
BC-13B	115	100	17.3	1.5	0.5	36	6/6/76-7/12/76	
BC-13C	108	22	25.2	5.0	1.6	202	9/29/76-4/19/77	
		96	16.1	4.4	0.4	83	9/29/76-12/21/76	
BC-17A	104	96	18.1	3.0	-1.0	142	9/22/76-3/11/77	

¹This is the vector mean resolved into alongshelf (315°T) and cross shelf (45°T) components.

TABLE 1B
TIDAL CURRENT STATISTICS

Station	Depth	Meter Depth	Lat N	Long W	O ₁												K ₁												N ₂												M ₂											
					major						min						major						min						major						min																	
					Yr	JD	H	G	D	H	R	H	G	D	H	R	H	G	D	H	R	H	G	D	H	R																										
BC3	114	20	55	02	165	10	76	150	7.9	245	52	1.7	C	9.8	279	57	1.0	C	6.5	26	37	1.8	C	26.4	71	38	7.6	C																								
BC3	114	100	55	02	165	10	76	150	7.8	265	52	1.2	C	10.4	281	48	2.1	C	4.9	11	50	0.6	C	21.0	61	47	4.4	C																								
BC13B	115	100	55	30	165	49	76	158	5.6	272	71	2.2	C	8.0	289	68	2.8	C	5.3	3	50	2.2	C	18.9	67	54	9.6	C																								
BC17	104	96	56	34	167	24	76	266	4.5	312	109	1.8	C	9.1	326	105	4.3	C	6.4	27	61	4.0	C	15.9	81	53	10.5	C																								
BC4	51	30	58	37	168	14	75	251	7.4	330	140	3.1	C	11.7	350	133	6.2	C	9.6	45	49	7.2	C	27.3	118	80	22.2	C																								
BC4	51	47	58	37	168	14	75	251	7.9	331	128	2.6	C	10.9	0	131	4.8	C	4.9	28	46	3.3	C	30.2	107	51	15.1	C																								
BC9	41	33	58	12	167	43	77	133	8.5	332	130	0.9	C	13.0	359	134	2.9	C	7.0	60	47	5.1	C	18.7	120	51	14.6	C																								
BC18	31	20	58	40	167	07	77	132	12.7	333	113	0.6	A	20.5	356	116	0.1	A	6.3	130	109	4.8	C	21.2	186	103	13.8	C																								
BC16	80	37	57	58	165	16	77	133	7.7	308	102	1.3	A	11.4	328	108	1.5	A	6.8	68	69	6.8	C	20.8	101	82	15.1	C																								
BC2	65	50	57	04	163	22	75	210	8.6	292	77	1.1	A	14.1	309	81	1.6	A	5.9	76	81	2.9	C	20.4	145	80	12.1	C																								

¹ Amplitudes H are cm/sec, phases G are referred to Greenwich, and direction D of major axis is compass degrees. C refers to clockwise rotation, A to anti-clockwise. To obtain phase and direction of minor axis, add 90° to major axis direction; then add 90° to major axis phase if rotation is clockwise, or subtract 90° if anticlockwise.

vector mean flow was ~ 20 cm/sec into the Bering Sea between March and May and ~ 5 cm/sec for the remainder of the observation period (figure 6). A forcing mechanism for net inflow appears to be baroclinic flow along the Pacific side of the Alaska peninsula. This feature may be similar to the Kenai Current (Schumacher and Reed, 1980). The fluctuations were coherent with estimated atmospheric pressure gradient fluctuations normal to the peninsula. Changes in magnitude and direction of the atmospheric pressure gradient (hence winds) apparently drove flow reversals (up to 2.5-day duration) which occurred in 18% of the winter and 31% of the summer 35 hr filtered current observations. The authors note that large-scale winds may be from a different direction than those through the pass, since the latter winds are directly down the local pressure gradient.

3. Hydrographic Characteristics

The outer shelf can be defined in terms of vertical structure (figure 9), where the energy balances generating such structure appear tied to local bathymetry, and hence, the domains are nearly fixed in space (Kinder and Schumacher, 1981a). Since the water depth over the outer shelf typically exceeds the sum of the depth of wind and tidally stirred layers, there is a layer at mid-depths where energy for vertical mixing is low. Further, while waters over the middle shelf exhibit different temperatures and salinities (figure 10; TABLE 2), they are approximately the same density. As noted by Coachman and Charnell (1977, 1979) this juxtaposition of water types, under the influence of a pressure gradient, will result in interleaving of waters: the large-scale exchange is in the form of an intrusion of slope waters cross-shelf in a bottom layer and a seaward movement of middle shelf water at mid-depths. The seaward mid-layer movement is in the form of interleaving sheets and layers at finestructure scales (1-10m thick).

TABLE 2

HYDROGRAPHIC CHARACTERISTICS
OF
MIDDLE AND OUTER SHELF WATER

	<u>MIDDLE</u>	<u>OUTER</u>
vertical structure	<p>summer: two-layered with the upper layer 10 to 30m. Similar structure observed under ice.</p> <p>winter: well mixed (also observed during storms)</p>	<p>surface mixed layer (40-50m in winter, 10-30m in summer); stratified interior; bottom mixed layer (10-30m thick).</p>
depth	<p>$50 \leq \text{depth} \leq 100\text{m}$ thickness of surface+ bottom mixed layers</p>	<p>$\leq 100\text{m}$, greater than surface+ bottom mixed layers. Interior region contains (fine-structure).</p>
temperature ¹	<p>summer: upper layer: 8 to 11°C lower layer: -1 to 4°C</p> <p>winter: -1.5 to 3°C</p>	<p>7 to 10°C 3 to 5°C</p> <p>1 to 3°C upper 3 to 5°C lower</p>
salinity	<p>upper layer: 31.9 to 32.2 ‰ lower layer: 32.0 to 32.4 ‰</p>	<p>31.8 to 32.8 ‰ 32.5 to 33.5 ‰</p>

¹Note: The values presented represent maxima and minima since winter 1975/76 was one of extreme ice cover while 1979/80 was a winter of minimal ice cover.

The estimated fluxes (figure 11, from Coachman, et al., 1980) required to maintain a nearly steady state salinity distributions (given the extant freshwater flux) and recent current data (Coachman, 1980) both imply convergent transport at the middle front between middle and outer shelf domains. The result is that over the region about 50 to 75 km wide of a little steeper bottom slope, center ~ over the 100m isobath enhanced horizontal gradients are generated by convergence (middle front). The salt flux model assumed no horizontal flux in the upper layer over the outer shelf, and considering the observed weak vector current motion, is consistent with numerous observations indicating a region of less saline (≤ 32.0 gm/kg) water in the vicinity of the middle front. Over the middle front and across the middle shelf domain, fluxes into the surface layer are reduced during stratification. Hence, the surface layer here is last to regain salt to raise the salinities reduced by ice melt.

At the southeastern portion of the outer shelf domain, in the vicinity of Unimak Pass, both horizontal and vertical salinity gradients (figure 12) are stronger than those observed elsewhere over the outer shelf domain. It is likely that less saline (< 31.5 gm/kg) waters from the Gulf of Alaska flow into this region, resulting in greater gradients.

St. George Island lies at the northwestern corner of the outer shelf domain. Bathymetry shoals to less than 50m rather abruptly around this island. Hydrographic data and satellite infrared imagery indicate transitions occurred between two-layered and well mixed water separated by a structural or inner front (Schumacher, et al., 1979). However, stratified water is found within 10 km of St. George, the inner front appears more diffused and ill defined here where compared to St. Paul or in the vicinity of Nunivak Island. Satellite images show that the inner front does not always encompass the island.

REFERENCES

- Beardsley, R.C. and C.D. Winant, 1979. Mean circulation in the mid-Atlantic bight. J. Phys. Oceanogr., 9(3): 612-619.
- Coachman, L.K. 1980. PROBES Progress Report: Water Circulation and Mixing.
- Coachman, L.K. and R.L. Charnell, 1977. Finestructure in outer Bristol Bay, Alaska. Deep-Sea Res. 24(10): 809-889.
- Coachman, L.K. and R.L. Charnell, 1979. Lateral water mass interactions-a case study, Bristol Bay, Alaska. J. Phys. Oceanogr., 9(2): 278-287.
- Coachman, L.K., T.H. Kinder, J.D. Schumacher and R.B. Tripp, 1980. Frontal systems of the southeastern Bering Sea shelf. In Stratified Flow, 2nd Int. Assoc. Hydraulic Res. Symposium, Trondheim, June 1980, T. Carstens and T. McClimans, Eds. TAPIR Publishers, Norway: pp. 917-933.
- Csanady, G.T., 1978. The arrested topographic wave. J. Phys. Oceanogr., 8(1): 47-62.
- Kinder, T.H., L.K. Coachman and J.A. Galt, 1975. The Bering Slope Current system. J. Phys. Oceanogr., 5: 231-244.
- Kinder, T.H. and L.K. Coachman, 1978. The front overlaying the continental slope of the eastern Bering Sea. J. Geophys. Res. 83: 4551-4559.

Kinder, T.H., J.D. Schumacher and D.V. Hansen, 1980. Observation of a baroclinic eddy: an example of mesoscale variability in the Bering Sea. J. Phys. Oceanogr., 10(8): 1228-1245.

Kinder, T.H. and J.D. Schumacher, 1981a. Hydrographic structure over the southeastern Bering Sea. In The Eastern Bering Sea Shelf: Oceanography and Resources, Vol. 1, D.W. Hood and J.A. Calder, eds. NOAA, Office of Marine Pollution Assessment: pp 31-52.

Kinder, T.H. and J.D. Schumacher, 1981b. Circulation over the continental shelf of the southeastern Bering Sea. In The Eastern Bering Sea Shelf: Oceanography and Resources, D.W. Hood and J.A. Calder, eds. NOAA, Office of Marine Pollution Assessment: pp. 53-75.

Pearson, C.A., H. Mofjeld and R.B. Tripp, 1981. Tides of the eastern Bering Sea shelf. In The Eastern Bering Sea Shelf: Oceanography and Resources, D.W. Hood, and J.A. Calder, eds. NOAA, Office of Marine Pollution Assessment: pp. 111-130.

Schumacher, J.D., T.H. Kinder, D.J. Pashinski and R.L. Charnell, 1979. A structural front over the continental shelf of the eastern Bering Sea. J. Phys. Oceanogr., 9: 79-87.

Schumacher, J.D. and R.K. Reed, 1980. Coastal flow in the northwest Gulf of Alaska: the Kenai Current. J. Geophys. Res., 85: 6080-6088.

Schumacher, J.D., C.A. Pearson and J.E. Overland, 1981. Preliminary results from current, hydrographic and meteorological observations: Unimak Pass, Alaska. In RU541 Quarterly Report to OCSEAP: 43 pp.

FIGURE LEGENDS

- Figure 1. The Bering Sea. The line extending from Bristol Bay to the shelf break indicates the location of hydrographic features on figure 9.
- Figure 2. Drift buoy trajectories (from Kinder, Schumacher and Hansen, 1980).
- Figure 3. Mean currents (from Kinder and Schumacher, 1981b), note that vector mean flow over the middle shelf domain is virtually zero.
- Figure 4. Progressive vector diagram (PVD) from currents observed over (A) outer and (B) middle shelf domains. For the record in (A), the mean alongshelf (indicated by dashed line) speed was 2.6 cm/sec and mean cross shelf speed was 2.0 cm/sec. Over the Middle shelf, the vector mean was 1.0 cm/sec in the cross-shelf direction.
- Figure 5. Current ellipses for the M_2 and K_1 constituents (from Pearson, Mofjeld and Tripp, 1981).
- Figure 6. Location and bathymetry of Unimak Pass. Current meter moorings (\cdot) are also shown.
- Figure 7. PVD and scatter plot presentations of low pass filtered current data from Unimak Pass. Crosses on PD's are 5-day time ticks.

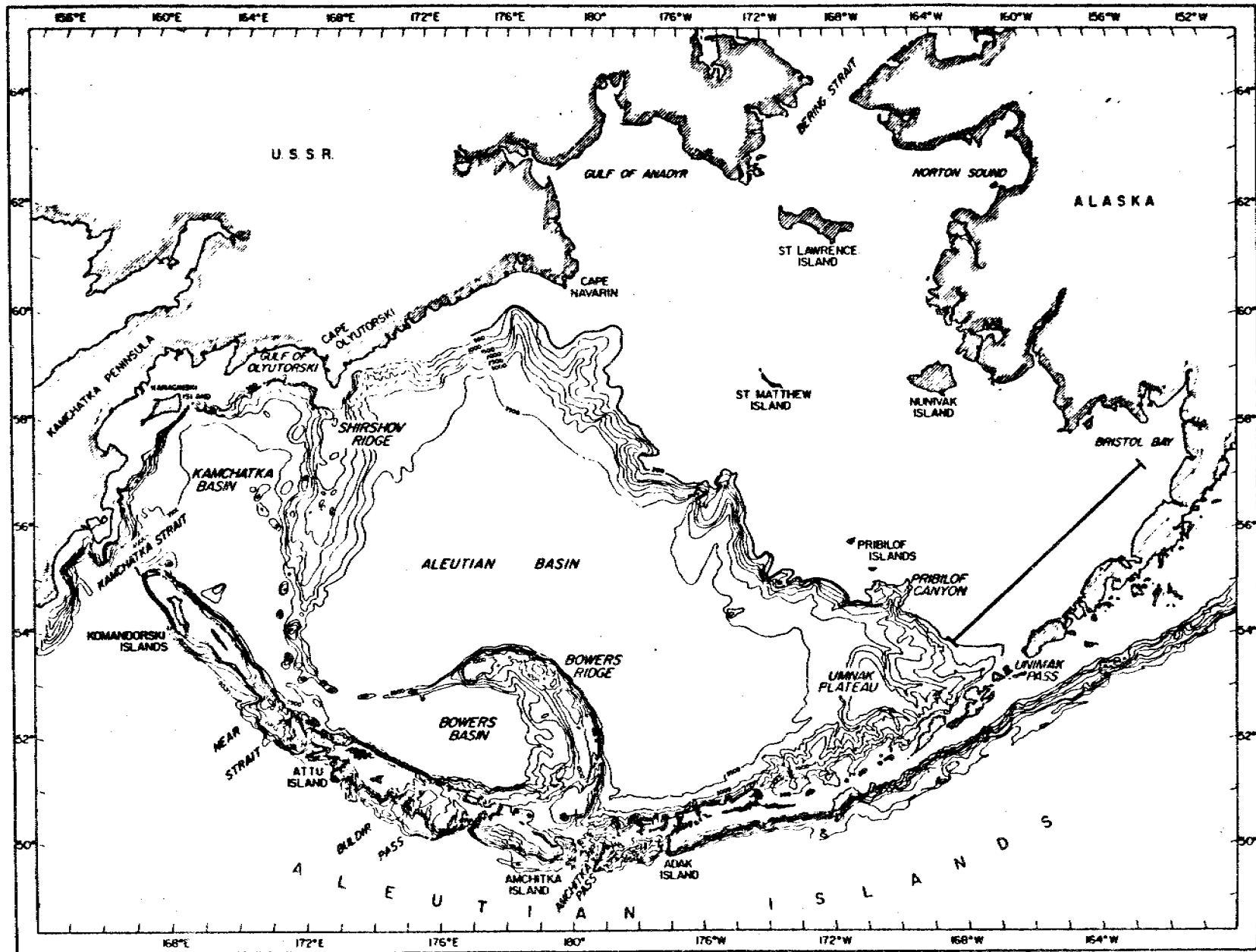
Figure 8. An example of surface atmospheric pressure during a current reversal. The arrow represents the direction of the pressure gradient. Contours are every 4 mb. (From Schumacher, Pearson and Overland, 1981).

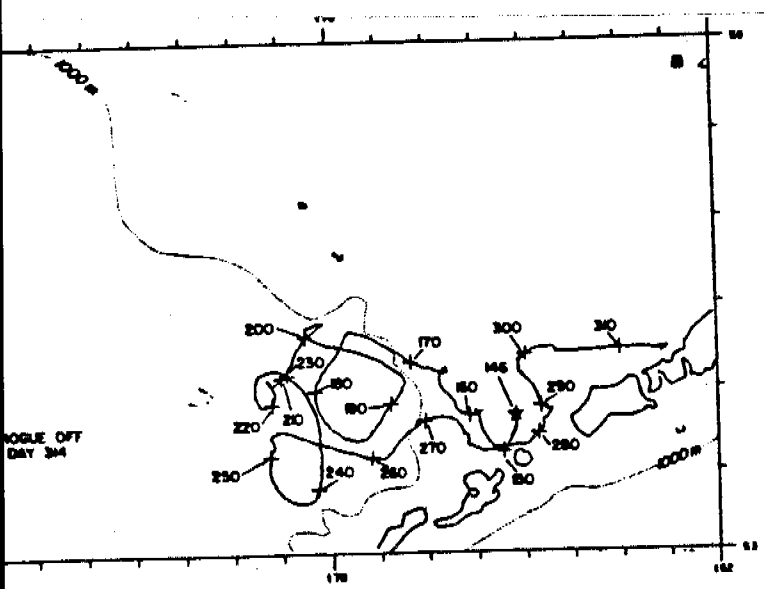
Figure 9. Hydrographic characteristics of southeast Bering Sea shelf waters.

Figure 10. Temperature-salinity correlations, middle domain (SHELF) and oceanic domain (ALASKA STR./BERING). (From Coachman and Charnell, 1979).

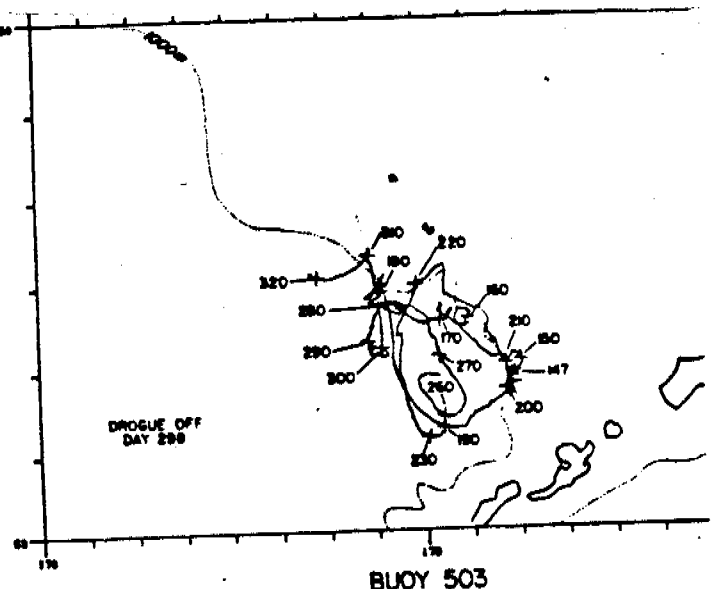
Figure 11. Schematic diagram of the salt balance model. Values of vertical flux and horizontal eddy coefficient for the tidal-diffusive layer for a constant net salt flux = 1 gm/cm sec are shown beneath in relation to their cross-shelf position. (From Coachman, et. al., 1980). Note: the crosses represent baroclinic flow toward the northwest to preserve continuity. Baroclinic flow along the fronts is also an observed phenomenon.

Figure 12 Hydrographic data from Unimak Pass presented as A) temperature B) salinity and C) sigma-t sections. The Δ values are the magnitude of surface minus bottom 1m averaged quantities.

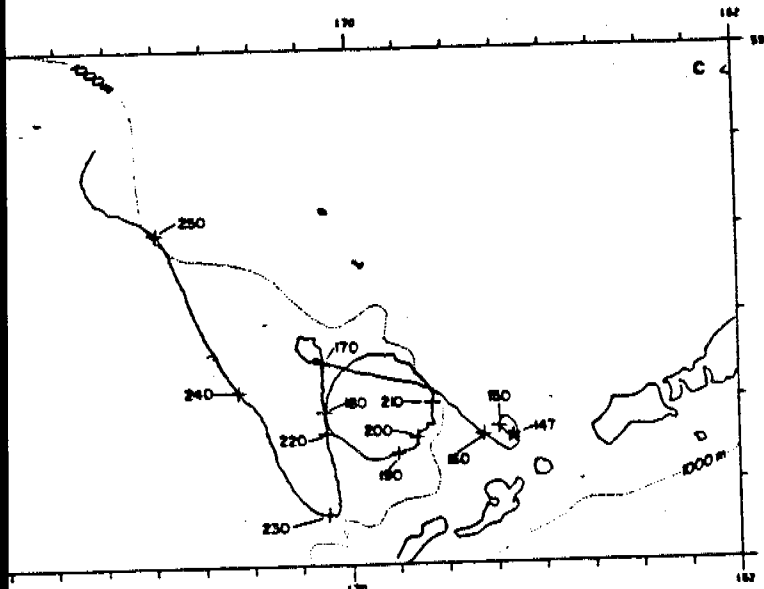




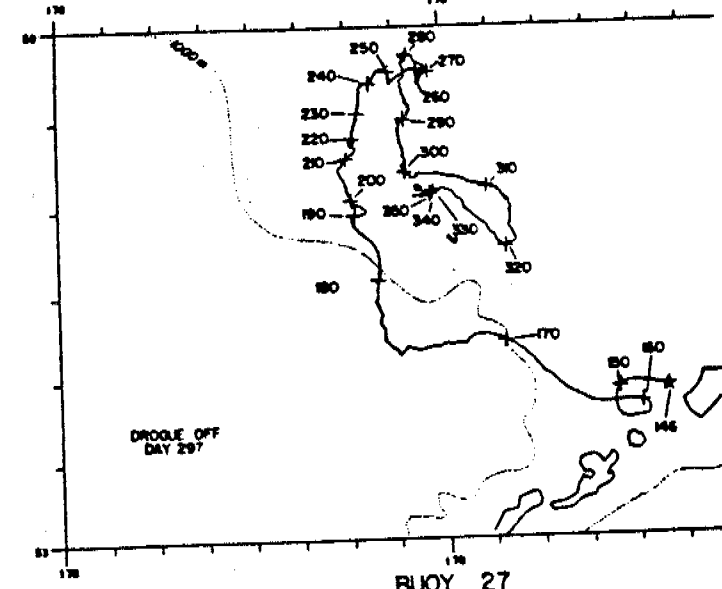
BUOY 56



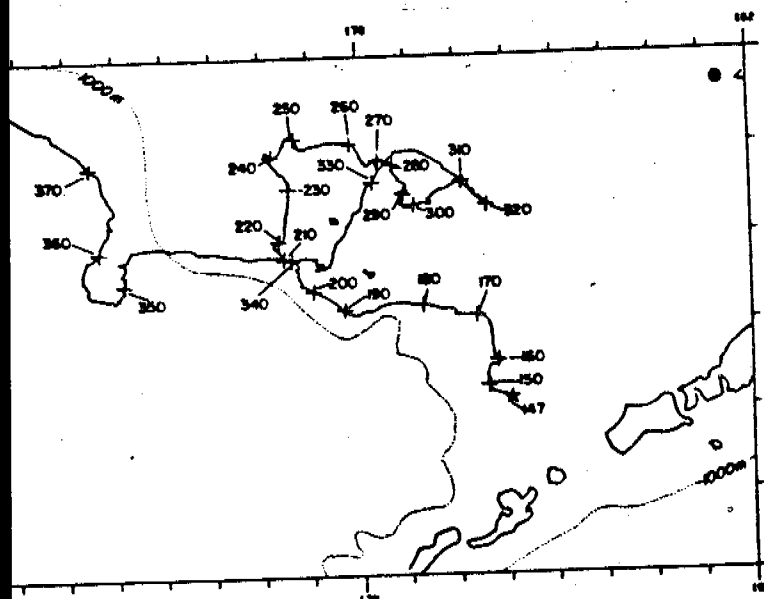
BUOY 503



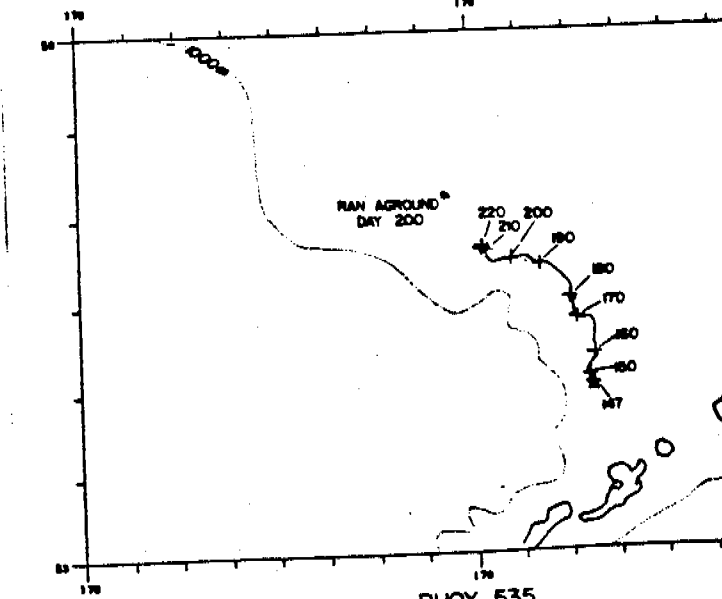
BUOY 544



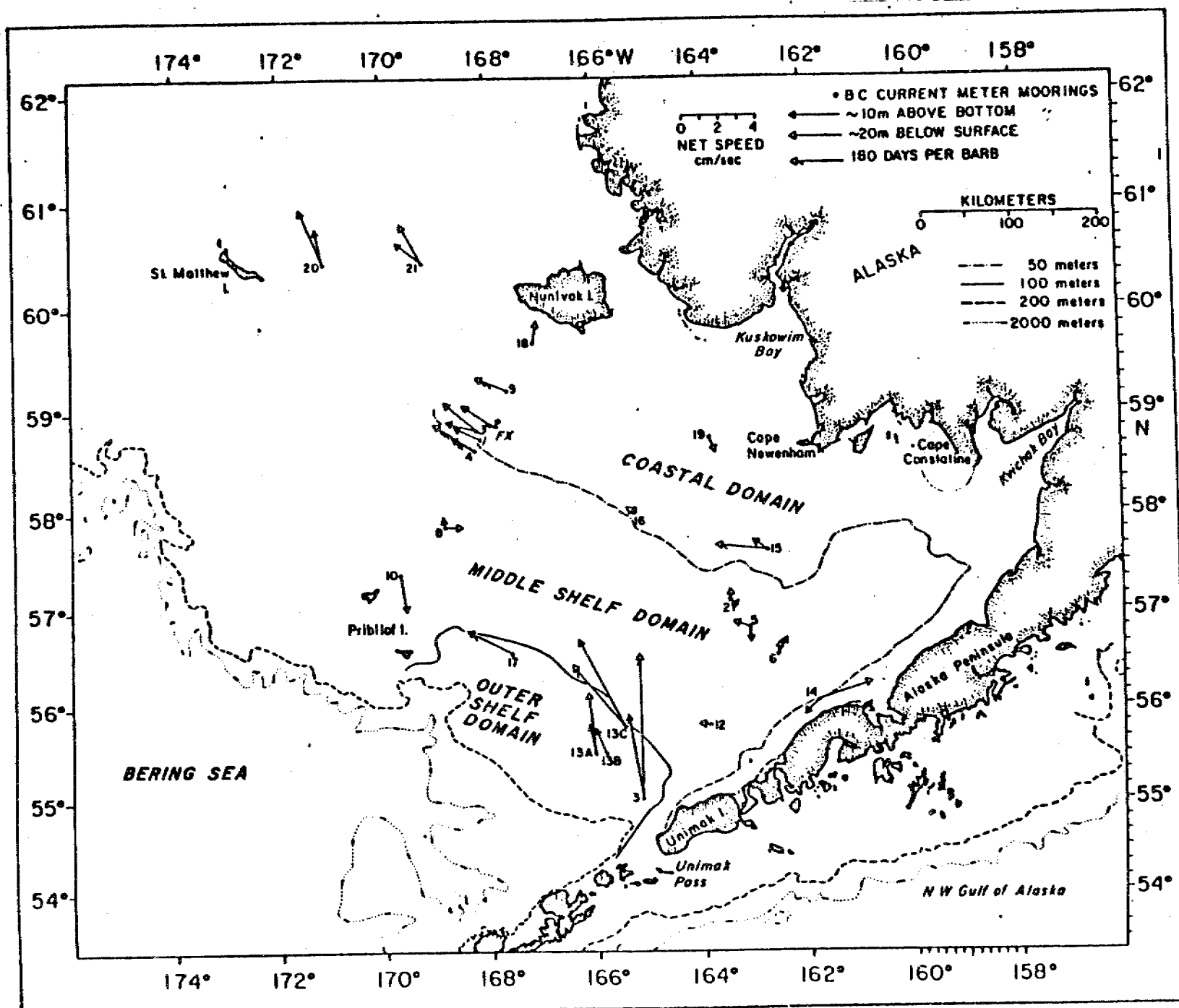
BUOY 27

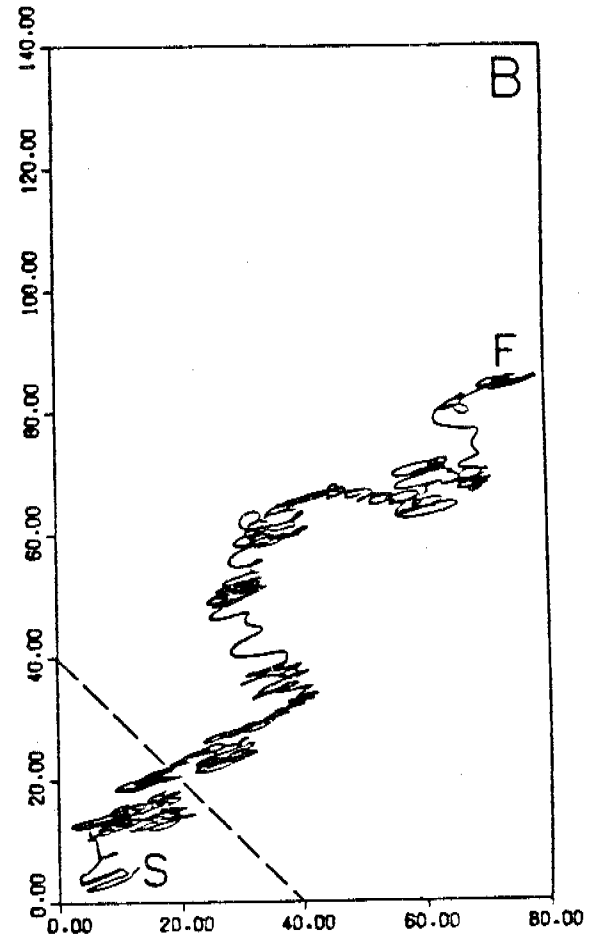
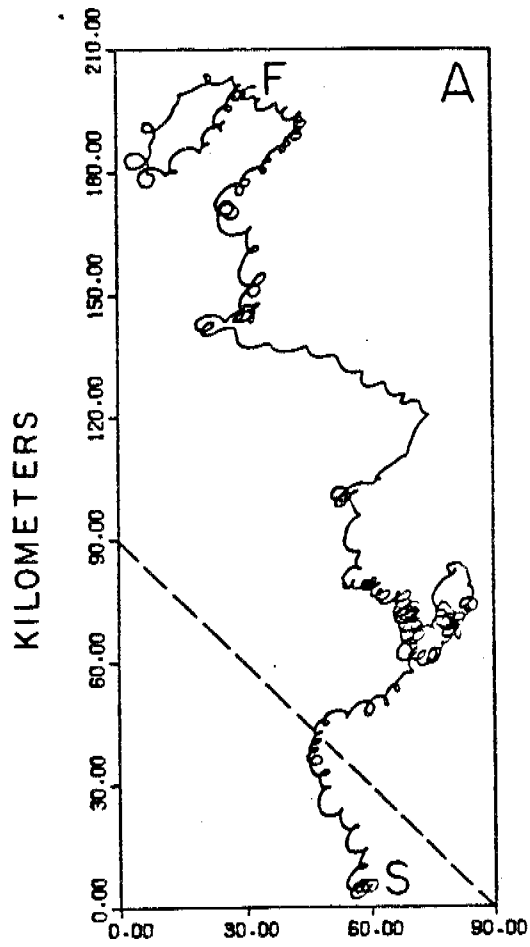


BUOY 11



BUOY 535





KILOMETERS

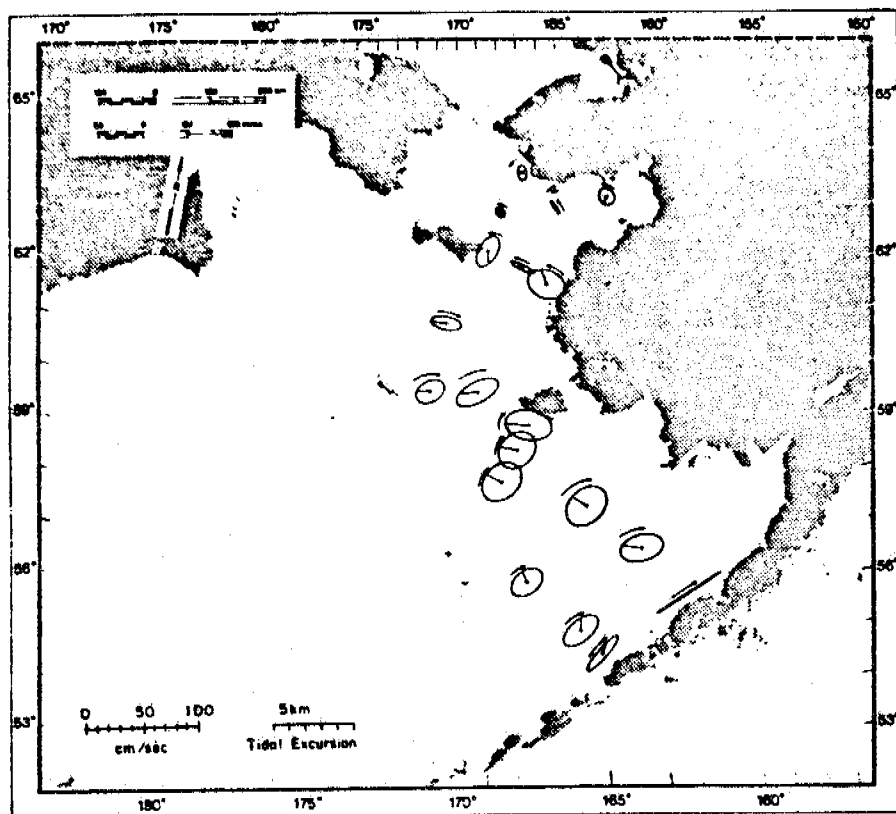


Figure 8-13. M_2 current ellipses for stations listed in Table 8-2. For stations with records from two depths the ellipse for the deeper meter is plotted. Ellipses are centered on station location; line from center indicates constituent current vector when the M_2 Greenwich equilibrium phase angle is 0° . Arrows indicate sense of rotation.

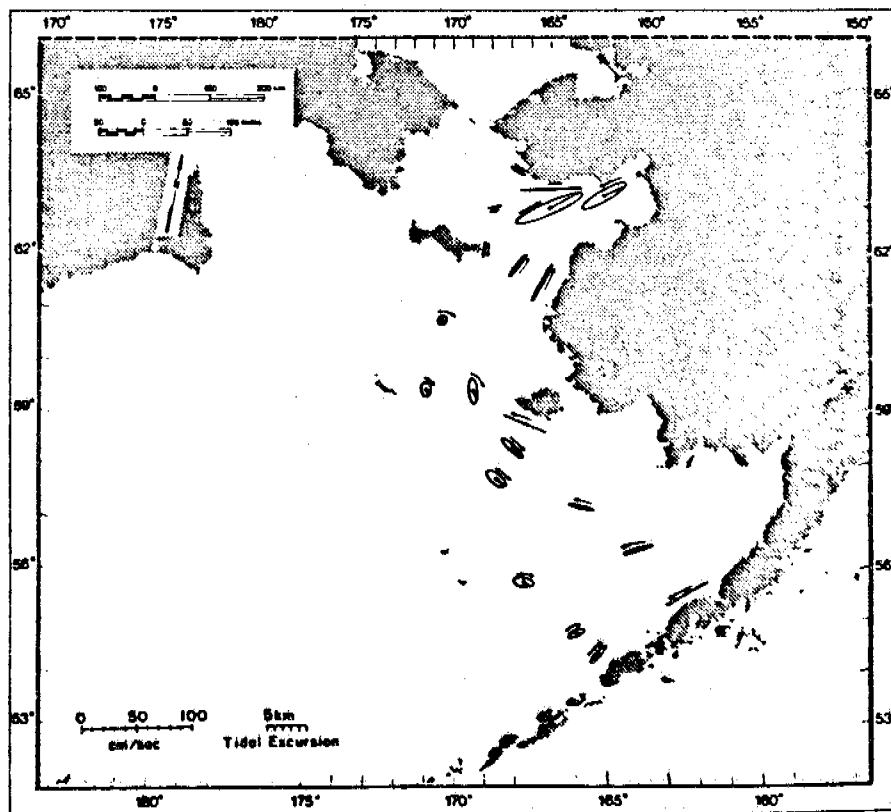
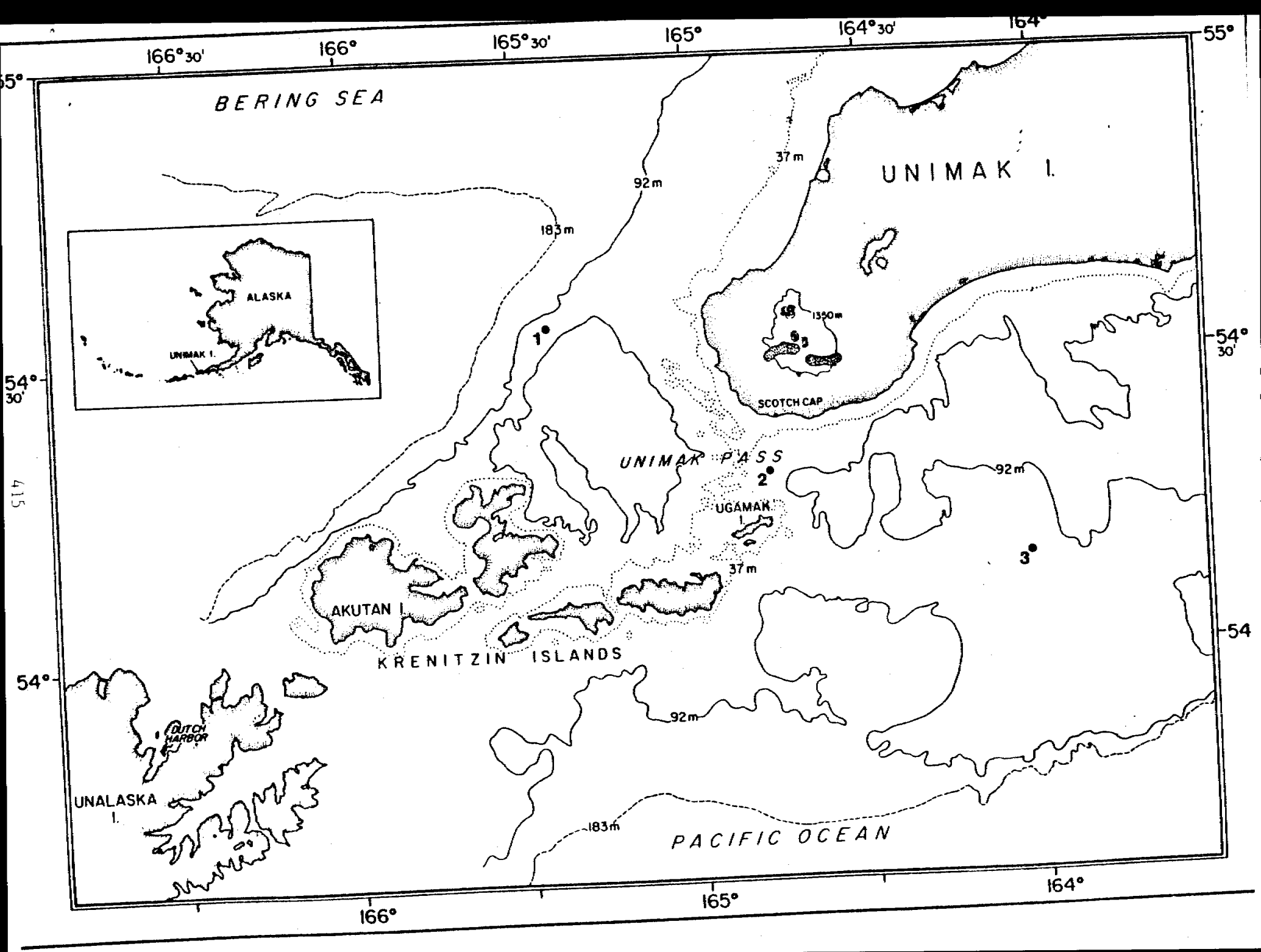
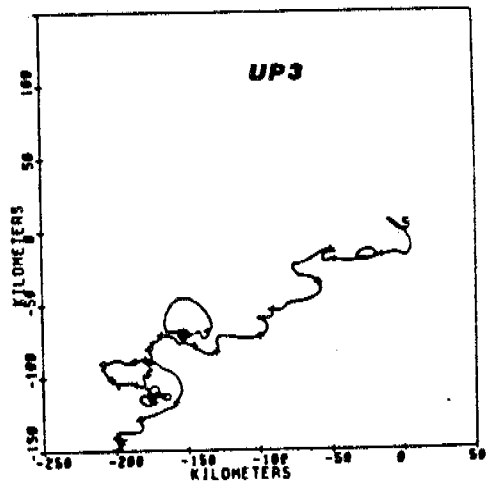
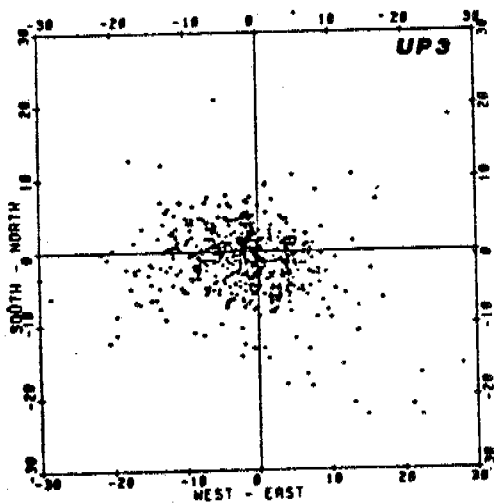
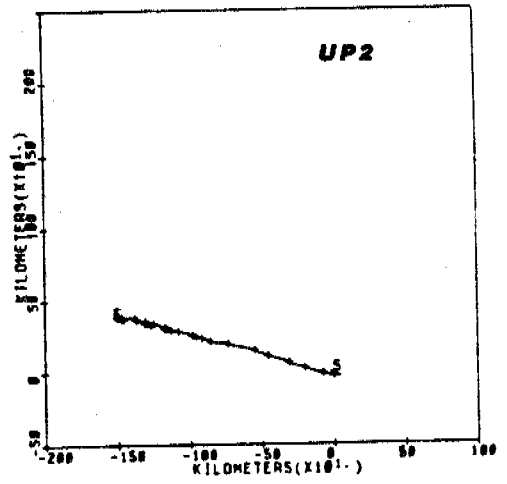
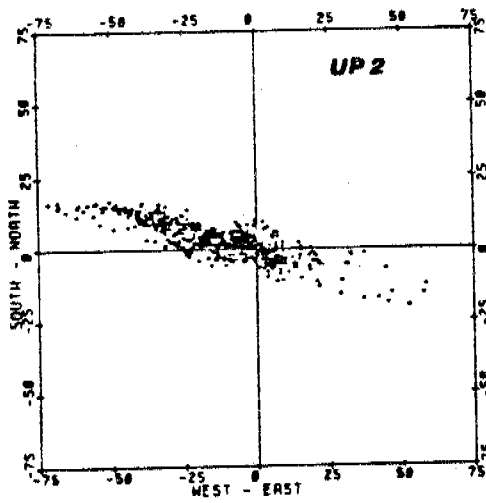
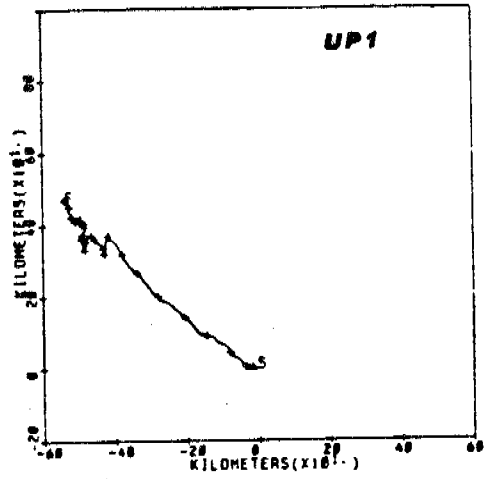
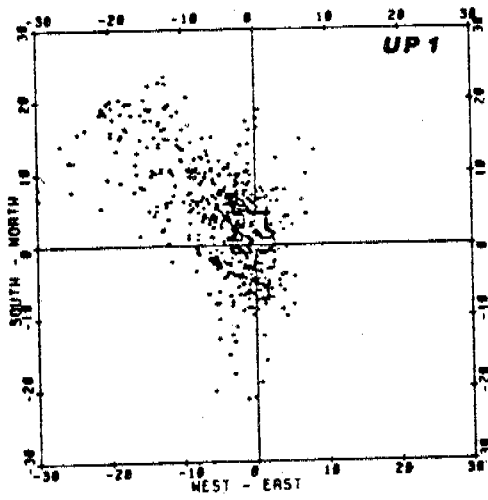
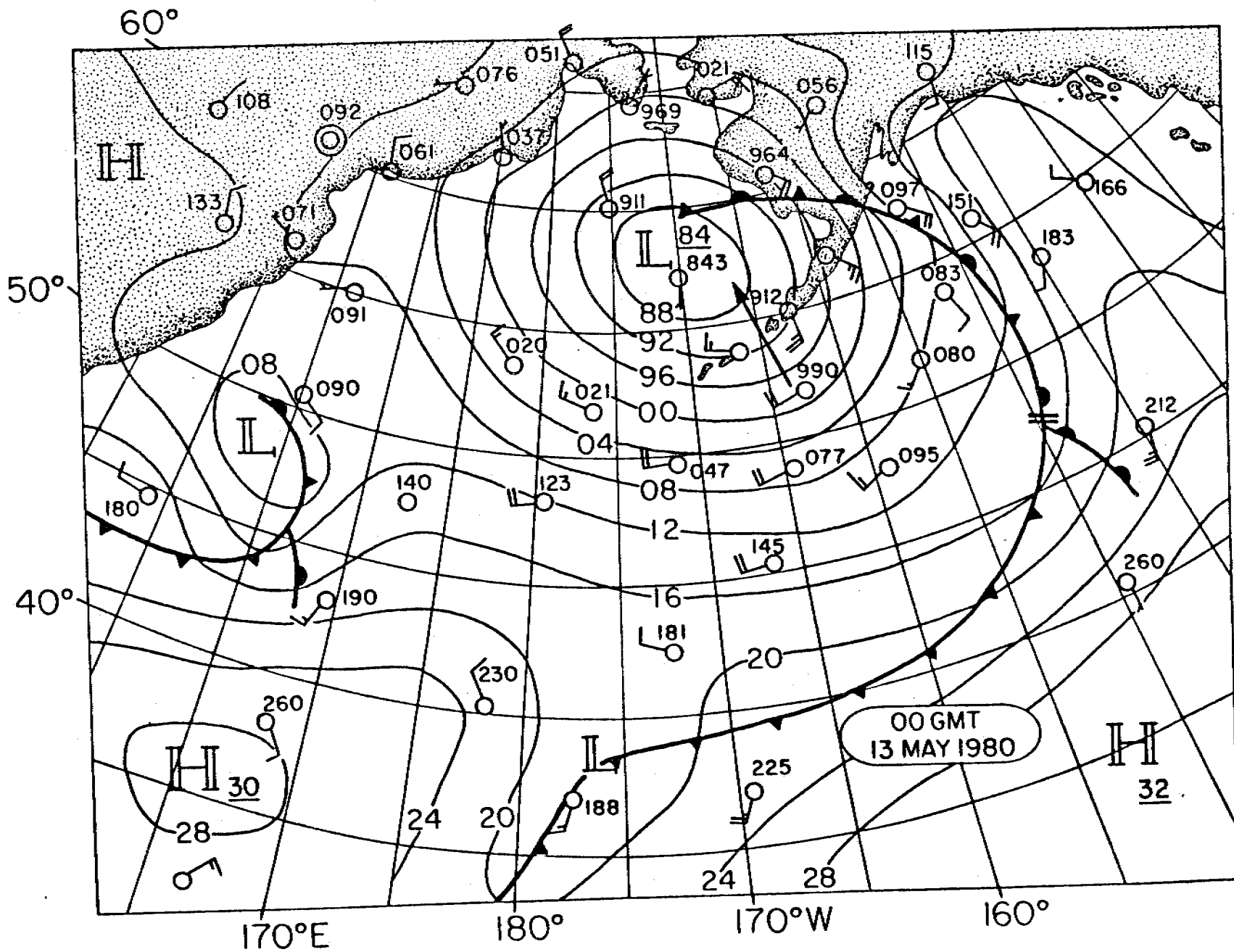


Figure 8-14. Same as 8-13 but for K_1 .

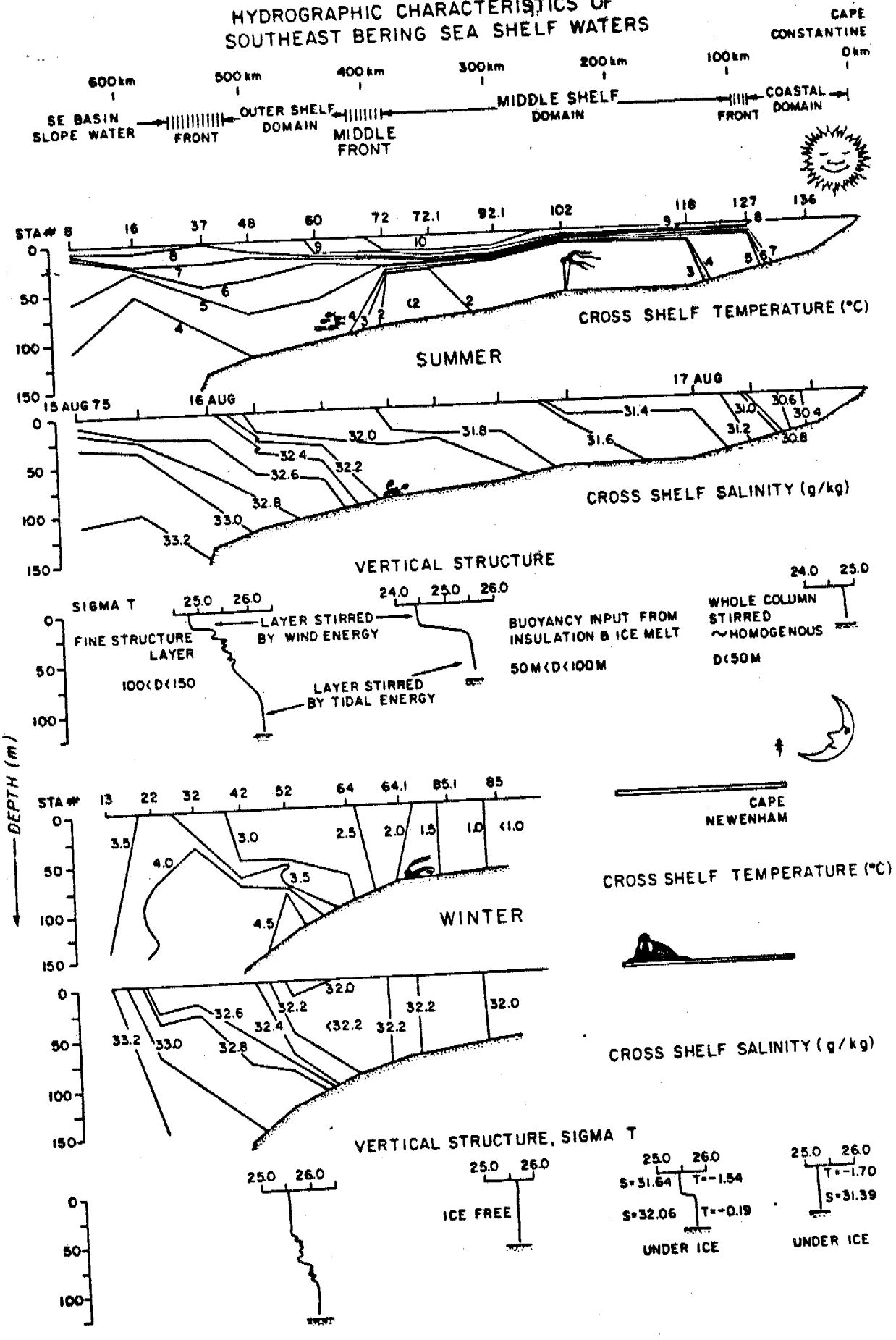




417



HYDROGRAPHIC CHARACTERISTICS OF SOUTHEAST BERING SEA SHELF WATERS



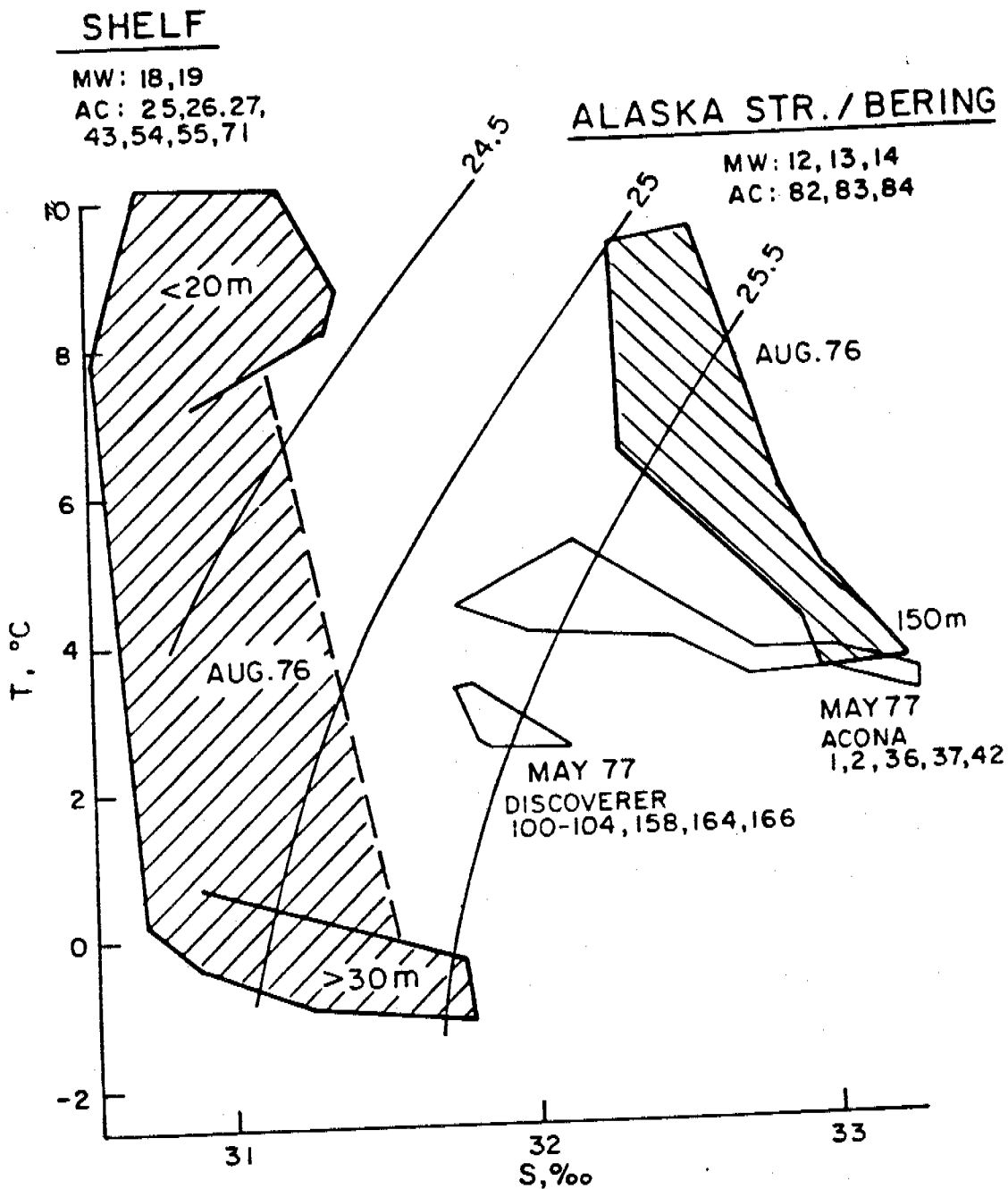
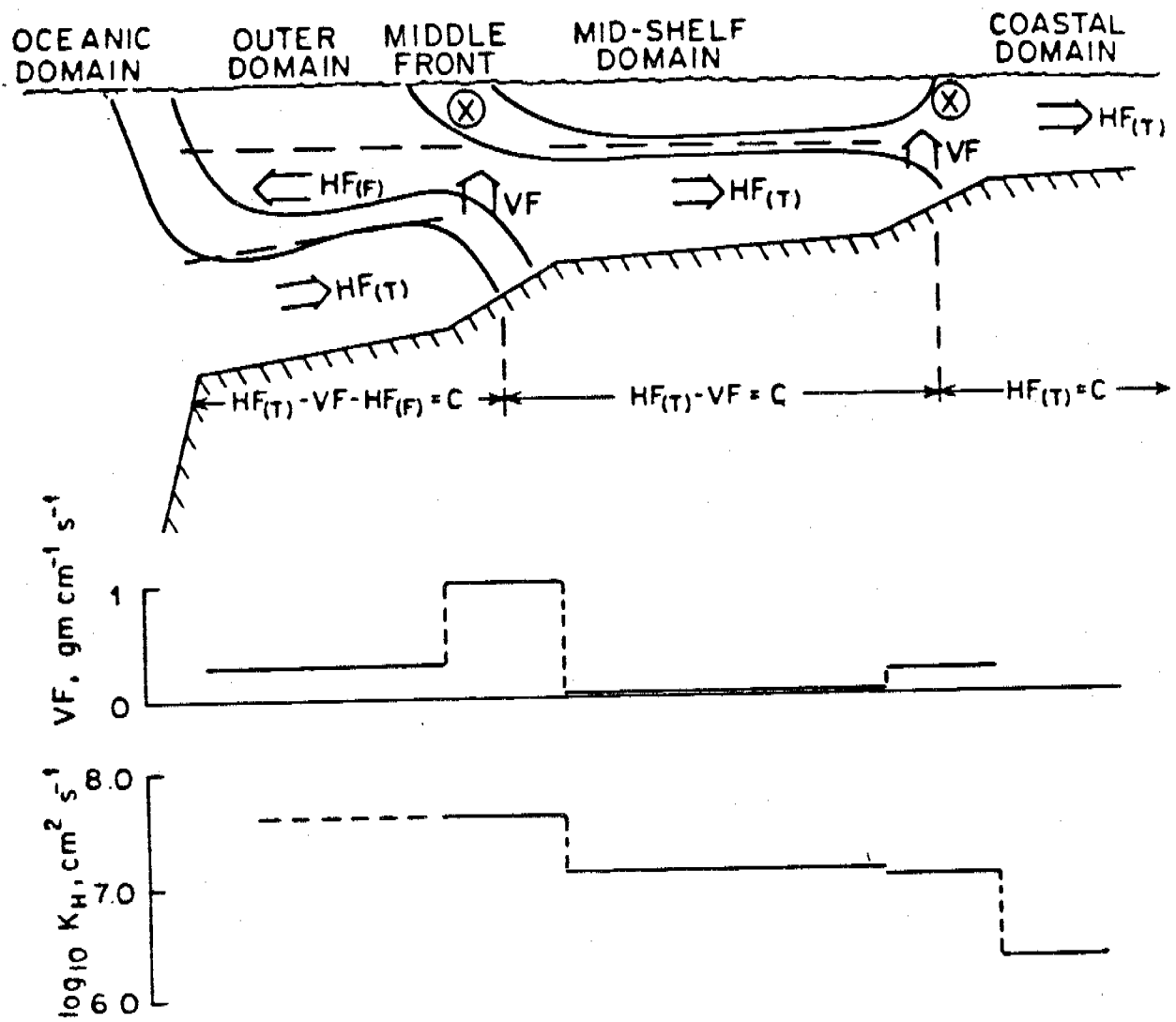
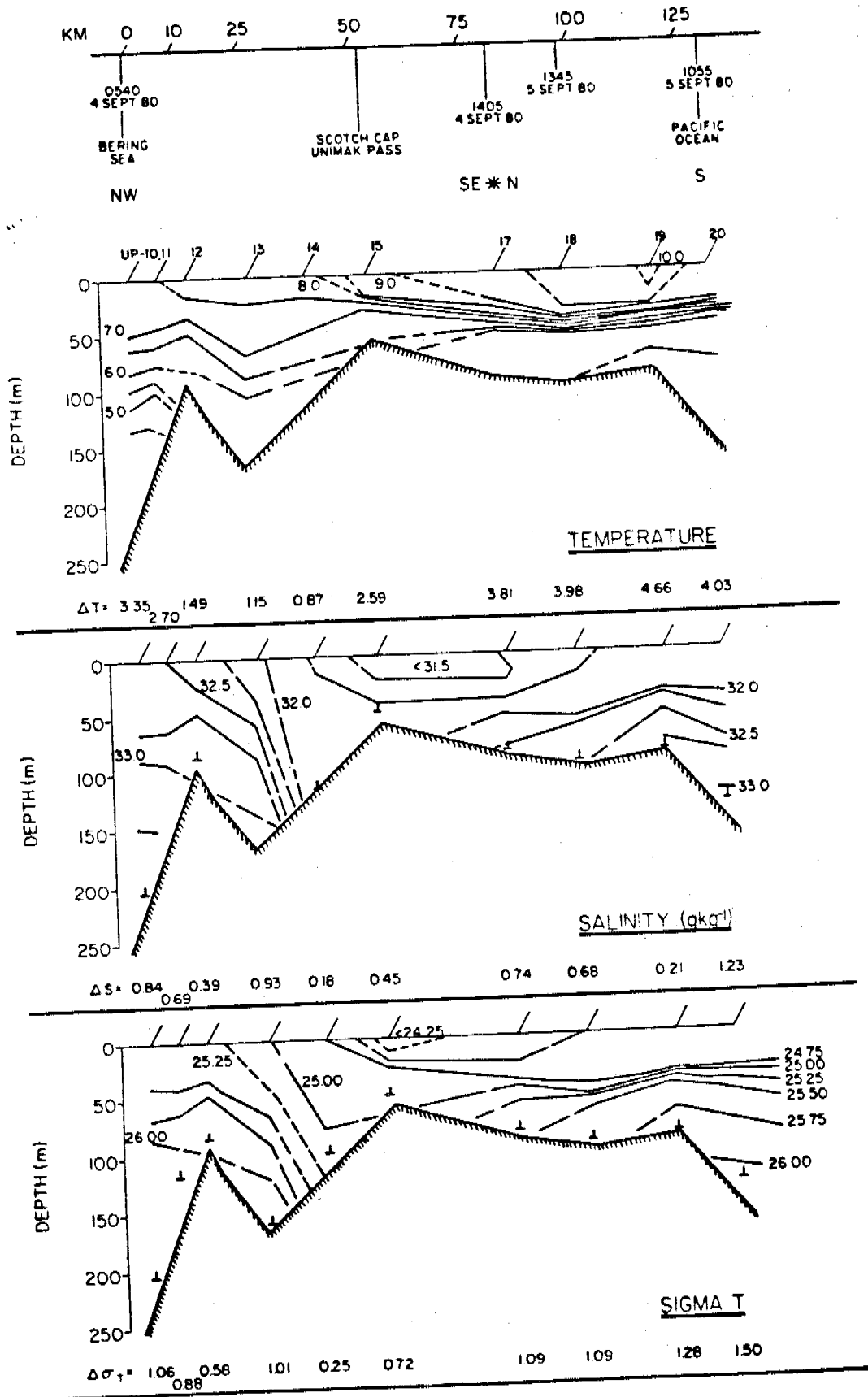


Figure 4-5. Temperature-salinity correlations, middle domain (SHELF) and oceanic domain (ALASKA STR./BERING). Envelopes drawn from data gathered in August 1976 and May 1977 illustrate the warmer and saltier oceanic water at the same density as the cooler and fresher shelf water, and interleaving occurs across the outer domain. (From Coachman and Charnell 1979.)





IV. B

EFFECTS OF WAVE-INDUCED MOORING NOISE ON TIDAL AND
LOW-FREQUENCY CURRENT OBSERVATIONS¹

by

Carl A. Pearson²

James D. Schumacher

Robin D. Muench³

Pacific Marine Environmental Laboratory
3711 15th Avenue N.E.
Seattle, Washington 98105

¹ Contribution 486 from the NOAA Pacific Marine Environmental Laboratory

² National Ocean Survey, assigned to PMEL

³ Presently at: Science Applications, Inc., NW
13400B Northrup Way, Suite 36
Bellevue, Washington 98005

ABSTRACT

Because of the controversy over the effects of surface wave motion on current records, we have compared summer and winter M_2 tidal current speeds measured by Aanderaa current meters on subsurface moorings from several locations on the Gulf of Alaska and Bering Sea continental shelf. Seasonal differences were slight and in most cases not significantly correlated with observed mean wave height measured at Buoy EB-03. We conclude that the seasonally averaged low-frequency currents measured by Aanderaa current meters on moorings with the float at least 18 meters below the surface were not seriously contaminated by surface-wave-induced mooring motion.

INTRODUCTION

Over the past decade, a large number of current observations have been obtained from continental shelf regions using a variety of current meters on taut-wire moorings. For reasons including cost, reliability, and availability, the instruments used have often been nonvector-averaging Savonius rotor and vane units, which were not necessarily the best-suited equipment for the highly variable current regimes in which they were deployed. Consequently several investigators (e.g. Halpern and Pillsbury, 1976a; Beardsley, Boicourt, Huff and Scott 1977; Hayes, 1979; Mayer, Hansen and Ortman, 1979) have pointed out that this type of current meter may be subject to speed errors due to wave-induced mooring motion, or rotor pumping.¹

If rotor pumping adds a constant speed to the current record, then the observed energy will be elevated by an approximately constant proportion across the entire spectrum. That is, the percentage increase in variance will be approximately constant for all frequencies. Halpern and Pillsbury (1976a) found this to be generally true at frequencies below 0.7 cph, where they noted a 1:1 correspondence between the shapes of spectra from two adjacent current records which were from similar depths but had different mooring configurations. One mooring had a 3 m deep subsurface float, the other an 18 m deep float. They also computed an energy ratio of 2.2 (greater energy at the mooring having the shallower float) at the M_2 tidal frequency, and 2.5 at lower frequencies.

¹ Halpern and Pillsbury (1976b) noted that another source of error due to mooring noise is the tilting of the mooring during high flow. However, pressure sensors on our current meters showed about the same range as the tide, so this was not a problem.

We have obtained a large number of current observations from the Alaskan continental shelves using Aanderaa RCM-4 current meters on taut-wire moorings. In the Gulf of Alaska storm frequency and intensity is considerably greater in winter than in summer, implying a higher sea state in winter and correspondingly higher probability of contamination of the current records by rotor pumping. In this note, we investigate the effects of rotor pumping on tidal and lower frequency currents using tidal analysis.

DATA ACQUISITION AND ANALYSIS

A mooring typical of those used in the northern Gulf of Alaska is shown in figure 1. The subsurface float was usually 1 m in diameter and provided a net buoyancy of approximately 400 kg. This float was about 18 m below the surface, which placed the uppermost current meters at a depth of about 20 m. Depending upon the bottom depth, additional meters were placed 50 m and 100 m below the surface and 10 m above the bottom. The moorings used in this analysis were located on the Alaskan continental shelf in water depths between 60 m and 190 m at the locations indicated in figure 2.

Aanderaa RCM-4 current meters record speed by summing the number of rotor turns for (in our case) 15-, 20-, or 30-minute intervals. Direction is recorded at the time of sampling by measuring compass and vane orientation. Therefore, speed recorded at time t_n is integrated over $\Delta t = t_n - t_{n-1}$, while direction is instantaneous at time t_n . Speeds at t_n and t_{n-1} were averaged before converting to east and north components of velocity at time t_n . These components were then low-pass filtered (filter half-amplitude response was at a period of 2.9 hours), and a second-order polynomial was used to interpolate the observations to whole hours.

Mean surface wave heights and periods for the northern Gulf of Alaska during the observations were obtained using data from NOAA environmental buoy EB-03 (fig. 2). The mean winter (November-February) wave height (H) was 3.3 m with a mean period (T) of 7.9 s. During summer (June-August) the mean wave height and period were 1.5 m and 6.5 s, respectively. The wave-associated horizontal component of water particle speed at depth z averaged over a wave period T is given by

$$\bar{v} = \frac{2H}{T} e^{-\sigma^2 z/g}$$

where g is the acceleration of gravity and $\sigma = 2\pi/T$. At a depth of 20 m, $\bar{v} = 6.8 \text{ cm s}^{-1}$ for summer and 23 cm s^{-1} for winter, which is of the same order of magnitude as the tidal currents.

Figure 3 shows typical winter and summer variance spectra from the Gulf of Alaska. Figure 3A is from the 20 m deep current meter at location WGC2 whose mooring configuration is described above, while figure 3B is from SLS-B whose 45 m deep float was below the depth of most surface wave motion (Hayes, 1979). Both spectra show higher energy levels in winter, with the largest winter-summer difference at subtidal frequencies. In the Gulf of Alaska winter currents are more energetic due to greater meteorological forcing (e.g. Lagerloef, Muench and Schumacher, 1981). This condition is similar to one in which noise has been added and the continuum raised except that the ratio of increase in the tidal bands is small. Assuming a barotropic tide, tidal currents should be coherent with the astronomic forcing, and the harmonic constants should be constant through the year. Since rotor pumping tends to raise tidal and lower frequency bands by an approximately constant proportion, a comparison of winter and summer tidal amplitudes will indicate contamination of the current records at tidal and lower frequencies.

In the Gulf of Alaska and southern Bering Sea the tide is predominantly semidiurnal, and the principal lunar semidiurnal tide (M_2) is the largest constituent. We found the semidiurnal currents to be coherent with the semidiurnal tides measured by pressure gauges. Current phases and ellipse-axis orientations at most stations were similar at different depths at the same location, at nearby moorings, and seasonally, indicating a predominantly barotropic semidiurnal tide. Current spectra are typically red indicating that the continuum noise level is lower at the semidiurnal frequencies than at diurnal frequencies, and therefore the signal to noise ratio is highest for M_2 .

An RMS M_2 tidal speed was computed and used for the comparison of summer and winter conditions. A response tidal analysis (Munk and Cartwright, 1966) was used to compute the east and north components of the M_2 tidal currents for summer (June-August) and winter (November-February). A 95% confidence interval for amplitude was computed from

$$\pm 1.96 \left(\frac{R}{9} \cdot \frac{27.3}{L} \right)^{\frac{1}{2}}$$

where R is the residual variance in the semidiurnal band centered on two cycles per lunar day and having a width of nine cycles per lunar month (27.3 days), and L is the series length in days. The residual series was computed by carrying out a self-prediction based on the analysis, then subtracting the predicted from the original series. The RMS tidal speed was then computed from

$$M_2 = \left(\frac{u^2 + v^2}{2} \right)^{\frac{1}{2}}$$

where u and v are the east and north component amplitudes of M_2 .

RESULTS

The results of the tidal computations show that there was little winter-summer difference of the RMS M_2 speeds (fig. 4). At mooring K7, amplitudes for both winter and summer periods were identical at 7.4 ± 0.6 cm s^{-1} . Amplitudes at mooring K6 were nearly identical to those at K7, or 7.4 ± 0.7 cm s^{-1} in summer and 7.5 ± 0.6 cm s^{-1} in winter. Tidal currents at mooring K11, located southwest of Kodiak Island, were slightly higher in summer than during winter; however, the summer record at K11 was early summer (22 May-28 July). At moorings WGC1, WGC2 and 62², the amplitudes were slightly ($\leq 10\%$) higher during winter than in summer. The summer-winter differences at most moorings were within 95% confidence intervals. For comparison we have included analysis of current records from the southern Bering Sea, BC3 (fig. 2). This mooring was south of the maximum ice extent and was not affected during winter by surface ice cover. Winter amplitude was slightly higher than the summer amplitude, but the difference was barely significant at the 95% level.

We have also plotted the RMS M_2 speeds from monthly 29-day harmonic analyses of the records versus the mean monthly wave height at EB-03 (fig. 5). A slight linear trend is evident for WGC2 with a slope of 3% of the mean M_2 speed per meter of wave height. The correlation coefficient of 0.84 is significant at the 95% confidence level, and agrees with the finding that summer-winter differences in the M_2 amplitudes are 10% or less. Similar analyses were performed on the other records, but none showed significant correlations between M_2 amplitude and wave height. The lack of a strong correlation between surface wave height and recorded current speed shows that the data were not seriously contaminated by rotor pumping.

² The current meters at mooring 62 were at a depth of 50 m below an 18 m subsurface float.

DISCUSSION

Our results show that, on a seasonal average, the effect of mooring motion on the semidiurnal tidal currents was slight, e.g. $\leq 10\%$. Since rotor pumping tends to raise the entire low-frequency spectrum by an approximately constant proportion, we infer that the effect on other low frequencies was also slight.

This is in contrast with the findings of Mayer et al. (1979), who found that the semidiurnal energy varied by a factor of two during the year with a clear minimum in summer; and Halpern and Pillsbury (1976a), who found a greater than twofold energy increase due to surface wave motion. The major difference among the moorings was the depth of the subsurface float: 18 m for ours, 8 m for Mayer et al., 3 m for Halpern and Pillsbury. Since the influence of wave motion decreases exponentially with depth, a mooring with a shallow subsurface float is likely to be contaminated much more than one at 18 m or deeper. We conclude that the depth of the subsurface float is a critical factor when using Aanderaa current meters. In our case a depth of at least 18 meters gave satisfactory results for seasonally averaged low frequency currents.

Finally, we wish to stress that our results are for seasonal averages, and that measurements taken during a severe storm should be viewed with caution. Comparison of tidal current speeds observed during a storm with predicted tidal speeds is difficult, due to the brief duration of storms and the unknown magnitude of the wind-driven flow, and attempts at such comparisons yielded inconclusive results. Nevertheless, since severe storms occur relatively infrequently, their contribution to the seasonal mean is small.

ACKNOWLEDGEMENTS

We wish to thank T. Kinder, D. Halpern, J. Holbrook and J. Blaha for their helpful comments, and our many colleagues at PMEL who assisted in the preparation of this manuscript. This study was supported in part by the Bureau of Land Management through interagency agreement with the National Oceanic and Atmospheric Administration, under which a multi-year program responding to needs of petroleum development of the Alaskan continental shelf is managed by the Outer Continental Shelf Environmental Assessment Program (OCSEAP) Office.

REFERENCES

- Beardsley, R.C., W. Boicourt, L.C. Huff and J. Scott (1977) CMICE 76: a current meter intercomparison experiment conducted off Long Island in February-March 1976. Woods Hole Oceanographic Inst. Technical Report WHOI 77-62, 123 pp.
- Halpern, D. and R.D. Pillsbury (1976a) Influence of surface waves on sub-surface current measurements in shallow water. Limnology and Oceanography 21, 611-616.
- Halpern, D. and R.D. Pillsbury (1976b) Near-surface moored current meter measurements. MTS Journal, 10, 32-38.
- Hayes, S.P. (1979) Variability of current and bottom pressure across the continental shelf in the northeast Gulf of Alaska. Journal of Physical Oceanography, 9, 88-103.
- Lagerloef, G., R.D. Muench and J.D. Schumacher (1981) Very low frequency variations in currents near the northeast Gulf of Alaska Shelf break. Journal of Physical Oceanography, in press.
- Mayer, D.C., D.V. Hansen and D.A. Ortman (1979) Long-term current and temperature observations on the middle Atlantic shelf. Journal of Geophysical Research, 84, 1776-1792.
- Munk, W.H. and D.E. Cartwright (1966) Tidal spectroscopy and prediction. Philosophical Transactions of the Royal Society of London, Series A, 259, 533-581.

FIGURE CAPTIONS

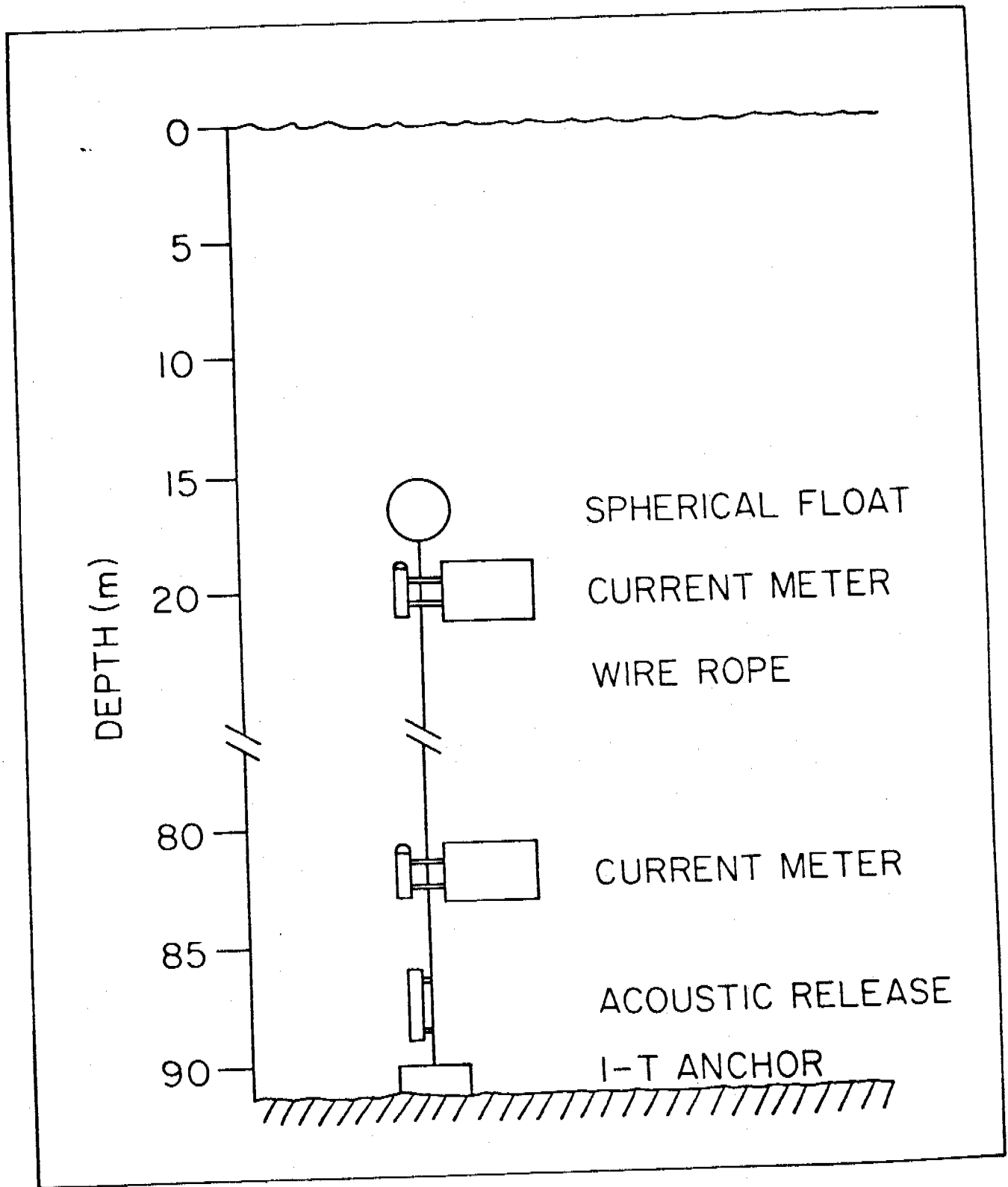
Figure 1. Typical configuration of mooring used on Gulf of Alaska shelf. The number of current meters and their vertical spacing varied with different stations and depended upon such factors as water depth and stratification.

Figure 2. Locations of stations used in this study. EB-03 is a NOAA Environmental buoy which recorded mean wave height and period.

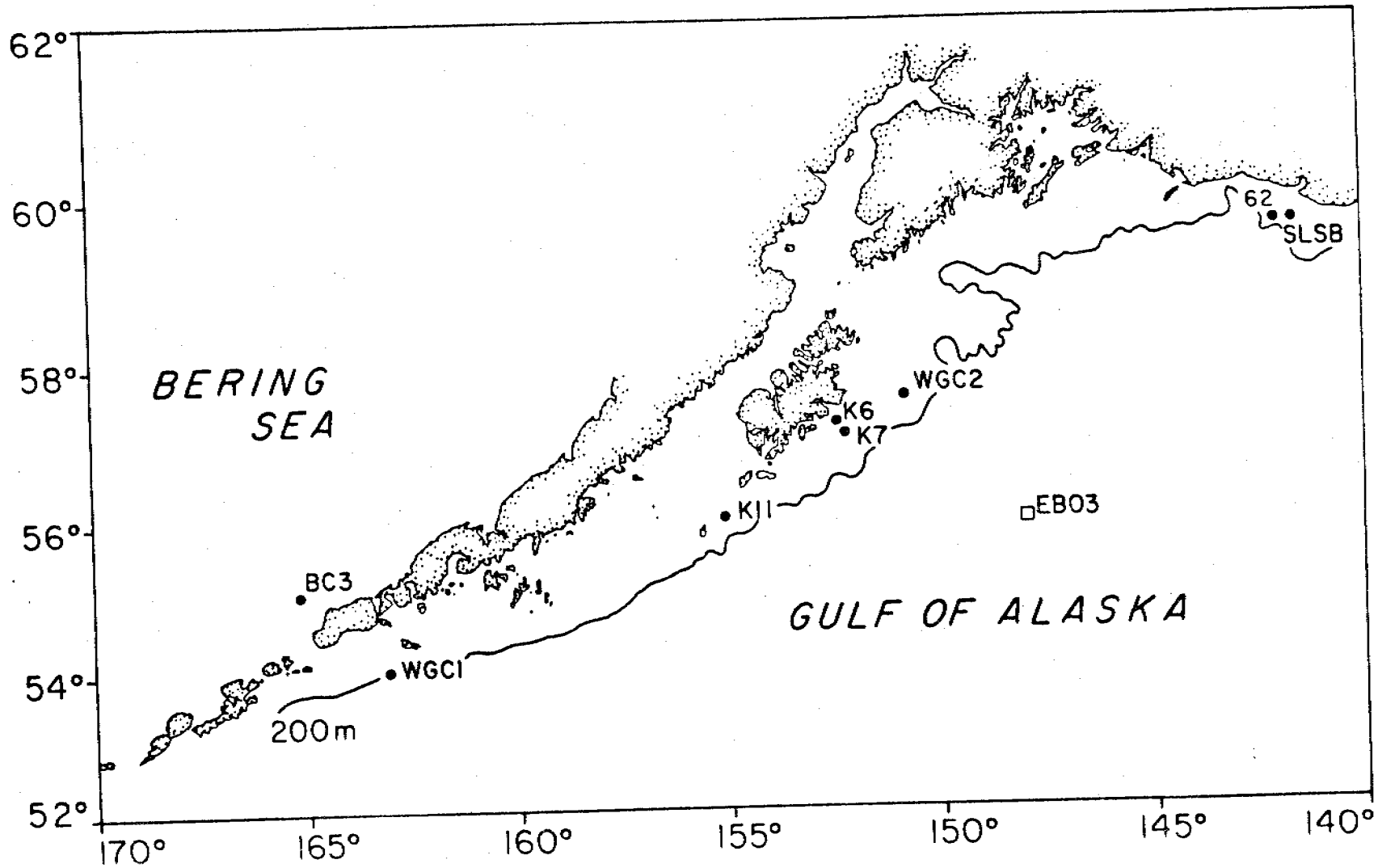
Figure 3. a. Winter (November 15, 1976-February 13, 1977 solid line) and summer (June 1 - August 29, 1976 dashed line) autospectra from station WGC2, depth 20 m.
b. Winter and summer autospectra from station SLS-B, depth 48 m.

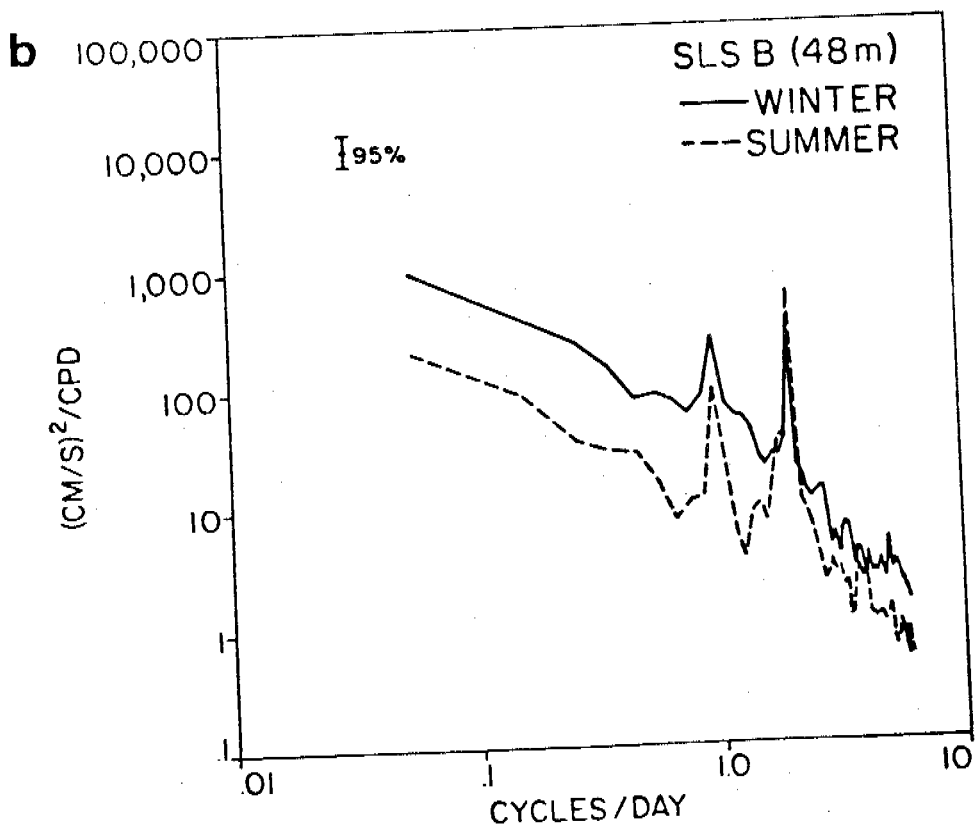
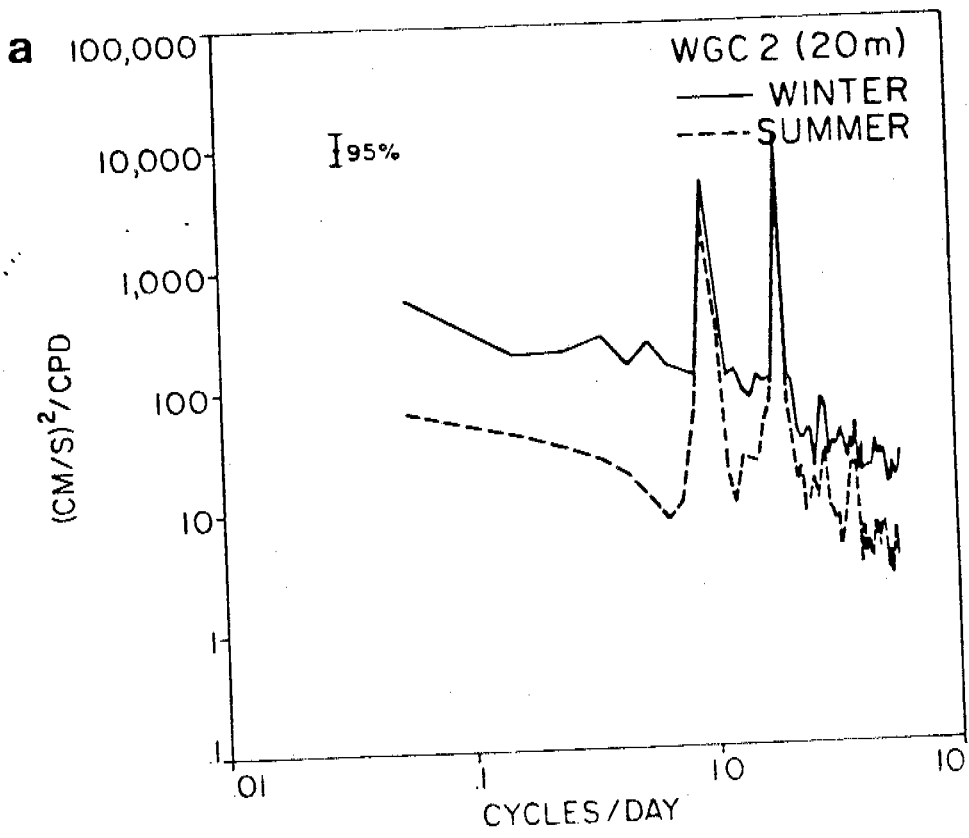
Figure 4. Mean monthly wave heights (solid line) and periods (dashed lines) for EB-03 (bottom); and seasonal RMS M_2 current speeds for various stations (top). Horizontal bar indicates length of series, vertical bar is 95% confidence interval. All had the subsurface float at about 18 m depth. The station 62 current meters were at a nominal depth of 50 m, while the others had a nominal depth of 20 m.

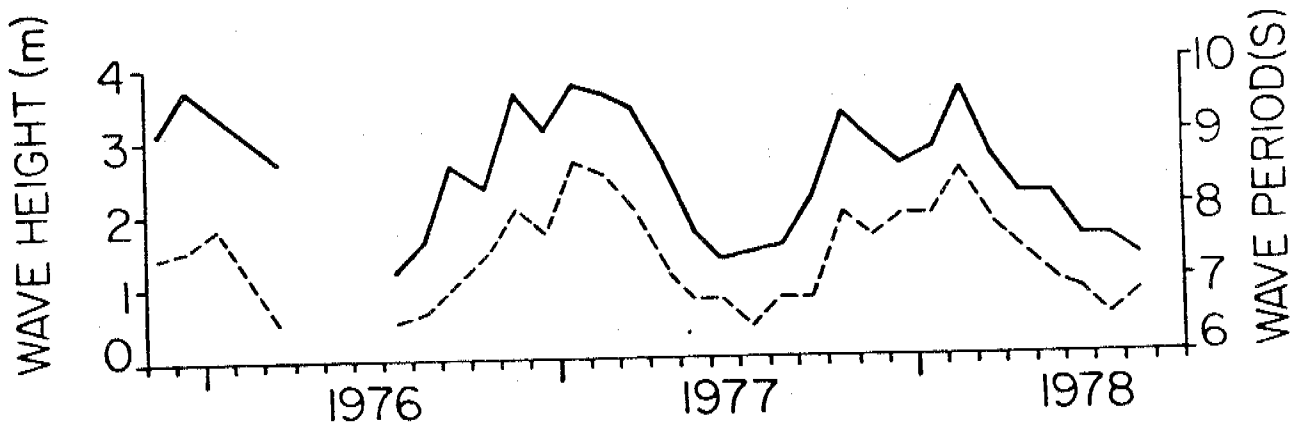
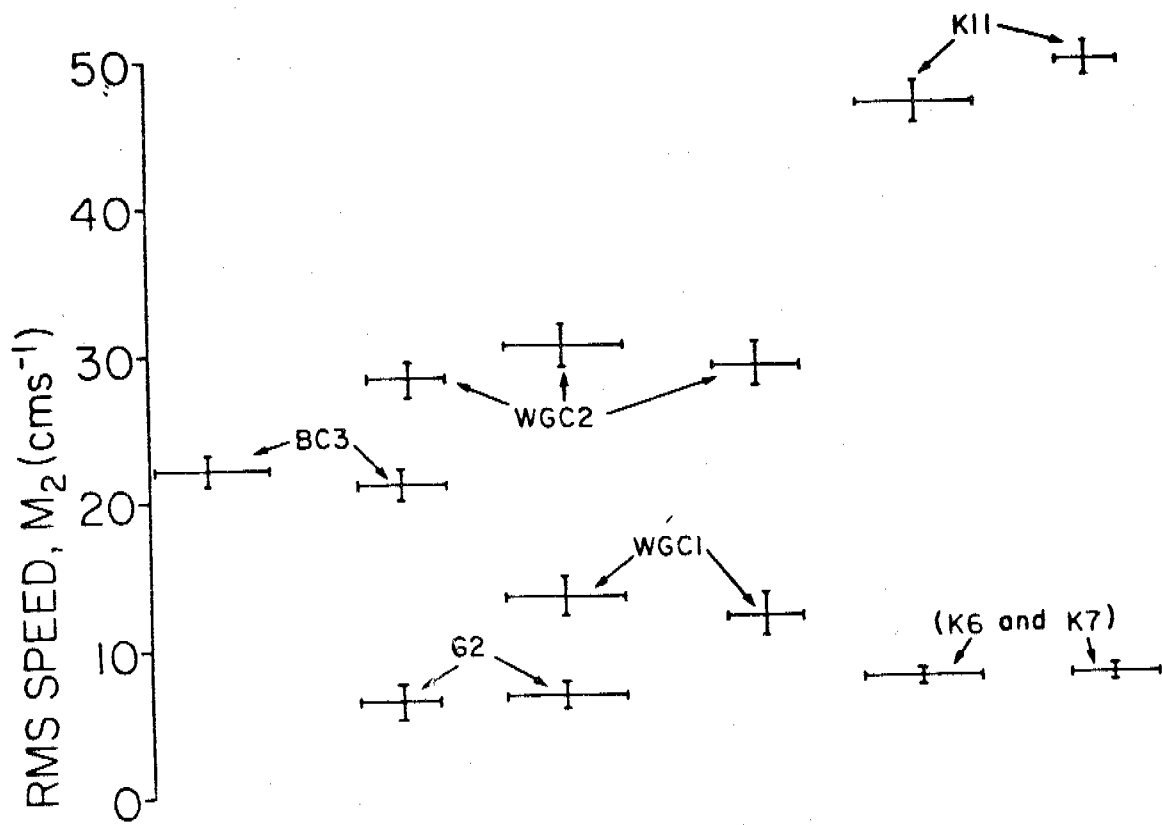
Figure 5. Mean monthly RMS M_2 speeds plotted against mean monthly wave height. Regression line is for station WGC2.

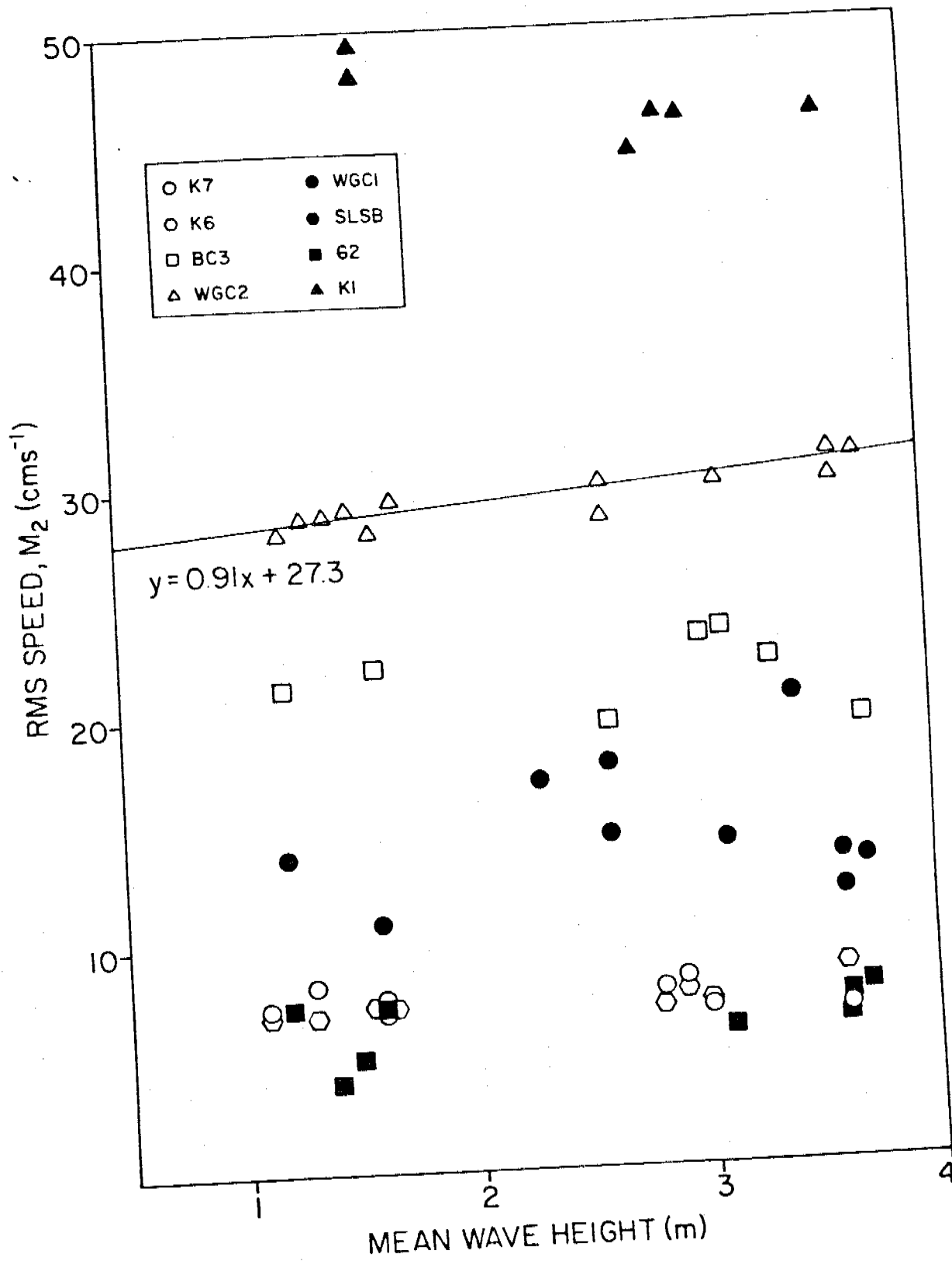


434









by
J. D. Schumacher
and
Lt. D. Sigrist
TABLE OF CONTENTS

INTRODUCTION	1-2
OVERVIEW	2
CHRONOLOGY	3-6
CHIEF SCIENTIST'S CRUISE REPORT	7-16
OPERATIONS	17-19
PROBLEMS AND RECOMMENDATIONS	20
CONCLUSIONS	20
COMPILATION	20
APPENDIX I SAILING ORDERS	
APPENDIX II PROJECT INSTRUCTIONS WITH AMMENDMENTS	
APPENDIX III HELICOPTER OPERATIONS REPORT	
APPENDIX IV LETTERS TRANSMITTING DATA	

INTRODUCTION

The Outer Continental Shelf Environmental Assessment Program is designed to accomplish the following:

1. Provide comprehensive and biological data and information on the Alaska Outer Continental Shelf (OCS) lease area;
2. Define the probable environmental impact of oil exploration, production, storage, and trans-shipment on the OCS;
3. Refine our understanding of key ecological dynamic processes;
4. Provide a basis for a priori predicative or diagnostic models of the ecosystem response to loading by petroleum and petroleum by-products.

Leg I is designed to study the physical, chemical, and biological oceanography of the North Aleutian Shelf, Bristol Bay and St. George Basin areas, and to recover/redeploy sub-surface moorings north of Port Moller. Operations included:

1. Logistics support for NOAA helicopter;
2. CTD casts with water samples (Niskin) and transmissometer sensor;
3. Butterfly water sampler casts;
4. Benthic sampling with a Smith-MacIntyre grab sampler and Pimatmat corer;
5. Recovery and deployment of current meter arrays;
6. Marine bird observations on a not-to-interfere basis;
7. Servicing of shore-based meteorological station;
8. Small boat support for water and bottom sampling operations inside the Port Moller area.
9. Marine Mammal Reporting Program under RP-13-80 to be reported under separate cover;
10. Marine Weather Observations;
11. IGOSS XBT drops;
12. SEABEAM Trackline data, S-N707-SU-80, on a not-to-interfere basis.

Scientific/Technical personnel for this Leg included:

Dr. James Schumacher, Chief Scientist	PMEL	SEATTLE
Chuck Katz	"	"
Bill Parker	"	"
Dwight Daniels	"	"
Sharon Walker	"	"
Bruce Titus	"	"
Bobbie Rice	"	"
Sam Tritt	"	"
Kimberly Hansen	"	"
Robert Griffiths	Oregon State University	
Bill Broich	"	"
Bruce Caldwell	"	"
George Roubal	University of Louisville	
Emily Irvin	"	"
Nancy Butowski	University of California	
R.B. Christman, Lt., NOAA		Helo Pilot
Bob Nield, NOAA		Helo Mechanic

OVERVIEW

SURVEYOR departed PMC for Kodiak, Alaska for fueling and final cruise preparations and, thence to the working grounds in Bristol Bay and the Bering Sea.

Enroute to Kodiak and the working grounds, SEABEAM data was obtained per project instructions S-707-SU-80. Initial operations included the recovery of current meter arrays deployed by SURVEYOR on LEG IV, RP-4-SU-80A and deployment of new sub-surface moorings north of Port Moller. Two additional sub-surface moorings for the University of Washington, were deployed following the work off Port Moller. Operations then shifted to the North Aleutian grid where CTDcasts with Niskin bottles, Smith-MacIntyre grabs, Pimatmat cores, and butterfly water samplers were used. During transits between sampling stations, 10 minute bird transects were conducted on a not-to-interfere basis. NOAA helicopter N57RF joined SURVEYOR off Port Moller and transferred scientific personnel ashore to service the wind station at Lagoon Point, and take samples inside Port Moller and Izembek Lagoon.

With the helicopter completing its work and returning to Kodiak operations shifted to the Probes Line (PL) and Saint George Basin (SG) stations. CTD's, water and bottom sampling operations continued according to project instructions. Final operations included CTD casts with water samples in the vicinity of Unimak Pass. SURVEYOR arrived at the USCG Base, Kodiak, on 19 February, ending Leg I.

CHRONOLOGY

- 01/20/81 Underway form PMC at 1100(L), for Kodiak, Alaska, beginning .RP-4-SU-81A.
- 01/21/81 Underway as before via Inside Passage.
- 01/22/81 Underway as before via Inside Passage. Medical evacuation at Ketchikan, Alaska, between 1445 to 1715.
- 01/23/81 Underway as before, entering the Gulf of Alaska, near Cape Decision, at 0330. IGOSS XBT drops commenced at 0900.
- 01/24/81 Underway as before, beginning a short SEABEAM trackline per S-N707-SU-80 instructions at 1615. Due to moderate seas, data were only marginally acceptable; SEABEAM trackline terminated at 2000.
- 01/25/81 Arrived Kodiak, Alaska, USCG Base, at 0900. During the short touch-and-go, SURVEYOR fueled while preparations continued for Leg I.
- 01/26/81 Underway form Kodiak at 1610 for working grounds near Port Moller (Bristol Bay). A short test of the Pimatmat core sampler was made off Kodiak Island at 2300.
- 01/27/81 Enroute to Unimak Pass, running a short SEABEAM trackline (Chirikov Box) between 0930 to 1420. IGOSS XBT drops continue in water depths greater than 200 fathoms. Bird observation transects begin on a not-to-interfere basis during daylight hours.
- 01/28/81 Transisting Unimak Pass at 1700, enroute for sub-surface mooring site TP-5, off Port Moller. An initial CTD station line off Unimak Pass was cancelled due to moderate seas and winds.
- 01/29/81 Between 1135 to 1430, sub-surface moorings TP-5 and TP-6 were recovered without incident. An initial CTD cast at site TP-5 indicated poor alignment between the CTD depth frequency and actual depth of the fish. Furthermore, minor problems with the Jered Winch compounded the situation. CTD's were completed at stations NA29 and NA30, with additional Smith-MacIntyre grab samples.
- 01/30/81 Completed CTD's at stations NA31 and NA32, however, a CTD cast at station TP-2 indicated the depth sensor on fish #6211 was not properly operating. Replacement fish #6234 was installed in the rosette sampler. The remainder of the afternoon was spent recovering mooring TP-2 and deploying moorings TP2B and TP7, without incident. The remainder of the evening was spent completing CTD's, Smith-MacIntyre grabs, and butterfly water samples at stations NA40, 39, 38, 37, 36, and 35. The Pimatmat core sampler was used at station NA40, unsuccessfully, due to the sandy bottom.
- 01/31/81 Completed remaining sample stations NA34, 46, 45, 44, 43, 42, and 41. A winch malfunction at station NA34 caused the rosette sampler to hit the hull, destroying one Niskin bottle and damaging two others. The remainder of the afternoon was spent recovering mooring TP-4 and deploying mooring TP-9. At 1645, SURVEYOR set course for station SG11.

02/01/81 Completed CTD stations SG11, SG12, and PL10, Smith-MacIntyre grab samples on SG11, and SG12. Accomplished deployment of University of Washington sub-surface moorings PR-1B and PR-2B without incident. Completed 2 successful Pimatmat cores and one Smith-MacIntyre grab on station PR-1B. An electronics problem with the CTD signal processor was cleared up in the early evening, permitting completion of stations PL-7 and SG28. At 2330 course was set for mooring site TP-8.

02/02/81 Underway as before to site TP-8, no operations enroute. Sub-surface mooring TP-8 was completed at 1145. Information regarding all previous deployments and recoveries was forwarded to USCG, Juneau, for insertion into "Local Notice to Mariners". At 2100, line NA52 (stations NA47 to NA52, inclusive) was finished and SURVEYOR set course for station NALA. (Note: Loran rate 9990Z was erratic throughout the day as the Coast Guard was attempting to resolve problems at the Narrow Cape Loran Slave Station.)

02/03/81 Completed CTD casts, Butterfly water samples, and Smith-MacIntyre grabs on stations NALA - NA4A, and NA6 - NA10. Large patches of "grease ice" encountered in Bristol Bay, but did not interfere with operations.

02/04/81 Continuing CTD's, Smith-MacIntyre grabs, and water sampling operations on the North Aleutian Shelf. Completed stations NA5 and NA11-NA17. The CTD rosette sampler began acting up, again, in the late afternoon, (The Niskin bottles were tripping erratically). After replacing the slip rings (in the winch) and other selected components, it was determined the CTD sea cable was bad. Approximately 200 meters of wire were removed from the winch, but the short was still not isolated. SURVEYOR hove to on station NA22 while repairs to the system were made.

02/05/81 With the CTD sea cable problem still not yet resolved, SURVEYOR set course for station PM3 (to anchor). Enroute to PM3, SURVEYOR contacted CPM-6 for assistance to rectify the sea cable problem. Prior to arrival at PM3, the sea cable was repaired and SURVEYOR began the CTD time series (while anchored) at 1600.

02/06/81 Continuing CTD time series at station PM3. At 1000 the Boston Whaler with a party of five was sent into Port Moller and Herendeen Bay to collect water and bottom samples. At 1015 Helicopter N57RF arrived with pilot Lt. Christman and mechanic Bob Nield. During the afternoon, the helo made two trips ashore; to service the meteorological station at Lagoon Point and collect bottom/water samples in Port Moller. CTD time series operations terminated at 1820, when SURVEYOR hauled anchor and set course for station NA22, arriving at 2340. The CTD delivered by helicopter earlier in the same day was installed and ready for use at station NA22.

02/07/81 Completed CTD station NA22, proceeding offshore, finishing stations NA21 to NA17. Helicopter operations were cancelled at 0900 when it was discovered that a main bearing assembly in the rotor system was defective. The remainder of the day was spent on stations NA23 - NA28 and NA28 - NA33, running CTD casts with water samples and Smith-MacIntyre bottom grabs.

02/08/81 Operations continue on the North Aleutian Shelf grid completing CTD casts with water samples at stations NA34-NA40, NA41-NA46, and NA47-NA49; also Smith-MacIntyre grab samples at selected stations. Helicopter operations postponed pending arrival of replacement bearing assembly in Cold Bay on February 9.

02/09/81 Water sampling, CTD casts, and Smith-MacIntyre grab sampling operations continue. Completed stations NA50-NA58A. At 1030, the helicopter departed for Cold Bay for repairs and transfer of scientist Bill Parker ashore to meet a commercial flight to Seattle. The helicopter returned at 1445 and departed shortly thereafter with a party of five scientists for Izembek Lagoon. After returning the scientific party, the helicopter refueled and then returned to Cold Bay with Ltjg Croom, completing helicopter operations for Leg I. SURVEYOR continued sampling operations on stations NA59-NA65A.

02/10/81 Underway as before to station NA72. Completed stations NA68-NA72, setting course for Probes Line station PL4 at 0815. Three attempts using the Pimatmat sampler at station PL4 were made, without success. CTD's, water and bottom sampling operations continue on the Probes Line. The first Pimatmat core attempted on station PL6 was successful. Final operations for the day were at station SG28.

02/11/81 Completed successful Pimatmat cores on stations PL8, 10, 12, & 14. CTD's, bottom and water sampling operations on the remaining Probes Line stations and SG13. The CTD mounted transmissometer malfunctioned early in the day and was not repairable, eliminating its use for the remainder of the Leg. Arrived at station SG14, at 2330, winds and seas building, sub-freezing temperatures.

02/12/81 On station SG14 completing the CTD cast at 0030. Winds and seas precluded use of the Smith-MacIntyre grab sampler; SURVEYOR hove to on station SG14, completing the bottom grab at 0700. Stations SG21, 22, and 23 completed by the end of the day.

02/13/81 Continuing bottom and water sampling work in the Saint George Basin, completing stations SG24-27. Completed one CTD cast on station SG28, however marginal wind and sea conditions prevented a second CTD cast and Smith-MacIntyre grab. SURVEYOR hove to in the vicinity of SG28 until 1940, at which time course was set for SG43. Winds in excess of 35 knots and seas building to 10-12 feet precluded any additional work.

02/14/81 Unsatisfactory sea conditions continue as SURVEYOR remains in the vicinity of SG43.

02/15/81 With moderate seas and winds, SURVEYOR resumed water and bottom sampling operations at SG43 at 0930. Completed station SG45, arriving at station SG28 at 2300.

02/16/81 Completed station SG23, 29, 48, and 47 with operations shifting to Unimak Pass, completing UP10, 11, 12.

02/17/81 CTD and water sampling operations continue near Unimak Pass, completing stations UP13, 14, and 15. Operations terminated at 0800 when SURVEYOR set course for Kodiak, Alaska.

02/18/81 Enroute to Kodiak, Alaska

02/19/81 Arrived USCG Base, Kodiak, at 0900 completing operations
for Leg I.

I. Purpose

The Southeastern portion of the Bering Sea Shelf supports one of the world's richest fisheries and has potentially large quantities of petroleum. In order that logical decisions can be made with respect to leasing, fate and impact of petroleum development must be known. The Outer Continental Shelf Environmental Assessment Program has funded a series of three cruises to elucidate transport processes in the Aleutian Shelf and Saint George Basin lease areas. The general goal of RP-4-SU-81A, Leg I, was to collect such data during winter conditions. In addition, two current meter moorings were deployed and nutrient samples collected for our colleagues in the National Science Foundation funded Processes of Resources of the Bering Sea Shelf (PROBES) study.

II. Disiplinary Reports

- A. Physical Oceanography: RU549/PMEL
- B. Microbiology: RU595/Oregon State University
RU29/University of Louisville
- C. Suspended Particulate Matter: RU/PMEL
- D. Bird Observations: RU/University of California Irvine
- E. Methane: RU/PMEL

III. Comments and Problems

IV. Acknowledgements

A. Physical Oceanography: RU541/PMEL

1. Mooring Recoveries: All equipment deployed in August 1980 was successfully recovered:

Mooring ID	Recovered JD/GMT	Instruments
TP-5	029/2239	ACM94, PG107, RCM-4 with Transmissometer 2505
TP-6	030/0115	ACM97, PG120, RCM-4 3293 RCM-4 with transmissometer 2500
TP-2A	030/1955	ACM95, PG205, RCM-4 with Transmissometer 2502
TP-4	031/2245	ACM96, PG209, RCM-4 with Transmissometer 2501
TP-1A	037/2331	Data logger 322 with wind speed direction, air temperature and gust sensors. Note: The arm up which the direction sensor was mounted was not perpendicular when serviced.

2. Mooring Deployments: Six moorings were deployed and the meteorological station (TP-1) was serviced. Mooring positions, time, and Loran-C rates are given in Table 1, and the order of instruments on each NASTE mooring is as follows:

TP-2B	41" ORE float, ACM, Sediment trap, 28" ORE float, RCM-4 transmissometer, AMF release with PG.
TP-7	41" ORE, ACM, Sediment trap, RCM-4 with transmissometer, AMF release with PG.
TP-9	41" ORE, ACM, RCM-4, 28" ORE, Sediment trap, RCM-4 with transmissometer, AMF release with PG.
TP-8	41" ORE, ACM, Sediment trap, 28" ORE, RCM-4 with transmissometer, AMF release with PG.

TABLE 1
 NOAA Ship Surveyor S132
 RP-4-SU-81A
 (OCSEAP)

Array Deployment

<u>Array</u>	<u>Date</u>	<u>GMT Time</u>	<u>Latitude</u>	<u>Longitude</u>	<u>9990X</u>	<u>9990Y</u>	<u>9990Z</u>
TP-2B	1/30/81	2229Z	56 04.6	161 18.2	18610.60	33748.91	46605.81
TP-7	1/31/81	0121Z	56 01.95	161 13.1	18606.13	33747.91	46573.47
TP-9	2/1/81	0151Z	56 29.7	161 42.3	18652.50	33695.78	46758.26
PR-2B	2/1/81	2023Z	56 18.8	165 31.8	18615.04	34386.29	48283.50
PR-1B	2/2/81	0008Z	56 52.1	166 16.9	18509.59	34613.24	48547.75
TP-8	2/2/81	2247Z	55 52.2	162 03.0	18587.50	33913.84	46903.87

3. Hydrography: Conductivity, temperature and depth observations were collected at 132 stations (see Fig1) on 158 casts, including a 24 hour time series at station PM3 and all but two of the North Aleutian (NA) stations. Preliminary analysis of these data indicate that middle-shelf domain waters ($Z > 50\text{m}$) were well mixed (the magnitude of surface minus bottom density was less than 0.03); however, in a 30km wide band beginning about 5km offshore of Port Moller stratification existed. Maximum stratification was about 0.3 sigma-t units and was salinity controlled. CTD data from the time series at PM3 indicated a tidal frequency signal in mean salinity which ranged from about 30.0g/kg, on ebb tide to 31.0g/kg on flood tide. At several points in the tidal cycle stratification existed even in these shoal (depth about 17m) waters; however, the magnitude of this stratification never exceeded 0.2 sigma-t units. Changes in hydrographic conditions between the first and second occupation of the Port Moller section (NA40 to NA34) suggest that in addition to a general cooling trend, there was an offshore flux of lower salinity surface water accompanied by a compensating inshore flux of more saline, warmer near-bottom water. During a two day period prior to the second occupation of the Port Moller section, winds had a dominant alongshore (towards 250° T) component, were relatively dry and cold. These winds could account for the general heat loss and as shown in current data from about 50km off Port Moller (TP-3A), result in coastal divergence of an upper layer. Such dynamics would result in hydrographic conditions similar to those observed, and may also be important in generating coastal "jets". The magnitude and duration of such events is an important transport mechanism for both methane distribution and spilled oil trajectory models.

B. Microbiology Studies:

1. RU595/Oregon State University

The main objective of this component was to determine rates of methane oxidation and methane production in the Saint George Basin and North Aleutian Shelf regions under winter conditions. As was the case during the August-September 1980 cruise, our work will aid the chemists in determining rates of transport in the waters of the study areas by defining biological sources and sinks of methane.

During this cruise we collected 149 water and 40 sediment samples from 70 locations. Rates of methane production were assayed in all sediments collected using gas chromatography on board ship. The water samples were assayed for methane oxidation rates and relative microbial activity. The results at these measurements will not be known until we return to our home laboratory.

Thanks to the efforts of the ships crew, we were able to collect samples in Port Moller using a small boat and a helicopter in areas that we were not able to sample last summer. The measurements of methane production that we made and measurements of methane concentration in the water samples by Mr. Katz, strongly suggest that the major source of methane in Port Moller is not the cannery at Port Moller as previously suggested but at the head of Herendeen Bay. Finding this source of methane was important to better understand the flux of methane in the Port Moller area. More detailed sampling of this region will be made during the next cruise so that the source areas can be more clearly def

2. RU29/University of Louisville

Information concerning transport and dispersal of crude oil on the surface and within the water column of the Bering Sea is of obvious economic and environmental importance. Once possible routes of transport are physically and chemically determined, the biological effect of crude oil must be considered with respect to toxicity in and removal from this mediterranean ecosystem.

Since many of the food chains in marine arctic ecosystems are relatively short, fragile, and depend fundamentally on microorganisms, it is necessary to determine both effects of crude oil on microbial mediated processes, e.x. nutrient cycling, and the effect of microorganism on crude oil transport e.x. complete and/or incomplete biodegradation of petroleum hydrocarbons. With this in mind the University of Louisville began analysis on samples (97) taken from and around two previously located sources of methane in the Bering Sea/Bristol Bay ecosystem, i.e. Port Moller, North Aleutian Shelf and the Saint George Basin area. Fifty stations were occupied and forty-five surface-water, six mid-water, nineteen bottom water samples and (27) twenty seven Smith-MacIntyre sediment grab samples were obtained. Water samples were obtained using a sterile Niskin butterfly sampler, which allows an uncontaminated water sample at any depth taken. Analysis to determine microbial population microscopically:

1. Enumeration of total microbial population microscopically
2. Enumeration metabolically for crude oil degrading microbial community using a radio tracer most probable technique.
3. Crude oil biodegradation potentials with and without nutrient additions, using selected classes of crude oil hydrocarbons to determine degradation rates and ranges metabolically.

Due to length of incubation times, analysis will be completed at the University of Louisville, Louisville, KY.

C. Suspended Particulate Matter RU/PMEL

The objective of the suspended material studies was to document the distribution and nature of the suspended particulate matter (SPM) over the North Aleutian Shelf and Saint George Basin. Two beam transmissometers were used to obtain continuous traces of turbidity both vertically and horizontally. One transmissometer was interfaced to the CTD, and provided continuous vertical profiles of turbidity, temperature and salinity at every station. Continuous readings of surface water turbidity, temperature and chlorophyll concentration and a fluorometer into the ship's forward seawater pump system. About 200 discrete water samples collected from rosette casts and 15 samples collected from the onboard flow-through system were filtered through preweighed Nucleopore filters and will be used to calibrate the turbidity measurements in terms of mass concentration of SPM.

Size distributions of SPM in 358 discrete water samples were analyzed using ZBI Coulter Counter interfaced to a HP9825 mini-computer. Organic/inorganic ratios will be measured on all filters from discrete water samples. Eleven special samples were taken from the North Aleutian Shelf region for mineralogy analysis.

D. Bird Observations: University of California at Irvine

A total of 280 bird transects were conducted from the ship during the cruise. The largest concentrations of birds, mainly King eiders, (*Somateria spectabilis*) and white-winged scoters (*Melanitta deglandi*) were found near the coast between Port Heiden and Port Moller. They comprised 75% of the total birds observed. These two migratory species are known to hug the coastline and move north as the ice permits. A large flock (>200) of cormorants (*Phalacrocorax* sp.) were also observed in this coastal, ice free area. All three species are benthic feeders and are limited to shallow areas. The cormorants are generally not found in such large groups. The majority of birds in this cormorant group were in breeding plumage with white flank patches.

Glaucous-winged gulls (*Larus glaucescens*) were most commonly seen and evenly distributed along each transect line. Over 33% of the gulls observed were in first or second winter plumage. An occasional glaucous gull (*Larus hyperboreus*) was observed. Kittiwakes (*Rissa* sp) were evenly distributed over Bristol Bay in very low numbers, this is a notable difference from the early autumn season. During August and September of 1980, Kittwaks were more than twice as numerous as gulls.

There was an increase in the number of alcids along the shelf break. Common murres were found in low numbers in Bristol Bay where as the thick-billed murres were numerous in the Outer Shelf domain. Tufted puffins (*Lunda cirrhata*) in winter plumage were observed in low numbers. Crested auklets (*Aethia cristatella*) were twice as abundant as tufted puffins. The total number of alcids are probably under-estimated due to lower visibility during rough sea states.

Conspicuously absent from the winter season were shearwater (*Puffinus* sp.) petrels (*Oceanodroma* sp.), jaegers (*Stercorarius* sp.), and terns (*Sterna* sp.). Incidentals, comprising less than 10% of all observations occurred as follows:

- Oldsquaw (*Clangula hyemalis*)
- Parakeet auklet (*Cyclorhynchus psittacula*)
- Least auklet (*Aethia pusilla*)
- murrelets (*Brachyramphus* sp.)
- Northern fulmer (*Fulmarus glacialis*)
- loon (*Gavia* sp.)
- petrel (*Oceanodroma* sp.)

One air survey by helicopter was conducted over a 17 mile transect. Large flocks of eiders were observed and easily identified from above. Ship following attractions exhibited by some seabird species were not detectable at this time due to lack of data.

E. Methane Tracer Studies: RU153/PMEL

The objective of this component was to assess winter distributions and concentrations of dissolved methane on the North Aleutian Shelf (NAS) and in the Saint George Basin in order to model diffusive transport processes. On the NAS, horizontal diffusion is quantified by tracing the dispersion of methane as it emanates from Port Moller/Herendeen Bay. A bottom source of methane in the vertically stratified waters of Saint George Basin allows quantitation of vertical diffusion. Given the advective field and the rates at which methane is produced or lost via air-sea exchange and microbiological alteration, the steady state and time dependent distributions of dissolved methane will yield estimates of the horizontal and vertical eddy diffusivities.

Sampling Summary

In total, methane measurements were made at 116 unique stations. This total includes 7 stations occupied by small boat in Herendeen Bay, and 9 stations occupied by helicopter in Port Moller (5), Lagoon Point (1) and Izembek Lagoon (3). A total of 911 samples were analyzed for dissolved methane (a record number of analyses!) Ancillary measurements of dissolved oxygen and nutrients were made at selected stations. A total of 116 samples were analyzed for dissolved oxygen while 111 nutrient samples were collected and frozen for future analysis.

Results - North Aleutian Shelf

As has been observed in the past, the source of methane in Port Moller/Herendeen Bay could be traced to the northeast along the coast for approximately 150km. The width of the plume was approximately 20km. Although methane concentration at the mouth of Port Moller were reduced by approximately a factor of two from summer values (2600 cf. 5000 nLL^{-1}), the ambient levels of methane were also halved (250 cf. 500 nLL^{-1}). This, the concentration ratio above ambient still remained 10:1 as observed in summer. A maximum methane concentration of 2400 nLL^{-1} was measured at the head of Herendeen Bay. This value is comparable to the maximum last September at the Port Moller cannery pier. Concentration decreased monotonically toward the mouth of Herendeen Bay to approximately 200 nLL^{-1} . Concentration within Port Moller also decreased toward the entrance from approximately 1000 to 2000 nLL^{-1} . Thus, it appears that although methane is produced throughout the Port Moller/Herendeen Bay area, the predominate source are the reducing muds at the head of Herendeen Bay. Twenty-five hour time series measurements made at PM3 at the entrance to Port Moller showed a semidiurnal fluctuation in methane concentrations. On ebb tide, relatively methane-rich 2600 nLL^{-1} , low salinity water moved out of Port Moller. Upon flood, methane-poor (400 nLL^{-1}) relatively high salinity water returned. This is in good agreement with the methane source and the semidiurnal tidal regime. A methane flux calculated from these time series data will be utilized in modeling the horizontal diffusion.

The distribution of methane outside the plume was homogeneous, both laterally and vertically. Methane concentration averaged approximately 250 nLL^{-1} which is a factor of three times supersaturation with respect to equilibrium with the atmosphere. Dissolved oxygen data showed that shelf waters were everywhere at or near saturation.

Saint George Basin

Dissolved methane from the Saint George Basin indicated that concentrations had dropped by a factor of two from last September. Surface concentrations were relatively uniform at 250 nLL^{-1} . Near bottom concentrations were elevated substantially only with the central portion of the Basin. The highest concentration of methane at depth were approximately 400 to 800 nLL^{-1} . In order to determine the time-dependent vertical distribution of methane, station SG28 was occupied on 4 occasions. Preliminary data from last summer indicated a stability over a minimum of 7 days. Preliminary data from this cruise indicated a stability over a 3 day period, the changes being dependent upon intensity of stratification.

III. Comments and Problems

several of the problems which were encountered on the first NSATE cruise (August-September 1980) no longer existed.

1. A reasonable schedule for RF transmission was devised which eliminated noise in the integrators used in methane concentration determinations.
2. Under the direction of Ensign Bill, navigation during small boat operations was not a problem and these operations included successful sampling in Herendeen Bay. Some time was lost due to electrical problems associated with the CTD system; however, the combination of bad sea cable and shorted slip rings (ie. problems in series) is more difficult to resolve than a single problem at one time. It seems advisable that all electronic technicians going to sea should have completed the short course given by Plessey. The ET's are required to maintain numerous electronic systems onboard, many critical to safe ship operation. Although CTD operations are not related to general operations, they are one of the prime functions related to oceanographic research ships.

The analog chart for the CTD was, as usual, only marginally useful and often generated erroneous traces; however, digital data logger dumps provided by Ens. Ferguson enabled us to determine that the CTD "fish" was functioning properly. Software could be written to use a CRT screen rather than the chart recorder. Not only would this eliminate messy pens and a mechanical/electrical device which is more trouble than it's worth, but it would also enable real-time decisions regarding depths to trip sample bottles to be made more effectively.

IV. Acknowledgements

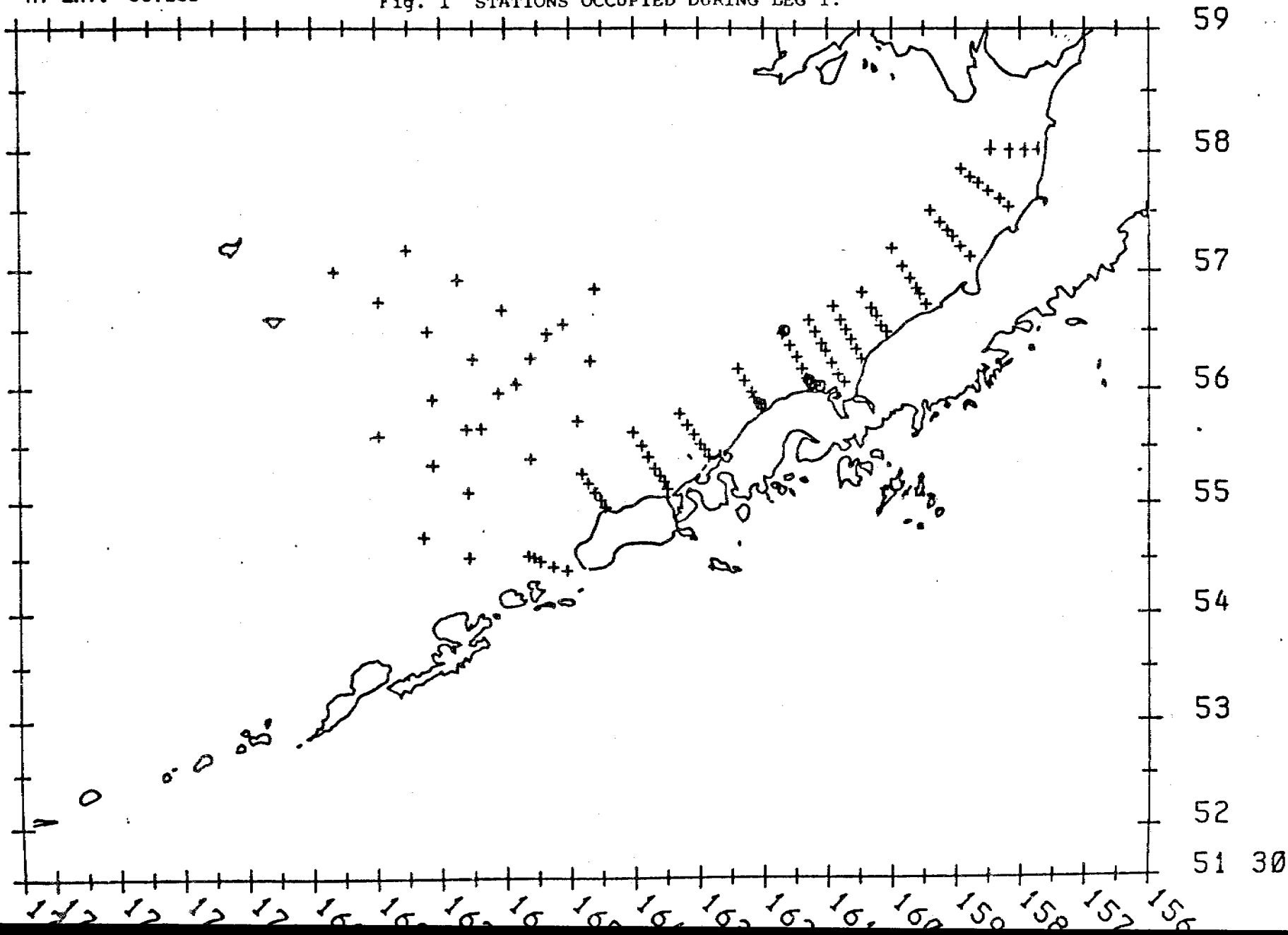
Under the given constraints, which include the inherent difficulties of conducting multi-disciplinary oceanographic research, severe weather (icy decks) and this was the first operation of the year. This latter constraint points to the need for practice for each watch until that watch functions as a team. For Leg 1, the transition to competent team work occurred quite rapidly. The high degree of organization of activities requiring up to five separate operations at a station, was skillfully orchestrated by Lt. Dennis J. Sigrist who deserves special thanks for an excellent cruise. Members of the Deck Department, Survey Department and watch officers contributed significantly to successful operations, as did all those members of the ships compliment, under the direction of Capt. Bruce I. Williams, who help the SURVEYOR function as well as she does.** It was not only a scientifically successful Leg, but also a personal pleasure.

Jim Schumacher
Chief Scientist
NOAA/PMEL

**This includes the Steward Department who enabled me to expand my horizon beyond my belt size and XO's POD, which expanded my mental capacities with a smile.

SCALE 5499170
AT LAT. 55.250

Fig. 1 STATIONS OCCUPIED DURING LEG I.



OPERATIONS

CTD Niskin/Water Samples

A rosette sampler with CTD (1500 meter) and five liter Niskin bottles were used throughout the Leg. A transmissometer, to measure transparency, was also attached to the rosette sampler.

CTD data were logged in the following formats:

- 1) Analog: XXXY recorder, Temperature/Conductivity/Transmissometer vs. Depth.
- 2) Digital: 9 track using PMC software (LMACTD) all four channels.

Using DDL2 and SURVEYOR modified DDL2, digital data dumps were provided to the scientific personnel for each cast.

Unfortunately, both CTD fish were found to be defective early in the cruise. The spare CTD was totally inoperative due to loose circuit boards but was repaired by the ET Department (calibration was, of course, invalidated). A post-calibration will be required on CTD #6234 to validate the data. A third CTD, delivered by helicopter, was installed on 06 February, following the time series at PM3.

Deployment of PR-1B & PR-2B

These two sub-surface meter moorings were deployed for Dr. R.B. Tripp, University of Washington.

The 28" sub-surface float, current meters and viny floats were first deployed over the starboard side while SURVEYOR drifted to port. A two-wheel anchor and acoustic release was then attached to the array and lowered over-the-side using the GEAR-MATIC winch on the main crane. When the anchor weight reached bottom, the gravity release freed, and deployment was completed. These deployments were made without incident in about one-half hour.

Recovery of TP-2, TP-4, TP-5, and TP-6

SURVEYOR recovered four current meter moorings deployed on Leg IV, RP-4-SU-80A. Loran-C proved to be repeatable within 100 feet, or less, in all cases. When sea conditions were favorable a small boat was launched to attach a line from the ship to the large top float. At other times, with winds above 15-20 knots, SURVEYOR drifted onto the array with the wind on the port beam while the buoy was lasoed on the starboard side. The line was then hauled in by the foredeck capstan until a chain stop hook could be employed to restrain the array and allow for separation. The starboard foredeck crane was then attached to the sub-surface float of the array to bring aboard the remaining portion. The entire array, using this method, was retrieved without incident in a period of about one hour.

IGOSS Observations were taken in accordance with Sailing Orders and will be reported under separate cover.

Deployment of TP-2B, TP-7, TP-8, & TP-9

These sub-surface current meter moorings were deployed in the reverse manner of the aforementioned recoveries, however, the top sub-surface float was connected to a trigger (gravity) release, and when the array was lowered to the bottom, with the majority of the weight removed, the trigger released the top float and deployment was complete. The small boat was not required for deployment. Appropriate information was sent to the Coast Guard for insertion into the "Local Notice to Mariners". Because sea and wind conditions were very favorable, the deployments were made without incident and required about one hour for completion.

Pimatmat Coring Sampler

The Pimatmat bottom sampler, a four barrel core, was deployed midships using the GEAR-MATIC winch and main crane. The corer would trip on the bottom taking four simultaneous cores. Since the Pimatmat is designed to sample mud bottoms, it was desirable to determine bottom composition with the Smith-MacIntyre first.

Smith-MacIntyre Grab Sampler

A Smith-MacIntyre grab sampler was used for the majority of bottom sample stations conducted during this Leg. The grab sampler was lowered from the starboard fantail using the hydraulic boom and the Rowe winch. After being cocked open, the grab would be lowered to the bottom at about 25 meters/minute, closing on impact. The scientific personnel would remove the required amount of sample when on deck. At selected stations, a butterfly water sampler was attached to the Smith-MacIntyre, and would trip (fill with water) concurrently when the grab was on the bottom.

Butterfly Water Samplers

The butterfly samplers provided in situ water samples; and were attached to the Smith-MacIntyre grab sampler; 10 meters (approximately) above the CTD fish; and from a separate winch midships, on the starboard side. The samplers on the Smith-MacIntyre grab sampler was tripped on contact with the bottom. The plastic bags, containing the water samples, were removed on deck and processed by the scientific party.

Bird Observations

Bird Observations were conducted throughout the Leg on a not-to-interfere basis. The bird observer, Nancy Butowski, tabulated all sightings during the 10 minute transect periods (while underway at a constant speed and heading).

Marine Mammal Observations

Observations were conducted in accordance with RP-13-80. A few sightings of mammals occurred in the project area and will be reported on the forms provided.

SEABEAM Trackline Data

SEABEAM trackline data, project instructions S-N707-SU-80, were obtained enroute to Kodiak and Unimak Pass. One line was completed between designated points E to F heading toward Kodiak and another line in the Chirikov box while transiting to Unimak Pass. The data will be reported under separate cover. Problems with the Loarn-C SURVEY program precluded automated use of the system. Ship positions and swath width were manually plotted.

Helicopter Operations

NOAA Helicopter N57RF piloted by Lt. R.B. Christman, NOAA, and mechanic Bob Nield, joined SURVEYOR off Port Moller on 06 February. A series of flights into the Port Moller area, Lagoon Point, and Izembek Lagoon, provided the scientific party the opportunity to obtain the mud and water samples they desired and service of the meteorological station at TP-1. A complete report on helicopter operations, by Lt. Christman, will be included as an appendix to the cruise report.

Navigation and Smooth Plot

Navigation control consisted primarily of Loran-C coupled to an InterNav CC2 converter. The JMR Satellite Navigation system was used to verify Loran positions and time delays. To further enhance the reliability and repeatability of the Loran-C system, one of SURVEYOR's PDP 8e computers was set up with RK321 Loran-C Utility program. SURVEYOR followed guidelines of the OCSEAP Navigation Subinstructions. Smooth plotting was done on OS sheets appropriate for the area.

Problems and Recommendations

SURVEYOR's CTD system required an inordinate amount of attention and pampering, even after replacing two CTD fish, installing a new set of slip rings on the winch, reterminating and rewiring the sea-cable a number of times, and using an inordinate amount of ET overtime to accomplish the repairs. A third CTD fish, #6201, was flown by helicopter to SURVEYOR and installed on 06 February. SURVEYOR's two original fish required internal repairs, invalidating their calibration. Fish #6234, used prior to the installation of #6201, will require a post-calibration to validate the data. To complicate the situation, the sea-cable developed a short between the rosette signal conductor and armor shield. This cable was replaced during the following Kodiak import. Hopefully, the system will remain functional for the remaining two Legs of "A" Cruise.

Weather was excellent during the first two weeks of the project, however, conditions deteriorated when operations shifted to the Saint George Basin causing a loss of about two days to rough seas.

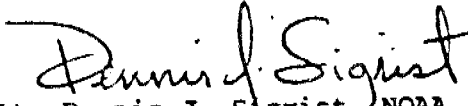
Conclusions

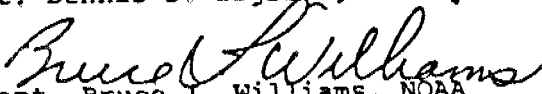
Even though the vessel CTD system was a cause of constant concern during this Leg, all major project objectives were accomplished as planned. This was, in part, due to the unseasonably fine weather during the first two weeks of the project and the continuing support provided by SURVEYOR's officers and crew and the visiting scientific party. Helicopter operations proceeded without incident due to the excellent support provided by the crew of N57RF.

Dr. Jim Schumacher did an excellent job coordinating the varied requirements of the scientific party. The "Station Activity Plan" form, listing specific operations for each station, proved to be an effective way of organizing the scientific party and ships' personnel into a working team. We will look forward to seeing our friends from PMEL (and other institutions represented) on subsequent cruises.

Compilation

The Chief Scientists' Report was compiled by Dr. James D. Schumacher, PMEL. Other sections were prepared by Lt. Dennis J. Sigrist, NOAA.

Compiled by:  Lt. Dennis J. Sigrist, NOAA

Approved by:  Capt. Bruce I. Williams, NOAA

IV. D

Preliminary Results

from

Current Hydrographic and Meteorological

Data: Unimak Pass, Alaska

Prepared for OCSEAP as
partial fulfillment
of RU 549 & RU 367

by

J. D. Schumacher

C. A. Pearson

and

J. E. Overland

All at

Pacific Marine Environmental Laboratory
3711 15 Ave. NE
Seattle, WA 98105

1. INTRODUCTION

Proceeding westward along the Alaska Peninsula, the first connection of substantial cross-sectional area between north Pacific Ocean (Gulf of Alaska) and Bering Sea waters is Unimak Pass (Figure 1). Historically, there exists the supposition that waters of the Gulf of Alaska enter the Bering Sea through this pass; general inflow vectors appear on large scale circulation schemes (e.g., Hughes, Coachman and Aagaard, 1974; Takenouti and Ohtani, 1974; and Favorite, Dodimead and Nasu, 1976). Such schemes have led to a sense of consistent inflow to the Bering Sea. Data collected during Outer Continental Environmental Assessment Program (OCSEAP) confirmed that westward flow does occur, at times, through Unimak Pass. Five drift cards, deployed off Kodiak Island in the Alaska Stream, were recovered along the Bering Sea side of the Alaska Peninsula and on St. George Island (Muench and Schumacher, 1980). A satellite tracked drifter travelled close to Akutan Island west of the pass, was set to the north after crossing most of the pass and then drifted eastward along the Bering Sea side of Alaska Peninsula grounding on Amak Island (Kinder, Schumacher and Hansen, 1980; see their Figure 6a). The intermittent nature of inflow was suggested by the drifter's trajectory which crossed most Unimak Pass before being set in and the lack of an onshelf (or through the pass) component in the mean flow observed on both the Gulf of Alaska (Muench and Schumacher, 1980) and Bering Sea (Kinder and Schumacher, 1981a) side of the pass, however, drift cards and drift bottle studies (Favorite and Fisk, 1971) suggested no outflow from the Bering Sea.

To describe the nature of flow in Unimak Pass, three current meter moorings were deployed in March 1980 and recovered in August 1980. The locations of these moorings (Figure 1) provide current records from either side of the pass and from within the region of minimal cross-sectional area

between Scotch Cap and Ugamak Island. Because the pass is heavily travelled by shipping and barge traffic, mooring lengths were kept to a minimum (currents are from about 20 m above the bottom), but above the bottom boundary layer. The purpose of this report is to provide, in a timely manner, preliminary analysis of current, hydrographic and atmospheric pressure data. These data support the mean inflow schemes; however, about 25% of the current observations indicated energetic outflow pulses from the Bering Sea, lasting up to ~3 days and these pulses were related to meteorological forcing.

2. SETTING

Complex orography and bathymetry typify geomorphological contours in the vicinity of Unimak Pass (Figure 1). At its narrowest location, as defined by a line from Scotch Cap to Ugamak Island, the pass is 19 km wide with an average depth of ~55 m or a cross-sectional area of about 10^6 m^2 . The along-pass axis normal to this cross section is taken as 285°T . On either side of this cross-section, bottom depths increase to greater than 92-m deep depressions which shoal before reaching the shelf edge (183-m isobath). Further complexity exists due to the presence of the Krenitzin Islands southwest of Unimak Island and the passes between these islands and Unimak Pass proper.

Orography is also complex. On the Krenitzen Islands, there are many peaks in excess of 800 m and elevations up to 2500 m exist on the western end of Unimak Island, where there also are several glaciers. The effect of such features katabatic winds on a small scale (5-25 km) steering of meso-scale geostrophic winds was documented in other Alaskan regions (Muench and Schumacher, 1980; Reynolds, 1980). We expect similar conditions to obtain here.

3. METHODS

Aanderaa RCM-4 current meters were used on taut wire moorings with an anchor and acoustic release at the bottom and 450 kg buoyancy subsurface float 2 m above the current meter. A summary of location, duration and statistics of each station's current meter is given in Table 1.

Current data were resolved into north and east components and low-pass filtered to remove high-frequency noise. Two new data series were then produced using a Lanczos filter (cf. Charnell and Krancus, 1976). The first series, called the 2.9 hr. filtered data, was filtered such that over 90% of the amplitude was passed at periods greater than 5 hr, 50% at 2.86 hr, and less than 0.5% at 2 hr. This series was used to determine tidal constituents and to provide spectral estimates. The second series, called the 35 hr. filtered data, was filtered to remove most of the tidal energy, passed over 99% of the amplitude at periods of over 55 hr, 50% at 35 hr, and less than 0.5% at 25 hr. This was resampled at 6-hr intervals and was used for examining sub-tidal circulation.

Temperature and salinity data were collected using Plessey model 9040 CTD systems with model 8400 data loggers. These systems sampled five times per second for simultaneous values of conductivity, temperature and depth. Data were recorded during the down cast using a lowering rate of 30 m min^{-1} . Nansen bottle samples were taken at every other station to provide temperature and salinity calibration. Data from monotonically increasing depth were despiked to eliminate excessive values and were averaged over 1-m intervals to produce temperature and salinity values from which density and geopotential anomaly were computed.

eastward as about Port Moller (about 300 km). While such distributions may simply represent presence of human activity, they could be considered supportive of non-outflow from the Bering Sea; all 38 drift cards returned (~4% of the total released) all were found along the Bering Sea shoreline..

5. CURRENTS

We begin our examination of current behavior in the vicinity of Unimak Pass with mean and low-frequency (periods $\geq 1\frac{1}{2}$ days) flow. At periods between $1\frac{1}{2}$ and 10 days, currents over continental shelves respond mainly to meteorological forcing, generally manifested as Ekman fluxes and cross-shelf barotropic pressure gradients. Over periods longer than 10 days, baroclinic pressure gradients can generate substantial alongshore currents. For northern latitudes, where water temperatures are generally less than 10°C , the equation of state for seawater implies salinity contributes more than temperature to density (Gebhart and Mollendorf, 1977). In the Gulf of Alaska, the freshwater flux results in a substantial long-term (order months) baroclinic cross-shelf pressure gradient which contributes to the alongshore coastal flow or Kenai Current (Schumacher and Reed, 1980). Interactions between oceanic circulation, either meso-scale eddies or larger scale circulation features, also can force mean shelf flow (Csanady, 1978; Beardsley and Winant, 1980). We examine current records to elucidate which of these processes are important in the Unimak Pass region.

Mean and Low Frequency Currents Current record statistics from the 2.9 hr. filtered data and mooring information are given in TABLE 1.

Drift cards were made of plastic, 3" x 5" in size and had a specific gravity of about 0.9 which caused them to float nearly submerged at the water surface. The resultant low above-water profile minimizes wind effect upon the cards, consequently movements should be representative of surface water motions. It should be stressed that the cards were not intended to yield actual trajectories, rather to provide, by distribution of their recoveries, a description of possible areas for grounding of an oil spill occurring at a given location. No attempts were made to compute transit times, since there was no way of knowing how long the cards had lain upon the beaches from which they were recovered. This was particularly true in our study region, where the beaches are relatively uninhabited.

From 0000 GMT 11 Mar 1980 to 1200 GMT 11 Aug 1980 Unimak Pass pressure gradients were measured using the National Meteorological Center's twice daily final sea level pressure analyses for the Northern Hemisphere. From 0000 GMT 12 Aug 1980 to 1200 GMT 07 Sep 1980 gradients were obtained from the final sea level pressure analyses of the Alaska region prepared twice daily by the National Weather Service Forecast Office of Anchorage, Alaska. Each map was quality checked for station accuracy and pressure analysis, and then a pressure gradient vector was determined for 54°N, 165°W and recorded in terms of direction from true north and magnitude in mb/1° latitude.

4. DRIFT CARDS

Drift Cards. During the summer of 1979, two sets of 500 drift cards were released in Unimak Pass (Figure 2). Deployment and recovery positions and times are given in Appendix A. As shown in Figure 2, all recoveries were from the Bering Sea and were found predominantly along the peninsula as far

Vector mean flow was strongest in the pass, with moderate flow on the Bering Sea shelf and weak flow east of the pass. These entire record length (147 day) means, as determined from 35 hr filtered data, are shown in Figure 3A as arrows with one standard deviation bars on the major (containing maximum variance) and minor axes, and in 3B as magnitude and percent total number of records partitioned into twelve 30° sectors. These depictions show that currents were westward through the pass and constrained to flow predominantly along channel. On the Gulf shelf the vector mean was weak and current direction was highly variable, while over the Bering Sea shelf flow was about twice as strong and more uniform than in the gulf. The distribution of speed and magnitude of direction is also clearly shown in scatter plots of the current data (Figure 4A). Each dot represents the end of a six-hourly current vector and as density of crosses increases, so does number of observations. At UP1, currents were generally toward the northwest with mean speed in that direction of about 15 cm/s, however, there were 15 to 20 cm/s pulses to the south. Currents at UP2 followed the bathymetry with a strong tendency for west-northwest flow, however, pulses in the opposite direction existed. The magnitude of the largest pulses was about 60 cm/s. Over the gulf shelf at UP3, flow was highly variable in direction with a westward tendency, but with moderate (~20 cm/s) south-eastward pulses. Progressive vector diagrams (Figure 4B) depict flow as above, however, the 5-day time ticks suggest that over the observation period two levels of horizontal kinetic energy (HKE) obtained, a high energy period during the first 50 to 60 days followed by a period of weaker currents.

Time-series of the three 35 hr filtered current records (Figure 5) again indicates a transition from energetic flow (between 23 March and about 22 May) to weaker flow in summer. Further, the forcing which resulted in flow

TABLE 1
CURRENT RECORD STATISTIC AND MOORING INFORMATION

Mooring Position	Water Depth	Observation Period: Record Length	Velocity Components (cm/s)						Speed (cm/s)		Vector Mean Speed Dir (cm/s) (°T)	
			V (North-South)			U (East-West)			mean	max.	(cms)	(°T)
			mean	max.	st. dev.	mean	max.	st. dev.				
UP1 54.56°N 165.40°W	84	22 Mar 16 Aug 147	3.82	-77.8	32.6	-4.2	-63.4	22.6	35.9	91.3	5.8 at 311°	
UP2 54.30°N 164.76°W	80	Same	2.9	77.5	77.9	-12.1	173.8	68.2	64.3	183.8	12.7 at 284°	
UP3 54.16°N 164.01°	68	Same	-1.3	48.9	10.3	-1.5	45.9	12.8	14.6	52.7	2.0 at 233°	

Alaska and Bering Sea. The phase of the M_2 constituent at Sanak Island, 142 km east of Unimak Pass in the Gulf of Alaska, is 320° , while at stations BC3, 80 km north of the pass, the phase is 89° . The Tidal Current Tables (National Ocean Survey, 1979) give an average flood (direction $295^\circ T$) of 3.4 knots and an average ebb ($105^\circ T$) of 3.0 knots at a location off Scotch Cap.

The data from the three Unimak Pass current meter stations were analyzed for tides using a Munk-Cartwright response analyses. Results, in an ellipse representation are given in TABLE 2 for the six major constituents, and in Figure 6 for M_2 and K_1 . The ellipses are aligned with flow through Unimak Pass. Velocities at UP2, near the center of the pass, were 50%-60% of those predicted in the tidal current tables. The higher velocities for the NOS station resulted from its location in shallower water near a headland. (Scotch Cap).

The tidal current at all three locations is mixed predominately semidiurnal, meaning that there are substantial diurnal inequalities, mostly in the ebb currents. That is, there are generally two flood currents of approximately equal velocity each day, while one of the ebbs is weak and the other strong, with larger velocity than the floods. During extreme lunar declination the weaker ebb may disappear entirely so that there is one flood of variable velocity lasting most of the day, and one strong ebb.

Tidal excursion (in kilometers) during a semidiurnal period may be estimated by summing the appropriate constituent amplitudes and multiplying by 0.14. The excursion during mid-June 1980, when the moon (M_2+K_1) was near its maximum declination ($+O_1$), in perigee ($+N_2$), was a new moon ($+S_2$) and near summer solstice ($+P_1$), was approximately $0.14 (M_2+N_2+S_2+K_1+O_1+P_1) = 29$ km. This is seen in Figure 7, a progressive vector diagram for UP2 on June 12, 1980, where the excursion on the greater ebb is about 32 km. The difference is accounted for by a small non-tidal current and other minor tidal constituents.

reversals within Unimak Pass also had manifestations on either side of the pass. During mid May, an extended (about 2½ days) strong (about 40 cm/s) reversal occurred in Unimak Pass. Over the entire record, about 25% of the observations suggested a reversed flow component. We summarize the above current data as follows: 1) on the Bering Sea mean shelf approximately 50 km from Unimak Pass, mean flow exhibited moderate speeds (about 9 cm/s) and some preferential direction (about 50% of the records were in the NW quadrant); current here appeared related to that in Unimak Pass, particularly at times of current pulses, 2) currents within Unimak Pass were strongly constrained by bathymetry, mean speed was large (about 19 cm/s) and direction bimodal with reversals (from the Bering Sea into the Gulf of Alaska) occurring in about 25% of the records, 3) currents on the continental shelf about 50 km southeast of Unimak Pass were low (about 7 cm/s) in a mean sense and due to the high degree of directional variability, very weak (about 2 cm/s) as a vector mean; the lack of a significant vector mean suggests that interactions between the nearby Alaskan Stream and the shelf were not important for long-term current, 4) all three current records indicated that a high and low energy regime existed; seasonality also occurs in the northwest (Schumacher and Reed, 1980) and northeast (Lagerloef, Muench and Schumacher, 1981) Gulf of Alaska where alongshore wind stress dominates winter flow and is less important at other times.

Tides Tides in the vicinity of Unimak Pass, in both the Gulf of Alaska and the Bering Sea, are of the mixed, predominately semidiurnal type. The tide progresses from the Gulf to the Bering. Strong tidal currents are found in Unimak Pass due to the large phase differences of the tide between the Gulf of

Spectra and Kinetic Energy We use rotary spectra to elucidate energy distribution. Using this technique, we do not have to select axes since these analyses decompose the current vectors into clockwise and anticlockwise rotating components, where orientation at a given frequency is a result rather than an input parameter. The ensuing rotary spectra, partitioned into winter (the first 70 days starting 22 March) and summer (70 days starting 31 May) segments are shown in Figure 8. Several features are apparent: energy levels at subtidal frequencies were lower in summer at all locations; at UP1, the anticlockwise component tended to dominate at low frequencies during winter, but in summer the clockwise component contained more energy; at UP2, geometric constraints resulted in nearly rectilinear flow; and at UP3 the clockwise component was always greater but energy levels at the lowest frequency (0.06 cpd) were comparable during both segments.

Using results from the rotary analysis, we define major and minor orthogonal axes for each of the current records and some of these varied with season as follows:

Mooring	Winter		Summer	
	Major (°T)	Minor	Major (°T)	Minor
UP1	335	065	350	080
UP2	280	010	Same	
UP3	276	006	300	030

TABLE 2
TIDAL CHARACTERISTICS

		Major axis		Minor axis		rotation
		H, cm/s	G°	D°T	H, cm/s	
UP1 54°33.7N 165°24.0W	O ₁	21.9	271	328	10.8	C
	P ₁	8.5	303	321	4.0	C
	K ₁	25.4	304	318	12.1	C
	N ₂	6.6	328	354	0.2	C
	M ₂	35.0	20	335	5.3	C
	S ₂	6.9	64	317	0.2	C
UP2 54°18.1N 164°45.9W	O ₁	33.6	261	290	5.3	A
	P ₁	16.3	286	288	1.9	A
	K ₁	49.4	287	288	5.5	A
	N ₂	17.6	338	293	1.5	A
	M ₂	73.5	26	293	5.3	A
	S ₂	15.3	78	291	0.4	A
UP3 54°09.6N 164°00.4W	O ₁	4.0	238	340	3.3	C
	P ₁	1.8	250	338	1.3	C
	K ₁	5.4	249	330	4.2	C
	N ₂	2.6	291	315	0.9	C
	M ₂	11.3	342	297	3.5	C
	S ₂	2.5	59	262	0.7	A

Where amplitude, H is in cm/s. phase, G, is referred to Greenwich, D is the direction of the major axis on the flood and C indicates clockwise rotation, A anticlockwise rotation.

Each time series was decomposed into orthogonal components to determine distribution of horizontal kinetic energy with frequency, where all units are cm^2/s^2 and

$KE = \frac{1}{2} [(\bar{u})^2 + (\bar{v})^2]$ is the kinetic energy of the segment mean,

$KE' = \frac{1}{2} (u' + v')$ is the total fluctuating kinetic energy (prime indicates record segment variance),

KE'_{LF} is the amount of fluctuating kinetic energy in periods greater than 1.5 days, i.e., meteorological and longer period (>10 day) forcing,

KE'_T is the kinetic energy at tidal frequencies.

The resulting quantities are given in TABLE 3:

TABLE 3
DISTRIBUTION OF HORIZONTAL
KINETIC ENERGY

Mooring	KE		KE'	KE' _{LF}		KE' _T (%KE')
	Major	Minor		Major	Minor	
<u>A. Winter</u>						
UP1	37	11	770	55	12	675 (88)
UP2	192	1	2602	302	8	2248 (86)
UP3	4	2	164	38	20	69 (42)
<u>B. Summer</u>						
UP1	2	0	785	15	4	720 (92)
UP2	13	0	2786	68	7	2625 (94)
UP3	0	1	102	12	7	64 (63)

We note that \overline{KE} decreased by more than an order of magnitude between winter and summer at UP1 and UP2, with major axis mean speeds decreasing by a factor of about five and four respectively. While major axis speeds also decreased at UP3, they were always weak (2 to 3 cm/s). Although at UP3 KE' and KE'_{LF} were less than that in the two other current records, because KE'_T was also substantially less as percent of KE' , KE'_{LF} was a large fraction (about 35%) of the total horizontal kinetic energy during winter. We also note that axes selection was relatively less definitive at UP3, as was suggested in the scatter diagrams (Figure 4).

Synthesizing current analysis presented above, the following behavior of currents obtained:

1. Mean and subtidal frequency currents exhibited strong seasonal differences; e.g., 70 day vector mean flow in Unimak Pass decreased from about 20 cm/s in winter to about 5 cm/s in summer but mean direction was consistent (into the Bering Sea). During winter, strong mean flow through the pass was apparently related to a moderate (about 10 cm/s at 310°) vector mean flow at UP1; however, south of the pass at UP3, the relation of vector mean flow to that which obtained in the pass appeared to be weaker. During summer, weaker vector mean flow (about 5 cm/s) in the pass appeared to have much less impact on flow at UP1 and as in winter, also at UP3.
2. KE'_T dominated total HKE north of and within the pass, but on the Gulf of Alaska shelf $KE'_{LF} \cong KE'_T$ during winter.
3. The distributions of HKE suggested that some manifestation of meteorological forcing was responsible for the seasonal signal. We note that current records were obtained 20 m above the seafloor, and in

all cases this was at least 40 m below the surface, or below a typical Ekman layer depth. Thus, these records, while indicating impact of barotropic flow established by meteorological forcing, cannot be used to infer quantitatively the direct contribution of wind stress at the surface.

6. ATMOSPHERIC PRESSURE GRADIENT

Coastal wind observations from Alaska are generally contaminated due to local orographic effects, however, we can estimate meteorological forcing by using the observed synoptic scale atmospheric pressure gradient computed for Unimak Pass. If meteorological forcing in terms of storm events was responsible for the seasonal signal in the current HKE, then spectral analysis of the atmospheric pressure gradient time series should also exhibit strong seasonality. Spectra for the same two record segments used for currents are shown in Figure 9, and summarized below:

Period	Total KE'	KE' LF on 150°T
Winter	2.2	1.2
Summer	0.9	0.4

where the 150°T axis is normal to the Alaska Peninsula and total variance is independent of axes and units are $\text{mb}^2 / (1^\circ \text{L} \& \text{t})^2$. Clearly, total variance was greatest in winter at all frequencies, however, resolved on 150°T, ΔP spectra indicated higher energy in summer at a period of ~ 1.8 days. Further, during summer peaks in this spectra at 1.8 and 3.9 days were more distinct and were shifted in frequency from those in winter. We note that the 3.9 day peak during summer contained about 1/3 of the total energy at periods ≤ 10 days.

The impact of the pressure gradient (ΔP) on the observed currents is shown in Figure 10 where the currents are resolved along the major axes for the entire record and the pressure difference (Δ Pressure) is resolved on a $150^\circ T$ axis. Using this axis, negative Δ Pressure implies lower pressure over the Bering Sea than over the Pacific Ocean. This latter axis was selected assuming that shelf winds will tend to flow parallel to the coastal mountains. The strongest pressure gradients occurred during winter and changes in ΔP are visually correlated with flow reversals in Unimak Pass (UP2). During summer, the relation still obtains but magnitude of events was less.

7. HYDROGRAPHY

An important factor in long-term flow along the Gulf of Alaska coast is a cross-shelf density gradient which appeared to be in geostrophic balance (Royer, Hansen and Pashinski, 1979; Schumacher and Reed, 1980; Reed, Schumacher and Wright, 1981). The strength of the baroclinic component is related to the annual hydrological cycle (Royer, 1979); however, such features have not been defined along the Gulf side of the Alaska Peninsula. We examine summer CTD data for suggestions of a westward flowing coastal current and magnitude of vertical and horizontal gradients (fronts) in the vicinity of Unimak Pass.

Ten CTD stations were occupied between 4 and 5 September 1980 along a line running southeastward through Unimak Pass and then southward to the shelf edge (Figure 11). Over the Gulf shelf, thermal stratification (given on Figure 11 as $\Delta T = \left| \text{surface temperature} - \text{bottom temperature} \right|$ from the 1-m average data) exceeded $4.5^\circ C$ and resulted from a greater heat content in the upper layer than existed over the Bering Sea shelf. Although HKE within

Unimak Pass was large, thermal stratification was greater in the pass ($\sim 2.6^{\circ}\text{C}$) than over the Bering Sea shelf at station 14 ($\sim 0.9^{\circ}\text{C}$). In terms of salt content, a similar condition existed; maximum ΔS values (1.23 gkg^{-1}) occurred over the Gulf shelf, persisted within the pass ($\Delta S = 0.45 \text{ gkg}^{-1}$) and were minimal just west of the pass proper ($\Delta S = 0.18 \text{ gkg}^{-1}$). The result of heat and salt stratification on density is shown in the bottom panel of Figure 11, where density stratification ($\Delta\sigma_t$) showed the same characteristics. A region of low salinity ($\leq 31.5 \text{ gkg}^{-1}$) water appeared to be confined within about 20 km of the coast. The presence of less saline water over the gulf shelf south of the peninsula was also noted by Wright (1981) during February 1980. West of the pass, a haline front occurred in water depths between 125 and 150 m. This feature may be an extension of the middle front which exists over the southeast Bering Sea shelf (Coachman and Charnell, 1979; Kinder and Schumacher, 1980b). This front has a profound impact on nutrient fluxes (Iverson, et al, 1980; Coachman and Walsh, 1981) and may be important to dissolved oil transport. We note that the vertical salinity gradient ($\Delta S/\Delta Z \text{ gkg}^{-1} \text{ cm}^{-1}$) at station 13 was about $6 \times 10^{-5} \text{ gkg}^{-1} \text{ cm}^{-1}$ or sixty times the value reported for the middle front about 100 km to the north (Coachman, et al, 1980). In terms of a vertical mean horizontal salinity gradient ($\overline{\Delta S}/\Delta X \text{ gkg}^{-1} \text{ km}^{-1}$), the magnitude of the front between (13 and 14 CTD stations) observed in these data was $32 \times 10^{-3} \text{ gkg}^{-1} \text{ km}^{-1}$ or about three times larger than that given by Kinder and Coachman (1978). The bottom 50 m average horizontal salt gradient was $84 \times 10^{-3} \text{ gkg}^{-1} \text{ km}^{-1}$ or nearly four orders of magnitude greater than values given for the middle front (Coachman et al, 1980).

We estimate the impact that the observed mass distribution had on the velocity field by assuming a baroclinic geostrophic balance. This method

neglects factors such as wind stress, bottom friction and barotropic pressure gradients, however, during summer conditions (light winds) and in particular over the Bering Sea shelf (Kinder and Schumacher, 1981a) and in the Gulf of Alaska (Royer, Hansen and Pashinski, 1979; Schumacher and Reed, 1980) good agreement obtained between baroclinic geostrophic and observed flow. Dynamic relief between most station pairs was insignificant, however, substantial values obtained between the following pairs:

BAROCLINIC GEOSTROPHIC
CURRENTS

Station pair	Separation (km)	0/50db Dynamic Relief (dyn.m)	Speed (cm/s)	Direction (°T)
12/13	13	0.014	9.0	NE
13/14	13	0.015	10.0	NNE
14/15	13	0.011	7.0	NE
18/19	21	0.012	5.0	E

The inferred flow from the first three station pairs suggests moderate inflow through Unimak Pass which is consistent with current observations. Further, the direction of dynamic topography lines compares favorably with contours presented by Coachman and Charnell (1977), while magnitude appears stronger than their dynamic topographics for March and July CTD data. Between Gulf shelf and Alaska Stream waters (stations 18 and 19), there was a reversal of the baroclinic field. This feature has been noted as characteristic of the northwest Gulf of Alaska shelf (Reed, Muench and Schumacher, 1980; Schumacher and Reed, 1980) and appears to hold for baroclinic fields south of the Alaska Peninsula.

In summary, hydrographic data suggest that:

1. During summer, vertical stratification ($\Delta\sigma_t \sim 0.7$) existed within the pass and resulted from a combination of freshwater and insolation.
2. The horizontal gradient west of the pass appeared to be an extension of the middle front, however, gradients were stronger than those generally observed further northwest which suggests importance of less saline waters from south of the Alaska Peninsula.
3. Baroclinic flow generated by the mass distribution implied inflow through Unimak Pass with estimated speeds of 2 to 10 cm/s. Such flow may represent a baroclinic coastal flow similar to the Kenai Current.

8. DISCUSSION

We have shown that currents at the three locations are visually related to each other and to the atmospheric pressure gradient normal to the topography. We now quantify such relationships using linear correlation and coherence estimates. Correlations were calculated using record length major axes of 330° , 285° and 280° respectively for UP1, UP2 and UP3 and 150° for the pressure gradient and are given in TABLE 4:

TABLE 4
CORRELATION MATRIX
OF
35 HR. FILTERED DATA

A. Winter				
	UP1	UP2	UP3	ΔP
UP1	1.0*	-	-	-
UP2	0.70*	1.0*	-	-
UP3	0.37*	0.74(6)*	1.0	-
ΔP	0.66(12)	0.79(12)*	0.56(12)*	1.0*

B. Summer				
	UP1	UP2	UP3	ΔP
UP1	1.0*	-	-	-
UP2	0.23	1.0*	-	-
UP3	-0.16(24)	0.49(6)*	1.0*	-
ΔP	-0.17(-12)	0.63(18)*	0.30(12)*	1.0*

where the number in parenthesis is the lag in hours (no number means 0 lag) and column lags row. * indicates a significant correlation at the 95% level.

Winter correlations were consistently greater than during summer with the greatest correlation in either season between UP2 current and atmosphere pressure gradient. Currents on either side of the pass were both highly correlated (accounting for ~50% of subtidal variance) to flow within the pass during winter; in summer, currents in the pass were significantly more correlated to those on the Gulf shelf. The values in TABLE 4 substantiate visual relations between current record pairs and suggest that a linear relation between atmospheric pressure gradient and current in Unimak Pass accounted for 62% to 40% of the winter/summer variance. We note, however, that the energy in each of the records was not distributed equally throughout the frequency domain and linear correlations are performed in the time domain. Thus, we now consider coherence (similar to correlation but calculated in the frequency domain) between records.

In Figure 12 we show coherence squared estimates for each of the current record pairs, where row A is the cross-spectral energy, row B the phase (where the solid bar represents winter time confidence interval) and row C coherence squared. The solid line is for the winter record segment and dashed for summer, where the series were resolved on the major axes determined from rotary spectra (see Section 5). During winter at frequencies ≤ 0.3 cpd (~ 3 days), the phase suggests that currents at UP1 lag those at UP2 or UP3. The greatest coherence occurred between UP1 and UP2 at periods >10 days, however, currents were highly coherent (>0.8) over a wider frequency range (0.4 to 0.04 cpd) between UP2 and UP3. Between UP1 and UP3 (about 100 km) significant coherence existed at periods >5 days, and again the phase suggests flow into the Bering Sea at these periods. We note between 2 and 3 day periods, however, that currents at UP2 lagged those at UP1 and were coherent above the 95% level of significance. During winter, coherent inflow to the Bering Sea occurred at periods approximately >5 days and the variance accounted for was generally $>70\%$. Flow reversals with 2 to 3 day periods were coherent between UP1 and UP2, but not with the record from the Gulf shelf.

During summer, cross-spectral energy levels were lower except at periods <2.5 days. Currents at this frequency were highly (≥ 0.9) coherent between both UP1/UP2 and UP3/UP2 pairs, and the phase suggests that these were outflow events. For longer periods, coherence was less than in winter and was significant over the 100 km separation only at 2.5 and 1.8 day periods with the suggestion that currents at UP3 lagged UP1.

Coherence squared estimates between 35 hr filtered current and ΔP are shown in Figure 13, where ΔP is resolved on $150^\circ T$ and current series on the various winter/summer axes. In all cases, significant coherence is greater in winter than in summer at periods longer than about 3 days; during summer the

only significant coherence at such periods occurred within Unimak Pass. Coherence squared between ΔP and UP1 or UP2 has a second significant peak at periods of about 2 days which corresponds to the peak in the ΔP variance spectrum (Figure 9). Summing the percent of current variance at each frequency which was significantly coherent with ΔP , we determine that about 78% of the variance in the current record from UP2 was explained by ΔP in winter, and 39% during summer.

We suggest that when ΔP is negative, with the isobars decreasing from the Gulf of Alaska to the Bering Sea (as occurred during the 2½ day reversal in May, Figure 14), the ensuing wind field has a major component parallel to the isobars. Given such wind fields, Ekman fluxes will generate set up on the Bering Sea side and set down or coastal divergence on the Gulf side of the peninsula. The result would be barotropic outflow through Unimak Pass. Reversing ΔP would result in inflow through the pass. We note that while our general description of the wind field may hold along most of the peninsula, there are gaps in the orography, e.g. Unimak Pass and at Cold Bay, ^{which} induce orographically controlled wind flow down ΔP rather than parallel to isobars. An example is shown for OOGMT, 13 May 1980 (Figure 14). Coastal winds had an alongshelf component while the surface wind at Cold Bay was directed through a low region in the peninsula to the north at 25 knots. While the major portion of transport is out of the Bering for such storm events, surface current flow may be in the opposite direction due to channelling of wind from high to low atmospheric pressure. Although such local orographic effects will be important to the distribution of surface oil, on the larger scale we expect set up and set down to dominate current generation and transport through the Pass.

9. CONCLUSIONS

From the data and analysis presented in this report, we make the following conclusions about flow and forcing in the vicinity of Unimak Pass:

1. Mean flow was westward through Unimak Pass, however, reversals occurred in 18% of winter 35 hr filtered current observations and 31% of those made during summer.
2. Magnitude of low frequency current in Unimak Pass was seasonal and highly coherent at selective frequencies with an atmospheric pressure gradient normal to the Alaska Peninsula.
3. Current in the pass was generally more coherent with current on the Gulf shelf than that in the Bering Sea, with all coherences showing a seasonal trend.
4. Coherence existed between the pressure gradient and currents on either side of the pass, however, such estimates were typically less than those between ΔP and currents in Unimak Pass.
5. The observations suggest that currents driven by wind set up and coastal divergence on either side of the pass result in a large fraction of the observed flow through the pass.
6. Long-term forcing for inflow to the Bering Sea appeared to be related to a baroclinic coastal current flowing westward along the southern side of the Alaska Peninsula.
7. The inflow of less saline Gulf of Alaska shelf waters appeared to have strengthened horizontal gradients in the middle front located about 50 km west of the pass.

10. ACKNOWLEDGEMENTS

We acknowledge the aid of a large number of persons, not only in the preparation of this document but in carrying out the field work and processing which have led to its existence. Of these, special thanks must go to the compliment of the research vessels SURVEYOR, and THOMPSON (R.B. Tripp, Chief Scientist) for laboring under less than ideal conditions to carry out field operations. Lynn Long, Sharon Wirght, Bruce Fiddler, Gini May, Sally Schoenberg and Phyllis Hutchens of NOAA/PMEL are due thanks, also, for their help in processing the data and preparing this document. This study was supported in part by the Bureau of Land Management through interagency agreement with the National Oceanic and Atmospheric Administration, under which a multiyear program responding to needs of petroleum devlopment of the Alaskan continental shelf has been managed by the Outer Continental Shelf Environmental Assessment Program (OCSEAP) Office, Juneau, Alaska.

11. REFERENCES

- Beardsley, R.C. and C.D. Winant, 1979. On the mean circulation in the mid-Atlantic bight. J. Phys. Oc., 9: 612-619.
- Charnell, R.L. and G.A. Krancus, 1976. A processing system for Aanderaa current meter data. Tech. Memo. ERL-PMEL 6, NOAA, Boulder, Colo: 49 pp.
- Coachman, L.K. and R.L. Charnell, 1977. Finestructure in outer Bristol Bay, Alaska. Deep-Sea Res., 24(10): 809-839.
- Coachman, L.K. and R.L. Charnell, 1979. On lateral water mass interaction - a case study, Bristol Bay, Alaska. J. Phys. Oc. 9: 278-297.
- Coachman, L.K., T.H. Kinder, J.D. Shumacher and R.B. Tripp, 1980. Frontal systems of the southeastern Bering Sea shelf. In, Stratified Flows, 2nd IAHR Symposium, Trondheim, Norway, 1980. T. Carstens and T. McClimans Eds., TAPIR Publishers, Norway.
- Coachman, L.K. and J.J. Walsh, 1981. A diffusion model of cross-shelf exchange of nutrients in the southeastern Bering Sea. In press.
Deep-Sea Res.
- Favorite, F. and D.M. Fisk, 1971. Drift bottle experiments in the North Pacific ocean and Bering Sea--1957-50, 1962, 1966 and 1970. Data Report 67, Nat. Mar. Fish. Ser.; 20 pp.

- Favorite, F., A.J. Dodimead and K. Nasu, 1976. Oceanography of the subarctic Pacific region, 1960-1971. Int. N. Pacific Fish. Comm, Bull. 33: 187 pp.
- Gebhart, B. and J.C. Mollendorf, 1977. A new density relation for pure and saline water. Deep-Sea Res., 24: 831-848.
- Hughes, F.W., L.K. Coachman and K. Aagaard, 1974. Circulation, transport and water exchange in the western Bering Sea. In: Oceanography of the Bering Sea, D.W Hood and E.J. Kelley, Eds.: 59-98.
- Iverson, R.L., L.K. Coachman, R.T. Cooney, T.S. English, J.J. Goering, G.L. Hunt, Jr., M.C. Macauley, C.P. McRoy, W.S. Reeburgh and T.H. Whitledge, 1980. Ecological significance of fronts in the southeastern Bering Sea. In: Ecological Processes in Coastal and Marine Systems, Plenum Press.
- Kinder, T.H. and L.K. Coachman, 1978. The front overlaying the continental slope in the eastern Bering Sea. J. Geophys Res., 83: 4551-59.
- Kinder, T.H., J.D. Schumacher and D.V. Hansen, 1980. Observations of a baroclinic eddy: an example of meso-scale variability in the Bering Sea. J. Phys. Oc.
- Kinder, T.H. and J.D. Schumacher, 1981a. Circulation over the continental shelf of the southeastern Bering Sea. In: Bering Sea: Oceanography and Resources, D.W. Hood, ed. (in press).

- Kinder, T.H. and J.D. Schumacher, 1981b. Hydrography over the continental shelf of the southeastern Bering Sea. In: Bering Sea: Oceanography and Resources, D.W. Hood, ed. (in press).
- Lagerloef, G., R.D. Muench and J.D. Schumacher, 1981. Very low frequency variations in currents near the northeast Gulf of Alaska shelf break. J. Phys. Oc., in revision.
- Muench, R.D. and J.D. Schumacher, 1980. Physical Oceanographic and meteorological conditions on the northwest Gulf of Alaska. Tech. Memo ERL-PMEL-22, NOAA, Boulder, Colo.: 157 pp.
- National Ocean Survey, 1979. Tidal Current Table, Pacific Coast of North America and Asia. NOAA, Rockville, MD.
- Reed, R.K., R.D. Muench and J.D. Schumacher, 1980. On baroclinic transport of the Alaskan Stream near Kodiak Island. Deep-Sea Res., 27: 509-523.
- Reed, R.K., J.D. Schumacher and C. Wright, 1981. On coastal flow in the northeast Gulf of Alaska. Atmosphere-Ocean, in press.
- Reynolds, R.M., 1980. On the dynamics of coastal winds. PhD dissertation, Univ. of Washington: 173 pp.
- Royer, T.C., 1979. On the effect of precipitation and runoff on coastal circulation in the Gulf of Alaska. J. Phys. Oc., 9: 555-563.

Royer, T.C., D.V. Hansen and D.J. Pashinski, 1979. Coastal flow in the northern Gulf of Alaska as observed by dynamic topography and satellite-tracked drogued drift buoys. J. Phys. Oc., 9: 785-801.

Schumacher, J.D. and R.K. Reed, 1980. Coastal flow in the northwest Gulf of Alaska: the Kenai Current. J. Geophys. Res., 85: 6680-6688.

Wright, C., 1981. Observations in the Alaskan Stream during 1980. Tech. Memo. PMEL-ERL, in press.

12. FIGURE LEGENDS

1. Unimak Pass study area showing bathymetry (in meters), some orographic features and the location of three current meter moorings (dots).
2. Drift card release and recovery sites connected by straight lines.
3. Results from 35 hr. filtered current data presented as A) record length vector mean current (arrows) and orientation of major (containing greatest variance) and minor axes, where the length represents one standard deviation, B) percent of observations and mean speed (given by length) partitioned into twelve sectors.
4. Results from 35 hr filtered data presented as scatter plots and progressive vector diagrams. Note the different length scales.
5. Current vector time series from 35 hr filtered data.
6. Tidal current ellipses for M2 and K1 constituents where the arrow shows sense of rotation and the dot the direction of the current vector at 0° phase relative to Greenwich. The ellipses are shown at the same scale as land features.
7. A progressive vector diagram from 2.9 hr filtered current data at UP2 on 12 June 1980.

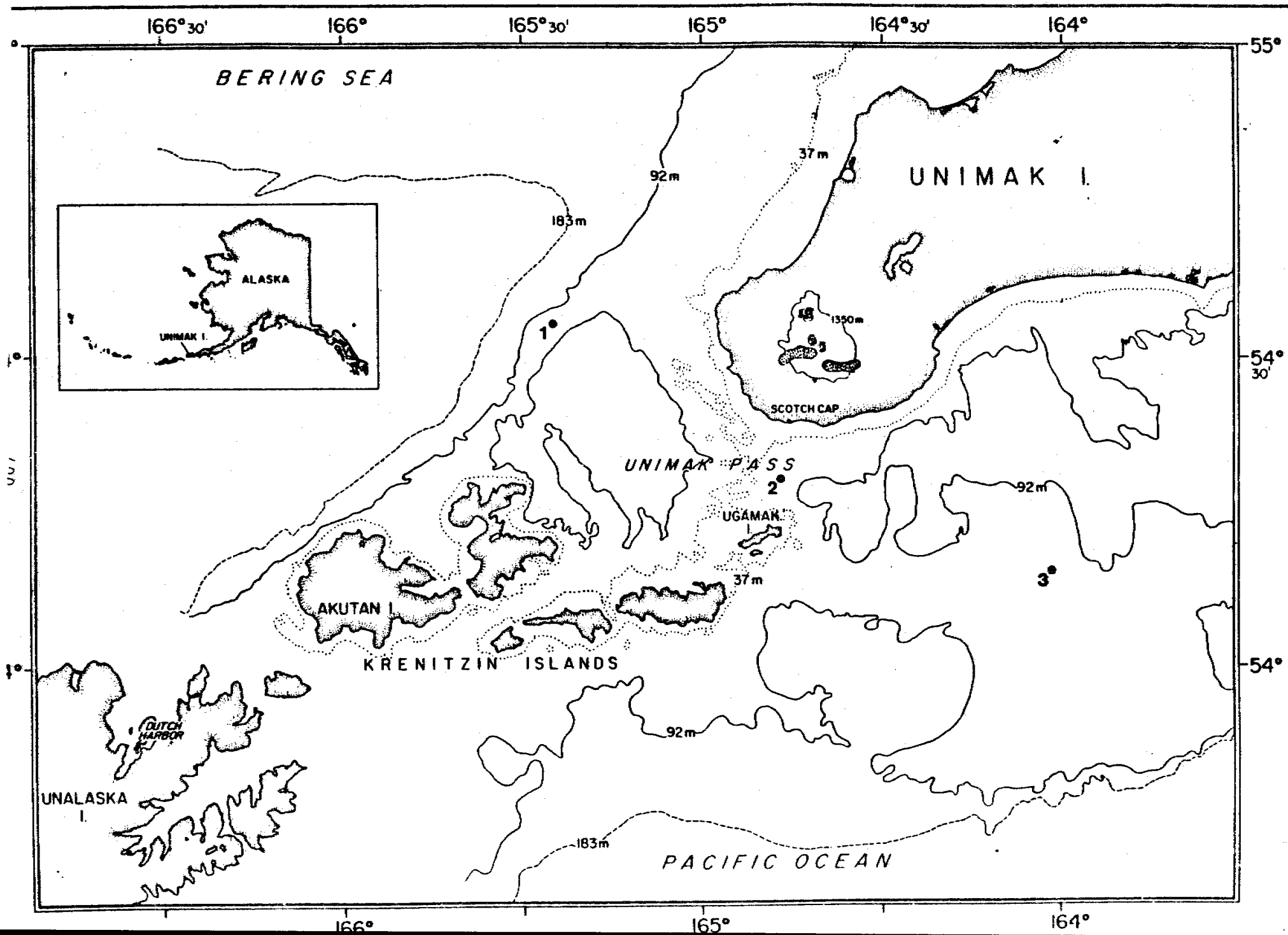
8. Rotary spectra for 70 day winter (22 March to 30 May 1980) and summer (31 May to 9 August 1980) segments of 2.9 hr filtered current data. Clockwise component is solid line.
9. Spectra of atmospheric pressure gradient resolved on 150°T and as total variance.
10. Time-series of 35 hr filtered current records resolved on total record length major axes and atmospheric pressure gradient resolved normal to the trend of the Alaska Peninsula. Vertical lines indicate some reversal events.
11. Hydrographic data presented as A) temperature ($^\circ\text{C}$), B) salinity and C) sigma-t sections. The Δ values are the magnitude of surface minus bottom 1m averaged values.
12. Row A) cross-spectral energy, B) phase and C) coherence squared for winter (solid line) and summer (dashed line) current record segments. The horizontal line in row C is the 90% level of significance.
13. Winter (solid line) and summer (dashed line) coherence squared between 35 hr filtered current records and atmospheric pressure gradient (ΔP).
14. An example of surface atmospheric pressure during a reversal event. The arrow represents the direction of ΔP across Unimak Pass. Contours are every 4 mb.

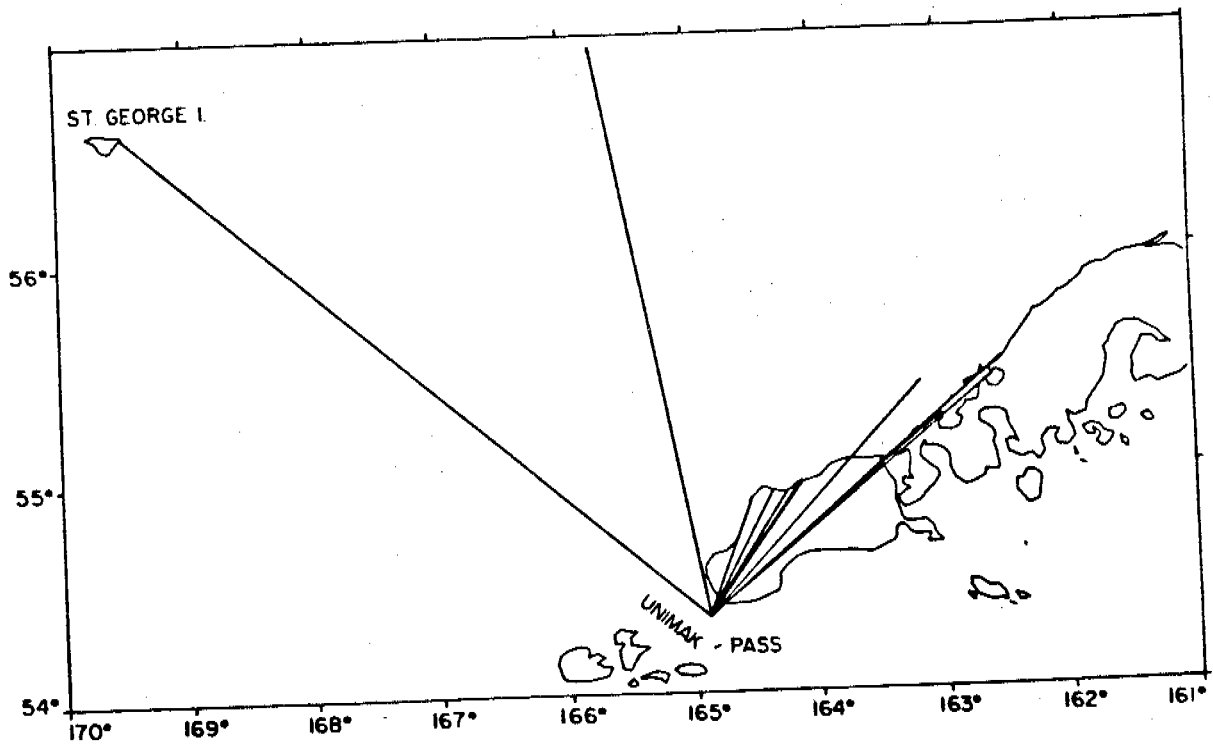
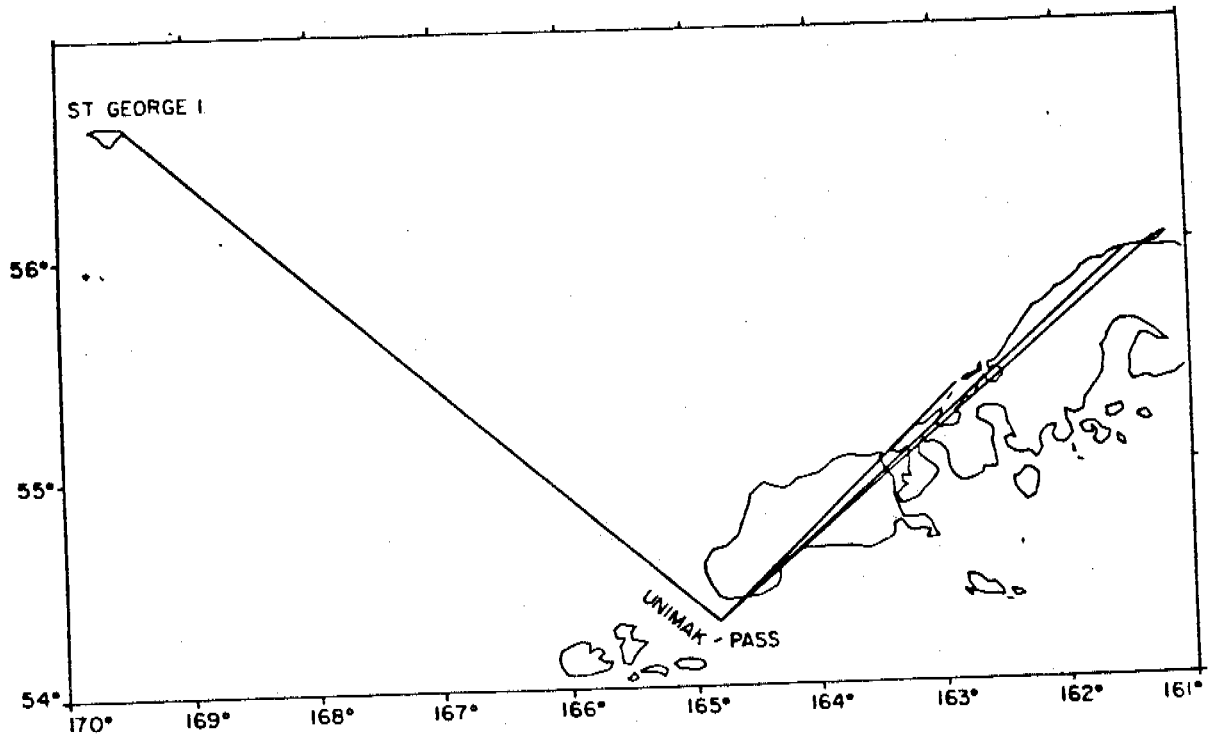
APPENDIX A
Drift Card Recoveries

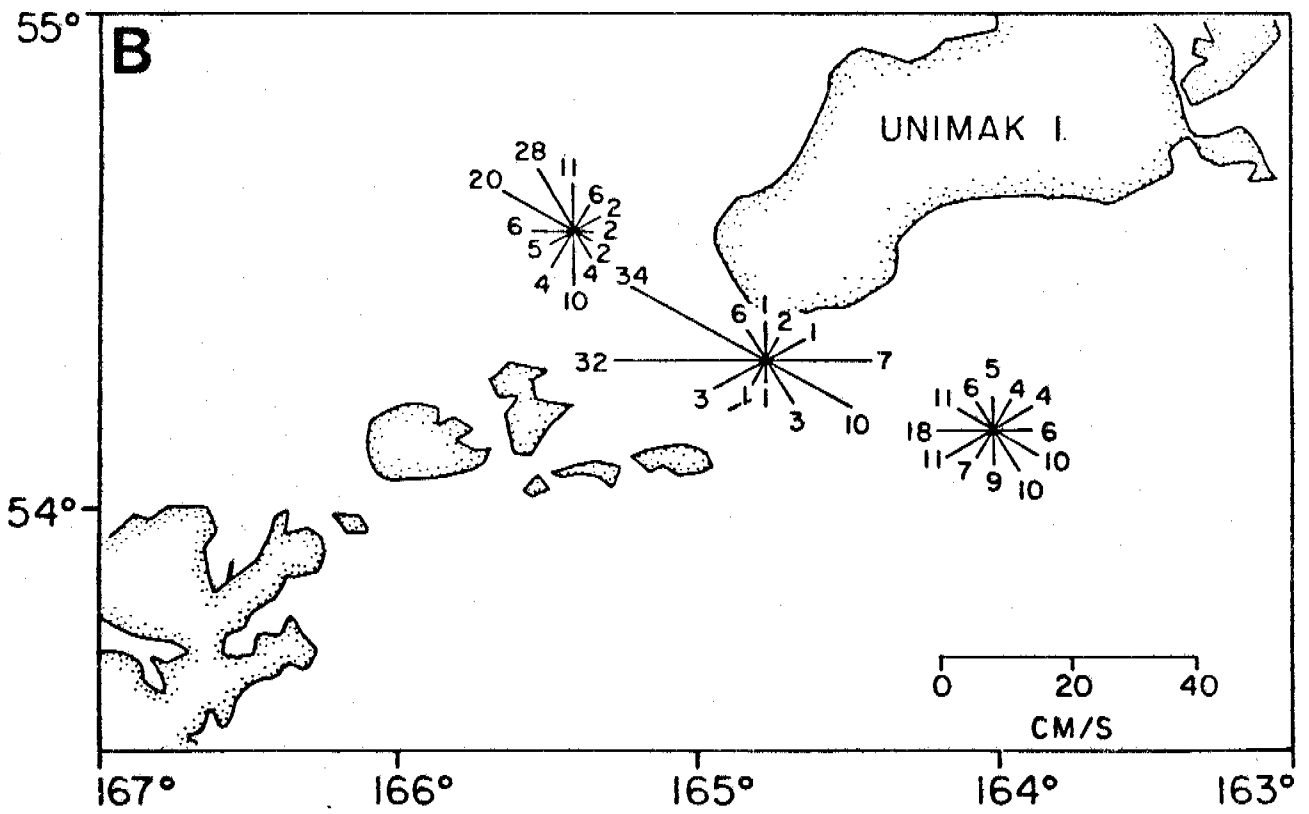
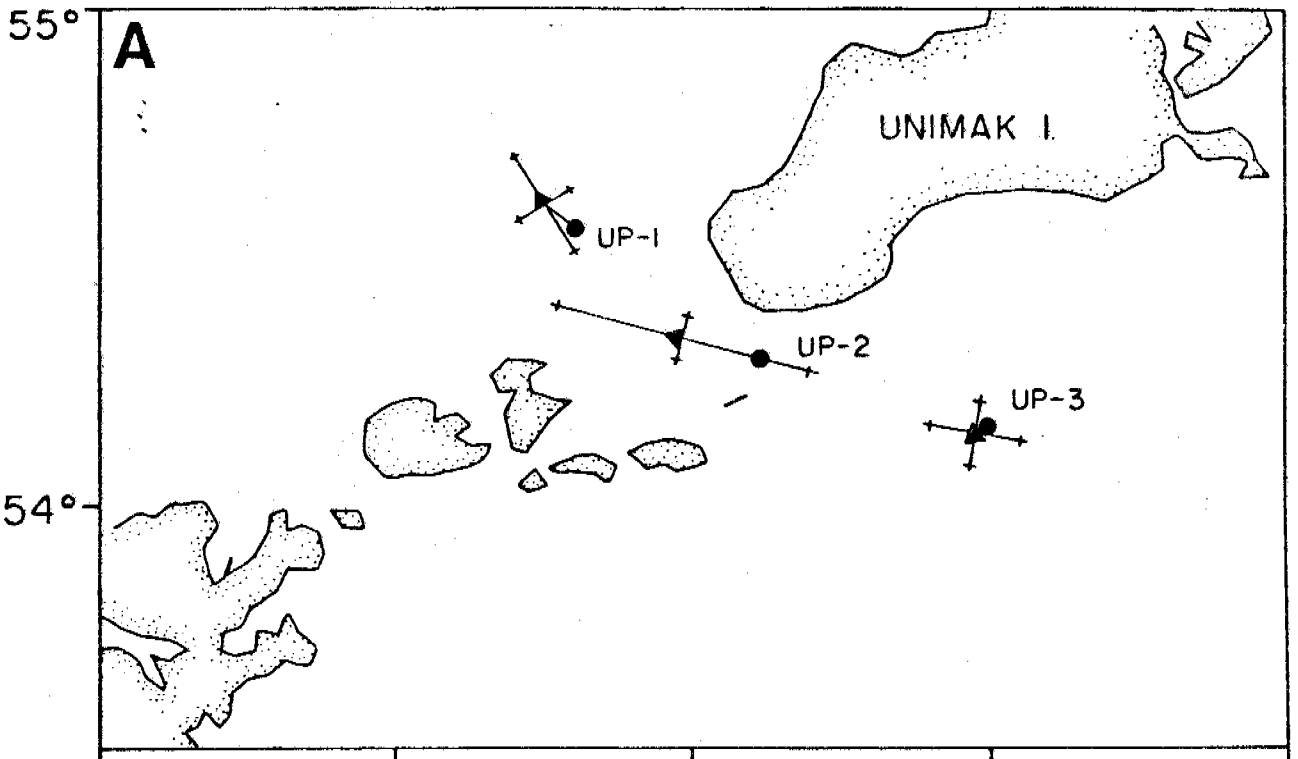
Release	9000-9499	7/4/79	54°21.0'N	164°53.6'W
Sites:	9500-9999	8/3/79	54°17.8'N	164°16.3'W

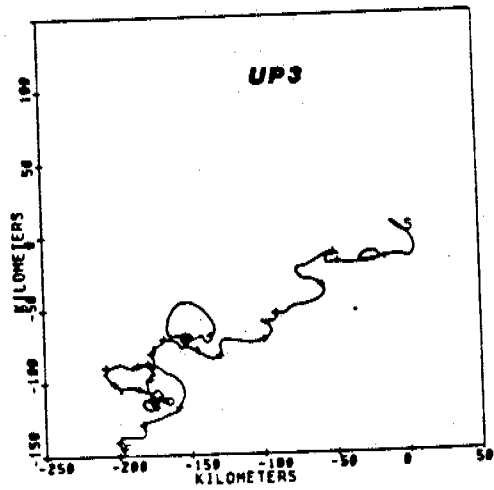
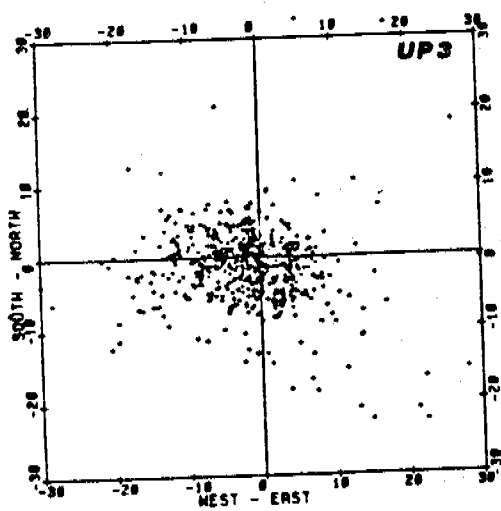
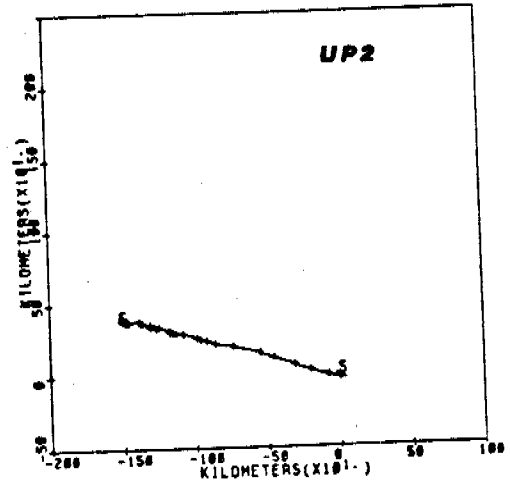
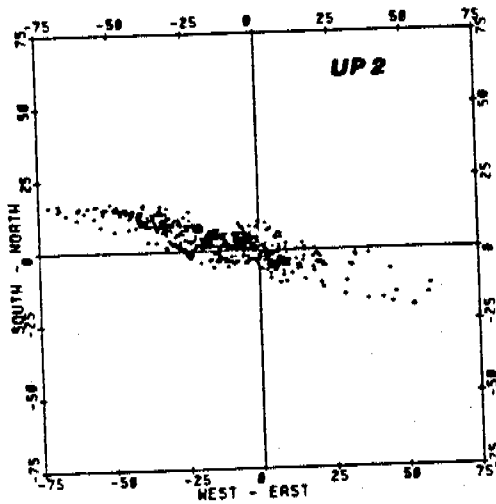
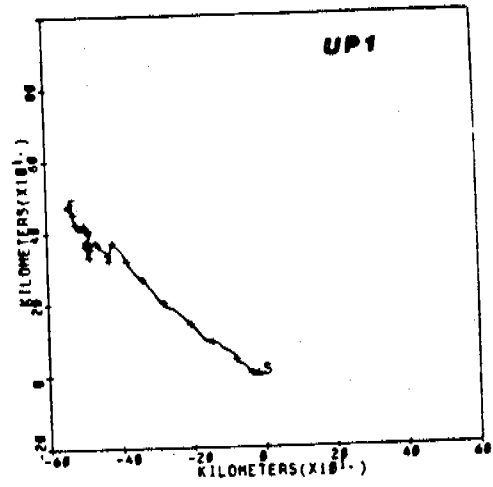
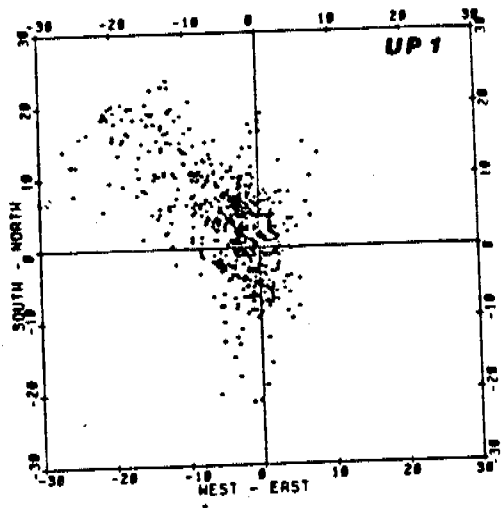
Recovery:

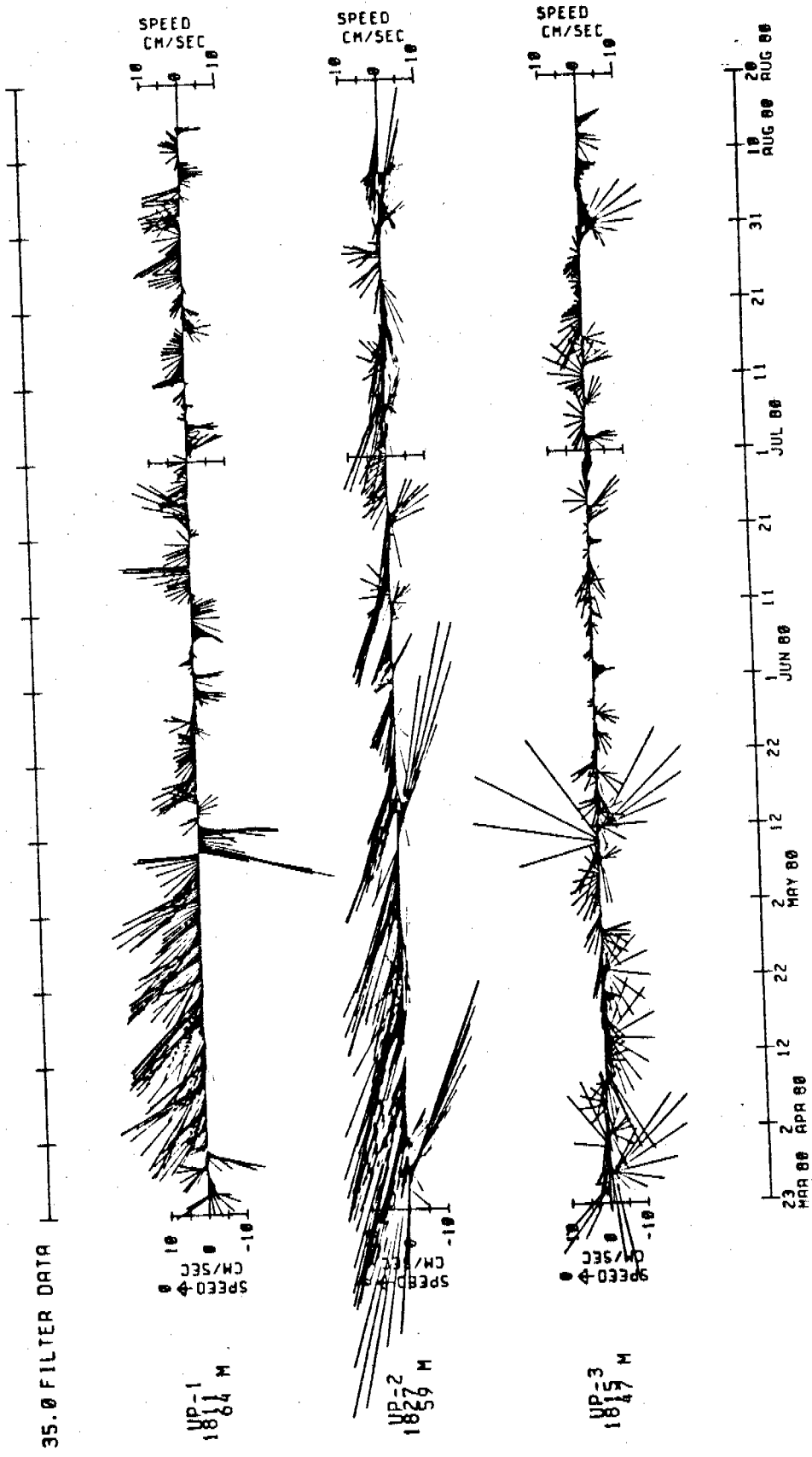
#	Date	Lat	Long	Location
9362	8-1-79	54°55'	164°22.5'	Urilia Bay, Unimak Isl.
9392	8-1-79	54°55'	164°22.5'	"
9418	8-2-79	"	"	"
9363	"	"	"	"
9351	"	"	"	"
9060	"	"	"	"
9344	"	"	"	"
9309	"	"	"	"
9048	"	"	"	"
9414	"	"	"	"
9328	8-4-79	54°56'	164°11.5'	Peterson Lagoon, Unimak Isl.
9122	8-6-79	54°57'	164°08'	Cape Lapin, Unimak Isl.
9627	9-8-79	56°	161°16'	Nelson Lagoon
9702	9-8-79	56°	161°16'	"
9907	9-8-79	56°	161°16'	"
9518	9-6-79	56°	161°16'	"
9628	"	"	"	"
9631	"	"	"	"
9978	"	"	"	"
9510	"	"	"	"
9540	9-23-79	55°57'	161°30'	West of Nelson Lagoon
9370	8-7-79	54°55'	164°22.5'	Urilia Bay, Unimak Isl.
9072	8-7-79	55°25'	162°35'	Cold Bay
9783	9-23-79	56°	161°16'	Nelson Lagoon
9623	9-23-79	56°	161°16'	"
9532	9-1-79	55°22'	162°52°	Operl Isl.
9467	9-18-79	55°30'	162°31'	NE of Mffet Pt.
9209	9-18-79	55°30'	162°31'	"
9164	8-7-79	54°55'	164°22.5'	Urilia Bay, Unimak Isl.
9018	7-18-79	54°55'	164°15'	Near Urilia Bay
9063	8-3-79	54°58'	164°08'	Point Lapin
9482	4-5-80	56°00.0	161°10.0	Nelson Lagoon
9874	"	"	"	"
9912	"	"	"	"
9379	6-15-80	56°27'	154°47'	Urilia Bay
9804	7-15-80	56°27'	154°47'	Tugidak Isl.
9278	7-15-80	64°34'	165°44'	Nome, AK
9028	5-19-80	55°54'	161°43'	NE of Cold Bay

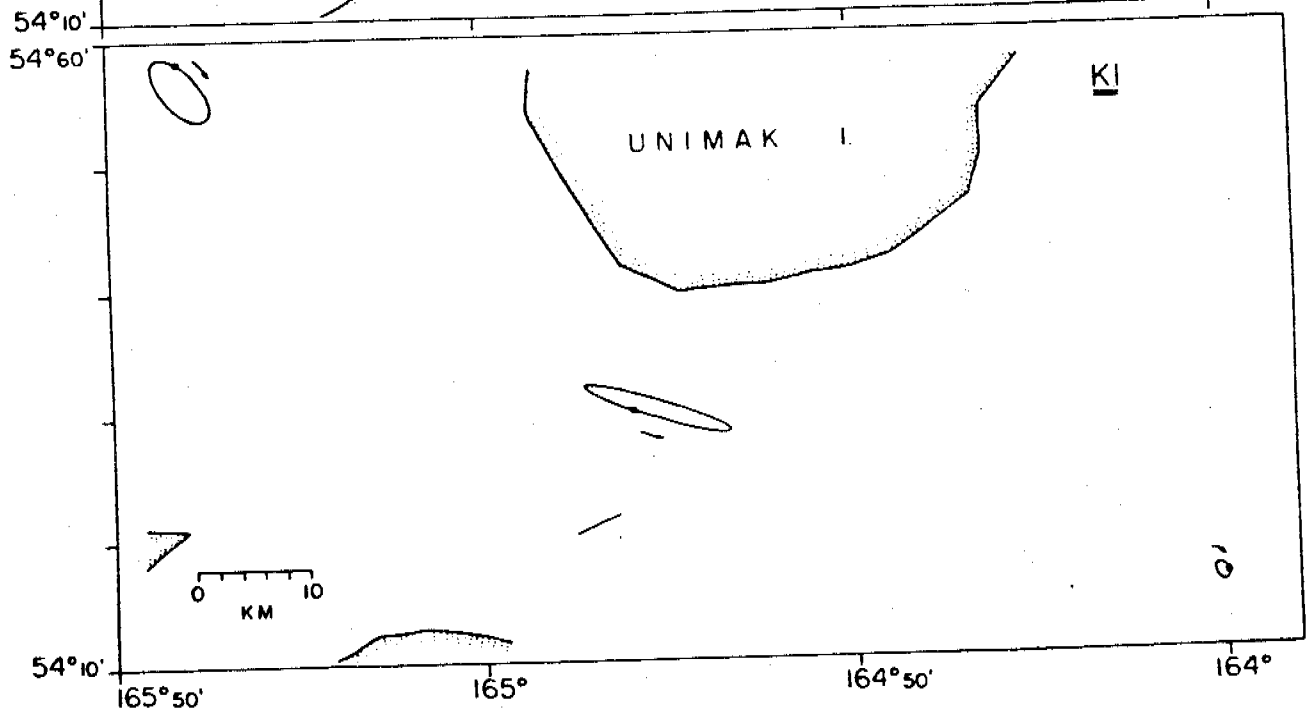
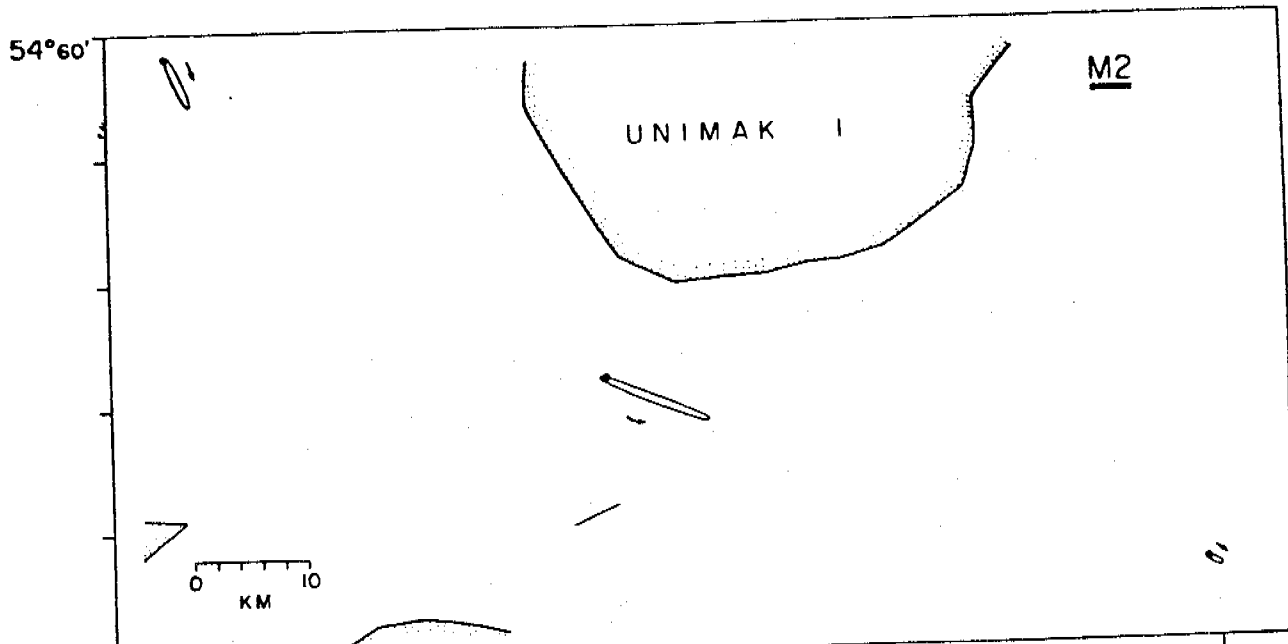


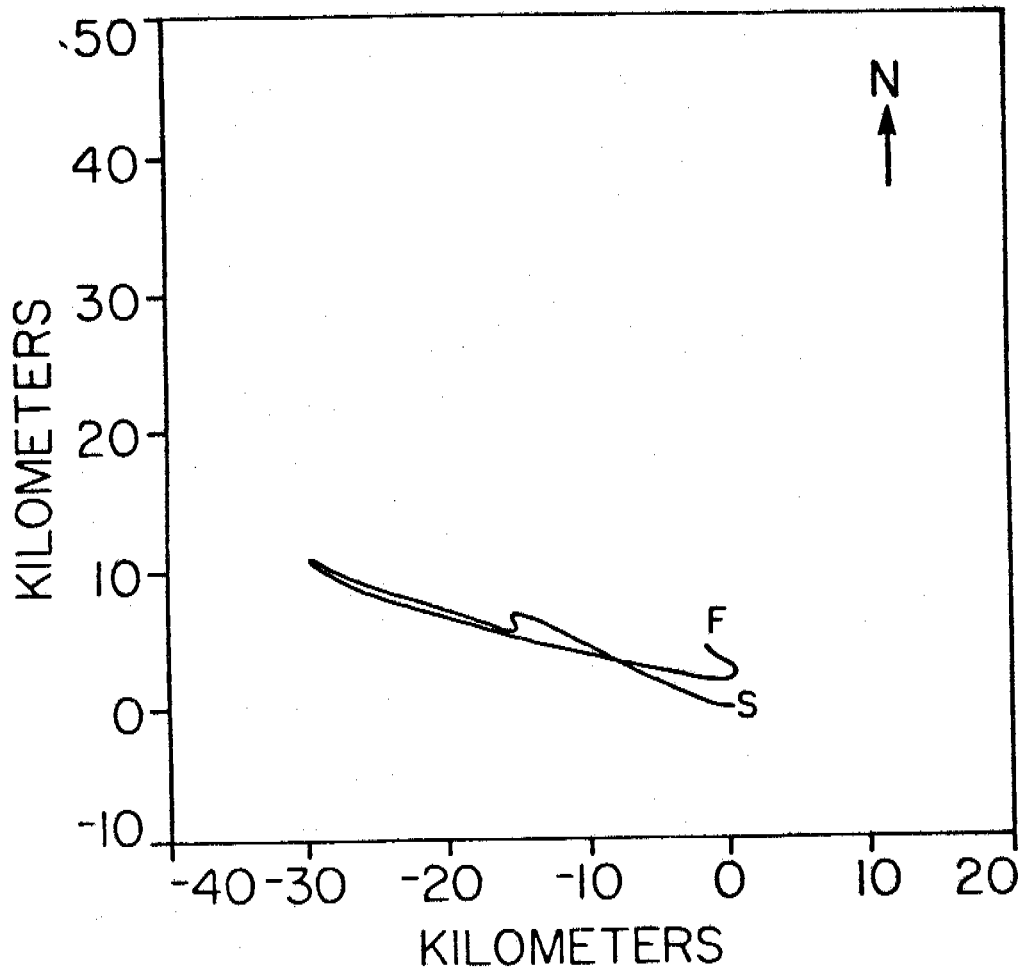


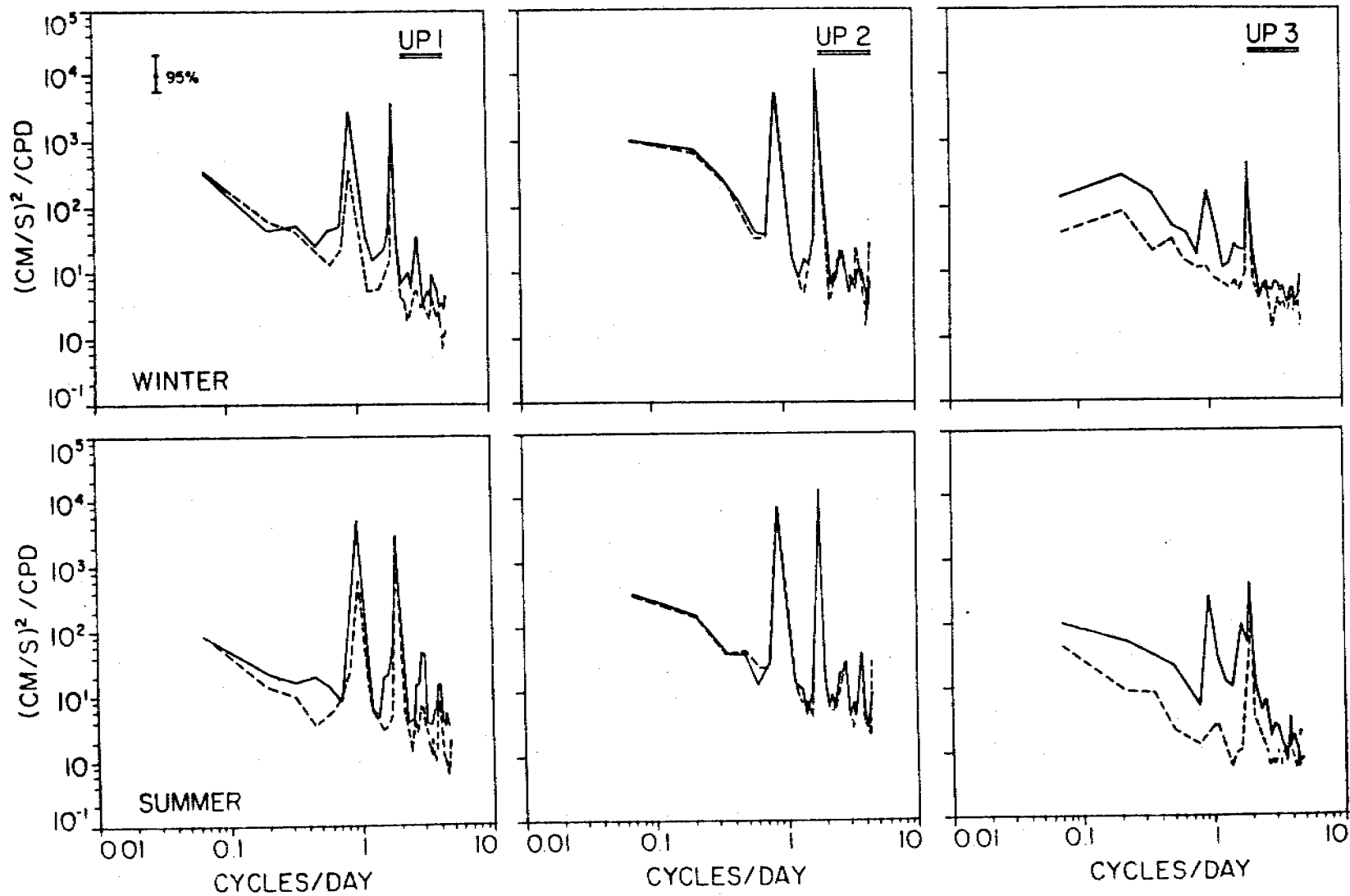


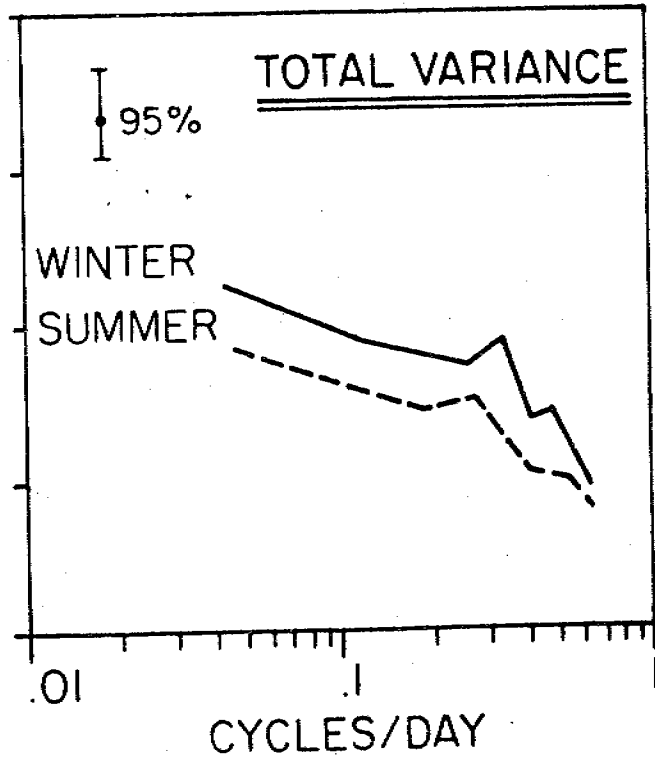
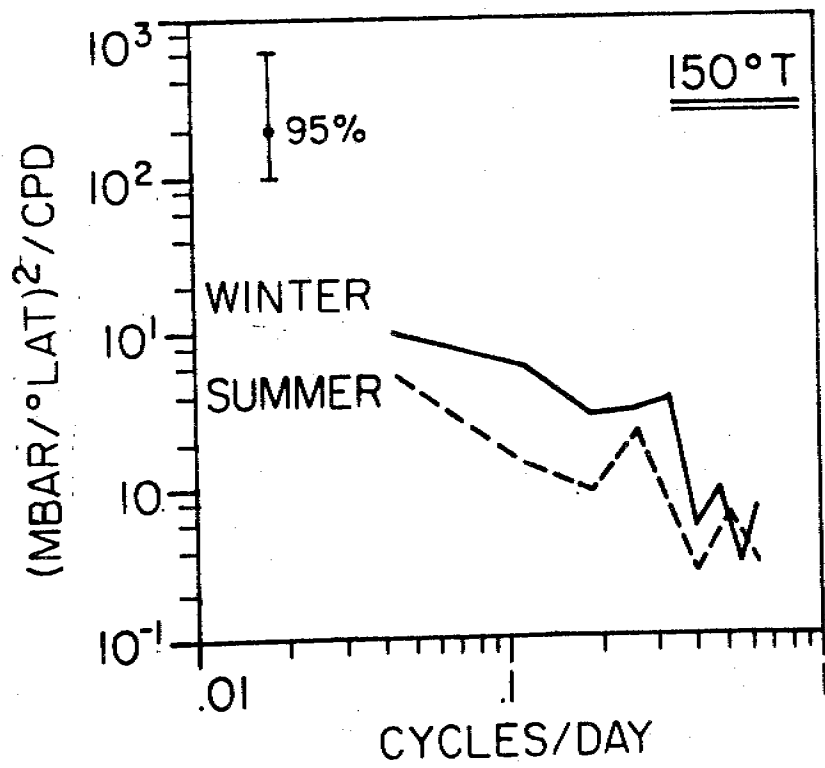


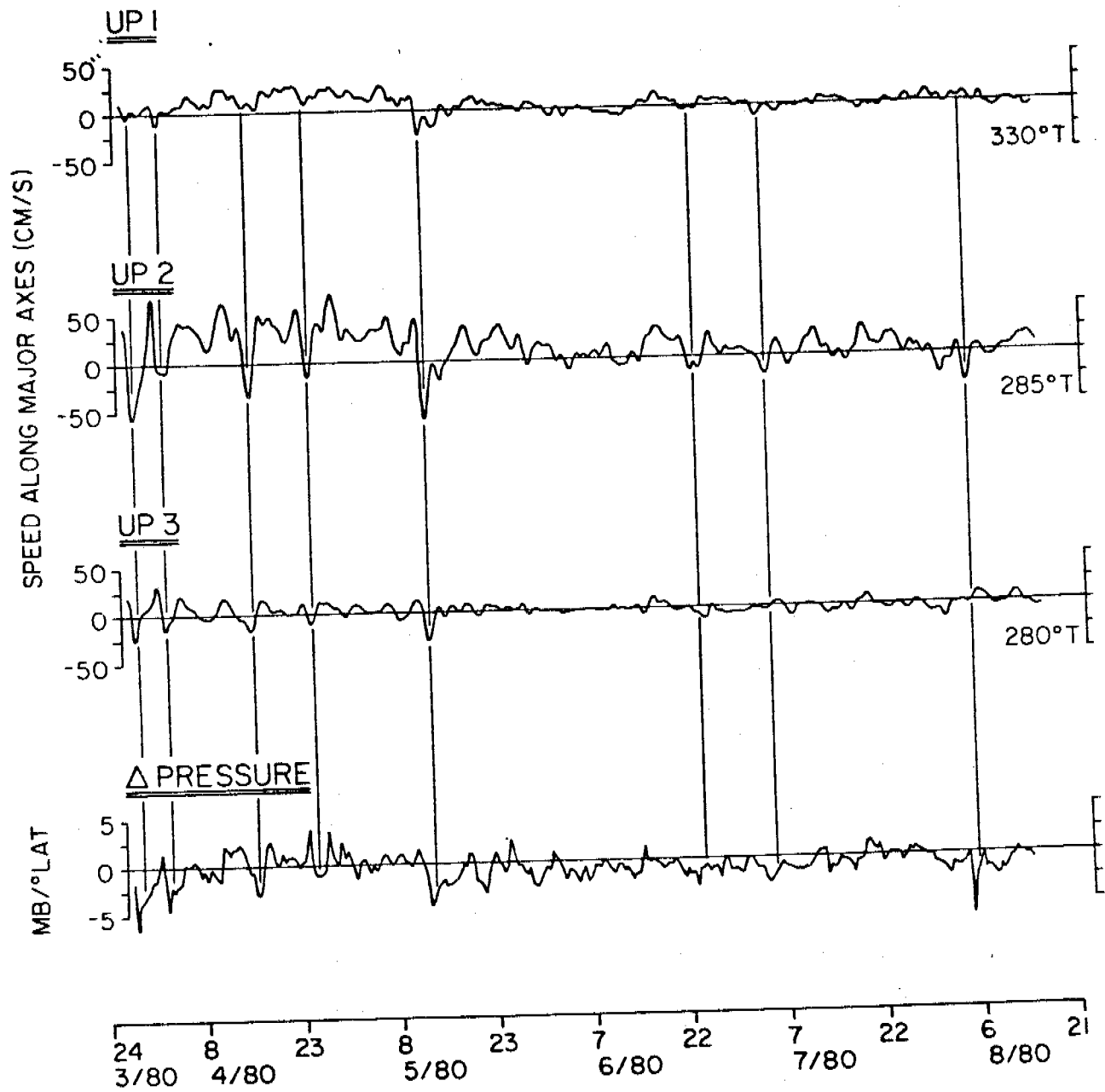


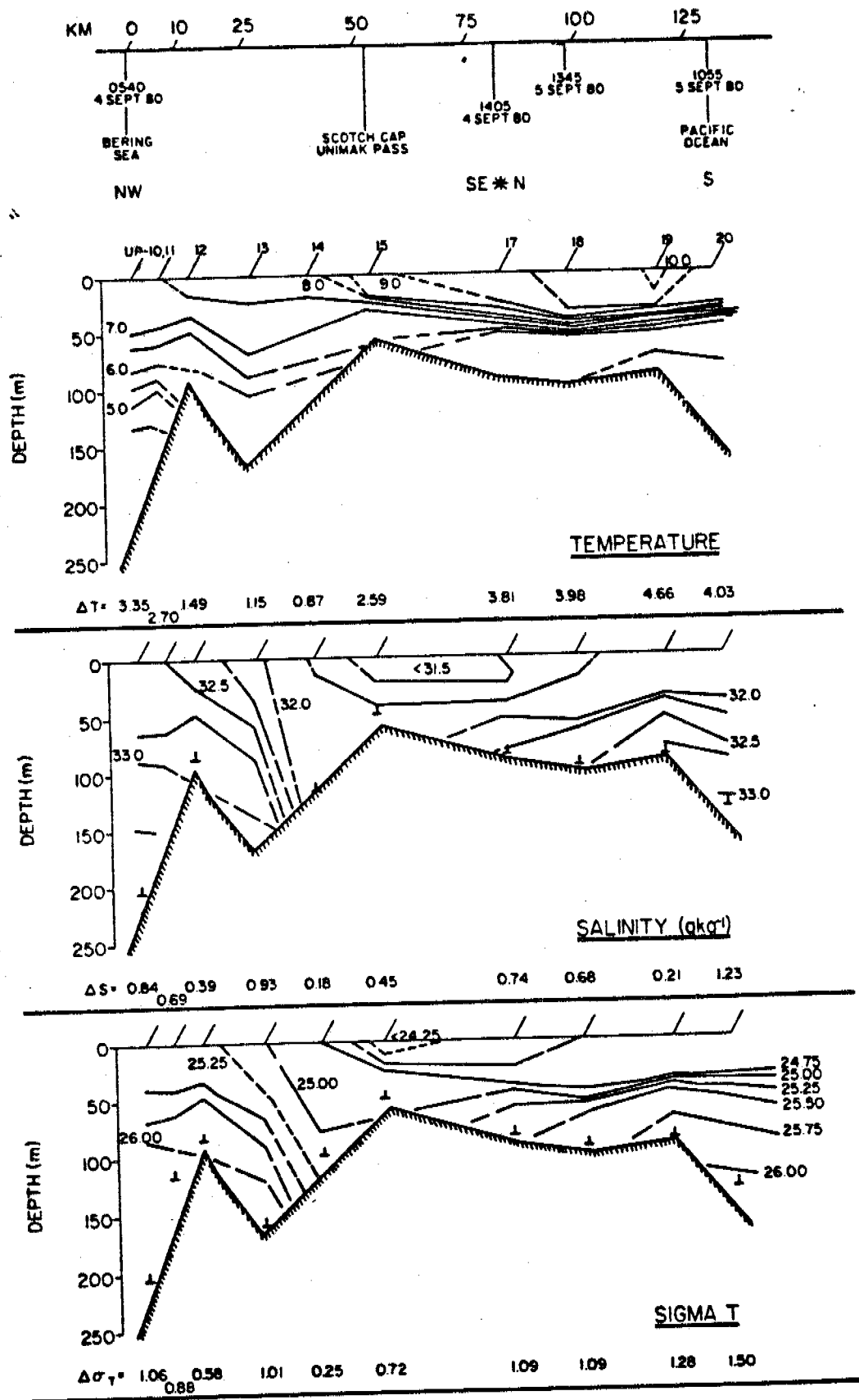


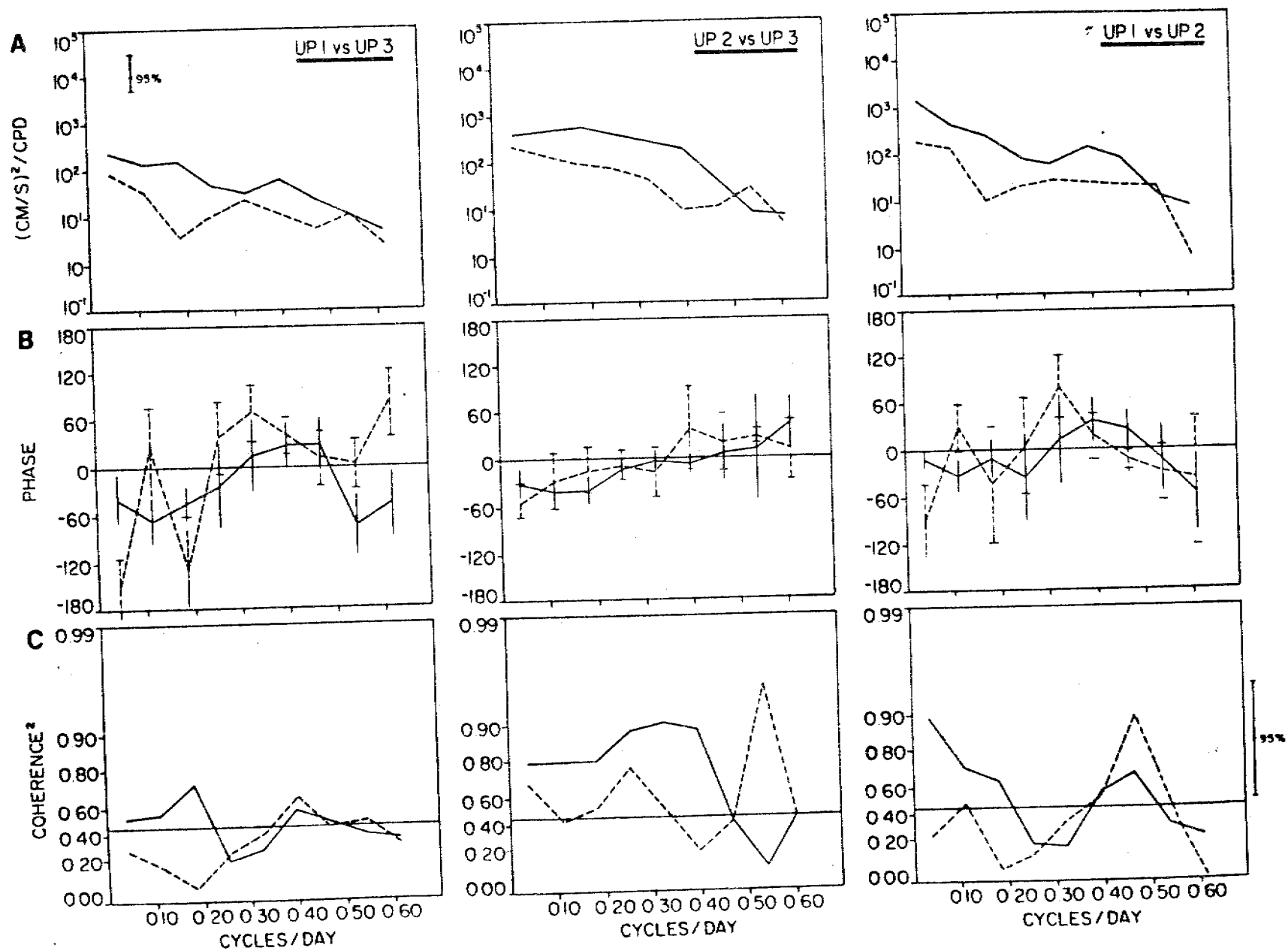


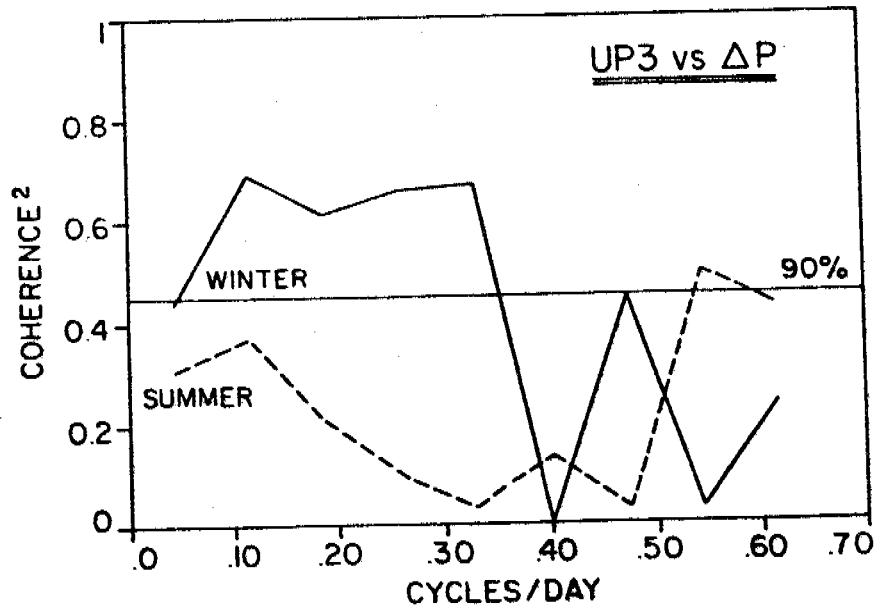
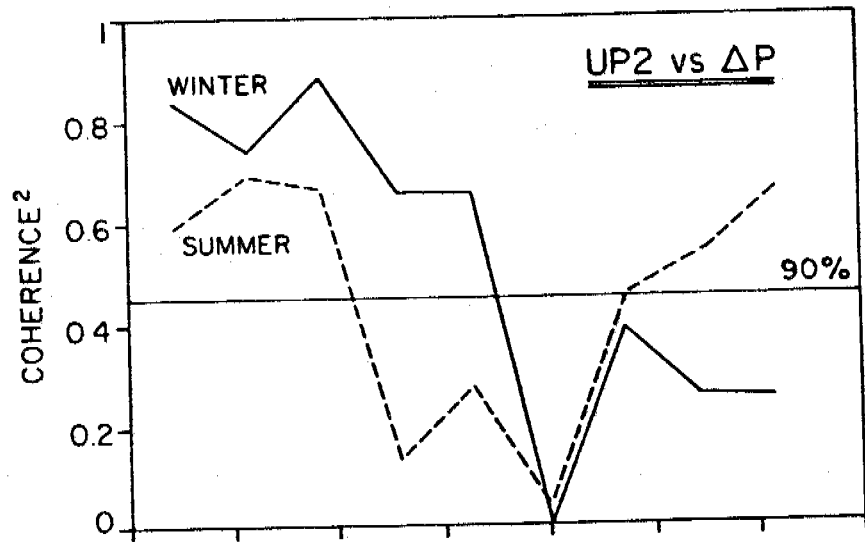
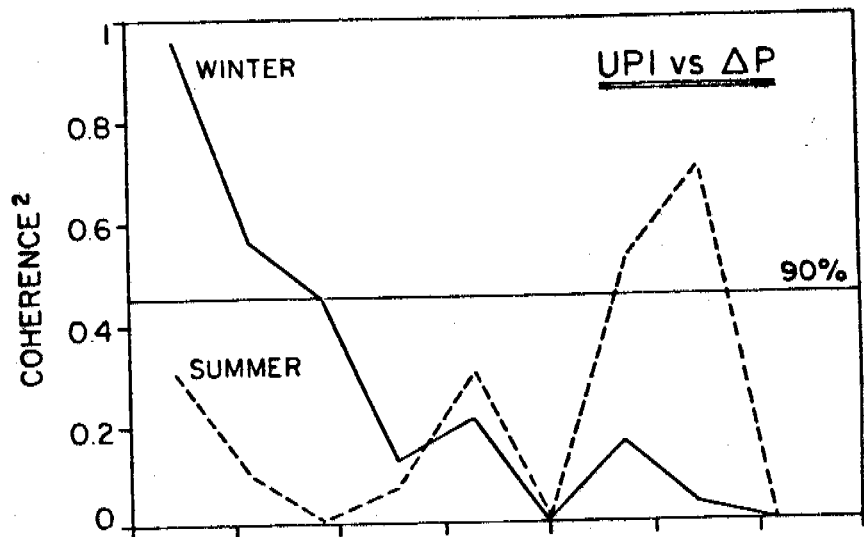


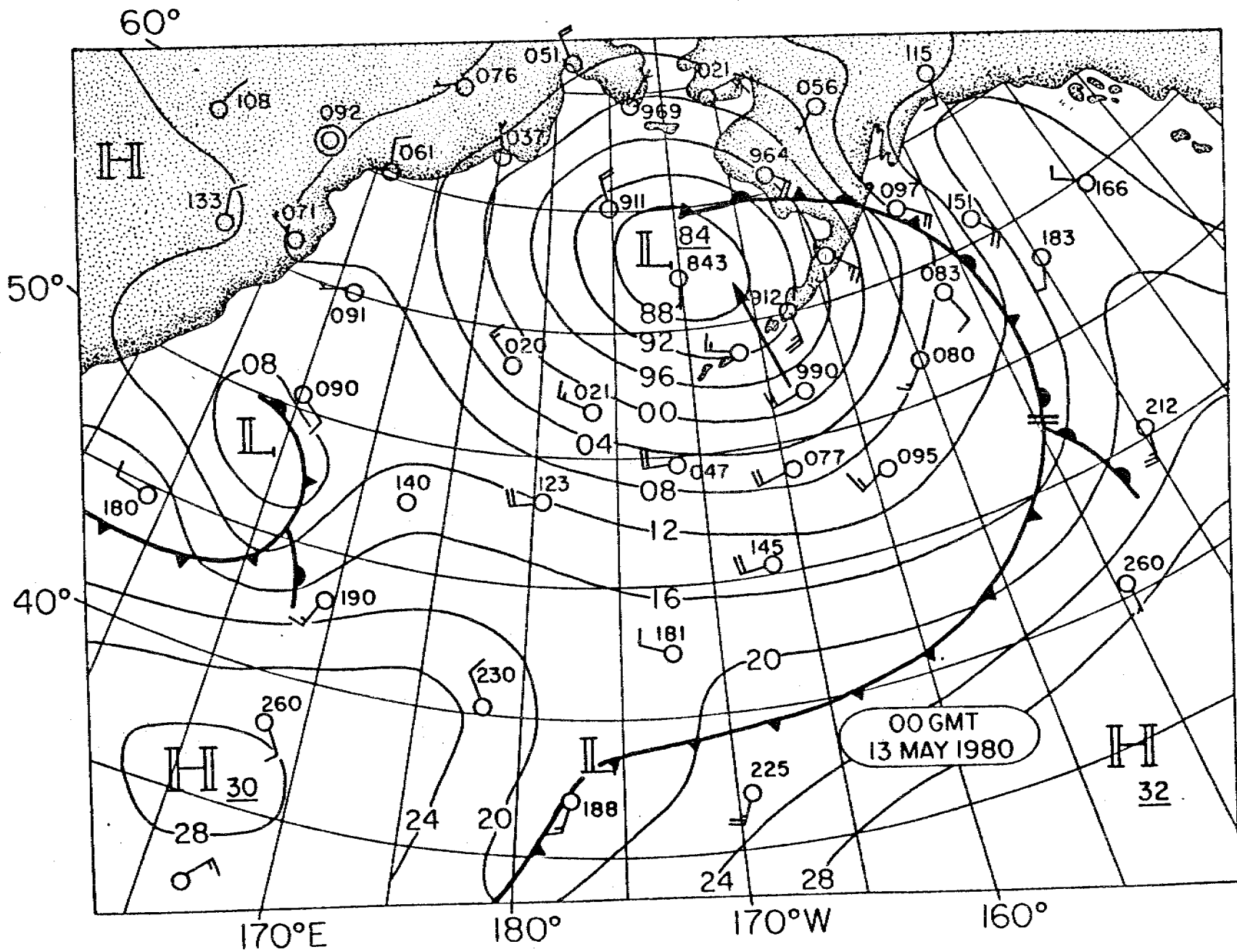












Hydrographic, Suspended Particulate Matter,
Wind and Current Observation During
Reestablishment of a Structural Front:
Bristol Bay, Alaska

by

C. A. Pearson

E. Baker

and

J.D. Schumacher

all at Pacific Marine Environmental Laboratory
3711 15th Ave. NE
Seattle, Washington 98105

prepared
for
Fall 1980 AGU

ABSTRACT

In summer a structural front located in the vicinity of the 50m isobath separates a well-mixed coastal domain from the two-layered middle shelf domain of the southeastern Bering Sea. This system was perturbed in mid-August by a strong storm (winds in excess of 30m sec^{-1}) which vertically mixed temperature, salinity and suspended particulate matter (SPM) throughout the water column. Using CTD and SPM data collected 1, 7, and 14 days after the storm, we document the subsequent reestablishment of frontal and domain characteristics. Prior to the second occupation of stations, a period of moderate (5 to 10 ms^{-1}) northeasterly winds appeared to drive an offshore Ekman flux, resulting in stratification across the entire study area with an SPM minimum at or near the maximum density gradient. By the third observational series, increasingly strong tides had reestablished the well-mixed coastal domain. These observations illustrate that distributions of both conservative and nonconservative properties of the water column are similarly governed by the balance between tidal stirring and buoyancy flux.

INTRODUCTION

The Bering Sea is the northernmost mediterranean sea of the North Pacific (Sayles, et al, 1979). The northeastern one-half of the sea is underlaid by a flat and shallow shelf (figure 1). The southeastern portion of this shelf supports one of the world's richest fisheries resource and potentially large quantities of petroleum. In order to make knowledgeable decisions regarding fate and impact of petroleum development, the Outer Continental Shelf Environmental Assessment Program (OCSEAP) had funded extensive field experiments since 1975 to describe the regional oceanography, and to understand important transport processes.

Physical oceanographic results from OCSEAP and Processes and Resources of the Bering Sea shelf (PROBES) e.g., Coachman and Charnell, 1977, 1979; Coachman, Kinder, Schumacher and Tripp, 1980; Kinder and Coachman, 1978; Kinder, Schumacher and Hansen, 1980; Kinder and Schumacher, 1981a and 1981b; Pearson, Mofjeld and Tripp, 1981; Reed, 1978; Schumacher, Kinder, Pashinski and Charnell, 1979 are summarized below in terms of features germane to the present study. During periods of positive buoyancy flux at the surface (ice melt and insolation), three distinct hydrographic domains exist. These domains are separated by regions of enhanced horizontal temperature and salinity gradients - fronts - which are located in the vicinity of the 50 and 100m isobaths. A typical summer hydrographic cross-section (figure 2) clearly shows these features and the relation between vertical structure, depths, and domains. Herein we will focus on the mixed coastal and two-layered middle shelf domains located adjacent to the Alaska Peninsula. We note that there are no major sources of fresh water along the peninsula, and the amount of ice cover along the Peninsula is highly variable year to year.

The most common forcing mechanisms for coastal circulation are tides and winds, however, recent studies (Beardsley and Winant, 1980; Csanady, 1978) suggest that interactions between oceanic circulation and the shelf may also be important. For the southeastern Bering Sea shelf, Kinder and Schumacher (1981b) have summarized current data (figure 3) and note that tides dominate horizontal kinetic energy (HKE). Tides are thought to be responsible for the cross-shelf flux of salt required to maintain the observed mean salt balance; over most of this shelf, tidal diffusion appears to be the dominant transport mechanism (Coachman et al., 1980). There is little or no evidence that weakly organized oceanic circulation (the Bering Slope Current) results in advection on the shelf proper (Kinder, Schumacher and Hansen, 1980). Further, the vast size of this shelf makes it unlikely that any oceanic/outer shelf eddies could propagate into the middle shelf or coastal domains. In

these latter areas tides account for $\geq 90\%$ of the HKE and current spectra indicate only a small fraction ($\leq 10\%$) of the HKE lies in the periods (2 to 10 days) associated with meteorological forcing (Kinder and Schumacher, 1981b). While winds may not be important over long time scales (0 months), they provide (via wind stress and wave generation) energy to typically generate a 20 to 30-m mixed upper layer and aperiodic eastward travelling storms can result in significant pulses of advection. During August, however, winds are generally weak, 40% of wind speeds are ≤ 5 m/sec with monthly vector mean winds ≤ 2.5 m/sec toward the northeast (Brower, *et al.*, 1977).

The purpose of this preliminary note is to present hydrographic, suspended particular matter (SPM) wind and current data collected along the Alaska Peninsula (figure 4) during a 14-day period in August 1980. These data show that a storm significantly altered mean hydrographic conditions, stirring middle shelf domain waters throughout the water column and thus had a profound impact on vertical transport. Further, Ekman fluxes (coastal divergence and convergence) appear to play an important role in reestablishment of stratification and together with enhanced tidal mixing (using the mean of the speed cubed as a measure of mixing energy) resulted in a return to mean conditions within 14 days.

DATA ACQUISITION AND PROCESSING

Hydrographic data were collected using Plessey model 9040 system with model 8400 data logger. This system sampled five times per second for values of temperature, conductivity, and pressure. Data were recorded only during the down-cast using a lowering rate of 30 m/min. Nansen bottle samples were taken at most stations to provide temperature and salinity calibration. The correction factors for these data were $S = -0.04 \text{ g kg}^{-1}$ and $T = -0.01^\circ\text{C}$.

Data from monotonically increasing depth were "despiked" to eliminate excessive values and were averaged over 1-m intervals to produce temperature and salinity values from which density was computed.

Seven Neil Brown vector averaging acoustic current meters (ACM) were suspended beneath a surface float, at depths of 5, 10, 15, 20, 29, 39, and 50 meters, in water depth of 65 meters. Here we present results from the 5 and 39 meter depths. The ACM's emit continuous high frequency acoustic signals which are phase advanced or delayed as they travel with or against the current. The relative phase is converted to a voltage which is directly proportional to the water velocity. Currents are measured along two right angle horizontal paths. At a pre-determined interval, in this case one minute, the component velocities are averaged and recorded. Ten minute segments of the original one minute sample interval data were averaged. These data were then low-pass filtered (half amplitude at a period of 2.9 hours) and a second order polynomial was used to interpolate to whole hours. A Munk-Cartwright response tide analysis was then performed on the data, and a predicted tide series was subtracted from the original series. Finally, a 25 hour running mean was applied to the detided series, and the meaned series was resampled at a six hour interval.

Winds were recorded at 1 hour intervals onboard the NOAA ship SURVEYOR. The wind sensor is located about 20 m above the sea surface. During the first five days, the ship was operating within about 75 km of mooring TP3. After this time, the ship operated from inner Bristol Bay to the Pribilof Islands.

SPM measurements, given in terms of light attenuation coefficient, were made with a continuously recording 0.25 m beam transmissometer inter-faced to the CTD. The light source was a light emitting diode with a wavelength of 660 μm . This wavelength eliminates attenuation problems due to dissolved humic acids. Accuracy and stability are sufficient to provide data with an error less than 0.5% of true light attenuation.

RESULTS

Hydrography and Light Attenuation The line of CTD stations normal to the peninsula (figure 4) was occupied on 19, 24 and 31 August 1980. Temperature, salinity, σ_t and light attenuation sections are shown in figures 5, 6 and 7. The time to a complete line was about six hours. About one day prior to running the first section, the remnants of typhoon Marge passed eastward through the study area. This storm resulted in winds up to 30 ms^{-1} and 6 to 8 m waves. The turbulence associated with this storm mixed the water column at least 45 km seaward of the coast (figure 5). Suspended particulate matter was also well mixed within 10 km of the shore and seaward of station 45 isopleths exhibited weak monotonically increasing vertical gradients.

During the second occupation of this section (figure 6), the entire shelf region was thermally stratified, with surface minus bottom temperature difference (ΔT) from 0.6 to 2.7°C . Colder bottom waters intruded onshore, with a displacement of the 8.5°C -isotherm of about 10 km. A similar change of mixed to stratified structure was observed in isohalines with the strongest stratification ($\Delta S = 0.13 \text{ g kg}^{-1}$) over the normally mixed coastal domain. Again, the data suggested an onshore flux, e.g. at station 42 bottom salinity increased by 0.05 g kg^{-1} , while upper layer salinities decreased. Light attenuation values indicated a 50% reduction in nearshore concentration of SPM, while over the middle shelf domain ($z \geq 50 \text{ m}$) a subsurface minimum layer was established.

Hydrographic conditions observed on 31 August (figure 7) showed a return to more typical stratification distributions (c.f. figure 2); middle shelf waters were stratified with $\Delta \sigma_t \geq 0.43$ and coastal domain waters were vertically well mixed. We note that stratification was now stronger than that observed on May 31 (inset, figure 4) by about a factor of three. SPM profiles

also indicated mixed conditions in the coastal domain and a minimum layer was clearly established near or below the pycnocline.

Winds and Currents Alongshore (v positive $60^\circ T$, see figure 4) winds are shown in Figure 8. The passage of the storm resulted in maximum alongshore wind speeds of about 25 ms^{-1} . About 3.5 days after the storm's peak speeds, a period of relatively steady alongshore winds existed for about 3 days with a mean speed of -5.5 ms^{-1} . We note that with the exception of the storm winds and those on 24 August, onshore wind speeds (not shown) were only about 1 ms^{-1} .

Currents at 5 and 39 m below the surface are shown in the next two panels of figure 8, where the alongshore axis is the same as for the wind and the onshore axis is u positive $150^\circ T$. Near-surface currents reversed from onshore to offshore concomitant with the wind reversal and this initial offshore pulse lasted for about 3 days. While near surface currents were offshore those at 39 m were onshore for the same time period. The visual correlation between wind and near-surface current did not extend to currents at 39 m depth. The along-shore current appeared to be similar at the two depths.

In the bottom panel of figure 8 we present 25-hr average $\overline{s^3}$ values. The flux of turbulent energy generated at the sea floor, E_t , was estimated by assuming that the mean rate of work of tidal currents against bottom stress ($\tau = \rho_0 C_D u u$) is $\overline{\tau \cdot u}$ where u is the mean flow velocity near the bottom (Fearhead, 1975). Here we have used hourly values of current speed from the 39 m depth current record, and have not included either a drag coefficient or density (including these parameters yields dimensions of tidal power but $\overline{s^3}$ gives a relative measure of this quantity). By the third occupation of the CTD section, tidal mixing power had increased by about a factor of three.

DISCUSSION AND SUMMARY

The destruction and subsequent reestablishment of typical summer middle shelf and coastal domain hydrographic features was related to winds and tides. The initial vertical mixing of the water column resulted from a combination of wind-wave and current shear turbulence which destroyed vertical structure at least 40 km, or twice the usual distance, from the shore. Longshore winds then reversed and generated an offshore Ekman flux in the near surface waters and a continuity preserving onshore flux at depth. The offshore flux transported warmer less saline surface water offshore, while the onshore flux at depth provided colder more saline waters; the net result was stratification across the entire study area. As tidal mixing power increased, coastal domain waters became vertically mixed and middle shelf domain waters returned to a two-layered configuration.

Near-surface current spectra (not shown) indicated that of the total fluctuating horizontal kinetic energy ($KE_C = \frac{1}{2} [u'^2 + v'^2]$) per unit mass, subtidal energy was $31.6 \text{ cm}^2 \text{ s}^{-2}$ or about 6%. This is consistent with previous studies (Kinder and Schumacher, 1981b). We note that 50% of the subtidal HKE was contained in the 2 to 5 day period bands. The wind spectrum contained little energy ($1.3 \text{ m}^2 \text{ s}^{-2}$ or about 10% of the total KE_w) at tidal or higher frequencies, however, 25% of the KE_w was contained in 2 to 5 day periods with the remainder at periods ≥ 7 days.

The visual correlation between longshore winds and onshore currents, suggesting Ekman dynamics, was substantiated by a linear correlation coefficient between the two low-pass filtered time-series of $r=0.83$ at 0 lag. In frequency, the maximum coherence between hourly wind and current components was at a period of 2.9 days with a coherence squared of 0.995 or about 99% of the variance. A second maximum occurred at 4.8 days with a coherence squared of

0.91 (for both estimates the 95% level of significance was 0.78). Onshore currents alongshelf winds were correlated to a lesser extent at lower depths, with correlations decreasing (0.57, 0.53, and 0.42) and lags increasing (0, 6 and 60 hours) at 10, 15 and 29 m respectively. The current record from 39m depth had a negative correlation ($r = -0.68$ at 48 hours) with alongshore winds. These results suggest that longshore winds generated off/onshore Ekman fluxes in an upper layer with, at times (e.g. 21 to 24 August), a compensating flow lower in the water column. During this particular event, coastal divergence would result in a barotropic pressure gradient toward shore. If this were geostrophically balanced, then an alongshore current (in this reference frame a negative value) would be generated. The observations indicated such flow during both 21 to 24 August and 30 August to 1 September wind events.

An empirical estimate of 5 m onshore current response to alongshore wind was 10^{-2} to 1, or a 10 ms^{-1} wind generated a 10 cm s^{-1} current. Theoretically, we can employ the shallow sea model developed by Csanady (1980) which assumes a semi-infinite ocean bounded by a straight coastline, constant water depth $H=h+h'$, where h is a slightly less dense upper layer and the wind begins at time $t=0$, exerting a stress $\tau_0 = \rho F$ at the water surface, directed parallel to the coast, constant in space and in time $t > 0$ but $t < \text{inertial period}$. Non-linear accelerations and frictional stress are neglected (thus the upper limit on t). The full solution contains some inertial oscillations and an aperiodic part describing a "coastal jet" structure near shore and Ekman drift offshore. Csanady's results indicate two fields germane to our study area; near shore, or within one internal radius of deformation and intermediate, or that shelf region lying between the internal and surface or barotropic radius of deformation. Carefully selecting a time period when stratification holds over the coastal domain (23 August) and wind stress was quasi-steady at $\sim 1.4 \text{ dyne cm}^{-2}$ for about 12 hours, we solve the following equations:

I. Near-shore ($x \leq 6$ km):

$$\begin{aligned} v &= \frac{Ft}{h} \\ v' &= 0 \end{aligned} \tag{1}$$

II. Intermediate field ($200 \text{ km} \geq x \geq 6 \text{ km}$)

$$u = \frac{F}{f(h+h')} \frac{h'}{h} \tag{2}$$

$$u' = \frac{-F}{f(h+h')}$$

$$v = \frac{Ft}{h+h'} = v' \tag{3}$$

where:

$$F = \tau/\rho = -1.4 \text{ c}^2 \text{ s}^{-2}$$

$$h' = 4 \times 10^3 \text{ c}$$

$$h = 2 \times 10^3 \text{ c}$$

$$t = 4.3 \times 10^4 \text{ s}$$

$$f = 10^{-4} \text{ s}$$

the prime indicates lower layer and v is alongshore and u is onshore as previously defined. Using the observed values, the following values were calculated:

TABLE 1

Comparison between Csanady's model and observations on the north Aleutian shelf

	Model	Observed
near-shore	$v = -30.0 \text{ cs}^{-1}$	*
intermediate-field	$u = -5.0 \text{ cs}^{-1}$	-10.0 cs^{-1}
	$u' = +2.5 \text{ cs}^{-1}$	2.5 cs^{-1}
	$v=v' = -10.0 \text{ cs}^{-1}$	$- 5.0 \text{ cs}^{-1}$ (upper layer)
		$- 2.5 \text{ cs}^{-1}$ (lower layer)

* Current meters presently in the water may allow a comparison with near-shore model velocity.

The agreement between model and observed values was good, considering that winds were not steady state, the model yields an integrated upper and lower layer velocity rather than a measurement at one specific depth, and that the "bottom layer" observed currents were obtained 25 m above the seafloor.

In summary, preliminary analysis of wind, current, hydrographic and SPM data suggest the following:

- 1) Storms radically alter mean hydrographic domains. The enhanced turbulence vertically mixed middle shelf water and increased SPM concentrations. These two factors could dominate vertical transport of oil, resulting in greater concentrations on the bottom in a shorter time than detrital rain.
- 2) Although tides dominate HKE, in the vicinity of coastal boundaries Ekman fluxes are important to transport and water mass distributions.

- 3) The effectiveness of tidal mixing power was evident between 24 and 31 August. During this period, tidally generated turbulence reduced vertical stratification from 0.20 and 0.31 sigma-t units to zero.
- 4) It appears that the dynamics of coastal flow may adhere to physics in Csanady's (1980) model. Bottom pressure, current and wind measurements presently underway will help elucidate alongshore and cross-shelf pressure and velocity fields, provide improved wind measurements, and allow further comparisons with models of coastal dynamics.

ACKNOWLEDGEMENTS

We thank all those who assisted in data collection, processing, manuscript preparation and lent moral support, in particular: the compliment of the NOAA SHIP SURVEYOR, Dick Tripp for PROBES data, Dave Pashinski, Lynn Long, Dave Katchel, Joy Golly, Gini May, Phyllis Hutchens and Glenn Cannon. This study was supported in part by the Bureau of Land Management through an interagency agreement with the National Oceanic and Atmospheric Administration, under which a multi-year program responding to needs of petroleum development of the Alaskan continental shelf is managed by the Outer Continental Shelf Environmental Assessment Program (OCSEAP) office, Juneau.

REFERENCES

- Beardsley, R.C. and C.D. Winant, 1979. Mean circulation in the mid-Atlantic bight. JPO, 9(3): 612-619.
- Brower, W.A., H.F. Diaz, A.S. Prechtel, H. Searby and J.L. Wise, 1977. Climatic atlas of the outer continental shelf waters and coastal regions of Alaska. Vol II NOAA/OCSEAP. Final Report (RU 347): 443 pp.
- Coachman, L.K. and R.L. Charnell, 1977. Finestructure in outer Bristol Bay, Alaska. Deep-Sea Res. 24(10): 809-889.
- Coachman, L.K. and R.L. Charnell, 1979. Lateral water mass interactions-a case study, Bristol Bay, Alaska. JPO, 9(2): 278-287.
- Coachman, L.K., T.H. Kinder, J.D. Schumacher and R.B. Tripp, 1980. Frontal systems of the southeastern Bering Sea shelf. In Stratified Flow, 2nd Int. Assoc. Hydraulic Res. Symposium, Trondheim, June 1980, T. Carstens and T. McChmans Eds., TAPIR Publishers, Norway.
- Csanady, G.T., 1978. The arrested topographic wave. JPO 8(1): 47-62.
- Csanady, G.T., 1980. The coastal jet conceptual model in the dynamics of shallow seas. In the Sea, Vol 6: 117-144.
- Fearhead, P.G. On the formation of fronts by tidal mixing around the British Isles. Deep-Sea Res., 22(5): 311-322.

Kinder, T.H. and L.K. Coachman, 1978. The front overlaying the continental slope of the eastern Bering Sea. J. Geophys. Res. 83: 4551-4550.

Kinder, T.H., J.D. Schumacher and D.V. Hansen, 1980. Observation of a baroclinic eddy: an example of mesoscale variability in the Bering Sea. JPO, 10(8): 1228-1245.

Kinder, T.H. and J.D. Schumacher, 1981a. Hydrographic structure over the continental shelf of the southeastern Bering Sea. In The Bering Sea: Oceanography and Resources, D. W. Hood, Editor, in press.

Kinder, T.H. and J.D. Schumacher, 1981b. Circulation over the continental shelf of the southeastern Bering Sea. In the Bering Sea: Oceanography and Resources, D. W. Hood, Editor, in press.

Pearson, C.A., H. Mofjeld and R.B. Tripp, 1981. Tides of the eastern Bering Sea shelf. In The Bering Sea: Oceanography and Resources, D. W. Hood, Editor in press.

Reed, R.K., 1978. Heat budget in the eastern Bering Sea. J. Geophys. Res. 83: 5613-5619.

Sayles, M.A., K. Aagard and L.K. Coachman, 1979. Oceanographic Atlas of the Bering Sea basin. Univ. Washington Press, Seattle: 158 pp.

Schumacher, J.D., T.H. Kinder, D.J. Pashinski and R.L. Charnell, 1979. A structural front over the continental shelf of the eastern Bering Sea. JPO, 9(1): 79-87.

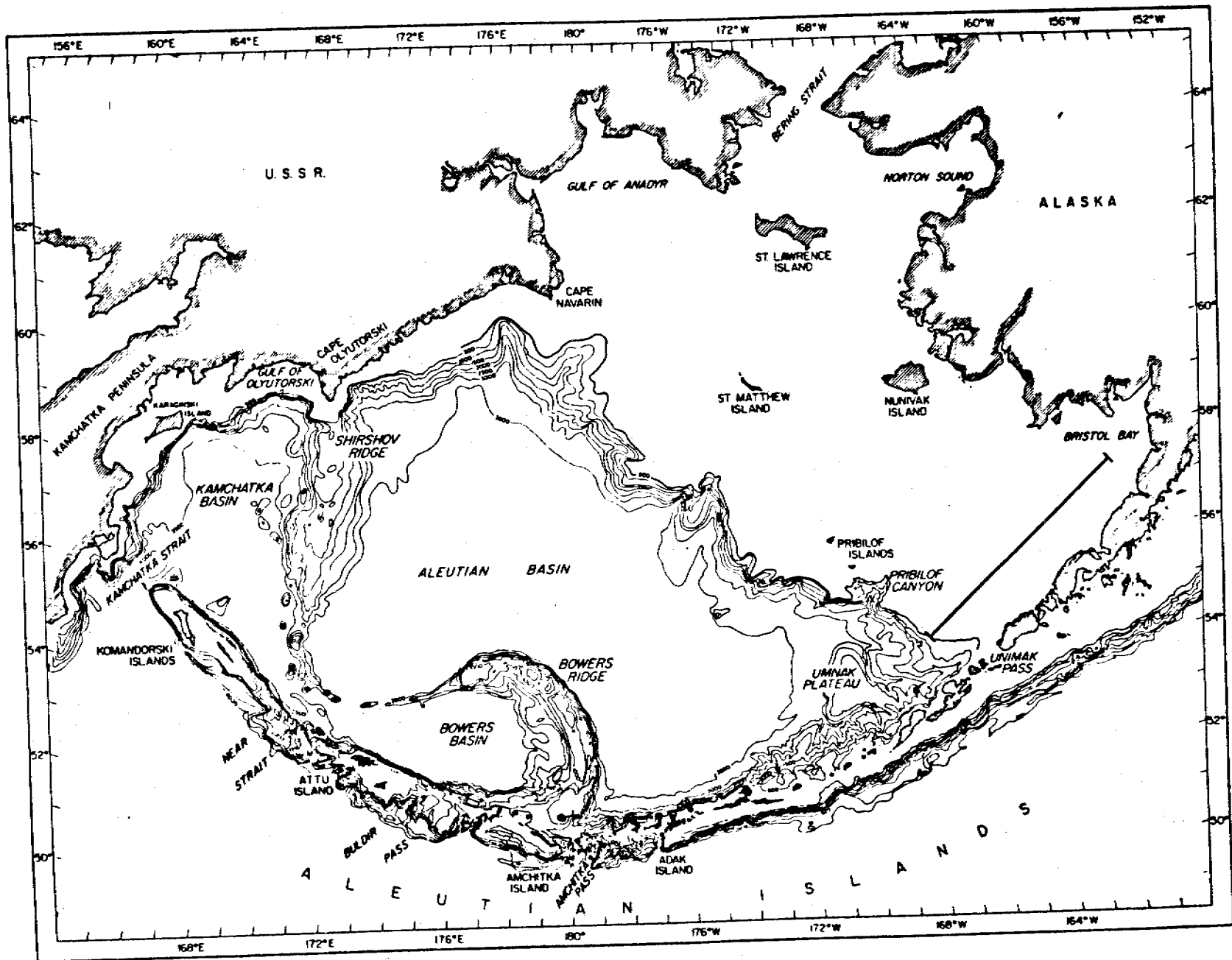
Wu, J., 1969. Windstress and surface roughness at the air-sea interface. J. Geophys. Res., 74(2): 444-445.

Wynant, C.D., 1980. Coastal circulation and wind-induced currents. In Annual Reviews of Fluid Mechanics, Vol 12: 271-302.

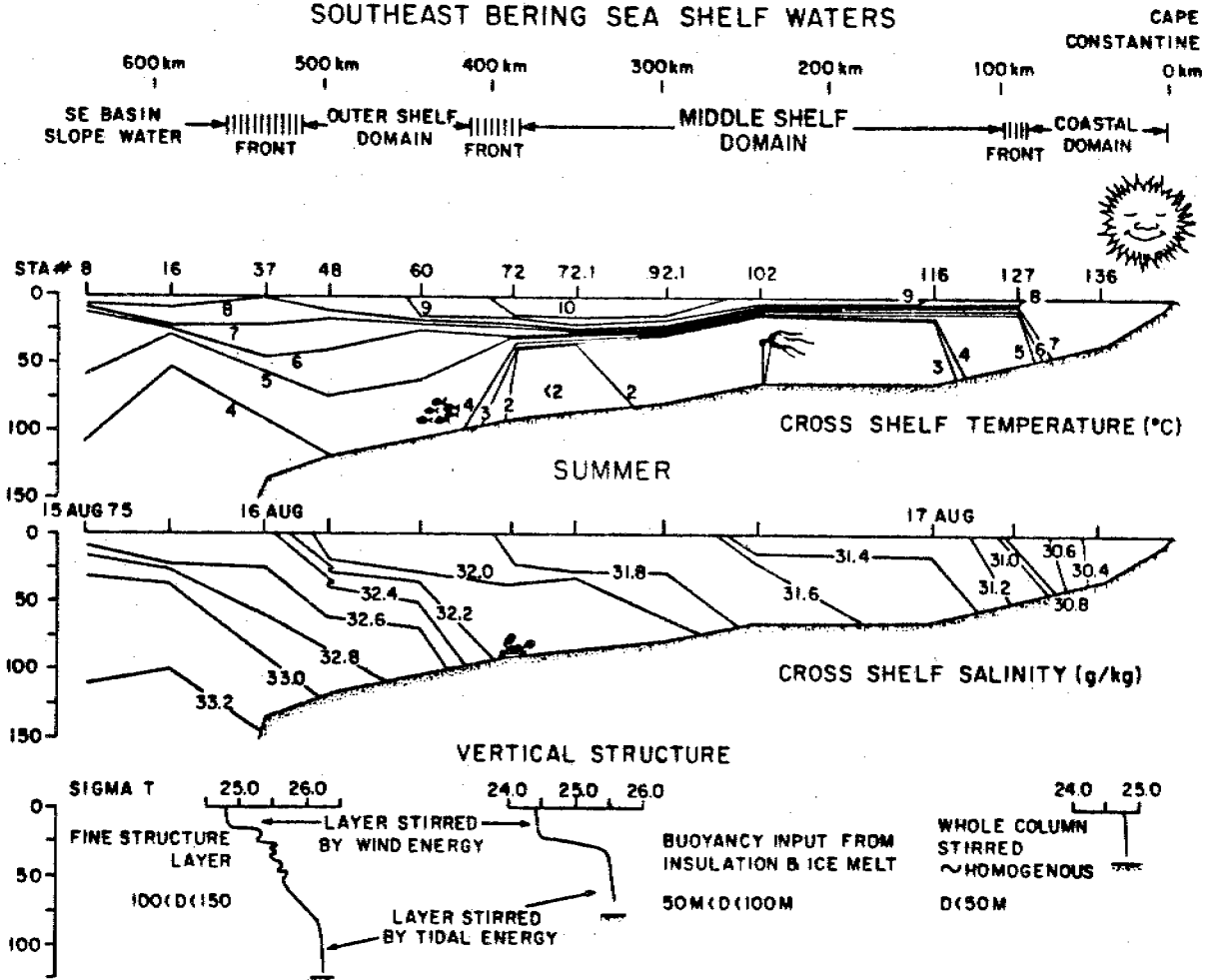
FIGURE LEGENDS

- Figure 1. The Bering Sea. The line extending from Bristol Bay (off Cape Costantine) to the shelf break indicates location of hydrographic features on figure 2. Depths are in meters.
- Figure 2. Hydrographic characteristics of southeast Bering Sea shelf waters during typical summer conditions.
- Figure 3. Spatial configurations of hydrographic domains. Also shown are net current vectors (from Kinder and Schumacher, 1981b).
- Figure 4. North Aleutian Shelf study area, showing location of hydrographic data section (NA41 to NA46) and mooring TP3. Also shown are CTD data from 31 May 1980 and axes used for current and wind data.
- Figure 5. Hydrographic and light attenuation sections from 19 August 1980. Note the location of the 8.5°C isotherm.
- Figure 6. Hydrographic and light attenuation sections from 24 August 1980. Contour intervals are 0.5°C, 0.25 gm kg⁻¹, 0.25 σ_t units and 0.2 m⁻¹ for light attenuation. Magnitude of upper minus lowest 1m average parameter is presented under a given station as a Δ . Note, lowest 1m average salinity at station 42 was 31.71 gm kg⁻¹.
- Figure 7. Hydrographic and light attenuation sections from 31 August 1980.

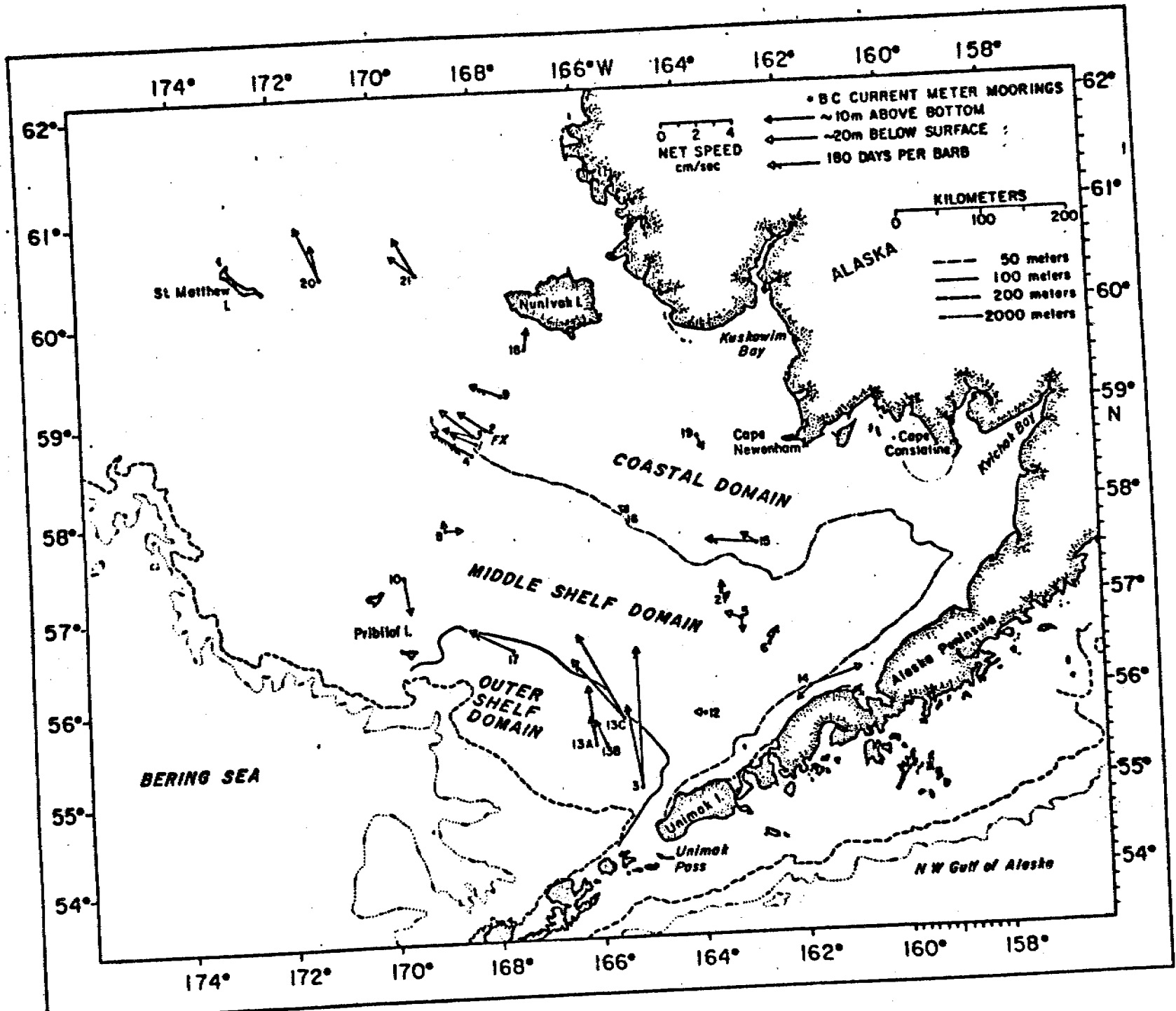
Figure 8. a) Alongshore windspeed, b) onshore current at 5 and 39m, c) alongshore current at 5 and 39m and d) 25-hr. average tidal mixing parameter $\overline{s^3}$ from the 39m depth current record.



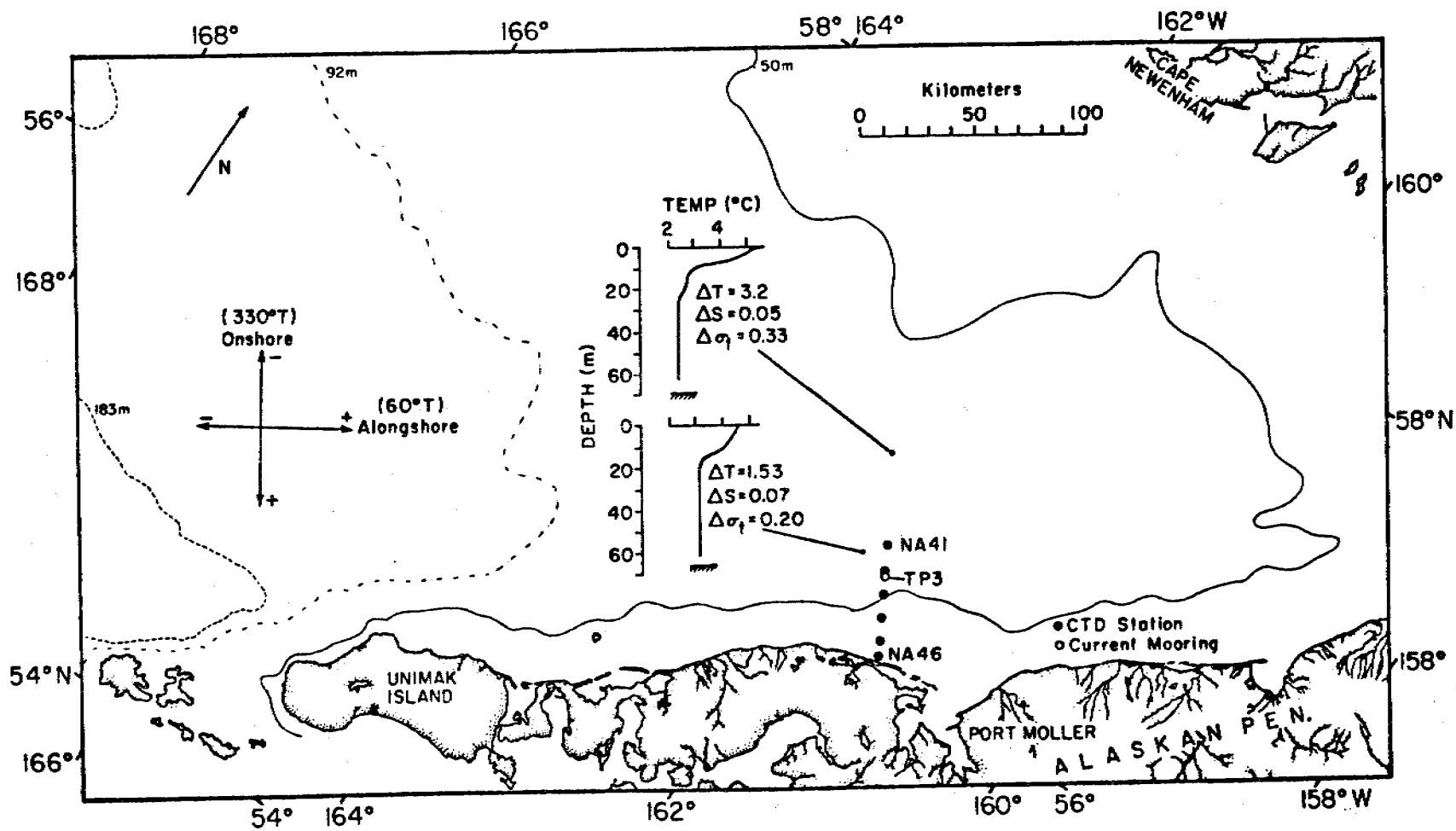
HYDROGRAPHIC CHARACTERISTICS OF SOUTHEAST BERING SEA SHELF WATERS

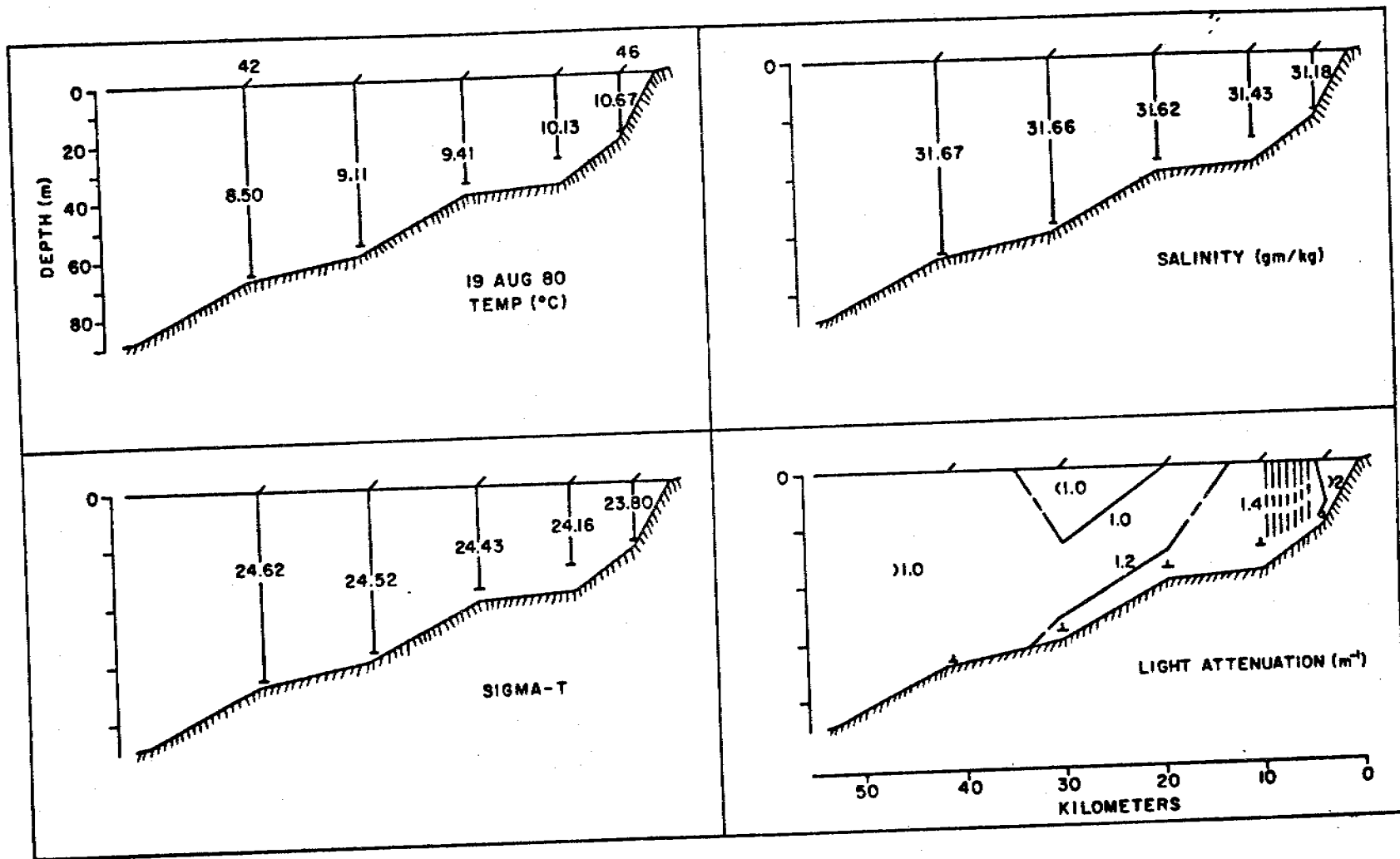


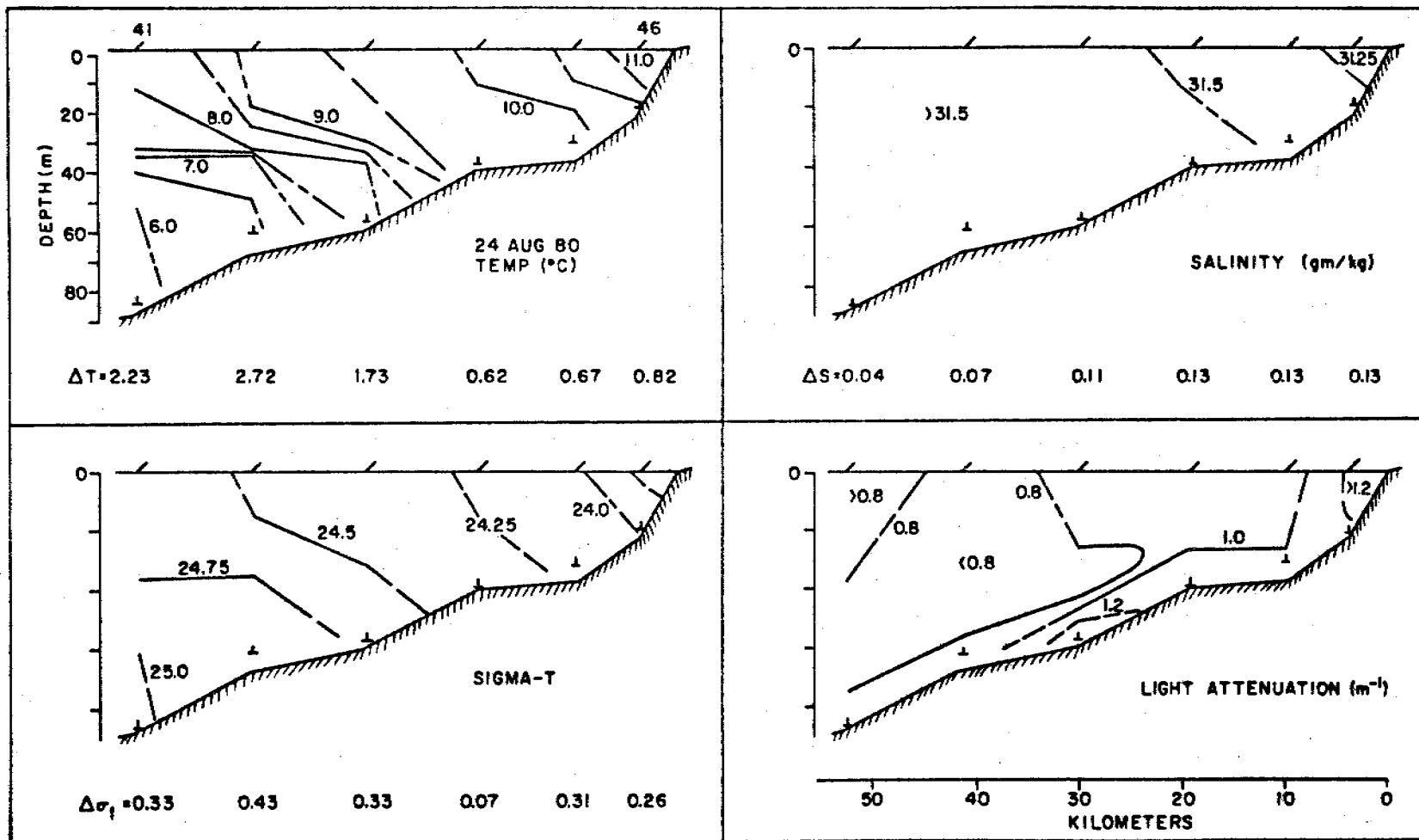
523

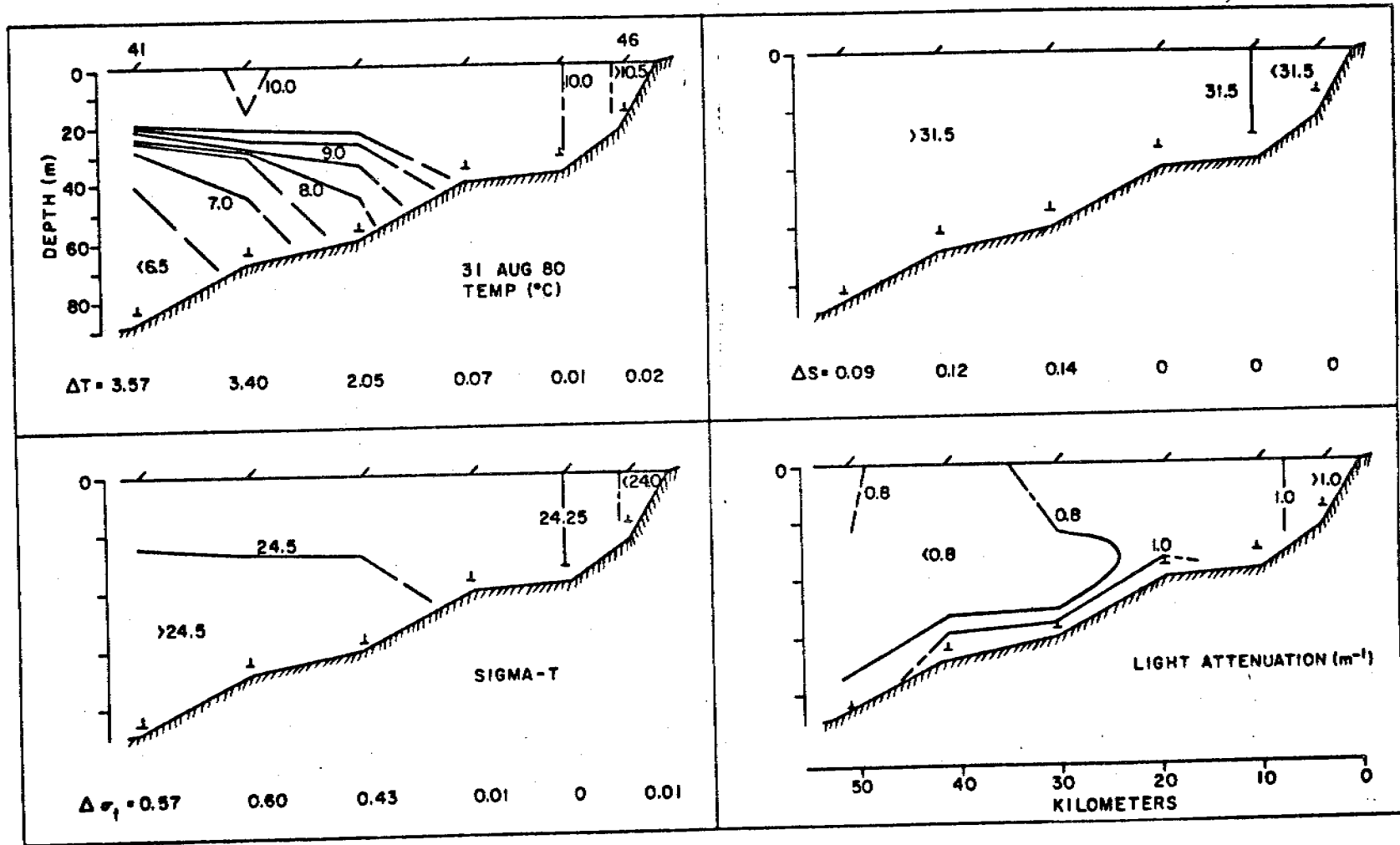


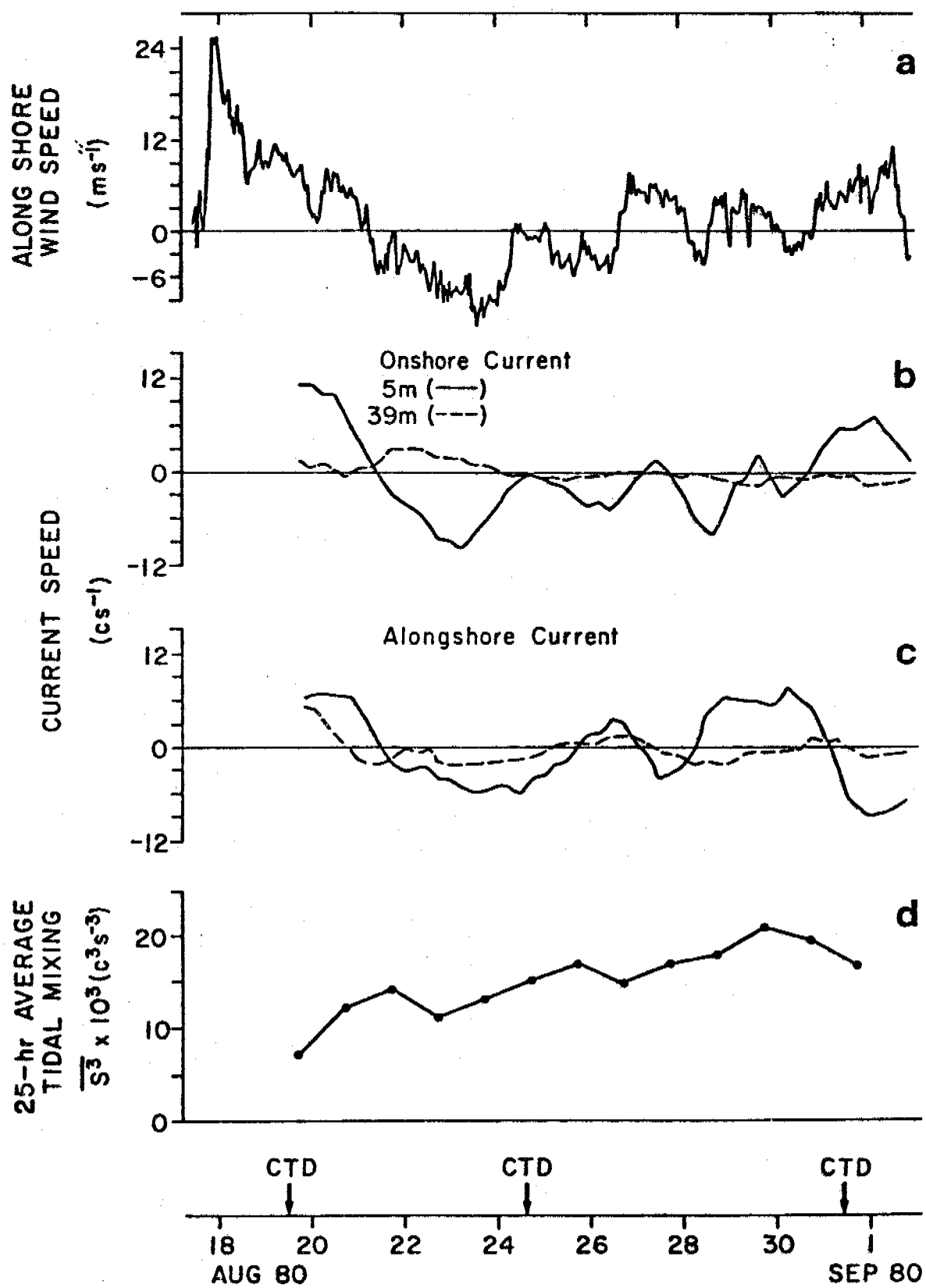
524











IV. F

Guide to R2D2-Rapid Retrieval Data Display¹

Carl A. Pearson²

Pacific Marine Environmental Laboratory

3711 15th Ave. N.E.

Seattle, Washington 98105

ABSTRACT

R2D2 is a set of Fortran programs, linked by a procedure file, for rapid retrieval and display of hydrographic, current meter and pressure gauge data. Data are stored as random access disk files for rapid access and sorting. Programs are interactive and have graphics capability. A wide range of display and analysis outputs are available, including time series plots, data listings, statistics, spectral and tide analysis, empirical orthogonal function analysis, and maps of properties. Routines are described from a user's point of view, with output examples.

¹Contribution No. 511 from NOAA PMEL

²National Ocean Survey, assigned to PMEL

CONTENTS

	Page
Abstract	
I. Introduction	533
II. Program notes and user's guide	537
A. General R2D2 Structure	539
1. External files used in R2D2 programs	540
2. Beginning R2D2	541
B. R2START	542
C. Hydrographic (STD) data routines	545
1. Sorting	546
a. Summary listing of file	548
b. Select individual reference number	550
c. Sort by reference number range	552
d. Sort by latitude and longitude	553
e. Sort by time period	554
f. Sort by depth range	555
g. Sort by cruise name	556
h. List stations selected	557
i. Plot stations selected	559
2. Write selected stations from Master File to PF	561
3. Data analysis and display routines	563
a. Data listings	565
b. Area distributions	567
c. Profiles	571
d. Time series profiles	574
e. T-S diagrams	576
f. Transections	579
D. Current meter/pressure gauge programs	582
1. Sorting	583
a. Summary listing of file	586
b. Sort by project, mooring, meter names	588
c. Add TAPE4 files	589
d. Plot mooring locations	590

2.	Data analysis and display routines	592
a.	Data listings	594
b.	Statistics	597
c.	Time series plots(all parameters, one record).	600
d.	Time series plots(one parameter, all records).	602
e.	U-V scatter diagrams	605
f.	PVD plots	607
g.	Histograms	609
h.	Current roses	612
i.	Summary current vectors	615
j.	Lagged linear correlations	617
k.	Empirical orthogonal functions	622
l.	Write data in TAPE4 format	625
m.	Selecting filter type, time period for individual records	627
n.	Selecting filter type, time period for all records	628
o.	Axis rotation	629
3.	Spectral, tide analysis	630
a.	Scalar spectra	633
b.	Components, total spectra	635
c.	Rotary spectra	637
d.	Scalar cross-spectra	640
e.	Rotary cross-spectra	643
f.	29-day harmonic tide analysis	646
g.	Successive tide analysis	650
h.	Plotting spectra	651
i.	FFT and Spectral averaging	652
4.	TAPE4 format	653
E.	Ending R2D2	655
F.	Miscellaneous routines	656
1.	Map drawing	656
2.	Plotting	659
III.	Associated user programs	661
A.	R2PLOT: Offline plotting	661
B.	UPLT	662
IV.	Data structure, maintenance programs	663
A.	STD	663
1.	Data structure	663
2.	Data loading	665
3.	Editing header files	666

B. Current meter/pressure gauge data	668
1. Data structure	668
2. Data loading	671
3. Editing header files	672
Acknowledgements	674
References	675

I. Introduction

The large amount of current meter, pressure gauge and CTD/STD data collected by the Coastal Physics Group of PMEL has required the development of a computer-based system for easy and efficient data retrieval, analysis and display. The requirements of such a system were: 1) data be readily accessible and capable of being sorted to the user's specification; 2) no programming be required of the user; 3) the programs be interactive and as "user proof" as possible; and 4) a wide variety of graphical and printed output products be available for analysis. This system was named Rapid Retrieval Data Display, or "R2D2", and currently resides on the ERL CYBER 170/750 Computer in Boulder, Colorado. An early version is described in Pearson, Krancus and Charnell (1979).

Data are stored as two-level random access packed binary files. The files are divided by type (STD and current meter/pressure gage) and geographical area (Gulf of Alaska, Bering Sea and Puget Sound). Thus there are 6 Master Data Files (MDF's). For each data set there is a header field, which contains information such as reference number, station name, date and times, latitude and longitude, depth, record length, and other information. The header information is used for sorting. The random access data storage location is keyed to the reference number, which is assigned when the data are originally loaded in the file.

MDF's are stored on a private disk pack. Six Master Header Files (MHF's) containing header information only, are stored as permanent files on NOAA family disks. The random access storage structure of the data and header files is identical, so that they may be used interchangeably by the program for sorting.

The user may access the data through a User Data File (UDF). A UDF is created by sorting a MHF and then selecting the R2D2 program option which

creates and submits a batch job, which then reads the selected data sets from the MDF and writes them on the UDF permanent file under the user's number. Thereafter, the user may attach the UDF, then sort to select the desired data sets for further data analysis and display.

STD data are stored as 1-m averaged salinity and temperature. Depth is computed from the array subscript, and σ_t from the equation of state. Current meter data is hourly 2.86 hour filtered east and north velocity components, and temperature, pressure and salinity, and six-hourly 35 hour filtered east and north component velocities (see Krancus, Pearson and Charnell (1979) for a description of current meter data processing). There are presently (1981) about 12000 STD casts and 600 current meter records on file.

The user accesses the R2D2 programs by remote terminal and executes a "procedure file" called R2D2. The procedure file is a series of control language commands which attach and execute the programs. Registers set from within the programs control flow through the procedure file (fig. 1).

Like the data files, programs have been divided by type to minimize central memory requirements. The main programs are: 1) R2START, which checks the user's access authorization, and allows the user to select the desired data type and file; 2) STDMAIN, which sorts and displays hydrographic data; 3) CMSORT, which sorts the current meter files and provides options for listing and plotting header information; 4) SPECT, which contains auto-, cross-spectral and tidal analysis routines; 5) CMLOOK, which has options for a variety of current meter data display and analysis routines, including data listings, PVD and time-series plots, cross correlation, empirical orthogonal functions and others. All programs are written in FORTRAN.

Printed and plotted output may be through the user's terminal as well as routed to the PMEL RJE terminal (or with slight modification to any terminal linked to the central computer).

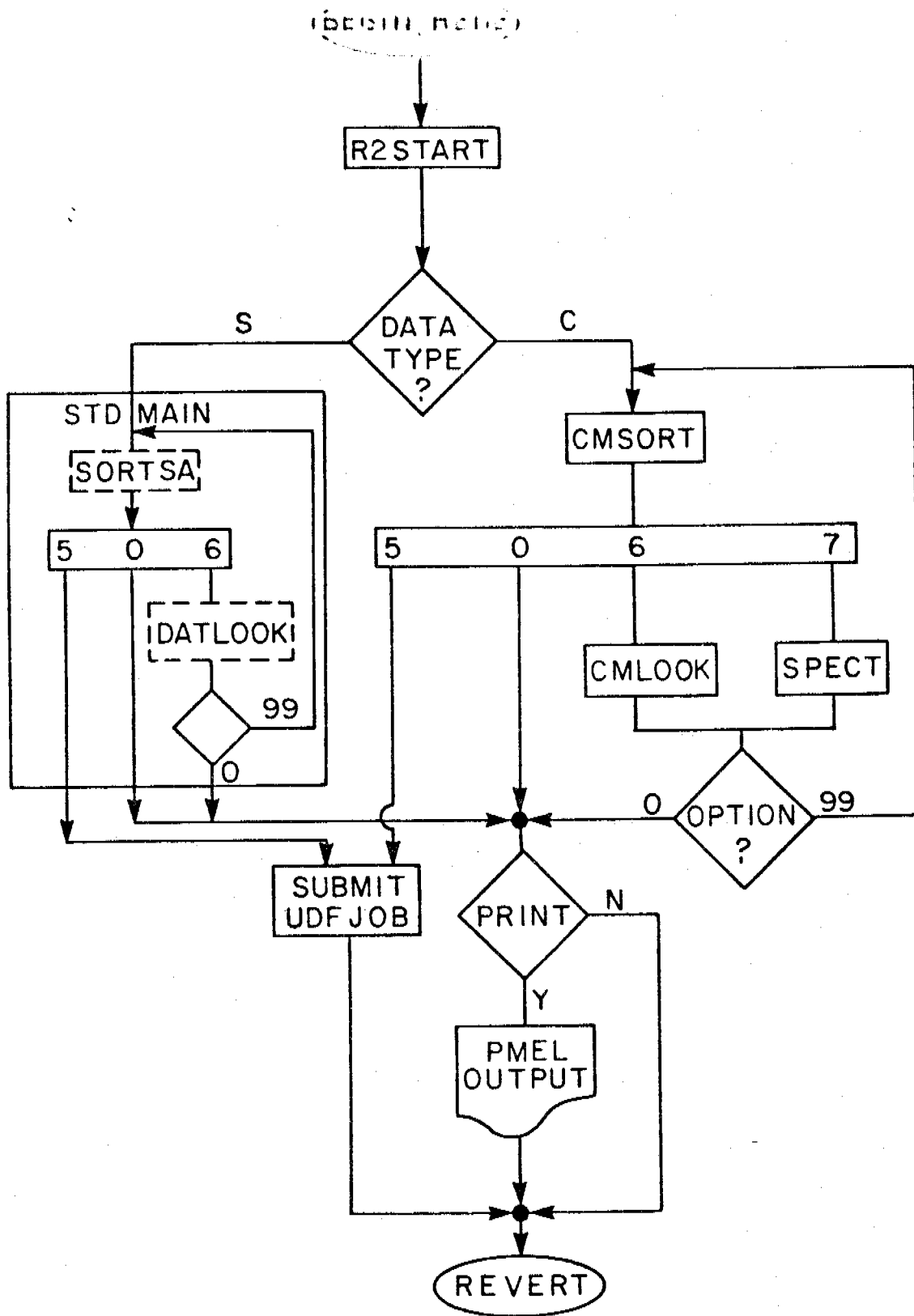


Fig. 1. General R2D2 structure.

The remainder of this report will contain a detailed description and user's guide of the R2D2 programs (section II), and associated programs such as R2PLOT and UPLT (section III); and documentation of the data structure and the loading and editing programs (section IV).

II. Program notes and user's guide

This section describes the R2D2 sorting, analysis and display routines from the user's point of view. That is, each of the major options will be described with reference to how to get there, explanations of options available, some examples of output, and notes on algorithms used. It serves as a user's guide, giving directions and descriptions of available products. Accompanying this is a schematic of the detailed R2D2 structure (fig. 2), which may be thought of as a map, providing a quick reference on how to get from one point to another.

R2D2 is not static. Routines are occasionally changed or added to increase efficiency or expand versatility. Therefore this report should be put in a loose-leaf binder, and pages replaced as changes are made. If you wish to receive updates, please notify the author of this report.

This section is subdivided as follows: Section II-A describes the general R2D2 program structure; II-B describes R2START, which checks the user access code, sets registers and attaches data files; II-C describes STDMAIN, the STD sorting and display program; II-D describes the current meter/pressure gauge programs (CMSORT, CMLOOK and SPECT); II-E ending R2D2; II-F describes miscellaneous routines such as those used for drawing maps and plotting.

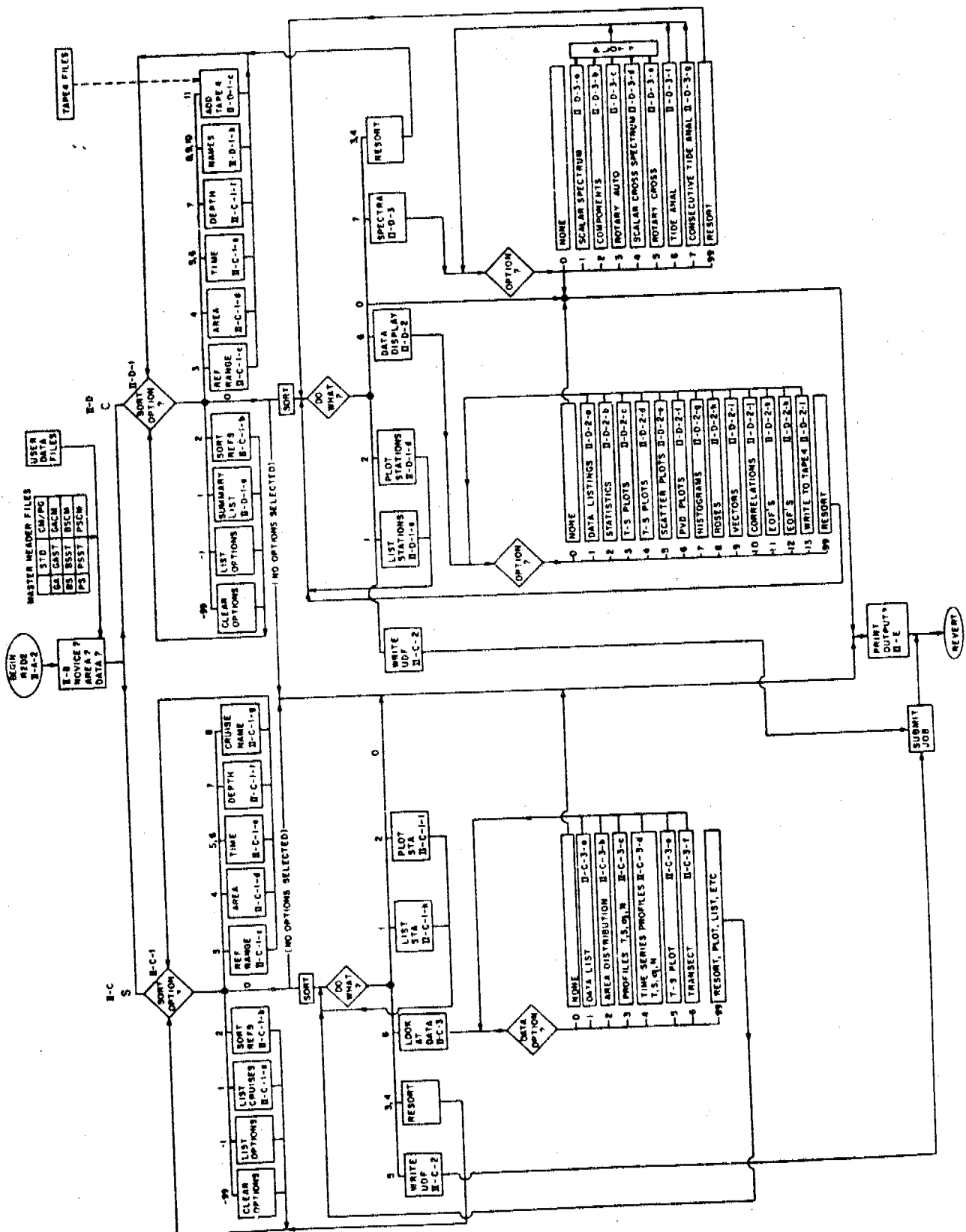


Fig. 2. Detailed schematic of R2D2.

II-A General R2D2 structure.

R2D2 is the name of a procedure file which resides as an indirect access file on user number RLC. Figure 1 shows the general R2D2 structure. R2D2 attaches and executes the programs, with flow controlled by registers R1, R2 and R3. The control registers are set both from within programs and in the procedure file. They are also used to transfer information from one program to another.

Programs are stored as core images. That is, programs and libraries have been previously loaded into core, and the core image saved as a direct access permanent file, which may then be attached and executed.

II-A-1 external files used in R2D2 programs

Several local files are used by R2D2 which will be read and/or written by the various programs. These files are:

- INPUT - used to read input through the user's interactive terminal (used in all programs)
- OUTPUT - used to print output to the user's terminal (all programs)
- TAPE1 - a scratch file used by the PLOT10 routines for plotting on Tektronix terminals (STDMAIN, CMSORT, CMLOOK, SPECT)
- TAPE2 - PLOT10 output file used for plotting on Tektronix terminals, equivalenced to OUTPUT (STDMAIN, CMSORT, CMLOOK, SPECT)
- TAPE3 - a permanent file containing mercator coordinates of coastline, of each of the three geographical areas used by the map drawing routine (STDMAIN, CMSORT, CMLOOK)
- TAPE4 - used to read or write data in the "TAPE4 format", an unformatted sequential type file which permits the use of R2D2 data in other programs, and non-R2D2 data in R2D2 (STDMAIN, CMSORT, CMLOOK, SPECT)
- TAPE5 - A scratch file which contains the header information of the selected data records (STDMAIN, CMORT, CMLOOK, SPECT)
- TAPE6 - A file containing formatted output which may be routed to a central printer (all programs)
- TAPE7 - The data permanent file, which may be either a Master Header File or a User Data File (all programs)
- TAPE98 - A direct access permanent file, defined in the program and used to store plots for offline plotting (STDMAIN, CMSORT, CMLOOK, SPECT)
- TAPE99 - A scratch file used for temporarily storing plots or data. Also used as the authorized user list in R2START, and as the Submit File which reads the Master Data File (all programs)

II-A-2 Beginning R2D2.

To begin R2D2, the user logs into the Boulder ERL CDC 750 computer and then enters the following commands, followed by a carriage return....

```
GET,R2D2/UN=RLC
```

```
R2D2
```

This begins execution of R2D2. The first control statement executed by R2D2 is to begin a procedure file called BANNER. This is a procedure file on the user's user number which writes a banner to TAPE6. If BANNER is not found, a message will be printed to that effect, and execution will continue. An example of a BANNER file is:

```
.PROC,BANNER,LIST.  
HEADING(LIST) H. SOLO
```

R2D2 then attaches and executes R2START.

II-B R2START

After entering the command R2D2, the first output seen by the user should be....

THE COASTAL PHYSICS GROUP

PRESENTS

R RAPID

2 RETRIEVAL

R DATA

2 DISPLAY

BUILT A LONG TIME AGO

... ON A DATA BASE FAR, FAR AWAY

(At this point, the user's user number is checked against a list of authorized users. If not on the list, the following would be printed:

SORRY, INCORRECT PERMISSION

and execution terminated. If found, R2D2 then continues...)

GOOD MORNING (your name)

R2D2 AT YOUR SERVICE

message, if any

ARE YOU A NOVICE USER?

For this and all subsequent yes or no questions, enter a Y for yes, N for no, or just a carriage return for an explanation of the question. If the answer to this question is Y, a switch will be set to print instructions before each subsequent question is asked.

DATA TYPE?

Enter S if you are going to select an STD data set, or C for current meter/pressure gauge data.

FILE?

Enter 0 if no random access file is to be attached i.e., only TAPE4 files are being used. In this case R2D2 proceeds to the next program immediately. To attach a Master Header File enter GA, BS or PS for a Gulf of Alaska, Bering Sea or Puget Sound header file, respectively. To attach a User Data File, enter the name of the data file. If a User Data File name is entered, the next question is....

ENTER DATA FILE USER NUMBER?

In this case enter the user number on which the User Data File resides. Do not, however, enter a password. If all goes well, R2D2 will print....

(file name) HAS BEEN ATTACHED

and proceed to the next program. If the file could not be attached an error message is printed and execution terminated.

Figure 3 is an example of an R2D2 start.

GET, R2D2/UN=RLC
/R2D2
THE COASTAL PHYSICS GROUP

PRESENTS

R RAPID

2 RETRIEVAL

D DATA

2 DISPLAY

BUILT A LONG TIME AGO
...ON A DATA BASE FAR FAR AWAY

GOOD MORNING CARL
R2D2 AT YOUR SERVICE

ARE YOU A NOVICE USER ? N
NOTE: FOR INSTRUCTIONS TO QUESTIONS, PRESS RETURN KEY
DATA TYPE ? S
FILE? NASTE
ENTER DATA FILE USER NUMBER ? CAP
NASTE HAS BEEN ATTACHED

Fig. 3. Starting R2D2.

II-C Hydrographic (STD) data routines

The program STDMAIN contains all the sorting, analysis and display routines for the STD data type. The program STDMAIN itself is short and serves primarily to call the two major subroutines: SORTSTA, which sorts the data; and DATLOOK, which does the data display.

II-C-1 Sorting

DATA TYPE: S (II-B)

After the user selects data type S and the appropriate data file, R2D2 attaches and executes STDMAIN, continuing thus.....

YOU MAY NOW SORT

ENTER SORT OPTION?

The options are:

- 99 CLEAR PREVIOUS OPTIONS
- 1 LIST OPTIONS CURRENTLY SELECTED
- 0 SORT WITH OPTIONS SELECTED
(If none selected, no sorting will be done)
- 1 SUMMARY LISTING OF FILE (II-C-1-a)
- 2 SELECT INDIVIDUAL REFERENCE NUMBERS (II-C-1-b)
- 3 SORT BY REFERENCE NUMBER RANGE (II-C-1-c)
- 4 SORT BY LATITUDE AND LONGITUDE (IIC-1-d)
- 5 SORT BY TIME PERIOD (JULIAN DATES)(II-C-1-e)
- 6 SORT BY TIME PERIOD (GEGORIAN DATE)(II-C-1-e)
- 7 SORT BY STATION DEPTH (II-C-1-f)
- 8 SORT BY CRUISE NAME (II-C-1-g)

These options are described in sections II-C-1-(a thru g). When the desired sort options have been selected, option 0 is entered to initiate sorting. Any stations which meet all the specified criteria are selected. A maximum of 600 stations may be used for subsequent data analysis, but any number may be selected for listing and/or plotting of the header information.

When the sorting process is complete, the total number of stations selected is printed, i.e.

128 STATIONS HAVE BEEN SELECTED

WHAT WOULD YOU LIKE TO DO?

Now the options are....

0 TO DO NOTHING MORE (II-E)

1 TO LIST STATIONS SELECTED (II-C-1-h)

2 PLOT LOCATIONS OF STATIONS SELECTED (II-C-1-i)

3 RESORT

4 SORT AGAIN, KEEPING STATIONS ALREADY SELECTED

5 WRITE SELECTED RECORDS FROM MASTER TAPE TO PF (II-C-2)

6 LOOK AT DATA FOR STATIONS SELECTED (II-C-3)

These options are discussed in following sections.

Notes on sorting:

Option 2 selects the specified records immediately. For options 3-8, sorting is done only after the desired sort options are selected and sort option 0 entered. The sort option routines simply set up the sort parameters. The quickest sorting is done if option 3 is included, since only the specified range of reference numbers needs to be checked. Otherwise the whole file, which may be several thousand records in the case of a Master Header File, must be sorted.

II-C-1-a SUMMARY LISTING OF FILE (fig. 4)

DATA TYPE: S (II-B)

SORT OPTION: 1 (II-C-1)

This option prints a summary of all or part of the file contents by cruise name. For each cruise, output includes cruise name, ship name, Chief Scientist's name, the extreme latitudes and longitudes, start and end times, reference number ranges and number of records.

R2D2 will ask...

ALL OF THEM?

If answer is Y the entire file will be summarized. If N the next question is...

ENTER REFERENCE NUMBER RANGE: FIRST, LAST?

If the reference number entered for LAST is larger than the actual last reference number in the file, LAST will be reset accordingly.

DO YOU WANT TO PRINT ON YOUR TERMINAL?

If the answer is N, output will be written on TAPE6 only.

Subroutine name: INDEX

Called from: SORTSTA (II-C-1)

Program: STDMAIN (II-C)

YOU MAY NOW SORT
ENTER SORT OPTION ? 1
ALL OF THEM ? Y
DO YOU WANT TO PRINT ON YOUR TERMINAL ? Y

RP4SU80AL4 SURVEYOR CURL
LATITUDES 53.46 TO 58.34
LONGITUDES 151.68 TO 169.41
802280128 TO 802491511
YOUR REFERENCE NO 1 TO 198
MASTER REFERENCE NO 2676 TO 2873
198 CASTS

TOTAL CASTS = 198

Fig. 4. Summary listing of hydrographic file contents.

II-C-1-b SELECT INDIVIDUAL REFERENCE NUMBER (fig.5)

DATA TYPE: S (II-B)

SORT OPTION: 2 (II-C-1)

This option allows the user to select individual records by reference number, without regard to the actual order in the file. Since files are random access, this is the most efficient way to select a few records. Up to 600 records may be selected. Unlike the other sort options, this one immediately gets the records selected, rather than waiting for sort option 0 to be entered.

R2D2 will print....

ENTER N REF NUMBERS (IE REF1, REF2,...REFN)

FOLLOWED BY AN EXTRA CARRIAGE RETURN

The user now enters from 1 to 600 reference numbers, separated by commas. Two carriage returns in a row terminates entry.

The program continues...

YOU HAVE SELECTED:

(list of reference numbers)

IS THAT OK?

If not OK, the numbers may be re-entered. Otherwise the desired records are selected. If a particular record cannot be found, a message to that effect is printed.

Subroutine name: SELECT

Called from: SORSTA (II-C-1)

Program: STDMAIN (II-C)

```

ENTER SORT OPTION ? 2
ENTER N REF NUMBERS (IE REF1,REF2,..REFN)
  FOLLOWED BY AN EXTRA CARRIAGE RETURN
? 44,45
?
YOU HAVE SELECTED:
44 45
  IS THIS OK? Y
  ENTER SORT OPTION ? 3
  ENTER REFERENCE NUMBER RANGE: REF1,REF2 ? 10,100
  REF NO. RANGE IS 10 TO 100
  IS THIS OK? Y
  ENTER SORT OPTION ? 4
  ENTER: LAT1,LAT2,LOH1,LOH2
? 55,59,156,163

AREA IS BOUNDED BY:
LATITUDES 55.00 TO 59.00
LONGITUDES 156.00 TO 163.00
  IS THIS OK? Y
  ENTER SORT OPTION ? 5
  IF YOU ENTER 0 FOR YEAR, THE YEAR WILL BE DISREGARDED
  ENTER: STARTDAT,ENDDAY? 802200000,802302400

TIME PERIOD IS:
FROM 802200000 TO 802302400
  IS THIS OK? Y
  ENTER SORT OPTION ? 6
  IF YOU ENTER 0 FOR YEAR, THE YEAR WILL BE DISREGARDED
  ENTER: START YEAR,MON,DAY,END YEAR,MON,DAY
  (USE NUMBER FOR MON)
? 80,8,22,80,8,25
TIME PERIOD IS:
FROM 80 AUG 22 TO 80 AUG 25
  IS THIS OK? Y
  ENTER SORT OPTION ? 7
  ENTER D1,D2 ? 10,100
  UPPER DEPTH IS 10
  LOWER DEPTH IS 100
  IS THIS OK? Y
  ENTER SORT OPTION ? 8
  CRUISE NAME ? RP4SU80AL4
  CRUISE = RP4SU80AL4
  IS THIS OK? Y
  ENTER SORT OPTION ? -1
  LATS 55. 59. LONS 156. 163.
  TIME PERIOD (JD) 802350000,TO 802382400
  CRUISE RP4SU80AL4
  STATION DEPTH RANGE 10. TO 100.
  REFS 10 TO 100
  ENTER SORT OPTION ? 0
  56 RECORDS HAVE BEEN SELECTED
  WHAT WOULD YOU LIKE TO DO ?

```

Fig. 5. Hydrographic file sorting options.

II-C-1-c SORT BY REFERENCE NUMBER RANGE (fig.5)

DATA TYPE: S,C (II-B)

SORT OPTION: 3 (II-C-1, II-D-1)

This option allows sorting on a range of reference numbers. Use of this option is more efficient because only the specified range of numbers is tested during sorting. No actual sorting is done until sort option 0 is selected

R2D2 will print....

ENTER REFERENCE RANGE: REF1, REF2?

The user enters the first and last reference numbers in the desired range, separated by commas. If the entered reference numbers are larger than the actual last reference number LAST on file, this is noted and REF2 is changed to LAST.

R2D2 continues.....

REF NO RANGE IS (REF1) to (REF2)

IS THIS OK?

If not OK the reference number range may be re-entered.

Subroutine name: REFSORT

Called from: SORTSTA (II-C-1), SORTSET (II-D-1)

Programs: STDMAN (II-C), CMSORT (II-D-1)

II-C-1-d SORT BY LATITUDE AND LONGITUDE (fig. 5)

DATA TYPE: S, C

(II-B)

SORT OPTION: 4

(II-C-1, II-D-1)

This routine sets up latitude and longitude boundaries for sorting and map drawing. Latitudes and longitudes are entered as decimal degrees, with latitude positive north and longitude positive west.

R2D2 prints....

ENTER: LAT1, LAT2, LON1, LON2?

LAT1, LAT2 are the latitude boundaries and LON1, LON2 are the longitude boundaries. After the user enters the latitudes and longitudes R2D2 prints out the boundaries and asks for an OK.

Subroutine name: AREA

Called from: SORTSTA (II-C-1), SORTSET (II-D-1), MCHART (II-F-1)

Programs: STDMAIN (II-C), CMSORT (II-D-1), CMLook (II-D-2)

II-C-1-e SORT BY TIME PERIOD (fig. 5)

DATA TYPE: S,C (II-B)

SORT OPTION: 5,6 (II-C-1, II-D-1)

This routine sets up the parameters for sorting by time period. The time period may be entered either as a year-julian day-time word (option 5) or as year, month, day (option 6). In option 5 the time word is a nine digit integer in the form

YYDDDHMM

where YY is the year, DDD is Julian date, HH is hour (GMT) and MM the minute.

In option 6 the date is entered as YEAR, MON, DAY, where MON is the number of the month (i.e. 3 = March) and DAY is the day of the month. These are then converted to the YYDDDHMM form for sorting.

If 0 is entered for the year, the year will be disregarded in sorting. This is useful for selecting all records of a particular season, for example.

Subroutine name: TIMSORT

Called from: SORTSTA (II-C-1), SORTSET (II-D-1)

Programs: STDMAIN (II-C), CMSORT (II-D-1)

II-C-1-f Sort by Depth Range (fig 5)

DATA TYPE: S,C

(II-B)

SORT OPTION: 7

(II-C-1, II-D-1)

This option is used to sort on the basis of station depth. A range of depths from D1 to D2 is specified, where D1 is the upper depth and D2 the lower. Records are selected whose depth D fall within the range $D1 \leq D \leq D2$.

Subroutine name: DEPSORT

Called from: SORTSTA(II-C-1), SORTSET(II-D-1)

Programs: STDMAIN (II-C), CMSORT (II-D-1)

II-C-1-g SORT BY CRUISE NAME (fig. 5)

DATA TYPE: S (II-B)

SORT OPTION: 8 (II-C-1)

This option is used to select STD records on the basis of cruise name. The cruise name must be entered exactly as it appears in the header field. If the exact name isn't known, option 1 (II-C-1-a) may be used to obtain a summary list by cruise name.

Subroutine name: CRUSORT

Called from: SORTSTA (II-C-1)

Program: STDMAIN (II-C)

II-C-1-h LIST STATIONS SELECTED (fig. 6)

DATA TYPE: S (II-B)
SORT OPTION: 0 (II-C-1)
WHAT WOULD YOU LIKE TO DO? 1 (II-C-1)

This option lists the header information of the selected records. Information listed includes reference numbers, cruise name, cast number, station name, latitude, longitude, time, depth and master reference number. If more than 10 records have been selected, R2D2 prints.

YOU HAVE (n) STATIONS
DO YOU WANT TO PRINT ALL OF THEM?

If the answer is no...

TYPE IN THE NUMBERS I,J,K TO LIST EVERY KTH STATION FROM I THRU J

Then a subset of the records will be printed. For example, if 100 have been selected, and I,J,K is entered as 30,50,5, the records 30,35,40,45,50 will be printed on the terminal. All 100 will be written on TAPE6.

Subroutine: IJK
Called from: SORTSTA (II-C-1)
Program: STDMAIN (II-C)

WHAT WOULD YOU LIKE TO DO ? 1
 YOU HAVE 56 STATIONS.
 DO YOU WANT TO PRINT ALL OF THEM? N
 TYPE IN NUMBERS I, J, K TO LIST EVERY K-TH STATION
 FROM I THRU J
 ? 1,56,5

REF	CRUISE	CAST	STA	LAT	LONG	DATE	DEP	MREF
44	RP4SU80AL4	44	NA-18	57.04	159.83	802360546	59.	2719
32	RP4SU80AL4	32	NA-8	57.67	158.50	802350836	38.	2707
37	RP4SU80AL4	37	NA-15	57.20	158.94	802351915	43.	2712
42	RP4SU80AL4	42	NA-17	57.19	160.01	802360307	60.	2717
47	RP4SU80AL4	47	NA-21	56.80	159.57	802360956	39.	2722
52	RP4SU80AL4	53	NA-23	56.82	160.48	802361938	65.	2727
57	RP4SU80AL4	58	NA-32	56.34	160.55	802370325	41.	2732
62	RP4SU80AL4	63	NA-38	56.22	160.93	802370922	35.	2737
67	RP4SU80AL4	68	NA-41	56.46	161.72	802371740	96.	2742
72	RP4SU80AL4	73	NA-45	56.09	161.35	802372257	35.	2747
77	RP4SU80AL4	78	NA-49	55.97	162.19	802380616	62.	2752
82	RP4SU80AL4	83	NA-40	56.05	160.75	802382326	17.	2757

WHAT WOULD YOU LIKE TO DO ?

Fig. 6. List of hydrographic stations selected.

II-C-1-i PLOT STATIONS SELECTED (fig. 7)

DATA TYPE: S (II-B)
SORT OPTION: 0 (II-C-1)
WHAT WOULD YOU LIKE TO DO? 2 (II-C-1)

This option plots the locations of the selected stations on a mercator chart. There are four plot options...

ENTER: 1 FOR STATION REFERENCE NUMBERS
2 FOR SHIP-ASSIGNED CAST NUMBERS
3 FOR STATION NAMES
4 FOR LOCATIONS ONLY

After the plot option is entered R2D2 either asks for the map boundaries (see II-C-1-d) or prints out the already entered boundaries and asks if they are OK. If necessary a new mercator chart is computed (see II-F-1). Stations not within the map boundaries are not plotted. Stations which would plot within 0.05 inch of the previously plotted station also are not plotted.

Subroutines: GETSTA, CHARTEM
Called from: SORTSTA (II-C-1)
Program: STDMAIN (II-C)

WHAT WOULD YOU LIKE TO DO ? 2
 PLOT OPTION ? 1
 YOUR PRESENT MAP BOUNDARIES ARE:
 LATITUDES 55.00 TO 59.00
 LONGITUDES 156.00 TO 163.00
 IS THIS OK? Y
 WHICH MAP FILE? 2
 ENTER SCALE, ATLAT, TIC, YLEN
 ? 0,0,0.25,6
 SCALE = 2926296. AT LATITUDE 57.000
 TIC MARKS EVERY .25 DEGREE
 CHART HEIGHT = 6.00, LENGTH = 5.72
 IS THIS OK? Y
 ARE YOU USING A TEKTRONIX TERMINAL? Y
 ENTER BAUD RATE ? 1200
 DO YOU WANT TO PLOT THIS ON YOUR TERMINAL ? Y

SCALE 2926296
 AT LAT. 57.000

STATION REF NOS.
 00AUG 22 TO 00AUG 24

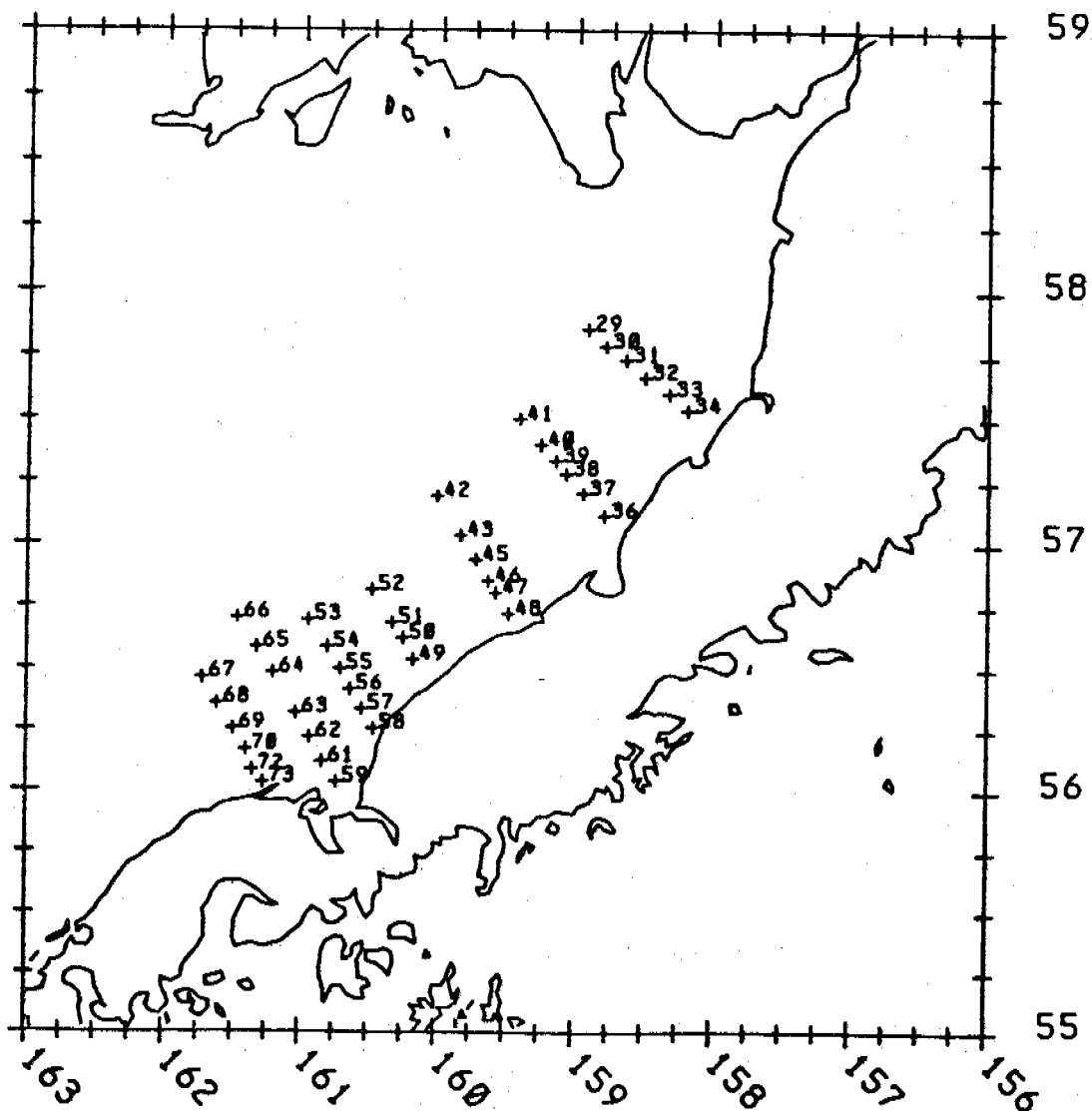


Fig. 7. Plot of hydrographic stations selected.

II-C-2 WRITE SELECTED STATIONS FROM MASTER FILE TO PF

DATA TYPE: S, C (II-B)
SORT OPTION: 0 (II-C-1, II-D-1)
WHAT WOULD YOU LIKE TO DO? 5 (II-C-1, II-D-1)

This option is used to create a submit file which will write records from a Master Data File to a User Data File. The user first sorts one of the Master Header Files to obtain the desired records. If a Master Header File has not been used for sorting execution will terminate.

If all goes well, R2D2 will ask for user and charge numbers for the submit file...

USER,?

Enter user number, password under which the submit job will run, but not the word "USER". The User Data File will then be stored under that user number.

CHARGE,?

Similarly enter the charge number, but not the word "CHARGE".

ENTER PERMANENT FILE NAME?

This is the name of the direct access User Data File, one to seven characters.

The submit file is written on local file TAPE99. Upon completion of this routine, program execution stops and R2D2 REPLACE's TAPE5(the file containing the list of selected stations) as R2LIST, and then SUBMIT's TAPE99. The job name will be printed. Since the Master Data File resides on a private disk

pack which usually must be mounted, the job will take a few minutes or more to run. The user may check job status by entering...

STATUS,JN.

Upon completion, job output is REPLACE'd, again under the permanent file name R2LIST. This file may be examined by typing in...

GET,R2LIST

LNH,F=R2LIST

If all went well there will be a list of records selected followed by the dayfile. If the job did not run, the user and charge numbers may have been incorrectly entered, or the permanent file name may have already existed.

Subroutine: WRITFIL

Called from: SORTSTA (II-C-1), CMSORT (II-D-1)

Program: STDMAIN (II-C), CMSORT (II-D-1)

II-C-3 LOOK AT DATA FOR STATION SELECTED

DATA TYPE: S (II-B)
SORT OPTION: 0 (II-C-1)
WHAT WOULD YOU LIKE TO DO? 6 (II-C-1)

Selection of this option gives access to the STD data analysis and display section of R2D2. A User Data File must have been attached and sorted. If this option is attempted with a Master Header File,

MASTER FILES DO NOT CONTAIN DATA.

WHAT WOULD YOU LIKE TO DO?

will be printed.

Otherwise, R2D2 will print....

TYPE OF DATA OUTPUT?

The options available are.....

0 END R2D2 SESSION (II-E)
1 DATA LISTINGS (II-C-3-a)
2 AREA DISTRIBUTIONS (II-C-3-b)
3 PROFILES (II-C-3-c)
4 TIME SERIES PROFILES (II-C-3-d)
5 T-S DIAGRAMS (II-C-3-e)
6 TRANSECTIONS (II-C-3-f)
99 RESORT, LIST, PLOT, ETC.

Option 0 terminates the R2D2 session. Option 99 returns to the SORTSTA subroutine at the point of "WHAT WOULD YOU LIKE TO DO?" (see II-C-1)

The other options are discussed in the following sections.

Subroutine: DATLOOK

Program: STDMAIN (II-C)

II-C-3-a DATA LISTINGS (fig. 8)

DATA TYPE S (II-B)
SORT OPTION: 0 (II-C-1)
WHAT WOULD YOU LIKE TO DO? 6 (II-C-1)
TYPE OF DATA OUTPUT: 1 (II-C-3)

This option provides a full or abbreviated listing of the 1 m average temperature, salinity, sigma-t and dynamic height of each record selected.

The program asks...

DO YOU WANT TO PRINT ON YOUR TERMINAL?
and then....

ENTER 0 FOR NONE
1 FOR COMPLETE LIST
2 FOR SHORT LIST

The short list prints every meter for depths 0-100 m, every 5 m for 100-500 m and every 25 m for over 500 m depth. Since 4 depths are printed on each line of TAPE6, a 1500m cast will be printed on one standard computer page using the short list, or 7 pages using the complete list.

If the uppermost depth Z_0 of the cast is not at 0 m, temperature and salinity will be extrapolated to 0 m by assuming that T and S above Z_0 are equal to T and S at Z_0 . Extrapolated values are denoted by an *.

Subroutine: DATLIST
Called from: DATLOOK (II-C-3)
Program: STDMAIN (II-C)

TYPE OF DATA OUTPUT ? 1
 DO YOU WANT TO PRINT ON YOUR TERMINAL ? Y
 ENTER 1 FOR COMPLETE LIST, 2 FOR SHORT LIST, 0 FOR NONE
 ? 1
 ENTER MAXIMUM DEPTH, OR -2 FOR BOTTOM
 ? 40

REF	CRUISE	CAST	STA	LAT,N	LOH,W	DATE	DEP	MREF	PG
45	RP4SU80AL4	45	NA-19	56.94	159.72	002360710	44	2720	1
DEP	TEMP	SAL	SIGT	DYN M	DEP	TEMP	SAL	SIGT	DYN M
0	9.49	31.49	24.32	0.000	1	9.49	31.49	24.32	.004
2	9.49	31.49	24.32	.007	3	9.49	31.49	24.32	.011
4	9.49	31.49	24.32	.014	5	9.49	31.49	24.32	.018
6	9.49	31.49	24.32	.022	7	9.49	31.49	24.32	.025
8	9.48	31.48	24.32	.029	9	9.48	31.49	24.32	.033
10	9.47	31.48	24.31	.036	11	9.46	31.49	24.33	.040
12	9.46	31.49	24.33	.043	13	9.47	31.49	24.32	.047
14	9.45	31.49	24.32	.051	15	9.43	31.48	24.32	.054
16	9.41	31.48	24.33	.058	17	9.38	31.45	24.32	.061
18	9.22	31.48	24.36	.065	19	9.08	31.45	24.35	.069
20	8.98	31.47	24.39	.072	21	8.80	31.47	24.41	.076
22	8.65	31.45	24.41	.079	23	8.55	31.52	24.49	.083
24	8.53	31.53	24.50	.086	25	8.51	31.52	24.50	.090
26	8.48	31.53	24.51	.093	27	8.47	31.53	24.51	.097
28	8.46	31.53	24.51	.100	29	8.45	31.53	24.51	.103
30	8.43	31.53	24.51	.107	31	8.43	31.53	24.51	.110
32	8.38	31.52	24.51	.114	33	8.35	31.53	24.53	.117
34	8.34	31.54	24.53	.121	35	8.33	31.54	24.53	.124
36	8.32	31.53	24.53	.127	37	8.30	31.54	24.54	.131
38	8.30	31.55	24.55	.134	39	8.30	31.54	24.54	.138
40	8.28	31.54	24.54	.141					

TYPE OF DATA OUTPUT ?

Fig. 8. Hydrographic data listing.

II-C-3-b AREA DISTRIBUTIONS (figs. 9, 10)

DATA TYPE: S (II-B)
SORT OPTION: 0 (II-C-1)
WHAT WOULD YOU LIKE TO DO?: 6 (II-C-1)
TYPE OF DATA OUTPUT: 2 (II-C-3)

This option lists and plots various parameters of the selected stations.

The options are ...

- 0 TO ESCAPE
- 1 TEMPERATURE AT DEPTH D
- 2 SALINITY AT DEPTH D
- 3 SIGMA-T AT DEPTH D
- 4 TEMP DIFFERENCE BETWEEN DEPTHS D1 & D2
- 5 SALIN DIFFERENCE BETWEEN D1 & D2
- 6 SIGMA-T DIFFERENCE BETWEEN D1 & D2
- 7 TEMP AVERAGE BETWEEN D1 & D2
- 8 SALIN AVERAGE BETWEEN D1 & D2
- 9 SIGMA-T AVERAGE BETWEEN D1 & D2
- 10 DYNAMIC HEIGHT BETWEEN D1 & D2
- 11 DEPTH OF A SIGMA-T SURFACE
- 12 TEMPERATURE OF A SIGMA-T SURFACE
- 13 SALINITY OF A SIGMA-T SURFACE
- 14 MIXED LAYER DEPTH (MLD)

Options 1-3 require entry of depth D, and options 4-10 require upper depth D1 and lower depth D2. A -1 entered for a depth means the topmost

depth of the cast and -2 means deepest depth. Options 11-13 require entry of a sigma-t value of the isopycnal.

If option 14 is selected, the user must enter...

- 1 FOR MLD DEFINED BY SIGMA-T DIF, TOP TO DEP
- 2 FOR MLD DEFINED BY SIGMA-T GRADIENT PER M
- 3 FOR MLD DEFINED BY TEMP DIF, TOP TO DEP

That is, 1 gives the depth D at which σ_t exceeds σ_t at the surface by a given amount, 2 gives the depth D at which σ_t exceeds σ_t at D-1 by a given amount, and 3 gives the depth D at which the temperature exceeds the surface temperature by a given amount.

Once the option number and required input have been entered, R2D2 asks for verification.

If option = 10 and D1 = -1 the user has the choice of whether or not to extrapolate to the surface if the actual topmost depth is greater than 0. Extrapolated values are indicated by a *, and are computed by assuming that the temperature and salinity values above the topmost depth are equal to those at the topmost depth.

Finally, the user has the option of whether or not to print on the terminal (see II-C-1-h), and then R2D2 proceeds to compute the requested parameter for each station, as well as the mean and standard deviation for the entire set. The station parameters may then be plotted on a chart if desired, as described in II-C-1-i.

Subroutine: DEPDATA

Called from: DATLOOK (II-C-3)

Program: STDMAIN (II-C)

TYPE OF DATA OUTPUT ? 2
ENTER OPTION? 1
ENTER DEPTH D ? -1

YOU HAVE SELECTED TEMP AT SURFACE
IS THIS OK? Y
DO YOU WANT TO PRINT ON YOUR TERMINAL ? Y
YOU HAVE 45 STATIONS.
DO YOU WANT TO PRINT ALL OF THEM? N
TYPE IN NUMBERS I, J, K TO LIST EVERY K-TH STATION
FROM I THRU J
? 1,45,5

REF.	CRUISE	STA.	TEMP AT	SURFACE
29	RP4SU88AL4	NA-5	11.08	0.
34	RP4SU88AL4	NA-10	10.89	0.
39	RP4SU88AL4	NA-13	9.59	0.
44	RP4SU88AL4	NA-18	8.49	0.
49	RP4SU88AL4	NA-26	10.11	0.
54	RP4SU88AL4	NA-29	9.27	0.
59	RP4SU88AL4	NA-40	10.68	0.
64	RP4SU88AL4	NA-35	8.98	0.
69	RP4SU88AL4	NA-43	9.56	0.

MEAN = 9.89 STANDARD DEVIATION = .86
DONE
DO YOU WANT A PLOT?

Fig. 9. Hydrographic data distributions: printout.

SCALE 2926296
AT LAT. 57.000

TEMP AT SURFACE
80AUG 22 TO 80AUG 24

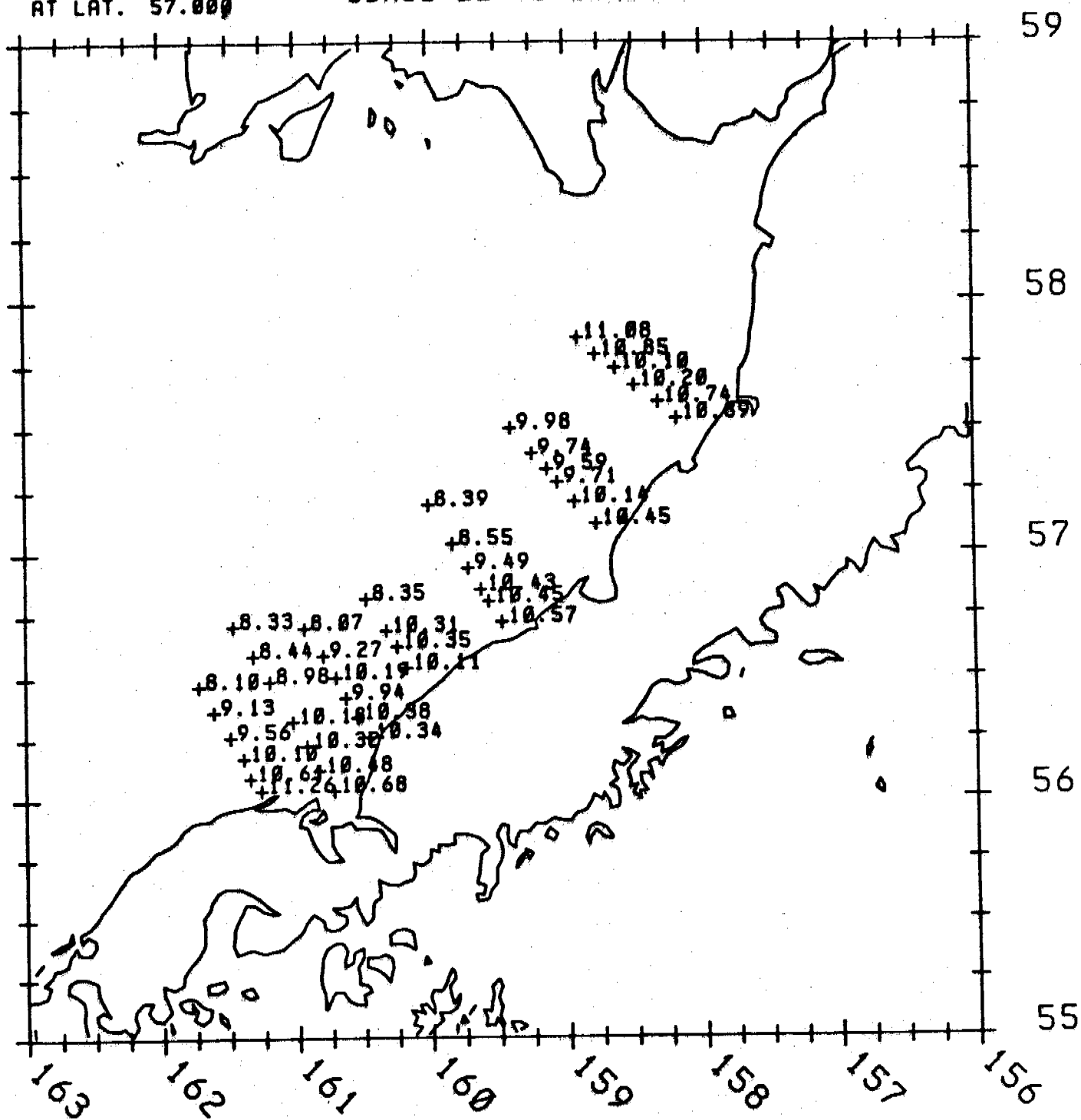


Fig. 10. Hydrographic data distributions: plot.

II-C-3-c PROFILES (fig. 11)

DATA TYPE: S (II-B)
SORT OPTION: 0 (II-C-1)
WHAT DO YOU WANT TO DO? 6 (II-C-1)
TYPE OF DATA OUTPUT: 3 (II-C-3)

This option plots temperature, salinity and sigma-t versus depth, or Brunt-Väisälä frequency (N) versus depth. If more than 2 records have been selected, R2D2 prints...

YOU HAVE (n) STATIONS, DO YOU WANT TO DO THEM ALL?

If the answer is no, the program returns to the main subroutine (II-C-3).
Otherwise it continues...

PROFILE TYPE, MAXIMUM DEPTH?

Profile type 1 gives the T, S, σ_t vs depth plot and type 2 gives N vs depth. Maximum depth is the maximum depth, in meters, to which the cast will be plotted. Enter a -2 for actual cast depth. The plot will be scaled to depths of 40, 80, 200, 400, 800, 1600, 3200 or 6400 meters, whichever is greater than or equal to the entered depth.

The Brunt-Väisälä frequency in cycles per hour is calculated from

$$N = \left(\frac{g}{\rho_0} \frac{\delta \rho}{\delta z} \right)^{\frac{1}{2}}$$

where $g = \text{gravity} = 980 \text{ cm s}^{-2}$

ρ_0 reference density = 1.026 gm cm^{-3}

$\frac{\delta\rho}{\delta z}$ = the density gradient at depth z , estimated from a least square fit of σ_t over $z \pm 5 \text{ m}$. The sign of N depends on the sign of $\frac{\delta\rho}{\delta z}$. In the program the algorithm is

$$N \cong \left(\frac{g}{\rho_0} \frac{\Delta\sigma_t/1000}{100\text{cm}} \right)^{\frac{1}{2}} \frac{3600}{2\pi} = 56 (\Delta\sigma_t)^{\frac{1}{2}} \text{ cph.}$$

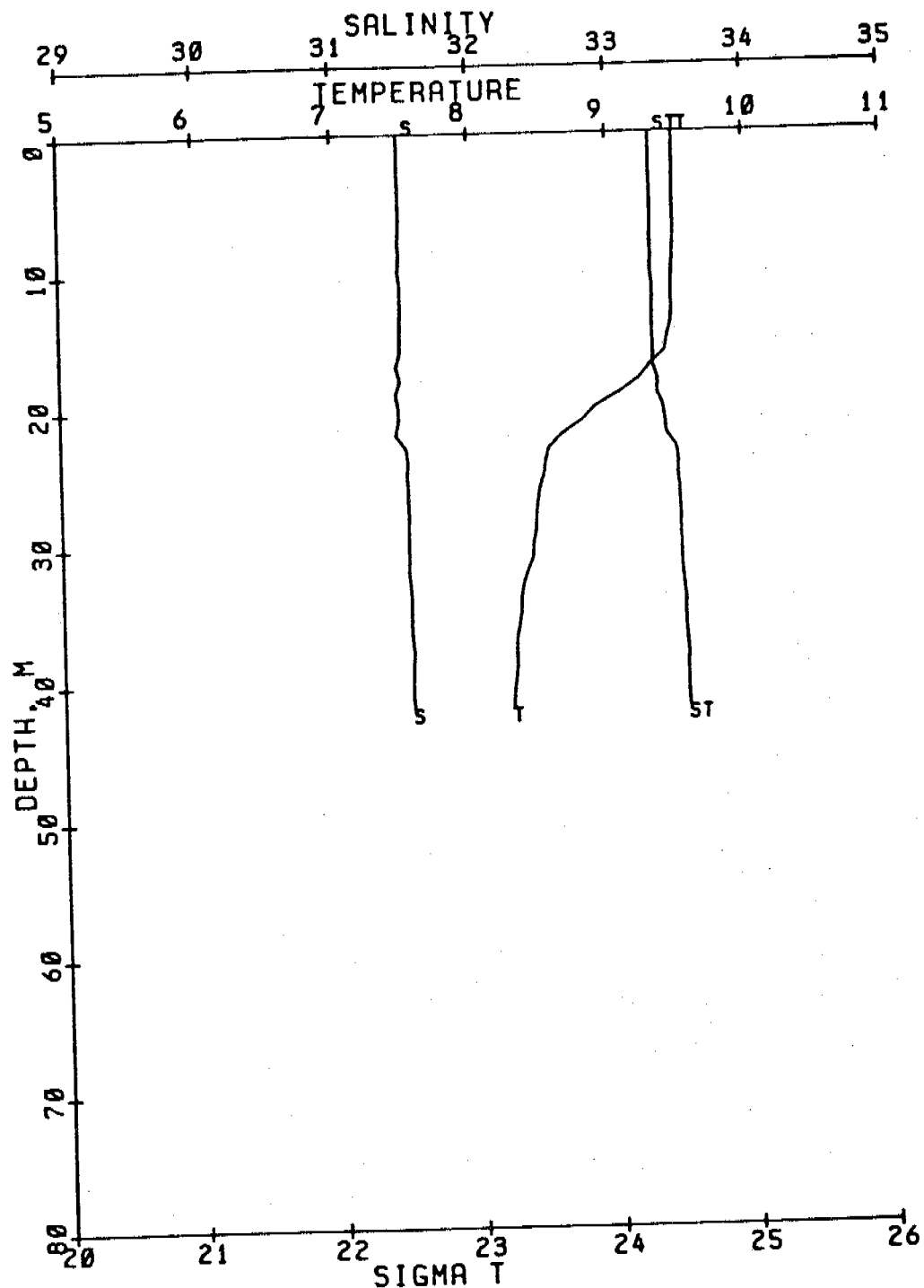
where $\Delta\sigma_t$ is the slope of the least square fit.

Subroutine: PROFILE

Called from: DATLOOK (II-C-3)

Program: STDMAIN (II-C)

TYPE OF DATA OUTPUT ? 3
 PROFILE TYPE, MAXIMUM DEPTH ? 1,-2
 DO YOU WANT TO PLOT THIS ON YOUR TERMINAL ?



REF. NO. 45 2720 STA. NA-19 56.94 N
 TIME = 802360710 RP4SU80AL4-45 159.72 W

Figure 11. Hydrographic data profile.

II-C-3-d TIME SERIES PROFILES (fig. 12)

DATA TYPE: 5 (II-B)
SORT OPTION: 0 (II-C-1)
WHAT DO YOU WANT TO DO? 6 (II-C-1)
TYPE OF DATA OUTPUT: 4 (II-C-3)

This option plots temperature, salinity, density or Brunt-Väisälä frequency of one or more records on a single plot. This is especially useful for time series stations, i.e. several casts at the same location. Plots may be on top of each other or separated by a specified offset. R2D2 will ask...

PARAMETER, PLOT HEIGHT, DEPTH SCALE, OFFSET?

where

PARAMETER = 1 FOR TEMPERATURE
 2 FOR SALINITY
 3 FOR SIGMA-T
 4 FOR BRUNT-VAISALA FREQUENCY

PLOT HEIGHT = DEPTH AXIS IN INCHES

DEPTH SCALE = METERS/INCH

OFFSET = INCHES BETWEEN PROFILES

Total depth = plot height x depth scale. For parameters 1, 2 and 3, one inch offset = one unit. For parameter 4, one inch offset = 10 cph. (see II-C-3-c for description of the Brunt-Väisälä frequency algorithm.)

Subroutine: PROFILS

Called from: DATLOOK (II-C-3)

Program: STDMAIN (II-C)

TYPE OF DATA OUTPUT ? 4
 PARAMETER, PLOT HEIGHT, DEPTH SCALE, OFFSET ? 1,6,10,.5
 YOU HAVE SELECTED TEMP., C PROFILES FOR 6 STATIONS
 PLOT HEIGHT = 6. INCHES, LENGTH = 9.
 MAXIMUM DEPTH = 60. METERS
 OFFSET = .50 INCHES
 IS THIS OK? Y
 DO YOU WANT TO PLOT THIS ON YOUR TERMINAL ?

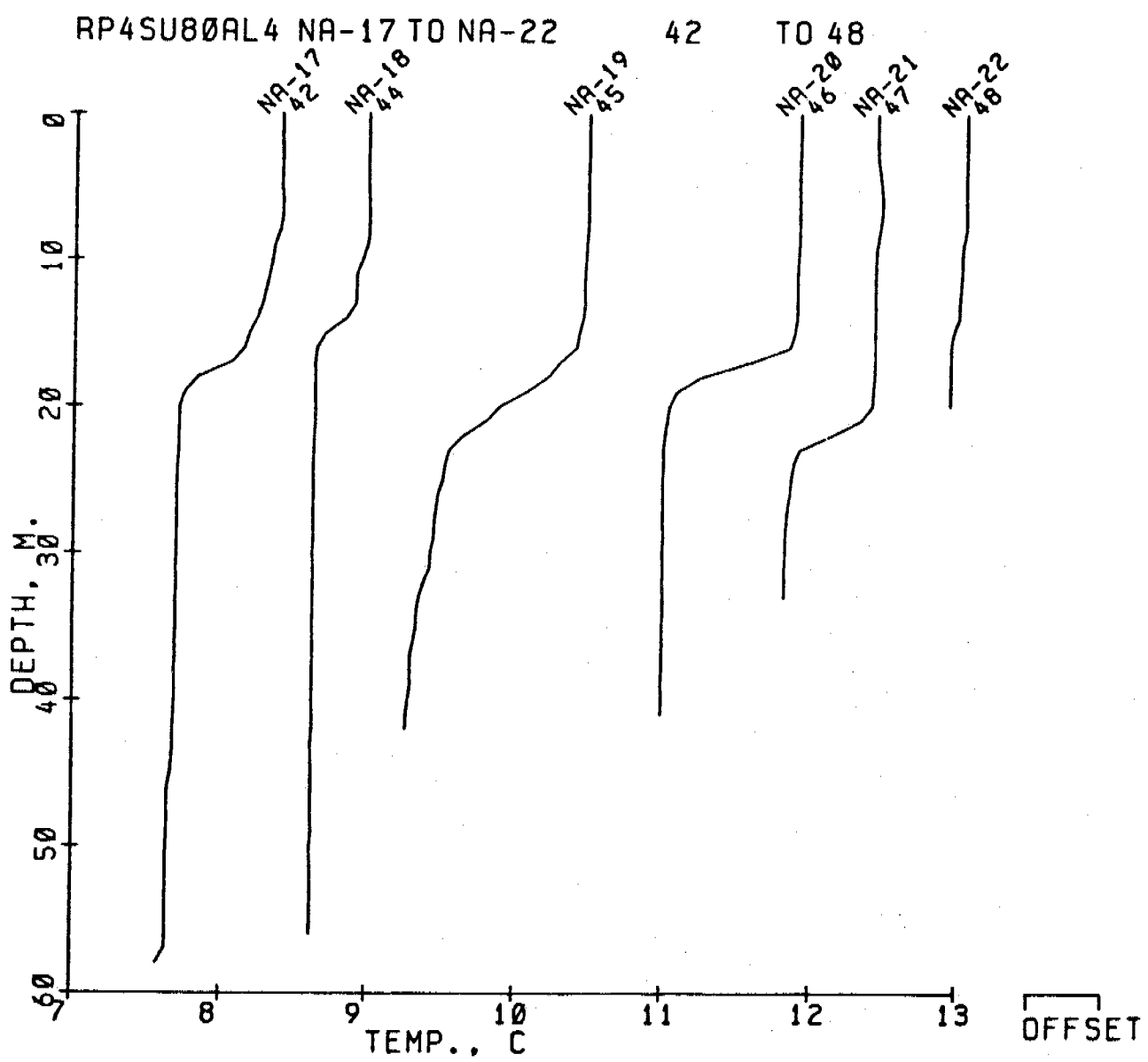


Fig. 12. Hydrographic data time series profile.

II-C-3-e T-S DIAGRAMS (fig. 13)

DATA TYPE: S (II-B)
SORT OPTION: 0 (II-C-1)
WHAT WOULD YOU LIKE TO DO? 6 (II-C-1)
TYPE OF DATA OUTPUT: 5 (II-C-3)

T-S diagrams are plots of temperature vs. salinity, with lines of equal density superimposed. Options available include: all stations on the same plot or each on a different plot; variable temperature and salinity scales; depth ticks; and variable maximum depth. The routine will begin...

ENTER 0 TO ESCAPE

1 FOR ALL ON THE SAME PLOT

2 FOR INDIVIDUAL PLOTS

and then...

DO YOU WANT THE DEFAULT TS DIAGRAM?

The default is a 9" (temperature axis, -2°C to 16°C) x 6" (salinity axis, 24 ‰ to 36 ‰), to the deepest depth with no tick marks. If the default is not desired, R2D2 continues...

ENTER: TMIN, DT, TLEN, SMIN, DS, SLEN, DMAX, TICKS

where...

TMIN = MINIMUM TEMP
DT = DEGREES/INCH ON PLOT
TLEN = LENGTH OF TEMP AXIS, INCHES
SMIN = MINIMUM SALINITY
DS = PPT/INCH ON PLOT
SLEN = LENGTH OF SALINITY AXIS, INCHES
DMAX = MAXIMUM DEPTH (-2 GIVES BOTTOM)
TICKS = INTERVAL (METERS) OF DEPTH TICKS
(TICKS = 0 MEANS NO TICKS)

After asking for an OK on the input parameters, the plots are computed.
A * indicates that the plot would have continued outside the plot boundaries.

Subroutine: TS

Called from: DATLOOK (II-C-3)

Program: STDMAIN (II-C)

```

TYPE OF DATA OUTPUT ? 5
YOU HAVE 6 STATIONS
ENTER 0 TO ESCAPE
    1 FOR ALL ON THE SAME PLOT
    2 FOR INDIVIDUAL PLOTS
? 2
DO YOU WANT THE DEFAULT TS DIAGRAM? N
ENTER: THIN,DT,TLEN,SMIN,DS,SLEN,DMAX,TICK
? 7,.5,6,30,.5,6,-2,0
TEMP RANGE IS 7.0 TO 10.0
SALIN RANGE IS 30.0 TO 33.0
ON A 6.0 BY 6.0 INCH PLOT
MAXIMUM DEPTH = -2.
NO DEPTH TICKS
IS THIS OK? Y
STATION 42
DO YOU WANT TO PLOT THIS ON YOUR TERMINAL ?

```

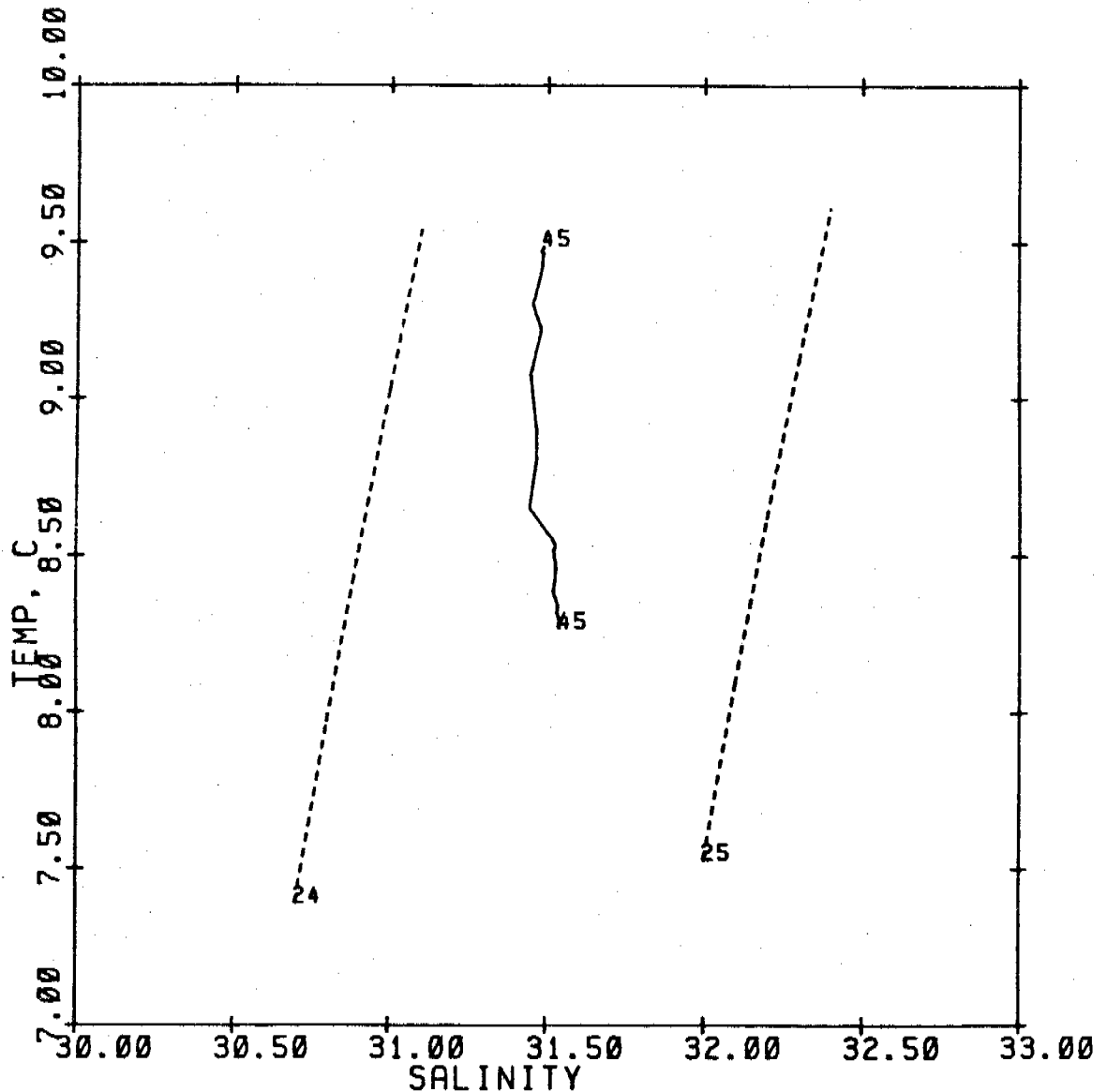


Fig. 13. Hydrographic data temperature-salinity diagram.

II-C-3-f TRANSECTIONS (fig. 14)

DATA TYPE: S	(II-B)
SORT OPTION: 0	(II-C-1)
WHAT WOULD YOU LIKE TO DO? 6	(II-C-1)
TYPE OF DATA OUTPUT: 6	(II-C-3)

This option plots vertical sections of temperature, salinity or sigma-t for a selected line of stations. After selecting the parameter to plot, R2D2 prints...

ENTER PLOT HEIGHT, LENGTH (IN INCHES), SCALE, DEPTH INTERVAL (METERS/INCH ON Y AXIS), AND DATA CONTOUR INTERVAL

NOTE: IF SCALE IS 0, SCALE IS COMPUTED FROM LENGTH
IF SCALE IS GIVEN, LENGTH IS COMPUTED FROM SCALE.

The station spacing is determined by the distance between individual stations, so a crooked line is in effect straightened out. The deepest depth plotted is the product of plot height and depth interval, i.e. a plot height of 6 and a depth interval of 20 gives a total depth of 120 m. Scale is the ratio of real distance to plot distance, so that a scale of 100,000 means 1 cm = 1 km. The data contour interval is the interval at which values will be plotted for contouring. For example, if the data contour interval is 0.1, an annotation will be made at whatever depth the parameter increases or decreases by 0.1. Surface and bottom values are also plotted, and a *

is plotted at the station bottom depth. When reversals are encountered, i.e., the same value as before is found, a tick mark is made but the value number is not plotted. Parameter values and depths are also written on TAPE6.

Subroutine: SECTION

Called from: DATLOOK (II-C-3)

Program: STDMAIN (II-C)

TYPE OF DATA OUTPUT ? 6
 ENTER: 1 FOR TEMP, 2 FOR SALINITY, 3 FOR SIGMA T
 OR 0 TO ESCAPE
 ? 1
 ENTER PLOT HEIGHT, LENGTH (IN INCHES), SCALE,
 DEPTH INTERVAL (METERS/INCH ON Y AXIS),
 AND DATA CONTOUR INTERVAL
 NOTE: IF SCALE IS 0, SCALE IS COMPUTED FROM LENGTH.
 IF SCALE IS GIVEN, LENGTH IS COMPUTED FROM SCALE
 ? 6, 6, 0, 10, .5
 YOU HAVE 6 STATIONS ON A 6.0° HIGH
 BY 6.0° LONG PLOT; MAXIMUM DEPTH IS 60.M
 TEMP CONTOUR INTERVAL IS .50
 SCALE = 489198.
 IS THIS OK? Y

42 DEPTH TEMP
 0.0 8.39 17.5 8.00
 44 DEPTH TEMP
 0.0 8.49
 45 DEPTH TEMP
 0.0 9.49 19.5 9.00 25.5 8.50
 46 DEPTH TEMP
 0.0 10.43 17.5 10.00 38.5 9.50 39.5 9.50 40.5 9.50
 47 DEPTH TEMP
 0.0 10.45 22.5 10.00
 48 DEPTH TEMP
 0.0 10.57 14.5 10.50
 DO YOU WANT TO PLOT THIS ON YOUR TERMINAL ?

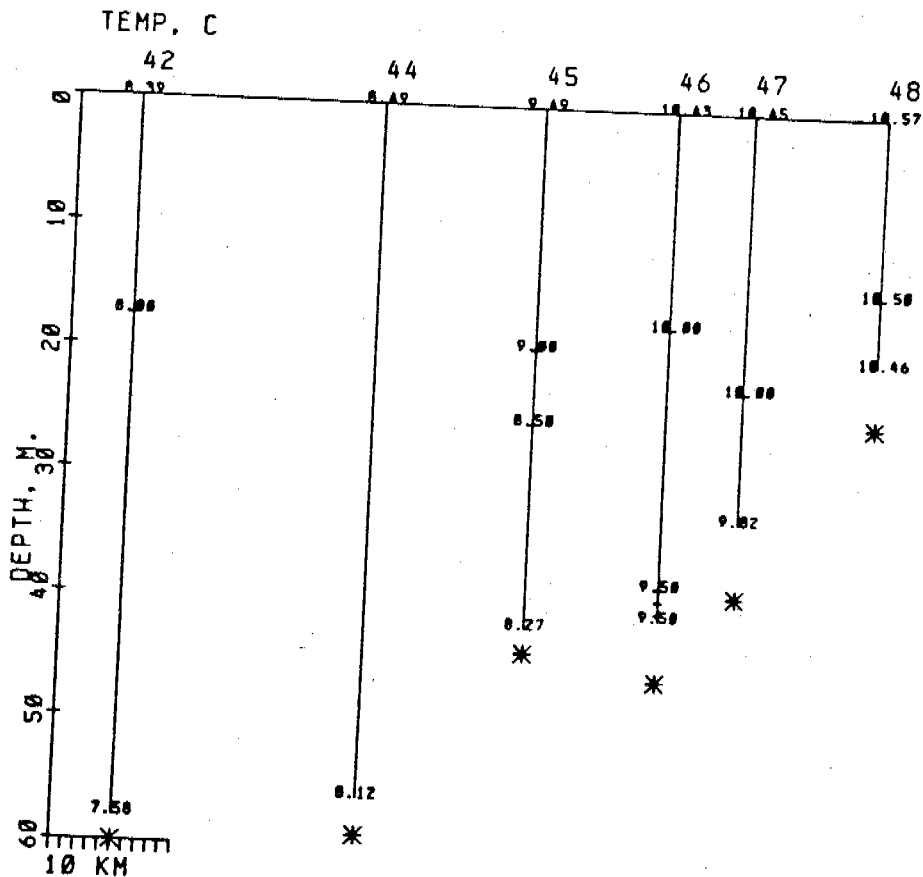


Fig. 14. Hydrographic data transection.

II-D The current meter/pressure gauge programs

The current meter/pressure gauge data analysis and display package consists of three main programs: CMSORT, which does the sorting, listing and plotting of the header information; CMLOOK, which contains routines for data listing, statistics, time series plots, progressive vector diagrams, scatter diagrams, histograms, current roses, summary current vector plots, correlations and empirical orthogonal functions; and SPECT, which does auto- and cross-, scalar and rotary, spectral analysis, and 29-day harmonic tide analysis. Program CMSORT corresponds to subroutine SORTSTA in STDMAIN, and CMLOOK and SPECT correspond to subroutine DATLOOK. The current meter routines have been divided into three separate programs because of the greater amount of central memory required by larger arrays and more subroutines. Control registers set from within the programs allow the procedure file to transfer between the three programs.

II-D-1 Sorting current meter/pressure gauge files

DATA TYPE: C

(II-B)

This program does the sorting, listing and plotting of the header information of the current meter/pressure gauge files. It also transfers control to CMLOOK and SPECT.

After selecting data type C and attaching the appropriate file (see R2START, II-B), CMSORT begins by asking...

ENTER SORT OPTION?

The options are...

- 99 = CLEAR PREVIOUS OPTIONS
- 1 = LIST OPTIONS CURRENTLY SELECTED
- 0 = END ENTERING OPTIONS AND SORT
- 1 = SUMMARY LISTING OF HEADER FILE (II-D-1-a)
- 2 = GET INDIVIDUAL RECORDS BY REFERENCE NUMBER (II-C-1-b)
- 3 = SORT BY REFERENCE NUMBER RANGE (II-C-1-c)
- 4 = SORT BY LATITUDE AND LONGITUDE (II-C-1-d)
- 5 = SORT BY JULIAN DATE (II-C-1-e)
- 6 = SORT BY GREGORIAN DATE (II-C-1-e)
- 7 = SORT BY DEPTH RANGE (II-C-1-f)
- 8 = SORT BY PROJECT NAME (II-D-1-b)
- 9 = SORT BY MOORING NAME (II-D-1-b)
- 10 = SORT BY METER NAME (II-D-1-b)
- 11 = ADD YOUR TAPE4 FILES (II-D-1-c)

Options 3-10 set up keys which are used for sort criteria. These options are described in the referenced sections. Option -99 clears previously set sort keys. Option -1 lists the currently selected keys.

Selection of option 0 ends the entering of sort options and initiates sorting, if any of the sort keys have been set. The number of records which have been selected is printed...

(n) RECORDS HAVE BEEN SELECTED
WHAT DO YOU WANT TO DO?

The options now are...

0	END R2D2 SESSION	(II-E)
1	LIST RECORDS SELECTED	(II-D-1-a)
2	PLOT MOORING LOCATIONS	(II-D-1-d)
3	RESORT	
4	SORT AGAIN, KEEPING STATIONS ALREADY SELECTED	
5	WRITE SELECTED RECORDS FROM MASTER FILE TO PF	(II-C-2)
6	DATA PLOTS, LISTINGS, CORRELATIONS, EOF, ETC	(II-D-2)
7	SPECTRAL, TIDE ANALYSIS	(II-D-3)

Option 3 clears the sort keys and previously selected records, and restarts the sort process. Option 4 also clears the sort keys, but retains the records previously selected.

Options 6 and 7 transfer to the CMLLOOK and SPECT routines respectively. The user may return to this point (WHAT DO YOU WANT TO DO?) by selecting option 99 in those programs. Selection of 6 or 7 is possible only if a Data File or TAPE4 is attached, since Header Files do not contain data.

In the special case when FILE = 0 (II-B), user selection of sort options is skipped, and sort option 11 automatically selected.

Program: CMSORT

II-D-1-a SUMMARY LISTING OF HEADER FILE (fig 15)
or LIST RECORDS SELECTED

DATA TYPE: C (II-B)
SORT OPTION: 1 or 0 (II-D-1)
WHAT DO YOU WANT TO DO? 1 (II-D-1)

This option does a short or complete listing of the header information for either the complete file or the selected records. The short, or summary, list prints on one line per record the reference number, mooring name, meter number, meter depth, start and end times and length of the 2.86 hr filtered data, latitude and longitude, mooring depth and master reference number. The complete list includes the above plus information on the 35 hr filtered data and some statistics (calculated during initial loading of the data, see IV-B-2). It takes 15 lines per record or 4 records per page. R2D2 will print...

ENTER LIST OPTION?

which are...

ENTER 0 TO ESCAPE

1 FOR A SUMMARY LISTING

2 FOR A COMPLETE LISTING

ENTER A NEGATIVE NUMBER TO SUPPRESS TERMINAL LISTING

Subroutine: CMHSUM

Program: CMSORT (II-D-1)

ENTER SORT OPTION ? 1
 ENTER LIST OPTION ? 1

REF	MOORING	METER	DEP	START	END	LEN	LAT	LOM	DEP	MREF
1	UP-1	1811	64	800821400	802292100	3536	54.56	165.40	84.	42
2	UP-2	1827	59	800821000	802291700	3536	54.30	164.76	80.	43
3	UP-3	1815	47	800820400	802291300	3538	54.16	164.01	69.	44
4	TP3A	N99	5	802320500	802461200	344	56.40	161.66	654.	46
5	TP3A	N98	10	802320500	802461200	344	56.40	161.66	654.	47
6	TP3A	N90	15	802320500	802461200	344	56.40	161.66	654.	48
7	TP3A	N89	19	802320500	802461200	344	56.40	161.66	654.	49
8	TP3A	N100	29	802320500	802461200	344	56.40	161.66	654.	50
9	TP3A	N87	39	802320500	802461200	344	56.40	161.66	654.	51
10	TP3A	N88	50	802320500	802461200	344	56.40	161.66	654.	52

ENTER LIST OPTION ? 2

DATA SET 1 UNIMAK PAS UP-1 1811 64 MASTER REF.= 42
 LAT, LONG, BOTDP= 54.56 165.40 84.00

2.86 HR START-STOP, NUMBER OF POINTS= 800821400 - 802292100 3536
 35.0 HR START-STOP, NUMBER OF POINTS= 800850600 - 802270600 569

	TEMPERATURE	PRESSURE	SALINITY	2.86 HR SPD	35.0 HR SPD
MEANS =	4.18	170.21	29.03	35.85	9.18
VARIANCES =	.57	1.32	.07	317.93	48.93
MINIMUMS =	2.76	166.70	28.21		
MAXIMUMS =	6.61	173.65	31.34		
DRIFTS =				5.64 @ 312.0	5.77 @ 311.2

Fig. 15. Summary listing of CM/PG file contents and list of records selected.

II-D-1-b SORT BY PROJECT NAME

" " MOORING NAME

" " METER NUMBER

DATA TYPE: C (II-B)

SORT OPTION: 8,9,10 (II-D-1)

Options 8, 9 and 10 allow sorting by project name, mooring name or meter number, respectively. Up to 5 names may be selected for each option, but they must match exactly those in the headers. If the exact name is unknown, sort option 1 (II-D-1-a) may be used to get a list. To end entering names, type in the word "END". R2D2 will ask for an OK on the entered names before returning.

Subroutine: NAMSORT

Program: CMSORT (II-D-1)

II-D-1-c ADD YOUR TAPE4 FILES

DATA TYPE: C (II-B)

SORT OPTION: 11 (II-D-1)

This option permits the use, in R2D2, of current meter, pressure gauge or wind data which are not in the R2D2 data files. To use this option, TAPE4 must have been made a local file prior to beginning R2D2. There may be any number of records on TAPE4, but only one file. The TAPE4 format is described in II-D-4

Subroutine: SET4

Program: CMLOOK

II-D-1-d PLOT MOORING LOCATIONS (fig 16)

DATA TYPE: C (II-B)
SORT OPTION: 0 (II-D-1)
WHAT DO YOU WANT TO DO? 2 (II-D-1)

This option plots station locations on a mercator chart (II-F-1) with user defined map boundaries (II-C-1-d). Locations are denoted by a *. If the station location is outside the map boundaries it is not plotted.

Subroutine: MORPLT

Program: CMSORT

SCALE 1461066
AT LAT. 54.000

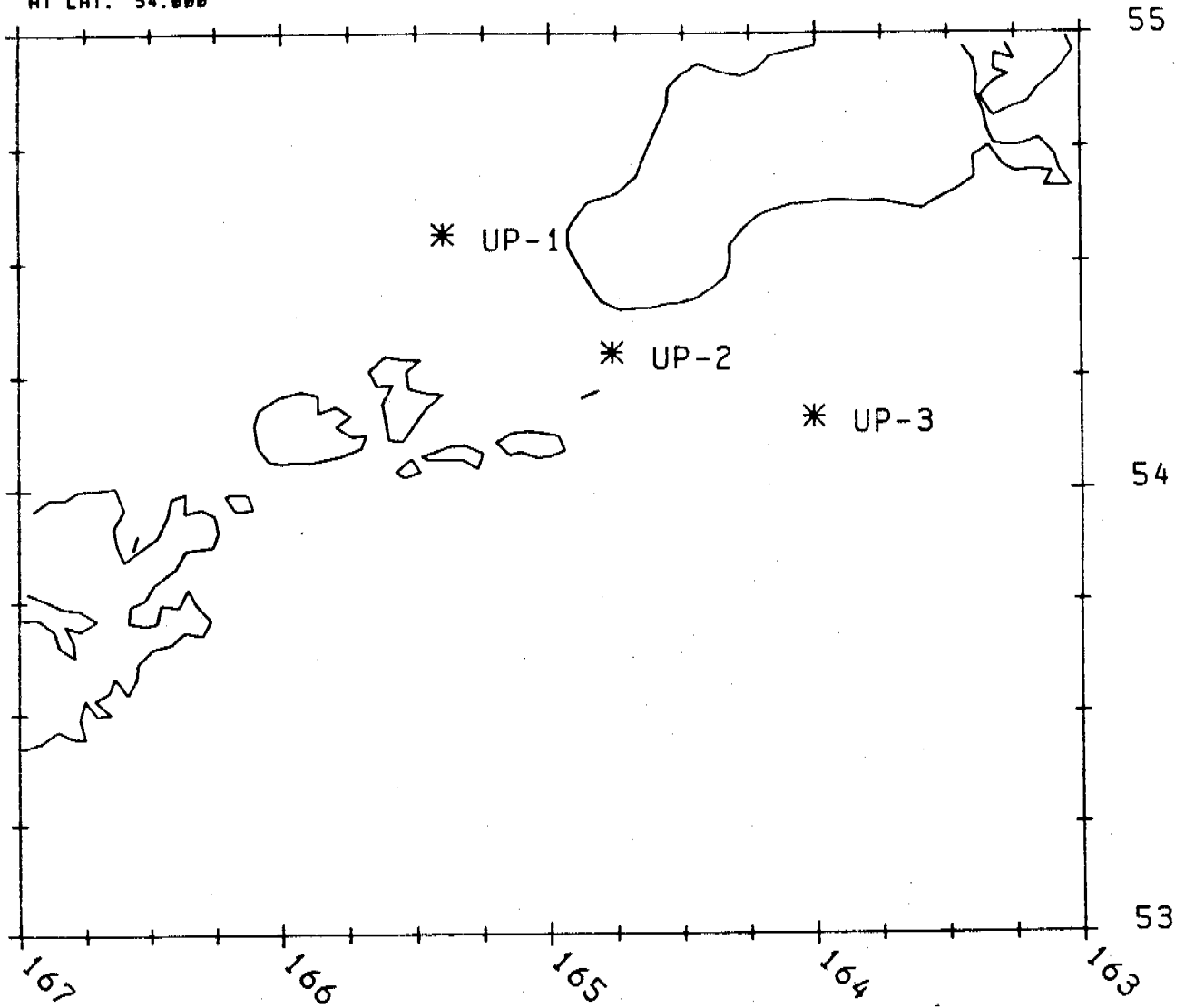


Fig. 16. Plot of CM/PG mooring locations.

II-D-2 DATA PLOTS, LISTINGS, CORRELATIONS, EOF, ETC

DATA TYPE: C (II-B)
SORT OPTION: 0 (II-D-1)
WHAT DO YOU WANT TO DO? 6 (II-D-1)

Selection of option 6 after sorting provides access to the data analysis and display program CMLOOK. A data file must have been sorted. If this option is attempted using a Master Header File, R2D2 will print...

MASTER FILES DO NOT CONTAIN DATA

WHAT DO YOU WANT TO DO?

Otherwise, CMLOOK will begin with...

ENTER DATA OPTION.

and the options are...

0 = END R2D2 (II-E)
1 = DATA LISTINGS (II-D-2-a)
2 = STATISTICS ON DATA SEGMENTS (II-D-2-b)
3 = TIME SERIES PLOTS (ALL PARAMETERS, ONE RECORD) (II-D-2-c)
4 = TIME SERIES PLOTS (ONE PARAMETER, ALL RECORDS) (II-D-2-d)
5 = UV SCATTER DIAGRAMS (II-D-2-e)
6 = PVD PLOTS (II-D-2-f)
7 = HISTOGRAMS (II-D-2-g)

- 8 = CURRENT ROSES (II-D-2-h)
- 9 = SUMMARY CURRENT VECTORS (II-D-2-i)
- 10 = LAGGED LINEAR CORRELATIONS (II-D-2-j)
- 11 = EMPIRICAL ORTHOGONAL FUNCTIONS (EOF) (II-D-2-k)
- 12 = EOF WITH USER SUPPLIED MATRIX (II-D-2-k)
- 13 = WRITE DATA TO TAPE4 (II-D-2-l)
- 99 = RESORT, LIST, PLOT ETC HEADER INFO

Options 1-13 are described in the following sections. After each option is completed, the program returns to "ENTER DATA OPTION". Selection of option 99 returns to CMSORT at "WHAT DO YOU WANT TO DO?" (see II-D-1)

Program: CMLook

II-D-2-a DATA LISTINGS (fig 17)

DATA TYPE: C	(II-8)
SORT OPTION: 0	(II-D-1)
WHAT DO YOU WANT TO DO? 6	(II-D-1)
DATA OPTION: 1	(II-D-2)

After asking for filter type and start and end times (see II-D-2-m) and major axis direction (II-D-2-o), R2D2 will print...

LIST OPTION?

The options are...

0 TO ESCAPE

1 FOR FULL DATA LIST

2 FOR AVERAGES

3 FOR BOTH 1 AND 2

(USE NEGATIVE NUMBER TO SUPPRESS TERMINAL OUTPUT)

Option 1 provides a complete list of all data on the record with a time word (II-D-2-m defines the time word). This includes hourly component speeds, vector speed and direction, temperature, pressure and salinity for 2.86 hr filtered current meter data, and 6-hourly component speeds and vector speed and direction for the 35 hour filtered data. Aanderaa data logger substitutes wind gust for salinity. Pressure gauges have pressure in millibars, and some have temperature. TAPE4 data may contain some or all of the above parameters.

Option 2 prints only averages computed for a specified time period. If option 2 or 3 is selected, R2D2 will ask...

HOW MANY HOURS DO YOU WANT TO AVERAGE?

Averaging is done over this time interval starting at the specified start time, and also for the entire record length.

If terminal output was not suppressed by entering a negative option number, R2D2 will estimate the number of lines of output which will be printed on the terminal, and if over 200 will ask if the user wants to reconsider. If so the parameters may be re-entered.

Subroutine: CMDAT

Program: CMLLOOK (II-D-2)

ENTER DATA OPTION ? 1
 1 UP-1 1811 64
 FILTER TYPE ? 1
 START,END=800821400 802292100 LEN=3536
 NEW START, END TIME ? 0,800822400
 NEW START,END=800821400 800822400 LEN=11
 MAJOR AXIS DIRECTION? 0
 LIST OPTION ? 3
 HOW MANY HOURS DO YOU WANT TO AVERAGE ? 6

UP-1 1811 DEPTH = 64 LAT = 54.56 LON = 165.40
 AVERAGING INTERVAL = 6. HOURS

TIME	90 T	0 T	TEMP	PRESS	SAL	SPEED	DIR	TIME
800821400	12.0	3.3	3.36	172.58	28.96	12.5	74.7	
800821500	6.2	24.5	3.44	172.56	29.03	25.2	14.2	
800821600	-11.4	42.4	3.35	172.83	28.96	43.9	345.0	
800821700	-20.8	53.5	3.29	173.27	28.92	57.4	338.7	
800821800	-11.8	53.7	3.28	173.62	28.88	54.9	347.6	
800821900	2.7	37.5	3.29	173.62	28.88	37.6	4.1	
MEANS, 800821400 TO 800821900								
	-3.8	35.8	3.33	173.08	28.94	38.6		
				NET VELOCITY =		36.0	353.9	T
800822000	15.6	9.1	3.27	173.65	28.90	18.1	59.9	
800822100	24.0	-19.0	3.22	173.62	28.87	30.6	128.4	
800822200	31.5	-46.0	3.19	172.97	28.86	55.7	145.6	
800822300	38.5	-67.6	3.33	172.24	28.99	77.8	150.3	
MEANS, 800822000 TO 800822400								
	28.6	-39.3	3.30	172.83	28.94	52.5		
				NET VELOCITY =		48.7	144.0	T
MEANS, 800821400 TO 800822400								
	10.9	1.6	3.32	172.96	28.94	44.9		
				NET VELOCITY =		11.0	81.5	T

Fig. 17. CM/PG data listing.

II-D-2-b STATISTICS ON DATA SEGMENTS (fig 18)

DATA TYPE: C (II-B)
 SORT OPTION: 0 (II-D-1)
 WHAT DO YOU WANT TO DO? 6 (II-D-1)
 DATA OPTION: 2 (II-D-2)

After asking for time period and filter type (II-D-2-m) and major axis direction (II-D-2-o), this routine computes the mean, minimum, maximum, standard deviation, variance, skewness and kurtosis for each parameter. If the input series is not pressure gauge data, it goes on to compute net velocity and direction, and axis of greatest variance.

The statistics are computed as follows:

$$\text{mean} = \bar{x} = \frac{1}{n} \sum x$$

$$\text{maximum} \geq x_n$$

$$\text{minimum} \leq x_n$$

$$\text{standard deviation} = s = \left(\frac{\sum (x - \bar{x})^2}{n} \right)^{1/2}$$

$$\text{variance} = \frac{\sum (x - \bar{x})^2}{n}$$

$$\text{skewness} = \frac{\sum (x - \bar{x})^3 / n}{s^3}$$

$$\text{kurtosis} = \frac{\sum (x - \bar{x})^4 / n}{s^4}$$

$$\text{net velocity} = (\bar{u}^2 + \bar{v}^2)^{1/2}$$

u = east, v = north

$$\text{direction} = \tan^{-1} (\bar{u} / \bar{v})$$

The axis of greatest variance is defined by the first mode eigenvector of the velocity component covariance matrix. The variance on the axis of greatest variance is the first mode eigenvalue. (See also the EOF option description, II-D-2-k)

Subroutine: DATSTAT

Program: CMLOOK (II-D-2)

ENTER DATA OPTION ? 2
 1 UP-1 1811 64
 FILTER TYPE ? 1
 START,END=800821400 802292100 LEN=3536
 NEW START, END TIME ? 0,0
 NEW START,END=800821400 802292100 LEN=3536
 MAJOR AXIS DIRECTION? 300

UP-1 1811 64 800821400 TO 802292100 LEN = 3536 2.9 FILTER DATA

PARAMETER	MEAN	MINIMUM	MAXIMUM	ST DEV	VARIANCE	SKENNESS	KURTOSIS
30 T	1.18	-62.00	56.05	22.72	516.26	.13	2.22
300 T	5.52	-83.08	81.22	32.49	1055.29	-.47	2.48
TEMP	4.18	2.76	6.61	.76	.57	.26	2.04
PRESS	170.21	166.70	173.65	1.15	1.32	-.48	2.95
SAL	29.03	28.21	31.34	.26	.07	-.29	5.08
SPEED	35.85	.75	91.25	17.83	317.93	.43	2.56

NET VELOCITY = 5.64 AT 312.0T
 AXIS OF GREATEST VARIANCE = 330.2 T
 VARIANCE = 1332.58 = 84.79 0/0

II-D-2-c TIME SERIES PLOTS (ALL PARAMETERS, ONE RECORD) (fig 19)

DATA TYPE: C	(II-B)
SORT OPTION: 0	(II-D-1)
WHAT DO YOU WANT TO DO? 6	(II-D-1)
DATA OPTION: 3	(II-D-2)

This option does time series plots. For 2.86 hr current meter data this includes major and minor axes, speed, temperature, pressure and salinity. The 35 hr data plot has component speeds and stick (vector speeds) plots. Pressure gauge records plot pressure and temperature. TAPE4 records with only one parameter should be plotted with option 4 (II-D-2-d).

After asking for time period and filter type (II-D-2-m) R2D2 will ask for scale parameters...

DAYS PER INCH, SCALE?

Days per inch sets the time scale and the SCALE parameter sets the speed (or pressure in millibars for pressure gauge records) axis. Defaults, set by entering "0,0", are 2 days and 100 units per inch for 2.86 hr filtered data, and 2 days and 40 units per inch for 35 hr filtered data. (For wind data SCALE = 20 units per inch).

Then the major axis direction is requested (II-D-2-o). If a parameter is not plotted, there is none of that data on the record.

Subroutine: TSPLT

Program: CMLOOK (II-D-2)

```

ENTER DATA OPTION ? 3
1 UP-1 1811 64
FILTER TYPE ? 1
START,END=800821400 802292100 LEM=3536
MEM START, END TIME ? 0,800920000
MEM START,END=800821400 800920000 LEM=227
DAYS PER INCH, SCALE? 2,100
MAJOR AXIS DIRECTION? 0
DO YOU WANT TO PLOT THIS ON YOUR TERMINAL ?

```

STATION: UP-1
 PROJECT: UNIMAK PAS
 LATITUDE: 54.56N
 LONGITUDE: 165.40W
 DEPTH: 84.0 METERS

METER: 1811
 DEPTH: 64 METERS

MEAN SPEED: 33.78 CM/S
 NET SPEED: 3.48 CM/S
 DIRECTION: 261.8°T
 VARIANCE: 1350.39

2.86 HOUR DATA PLOT

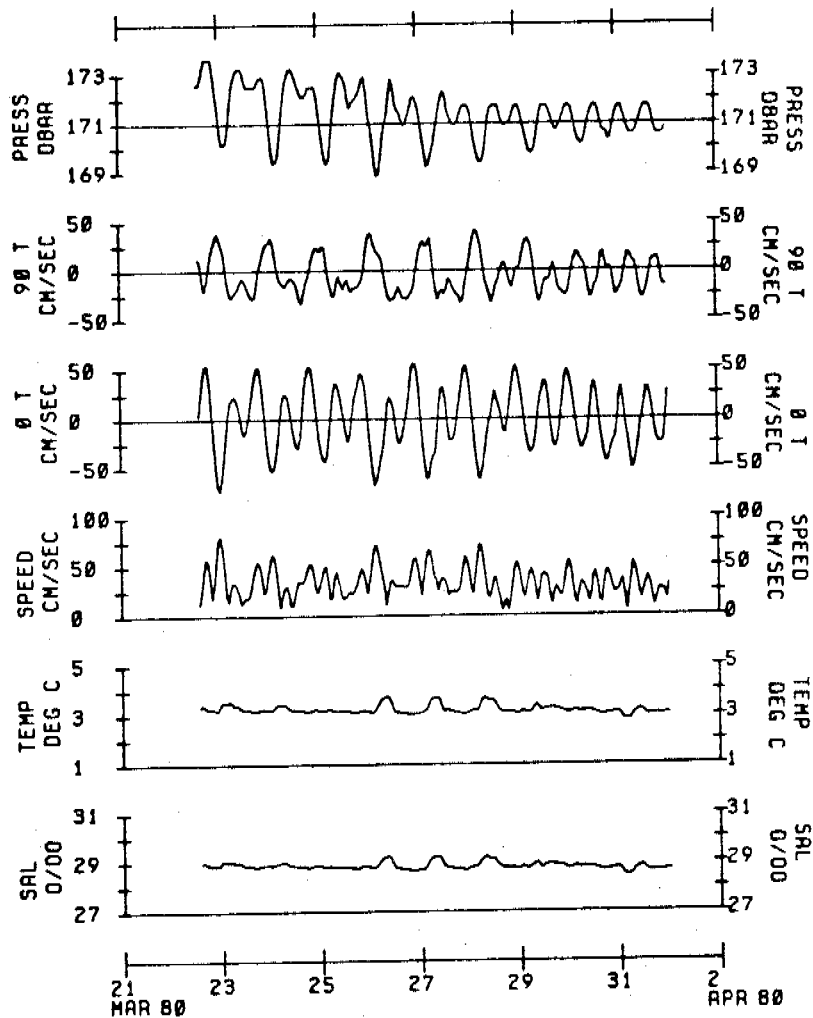


Fig. 19. CM/PG data time series plots (all parameters for one record).

II-D-2-d TIME SERIES PLOTS (ONE PARAMETER, ALL RECORDS) (fig 20)

DATA TYPE: C	(II-B)
SORT OPTION: 0	(II-D-1)
WHAT DO YOU WANT TO DO? 6	(II-D-1)
DATA OPTION: 4	(II-D-2)

This option does time series plots of one parameter for each record selected. Up to 20 records may be plotted at one time. To plot n parameters for a particular record, that record should be selected n times. For six or less records, plot height is 9.5 inches, and is plotted on 11" paper. More than six records are plotted on 34" paper. R2D2 first asks for time period and filter type (II-D-2-n), and then....

DAYS PER INCH?

which is the number of days per inch on the X (time) axis, entered as a whole number. Next R2D2 will ask for each record...

PARAMETER, SCALE?

where...

PARAMETER = 0 TO ESCAPE

- 1 FOR COMPONENT SPEED
- 2 FOR VECTORS (STICKS)
- 3 FOR TEMPERATURE

4 FOR PRESSURE

5 FOR SALINITY

6 FOR SPEED

7 FOR DIRECTION

SCALE = UNITS PER INCH ON Y AXIS

If the data are 35 hr filtered, 3, 4 and 5 are omitted. If the data are from a pressure gauge...

PARAMETER = 1 FOR PRESSURE

2 FOR TEMPERATURE

When current meter parameters 1 or 2 have been selected, the major axis direction (II-D-2-o) will also be requested. After each record has been processed, plotting procedes (II-F-2). If a parameter is not plotted, there was none of that data on the record.

Subroutine: TSPLTS

Program: CMLOOK (II-D-2)

```

ENTER DATA OPTION ? 4
FILTER TYPE ? 2
YOUR FILES ARE:
UP-1      1811    64 888858688 TO 882278688 LEM= 569 DT= 6.00 HR
UP-2      1827    59 888858888 TO 882278888 LEM= 569 DT= 6.00 HR
UP-3      1815    47 888841888 TO 882262488 LEM= 570 DT= 6.00 HR
NEW START, END TIME ? 0.001200000
DAYS PER INCH ? 5
UP-1      1811 AT 64 M
PARAMETER, SCALE ? 2,50
MAJOR AXIS DIRECTION? 300
UP-2      1827 AT 59 M
PARAMETER, SCALE ? 2,50
MAJOR AXIS DIRECTION? 285
UP-3      1815 AT 47 M
PARAMETER, SCALE ? 2,50
MAJOR AXIS DIRECTION? 280
DO YOU WANT TO PLOT THIS ON YOUR TERMINAL ? Y

```

35.0 FILTER DATA

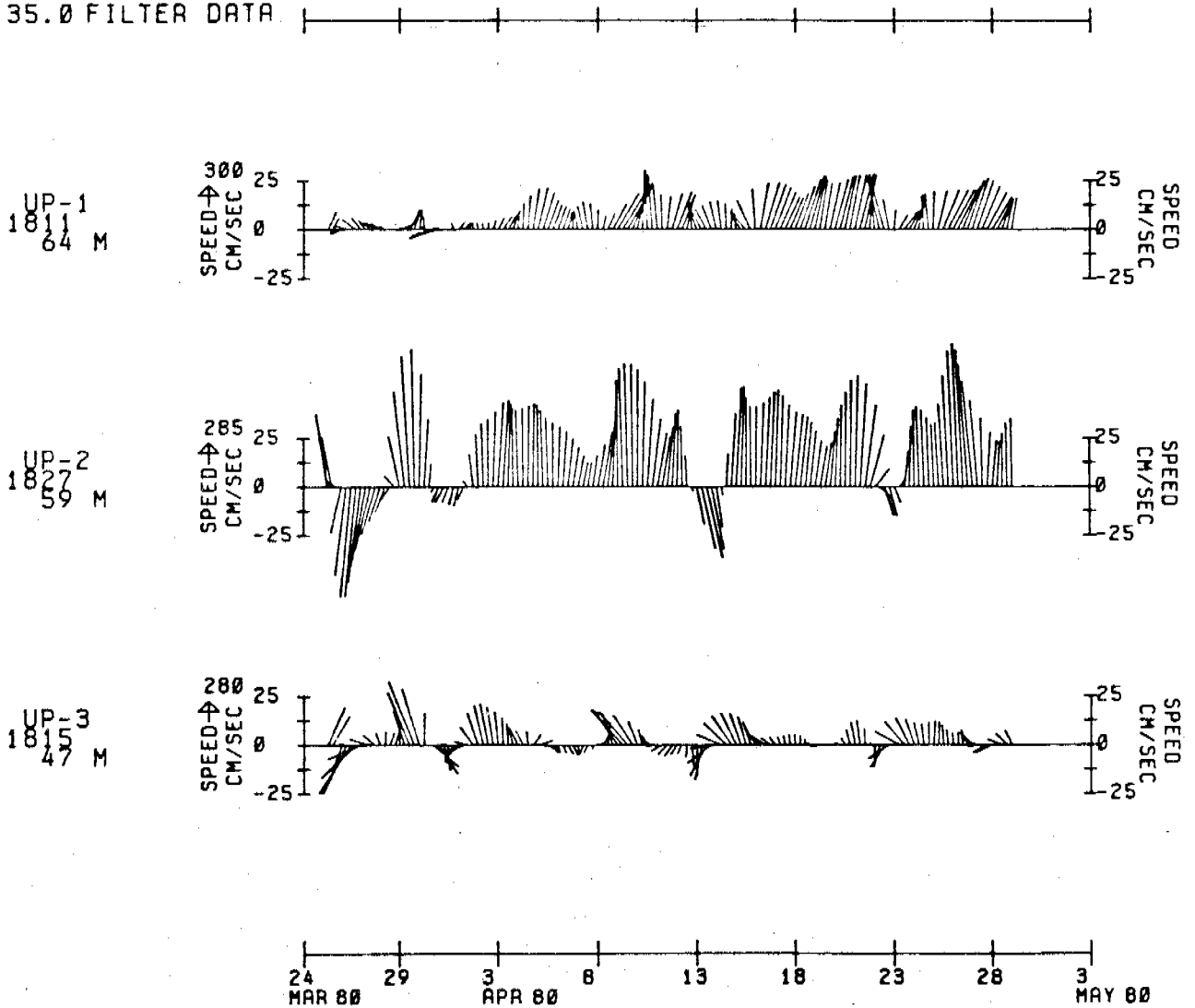


Fig. 20. CM/PG data time series plots (one parameter for each record)

II-D-2-e U-V SCATTER DIAGRAMS (fig 21)

DATA TYPE: C	(II-B)
SORT OPTION: 0	(II-D-1)
WHAT DO YOU WANT TO DO? 6	(II-D-1)
DATA OPTION: 5	(II-D-2)

This routine does scatter plots of u (east-west) component velocity vs. v (north-south) component velocity. Two plot types are available: a linear scale (option 1) or a square root speed scale, which preserves area (i.e. the area of a quadrant of 0 to 10 cm s^{-1} is equal to the area of a 90 to 100 cm s^{-1} quadrant). The plots are self-scaled, depending on the maximum component speed of the record time period. The record mean vector is also computed and plotted.

The program first requests plot type, filter type and desired time period (II-D-2-m) and then does the plot (II-F-2). Plot size is about 8" high x 6" wide.

Subroutine: SCAPLT

Program: CMLOOK (II-D-2)

ENTER DATA OPTION ? 5
PLOT OPTION ? 1
1 UP-1 1811 64
FILTER TYPE ? 2
START,END=800850600 802270600 LEN=569
NEW START, END TIME ? 0,801200000
NEW START,END=800850600 801200000 LEN=140
ARE YOU USING A TEKTRONIX TERMINAL?

UP-1 1811 AT 64M
FROM 800850600 TO 801200000
LAT 54.56N LON 165.40W
35. HR FILTER DATA N= 140

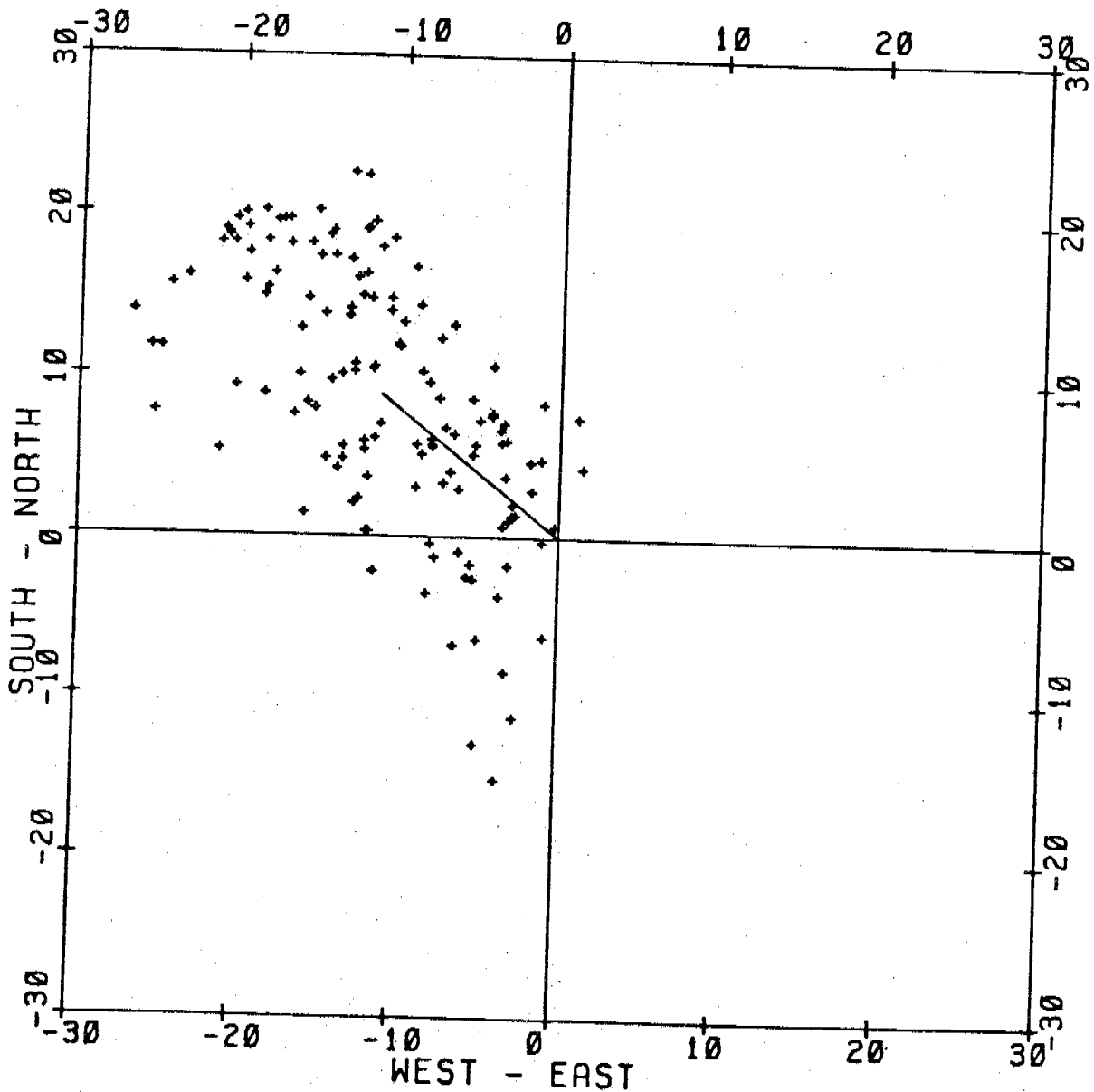


Fig. 21. CM data U-V scatter diagram.

II-D-2-f PVD PLOTS (fig 22)

DATA TYPE: C	(II-B)
SORT OPTION: 0	(II-D-1)
WHAT DO YOU WANT TO DO? 6	(II-D-1)
DATA OPTION: 6	(II-D-2)

This routine does PVD (progressive vector diagram) plots. These are plots of successive current or wind vectors connected end to end, simulating a Lagrangian path from Eulerian measurements. Plots are either self-scaled to 2, 5 or 10 x 10ⁿ kilometers per inch or the user may define the scale. A + symbol is plotted every 5 days. The program requests filter type and time period (II-D-2-m), and then the scale, in km/inch. A 0 is entered for self-scaling. R2D2 then plots (II-F-2). Plot size is about 8" high by 7" wide.

Subroutine: PVDPLT

Program: CMLOOK (II-D-2)

ENTER DATA OPTION ? 6
 1 UP-1 1811 64
 FILTER TYPE ? 2
 START,END=800850600 802270600 LEN=569
 NEW START, END TIME ? 0,0
 NEW START,END=800850600 802270600 LEN=569
 ENTER SCALE (KM/INCH) OR 0 FOR SELF-SCALING ? 0
 DO YOU WANT TO PLOT THIS ON YOUR TERMINAL ?

UP-1 1811 AT 64M
 FROM 800850600 TO 802270600
 LAT 54.56N LON 165.40W
 35. HR FILTER DATA N= 569
 + EVERY 5 DAYS

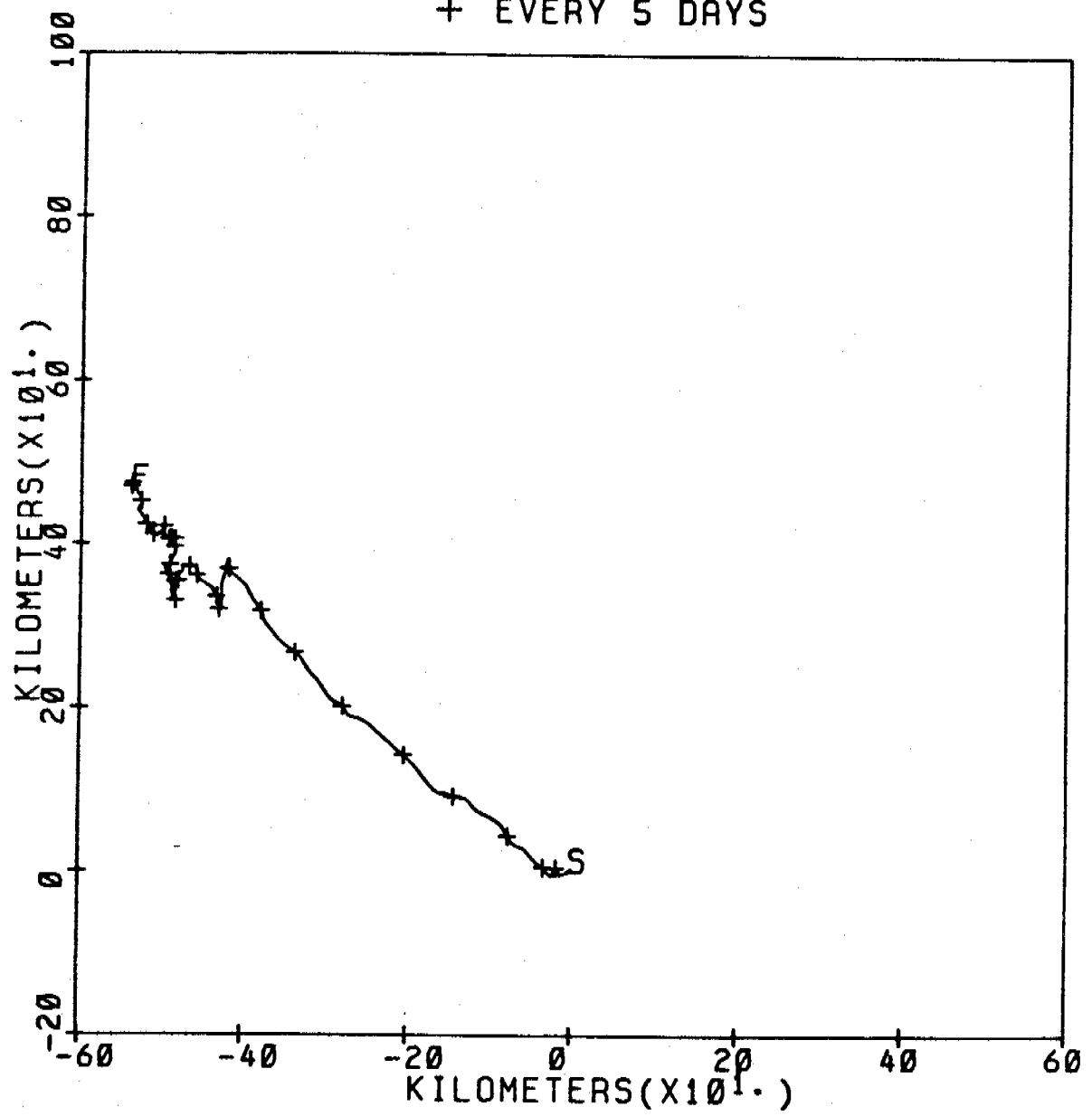


Fig. 22. CM data progressive vector diagram.

II-D-2-g HISTOGRAMS (fig 23)

DATA TYPE: C (II-B)
SORT OPTION: 0 (II-D-1)
WHAT DO YOU WANT TO DO? 6 (II-D-1)
DATA OPTION: 7 (II-D-2)

This routine does histograms of selected parameters. Either relative frequency or cumulative frequency plots may be done. Statistics (see II-D-2-b) are also computed and written on the plot.

The histogram is divided into 36 bins and the percentage of observations per bin computed. Bin width is determined by the standard deviation of the parameter to be plotted. A bin width is approximately 1/3 standard deviation, with a minimum of 0.1 and maximum of 20. The histogram is centered approximately at the mean. If any values exceed the bounds of the histogram, they are plotted in extra bins just outside the plot axes. The scale of the Y axis (percent observations) is determined by the bin with the maximum percentage.

R2D2 will first ask for filter type and time period (II-D-2-m) and then parameter and histogram type, where...

PARAMETER = 0 FOR NONE
1 FOR COMPONENT SPEED
2 FOR SPEED
3 FOR DIRECTION
4 FOR TEMPERATURE
5 FOR PRESSURE
6 FOR SALINITY

HISTOGRAM TYPE: 1 FOR RELATIVE FREQUENCY DISTRIBUTION
2 FOR CUMULATIVE FREQUENCY DISTRIBUTION

After selecting parameter and histogram type the plot will be done (II-F-2) and output printed on TAPE6. Plot size is about 7" x 7".

Subroutine: HISTO

Program: CMLOOK (II-D-2)

ENTER DATA OPTION ? 7

2 UP-2 1827 59

FILTER TYPE ? 2

START,END=800850000 802270000 LEN=569

NEW START, END TIME ? 0,0

NEW START,END=800850000 802270000 LEN=569

PARAMETER, HISTOGRAM TYPE ? 1,1

MAJOR AXIS DIRECTION? 285

UP-2 1827 AT 59M
FROM 800850000 TO 802270000
LAT 54.30N LON 164.76W
35. HR FILTER DATA N= 569

MEAN 12.70
MINIMUM -59.73
MAXIMUM 73.15
ST-DEV 20.38
VARIANCE 415.40
SKEWNESS -0.10
KURTOSIS 3.96

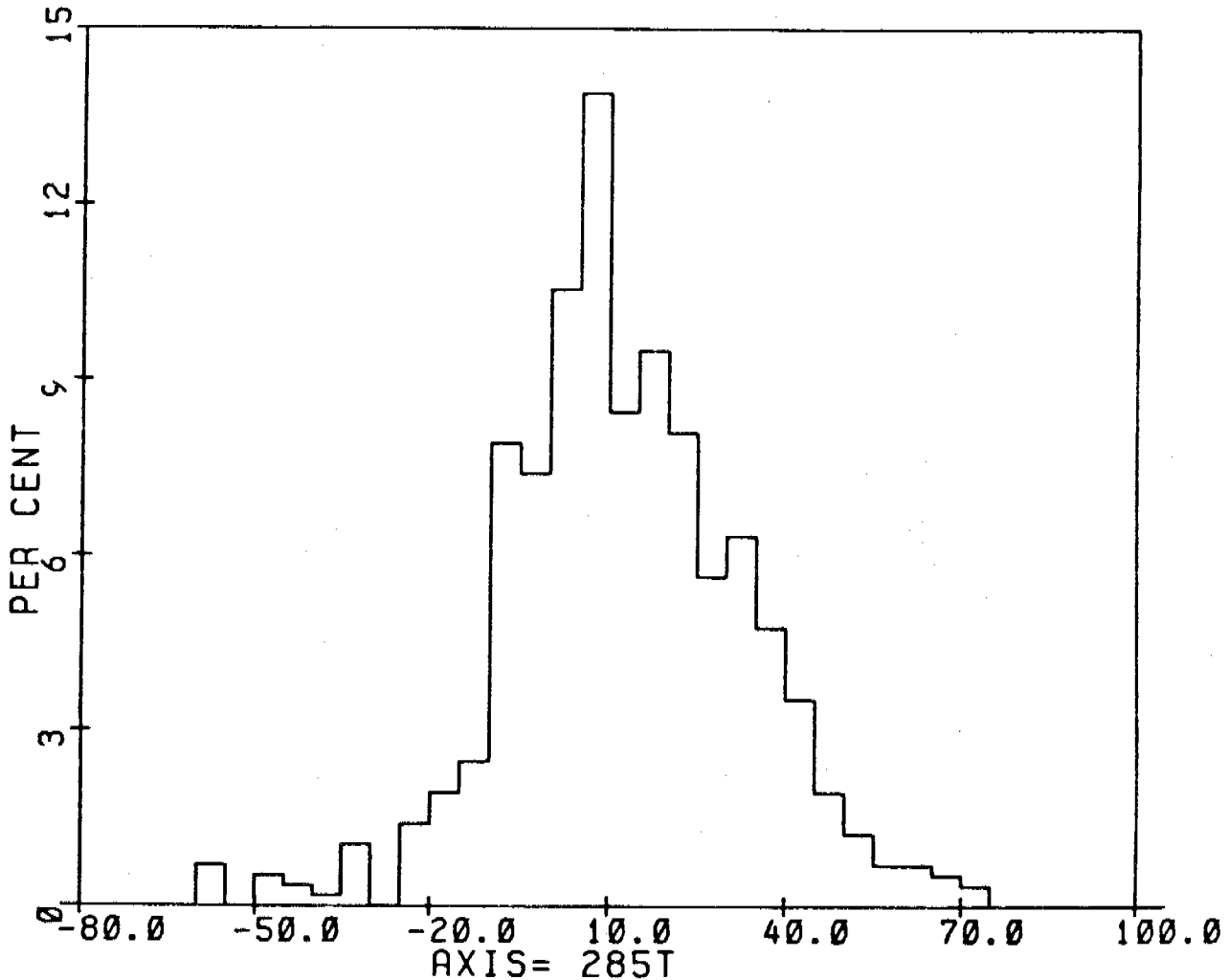


Fig. 23. CM/PG data histogram. 611

II-D-2-h CURRENT ROSES (fig 24)

DATA TYPE: C (II-B)
SORT OPTION: 0 (II-D-1)
WHAT DO YOU WANT TO DO? 6 (II-D-1)
DATA OPTION: 8 (II-D-2)

This option does current (or wind) roses, with or without a map, with an optional number of bins. The routine begins by asking...

ENTER NUMBER OF BINS (4 to 36)?

The compass is sectioned into the number of bins, NBIN, each section centered on $n \times 360^\circ / \text{NBIN}$, $n=0, 1, \dots, \text{NBIN}-1$. A line will be plotted in the direction of the section with lengths proportional to the mean speed of the observations in the bin. The percentage of observations represented by bin is printed next to its line

Next R2D2 asks...

DO YOU WANT THESE PLOTTED ON A MAP?

if so....

ENTER 1 TO PLOT ALL ON ONE MAP

2 TO PLOT SEPARATELY BUT USING SAME MAP

3 TO PLOT EACH ON A DIFFERENT MAP

and then the map parameters are requested (see II-F-1)

If plotting is to be done on a map the speed scale is $20 \text{ cm s}^{-1}/\text{inch}$.
If not, the scale is $10 \text{ cm s}^{-1}/\text{inch}$ on a plot 7" high x 6" wide.

For each record selected, R2D2 asks for filter type and time period (II-D-2-m) and then does the plot (II-F-2)

Subroutine: ROSE

Program: CMLOOK (II-D-2)

ENTER DATA OPTION ? 8
 ENTER NUMBER OF BINS (4 TO 36)? 12
 DO YOU WANT THESE PLOTTED ON A MAP? N
 2 UP-2 1827 59
 FILTER TYPE ? 2
 START,END=800850000 802270000 LEN=569
 NEW START, END TIME ? 0,0
 NEW START,END=800850000 802270000 LEN=569
 DO YOU WANT TO PLOT THIS ON YOUR TERMINAL ?

UP-2 1827 AT 59M
 FROM 800850000 TO 802270000
 LAT 54.30N LON 164.76W
 35. HR FILTER DATA N= 569

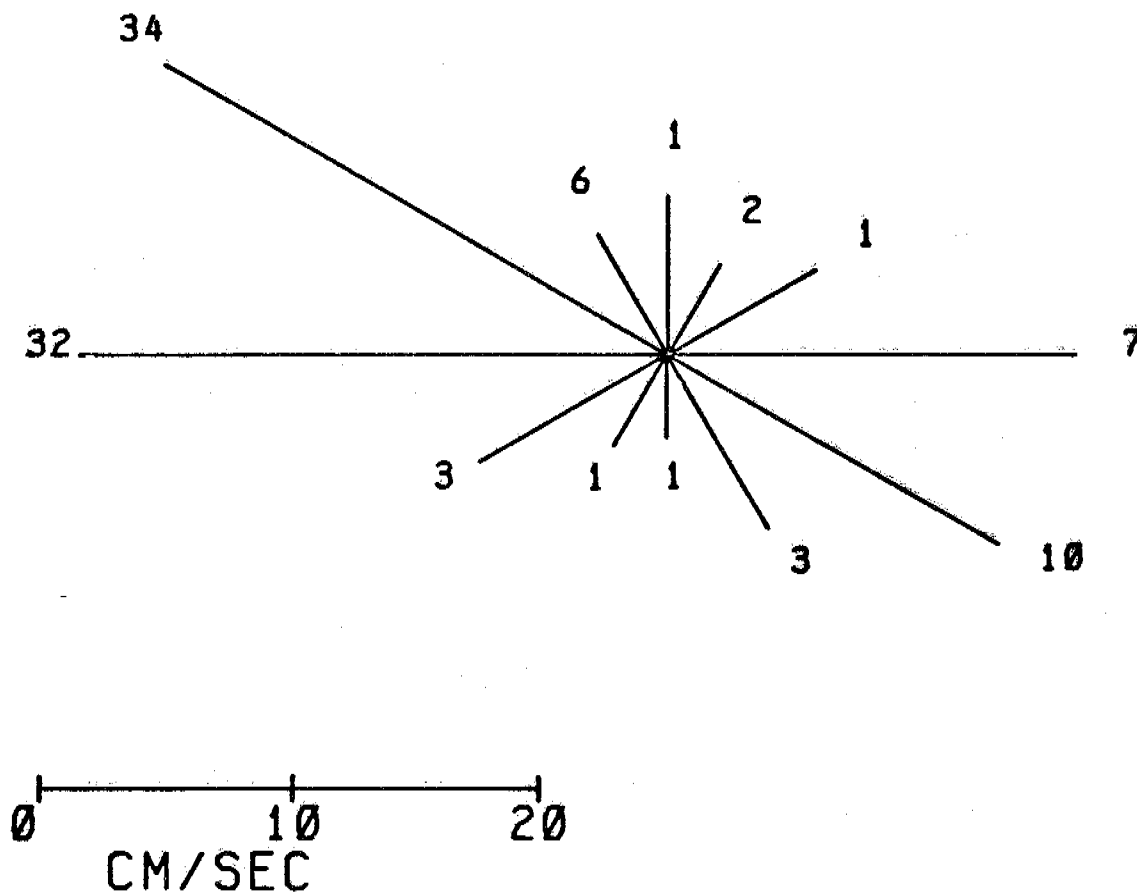


Fig. 24. CM data current rose plot.

II-D-2-i SUMMARY CURRENT VECTORS (fig 25)

DATA TYPE: C	(II-B)
SORT OPTION: 0	(II-D-1)
WHAT DO YOU WANT TO DO? 6	(II-D-1)
DATA OPTION: 9	(II-D-2)

This option plots a mean velocity vector on the end of which are plotted the axes of greatest and least variance. R2D2 will ask whether to plot on a map (see II-D-2-h) and for filter type and time period (II-D-2-m).

If done on a map, the scale is $20 \text{ cm s}^{-1}/\text{inch}$ on a 7" high x 6" wide plot. The axis of greatest variance is defined by the direction of the first mode eigenvector of the velocity component covariance matrix. (see also II-D-2-k) The axis length is proportional to the square root of the first mode eigenvalue, which is the standard deviation along the axis of greatest variance. The orthogonal axis length is proportional to the square root of the second mode eigenvalue. The values for the mean velocity and axis of greatest variance are printed and written on TAPE6, and then plotted (II-F-2).

Subroutine: VECPLT

Program: CMLook (II-D-2)

```

ENTER DATA OPTION ? 9
DO YOU WANT THESE PLOTTED ON A MAP? Y
ENTER 1 TO PLOT ALL ON ONE MAP
      2 TO PLOT SEPARATELY BUT USING SAME MAP
      3 TO PLOT EACH ON A DIFFERENT MAP
? 1
WHICH MAP FILE? 2
ENTER: LAT1,LAT2,LON1,LON2
? 53.5,55.5,163,167

AREA IS BOUNDED BY:
LATITUDES 53.50 TO 55.50
LONGITUDES 163.00 TO 167.00
IS THIS OK? Y
ENTER SCALE,ATLAT,TIC,YLEN
? 0,0,.25,6
SCALE = 1461199. AT LATITUDE 54.500
TIC MARKS EVERY .25 DEGREE
CHART HEIGHT = 6.00, LENGTH = 6.98
IS THIS OK? Y
1 UP-1 1811 64
FILTER TYPE ? 2
START,END=800850600 802270600 LEN=569
NEW START, END TIME ? 0,0
NEW START,END=800850600 802270600 LEN=569

FOR UP-1 AT 64 METERS 35.0 HR FILTERED DATA
MEAN SPEED = 5.77 DIRECTION T = -48.0
STANDARD DEVIATIONS: MAJOR AXIS = 8.88 @ -31.5 T
MINOR AXIS = 4.58
DO YOU WANT TO PLOT THIS ON YOUR TERMINAL ?

```

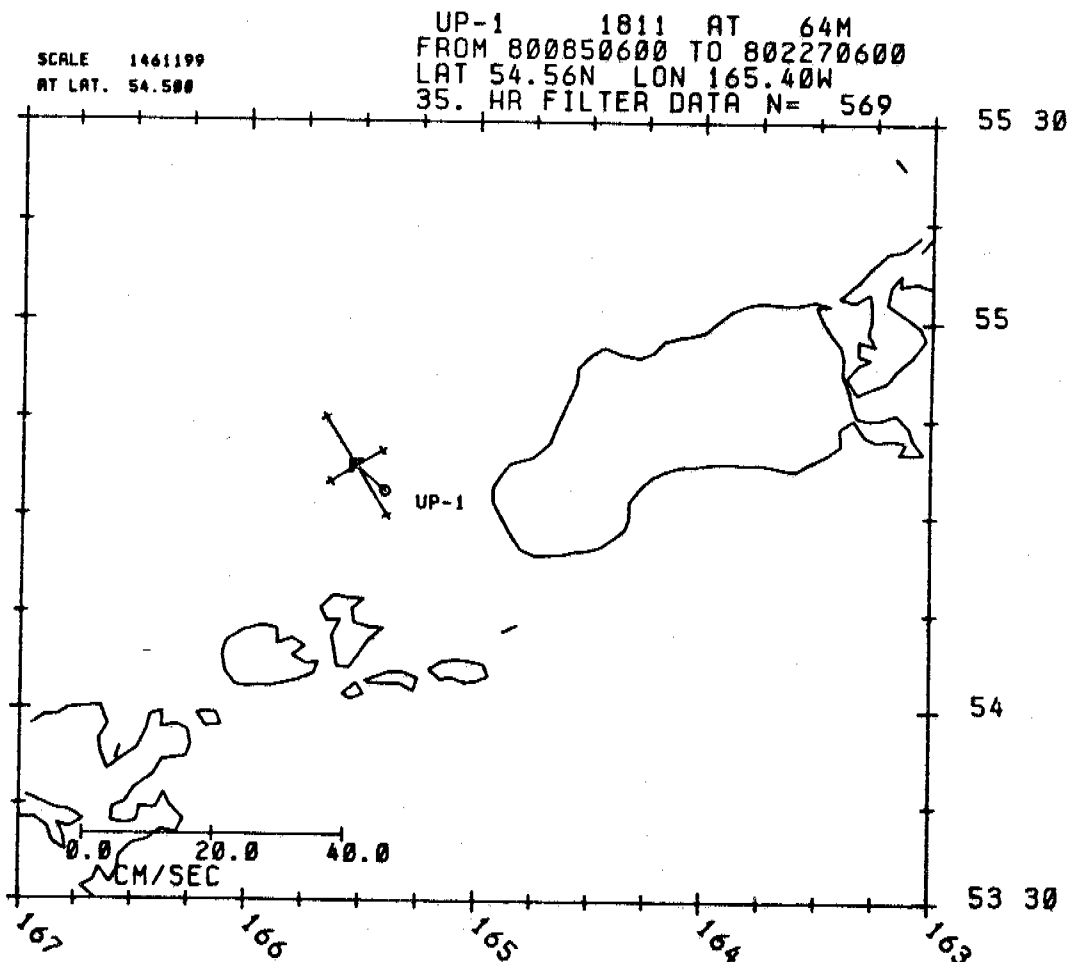


Fig. 25. CM data summary current vector plot.

II-D-2-j LAGGED LINEAR CORRELATIONS (fig 26)

DATA TYPE: C	(II-B)
SORT OPTION: 0	(II-D-1)
WHAT DO YOU WANT TO DO? 6	(II-D-1)
DATA OPTION: 10	(II-D-2)

This option computes linear covariance and correlation matrices for up to 12 records at 0 to n lags. It also computes the integral time scale matrix and matrix of confidence levels for the correlations.

The routine begins by asking for filter type, listing the selected records and asking for desired time interval (II-D-2-n). If more than 12 records had been selected, only the first 12 are used. The total number of data points may not exceed 12000 (i.e., number of records x data per record \leq 12000).

Next the number of lags is requested. Each lag is one time step in length, i.e., 1 hour for the 2.86 hr filtered data or 6 hours for 35 hr filtered data. Covariance and correlation matrices will be computed and printed for each lag.

After asking for an OK on the time interval and number of lags, the program proceeds to set up the data in the common time base. Any records which do not fall within the time window or whose data interval is not the common data interval (defined by the data interval of the last record of the set) are not included. R2D2 will ask for parameter number, where the user should...

ENTER 1 FOR COMPONENT SPEED

2 FOR SPEED

3 FOR TEMPERATURE

4 FOR PRESSURE

5 FOR SALINITY

or if a pressure gauge record

1 FOR PRESSURE

2 FOR TEMPERATURE

If component speed is the option, major axis direction is requested (II-D-2-o). The data are then loaded into arrays, record information printed, R2D2 asks if output is to be printed on the terminal, and then the correlation computations proceed. The correlations are computed from:

$$r_{xy} = \frac{\frac{1}{N-K} \sum_{i=1}^{N-K} (x_i - \bar{x})(y_{i+K} - \bar{y})}{\frac{1}{N-K} \left[\sum_{i=1}^{N-K} (x_i - \bar{x})^2 \cdot \sum_{i=1}^{N-K} (y_{i+K} - \bar{y})^2 \right]^{1/2}} \quad (1)$$

$$\text{where } \bar{x} = \frac{1}{N-K} \sum_{i=1}^{N-K} x_i = \text{mean series } x$$

$$\bar{y} = \frac{1}{N-K} \sum_{i=1}^{N-K} y_i = \text{mean series } y$$

N = number points

K = lag

and the numerator is the lagged covariance. Note that for each lag, new means and autocovariances are computed for both the lagged and non-lagged series. For example, if x and y have 100 points, at lag 3 the means and covariances are computed for x_{1-97} and y_{4-100} . This method is discussed in Jenkins and Watts (1968), p. 182.

After computing and printing the correlations for all requested lags the integral, or independent, time scale (Allen and Kundu, 1978) matrix is computed:

$$\tau_{xy} = \Delta t + \sum_{K=1}^{N-1} 2r_{xx}(K)r_{yy}(K)\Delta t$$

where r_{xx} and r_{yy} are the lagged autocorrelation coefficients for series x and y.

Now the correlations are computed from:

$$r_{xx} = \frac{\frac{1}{N} \sum_{i=1}^{N-K} (x_i - \bar{x})(x_{i+K} - \bar{x})}{\frac{1}{N} \sum_{i=1}^N (x_i - \bar{x})^2} \quad (2)$$

where $\bar{x} = \frac{1}{N} \sum_{i=1}^N x_i$ = mean of series x.

Means and autocovariances are computed just once. This method of computing the autocorrelation is discussed on p 181 of Jenkins and Watts. The two methods differ in that (1) provides a calculation of the sample correlation, and (2) converges and is a better estimate of the population correlation.

Finally, the 95% confidence levels for the correlation matrix are computed from:

$$CL_{xy} = \pm 1.96 \left(\frac{N\Delta t}{\tau_{xy}} \right)^{-\frac{1}{2}}$$

Linear regression coefficients for slope (a) and intercept (b) may be derived from the means and covariance matrix, viz

$$y = ax + b$$

where

$$a = \frac{C_{xy}}{C_{xx}}$$

$$b = \bar{y} - a\bar{x}$$

C_{xy} = covariance between series x and y

C_{xx} = variance of series x

\bar{x} = mean of series x

\bar{y} = mean of series y

The means and covariance matrix may also be used to calculate an estimate of flux. For example, if series x is velocity on some axis, and series y is salinity, salt flux per unit time in the x direction is

$$\begin{aligned}\frac{1}{n} \sum xy &= \frac{1}{n} \sum (\bar{x}+x') (\bar{y}+y') \\ &= \frac{1}{n} (\sum \bar{x}\bar{y} + \sum \bar{x}y' + \sum \bar{y}x' + \sum x'y') \\ &= \bar{x}\bar{y} + C_{xy}\end{aligned}$$

That is, the flux is the product of the means plus the covariance. The $\sum \bar{x}y'$ and $\sum \bar{y}x'$ terms drop out because the sum of products of a constant and a fluctuating term of zero mean is zero.

Subroutines: LINCOR, GET5, LODDAT, CROSSC

Program: CMLLOOK (II-D-2)

ENTER DATA OPTION ? 10
 FILTER TYPE ? 2
 YOUR FILES ARE:
 UP-1 1811 64 800850600 TO 802270600 LEN= 569 DT= 6.00 HR
 UP-2 1827 59 800850000 TO 802270000 LEN= 569 DT= 6.00 HR
 UP-3 1815 47 800841800 TO 802262400 LEN= 570 DT= 6.00 HR
 NEW START, END TIME ? 0,0

ENTER THE NUMBER OF LAGS? 0

NUMBER OF LAGS IS 0 (0 HOURS)

TIME INTERVAL IS FROM 800850600 TO 802262400
 DT= 6.00 HR, 568 POINTS
 IS THIS OK? Y

UP-1 1811
 PARAMETER ? 1
 MAJOR AXIS DIRECTION? 330

UP-2 1827
 PARAMETER ? 1
 MAJOR AXIS DIRECTION? 285

UP-3 1815
 PARAMETER ? 1
 MAJOR AXIS DIRECTION? 280

NUMBER 1 IS UP-1 METER 1811 AT 64 M 330 T

NUMBER 2 IS UP-2 METER 1827 AT 59 M 285 T

NUMBER 3 IS UP-3 METER 1815 AT 47 M 280 T

THE RESULTS WILL BE WRITTEN ON TAPE6
 DO YOU WANT THEM PRINTED ON YOUR TERMINAL ALSO? Y

MEANS OF SERIES

	1	2	3
	5.47	12.66	1.33

F O R L A G = 0 (568 POINTS)
 (COLUMN LAGS ROW)

COVARIANCE MATRIX

	1	2	3
1	78.89	119.19	21.71
2	119.19	415.30	98.56
3	21.71	98.56	51.77

CORRELATION MATRIX

	1	2	3
1	1.000	.658	.348
2	.658	1.000	.672
3	.348	.672	1.000

TIME SCALE MATRIX, HOURS (ALLEN AND KUNDU,78)

	1	2	3
1	167.34	89.97	32.07
2	89.97	74.44	41.37
3	32.07	41.37	48.07

95 % CONFIDENCE LEVEL OF CORRELATIONS

	1	2	3
1	.434	.318	.190
2	.318	.290	.216
3	.190	.216	.233

Figure 26. CM/PG lagged linear correlations.

11-D-2-k EMPIRICAL ORTHOGONAL FUNCTIONS (EOF) (fig. 27)

DATA TYPE: C	(11-B)
SORT OPTION: 0	(II-D-1)
WHAT DO YOU WANT TO DO? 6	(11-D-1)
DATA OPTION: 11, 12	(II-D-2)

This option does empirical orthogonal function analysis using either the covariance or correlation matrix for 0 lag as described in II-D-2-j (option 11), or a user-supplied matrix (option 12).

This routine uses the IMSL (International Mathematical and Statistical Libraries) subroutines EHOUSS, EQRT2S and EHOBKS, described in IMSL Reference Manual Edition 7, vol 1, to compute the eigenvalues and eigenvectors of the symmetric correlation or covariance matrix.

Use of the covariance matrix gives greatest weight to the series with greatest variance. The correlation matrix is equal to a normalized covariance matrix (as if each data series had been divided by its standard deviation so that it had unit variance), and therefore gives equal weight to each series, regardless of the original units.

If option 12 is selected, the user supplies the covariance or correlation matrix. R2D2 will ask for the order of the matrix, which should be an integer, greater than 1, to a maximum of 12. Then the lower part of a symmetric diagonal matrix is entered, N values for the Nth row (fig 27). After asking for an OK on the input matrix, the program proceeds with the solution of the eigenvalue problem.

The eigenvalues and columns of eigenvectors are ranked in descending order, i.e. mode 1 containing the greatest variance is first, mode 2 second etc. The eigenvalue is equal to the variance of the mode, and the sum of the eigenvalues equals the sum of the variance of all series. The eigenvectors are mutually orthogonal and the modes uncorrelated with each other. Mode 1 contains the greatest correlated variance, mode 2 the greatest correlated amount of the remaining variance, etc.

Output includes: eigenvalues and the percentage of total variance represented by each mode; the eigenvector matrix, columns representing the mode and rows the data series; and the matrix of percentage variance explained by each mode for each series.

If option 11 was selected, the user may also write from 0 to the maximum number of modes as time series in the "TAPE4 format" (see II-D-4) for further analysis and plotting. The EOF modes are computed from

$$Y_{M,t} = \sum_{n=1}^N x_{n,t} E_{n,M}$$

where $x_{n,t}$ is the demeaned data series n (divided by the standard deviation if the correlation matrix was used for the EOF analysis), $E_{n,M}$ is the eigenvector component for series n , mode M , and N is the total number of records in the analysis.

Subroutines: LINCOR, GET5, LODDAT, CROSSC, EOF5

Program: CMLOOK (II-D-2)

```

ENTER DATA OPTION ? 12
ENTER 1 FOR EOF BASED ON COVARIANCE MATRIX
      2 FOR EOF BASED ON CORRELATION MATRIX
? 2
ORDER OF MATRIX ? 3
ENTER LOWER PART OF SYMMETRIC MATRIX
ENTER N VALUES FOR NTH ROW
ROW 1 ? 1
ROW 2 ? .658,1
ROW 3 ? .34,.672,1

```

```

CORRELATION MATRIX
      1      2      3
1  1.000  .658  .340
2  .658  1.000  .672
3  .340  .672  1.000
IS THIS OK? Y

```

EOF ANALYSIS BASED ON CORRELATION MATRIX

```

EIGENVALUES
      MODE 1  MODE 2  MODE 3
0/0  2.13  .66  .21
      70.86  22.00  7.14

```

```

EIGENVECTORS
      MODE 1  MODE 2  MODE 3
1  -.540  -.717  .441
2  -.641  .010  -.767
3  -.546  .697  .465

```

```

MODE/INPUT VARIANCE EXPLAINED (PERCENT)
      MODE 1  MODE 2  MODE 3
1  61.89  33.94  4.17
2  87.38  .01  12.61
3  63.30  32.06  4.64

```

Fig. 27. CM/PG data empirical orthogonal function analysis.

II-D-2-1 WRITE DATA IN TAPE4 FORMAT (fig. 28)

DATA TYPE: C	(II-B)
SORT OPTION: 0	(II-D-1)
WHAT DO YOU WANT TO DO? 6	(II-D-1)
DATA OPTION: 13	(II-D-2)

This option writes data from selected records to a permanent file in the "TAPE4 format" (see II-D-4). This enables records from the R2D2 data base to be read by other programs.

The TAPE4 records have a header field and from 1 to 5 sets of data arrays. The current meter data arrays are written in order of east velocity, north velocity, temperature, pressure, and salinity. Pressure gauge records have pressure and temperature.

After asking for filter type and time interval (II-D-2-m), R2D2 asks for the number of parameters to write, where the user should enter...

2 FOR u,v

3 FOR u,v,T

4 FOR u,v,T,P

5 FOR u,v,T,P,S

or if it is a pressure gauge record...

1 FOR P

2 FOR P,T

After all selected records have been written R2D2 will ask for permanent file name and save (using the REPLACE command) the file as an indirect access permanent file.

Subroutine: WRITE4

Program: CMLook

ENTER DATA OPTION ? 13
1 UP-1 1811 64
FILTER TYPE ? 1
START,END=800821400 802292100 LEN=3536
NEW START, END TIME ? 0,0
NEW START,END=800821400 802292100 LEN=3536
NUMBER OF PARAMETERS? 2
2 UP-2 1827 59
FILTER TYPE ? 1
START,END=800821000 802291700 LEN=3536
NEW START, END TIME ? 0,0
NEW START,END=800821000 802291700 LEN=3536
NUMBER OF PARAMETERS? 2
3 UP-3 1815 47
FILTER TYPE ? 1
START,END=800820400 802291300 LEN=3538
NEW START, END TIME ? 0,0
NEW START,END=800820400 802291300 LEN=3538
NUMBER OF PARAMETERS? 2
ENTER PERMANENT FILE NAME ? UP123

UP123 HAS BEEN SAVED!

II-D-2-m SELECTING FILTER TYPE, TIME PERIOD FOR INDIVIDUAL RECORDS

This routine is called by many of the current meter data routines described in II-D-2. It sets up parameters which tell the other routines which data type the record currently under examination is, and the time period to examine. If the record is from the R2D2 data base (as a User Data File), the program will ask for filter type, where the user will...

ENTER 0 FOR NO DATA

1 FOR 2.86 HR FILTERED DATA

2 FOR 35 HR FILTERED DATA

Entering 0 will cause the record to be skipped.

Next record start, end times are printed, and new start, end times requested. The time words are nine digit integers in the form...

YYDDDHMM

where YY is the year, DDD julian day, HH is hour (GMT) and MM the minutes. By entering 0 for start and/or end time, the original start and/or end time is retained. Entering a -1 for start time causes the record to be skipped.

A message will be printed if the times are incorrectly entered, i.e. if the new start time is earlier than the original, etc.

After the times have been established, the meter number word is examined to determine data type. If the first two characters of meter number are PG or TG, it is pressure gauge data. If they are DL or WX it is wind data. Otherwise current meter data is assumed.

Subroutine: TIMES

Program: CMLOOK

II-D-2-n SELECTING FILTER TYPE, TIME PERIOD FOR ALL RECORDS

This option sets up a common time base for a group of records, as required by option 4, 10 and 11.

As in II-D-2-m, filter type and start, end times are entered. If 0 is entered for start and/or end time the latest original start time is used as the common start time, and the earliest end time as the common end time. This gives the longest possible common time period for all records. Selection of an earlier start time or later end time has different results, depending on option selected: for option 4 (II-D-2-d) it merely extends the time axis of the plot; for 10 (II-D-2-j) and 11 (II-D-2-k) it causes records not within the common time base to be rejected. Entering a -1 for start time causes the entire set of records to be rejected.

Subroutine: TIMES2

Program: CMLOOK

II-D-2-o MAJOR AXIS DIRECTION

This routine allows for axis rotation of vector series. It will ask...

MAJOR AXIS DIRECTION?

where one should...

ENTER MAJOR AXIS DIRECTION IN COMPASS DEGREES

MINOR AXIS = MAJOR +90

FOR STANDARD u,v ENTER 0

(v = 0, u = 90)

The north and east component series will be transformed by:

$$y_t = u_t \sin(A) + v_t \cos(A)$$

$$x_t = u_t \cos(A) - v_t \sin(A)$$

where y = major axis component

x = minor axis component

u = east component

v = north component

A = major axis direction.

Subroutine: AXIS

Program: CMLook

II-D-3 SPECTRAL, TIDE ANALYSIS

DATA TYPE: C (II-B)
SORT OPTION: 0 (II-D-1)
WHAT DO YOU WANT TO DO? 7 (II-D-1)

Selection of option 7 after sorting provides access to the program SPECT, which does the spectral and tide analysis. A data file must have been sorted first (see II-D-1).

The program will begin by asking...

ENTER TS OPTION?

where the user should...

ENTER 0 TO END R2D2 SESSION (II-E)
1 FOR SCALAR SPECTRA (II-D-3-a)
2 FOR COMPONENTS, TOTAL SPECTRA (II-D-3-b)
3 FOR ROTARY SPECTRA (II-D-3-c)
4 FOR SCALAR CROSS SPECTRA (II-D-3-d)
5 FOR ROTARY CROSS SPECTRA (II-D-3-e)
6 FOR 29 DAY HARMONIC TIDE ANALYSIS (II-D-3-f)
7 FOR SUCCESSIVE TIDE ANALYSES (II-D-3-g)
99 TO RESORT

If the option is entered as a negative number terminal output will be suppressed, but will still be written on TAPE6. Option 99 returns to the CMSORT program where it asks "What do you want to do?" (II-D-1).

After the option is entered, the program begins to process each of the selected records. Options 1, 2, 3, 6 and 7 require one record per analysis, 4 and 5 two. R2D2 will ask for an OK on each record until the required number has been accepted. When a record has been accepted, R2D2 will ask for parameter if the record is 2.86 hr filtered current meter data, where...

DATA TYPE = 2 FOR U & V
= 3 for TEMPERATURE
= 4 FOR PRESSURE
= 5 FOR SALINITY

or if a pressure gauge record

DATA TYPE = 1 FOR PRESSURE
= 2 FOR TEMPERATURE

NOTE: In the SPECT program, temperature ($^{\circ}\text{C}$), pressure (dbar) and salinity (‰) are multiplied by 100 prior to analysis.

Next the start time is requested as a YYDDHHMM time word (e.g., see II-D-2-m). If 0 is entered the original start time is retained.

After checking the time base the program prints the series length (the length from the new start time to the end, or 6000, whichever is less) and asks...

ENTER LEN, NAVE, T

where...

LEN = LENGTH OF SERIES TO BE ANALYZED (MUST BE EVEN)

NAVE = NUMBER OF PERIODOGRAM BANDS TO AVERAGE

T = SHORTEST PERIOD DESIRED, HOURS

The Fast Fourier Transform (FFT) algorithm used requires an even series length with no prime number greater than 47. If necessary, LEN will be truncated accordingly. The periodogram produced by the FFT will be averaged by a boxcar of length NAVE, from the fundamental period to T. The FFT and averaging is described in II-D-3-i. The program then prints the starting frequency f_1 , bandwidth Δf , number of bands NB and degrees of freedom N where

$$f_1 = f_0 \cdot \frac{(NAVE+1)}{2} \text{ cpd}$$

$$\Delta f = f_0 \cdot NAVE \text{ cpd}$$

$$NB = \frac{\frac{24}{T} - f_1}{\Delta f} + 1$$

$$N = 2 \cdot NAVE \text{ (4} \cdot NAVE \text{ if summed components)}$$

$$f_0 = \frac{24}{LEN \cdot \Delta t} \text{ cpd}$$

Δt = time interval, hours.

and asks for an OK. If not OK, the program returns to the point of entering LEN, NAVE, T.

Then the log confidence interval (Jenkins & Watts, 1968 p. 255) is computed and printed, using a chi square distribution for N degrees of freedom.

Finally the selected spectral analysis option is performed (II-D-3-a thru e) and plotted (II-D-3-h) if desired.

After all selected records have been processed for the option, the program returns to ask for a new TS option.

Program: SPECT

II-D-3-a SCALAR SPECTRA (fig. 29)

DATA TYPE: C	(II-B)
SORT OPTION: 0	(II-D-1)
WHAT DO YOU WANT TO DO? 7	(II-D-1)
TS OPTION: ±1	(II-D-3)

This option does autospectra on scalar series. If a u-v vector series (parameter = 2) had been selected, R2D2 will ask for axis direction, and the series will be resolved into that direction (compass degrees). Output includes some header information, series mean and variance, and for each frequency: frequency (cycles per day), period (days) and variance in units squared, or (100 x units) squared if T, P or S from a current meter. Series mean and variance are computed from the data series. See II-D-3-i for discussion of calculation of the spectrum. Plotting is described in II-D-3-h.

Subroutine: SPEC1

Program: SPECT (II-D-3)

ENTER TS OPTION ? 1
 FILTER TYPE ? 2
 UP-2 1827 59 800850000 TO 802270000 LEN = 569 DT = 6.00HR
 IS THIS OK? Y
 ENTER DESIRED START TIME OR 0 FOR SAME TIME ? 0
 LENGTH IS 569
 ENTER: LEN, HAVE, T ? 500, 5, 50
 STARTING FREQUENCY = .024000 BANDWIDTH = .040000
 12 BANDS, 10 DEGREES OF FREEDOM
 IS THIS OK? Y
 LOG 95% CONFIDENCE INTERVAL = .49 TO -.31
 AXIS DIRECTION? 300

UP-2 1827 59 54 18N 164 46W 35.0 AXIS= 300

125 DAYS STARTING 800850000
 MEAN = 13.77 VAR = 404.19

F, CPD	T, DAYS	VARIANCE
.02400	41.667	127.311
.06400	15.625	38.665
.10400	9.615	50.738
.14400	6.944	38.631
.18400	5.435	34.864
.22400	4.464	22.845
.26400	3.788	12.017
.30400	3.289	11.104
.34400	2.907	16.092
.38400	2.604	12.228
.42400	2.358	7.634
.46400	2.155	1.703

TOTAL = 357.834
DO YOU WANT A PLOT?

UP-2 1827 59 54 18N 164 46W 35.0 AXIS= 300

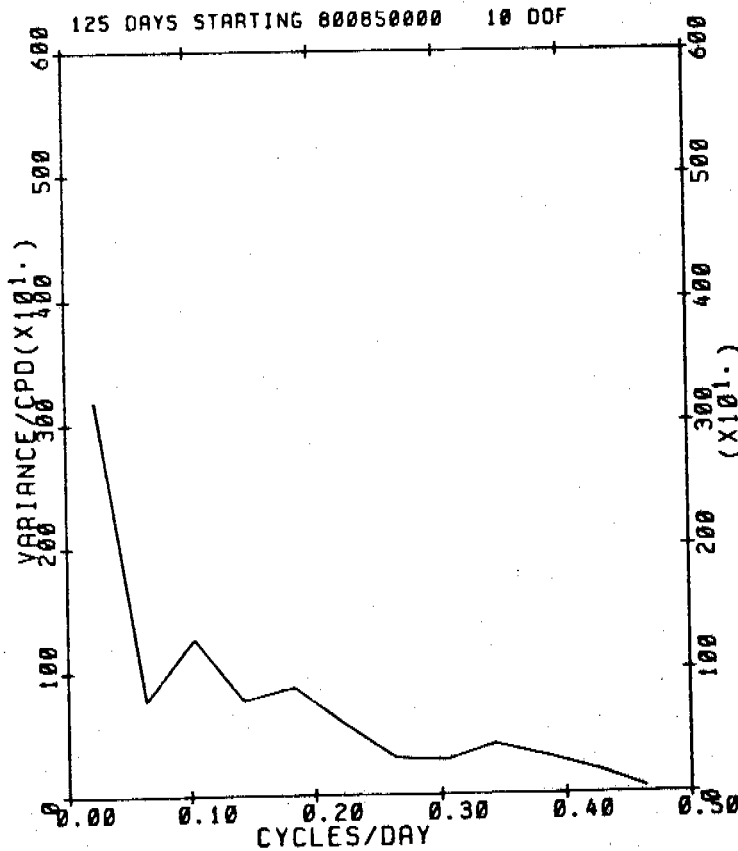


Fig. 29. Scalar auto-spectral analysis, plot.

II-D-3-b COMPONENTS, TOTAL SPECTRA (fig. 30)

DATA TYPE: C	(II-D)
SORT OPTION: 0	(II-D-1)
WHAT DO YOU WANT TO DO? 7	(II-D-1)
TS OPTION ± 2	(II-D-3)

This option does autospectra on orthogonal components of a vector series. R2D2 will ask for axis direction, in compass degrees, which will be the major axis. The minor axis is 90° to the right of the major. Entering 0 for axis direction gives the usual north and east components. (see also II-D-2-o).

Outputs include major and minor axis series means and variances, and the major, minor, and summed variance for the desired range of frequencies (II-D-3-i). Plots (II-D-3-h) may be done for the summed component spectrum (plot option 1) or the major and minor components together (plot option 2).

Subroutine: SPEC2

Program: SPECT

ENTER TS OPTION ? 2
 FILTER TYPE ? 2
 UP-2 1827 59 00050000 TO 002270000 LEN = 569 DT = 6.00HR
 IS THIS OK? Y
 ENTER DESIRED START TIME OR 0 FOR SAME TIME ? 0
 LENGTH IS 569
 ENTER: LEN, HAVE, T ? 500, 5, 50
 STARTING FREQUENCY = .024000 BANDWIDTH = .040000
 12 BANDS, 10 DEGREES OF FREEDOM
 IS THIS OK? Y
 LOG 95% CONFIDENCE INTERVAL = .49 TO -.31
 AXIS DIRECTION? 285

UP-2 1827 59 54 18N 164 46W 35.0 MAJOR= 285
 MINOR= 15
 125 DAYS STARTING 00050000
 285 AXIS MEAN = 14.29 VAR = 431.02
 15 AXIS MEAN = -.13 VAR = 12.10

F, CPD	T, DAYS	285 VAR	15 VAR	SUM
.02400	41.667	137.170	1.810	138.980
.06400	15.625	31.062	2.642	33.704
.10400	9.615	54.344	.267	54.611
.14400	6.944	33.535	.650	34.194
.18400	5.435	37.074	1.359	39.234
.22400	4.464	24.668	.177	24.844
.26400	3.708	12.808	.360	13.160
.30400	3.209	12.226	.230	12.456
.34400	2.907	18.011	.257	18.269
.38400	2.684	13.242	.420	13.670
.42400	2.358	8.432	.304	8.737
.46400	2.155	1.810	.620	2.438
TOTAL =		395.183	9.122	394.384

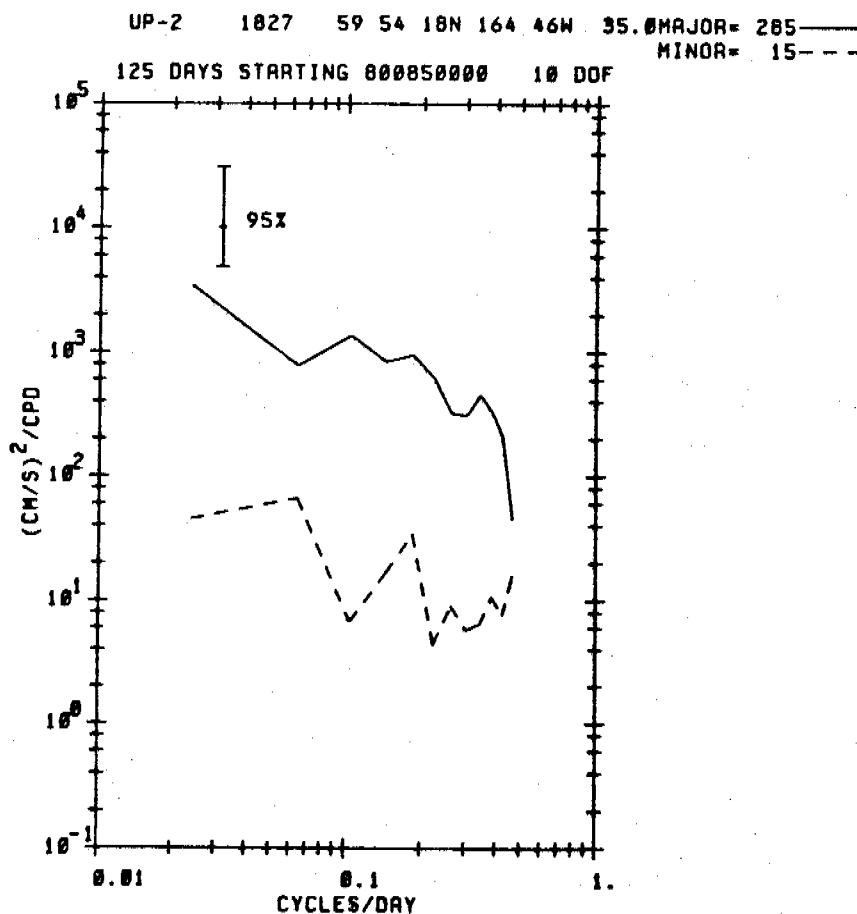


Fig. 30. Vector series auto-spectral analysis, plot.

II-D-3-C ROTARY SPECTRA (fig. 31)

DATA TYPE: C (II-B)
 SORT OPTION: 0 (II-D-1)
 WHAT DO YOU WANT TO DO? 7 (II-D-1)
 TS OPTION: ±3 (II-D-3)

This option does rotary component auto-spectra, as discussed by Mooers (1973). Briefly, the u and v component Fourier coefficients (see II-D-3-i) are transformed to clockwise and anticlockwise rotary component Fourier coefficients by:

$$C_R = (V_I - U_R) / \sqrt{2} = \text{real clockwise}$$

$$C_I = (V_R + U_I) / \sqrt{2} = \text{imaginary clockwise}$$

$$A_R = (V_I + U_R) / \sqrt{2} = \text{real anticlockwise}$$

$$A_I = (V_R - U_I) / \sqrt{2} = \text{imaginary anticlockwise}$$

and

$$C^2 = C_R^2 + C_I^2 = \text{clockwise variance}$$

$$A^2 = A_R^2 + A_I^2 = \text{anticlockwise variance}$$

$$Co = C_R A_R + C_I A_I = \text{covariance}$$

$$Q = C_R A_I - A_R C_I = \text{quadrature variance}$$

The rotary components may be used to define an ellipse, where...

$$C+A = \text{semimajor axis}$$

$$C-A = \text{semiminor axis}$$

$$\tan^{-1}(-Q/Co) = \text{major axis direction}$$

$$\frac{Co^2 + Q^2}{C^2 \cdot A^2} = \text{squared coherence between the rotary components, or ellipse axis stability}$$

Outputs include total series variance, and for each frequency: the clockwise, anticlockwise and summed variances; semimajor and semiminor axes; major axis direction; and axis stability. Plots (II-D-3-h) may be done of the summed variance spectrum (plot option 1) or the rotary components (plot option 2)

Subroutine: SPEC3

Program: SPECT

ENTER TS OPTION ? 3
 FILTER TYPE ? 2
 UP-2 1827 59 800850000 TO 802270000 LEN = 369 DT = 6.00HR
 IS THIS OK? Y
 ENTER DESIRED START TIME OR 0 FOR SAME TIME ? 0
 LENGTH IS 569
 ENTER: LEN,NAVE,T ? 500,5,50
 STARTING FREQUENCY = .024000 BANDWIDTH = .040000
 12 BANDS, 18 DEGREES OF FREEDOM
 IS THIS OK? Y
 LOG 95% CONFIDENCE INTERVAL = .49 TO -.31

UP-2 1827 59 54 18N 164 46W 35.0 CLOCKWISE
 ANTICLKWS

125 DAYS STARTING 800850000

TOTAL VARIANCE = 443.92

F,CPD	T,DAYS	CLOCKW	ANTICL	SUM	MAJ	MIN DIR	STABILITY
.0240	41.667	66.74	72.24	138.98	16.67	.33 -75.7	.951
.0640	15.625	18.41	15.30	33.70	8.20	.38 -69.0	.749
.1040	9.615	26.37	28.24	54.61	10.45	.10 -75.0	.982
.1440	6.944	17.69	16.50	34.19	8.27	.14 -77.4	.932
.1840	5.435	21.16	18.07	39.23	8.85	.35 -76.0	.875
.2240	4.464	12.76	12.09	24.84	7.05	.09 -75.9	.973
.2640	3.788	7.20	5.97	13.17	5.13	.24 -74.6	.982
.3040	3.289	6.23	6.23	12.46	4.99	.00 -78.0	.938
.3440	2.907	9.32	8.95	18.27	6.04	.06 -79.7	.970
.3840	2.684	5.95	7.72	13.67	5.22	.34 -76.4	.896
.4240	2.358	4.83	3.90	8.74	4.17	.22 -78.6	.889
.4640	2.155	1.44	1.00	2.44	2.20	.28 -77.7	.245

TOTAL = 198.09 196.21 394.30
 PLOT TYPE ?

UP-2 1827 59 54 18N 164 46W 35.0 CLOCKWISE ———
 ANTICLKWS - - -

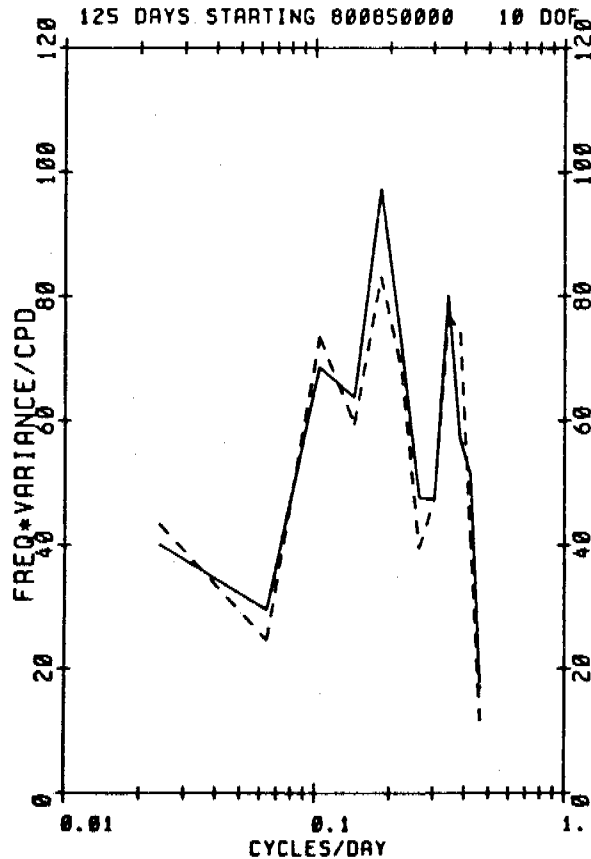


Fig. 31. Rotary auto-spectral analysis, plot

II-D-3-d SCALAR CROSS SPECTRA (fig. 32)

DATA TYPE: C (II-B)
 SORT OPTION: 0 (II-D-1)
 WHAT DO YOU WANT TO DO? 7 (II-D-1)
 TS OPTION: ±4 (II-D-3)

This option does cross spectral analysis between two scalar series. If the input series are vectors, R2D2 will request the axis direction into which to resolve the series (see II-D-3-a).

Outputs include variance of each of the input series, and for each frequency: autovariances, covariance, cross variance, phase and coherency (coherence squared). (see also II-D-3-i) The 95% significance level of coherency for N degrees of freedom is

$$1 - .05^{[2/(N-2)]}$$

If the Fourier coefficients of series X and Y are defined by X_R , X_I and Y_R , Y_I

$$X^2 = X_R^2 + X_I^2 = \text{variance of X}$$

$$Y^2 = Y_R^2 + Y_I^2 = \text{variance of Y}$$

$$Co = X_R Y_R + X_I Y_I = \text{covariance}$$

$$Q = X_R Y_I - Y_R X_I = \text{quadrature variance}$$

$$(Co^2 + Q^2)^{\frac{1}{2}} = \text{cross variance}$$

$$\tan^{-1}(Q/C) = \text{phase (X leads Y)}$$

$$k^2 = \frac{Co^2 + Q^2}{X^2 Y^2} = \text{coherency}$$

Plots may be done for the cross spectrum (plot option 1), phase spectrum (plot option 2) and coherency spectrum (plot option 3), as discussed in II-D-3-h.

Subroutine: SPEC4

Program: SPECT

```

ENTER TS OPTION ? 4
FILTER TYPE ? 2
UP-1 1811 64 800850600 TO 802270600 LEN = 569 DT = 6.00HR
IS THIS OK? Y
UP-2 1827 59 800850000 TO 802270000 LEN = 569 DT = 6.00HR
IS THIS OK? Y
ENTER DESIRED START TIME OR 0 FOR SAME TIME ? 0
LENGTH IS 568
ENTER: LEN,NAVE,T ? 500,5,50
STARTING FREQUENCY = .024000 BANDWIDTH = .040000
12 BANDS, 10 DEGREES OF FREEDOM
IS THIS OK? Y
LOG 95% CONFIDENCE INTERVAL = .49 TO -.31
UP-1 1811 64
AXIS DIRECTION? 300
UP-2 1827 59
AXIS DIRECTION? 285

```

```

UP-1 1811 64 54 34N 165 24W 35.0 AXIS= 300
UP-2 1827 59 54 18N 164 46W 35.0 AXIS= 285
125 DAYS STARTING 800850600
SERIES 1 VARIANCE = 70.54
SERIES 2 VARIANCE = 431.26
PHASE: SERIES 1 LEADS SERIES 2
95% SIGNIFICANCE LEVEL OF COHERENCY = .527

```

F, CPD	T, DAYS	VAR1	VAR2	COSPEC	VAR1X2	PHASE	CON2
.0240	41.667	54.75	136.02	81.42	81.69	-4.7	.891
.0640	15.625	6.27	30.87	11.27	12.30	-24.5	.792
.1040	9.615	4.68	54.58	10.32	13.96	-42.3	.763
.1440	6.944	1.71	33.45	.49	1.71	-73.2	.851
.1840	5.435	2.01	37.35	7.69	7.73	-6.2	.798
.2240	4.464	2.89	24.60	2.71	4.95	-56.0	.476
.2640	3.788	.56	12.64	.60	1.13	57.7	.177
.3040	3.289	.59	12.06	-.34	2.16	99.0	.649
.3440	2.987	.99	18.11	-.75	1.73	-115.6	.167
.3840	2.684	1.02	13.20	1.02	1.05	-15.2	.883
.4240	2.358	1.26	8.40	1.71	2.39	44.4	.539
.4640	2.155	.33	1.84	.03	.37	85.5	.231

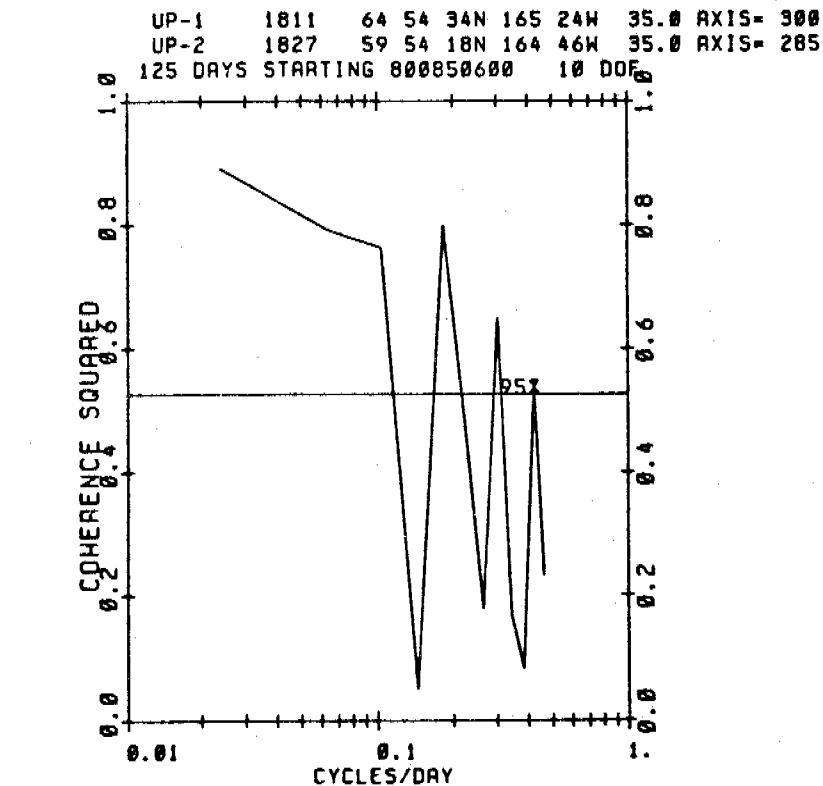


Fig. 32. Scalar cross-spectral analysis, plot.

II-D-3-e ROTARY CROSS SPECTRA (fig. 33)

DATA TYPE: C (II-B)
 SORT OPTION: 0 (II-D-1)
 WHAT DO YOU WANT TO DO? 7 (II-D-1)
 TS OPTION: ±5 (II-D-3)

This option does rotary inner cross spectra, as discussed by Mooers (1973). (See II-D-3-c for a description of the rotary autospectra and definition of terms).

Output includes input series variances and for each frequency: variance, phase and coherency for the clockwise, anticlockwise and combined components, and axis orientation difference. The 95% significance levels of coherency for N degrees of freedom are computed from

$$1-.05^{[2/(N-2)]}$$

Note that for the combined coherency (phasor in Mooers, 1973) the number of degrees of freedom is twice that for the components.

For the clockwise component

X_C^2 = clockwise variance of series X

Y_C^2 = clockwise variance of series Y

Co_C = clockwise covariance

Q_C = clockwise quadrature variance

$XY_C = (Co_C^2 + Q_C^2)^{1/2}$ = clockwise cross variance

$\phi_C = -\tan^{-1} (-Q_C/Co_C)$ = clockwise phase (X leads Y)

$k_C^2 = \frac{XY_C^2}{X_C^2 Y_C^2}$ = clockwise coherency

and similarly for the anticlockwise component, except that

$$\phi_A = -\tan^{-1}(+Q_A/Co_A)$$

For the combined spectra

$$XY_s = XY_C + XY_A = \text{summed variance}$$

$$\Delta\alpha_s = -(\phi_A + \phi_C)/2 = \text{axis difference, X clockwise from Y}$$

$$\phi_s = (\phi_A - \phi_C)/2 = \text{phase difference (X leads Y)}$$

Plots may be made of component cross variance, phase and coherence, and combined cross variance phase and coherence spectra (plot options 1-6 respectively). Section II-D-3-h describes the plots and II-D-3-i describes the FFT.

Subroutine: SPEC5

Program: SPECT (II-D-3)

```

ENTER TS OPTION ? 5
FILTER TYPE ? 2
UP-1 1811 64 800850600 TO 802270600 LEN = 369 DT = 6.00HR
IS THIS OK? Y
UP-2 1827 59 800850000 TO 802270000 LEN = 369 DT = 6.00HR
IS THIS OK? Y
ENTER DESIRED START TIME OR 0 FOR SAME TIME ? 0
LENGTH IS 568
ENTER: LEN, HAVE, T ? 500, 5, 50
STARTING FREQUENCY = .024000 BANDWIDTH = .040000
12 BANDS, 10 DEGREES OF FREEDOM
IS THIS OK? Y
LOG 95% CONFIDENCE INTERVAL = .49 TO -.31

UP-1 1811 64 54 34N 165 24W 35.0 CLOCKWISE
UP-2 1827 59 54 18N 164 46W 35.0 ANTICLKWS
125 DAYS STARTING 800850600
SERIES 1 VARIANCE = 106.99
SERIES 2 VARIANCE = 443.48
INNER CROSS SPECTRA (MODERS, 1973)
PHASE: SERIES 1 LEADS SERIES 2
95% SIGNIFICANCE LEVEL OF COMPONENT COHERENCY = .527
DAX: AXIS DIFFERENCE, SERIES 1-SERIES 2, DEG. TRUE
TOTAL COHERENCY = PHASOR; 95% SL = .283

```

F, CPD	T, DAYS	CLOCKWISE			ANTI-CLOCKWISE			TOTAL			
		UAR	PHASE	COH	UAR	PHASE	COH	UAR	DAX PHASE	COH	
.024	41.67	42.0	-27.	.796	42.1	-38.	.771	84.1	33.	-5.	.783
.064	15.63	8.2	-28.	.687	8.3	-64.	.652	16.5	46.	-18.	.661
.104	9.62	5.0	-29.	.448	12.2	-78.	.629	17.2	53.	-25.	.517
.144	6.94	2.3	-92.	.168	3.3	-111.	.396	5.6	101.	-10.	.266
.184	5.43	3.9	-25.	.553	4.1	-25.	.537	8.1	25.	-8.	.538
.224	4.46	2.7	-1.	.359	3.4	-108.	.506	6.1	54.	-53.	.430
.264	3.79	2.3	-112.	.732	1.2	-64.	.210	3.6	88.	24.	.430
.304	3.29	1.0	-129.	.643	.5	21.	.164	2.3	54.	75.	.483
.344	2.91	1.2	-145.	.108	2.6	-114.	.781	3.7	129.	16.	.381
.384	2.68	2.0	-140.	.402	3.3	-50.	.729	5.3	99.	41.	.570
.424	2.36	2.9	-108.	.669	2.0	-47.	.907	4.9	77.	31.	.731
.464	2.16	.6	-105.	.417	.1	-163.	.015	.6	134.	-29.	.198

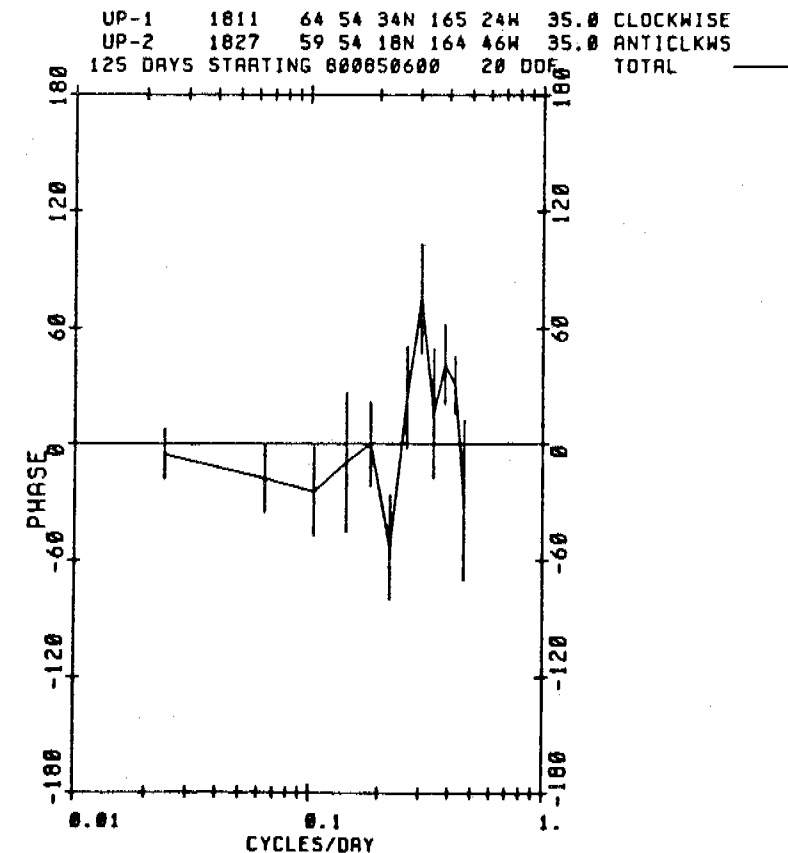


Fig. 33. Rotary cross-spectral analysis, plot.

II-D-3-f 29 DAY HARMONIC TIDE ANALYSIS (fig. 34)

DATA TYPE: C	(II-B)
SORT OPTION: 0	(II-D-1)
WHAT DO YOU WANT TO DO? 7	(II-D-1)
TS OPTION: ±6	(II-D-3)

This option does a 29-day harmonic tide analysis based on Schureman (1958) and Dennis & Long, (1971). A brief description of the method, as used in the program, follows.

The analysis begins by computing the primary orbital elements h , p_1 , s , p and N for the beginning of the observation time period, from formulas based on table 1 of Schureman. The secondary orbital functions are calculated from formulas in table 2 of Dennis & Long. Then Greenwich equilibrium arguments E and node factor reciprocals f are computed from the formulas in table 2 of Schureman and table 3 of Dennis & Long, respectively.

Next a Fourier transform is performed at the exact frequencies of the primary constituents O_1 , K_1 , N_2 , M_2 , S_2 and M_4 , from which is derived the amplitude $R'(A)$ and phase $\zeta'(A)$ of constituent A for the period of observation.

K_1 may be disturbed considerably by the nearby constituent P_1 and likewise S_2 by K_2 and T_2 . Therefore K_1 and S_2 are corrected using formulas 359-364 in Schureman, adjusted for the 29-day analysis by correction factors derived from tables 21-26. Then the amplitudes and phases of secondary constituents Q_1 , M_1 , P_1 , J_1 , $2N_2$, μ_2 , ν_2 , T_2 and K_2 are inferred from the primary constituents using the formulas 325-343 in Schureman, which are based on the equilibrium tide relationships.

Now that preliminary amplitudes and phases have been calculated, the disturbing effects on the primary constituents by the other constituents of the same species must be eliminated. This is done through the use of formulas 389 and 390 in Schureman.

Finally, the observed amplitudes and phases of the primary constituents are converted to harmonic constants

$$H(A) = R(A) \cdot f(A) \quad \text{amplitude}$$

$$G(A) = \zeta(A) + E(A) \quad \text{Greenwich phase}$$

and the secondary constituents inferred from these.

After entering the start time (II-D-3) R2D2 determines whether there are 696 hourly observations available (if not, a message will be printed and the program goes on to the next record) and then asks...

DO YOU WANT TO SAVE THE DETIDED SERIES?

If so, the detided series, as discussed below, will be saved as a permanent file in the TAPE4 format (see II-D-2-1 and II-D-4).

The tide analysis is performed on either a scalar series (i.e., pressure, temperature, salinity) or a vector current series. If a current series...

ENTER 1 FOR ANALYSIS ON AXIS

2 FOR U,V ANALYSIS WITH ELLIPSES

If 1 is entered the u, v current series will be resolved along the selected axis. Option 2 does the analysis on the u (east) component and the v (north) component, and then computes tidal ellipses for each of the constituents (described below).

Output includes Greenwich equilibrium arguments E and node factor reciprocals f for each of the constituents and the harmonic constants. The variance within the tidal bands for the observed and residual series are also computed. This is done by performing an FFT (see II-D-3-i) on the series and then summing the variance over the frequencies:

$$n \text{ cycle per lunar day} \pm 4 \text{ cycles per lunar month}$$

where $n = 1, 2, 3, 4$, a lunar day is 24.84 solar hours and a lunar month is 27.3 solar days.

The residual (detided) series is formed by computing a predicted series from the derived harmonic constants, and then subtracting the predicted series from the observed series.

95% confidence intervals of the harmonic constant amplitude H and phase G are computed from

$$CI(H) = \pm 1.96 \left(\frac{V_r}{9} \cdot \frac{27.3}{29} \right)^{\frac{1}{2}}$$

$$CI(G) = \pm \frac{CI(H)}{H} \text{ radians}$$

where V_r is the variance in the tidal band of the residual series. It should be noted that this applies to the primary constituents, and since the secondary constituents are inferred from them, the confidence intervals for the secondary constituents should be proportional to those of the primary constituents.

Ellipses are computed from the U and V component harmonic constants by

$$C_R = H_V \sin G_V - H_U \cos G_U$$

$$C_I = H_V \cos G_V + H_U \sin G_U$$

$$A_R = H_V \sin G_V + H_U \cos G_U$$

$$A_I = H_V \cos G_V - H_U \sin G_U$$

$$C = \frac{1}{2} (C_R^2 + C_I^2)^{\frac{1}{2}} = \text{clockwise amplitude}$$

$$A = \frac{1}{2} (A_R^2 + A_I^2)^{\frac{1}{2}} = \text{anticlockwise amplitude}$$

$$\theta = \tan^{-1}(C_I/C_R) = \text{clockwise phase}$$

$$\phi = \tan^{-1}(A_I/A_R) = \text{anticlockwise phase}$$

$$\text{semimajor axis} = C+A$$

$$\text{semiminor axis} = |C-A|$$

$$\text{major axis direction} = -\frac{1}{2}(\phi-\theta)$$

$$\text{major axis phase} = 90^\circ - \frac{1}{2}(\phi+\theta)$$

and the sense of rotation is determined by whether C or A is greater.

Subroutine: TIDES, TIHAR

Program: SPECT (II-D-3)

ENTER TS OPTION ? 6
 UP-2 1827 59 000021000 TO 002291700 LEN = 3536 DT = 1.00HR
 IS THIS OK? Y
 PARAMETER ? 2
 ENTER DESIRED START TIME OR 0 FOR SAME TIME ? 0
 DO YOU WANT TO SAVE THE DETIDED SERIES? N
 ENTER: 1 FOR ANALYSIS ON AXIS
 2 FOR U, V ANALYSIS WITH ELLIPSES
 ? 2

UP-2 1827 59 54 18M 164 46M 2.9 U + U
 29 DAY HARMONIC TIDE ANALYSIS
 STARTING 000021000
 O1, K1, M2, N2, S2, M4 FROM ANALYSIS, OTHERS INFERRED
 PHASES ARE REFERRED TO GREENWICH

MODE FACTOR RECIPRICALS AND GREENWICH EQUILIBRIUM ARGUMENTS

	F	E
O1	1.18035	-146.83
O1	1.18035	-74.46
M1	.61424	-195.27
P1	1.00000	-308.07
K1	1.18318	234.51
J1	1.15422	303.92
2M2	.96937	-347.66
MU2	.96937	-344.66
M2	.96937	-275.29
MU2	.96937	-272.29
M2	.96937	-202.91
L2	1.16318	-207.33
T2	1.00000	-137.47
S2	1.00000	300.00
K2	1.27237	289.86

ANALYSIS FOR EAST

OBSERVED SERIES MEAN = -20.41 VARIANCE = 4742.12
 SPECIES 1 VARIANCE = 888.15
 SPECIES 2 VARIANCE = 2654.28
 SPECIES 3 VARIANCE = 4.60
 SPECIES 4 VARIANCE = 4.82

RESIDUAL SERIES
 SPECIES 1 VARIANCE = 27.95
 SPECIES 2 VARIANCE = 12.27
 SPECIES 3 VARIANCE = 4.59
 SPECIES 4 VARIANCE = 3.27

CONST	F, CPD	H	+	G	+-
O1	.89324	5.81	3.35	71.2	33.0
O1	.92954	29.96	3.35	84.0	6.4
M1	.96643	2.13	3.35	96.0	98.3
P1	.99726	17.97	3.35	107.0	10.7
K1	1.00274	54.28	3.35	109.7	3.5
J1	1.03903	2.37	3.35	122.4	81.2
2M2	1.05969	2.45	2.22	89.1	52.0
MU2	1.06455	2.94	2.22	97.0	43.2
M2	1.09598	18.39	2.22	148.2	6.9
MU2	1.90084	3.57	2.22	156.1	35.7
M2	1.93227	68.49	2.22	207.3	1.9
L2	1.96857	1.92	2.22	233.3	65.3
T2	1.99726	.88	2.22	253.9	145.1
S2	2.00000	14.86	2.22	259.9	8.6
K2	2.00548	4.84	2.22	259.9	31.9
M4	2.86455	1.85	1.15	172.8	62.4

ANALYSIS FOR NORTH

OBSERVED = 5.26 VARIANCE = 758.22
 SPECIES 1 VARIANCE = 133.84
 SPECIES 2 VARIANCE = 437.24
 SPECIES 3 VARIANCE = 5.73
 SPECIES 4 VARIANCE = 4.85

RESIDUAL SERIES
 SPECIES 1 VARIANCE = 7.45
 SPECIES 2 VARIANCE = 4.31
 SPECIES 3 VARIANCE = 5.76
 SPECIES 4 VARIANCE = 3.35

CONST	F, CPD	H	+	G	+-
O1	.89324	2.73	1.73	228.9	36.3
O1	.92954	14.86	1.73	239.9	7.1
M1	.96643	1.00	1.73	259.0	95.3
P1	.99726	3.91	1.73	275.3	16.8
K1	1.00274	17.87	1.73	278.1	5.3
J1	1.03903	1.11	1.73	297.1	89.7
2M2	1.05969	1.00	1.32	257.2	69.7
MU2	1.06455	1.30	1.32	265.3	58.0
M2	1.09598	8.13	1.32	317.6	9.2
MU2	1.90084	1.58	1.32	325.6	47.8
M2	1.93227	27.70	1.32	17.9	2.9
L2	1.96857	.78	1.32	46.3	97.2
T2	1.99726	.26	1.32	68.7	291.4
S2	2.00000	4.38	1.32	78.9	17.2
K2	2.00548	1.19	1.32	75.2	63.2
M4	2.86455	.93	1.16	351.8	71.6

CONST	MAJOR	MINOR	DIR	PHASE	ROTATION
O1	6.29	1.27	113.0	66.3	ANTI-CLOCKWISE
O1	32.67	5.26	113.0	79.9	ANTI-CLOCKWISE
M1	2.33	.29	114.4	93.7	ANTI-CLOCKWISE
P1	18.88	1.22	107.9	100.6	ANTI-CLOCKWISE
K1	57.85	3.41	107.9	100.6	ANTI-CLOCKWISE
J1	2.61	.09	115.1	121.5	ANTI-CLOCKWISE
2M2	2.67	.20	113.5	87.2	ANTI-CLOCKWISE
MU2	3.21	.24	113.5	95.1	ANTI-CLOCKWISE
M2	20.86	1.30	113.6	154.4	ANTI-CLOCKWISE
MU2	3.89	.26	113.6	146.5	ANTI-CLOCKWISE
M2	73.76	4.22	113.6	154.4	ANTI-CLOCKWISE
L2	2.87	.09	-68.2	26.0	ANTI-CLOCKWISE
T2	.91	.02	-68.1	52.3	ANTI-CLOCKWISE
S2	15.49	.37	-73.6	73.5	ANTI-CLOCKWISE
K2	4.21	.09	-73.6	75.5	ANTI-CLOCKWISE
M4	1.48	.82	-48.6	79.4	ANTI-CLOCKWISE
M4				-8.0	ANTI-CLOCKWISE

ENTER TS OPTION ?

Fig. 34. 29 day harmonic tide analysis.

II-D-3-g SUCCESSIVE TIDE ANALYSES

DATA TYPE: C	(II-B)
SORT OPTION: 0	(II-D-1)
WHAT DO YOU WANT TO DO? 7	(II-D-1)
TS OPTION: ±7	(II-D-3)

This option performs 29-day harmonic tide analyses (as described in II-D-3-f) on successive segments of the data series, starting at the specified time (II-D-3). After each segment is analysed, 15 days is added to the start time, and another analysis performed. This continues until there are less than 696 hours remaining. The detided series cannot be saved using this option. Since the output from this option is often lengthy, it may be wise to suppress terminal output by entering -7 for TS option (II-D-3).

Subroutines: TIDES, TIHAR

Program: SPECT

II-D-3-h Plotting the spectra (figs. 29-33)

Output from each of the spectral analysis option (TS options 1-5, section II-D-3-a thru e) may be plotted. This includes variance spectra (all) and phase and coherency spectra (TS options 4 and 5). Plots may be on either linear or log frequency scale.

If a variance spectrum is to be plotted, the computed variance spectrum (units²/band) is normalized by dividing by the bandwidth (in cycles per day) to get variance in units²/cpd. Either energy density or variance preserving plots may be done. Energy density plots are done on a log energy scale, with 95% confidence intervals derived from a chi square distribution. Variance preserving spectra (e.g. Hayes, 1979) are normalized so that the area under the curve is proportional to the variance. Therefore the Y (variance) axis is linear, and is automatically scaled so that the largest variance fits within the plot boundaries. If a log frequency scale had been selected, the variances are multiplied by the frequency.

Phase spectra are plotted on an axis of $\pm 180^\circ$. A 95% confidence interval of the phase, for N degrees of freedom, is calculated from

$$\bar{F} = \pm \tan^{-1} \left(1.96 \cdot \left(\frac{1}{N} \left(\frac{1}{k^2} - 1 \right) \right)^{\frac{1}{2}} \right)$$

where k^2 is the coherency (Jenkins & Watts, 1968, p.380)

A 95% significance level for the coherence squared (coherency) for N degrees of freedom is calculated from

$$SL = 1 - .05^{[2/(N-2)]}$$

Subroutine: PLTSPC

Program: SPECT

II-D-3-1 The FFT and spectral averaging

The FFT used by the routines in SPECT is, according to the program documentation, a Cooley-Tukey Fast Fourier Transform written by Norman Brenner of M.I.T. and is described in the IEEE Audio and Electroacoustics Transactions of June 1967 and June 1969 special FFT issues. Series length is limited to even numbers whose primes do not exceed 47.

Before entering the FFT, the series is demeaned and tapered. The taper is a 10% cosine taper, where the first and last 10% of the data series of length n is multiplied by weights

$$W_i = 0.5 \left(1 - \cos \frac{i\pi}{n/10} \right) \quad i = 0, 1, \dots, n/10$$

The variances subsequently computed are then divided by 0.875 to make up for the energy lost by the taper.

The spectra are averaged by a boxcar of length NAVE to produce NB bands of width Δf , starting at f_1 (see II-D-3). For example, if the series length was 100 hours and NAVE=5, the frequencies would be .03, .08, .13cph, where the variance of the first frequency .03 cph is the sum over frequencies .01, .02, .03, .04, and .05. The spectral variances in the printed output are in accordance with Parseval's theorem, so that the sum of the variances over all frequencies (f_1 to the nyquist frequency) equals the total variance. Of course there will be discrepancies because of the tapering done on the original series.

Subroutine: FFT, TAPER, FOURT

Program: SPECT

II-D-4 The TAPE4 FORMAT

Perhaps a user wants to use R2D2 with data that is not in the R2D2 data base, or it may be desirable to use data from the data base in some other program. For these reasons the "TAPE4" format was developed for current meter, pressure gauge or wind data.

The TAPE4 format consists of an unformatted 9 word header field and from 1 to 5 sets of unformatted data arrays. The header field, with suggested output format is:

- 1) mooring name (A10)
- 2) meter number (A5)
- 3) meter depth, m (I5)
- 4) start time (I10)
- 5) end time (I10)
- 6) series length (I5)
- 7) data time interval, minutes(F5.0)
- 8) latitude, decimal degrees (F8.3)
- 9) longitude, decimal degrees (F8.3)

Start time and end time are written as 9 digit integers YYDDHHMM where YY is year, DDD julian day, HH hour and MM minutes.

The data arrays are written in order of east velocity, north velocity, temperature, pressure and salinity. Pressure gauge data has pressure and temperature. Data are written in arrays of maximum size 2000. If the actual series length is larger than 2000, the first 2000 of each parameter are written, then the next 2000, etc.

For example, if a current meter record of length 3500 is written, and

U, V, T are the parameters, the "TAPE4" file would be:

MOOR,MET,MDEP,IST,IET,NPT,DT,ALAT,ALON

U(I),I=1,2000

V(I),I=1,2000

T(I),I=1,2000

U(I),I=2001,3500

V(I),I=2001,3500

T(I),I=2001,3500

EOR

All selected records are written on one file, separated by end-of-records.

To write data from the data base to a TAPE4 file see II-D-2-1. To use a TAPE4 file in R2D2 see II-D-1-c.

II-E Ending R2D2

The R2D2 session may be ended by entering a 0 for "WHAT DO YOU WANT TO DO?" (II-C-1, II-D-1) or for the options in the main data programs (II-C-2, II-D-2, II-D-3). After 0 is entered, R2D2 will ask one final question...

DO YOU WANT OUTPUT PRINTED AT PMEL?

If the answer is yes, TAPE6 will automatically be routed to the PMEL RJE terminal. Otherwise it will remain as a local file until returned or the user logs off.

Another way to end R2D2 is to enter the word STOP for any input request. This is a NOS command which will immediately terminate program execution.

II-F Miscellaneous routines

Several routines which require user input are used in many different options, and are described in this section.

II-F-1 Map drawing (fig 7, 16)

This routine draws a Mercator projection map, with user specified boundaries and scale and optional coastline.

When first entering this routine during execution of one of the main programs, it will ask...

WHICH MAP FILE?

where one should

ENTER 0 FOR NONE

1 FOR GULF OF ALASKA

2 FOR BERING SEA

3 FOR PUGET SOUND

The Gulf of Alaska coastline extends from Cape Spencer to the Aleutians; the Bering Sea file includes the Aleutians and parts of Siberia and extends from the Alaskan Peninsula to Kotzebu Sound; and the Puget Sound file includes Puget Sound, Strait of Juan de Fuca to the Pacific coast, San Juan Islands and southern Strait of Georgia. Coastline resolution is about 5 km for the Alaska

files and 1 km for Puget Sound. If 0 is entered (for NONE) no file will be attached, but if TAPE3 already exists as a local file it will be read as a coastline file. The TAPE3 format is:

DLAT,DLON,IFLAG

where DLAT = meridional parts of latitude, decimal degree (positive north)

= M/60

DLON = longitude, decimal degrees (positive west)

IFLAG = 2 pen down when moving to this point

3 pen up " " " " "

Latitude is converted to meridional parts using Bowditch's (1962, p.1187)

formula

$$M = 7915.704468 \log \tan \left(45 + \frac{L}{2} \right) - 23.268932 \sin L - 0.0525 \sin^3 L - 0.000213 \sin^5 L$$

where L is degrees of latitude.

After attaching the coastline file, R2D2 will ask for latitude and longitude boundaries (II-C-1-d) if necessary, and then ask...

ENTER SCALE,ATLAT,TICK,YLEN

where

SCALE = CHART SCALE

ATLAT = LATITUDE OF SCALE

TICK = SPACING OF TICK MARKS IN DEGREES

YLEN = LENGTH OF LATITUDE AXIS IN INCHES

Scale may be entered as the scale from a mercator nautical chart, accompanied by the latitude for that scale. If scale is entered, the parameter YLEN is ignored and the map is drawn to scale, and may be overlaid on a nautical chart. If scale is entered as 0, ATLAT is ignored and the scale is computed from YLEN and the latitude boundaries. TICK specifies the spacing of the latitude and longitude tick marks. For example TICK = .25 will cause a tick mark every 15' on the plot. Values of latitude and longitude are written every whole degree and at the corners.

After the parameters are entered R2D2 will print the scale and plot dimensions, ask for an OK and proceed with the plot.

Subroutine: MCHART

II-F-2 Plotting

Plotting is done for the most part using standard Calcomp calls. An exception is the AXIS routine, which has been modified to accept a variable number of digits to the right of the decimal point, as in the NUMBER routine. The Calcomp routines write a plot file on TAPE99 of X,Y,IP

where X and Y are the pen coordinates in inches and IP is the pen position (2 = move with pen down, 3 = move with pen up).

After a plot file is written subroutine PLOTR is called. On the first call to PLOTR, R2D2 will ask...

ARE YOU USING A TEKTRONIX TERMINAL?

If not, R2D2 will proceed to save the plot on TAPE98 (see below). If the answer is yes...

ENTER BAUD RATE?

This enables plotting on a Tektronix graphic terminal, using the PLOT10 library routines. Plots are scaled in the vertical to fit a Tektronix 4012 screen (780 x 1023 screen coordinates). If the horizontal dimension of the plot is too large to fit the screen, the leftmost segment will be plotted first, then the next segment, and so on until the entire plot has been drawn. After each segment is plotted, a "?" will appear in the upper left corner accompanied by a "beep", which stops execution until something is entered. If an "E" is entered the plot will be ended, otherwise it will continue.

When the plotting has been completed R2D2 will ask...

DO YOU WANT TO SAVE THIS FOR OFFLINE PLOTTING?

If the answer is yes, or if one is not using a Tektronix terminal, the plot will be saved as a permanent file for later offline (Calcomp) plotting. Before the first plot is saved, R2D2 will attempt to DEFINE TAPE98 as a direct access permanent file. If an old TAPE98 already existed, it may be purged or its name changed, so that a new TAPE98 may be DEFINED. The plot is then written from TAPE99 to TAPE98 in arrays of 300, where 1 to 100 are X, 101 to 200 are Y, and 201 to 300 are IP (written as floating point). The value of IP following the last point plotted is set to -99, signifying the end of plot. Successive plots are separated by end-of-records, and all plots from one session are on one file. TAPE98 may be used later as input to procedure file R2PLOT for plotting on the PMEL Calcomp plotter (see III-A), or as input to any other plotting program.

Subroutines: PLOTR, TEKPLT

III. Associated user programs

III-A. R2PLOT: offline plotting

Procedure file R2PLOT reads a TAPE98 plot file (II-F-2) and writes a file which is routed to the PMEL RJE terminal for plotting on the Calcomp plotter. The user executes R2PLOT by entering...

```
GET,R2PLOT/UN=RLC
```

```
R2PLOT, pfn
```

where pfn is the name (usually TAPE98) of the TAPE98 direct access permanent file. All plots saved from one R2D2 session are on one file. Several TAPE98 files may be merged prior to executing R2PLOT using COPYBF.

R2PLOT begins by attempting to execute a BANNER file (see II-A-2), and then executes the program R2PLOT. R2PLOT uses subroutines PLOTS,SYMBOL,and PLOT from the Calcomp library CCLIB on UN=PMELIB. The user number and date are plotted first, and then the plots from the TAPE98 file, each separated by 2 inches. The output file is named PLOTS, which is REPLACE'd and then routed to the PMEL RJE. If the maximum plot dimension in the vertical exceeds 10.5", FC=PW. Otherwise FC=PN. When execution is complete, the final portion of the dayfile is printed.

Program: R2PLOT

III-B UPLT

UPLT is a procedure file which executes a program to plot positions on a mercator projection (see II-F-1). The user executes UPLT by entering

```
GET,UPLT/UN=RLC
```

The program reads local file TAPE4, which contains station name, latitude, longitude, symbol code and pen position. TAPE4 format is:

columns	format	
1-10	A10	name
11-14	F4.0	degrees latitude (+north)
15-20	F6.2	minutes latitude
21-24	F4.0	degrees longitude (+west)
25-30	F6.2	minutes longitude
31	1X	blank
32-33	I2	calcomp SYMBOL code
34	I1	calcomp PLOT pen position (3 = default)

Plotting of the station name is optional. Plotting proceeds until an end-of-record is encountered. Then TAPE4 may either be rewound, or the next record plotted.

If a station falls outside the map boundaries, a message is printed and it is not plotted.

Plotting is done using the R2D2 routines (II-F-2 and III-A).

IV. Data structure, maintenance programs

IV-A STD

IV-A-1 STD data structure

The R2D2 STD files are stored as two-level random access packed binary files. The master header files, stored as direct access permanent files on NOAA family disks, contain header information only. The Master Data Files contain headers and data, and are stored on a private disk pack.

The random access storage location is keyed to the unique station reference number, which is assigned sequentially when the data are loaded. The first level of indexing points to the locations of the second level of indexing, which has addresses of the data. The first level index is

$$IA = (IREF-1)/100 + 1 \text{ (truncated)}$$

where IREF is the reference number. IA is the subscript of array INDA (size 100) which contains the address for the array INDB. INDB contains 200 values, the first 100 of which are addresses for the header information for 100 casts, and the second 100 the packed data.

Thus, the header address subscript is...

$$IND = IREF - (IA - 1) \cdot 100$$

and the data address subscript = $IND + 100$

The header field consists of 13 words: reference number (I), cruise name (A), cast number (I), station name (A), decimal latitude (F), decimal longitude (F), time word (I), station depth (F) series length (I), depth of first data (F), ship name (A), chief scientist name (A) and master reference number (I).

The time word is described in II-C-1-e. In master files the reference number equals the master reference number. New reference numbers, starting with 1, are assigned sequentially when creating User Data Files.

The data are packed temperature-salinity words in arrays of variable length, defined in the header. The first 30 bits of the data word contains temperature and the last 30 are salinity. Temperature is recovered by masking the last 30 bits using logical AND. Salinity is recovered by shifting the salinity bits to the temperature space and then masking the last 30 bits.

IV-A-2 STD data loading

The STD data loading is done using submit file STDLOAD, which attaches the data and header files and runs program STDMS2.

TAPE1 contains one-meter averaged STD data in the Coastal Physics format. TAPE2 is the Master Header File and TAPE3 the Master Data File. The first input card contains the previous last reference number LAST in I5 format (i.e., the first of the new set will be LAST+1). If the input number is less than or equal to 0, the LAST will be read from TAPE2. The effect of entering LAST on the input card is to redefine LAST and overwrite subsequent data. The next input card contains ship name, chief scientist name and comments, in 8A10 format. A new card is read whenever a new cruise name is read from TAPE1.

The TAPE1 header information is read and printed, a reference number assigned, and header fields written on TAPE2 and TAPE3. Temperature and salinity are packed into one word and written in the data arrays on TAPE3. See II-A-1 for data structure. The full header information from TAPE1 is printed and the output stored in room 304 Showboat.

Program: STDMS2

IV-A-3 Editing STD header files

Occasionally the header information has been entered incorrectly when processing the STD data, or data must be deleted from R2D2. In those cases program STDEDIT is used to correct the R2D2 header file.

The header file is attached in the write mode as TAPE7. On execution, STDEDIT will ask....

- ENTER 0 TO END EDITING
- 1 TO DELETE CASTS
- 2 TO EDIT CRUISE NAME
- 3 " " CAST NUMBER
- 4 " " STATION NAME
- 5 " " LATITUDE
- 6 " " LONGITUDE
- 7 " " TIME
- 8 " " STATION DEPTH
- 9 " " ND
- 10 RESTORE DELETED CAST

Options 1 and 2 are done on a range of reference numbers, the rest one at a time. After each change the program will ask for an OK. Deletions are made by changing the reference numbers to 0.

Note that only the header file is changed. The Master Data File retains the original headers. The new header information is carried to the User Data Files via TAPE5, the list of selected stations (see II-C-2).

This program should be used only by the person responsible for maintaining the data base.

IV-B Current meter data

IC-B-1 Current meter data structure

Like the STD files, the current meter/pressure gauge files are stored as two-level random access packed binary files. The Master Header Files, stored as direct access permanent files on NOAA Family disks, contain header information only. The Master Data Files contain headers and data, and are stored on a private disk pack.

The random access storage location is keyed to the unique station reference number, which is assigned sequentially when the data are loaded. The first level of indexing points to the locations of the second level of indexing, which has the addresses of the data. The first level index is

$$IA=(IREF)/10+1 \text{ (truncated)}$$

where IREF is the reference number. IA is the subscript of array INDA (size 100) which contains the address for the array INDB. INDB contains 100 values, the first 10 of which contain addresses of header information for 10 records, and the next 90 for data of the 10 records.

The header address subscript is...

$$IND=IREF-(IA-1)\cdot 10$$

and the data address subscripts= $IND+10\cdot n$, where n is determined by data type, filter type, and data segment.

The header field consists of a 15 word integer array IVAR and 30 word floating point array FVAR, where

IVAR(1) = reference number (I)
IVAR(2) = project name (A)
IVAR(3) = mooring name (A)
IVAR(4) = meter number (A)
IVAR(5) = meter depth (I)
IVAR(6) = 2.86 hr filtered data start time (I)
IVAR(7) = 2.86 hr filtered data end time (I)
IVAR(8) = 2.86 hr filtered data length (I)
IVAR(9) = 35 hr filtered data start time (I)
IVAR(10) = 35 hr filtered data end time (I)
IVAR(11) = 35 hr filtered data length (I)
IVAR(12) = master reference number
IVAR(13-15) used internally by R2D2 routines
FVAR(1) = latitude, decimal degrees
FVAR(2) = longitude, decimal degrees
FVAR(3) = bottom depth
FVAR(4)-(23) data statistics computed during loading
FVAR(24)-(30) used internally by R2D2 routines.

The 2.86 and 35 hour filtered velocity components U & V are packed into one word. Basically, the least significant 30 bits of the original 60 bit words are masked off. Then the 30 most significant bits are left justified and contain a sign bit, an 11-bit biased exponent and an 18-bit integer coefficient (see Control Data Corp. Fortran Extended Version 4 reference

manual #60305601, p.III-4-1). The truncated V is then shifted 30 bits to the right and a new 60 bit u-v word formed by taking the logical product of the two.

The 2.86 hr filtered temperature, pressure and salinity words are packed in a somewhat different way. Each are multiplied by 1000 and rounded to the nearest integer. Then they are shifted and logically combined so that each occupies 20 bits of a 60 bit T-P-S word.

Up to 8000 2.86 hour filtered hourly data points may be stored, and 2000 35-hr filtered 6-hourly data. Storage location array subscripts are as follows:

IND	Headers
IND+10	2.86 hr filtered U-V points 1-2000
IND+20	" " " T-P-S " "
IND+30	" " " U-V " 2001-4000
IND+40	" " " T-P-S " "
IND+50	" " " U-V " 4001-6000
IND+60	" " " T-P-S " "
IND+70	" " " U-V " 6001-8000
IND+80	" " " T-P-S " "
IND+90	35 hr filtered U-V

Pressure gauge pressure and temperature data are packed in the same way as the U-V current meter data. Up to 16000 2.86 hr filtered P-T words may be stored, using both the U-V and T-P-S data areas.

IV-B-2 Current meter-pressure gauge data loading

Loading of the current meter data is a two-step process. Step one filters the data and step two loads the filtered records.

The filtering program, FILTR, applies two separate low-pass filters to the data. Input data are in the Coastal Physics "edited data format". Data processing is described in Krancus, Pearson and Charnell (1979). The filters are symmetrical Lanczos filters derived from the GENER1 routine in the FESTSA library.

The 2.86 hr filter is so called because the half amplitude response of the filter is at a period of 2.86 hours. Over 99% of the amplitude is passed at a period of five hours and less than 0.1% at 2 hours. Filtered data are resampled at 1 hour intervals and interpolated to whole hours using a second order polynomial. All parameters are 2.86 hr filtered. Kernel half width is 4 hours.

The 35 hr filter has half amplitude response at 35 hrs, passes 99% at 55 hours and less than 0.1% at 25 hours. This effectively removes the tides. U and V components are 35 hr filtered (pressure and temperature for pressure gauges) resampled at 6-hourly intervals and interpolated to 00, 06, 12, 18 hours GMT. Kernel half-width is 60 hours.

Program CMLoad adds the filtered data (TAPE9) to the Master Header File (TAPE2) and Master Data File (TAPE3). Statistics are computed (means, maxima, minima and variances of the parameters), stored in the header FVAR array, and printed. Data are packed and stored as described in IV-B-1.

IV-B-3 Editing CM/PG header files.

Errors in the Master Header File may be corrected using program CMEDIT. Header information may be edited or records may be deleted. Only the Master Header File is changed. Corrections are transferred via TAPE5 to User Data Files when they are created.

The Master Header File is attached in the write mode as TAPE7. CMEDIT begins by asking...

ENTER 1 TO EDIT THE HEADERS

2 TO DELETE DATA SETS

Records are deleted by changing the reference numbers of the sets to be deleted to 0.

If editing the headers, the program will ask...

ENTER REFERENCE NUMBER OR 0 TO END EDITING?

then...

ENTER INDEX?

where...

INDEXES ARE: 0 TO END ENTERING INDEXES

1 TO CHANGE PROJECT NAME

2 TO CHANGE MOORING NAME

3 TO CHANGE METER NUMBER

4 TO CHANGE METER DEPTH

5 TO CHANGE LATITUDE

6 TO CHANGE LONGITUDE

7 TO CHANGE BOTTOM DEPTH

When 0 is entered the new header is printed and if OK, will be written in place of the old header.

Note that times may not be changed. This is because the start and end times are computed in the filter program and are different for each filter. To correct the time base, the start time should be changed in the "edited data" record, and then refiltered and loaded.

This program should only be used by the person responsible for maintaining the data base.

Acknowledgements

R2D2 was conceived in 1977 from discussions between Robert Charnell, Gary Krancus and the author. Mr. Charnell, who was Coastal Physics group leader until he was lost at sea aboard the HOLO HOLO in December 1978, provided many ideas and a great deal of enthusiasm for the project. Gary Krancus was responsible for many of the program and data structure concepts, and wrote the early versions of CMSORT and CMLOOK. Many other people contributed ideas and helped in finding the "bugs", including James Schumacher, Michael Grigsby, Cathleen Wright, Gary Lagerloef and Rocky Geyer. D. James Baker kindly provided the FFT routines, Glen Watabayashi the Calcomp routines, and Clifford Fridlind the digitized coastlines. Thanks also to Phyllis Hutchens for typing and Joy Golly for drafting.

This work was supported in part by the Bureau of Land Management through interagency agreement with the National Oceanic and Atmospheric Administration, under which a multi-year program responding to needs of petroleum development of the Alaskan continental shelf is managed by the Outer Continental Shelf Environmental Assessment Program (OCSEAP) Office.

REFERENCES

- Allen, J.S. and P.K. Kundu, 1978. On the momentum, vorticity and mass balance on the Oregon Shelf, Journal of Physical Oceanography, 8, pp.13-27.
- Bowditch, N., 1962. American Practical Navigator, U.S. Navy Hydrographic Office, Wash. D.C., 1524 pp.
- Dennis, R.E., and E.E. Long, 1971. A user's guide to a computer program for harmonic analysis of data at tidal frequencies, NOAA Tech. Report NOS 41, U.S. Dept. of Commerce, Wash. D.C., 31 pp.
- Hayes, S.P., 1979. Benthic current observation at DOMES sites A, B, and C in the tropical North Pacific Ocean, from Marine Geology and Oceanography of the Pacific Marganese Nodule Province, J.L. Bischoff and D.Z. Pipes ed., Plenum Publishing, pp 83-112.
- Jenkins, G.M. and D.G. Watts, 1968. Spectral Analysis and Its Applications, Holden-Day, San Francisco, 525 pp.
- Krancus, G.A., C.A. Pearson and R.L. Charnell, 1979. A one-pass processing system for Aanderaa current meter data, in Proceedings Second Working Conference on Oceanographic Data Systems 1978, C.D. Tollios ed., pp 96-111.
- Mooers, C.N.K., 1973. A technique for the cross spectrum analysis of pairs of complex-valued time series, with emphasis on properties of polarized components and rotational invariants, Deep-Sea Research, 20, pp. 1129-1141.

Pearson, C.A., G.A. Krancus and R.L. Charnell, 1979. R2D2: An interactive graphics program for rapid retrieval and display of oceanographic data. In: Proceedings Second Working Conference on Oceanographic Data Systems, 1978, C.D. Tollios ed., pp. 318-329.

Schureman, P.W., 1958. Manual of harmonic analysis and prediction of tides, C&GS Special Publication No. 98, Revised(1940) Edition, U.S. Dept. of Commerce, Wash. D.C., 317 pp.

U.S. Department of Commerce
National Oceanic & Atmospheric Administration
Office of Marine Pollution Assessment
Alaska Office, RD/MPF24
P.O. Box 1808
Juneau, Alaska 99802

POSTAGE AND FEES PAID
U.S. DEPARTMENT OF COMMERCE
COM-210



OFFICIAL BUSINESS
PENALTY FOR PRIVATE USE, \$300

